Oxidative Medicine and Cellular Longevity

Alleviation of Drugs and Chemicals Toxicity: Biomedical Value of Antioxidants

Lead Guest Editor: Mohamed M. Abdel-Daim
Guest Editors: Khaled Abo-EL-Sooud, Lotfi Aleya, Simona G. Bungău, Agnieszka Najda, and Rohit Saluja

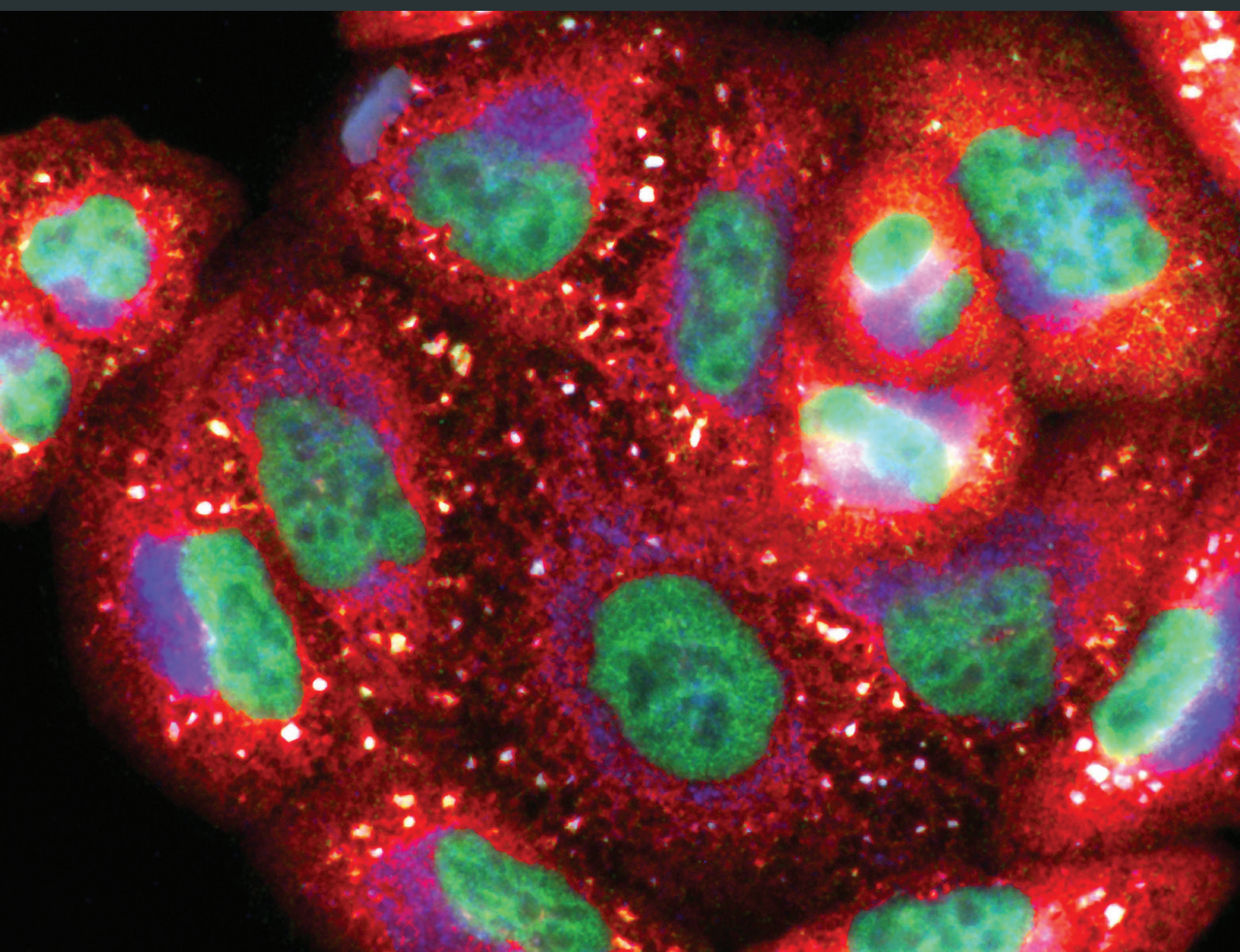

Alleviation of Drugs and Chemicals Toxicity: Biomedical Value of Antioxidants

Oxidative Medicine and Cellular Longevity

Alleviation of Drugs and Chemicals Toxicity: Biomedical Value of Antioxidants

Lead Guest Editor: Mohamed M. Abdel-Daim
Guest Editors: Khaled Abo-EL-Sooud, Lotfi Aleya, Simona G. Bungău, Agnieszka Najda, and Rohit Saluja

Editorial Board

Contents

Hindawi
Oxidative Medicine and Cellular Longevity
Volume 2018, Article ID 6276438, 2 pages
https://doi.org/10.1155/2018/6276438

Editorial

Alleviation of Drugs and Chemicals Toxicity: Biomedical Value of Antioxidants

Mohamed M. Abdel-Daim,[1] **Khaled Abo-EL-Sooud**,[2] **Lotfi Aleya**,[3] **Simona G. Bungău**,[4] **Agnieszka Najda**,[5] **and Rohit Saluja**[6]

[1]*Pharmacology Department, Faculty of Veterinary Medicine, Suez Canal University, Ismailia 41522, Egypt*
[2]*Pharmacology Department, Faculty of Veterinary Medicine, Cairo University, Giza, Egypt*
[3]*Chrono-Environment Laboratory, UMR CNRS 6249, Bourgogne Franche-Comté University, F-25030 Besançon Cedex, France*
[4]*Department of Pharmacy, Faculty of Medicine and Pharmacy, University of Oradea, Oradea, Romania*
[5]*Department of Vegetable Crops and Medicinal Plants, University of Life Sciences, Lublin, Poland*
[6]*All India Institute of Medical Sciences, Department of Biochemistry, Bhopal, Madhya Pradesh, India*

Correspondence should be addressed to Mohamed M. Abdel-Daim; abdeldaim.m@vet.suez.edu.eg

Received 12 November 2018; Accepted 12 November 2018; Published 17 December 2018

Understanding the mechanism of drug- and chemical-induced toxicities is the primary interest of many researchers worldwide to develop enhanced preventive and therapeutic strategies. Paracelsus (the father of toxicology) assumed that all chemicals and drugs as well as natural products—including antioxidants—could induce toxicity when received in high doses. His rule "the dose makes the poison" is now considered the core principle of traditional toxicology. Recently, researchers understood that toxicity is a complicated process affected by many factors, including developmental exposures, genetic predisposition, and doses [1].

Antioxidants exist naturally in many beverages, fruits, and vegetables, and they can be synthesized in laboratories [2]. They delay or ameliorate cellular oxidative damage; therefore, they have several health benefits in the prevention and treatment of diseases. They could be used alone or in combination with other medications as adjuvant treatments [3].

The study of free radicals and antioxidants leads to a revolution in medicine, which includes promising new solutions in health and disease management. In the last decade, the search for effective nontoxic natural compounds with antioxidant activity has been intensified. In addition to endogenous antioxidant defense systems, the use of plant-derived antioxidants is an appropriate alternative [4, 5]. In this special issue, many original studies and review articles focused on the value of antioxidants in ameliorating drug- and chemical-induced toxicities.

To evaluate chemical-induced cytotoxicity, Radaković et al. analyzed both the biochemical and genetic effects of adrenaline toxicity in rats. They concluded that adrenaline causes nitrative and oxidative stress through which they induce damage to cellular genes, proteins, and lipids, resulting in cardiomyocyte injury. Further, Abdelazim et al. examined the oxidative effects of zinc oxide nanoparticles (ZnONPs) on the muscles of Nile tilapia, as well as the potential protective role of vitamins (C and E) via enhancement of enzymatic and nonenzymatic antioxidant systems.

Other studies investigated the benefits of antioxidants in ameliorating the toxicity of common medications with frequent toxic effects. For example, Barakat et al. investigated the protective effects of boswellic acids (BAs) against doxorubicin- (DOX-) induced hepatotoxicity in mice. They concluded that BAs modulate the hemeoxygenase-1 (HO-1) and NF-E2-related factor 2 (Nrf2) pathways, resulting in reactive oxygen species (ROS) scavenging and reduction of DNA and lipids oxidative damage. Further, Liao et al. used dl-3-n-butylphthalide (dl-NBP) to alleviate DOX-induced

anxiety and depression-like behaviors through attenuation of ER stress, oxidative stress, neural apoptosis, and inflammatory reaction, providing the basis for potential preventive and therapeutic strategy against DOX-induced neurotoxicity.

The value of natural antioxidant compounds has been shown in several studies in this issue. For example, Saleh et al. concluded that berberine-rich fraction (BF) improved the infertility induced by gossypol acetate through anti-inflammatory and antioxidant mechanisms. Further, Duan et al. demonstrates that cadmium induces toxicity in the grass carp (*Ctenopharyngodon idellus)* liver through oxidative damage and activation of the caspase signaling cascade. However, treatment with Vitamin E and metallothionein alleviated cadmium hepatotoxicity through their antioxidant and antiapoptotic effects. Similarly, Palacios et al. used ascorbate to overcome the cardiovascular complications of the naphthoquinone derivative 2-(4-Hydroxyphenyl) amino-1,4-naphthoquinone in rats through inhibition of oxidative stress and reduction of blood pressure.

In addition, Abdel-Rahman and colleagues examined the antioxidant and hepatoprotective activities of the phytochemical (lycopene) against the endocrine disruptor xenoestrogen (Bisphenol A) through improving the liver function and oxidant-antioxidant balance and reducing DNA damage. In the same vein, Lebda et al. established the mechanism of miswak, *Salvadora persica*, extract ameliorative effects against ethanol-induced gastric ulcer in rats through the upregulation of transforming growth factor-β1 (TGF-β1) and endothelial nitric oxide synthase (eNOS) gene expression, improving the oxidant/antioxidant balance and mitigating the production of proinflammatory cytokines and apoptosis.

Other studies examined the value of synthetic antioxidants. For example, Guo et al. synthesized a novel dithiocarbamate, DpdtbA (di-2-pyridylhydrazone dithiocarbamate butyric acid ester), and investigated its anticancer activities. They found that it inhibits cellular growth through ROS formation and evoking p53, leading to the alteration of gene expressions related to cell survival. Further, Aly et al. used a molecular intersimple sequence repeat (ISSR) assay and cytogenetic biomarker analysis to examine the cyclophosphamide- (CP-) induced cytotoxicity and mutagenicity, as well as the potential preventive effects of the fullerene C_{60} nanoparticle (C_{60}) and virgin olive oil in rats.

In this issue, a review article by Wen and colleagues summarized the physiological and pathological roles of hydrogen sulfide (H_2S) in processes like atherosclerosis, hypertension, myocardial infarcts, and angiogenesis and examined its value as a target for drug development.

Conflicts of Interest

All guest editors declare that there are no conflict of interest or private agreement with the company or any other organizations.

Acknowledgments

The editors thank all authors who submitted their research to this special issue. They extend their thanks to all reviewers for their valuable comments and contribution to this special issue.

Mohamed M. Abdel-Daim
Khaled Abo-EL-Sooud
Lotfi Aleya
Simona G. Bungău
Agnieszka Najda
Rohit Saluja

References

[1] J. F. Robinson, J. L. A. Pennings, and A. H. Piersma, "A review of toxicogenomic approaches in developmental toxicology," *Methods in Molecular Biology*, vol. 889, pp. 347–371, 2012.

[2] S. Shaban, M. W. A. El-Husseny, A. I. Abushouk, A. M. A. Salem, M. Mamdouh, and M. M. Abdel-Daim, "Effects of antioxidant supplements on the survival and differentiation of stem cells," *Oxidative Medicine and Cellular Longevity*, vol. 2017, 16 pages, 2017.

[3] D. Bolignano, V. Cernaro, G. Gembillo, R. Baggetta, M. Buemi, and G. D'Arrigo, "Antioxidant agents for delaying diabetic kidney disease progression: a systematic review and meta-analysis," *PLoS One*, vol. 12, no. 6, article e0178699, 2017.

[4] K. El Bairi, M. Ouzir, N. Agnieszka, and L. Khalki, "Anticancer potential of Trigonella foenum graecum: cellular and molecular targets," *Biomedicine & Pharmacotherapy*, vol. 90, pp. 479–491, 2017.

[5] M. S. Brewer, "Natural antioxidants: sources, compounds, mechanisms of action, and potential applications," *Comprehensive Reviews in Food Science and Food Safety*, vol. 10, no. 4, pp. 221–247, 2011.

Hindawi
Oxidative Medicine and Cellular Longevity
Volume 2018, Article ID 1805354, 11 pages
https://doi.org/10.1155/2018/1805354

Research Article

Nitroso-Oxidative Stress, Acute Phase Response, and Cytogenetic Damage in Wistar Rats Treated with Adrenaline

Milena Radaković,[1] Sunčica Borozan,[2] Ninoslav Djelić,[1] Saša Ivanović,[3] Dejana Ćupić Miladinović,[3] Marko Ristanić,[1] Biljana Spremo-Potparević,[4] and Zoran Stanimirović[1]

[1]*Department of Biology, Faculty of Veterinary Medicine, University of Belgrade, Bulevar oslobodjenja 18, 11000 Belgrade, Serbia*
[2]*Department of Chemistry, Faculty of Veterinary Medicine, University of Belgrade, Bulevar oslobodjenja 18, 11000 Belgrade, Serbia*
[3]*Department of Pharmacology and Toxicology, Faculty of Veterinary Medicine, University of Belgrade, Bulevar oslobodjenja 18, 11000 Belgrade, Serbia*
[4]*Department of Physiology, Faculty of Pharmacy, University of Belgrade, Vojvode Stepe 450, 1221 Belgrade, Serbia*

Correspondence should be addressed to Milena Radaković; mradakovic@vet.bg.ac.rs

Received 30 March 2018; Revised 19 July 2018; Accepted 12 September 2018; Published 21 November 2018

Guest Editor: Mohamed M. Abdel-Daim

This study is aimed at analysing biochemical and genetic endpoints of toxic effects after administration of adrenaline. For this purpose, the study was carried out on Wistar rats and three doses of adrenaline were used: 0.75 mg/kg, 1.5 mg/kg, and 3 mg/kg body weight. To achieve these aims, we investigated the effects of adrenaline on catalase (CAT), Cu, Zn-superoxide dismutase (SOD), malondialdehyde (MDA), nitrite (NO_2-), carbonyl groups (PCC), and nitrotyrosine (3-NT). Total activity of lactate dehydrogenase (LDH), its relative distribution (LDH_1–LDH_5) activity, level of acute phase proteins (APPs), and genotoxic effect were also evaluated. The obtained results revealed that all doses of adrenaline induced a significant rise in CAT activity, MDA level, PCC, NO_2^-, and 3-NT and a significant decrease in SOD activity compared to control. Adrenaline exerted an increase in total activity of LDH, LDH_1, and LDH_2 isoenzymes. Further study showed that adrenaline significantly decreased serum albumin level and albumin-globulin ratio, while the level of APPs (α_1-acid glycoprotein and haptoglobulin) is increased. The micronucleus test revealed a genotoxic effect of adrenaline at higher concentrations (1.5 mg/kg and 3 mg/kg body weight) compared to untreated rats. It can be concluded that adrenaline exerts oxidative and nitrative stress in rats, increased damage to lipids and proteins, and damage of cardiomyocytes and cytogenetic damage. Obtained results may contribute to better understanding of the toxicity of adrenaline with aims to preventing its harmful effects.

1. Introduction

Adrenaline (epinephrine) is a naturally occurring catecholamine which is secreted by the medulla of the adrenal glands. As a drug, adrenaline was discovered over a century ago and has been used in human cardiopulmonary resuscitation since 1922 [1]. Adrenaline also finds application in treatment of cardiac arrest, asthma, allergic reactions, and glaucoma [2]. Adrenaline acts through the alpha and beta adrenergic receptors which leads to vasoconstriction, an increase in the rate and force of contraction of the heart, and dilatation of bronchi and cerebral vessels. During normal physiological conditions, there is no constant secretion of adrenaline, but under the stress condition, a high level of adrenaline is released to prepare body for "fight or flight" response [3].

However, adrenaline at other catecholamine at doses exceeding physiological levels may cause toxic effects [4, 5]. There are studies indicating toxic effects of adrenaline via signal transduction pathways [6, 7]. Also, it seems that adrenaline exerts detrimental effects via oxidative products of its metabolism [8–10]. In line with this, it was shown that autooxidation of catecholamine may generate reactive oxygen

species (ROS) [11]. One of the final products of oxidative metabolism-adrenochrome is able to stimulate oxidation of adrenaline in which superoxide anion ($O_2^{\cdot-}$) and hydrogen peroxide (H_2O_2) are formed. Besides, it was reported that catalase and quercetin diminished the DNA-damaging effect of adrenaline *in vitro* [12].

It is well known that overproduction of ROS can lead to disruption of redox balance and cause oxidative stress [13]. Namely, if antioxidative mechanisms fail to remove excess level of ROS, cells become prone to damage of DNA, proteins, and lipids [14]. Proteins are among major targets of ROS or reactive nitrogen species (RNS) and lead to changes in protein content such as carbonyl group formation and nitrotyrosine (3-NT) generation [15]. There are assumptions that high level of adrenaline may cause protein damage via free radicals [16]. It is worth noting that oxidative damage to proteins plays an important role in loss of physiological functions, thus favoring development of various diseases [17–19]. On the other hand, lipid peroxidation by ROS may initiate the peroxidation of membrane lipids and cause cellular injuries. In addition, oxidative DNA damages play a role in the mutagenesis and an increased risk of tumors [20, 21].

Although there are indications that adrenaline could increase the level of ROS, the cause-consequence relationship between them is not fully understood. For this purpose, we determined parameters of oxidative status: catalase (CAT) Cu, Zn-superoxide dismutase (SOD), malondialdehyde (MDA), nitrite (NO_2^-), lactate dehydrogenase (LDH), and carbonyl groups (PCC) after administration of adrenaline in Wistar rats. Also, we evaluated how adrenaline influenced the level of acute phase proteins (APPs), α_1-acid glycoprotein (AGP), haptoglobin (Hp), and level of 3-NT. Possible genotoxic effects of adrenaline on bone marrow cells using micronucleus test were also estimated. The results of this investigation should contribute to a better understanding of adrenaline toxicity with aims to preventing its harmful effects.

2. Materials and Methods

2.1. Animals. In this study, Wistar rats aged 18 weeks weighing 220–280 g were obtained from the Institute of Biomedical Research, University of Belgrade. Three experimental groups with adrenaline and two control groups (negative and positive) contained seven male Wistar rats. The animals were kept under controlled constant environmental conditions ($25 \pm 4^{\circ}$C, $55 \pm 5\%$ humidity) with a 12/12 h light/dark cycle. They received food and water *ad libitum*. Care and animal treatment were conducted according to the Guide for the Care and Use of Laboratory Animals (National Research Council [22]). The investigation was approved by the Ethical Committee of the Faculty of Veterinary Medicine (University of Belgrade).

2.2. Doses and Treatment. Three experimental doses of adrenaline were used: 0.75 mg/kg, 1.5 mg/kg, and 3 mg/kg body weight, corresponding to 15%, 30%, and 60%, respectively, of LD50 [23]. Cyclophosphamide was used as a positive control and 60 mg/kg body weight per rats was given, while the negative control group was treated with saline (0.9% NaCl) [24]. The intraperitoneal (i.p.) route of application was used in all experimental groups. After 24 hours of treatments, all rats were euthanized. From each animal, blood and bone marrow from both femurs were taken.

2.3. Blood Sampling. Blood samples for the biochemical analysis were taken from the rats by puncture of *v. jugularis* and collected into heparinized tubes. Plasma was obtained from blood by centrifugation at 3000 rpm for 10 min. Erythrocytes were rinsed three times in isotonic solution of NaCl (0.9%). Then, samples were frozen at −20°C until analysis. Haemoglobin concentration was estimated by the cyanomethaemoglobin method [25]. Haemolysates of erythrocytes were used for determination of activities of antioxidant enzymes (SOD, CAT) and level of MDA. Plasma was used for determination of NO_2^- concentration, 3-NT, protein carbonyl groups, total LDH level and its isoenzyme activity, and levels of APPs, Hp, and AGP.

2.4. Oxidative Stress Parameters. The Cu, Zn-superoxide dismutase (SOD) activity in erythrocytes was determined spectrophotometrically according to Misra and Fridovich [26] and expressed in units/gram of haemoglobin (U/g Hb). The relative activity of SOD was determined by means of vertical electrophoresis at 10% polyacrylamide gel electrophoresis (PAGE) and oxidation of nitro blue tetrazolium (NBT) following the Beauchamp and Fridovich method [27] (Hoeffer miniVE, Amersham, LKB, 2117, Bromma, Uppsala, Sweden). The band intensity was measured using TotalLab TL120, and results were expressed in arbitrary U/g Hb.

Catalase (CAT) activity in erythrocytes was assayed by means of the UV kinetic method at absorbance of 240 nm with the presence of H_2O_2 [28]. Activity was expressed as U/g Hb, calculated by using an extinction coefficient of $39.4\,M^{-1}\,cm^{-1}$.

The level of malondialdehyde (MDA) in erythrocytes was quantified by measuring the formation of thiobarbituric acid reactive substances (TBARS) [29, 30]. The absorbance of the colored MDA-TBARS complex was measured at a wavelength of 535 nm and expressed in nM MDA/g Hb.

Nitrite concentration (NO_2^-) in plasma was determined with Griess reagent [31] on a microplate reader at 540 nm (plate reader, Mod. A1, Nubenco Enterprises, ICN). The results were expressed in μM.

The determination of carbonyl groups (PCC) was performed spectrophotometrically with 2,4-dinitrophenylhydrazine at 365 nm [32]. The concentration of carbonyl groups was calculated on the basis of the absorption coefficient for this chromogen ($a = 22.000\,M^{-1}\,cm^{-1}$); the results are shown in μM.

Alpha 1-acid glycoprotein (AGP) determined using Native PAGE, haptoglobin (Hp), and 3-nitrotyrosine (3-NT) levels in plasma of rats was determined using SDS-PAGE and Imunobloth methods with polyclonal antibody produced in rabbit (Sigma-Aldrich, St. Louise, USA) and monoclonal anti-3-nitrotyrosine antibody produced in mouse (Sigma-Aldrich, St. Louise, USA) [33, 34].

2.5. Determination of LDH. Total lactate dehydrogenase (LDH) was determined by following the initial rate of pyruvate reduction to lactate [34]. The activity of LDH was expressed in units per liter (U/L). Isoenzyme forms of LDH (LDH_1-LDH_5) were detected by PAGE technique (Hoeffer MiniVE, LKB, 2117, Bromma, Uppsala Sweden) using Tris-glycine buffer and sodium-lactate as substrates in the presence of nitro blue tetrazolium chloride [35]. Band intensity was measured densitometrically using TotalLab TL 120. The relative activity of isoenzymes was shown in percentages.

2.6. Native Gel Electrophoresis of Plasma Proteins. Vertical polyacrylamide gel electrophoresis at pH 8.6 (alkaline-PAGE) was carried out with Hoeffer miniVE cell (Amersham, LKB, 2117, Bromma, Uppsala Sweden) at 120 V and room temperature for 2 h. The gel used (0.75 mm thick) consisted of 4.5% T staking gel and 8% T separation gel (T% is an expression representing the concentration of acrylamide plus bisacrylamide in the gel). The electrode and migration buffers consisted of 0.19 M glycine and 0.024 M Tris at pH 8.6. After electrophoresis, proteins were stained using Coomassie blue 0.1% [36]. The band intensity was measured using TotalLab TL120. Results were shown in percentages in relation to the total area. The albumin : globulin ratio was calculated by dividing albumin content by the sum of α-, β-, and γ-globulins.

2.7. Micronucleus Test. The preparation and staining of bone marrow cells for the micronucleus test were performed according to Schmid [37] and Mavournin et al. [38]. After 24 hours of treatment, the bone marrow cells were flushed out with fetal calf serum, and the cells were suspended through centrifugation, smeared, and stained with May-Grünwald and Giemsa solution. A total of 1000 polychromatic erythrocytes were scored for each animal at a magnification of 100x (oil immersion) using a microscope (Leica, Germany). The PCE/NCE ratio was calculated to determine the cytotoxic effects of the adrenaline. All slides were coded and scored blind.

2.8. Statistical Analysis. Statistical significance of differences of all examined parameters was determined by means of the ANOVA test followed by Dunnett test. Normality tests were first performed for all groups using the d'Agostino-Pearson omnibus test. Data were expressed as means ± stan dard error (S.E.). Significance level was set at $P < 0.05$. Statistical analysis was done using GraphPad Prism 7.0 Software, CA, USA.

3. Results

Results of the analysis of total activity of Cu, Zn-SOD enzyme in rats treated with adrenaline are shown in Figure 1. It was observed that adrenaline treatment significantly decreased ($P < 0.001$) the total enzyme activity by 26.09%, 38.09%, and 69.97%, respectively, in relation to the control group. Cyclophosphamide, as positive control, also reduces activity of SOD (48.54%, $P < 0.001$). The decreased activities of SOD biochemical assay were verified by the results of electrophoresis as shown in Figure 1(b).

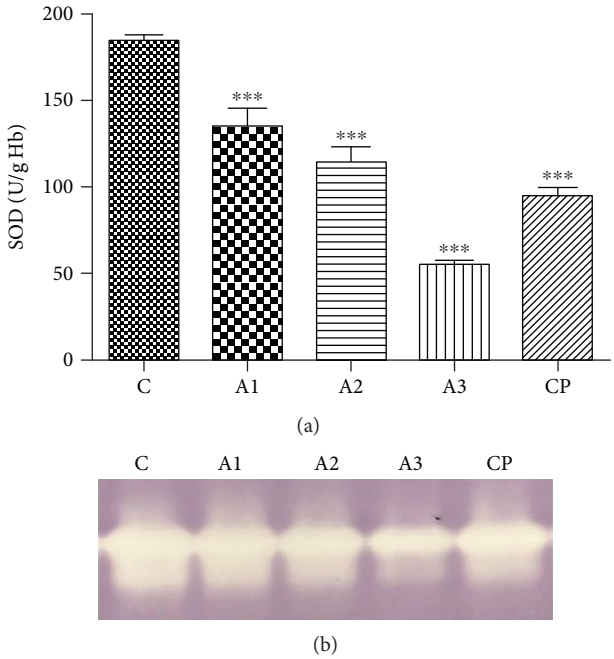

Figure 1: SOD activity after treatment with adrenaline (a), electrophoregram (b). Control group - C, groups treated with adrenaline doses (A1-0.75 mg/kg; A2-1.5 mg/kg; A3-3 mg/kg body weight); group treated with cyclophosphamide (CP). Data are expressed as means ± SE. $^{***}P < 0.001$ vs. control group.

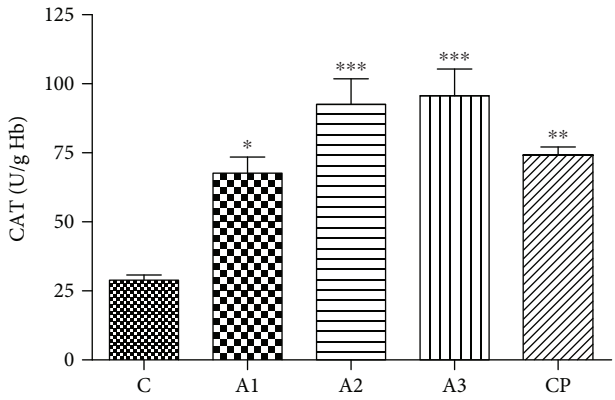

Figure 2: CAT activity after treatment with adrenaline. Control group - C, groups treated with adrenaline doses (A1-0.75 mg/kg; A2-1.5 mg/kg; A3-3 mg/kg body weight); groups treated with cyclophosphamide (CP). Data are expressed as means ± SE. $^{*}P < 0.05$, $^{**}P < 0.01$, $^{***}P < 0.001$ vs. control group.

Significant increase in CAT activity was identified at all concentrations of adrenaline (Figure 2). The lowest concentration of adrenaline (0.75 mg/kg) induced significant increases (67.66 ± 5.83 U/g Hb, $P < 0.05$) in activity of CAT while the higher concentrations (1.5 mg/kg and 3 mg/kg) of adrenaline induce a more evident increase (92.50 ± 9.35 U/g Hb and 95.65 ± 9.73 U/g Hb, $P < 0.001$) compared to the control group (28.92 ± 1.83 U/g Hb). Similarly, the activity of CAT was significantly increased ($P < 0.01$) after treatment with cyclophosphamide.

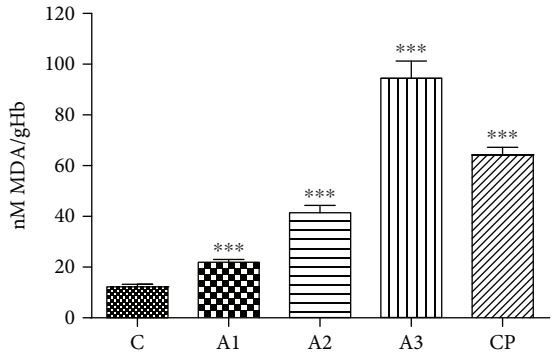

Figure 3: The level of MDA after treatment with adrenaline. Control group - C, groups treated with adrenaline doses (A1-0.75 mg/kg; A2-1.5 mg/kg; A3-3 mg/kg body weight); group treated with cyclophosphamide (CP). Data are expressed as means ± SE. $^{***}P < 0.001$ vs. control group.

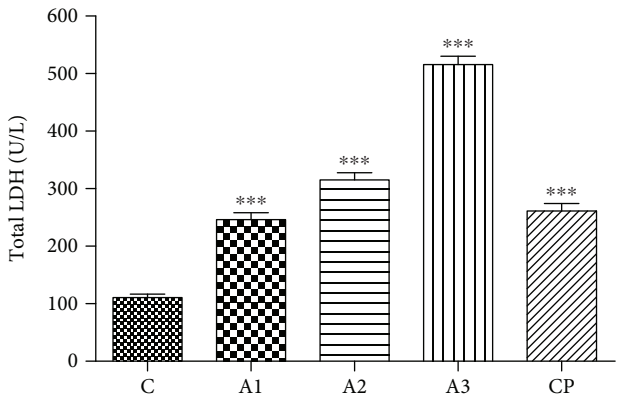

Figure 4: The total LDH level after treatment with adrenaline. Control group - C, groups treated with adrenaline doses (A1-0.75 mg/kg; A2-1.5 mg/kg; A3-3 mg/kg body weight); groups treated with cyclophosphamide (CP). Data are expressed as means ± SE. $^{***}P < 0.001$ vs. control group.

In Figure 3, MDA levels after treatment with adrenaline are shown. Adrenalin exerted a significant increase in a dose-dependent manner (1.84-, 3.41-, 7.78-, and 5.29-fold, $P < 0.001$) in MDA levels in rats compared to the untreated group (Figure 3). Also, cyclophosphamide induced a significant rise ($P < 0.001$) in MDA levels in respect to the control.

Results of the total LDH and its relative isoenzyme distribution in rats treated with adrenaline are shown in Figures 4 and 5. There was clearly an increase ($P < 0.001$) in total activity of LDH in the group treated with all doses of adrenaline compared to the control group. Cyclophosphamide induces a less profound effect than the group treated with 3.5 mg/kg dose of adrenaline, but the total activity of LDH is also significantly increased ($P < 0.001$) in comparison to the control.

In Figure 5, it was observed that the LDH_1 isoenzyme shows an evident increase ($P < 0.001$) in rats treated with adrenaline in respect to the control group. The lower but statistically significant effect ($P < 0.05$, $P < 0.001$) was evident in the activity of LDH_2 isoenzyme after adrenaline treatment compared to the control group. Similarly, significant intensity bands for LDH_1 and LDH_2 isoenzymes were noticed in

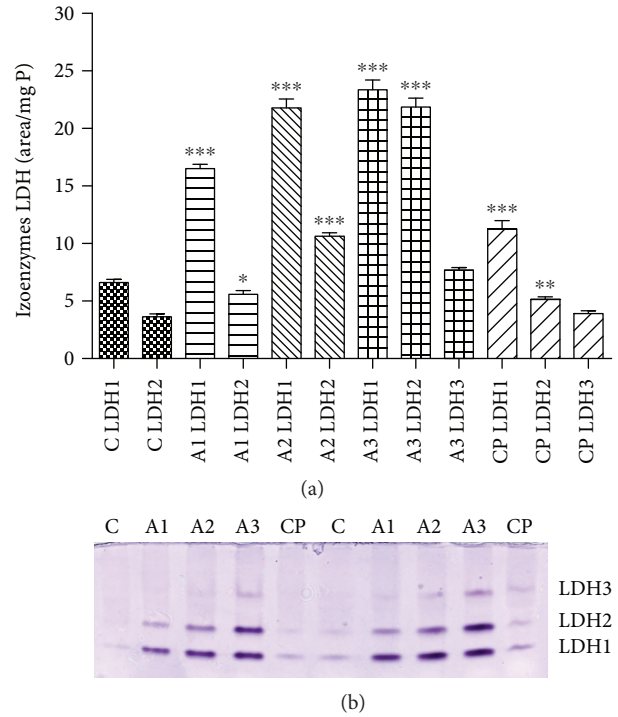

Figure 5: Relative distribution of LDH1-LDH5 isoenzymes (a) with electrophoretic profiles (b) after treatment with adrenaline. Control group - C, groups treated with adrenaline doses (A1-0.75 mg/kg; A2-1.5 mg/kg; A3-3 mg/kg body weight); group treated with cyclophosphamide (CP). Data are expressed as means ± SE. $^{*}P < 0.05$, $^{**}P < 0.01$, $^{***}P < 0.001$ vs. control group.

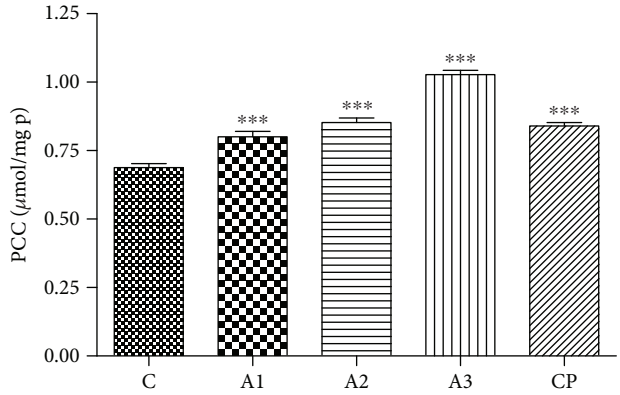

Figure 6: The PCC levels after treatment with adrenaline. Control group - C, groups treated with adrenaline doses (A1-0.75 mg/kg; A2-1.5 mg/kg; A3-3 mg/kg body weight); group treated with cyclophosphamide (CP). Data are expressed as means ± SE. $^{***}P < 0.001$ vs. control group.

the group of rats treated with higher concentrations of adrenaline. The activity of isoenzymes LDH_1 and LDH_2 was also significantly increased ($P < 0.01$, $P < 0.001$) in rats treated with cyclophosphamide.

The effect of adrenaline on PCC levels in rats is presented in Figure 6. Compared to untreated rats, the significant elevation ($P < 0.001$) of PCC levels after treatment with all tested doses of adrenaline was noticed (Figure 6). Rats treated with

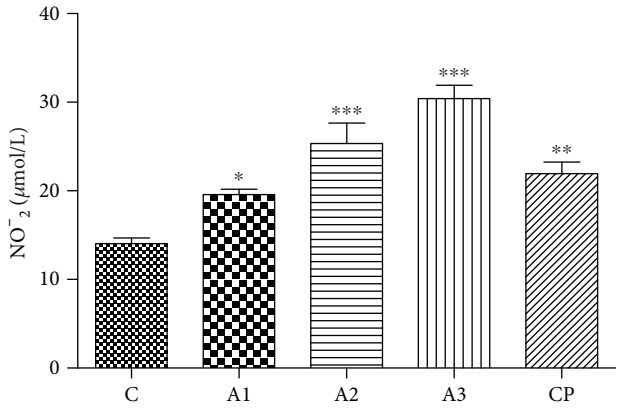

Figure 7: The level of NO2- in rats after treatment with adrenaline. Control group - C, groups treated with adrenaline doses (A1-0.75 mg/kg; A2-1.5 mg/kg; A3-3 mg/kg body weight); group treated with cyclophosphamide (CP). Data are expressed as means ± SE. $^*P < 0.05$, $^{**}P < 0.01$, $^{***}P < 0.001$ vs. control group.

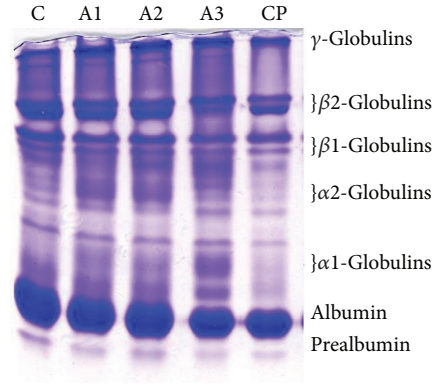

Figure 8: Representative electrophoregram of plasma proteins with Native PAGE after treatment with adrenaline. Control group- C, groups treated with adrenaline doses (A1-0.75 mg/kg; A2-1.5 mg/kg; A3-3 mg/kg body weight); groups treated with cyclophosphamide (CP).

cyclophosphamide also showed a significant rise ($P < 0.001$) in PCC levels in comparison to control.

The level of NO_2^- in rats after treatment with adrenaline is shown in Figure 7. Adrenaline induced a significant elevation of NO_2^- level in a dose-dependent manner. The highest concentration (3 mg/kg) of adrenaline induced the most distinct increases of NO_2^- ($P < 0.001$) compared to the control group. Positive control also induces a significant increment in the level of NO_2^- ($P < 0.01$).

The results of the electrophoretic distribution of plasma proteins are shown in Figure 8, while the results of their relative distribution are given in Table 1.

In our studies, reduced albumin concentration in adrenaline treatment has been demonstrated, and this decrease is dose-dependent. Adrenaline has been shown to reduce albumin concentration by 5.81%, 16.09%, and 18.75% depending on the dose level, while due to exposure to cyclophosphamide, the decrease of albumin is 9.62%. By comparing the results of albumin level in all groups with the control group, a statistically significant decrease in albumin was observed in the adrenaline-treated group with 1.5 and 3.0 mg/kg ($P < 0.01$). A significant increase in α1 fraction (AGP, α1-antitrypsin) versus the control group was observed in groups treated with adrenaline in doses of 0.75 mg/kg and 1.5 mg/kg ($P < 0.01$), and 3 mg/kg ($P < 0.001$), with increases by 42.97%, 45.09%, and 252.79%, respectably. The α2-fraction (Hp, ceruloplasmin, and α2-macroglobulin) was affected only by adrenaline treatment in doses of 0.75 mg/kg, 1.5 mg/kg, and 3.0 mg/kg and increases by 80.40% ($P < 0.05$), 150.67% ($P < 0.01$), and 79.36% ($P < 0.05$). A significant decrease ($P < 0.05$) of the β1-fraction (transferrin, haemopexin, and β-lipoproteins) versus the control group was noticed in groups treated with adrenaline in doses of 0.75 mg/kg (18.88%), 1.5 mg/kg (27.63%), and 3 mg/kg (19.32%). The β2-fraction (fibrinogen, C3, and β2-microglobulin) in groups treated with adrenaline was decreased by 27.78% (dose 0.75 mg/kg), 28.24% (1.5 mg/kg), and 50.69% (3 mg/kg), which was significantly lower ($P < 0.001$) than in the control group. In prealbumin and γ-globulin fractions, there were no significant differences between treated and control groups. A significant decrease ($P < 0.05$) in the ratio (A : G) versus control group was noticed in groups treated with adrenaline in doses of 1.5 mg/kg and 3 mg/kg.

The significant increase ($P < 0.001$) in AGP levels was noticed in rats treated with adrenaline, especially at higher doses (1.5 mg/kg and 3 mg/kg) in respect to the control group (Figure 9). Related results of AGP levels on electropherogram were also detected.

The effect of adrenaline treatment on level of haptoglobin (Hp) in rats is presented in Figure 10. The significant difference ($P < 0.01$, $P < 0.001$) was observed in the level of Hp in rats treated with 0.75 mg/kg, 1.5 mg/kg, and 3 mg/kg of adrenaline, versus the control group, respectively. These results conformed with the electrophoretic profile.

The effect of adrenaline treatment on level of 3-nitrotyrosine (3-NT) in rats is presented in Figure 11. A significant difference ($P < 0.001$) was evident in the level of nitrotyrosine in rats treated with all doses (1.5 mg/kg and 3 mg/kg) of adrenaline while a 0.75 mg/kg dose of adrenaline affects ($P < 0.01$) on the rise at the 3-NT level. In that manner, the intensity of the band was most evident at 3 mg/kg of adrenaline in the electrophoretic profile.

The results of the micronucleus (MN) test in bone marrow of rats treated with adrenaline are shown in Table 2. Adrenaline induced a significant increase ($P < 0.001$) in the frequency of micronucleated polychromatic erythrocytes (MNPCE) at higher concentrations (1.5 mg/kg, 3 mg/kg) when compared with the negative control group. Also, significant and dose-dependent decreases in polychromatic erythrocyte/normochromatic erythrocyte (PCE/NCE) ratio were seen in higher doses of adrenaline (1.5 mg/kg, 3 mg/kg). As expected, cyclophosphamide (60 mg/kg) induced a significant increase ($P < 0.001$) in MNPCE and decreases in the PCE/NCE ratio in respect to the control.

4. Discussion

In the last few decades, researchers focus on detecting harmful effects of chemical substances that are used as drugs in order to

Table 1: Relative distribution of proteins with Native PAGE after treatment with adrenaline.

Groups	Intensity, % (mean ± SD)							Ratio (A : G)
	Prealbumin	Albumin	α1-	α2-	β1-	β2-	γ-Globulins	
C	2.66 ± 0.52	57.62 ± 3.80	5.19 ± 0.56	2.96 ± 1.62	15.89 ± 1.49	8.64 ± 0.79	7.04 ± 0.52	1.36 ± 0.22
A1	4.57 ± 0.57**	54.32 ± 1.07	7.42 ± 1.03**	5.34 ± 1.20*	12.89 ± 0.70*	6.24 ± 1.27*	9.78 ± 1.38*	1.20 ± 0.15
A2	3.66 ± 0.25	48.39 ± 3.72**	8.53 ± 0.66**	7.42 ± 1.36**	11.50 ± 0.85**	6.20 ± 1.28*	9.43 ± 1.23	0.94 ± 0.22*
A3	2.05 ± 0.32	46.86 ± 2.54**	18.31 ± 3.01***	5.31 ± 1.32*	12.82 ± 1.52*	4.26 ± 2.57**	9.47 ± 1.56	0.88 ± 0.28*
CP	3.69 ± 0.47*	52.07 ± 1.25	6.07 ± 1.73	2.17 ± 1.52	16.14 ± 0.83	9.66 ± 0.84**	9.11 ± 1.42	1.08 ± 0.23

*$P < 0.05$, **$P < 0.01$, and ***$P < 0.001$. C: control group, groups treated with adrenaline doses (A1, 0.75 mg/kg; A2, 1.5 mg/kg; and A3, 3 mg/kg body weight); CP: group treated with cyclophosphamide.

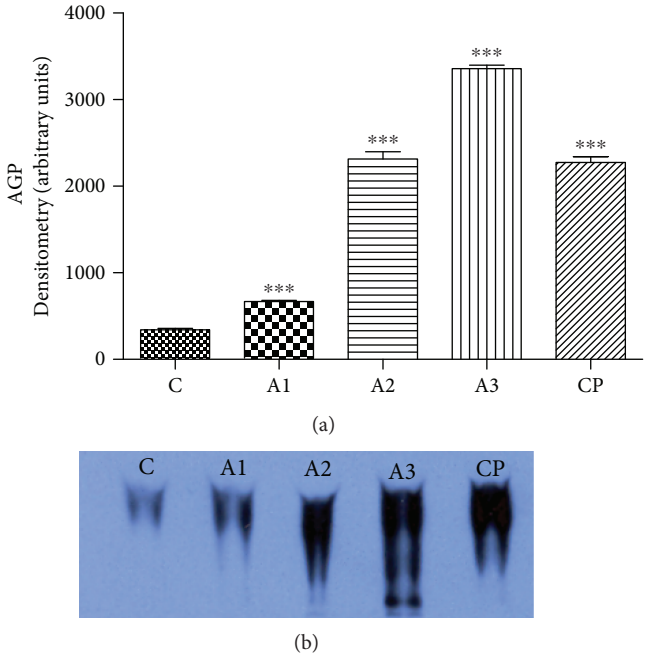

Figure 9: Immunohistochemical detection of APG on Native PAGE. The level of AGP (a) with electrophoregram (b) after treatment with adrenaline. Control group - C, groups treated with adrenaline doses (A1-0.75 mg/kg; A2-1.5 mg/kg; A3-3 mg/kg body weight); group treated with cyclophoshamide (CP). Data are expressed as means ± SE. **$P < 0.01$, ***$P < 0.001$ vs. control group.

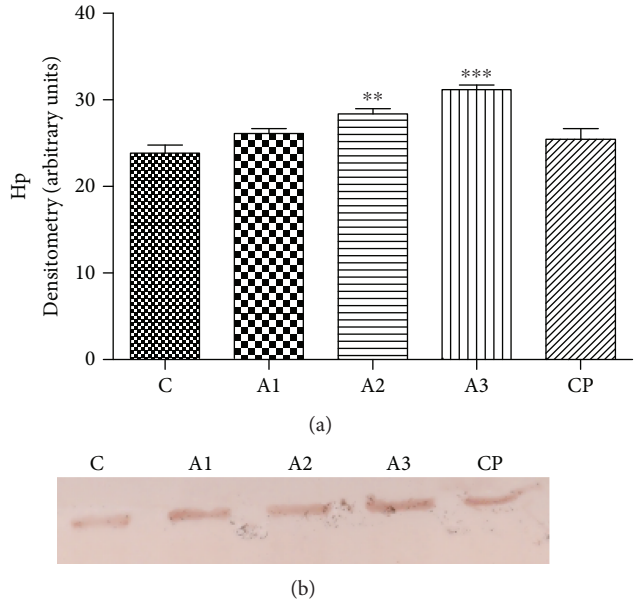

Figure 10: The level of haptoglobin (a) with electrophoregram (b) after treatment with adrenaline. Control group - C, groups treated with adrenaline doses (A1-0.75 mg/kg; A2-1.5 mg/kg; A3-3 mg/kg); group treated with cyclophosphamide (CP). Data are expressed as means ± SE. **$P < 0.01$, ***$P < 0.001$ vs. control group.

protect human health. In this study, we investigated toxic effects of adrenaline on Wistar rats using various parameters (SOD, CAT, MDA, NO_2^-, LDH, PCC, AGP, 3-NT, and APP) and obtained results unequivocally indicate that adrenaline at doses of 0.75 mg/kg, 1.5 mg/kg, and 3 mg/kg exerts oxidative and nitrative stress in rats.

In this study, SOD activity in erythrocytes was significantly decreased while CAT activity was significantly increased in rats treated with adrenaline compared to the untreated group. SOD and CAT are the most important antioxidant enzymes in the defense system against ROS [39]. These results may indicate that administration of adrenaline in rats caused disruption in oxidant/antioxidant balance. Superoxide anions generated in oxidative metabolism of adrenaline may stimulate oxidation of adrenaline and thus increase the amount of free radicals [11]. Decreased SOD activity in treated rats indicated that excess level of superoxide anions induced attenuation of SOD activity. On the other hand, increased CAT activity found in rats treated with adrenaline implies that CAT has an important protective role in removing free radicals produced in cells. This assumption is supported by studies of Djelić et al. [10] and Radakovic et al. [12] where catalase in cotreatment with adrenaline reduced DNA damage mediated by free radicals in human lymphocytes. Our results are in accordance with the study of Pereira et al. [40] who reported that adrenaline plays a role in the oxidative stress in the lymphoid organs since adrenodemedullation affected the activities of antioxidant enzymes.

We observed that the treatment with all doses of adrenaline clearly increased MDA levels in rat erythrocytes. Polyunsaturated fatty acids of the membrane are one of favored oxidation targets of ROS due to its oxygen-rich environment [41]. Our findings imply that adrenaline via free radicals induces enhancement in lipid peroxidation. This is in agreement with the study of Romana-Souza et al. [16] where treatment with a high level of adrenaline resulted in a significant

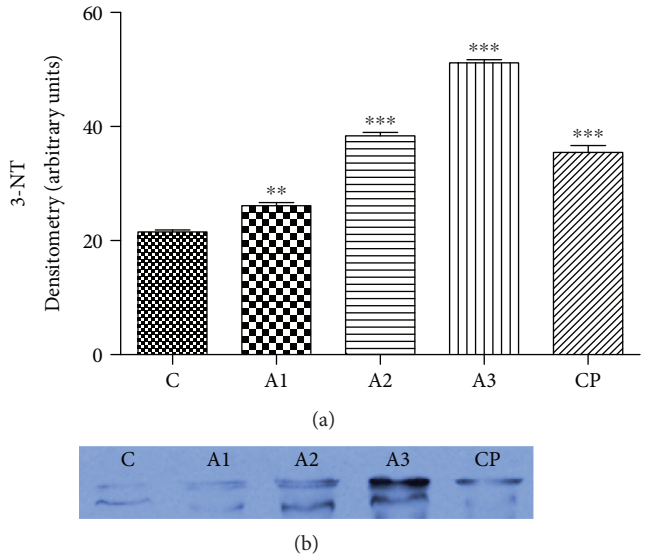

Figure 11: The level of nitrotyrosine (a) with electrophoregram (b) after treatment with adrenaline. Control group - C, groups treated with adrenaline doses (A1-0.75 mg/kg; A2-1.5 mg/kg; A3-3 mg/kg body weight); group treated with cyclophosphamide (CP). Data are expressed as means ± SE. $^{**}P < 0.01$, $^{***}P < 0.001$ vs. control group.

increment of lipid peroxidation in four days in murine dermal fibroblasts. An *in vitro* study of Bukowska et al. [42] demonstrated increased lipid peroxidation in human peripheral blood mononuclear cells after treatment with catechol. Increased lipid peroxidation indicates damage on cell membranes caused by adrenaline. Analysis of total LDH activity in this investigation confirms disturbance of the plasma membrane integrity since increased LDH activity was found in rats treated with adrenaline. In order to determine the type of damaged tissue, LDH isoenzyme distribution was estimated. A higher level of LDH_1 and LDH_2 isoenzymes was found in the treated group which points on damage of cardiomyocytes of adrenaline. A similar effect was revealed in rats treated with cyclophosphamide. Our results suggest that cell membrane damage in cardiac muscle is responsible for an increase in LDH leakage which resulted as a consequence of oxidative stress in rats exposed to adrenaline [43]. There is evidence that cardiotoxicity may originate from adrenochrome, an oxidative product of adrenaline [4]. It was demonstrated that adrenochrome promotes redox cycling process with subsequent production of ROS [44]. This oxidative product of adrenaline has been detected in the heart, skeletal muscle, liver, and blood [9]. In this study, oxidative damage of proteins has been manifested as an increased level of carbonyl groups, in plasma of rats treated with adrenaline. As a consequence of oxidative damage to proteins, their functions as receptors, enzymes, or transport or structural proteins can be disturbed [45]. Consistent with our results, Romana-Souza et al. [16] reported increased levels of carbonylated proteins in skin fibroblast cultures after treatment with adrenaline. They indicate that adrenaline stimulates production of ROS/RNS and increases protein oxidative damage considering that the detrimental effect was abolished when cells were treated with inhibitors of free radicals. In addition, increased protein carboxylation was detected in human blood cells after treatment with catechol [42].

We observed that rats treated with all doses of adrenaline induced significant elevation of nitrite oxide (NO) which is manifested as a rise in the level of nitrite concentration (NO_2^-). Excessive NO synthesis often causes myocardium damage and loss of contractile function [46]. The toxicity of NO is reflected to its ability to react with superoxide to produce potent oxidant peroxynitrite ($ONOO^-$) [47]. Therefore, this result points on nitrosative stress in rats treated with adrenaline. Namely, $ONOO^-$ may spontaneously decompose to yield NO_2^- and high reactive radical $^{\bullet}OH$. Forming $ONOO^-$ can take part of lipid peroxidation in reaction with unsaturated fatty acid-containing liposomes. In addition, $ONOO^-$ may influence on protein participation in signal transduction mechanisms [48]. It was found that high concentrations of $ONOO^-$ often lead to necrotic-type cell death [49]. Supportive evidence about the presence of nitrosative stress is revealed by our findings that an increase in the level of 3-NT was detected in the adrenaline-treated group. Consistent with our result is the study of Romana-Souza et al. [16] who reported an increased level of nitrotyrosine in mouse skin after treatment with a high level of adrenaline.

The mechanism of protein tyrosine nitration in biological systems has been well described [50]. Nitrotyrosine formation has been observed in various cardiovascular diseases [50–52]. An increased level of 3-NT may cause alternation of protein function, protein-protein interactions, and cell signaling [50, 53, 54]. Also, one of the consequences of adrenaline application is the acute phase response, which we demonstrated by evaluating APPs. One of the most important metabolic changes during the acute phase is the production of APPs which are released from the liver into the plasma [55]. This occurs within a few hours, and these proteins remain elevated as long as the inflammatory stimulus persists, making them perfect indicators of inflammation or injury, and useful for predicting the outcome of disease. Their only flaw is that they are poorly specific. APPs have been widely used in human and veterinary medicine as biomarkers of diseases, inflammatory processes, and various infections [56, 57]. Classification of APPs can be done according to the magnitude of the increase (positive APPs) or decrease (negative APPs) in their serum concentrations during the acute phase response [58]. Some of the APPs (α1-antitrypsin, and α2-macroglobulin) have antiprotease activity designed to inhibit phagocyte proteases and to minimize tissue damage. Others (α1-acid glycoprotein) have antibacterial or scavenging activity (haptoglobin, serum amyloid A, and C-reactive protein), by binding metabolites released from cellular degradation so they cannot be utilized by pathogen. Albumin, as a negative APP, is a major source of amino acids and is responsible for about 75% of the osmotic pressure of plasma. In this study, it has been shown that adrenaline reduced the albumin concentration by a dose-dependent level and also exposure to cyclophosphamide led to a decrease of albumin. Adrenaline causes an increased flux of free radicals, which can be due to the oxidation of thiol groups and the formation of albumin dimers or polymers, and consequently the reduction in osmotic pressure accurse.

Table 2: The frequency of micronuclei in bone marrow of Wistar rats treated with different doses of adrenaline.

Treatment	Treatment time (h)	Doses mg/kg	Total cell number	MNPCE (%)	PCE (%)
Negative control	24	0	5000	0.80 ± 0.37	49.24 ± 0.02
Adrenaline	24	0.75	5000	1.20 ± 0.49	47.92 ± 0.21
	24	1.5	5000	$2.80 \pm 0.37^{*}$	$46.40 \pm 0.44^{**}$
	24	3	5000	$5.40 \pm 0.24^{*}$	$43.43 \pm 1.19^{***}$
Cyclophosphamide	24	60	5000	$14.40 \pm 0.40^{*}$	$47.94 \pm 0.38^{***}$

Data are expressed as means ± SE. $^{**}P < 0.01$ and $^{***}P < 0.001$ vs. the control group.

The effect of the acute phase protein AGP in rats exposed to adrenaline was also estimated. A significant dose-dependent elevation in AGP following adrenalin treatment was observed. AGP is a positive APP with a normal concentration in the human plasma at 0.6–1.2 mg/mL [59]. The plasma concentration of AGP can increase from 2- to 10-fold when influenced by various factors, such as stress, inflammation drugs (phenobarbitone and rifampicin), burns, infections, and pregnancy. AGP possesses immunomodulatory activities and modulates neutrophil chemotactic migration and superoxide generation [60]. AGP significantly suppresses synthesis of IL-2, proliferation of lymphocytes, and platelet aggregation [61]. It has been shown that AGP protects neutrophil generation of ROS probably due to binding of free radicals [62]. AGP can bind to a number of metabolites such as heparin, histamine and serotonin, steroids, catecholamines, and pharmacological compounds. Increased AGP may affect pharmacokinetics by reducing the concentration of free drugs, by binding to the metabolically active fraction of the drug. Matsumoto et al. [63] reported that human AGP at physiological concentrations protects erythrocytes from H_2O_2. On the basis of the above-mentioned, we assume that the AGP level increases in response to oxidative stress after treatment with adrenaline. In this study, we detected an increased Hp level in rats treated with higher doses of adrenaline (1.5 and 3 mg/kg). Haptoglobin (Hp) is a positive acute-phase glycoprotein classified in $\alpha 2$ fraction together with fibrinogen and α-globulins with antiprotease activity [64]. Hp has a pronounced anti-inflammatory action, because of its ability to bind to heme of haemoglobin, forming an Hp-Hb complex. By forming this complex, Hp prevents the promotion of free radicals and its accumulation in endothelial cells which is catalysed by heme. Free Hb has the ability to catalyse the formation of hydroxyl radicals from H_2O_2. By binding to neutrophils, Hp may inhibit NADPH oxidase activation and therefore the production of reactive forms of oxygen associated with inflammation. The Hp-Hb complex, by removing free Hb, prevents renal injury that may occur when free Hb passes through the glomerular filter [65]. There is a great variability in antioxidant capacity, depending on Hp polymorphism, so individuals with Hp2-2 have a lower antioxidant capacity [65]. The Hp-Hb complex also binds nitric oxide or nitrogen monoxide (NO) [66]. This action is also phenotype-dependent. Due to its longer half-life, the Hp2-2/Hb complex scavenges more NO than the Hp1-1/Hb complex does [67, 68]. Haptoglobin can also modulate the immune response by binding to receptors on immune cells. Glucocorticoids and catecholamines activate haptoglobin synthesis whereas insulin exerts an opposite action. Since increased levels of extracellular Hb can occur due to impaired membrane integrity, we assumed that Hp scavenges free Hb as a result of lipid peroxidation. This fact coincides with our results of MDA analysis and leads to a conclusion that an elevated Hp level has a protective response to adrenaline-induced oxidative stress. Our findings unequivocally point that adrenaline induces an acute phase response. Although the APPs are a significant marker of inflammation and/or infection, it seems that these results give a new linkage between APPs and noninflammatory stress.

The possible genotoxicity of adrenaline was evaluated by a micronucleus test in bone marrow cells of rats. The results indicate that adrenaline expresses a genotoxic effect at higher concentrations (1.5 and 3 mg/kg) since it caused a significant induction of MN in the bone marrow of rats. This result is in compliance with the study of McGregor et al. [69] in which the adrenaline exhibited a mutagenic effect on mouse L5178Y lymphoma cells. In the Comet assay, adrenaline induced DNA damage in 3T3 cells of rats [6]. In our work, tested catecholamine (1.5 and 3 mg/kg) decreased the PCE/NCE ratio indicating its cytotoxicity in bone marrow. Muthuraman et al. [70] showed that adrenaline possessed a cytotoxic effect and affects DNA fragmentation in a dose-dependent manner in MDCK cells.

Several studies have implicated involvement of free radicals in the genotoxic action of adrenaline [12, 71]. Antioxidant enzymes CAT and SOD are the integral part of antioxidant defense mechanisms and have a considerable importance since they are involved in protection from free radicals. We assume that the antioxidants respond to oxidative stress caused by adrenaline since significant changes in the CAT and SOD activity in treated rats were detected. Martínez et al. [72] have classified catecholamines as potent oxidative mutagens. It has been suggested that catecholamine generates free radicals by autooxidation and redox cycling [44]. ROS have the ability to induce various types of DNA damage such as double-strand breaks (DSB), and this type of DNA damage is considered as a main contributor to MN induction [73]. We suggest that the increased induction of MN in the bone marrow of rats is a result of increased production of free radicals produced by oxidative metabolism of adrenaline. So, it should be expected that antioxidants could protect cells from toxic effects of adrenaline.

5. Conclusion

In summary, our results show that adrenaline induces oxidative and nitrative stress in Wistar rats, accompanied by changes in the activity of antioxidant enzymes, increased damage to lipids and proteins, increased level of NO_2^- and nitrotyrosine derivate, damage of cardiomyocytes, and genotoxic damage. Also, adrenaline exerts acute-phase response through increased level of AGP and Hp and decreased level of serum albumin level. Therefore, obtained results may contribute to better understanding of adrenaline toxicity with aims at preventing its harmful effects.

Data Availability

The data used to support the findings of this study are included within the article.

Conflicts of Interest

All authors declare that there are no conflicts of interest.

Acknowledgments

This work was funded by the Ministry of Education, Science and Technological Development of Serbia (Grants: OI173034 and III46002).

References

[1] J. A. Cooper, J. D. Cooper, and J. M. Cooper, "Cardiopulmonary resuscitation: history, current practice, and future direction," *Circulation*, vol. 114, no. 25, pp. 2839–2849, 2006.

[2] D. Dietz, *Toxicology and Carcinogenesis Studies of Epinephrine Hydrochloride (CAS NO. 59-31-2) in F344/N Rats and B6C3F1 Mice (Inhalation Studies)*, National Toxicology Program, Research Triangle Park, NC, USA, 1990.

[3] L. Gavrilovic, V. Stojiljkovic, J. Kasapovic et al., "Chronic physical stress changes gene expression of catecholamine biosynthetic enzymes in the adrenal medulla of adult rats," *Acta Veterinaria-Beograd*, vol. 62, no. 2-3, pp. 151–169, 2012.

[4] G. S. Behonick, M. J. Novak, E. W. Nealley, and S. I. Baskin, "Toxicology update: the cardiotoxicity of the oxidative stress metabolites of catecholamines (aminochromes)," *Journal of Applied Toxicology*, vol. 21, no. S1, pp. S15–S22, 2001.

[5] V. M. Costa, R. Silva, L. M. Ferreira et al., "Oxidation process of adrenaline in freshly isolated rat cardiomyocytes: formation of adrenochrome, quinoproteins, and GSH adduct," *Chemical Research in Toxicology*, vol. 20, no. 8, pp. 1183–1191, 2007.

[6] M. S. Flint, A. Baum, W. H. Chambers, and F. J. Jenkins, "Induction of DNA damage, alteration of DNA repair and transcriptional activation by stress hormones," *Psychoneuroendocrinology*, vol. 32, no. 5, pp. 470–479, 2007.

[7] A. Adameova, Y. Abdellatif, and N. S. Dhalla, "Role of the excessive amounts of circulating catecholamines and glucocorticoids in stress-induced heart disease," *Canadian Journal of Physiology and Pharmacology*, vol. 87, no. 7, pp. 493–514, 2009.

[8] T. Miura, S. Muraoka, Y. Fujimoto, and K. Zhao, "DNA damage induced by catechol derivatives," *Chemico-Biological Interactions*, vol. 126, no. 2, pp. 125–136, 2000.

[9] N. S. Dhalla, H. Sasaki, S. Mochizuki, K. S. Dhalla, X. Liu, and V. Elimban, "Catecholamine-induced cardiomyopathy," in *Cardiovascular Toxicity*, D. Acosta, Ed., pp. 269–318, Raven Press, New York, NY, USA, 2001.

[10] N. Djelić, M. Radaković, B. Spremo-Potparević et al., "Evaluation of cytogenetic and DNA damage in human lymphocytes treated with adrenaline in vitro," *Toxicology In Vitro*, vol. 29, no. 1, pp. 27–33, 2015.

[11] M. L. Genova, N. M. Abd-Elsalam, E. S. M. E. Mahdy et al., "Redox cycling of adrenaline and adrenochrome catalysed by mitochondrial complex I," *Archives of Biochemistry and Biophysics*, vol. 447, no. 2, pp. 167–173, 2006.

[12] M. Radaković, N. Đjelic, J. Stevanovic et al., "The investigation of DNA damage induced by adrenaline in human lymphocytes in vitro/Ispitivanja Oštećenja DNK Izazvanih Adrenalinom U Limfocitima Čoveka in vitro," *Acta Veterinaria*, vol. 64, no. 3, pp. 281–292, 2014.

[13] B. Halliwell and J. M. C. Gutteridge, "Role of free radicals and catalytic metal ions in human disease: an overview," *Methods in Enzymology*, vol. 186, pp. 1–85, 1990.

[14] A. Rahal, A. Kumar, V. Singh et al., "Oxidative stress, prooxidants, and antioxidants: the interplay," *BioMed Research International*, vol. 2014, Article ID 761264, 19 pages, 2014.

[15] E. Miller, A. Walczak, J. Saluk, M. B. Ponczek, and I. Majsterek, "Oxidative modification of patient's plasma proteins and its role in pathogenesis of multiple sclerosis," *Clinical Biochemistry*, vol. 45, no. 1-2, pp. 26–30, 2012.

[16] B. Romana-Souza, G. Santos Lima-Cezar, and A. Monte-Alto-Costa, "Psychological stress-induced catecholamines accelerates cutaneous aging in mice," *Mechanisms of Ageing and Development*, vol. 152, pp. 63–73, 2015.

[17] R. T. Dean, R. Dunlop, P. Hume, and K. J. Rodgers, "Proteolytic 'defences' and the accumulation of oxidized polypeptides in cataractogenesis and atherogenesis," *Biochemical Society Symposia*, vol. 70, pp. 135–146, 2003.

[18] E. R. Stadtman, "Protein oxidation and aging," *Free Radical Research*, vol. 40, no. 12, pp. 1250–1258, 2006.

[19] Q. Ding, E. Dimayuga, and J. Keller, "Oxidative damage, protein synthesis, and protein degradation in Alzheimers disease," *Current Alzheimer Research*, vol. 4, no. 1, pp. 73–79, 2007.

[20] S. Loft and H. E. Poulsen, "Cancer risk and oxidative DNA damage in man," *Journal of Molecular Medicine*, vol. 74, no. 6, pp. 297–312, 1996.

[21] J. E. Klaunig and L. M. Kamendulis, "The role of oxidative stress in carcinogenesis," *Annual Review of Pharmacology and Toxicology*, vol. 44, no. 1, pp. 239–267, 2004.

[22] National Research Council, *Guide for the Care and Use of Laboratory Animals*, National Academies Press, 2010.

[23] C. D. Barnes and L. G. Eltherington, *Drug Dosage in Laboratory Animals a Handbook*, University of California Pres-Barkley and Los Angeles, 1965.

[24] D. Anderson, J. B. Bishop, R. C. Garner, P. Ostrosky-Wegman, and P. B. Selby, "Cyclophosphamide: review of its mutagenicity for an assessment of potential germ cell risks," *Mutation Research/Fundamental and Molecular Mechanisms of Mutagenesis*, vol. 330, no. 1-2, pp. 115–181, 1995.

[25] L. Tentori and A. M. Salvati, "Hemoglobinometry in human blood," *Methods in Enzymology*, vol. 76, pp. 707–715, 1981.

[26] H. P. Misra and I. Fridovich, "The role of superoxide anion in the autoxidation of epinephrine and a simple assay for superoxide dismutase," *The Journal of Biological Chemistry*, vol. 247, no. 10, pp. 3170–3175, 1972.

[27] C. Beauchamp and I. Fridovich, "Superoxide dismutase: improved assays and an assay applicable to acrylamide gels," *Analytical Biochemistry*, vol. 44, no. 1, pp. 276–287, 1971.

[28] H. Aebi, "Catalase in vitro," in *Methods in Enzymology*, L. Packer, Ed., pp. 121–126, Academic Press, Orlando, FL, USA, 1984.

[29] J. M. Gutteridge, "Lipid peroxidation and antioxidants as biomarkers of tissue damage," *Clinical Chemistry*, vol. 41, 12, Part 2, pp. 1819–1828, 1995.

[30] N. Traverso, S. Menini, E. P. Maineri et al., "Malondialdehyde, a lipoperoxidation-derived aldehyde, can bring about secondary oxidative damage to proteins," *The Journals of Gerontology Series A: Biological Sciences and Medical Sciences*, vol. 59, no. 9, pp. B890–B895, 2004.

[31] I. Guevara, J. Iwanejko, A. Dembinska-Kiec et al., "Determination of nitrite/nitrate in human biological material by the simple Griess reaction," *Clinica Chimica Acta*, vol. 274, no. 2, pp. 177–188, 1998.

[32] R. L. Levine, D. Garland, C. N. Oliver et al., "Determination of carbonyl content in oxidatively modified proteins," *Methods in Enzymology*, vol. 186, pp. 464–478, 1990.

[33] H. Towbin, T. Staehelin, and J. Gordon, "Electrophoretic transfer of proteins from polyacrylamide gels to nitrocellulose sheets: procedure and some applications," *Proceedings of the National Academy of Sciences of the United States of America*, vol. 76, no. 9, pp. 4350–4354, 1979.

[34] T. Mahmood and P. C. Yang, "Western blot: technique, theory, and trouble shooting," *North American Journal of Medical Sciences*, vol. 4, no. 9, pp. 429–434, 2012.

[35] M. Yoshida and Y. Takakuwa, "Method for the simultaneous assay of initial velocities of lactate dehydrogenase isoenzymes following gel electrophoresis," *Journal of Biochemical and Biophysical Methods*, vol. 34, no. 3, pp. 167–175, 1997.

[36] B. D. Hames and D. Rickwood, *Gel Electrophoresis of Proteins, a Practical Approach*, Oxford University Press, New York, NY, USA, 1990.

[37] W. Schmid, "The micronucleus test," *Mutation Research/Environmental Mutagenesis and Related Subjects*, vol. 31, no. 1, pp. 9–15, 1975.

[38] K. H. Mavournin, D. H. Blakey, M. C. Cimino, M. F. Salamone, and J. A. Heddle, "The in vivo micronucleus assay in mammalian bone marrow and peripheral blood. A report of the U.S. Environmental Protection Agency Gene-Tox Program," *Mutation Research/Reviews in Genetic Toxicology*, vol. 239, no. 1, pp. 29–80, 1990.

[39] I. Fridovich, "Superoxide radical and superoxide dismutases," *Annual Review of Biochemistry*, vol. 64, no. 1, pp. 97–112, 1995.

[40] B. Pereira, L. F. B. P. Costa-Rosa, E. J. H. Bechara, P. Newsholme, and R. Curi, "Changes in the TBARs content and superoxide dismutase, catalase and glutathione peroxidase activities in the lymphoid organs and skeletal muscles of adrenodemedullated rats," *Brazilian Journal of Medical and Biological Research*, vol. 31, no. 6, pp. 827–833, 1998.

[41] E. N. Frankel, "Chemistry of free radical and singlet oxidation of lipids," *Progress in Lipid Research*, vol. 23, no. 4, pp. 197–221, 1984.

[42] B. Bukowska, J. Michałowicz, and A. Marczak, "The effect of catechol on human peripheral blood mononuclear cells (in vitro study)," *Environmental Toxicology and Pharmacology*, vol. 39, no. 1, pp. 187–193, 2015.

[43] M. Preus, A. Bhargava, A. Elrahmankhater, and P. Gunzel, "Diagnostic value of serum creatine kinase and lactate dehydrogenase isoenzyme determinations for monitoring early cardiac damage in rats," *Toxicology Letters*, vol. 42, no. 2, pp. 225–233, 1988.

[44] A. Bindoli, D. J. Deeble, M. P. Rigobello, and L. Galzigna, "Direct and respiratory chain-mediated redox cycling of adrenochrome," *Biochimica et Biophysica Acta (BBA) - Bioenergetics*, vol. 1016, no. 3, pp. 349–356, 1990.

[45] B. Halliwell and M. Whiteman, "Measuring reactive species and oxidative damage in vivo and in cell culture: how should you do it and what do the results mean?," *British Journal of Pharmacology*, vol. 142, no. 2, pp. 231–255, 2004.

[46] J. Zweier and M. Talukder, "The role of oxidants and free radicals in reperfusion injury," *Cardiovascular Research*, vol. 70, no. 2, pp. 181–190, 2006.

[47] J. Stamler, D. Singel, and J. Loscalzo, "Biochemistry of nitric oxide and its redox-activated forms," *Science*, vol. 258, no. 5090, pp. 1898–1902, 1992.

[48] N. Campolo, S. Bartesaghi, and R. Radi, "Metal-catalyzed protein tyrosine nitration in biological systems," *Redox Report*, vol. 19, no. 6, pp. 221–231, 2014.

[49] L. Virág, É. Szabó, and P. Gergely, "C. Szabó "Peroxynitrite-induced cytotoxicity: mechanism and opportunities for intervention"," *Toxicology Letters*, vol. 140-141, pp. 113–124, 2003.

[50] P. Pacher, J. S. Beckman, and L. Liaudet, "Nitric oxide and peroxynitrite in health and disease," *Physiological Reviews*, vol. 87, no. 1, pp. 315–424, 2007.

[51] C. Vadseth, J. M. Souza, L. Thomson et al., "Pro-thrombotic state induced by post-translational modification of fibrinogen by reactive nitrogen species," *Journal of Biological Chemistry*, vol. 279, no. 10, pp. 8820–8826, 2004.

[52] S. Pennathur, C. Bergt, B. Shao et al., "Human atherosclerotic intima and blood of patients with established coronary artery disease contain high density lipoprotein damaged by reactive nitrogen species," *Journal of Biological Chemistry*, vol. 279, no. 41, pp. 42977–42983, 2004.

[53] T. Koeck, X. Fu, S. L. Hazen, J. W. Crabb, D. J. Stuehr, and K. S. Aulak, "Rapid and selective oxygen-regulated protein tyrosine denitration and nitration in mitochondria," *Journal of Biological Chemistry*, vol. 279, no. 26, pp. 27257–27262, 2004.

[54] L. A. Abriata, A. Cassina, V. Tórtora et al., "Nitration of solvent-exposed tyrosine 74 on cytochrome *c* triggers heme iron-methionine 80 bond disruption: nuclear magnetic resonance and optical spectroscopy studies," *Journal of Biological Chemistry*, vol. 284, no. 1, pp. 17–26, 2009.

[55] H. Baumann and J. Gauldie, "The acute phase response," *Immunology Today*, vol. 15, no. 2, pp. 74–80, 1994.

[56] P. M. Ridker, "Inflammatory biomarkers and risks of myocardial infarction, stroke, diabetes, and total mortality: implications for longevity," *Nutrition Reviews*, vol. 65, no. 12, pp. 253–259, 2007.

[57] P. D. Eckersall and R. Bell, "Acute phase proteins: biomarkers of infection and inflammation in veterinary medicine," *The Veterinary Journal*, vol. 185, no. 1, pp. 23–27, 2010.

[58] H. H. Petersen, J. P. Nielsen, and P. M. H. Heegaard, "Application of acute phase protein measurements in veterinary clinical chemistry," *Veterinary Research*, vol. 35, no. 2, pp. 163–187, 2004.

[59] S. Colombo, T. Buclin, L. A. Décosterd et al., "Orosomucoid (α1-acid glycoprotein) plasma concentration and genetic variants: effects on human immunodeficiency virus protease inhibitor clearance and cellular accumulation," *Clinical Pharmacology & Therapeutics*, vol. 80, no. 4, pp. 307–318, 2006.

[60] T. Hochepied, F. G. Berger, H. Baumann, and C. Libert, "α_1-acid glycoprotein: an acute phase protein with inflammatory and immunomodulating properties," *Cytokine & Growth Factor Reviews*, vol. 14, no. 1, pp. 25–34, 2003.

[61] S. A. Elg, A. R. Mayer, L. F. Carson, L. B. Twiggs, R. B. Hill, and S. Ramakrishnan, "α-1 acid glycoprotein is an immunosuppressive factor found in ascites from ovarian carcinoma," *Cancer*, vol. 80, no. 8, pp. 1448–1456, 1997.

[62] A. L. Pukhal'skii, G. V. Shmarina, E. A. Kalashnikova et al., "Effect of semisynthetic analog of α_1-acid glycoprotein on immunomodulatory and antiinflammatory activity of natural glycoproteinglycoprotein on immunomodulatory and antiinflammatory activity of natural glycoprotein," *Bulletin of Experimental Biology and Medicine*, vol. 129, no. 5, pp. 480–483, 2000.

[63] K. Matsumoto, K. Nishi, Y. Tokutomi, T. Irie, A. Suenaga, and M. Otagiri, "Effects of α_1-acid glycoprotein on erythrocyte deformability and membrane stabilization," *Biological and Pharmaceutical Bulletin*, vol. 26, no. 1, pp. 123–126, 2003.

[64] E. Gruys, M. J. M. Toussaint, T. A. Niewold, and S. J. Koopmans, "Acute phase reaction and acute phase proteins," *Journal of Zhejiang University Science*, vol. 6B, no. 11, pp. 1045–1056, 2005.

[65] S. Fagoonee, J. Gburek, E. Hirsch et al., "Plasma protein haptoglobin modulates renal iron loading," *The American Journal of Pathology*, vol. 166, no. 4, pp. 973–983, 2005.

[66] I. Azarov, X. He, A. Jeffers et al., "Rate of nitric oxide scavenging by hemoglobin bound to haptoglobin," *Nitric Oxide*, vol. 18, no. 4, pp. 296–302, 2008.

[67] A. P. Levy, R. Asleh, S. Blum et al., "Haptoglobin: basic and clinical aspects," *Antioxidants & Redox Signaling*, vol. 12, no. 2, pp. 293–304, 2010.

[68] A. I. Alayash, "Haptoglobin: old protein with new functions," *Clinica Chimica Acta*, vol. 412, no. 7-8, pp. 493–498, 2011.

[69] D. B. McGregor, C. G. Riach, A. Brown et al., "Reactivity of catecholamines and related substances in the mouse lymphoma L5178Y cell assay for mutagens," *Environmental and Molecular Mutagenesis*, vol. 11, no. 4, pp. 523–544, 1988.

[70] P. Muthuraman, P. C. Nagajyothi, M. Chandrasekaran et al., "Differential sensitivity of Madin-Darby canine kidney (MDCK) cells to epinephrine," *The Journal of Nutrition, Health & Aging*, vol. 20, no. 5, pp. 486–493, 2016.

[71] M. E. Crespo and M. P. Bicho, "Membrane-mediated effects of catecholamines on the DNA of human leukocytes: the role of reactive oxygen species," *Neurosignals*, vol. 4, no. 2, pp. 78–85, 1995.

[72] A. Martínez, A. Urios, and M. Blanco, "Mutagenicity of 80 chemicals in *Escherichia coli* tester strains IC203, deficient in OxyR, and its *oxyR*$^+$ parent WP2 *uvrA*/pKM101: detection of 31 oxidative mutagens," *Mutation Research/Genetic Toxicology and Environmental Mutagenesis*, vol. 467, no. 1, pp. 41–53, 2000.

[73] F. van Goethem, D. Lison, and M. Kirsch-Volders, "Comparative evaluation of the in vitro micronucleus test and the alkaline single cell gel electrophoresis assay for the detection of DNA damaging agents: genotoxic effects of cobalt powder, tungsten carbide and cobalt–tungsten carbide," *Mutation Research/Genetic Toxicology and Environmental Mutagenesis*, vol. 392, no. 1-2, pp. 31–43, 1997.

Hindawi
Oxidative Medicine and Cellular Longevity
Volume 2018, Article ID 9125601, 13 pages
https://doi.org/10.1155/2018/9125601

Research Article

Neuroprotective Effects of dl-3-n-Butylphthalide against Doxorubicin-Induced Neuroinflammation, Oxidative Stress, Endoplasmic Reticulum Stress, and Behavioral Changes

Dehua Liao,[1,2] Daxiong Xiang,[2] Ruili Dang,[3] Pengfei Xu,[3] Jiemin Wang,[2] Wenxiu Han,[3] Yingzhou Fu,[1] Dunwu Yao,[1] Lizhi Cao,[1] and Pei Jiang[3]

[1]*Department of Pharmacy, Hunan Cancer Hospital, Changsha 410011, China*
[2]*Institute of Clinical Pharmacy & Pharmacology, Second Xiangya Hospital, Central South University, Changsha 410011, China*
[3]*Department of Pharmacy, Jining First People's Hospital, Jining Medical University, Jining 272000, China*

Correspondence should be addressed to Pei Jiang; jiangpeicsu@sina.com

Received 22 January 2018; Revised 16 May 2018; Accepted 6 June 2018; Published 16 August 2018

Academic Editor: Mohamed M. Abdel-Daim

Doxorubicin (DOX) is a broad-spectrum antitumor drug while its use is limited due to its neurobiological side effects associated with depression. We investigated the neuroprotective efficacy of dl-3-n-butylphthalide (dl-NBP) against DOX-induced anxiety- and depression-like behaviors in rats. dl-NBP was given (30 mg/kg) daily by gavage over three weeks starting seven days before DOX administration. Elevated plus maze (EPM) test, forced swimming test (FST), and sucrose preference test (SPT) were performed to assess anxiety- and depression-like behaviors. Our study showed that the supplementation of dl-NBP significantly mitigated the behavioral changes induced by DOX. To further explore the mechanism of neuroprotection induced by dl-NBP, several biomarkers including oxidative stress markers, endoplasmic reticulum (ER) stress markers, and neuroinflammatory cytokines in the hippocampus were quantified. The results showed that dl-NBP treatment alleviated DOX-induced neural apoptosis. Meanwhile, DOX-induced oxidative stress and ER stress in the hippocampus were significantly ameliorated in dl-NBP pretreatment group. Our study found that dl-NBP alleviated the upregulation of malondialdehyde (MDA), nitric oxide (NO), CHOP, glucose-regulated protein 78 kD (GRP-78), and caspase-12 and increased the levels of reduced glutathione (GSH) and activities of catalase (CAT), glutathione reductase (GR), and glutathione peroxidase (GPx) in the hippocampus of rats exposed to DOX. Additionally, the gene expression of interleukin-6 (IL-6), interleukin-1β (IL-1β), and tumor necrosis factor-alpha (TNF-α) and protein levels of inducible nitric oxide synthase (iNOS) were significantly increased in DOX-treated group, whereas DOX-induced neuroinflammation was significantly attenuated in dl-NBP supplementation group. In conclusion, dl-NBP could alleviate DOX-induced anxiety- and depression-like behaviors via attenuating oxidative stress, ER stress, inflammatory reaction, and neural apoptosis, providing a basis as a therapeutic potential against DOX-induced neurotoxicity.

1. Introduction

Doxorubicin (DOX) is an anthracycline antibiotic used commonly in multidrug chemotherapy regimens to treat solid tumors [1, 2]. However, its use as a drug has been reported to cause some adverse effects like heart arrhythmias, neutropenia, cardiotoxicity, kidney injury, as well as neuron damage in the brain [1, 3, 4]. Notwithstanding the fact that DOX poorly crosses the blood-brain barrier, it still penetrates the brain at doses sufficient to cause cytotoxicity [5]. More and more evidence showed that neurotoxicity is accompanied with long-term use of DOX and may cause many neuropsychiatric diseases including depression, anxiety, and impaired cognitive function [6, 7]. Clinical study also showed that DOX treatment has a negative impact on cognitive function in women with breast cancer [8].

Several studies suggested that the pathogenesis of anxiety and depression is associated with oxidative stress and neuroinflammatory response particularly in the hippocampal region [9–11]. Hydroxyl radicals and superoxide radicals

along with hydrogen peroxide are produced after administration of DOX, leading to the alterations of oxidative stress and antioxidant defense system. It is assumed that the formation of free radicals induces oxidative stress and plays a crucial role in the mechanism of DOX-induced neurotoxicity [12, 13]. Moreover, the generation of superoxide anions induced by DOX can elevate the level of circulating necrosis factor-alpha (TNF-α) which can directly cross the blood-brain barrier and activate glial cells to initiate the local production of proinflammatory cytokines, exacerbating oxidative stress and neural apoptosis [14]. In addition, DOX-evoked reactive oxygen species (ROS) activate nuclear factor kappa B (NF-κB) signaling pathway, which in turn triggers the activation of proinflammatory cytokines, such as interleukin-6 (IL-6), interleukin-1β (IL-1β), and TNF-α [11], and inducible nitric oxide synthase (iNOS) expression. Moreover, DOX specifically activates part of the endoplasmic reticulum (ER) stress response pathway, thus contributing to its proinflammatory effect in the hippocampus [15]. These inflammatory mediators have been shown to be involved in neuroinflammation both in animal models and patients undergoing chemotherapy [16]. The resulting neuroinflammation can trigger apoptotic cell death and depletion of neurotrophic factors, causing neurobehavioral alterations [11, 17]. Besides, previous study showed that ER stress and disrupted neurogenesis in the brain are associated with cognitive impairment and depression-like behavior in rats following chronic stress exposure [18]. Cai et al. have also reported that ER stress plays an important role in potential memory impairments in rats treated with microcystin leucine arginine [19]. Therefore, it might be beneficial to reduce the production of ROS and inhibit the release of neurotoxic agents in the treatment of DOX-induced depression.

Recent studies have highlighted that dl-3-n-butylphthalide (dl-NBP) displays an important role in mitigating brain damage [20, 21]. dl-NBP is a synthesized compound based on l-3-n-butylphthalide which is extracted from the seeds of *Apium graveolens* Linn. dl-NBP had been approved by the State Food and Drug Administration of China for clinical use in patients with stroke in 2002 [22]. As a fat-soluble small molecule compound, dl-NBP could cross the blood-brain barrier efficiently. dl-NBP has a variety of protective effects on brain tissues as a multitarget drug. Previous study has found that dl-NBP reduces focal cerebral ischemia volume in rats and improves local cerebral ischemia brain-induced edema, brain energy metabolism disorder, and apoptotic neuronal cell death [21]. Several studies have reported the neuroprotective effects of dl-NBP, for example, dl-NBP enhanced the ability of learning and memory in animal models of Alzheimer's disease and provided neuroprotection in the mice models after traumatic brain injury [23, 24]. It has also been reported that dl-NBP relieves hypoxia-induced damage in vitro [20] and prolonged animal survival in the mouse model of amyotrophic lateral sclerosis [24]. In addition, studies also showed that dl-NBP could resist HSPB8 K141N mutation-induced oxidative stress [22] and attenuate amyloid-β-induced inflammatory responses in cultured astrocytes [25, 26], highlighting the neuroprotective effect of dl-NBP via alleviating oxidative stress and inflammatory responses.

Based on the above findings, the purpose of our study was to investigate the potential protective effects of dl-NBP against DOX-induced neurotoxicity and depression-like behaviors in rats. In addition, the possible underlying mechanisms, including antioxidant, anti-inflammatory, and anti-ER stress as well as antiapoptotic effects of dl-NBP, were also examined.

2. Materials and Methods

2.1. Animals. Sprague-Dawley rats (male, 180–220 g; the Experimental Animal Center of Hunan Cancer Hospital) were initially housed in groups in a temperature-controlled ($23 \pm 2^{\circ}$C) environment under a 12/12 h light/dark cycle with free access to food and water, prior to sucrose preference test (SPT). This study was approved by the Animal Care and Use Committee of Hunan Cancer Hospital (protocol number 027/2016). All experiments were performed in accordance with the Guide for Care and Use of Laboratory Animals (Chinese Council).

2.2. Experimental Design. Animals were divided randomly into three groups ($n = 8$): (1) control, (2) DOX, and (3) DOX + dl-NBP. The untreated control group was injected with 1.5 ml of normal saline. Rats in the DOX group were given DOX every two days for a total of seven injections via intraperitoneal injection at a dose of 2.5 mg/kg for each injection. The dose and treatment duration was chosen based on our previous research showing the DOX-induced neurotoxicity and depression-like behaviors [27]. The DOX + dl-NBP group received dl-NBP (30 mg/kg) daily by gavage for three weeks starting one week before giving DOX. The dose of dl-NBP was selected because of previous investigation showing neuroprotective effects of this drug against cerebral ischemia and brain injury [22]. In addition, dl-NBP was administrated one week before DOX treatment to fully activate the antioxidant system, protecting the brain against the relative high dose of DOX challenge. The body weight of these rats was monitored throughout the experiment, and drug doses were adjusted accordingly.

At the end of the three weeks, behavioral tests were carried out following the sequence of SPT, elevated plus maze (EPM) test, and forced swimming test (FST). After behavioral tests, the rats were anesthetized with sodium pentobarbital (50 mg/kg) via intraperitoneal injection [28]. Blood samples were taken from cardiac coronary artery after anesthesia, and the brains were quickly removed after cardiac perfusion with phosphate-buffered saline (PBS) (pH = 7.2). The left hemisphere of the brain was maintained in 4% paraformaldehyde and then embedded in paraffin, prepared for histopathological examination and immunohistochemical staining. For the right hemisphere, the hippocampus was dissected and used for oxidative stress measurement and Western blot and polymerase chain reaction (PCR) analysis. The biochemical parameters such as malondialdehyde (MDA), nitric oxide (NO), reduced glutathione (GSH), glutathione peroxidase (GPx), glutathione reductase (GR),

catalase (CAT), IL-1β, IL-6, TNF-α, glucose-regulated protein 78 kD (GRP-78), iNOS, p65, inhibitor of NF-κB (IκB), CHOP, and caspase-12 were determined in our study.

2.3. Behavioral Test

2.3.1. Elevated Plus Maze Test. EPM test was performed to assess the anxiety-like behavior in rats. The apparatus of EPM was consisted of two open arms ($35 \times 5\,cm^2$) which were perpendicular to two closed arms ($35 \times 5\,cm^2$) with a small central square ($5 \times 5\,cm^2$) between arms. The maze was elevated 50 cm from the floor in a dimly illuminated room. Each rat was placed at the center of maze with head facing towards the open arm and allowed to freely explore for 5 min. The total number of entries into the open arm, closed arm, and time spent in open arm during the test were recorded and evaluated [29].

2.3.2. Sucrose Preference Test. SPT was utilized to determine anhedonia response which is a core symptom of major depression in rats. Prior to SPT, all the rats were housed individually and habituated to 48 h of forced 1% sucrose solution consumption in two bottles on each side. Then after 14 h of water deprivation, the rats were given access to two preweighed bottles, one containing 1% sucrose solution and another containing tap water. The position of the bottles was alternated to avoid bias from place preference. The bottles were weighed again after 1 h, and the weight difference was considered to be the rat intake from each bottle. The preference for sucrose was measured as a percentage of the consumed 1% sucrose solution relative to the total amount of liquid intake [30, 31].

2.3.3. Forced Swimming Test. Antidepressant efficacy and depression-like behavior in rodents were screened by using FST. The test was performed as previously described with minor modifications [28]. In brief, each rat was placed in a plastic cylinder (45 cm height and 25 cm diameter) containing approximately 35 cm of water ($24 \pm 1^{\circ}C$) for a 15 min pretest. After swimming, rats were dried with towels and placed back in their home cage. Twenty-four hours later, the rats were exposed to the same experimental conditions outlined above for a 5 min FST, and immobility time was recorded in our study.

2.4. Biochemical Parameter Assay. A 10% (*w*/*v*) homogenate of the hippocampus in 0.1 M phosphate-buffered saline (PBS) at pH 7.4 was prepared and centrifuged at 9500 rpm for 20 min at $4^{\circ}C$. The supernatant was used for the measurement of biochemical parameters of MDA, NO, GSH, GPx, and CAT.

2.4.1. Measurements of MDA and NO Content. The MDA formation was spectrophotometrically measured by the thiobarbituric acid (TBA) reaction [32]. Briefly, 1 ml of 15% trichloroacetic acid was added to 500 μl of brain homogenate supernatant and mixed well, and then, the solutions were centrifuged at 3000 rpm for 10 min. One milliliter of the supernatant was added to 0.5 ml of 0.7% TBA, and then, the mixture was heated for 60 min at $90^{\circ}C$. The absorbance was recorded at 532 nm using UV spectrophotometer. The content of NO was determined according to Montgomery and Dymock's method [33]. The reddish-purple azo dye product was measured spectrophotometrically at 540 nm.

2.4.2. Determination of Antioxidant Parameters. The content of reduced GSH was determined by the method of Maris [34]. GSH was reacted with 5,5′-dithio-bis-2-nitrobenzoic acid generating a yellow chromophore, and the absorbance was measured at 412 nm using a UV spectrophotometer. Total GSH content was expressed as nmol/mg protein.

The CAT activity was measured in brain homogenate following the method of Sinha [35]. A decrease in absorbance due to H_2O_2 degradation was monitored at 240 nm for 1 min, and the enzyme activity was expressed as U/mg protein.

The GR activity was assessed according to the previously described method, which was determined by measuring the rate of NADPH oxidation at 340 nm due to the formation of GSH, from GSSG, by the action of GR present in the sample [36]. The unit of enzyme activity was expressed as U/mg protein.

The GPx activity was analyzed as described previously, which was measured by a spectrophotometric method based on the disappearance of NADPH [37]. GPx catalyzes the oxidation of GSH by cumene hydroperoxide. The GPx activity was determined by subtracting the excess GSH after the enzymatic reaction of the total GSH in the absence of the enzyme. GSH reacts with DTNB to form a yellow-colored chromophore which was measured with a spectrophotometer at 412 nm. The enzyme activity was expressed as U/mg protein.

2.5. Western Blot Analysis. For Western blot analysis, total protein was prepared from the hippocampus, and the concentration was determined using Bradford method [27]. In brief, the hippocampus sample was loaded on a precast 12% SDS-PAGE gel with 10 μg proteins in each lane. Proteins in the gels were transferred to a 0.45 μm PVDF membrane at 15 V for 15 min in a transfer buffer, pH 8.1 (47.8 mM Tris/HCl, 0.293% glycine, 20% methanol) and blocked for 1 h in 5% nonfat dry milk in TBS-T (25 mM Tris, pH 7.5, 150 mM NaCl, 0.05% Tween-20). The membranes were probed overnight at $4^{\circ}C$ with primary antibodies as follows: anti-iNOS (Proteintech; 1 : 500), anti-IκB (Cell Signaling; 1 : 1000), anti-p65 (Proteintech; 1 : 800), anti-GRP78 (Proteintech; 1 : 1000), anti-CHOP (Cell Signaling; 1 : 1000), anti-caspase-12 (Proteintech; 1 : 1000), and anti-β-actin (Proteintech; 1 : 4000). After that, the membranes were washed and probed with HRP-conjugated secondary antibody for 40 min at room temperature. The bound antibodies were visualized using an enhanced chemiluminescent detection system (Amersham Pharmacia Biotech, Piscataway, NJ, USA) and then exposed to X-ray films (Kodak Xomat, Rochester, NY, USA). The density of protein bands was quantified using ImageJ software (National Institutes of Health, Bethesda, MD, USA). The density ratio represented the relative intensity of each band against β-actin as the loading control and normalized to those in the control group.

Table 1: Primers used in real-time PCR analyses of mRNA expression.

Target gene		Primer sequences	Size (bp)
IL-1β	Forward	5′-AGGTCGTCATCATCCCACGAG-3′	119
	Reverse	5′-GCTGTGGCAGCTACCTATGTCTTG-3′	
IL-6	Forward	5′-CACAAGT CCGGAGAGGAGAC-3′	167
	Reverse	5′-ACAGTGCATCATCGCTGTTC-3′	
TNF-α	Forward	5′-GAGAGATTGGCTGCTGGAAC-3′	82
	Reverse	5′-TGGAGACCATGATGACCGTA-3′	
β-Actin	Forward	5′-CATCCTGCGTCTGGACCTGG-3′	116
	Reverse	5′-TAATGTCACGCACGATTTCC-3′	

2.6. Real-Time PCR Analysis. The mRNA levels of inflammatory factors IL-1β, IL-6, and TNF-α were quantified by quantitative real-time polymerase chain reaction. The reference sample for the study was dissected from the rats in the control group. Total RNA was extracted from the hippocampus using TRIzol reagent (Invitrogen Corp., Carlsbad, CA, USA). The RNA concentration was determined for quantity by using the spectrophotometry (Jingke, Ningbo, China). Complementary DNA (cDNA) was generated from 2 μg of total RNA by RevertAid First Strand cDNA Synthesis Kit (Thermo Fisher Scientific, Tewksbury, MA, USA) using oligo (dT)12-18 as a primer in a total volume of 20 μl. Quantitative PCR was performed on Bio-Rad Cx96 Detection System (Bio-Rad, Hercules, CA, USA) using SYBR green PCR kit (Applied Biosystems Inc., Woburn, MA, USA) and gene-specific primers. The primer sequences were selected according to our previous study [27], and the sequences of gene-specific primers are listed in Table 1. The PCR amplification program consisted of a preincubation at 95°C for 10 min to activate the FastStart Taq DNA polymerase, followed by 40 cycles of denaturation at 95°C for 15 s and a 30 s annealing and elongation step at 60°C. After the amplification procedure, subject all PCR reactions to a melting curve analysis with continuous fluorescence measurement from 65°C to 95°C. Typically, collect one data point in each cycle by a stepwise increase of the temperature by 0.5°C per cycle. Melting curve analysis showed the single and sharp transition, indicating the specificity of the amplifications (Figure S1). The signals were normalized to β-actin as an internal standard. All PCR experiments were performed in triplicate. Relative change in mRNA expression was evaluated by using the $2^{-\Delta\Delta Cq}$ method.

2.7. Histopathological Examination. For each rat, brain samples were collected and fixed in 4% paraformaldehyde in PBS (pH 7.2) at room temperature overnight and processed routinely for embedding in paraffin. The paraffin-embedded tissue sections (5 mm) were stained with hematoxylin and eosin using standard techniques, and then examination was done through the light electric microscope (Olympus, USA).

2.8. TUNEL Assay. Terminal deoxynucleotidyl transferase-mediated deoxyuridine triphosphate nick end labeling (TUNEL) assay was used to evaluate neurocyte apoptosis. The TUNEL method was employed using an apoptosis detection kit (KeyGen Biotech, Nanjing, China). TUNEL-positive tubular cell numbers were counted at random in 20 nonoverlapping cortical fields under 200x magnification. This ratio represented the apoptotic index of the sample and was compared between groups.

2.9. Immunohistochemical Staining. For immunohistochemical, hippocampus sections were incubated overnight with anti-iNOS antibody (Santa Cruz Biotechnology, 1 : 500 in PBS, *v*/*v*). Sections were then washed with PBS and incubated with secondary antibodies. For quantitative analysis, original immunohistochemical photographs were assessed by densitometer using MacBiophotonics ImageJ 1.41a software [38, 39].

2.10. Statistical Analysis. In this study, all data were analyzed using the Statistical Package for Social Science (SPSS) version 18 (SPSS Inc., Chicago, IL, USA). All brain parameters were presented as means ± SEM and analyzed statistically by one-way analysis of variance (ANOVA) with least significant difference (LSD) post hoc multiple comparisons. The prior level of significance was established at $p < 0.05$.

3. Results

3.1. Effects of dl-NBP Pretreatment on DOX-Induced Body Weight Gain and Anxiety- and Depression-Like Behaviors. As shown in Figure 1(a), DOX-treated rats showed significant decreases in body weight gain when compared to the control animals, whereas dl-NBP pretreatment had no influence on the body weight gain in DOX-treated rats, which was consistent with the results of previous studies [40, 41]. EPM tests were performed for anxiety-like behavior assessment. As shown in Figures 1(b)–1(d), DOX administration induced an anxious effect as evident by reduction of time spent in the open arms ($F_{2,21} = 18.25$; $p < 0.01$) and number of entries in the open arm ($F_{2,21} = 16.32$; $p < 0.01$) as compared to the normal control group. Number of entries ($p < 0.01$) and time spent in the open arms ($p < 0.01$) were significantly increased in the dl-NBP-pretreated group when compared with DOX-

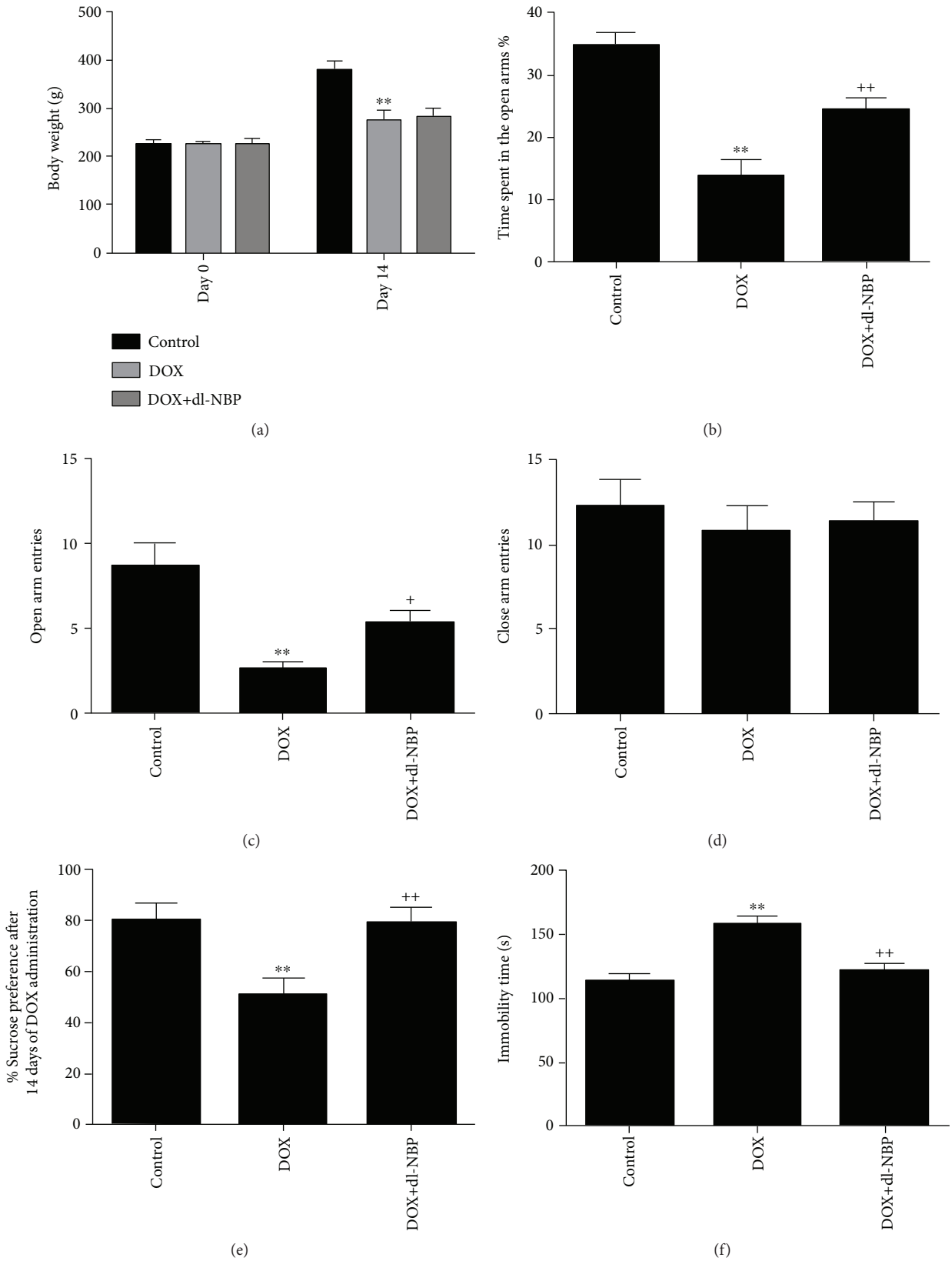

Figure 1: Body weight gain and behavioral test. Effects of DOX and dl-NBP on body weight gain (a); EPM test: time spent in the open arms (b); open arm entries (c); closed time entries (d); SPT: sucrose preference (e); and FST: immobility time (f). Data are expressed as means ± SEM ($n = 8$). $^{**}p < 0.01$ compared to the control group. $^{+}p < 0.05$ and $^{++}p < 0.01$ compared to the DOX-injected group.

treated group. There was no significant difference concerning the parameters of closed arm entries in the three groups.

Depression-like behaviors were assessed by using SPT and FST. In SPT, DOX-exposed rats showed a significant reduction in the sucrose preference ($F_{2,21} = 9.64$; $p < 0.01$) as compared to the normal control group, indicating depression-like behavior caused by DOX exposure (Figure 1(e)). However, dl-NBP pretreatment significantly alleviated DOX-induced depression-like behavior ($F_{2,21} = 9.64$; $p < 0.01$) as indicated by the marked increase in sucrose preference. Figure 1(f) depicts that immobility time in FST was significantly increased after administration of DOX ($F_{2,21} = 10.35$; $p < 0.01$) when compared with the control group, which was also alleviated by dl-NBP treatment.

3.2. Effects of DOX and dl-NBP on Oxidative Stress Markers. As shown in Figures 2(a) and 2(b), administration of DOX significantly increased levels of NO ($F_{2,21} = 9.79$; $p < 0.01$) and MDA ($F_{2,21} = 8.52$; $p < 0.01$) as compared to the normal control group, whereas treatment with dl-NBP significantly blocked the increasing of NO and MDA when compared to the DOX group. The parameter of CAT activity, GR activity, and GPx activity and the content of GSH are the major biomarkers of antioxidative defense system. The activities of CAT and GR were significantly decreased in rats treated with DOX as compared to the normal control group, whereas dl-NBP treatment caused a significant increase in the activity of CAT and GR as compared to DOX group ($p < 0.01$) (Figures 2(c) and 2(d)). The activity of GPx was not decreased after administration of DOX when compared with the control group, but the treatment with dl-NBP significantly increased GPx activity (Figure 2(e)) as compared to DOX-treated rats ($F_{2,21} = 4.56$; $p < 0.05$) (Figure 2(e)). DOX administration decreased the content of GSH significantly ($F_{2,21} = 5.93$; $p < 0.05$), whereas probably due to the fact that GSH was oxidized to neutralize DOX-induced excessive free radicals, slight, but nonsignificant increase of GSH concentration was observed in dl-NBP-treated rats compared with the DOX group (Figure 2(f)).

3.3. Effects of DOX and dl-NBP on Neuroinflammation Biomarkers. The gene expressions of IL-1β (Figure 3(a), $F_{2,21} = 13.32$; $p < 0.01$), IL-6 (Figure 3(b), $F_{2,21} = 3.87$; $p < 0.05$), and TNF-α (Figure 3(c), $F_{2,21} = 11.41$; $p < 0.01$) were significantly increased in the DOX group. However, except IL-6, these elevated gene expressions were significantly attenuated by dl-NBP supplementation. The DOX + dl-NBP group showed significantly decreased gene expressions of IL-1β (Figure 3(a), $p < 0.01$) and TNF-α (Figure 3(c), $p < 0.05$) when compared to the rats in the DOX group. The DOX group showed a significant increase in protein expression of p65 (Figure 3(f), $F_{2,21} = 13.46$; $p < 0.01$) and iNOS (Figure 3(g), $F_{2,21} = 7.02$; $p < 0.01$) when compared to the control group. Consistent with the modulating effects of dl-NBP on the inflammatory cytokines, dl-NBP decreased the protein expression of p65 (Figure 3(f), $p < 0.01$) and iNOS (Figure 3(g), $p < 0.01$), and the immunohistochemical staining results of iNOS were in accordance with Western blot analysis (Figure 3(h)). The protein expression of IκB was significantly suppressed in the DOX group (Figure 3(e), $F_{2,21} = 14.65$; $p < 0.01$) as compared to the control group; the treatment of dl-NBP significantly mitigated the reduction of IκB protein level (Figure 3(e), $p < 0.01$) when compared to the rats treated with DOX alone.

3.4. Effects of DOX and dl-NBP on ER Stress. As the indicator of ER stress, the protein levels of GRP78, CHOP, and caspase-12 were monitored by Western blot to explore the mitigation effect of dl-NBP on DOX-induced hippocampcal ER stress [38]. As shown in Figure 4, the protein expressions of GRP78 (Figure 4(b), $F_{2,21} = 7.85$; $p < 0.01$), CHOP (Figure 4(c), $F_{2,21} = 26.25$; $p < 0.01$), and caspase-12 (Figure 4(d), $F_{2,21} = 8.78$; $p < 0.01$) were significantly increased after administration of DOX compared to the control group. Meanwhile the upregulation of GRP78 (Figure 4(b), $p < 0.01$), CHOP (Figure 4(c), $p < 0.01$), and caspase-12 (Figure 4(d), $p < 0.05$) protein expression were effectively inhibited by dl-NBP treatment.

3.5. Effects of DOX and dl-NBP on Histopathological Changes and Neural Apoptotic Markers. Histopathological alternation in the hippocampus from different treated groups is presented in Figure 5(a). Compared with the normal histology in the control group, the hippocampus showed more frequent nuclear pyknosis in the DOX exposure group. In contrast, the treatment with dl-NBP was able to prevent the histopathological alternation evoked by DOX treatment. TUNEL test was used to assess apoptotic cells in the hippocampus of rats receiving different treatments. As revealed in Figure 5(b), fewer apoptotic cells were detected in the hippocampus of the normal treated control group. However, in the hippocampus of rats exposed to DOX, more TUNEL-positive cells were found as compared to the control group. Pretreatment with dl-NBP also markedly reduced TUNEL-positive cells, indicating the proapoptotic effects of DOX and antiapoptotic effects of dl-NBP in the hippocampus.

4. Discussion

Our study demonstrated the protective effect of dl-NBP against DOX-induced neurotoxicity in rats. We investigated the anxiety- and depression-like behaviors in rats exposed to DOX, and pretreatment with dl-NBP normalized behavioral changes in rats treated with DOX. Our study revealed that oxidative stress, neuroinflammation, ER stress, and cell death play a vital role in DOX-induced hippocampal damage. Moreover, we demonstrated that dl-NBP could partly alleviate these changes, suggesting the protective role of dl-NBP against DOX-induced neurotoxicity. Thus, our results provide a substantial support to those previously observed reports [42, 43] of neuroprotection by targeting oxidative stress, neuroinflammation, and ER stress cascade. dl-NBP might be an effective adjuvant therapy to prevent DOX-induced neurotoxic side effects in clinical practice.

As a chemotherapeutic agent, the long-term use of DOX tends to induce neurotoxicity and may cause neuropsychiatric diseases including anxiety and depression. Our

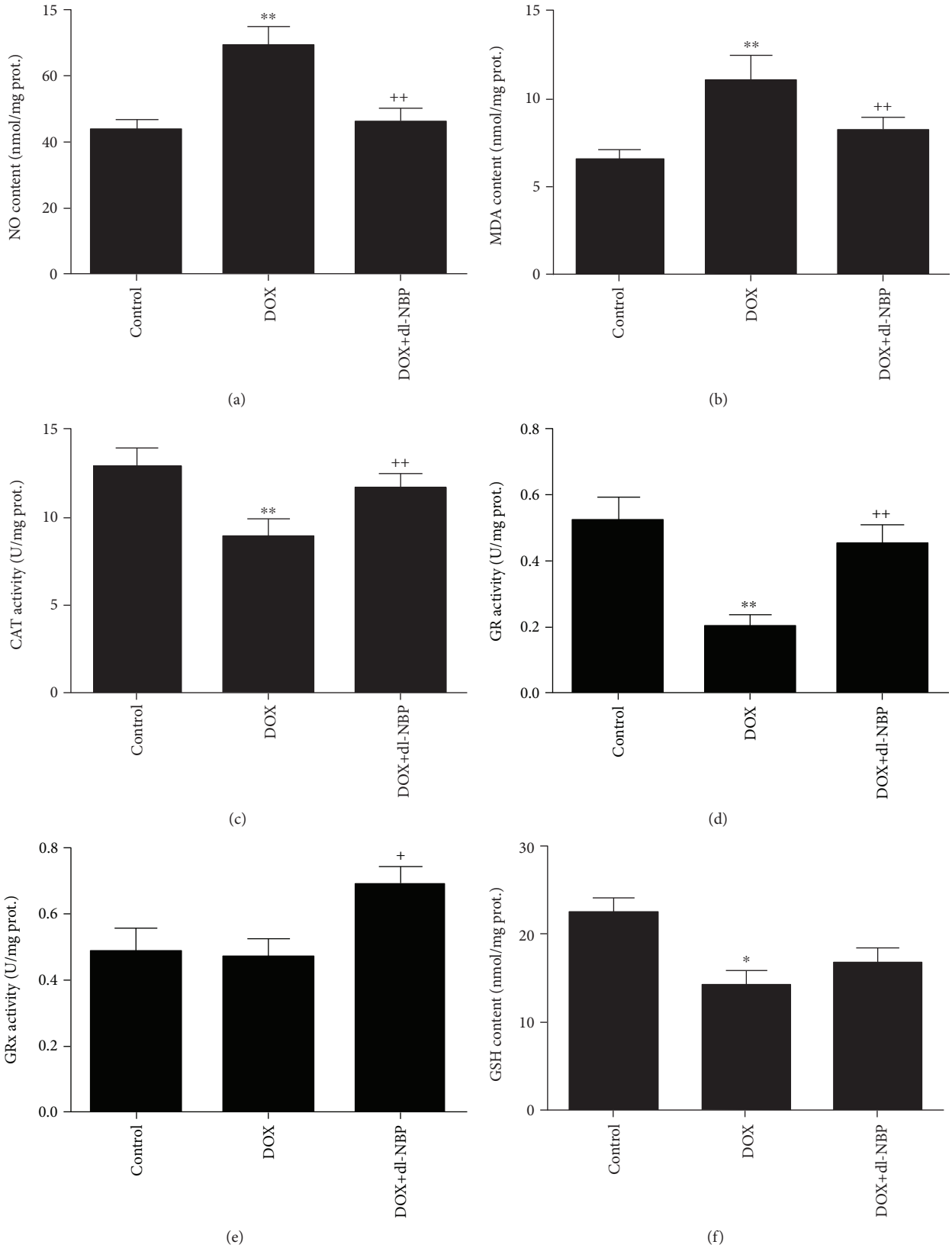

Figure 2: Effects of DOX and dl-NBP on oxidative stress markers in the hippocampus: NO content (a), MDA content (b), CAT activity (c), GR activity (d), GPx activity (e), and GSH content (f). Data are expressed as means ± SEM ($n = 8$). $^{*}p < 0.05$ and $^{**}p < 0.01$ compared to the control group. $^{+}p < 0.05$ and $^{++}p < 0.01$ compared to the DOX-injected group.

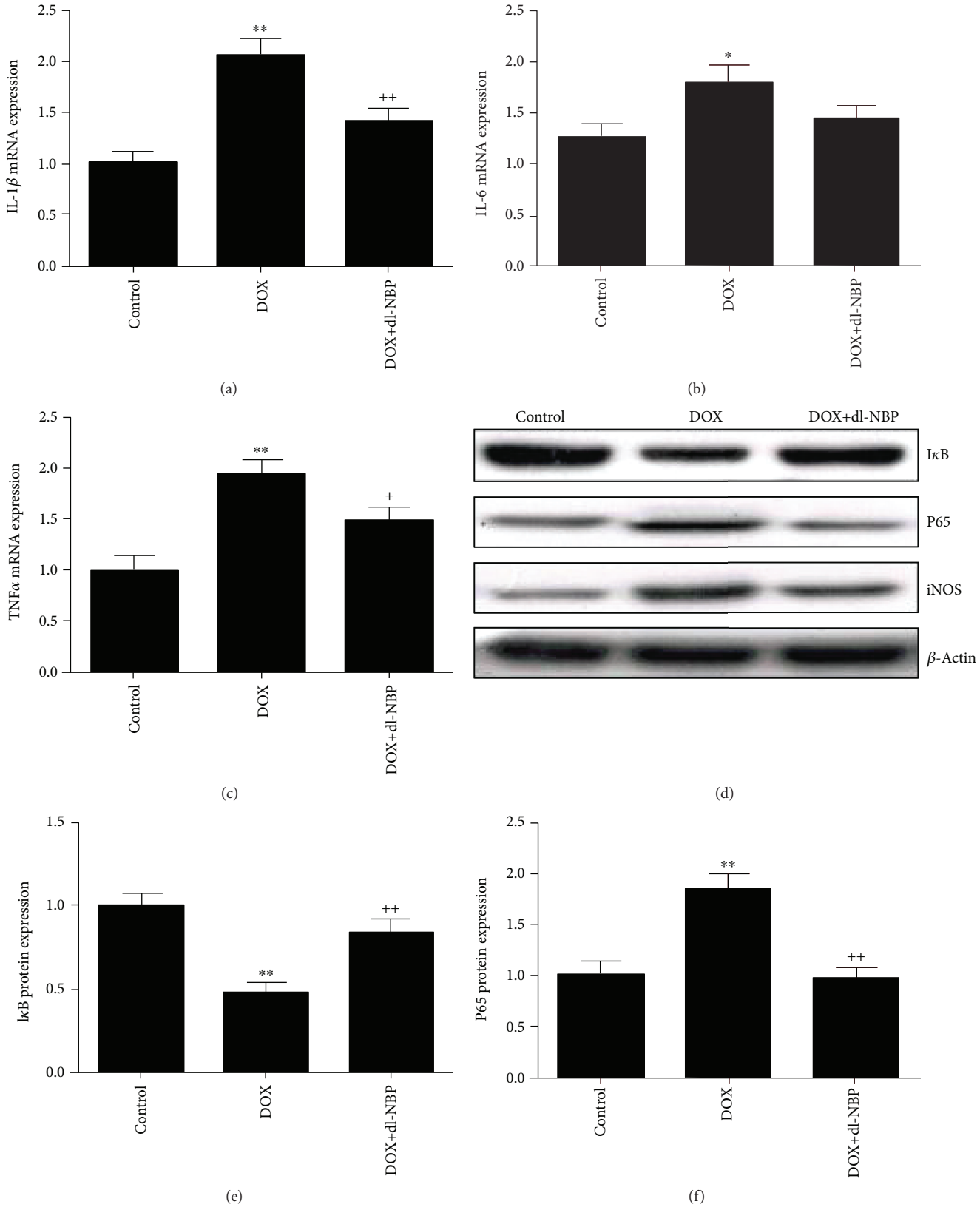

Figure 3: Continued.

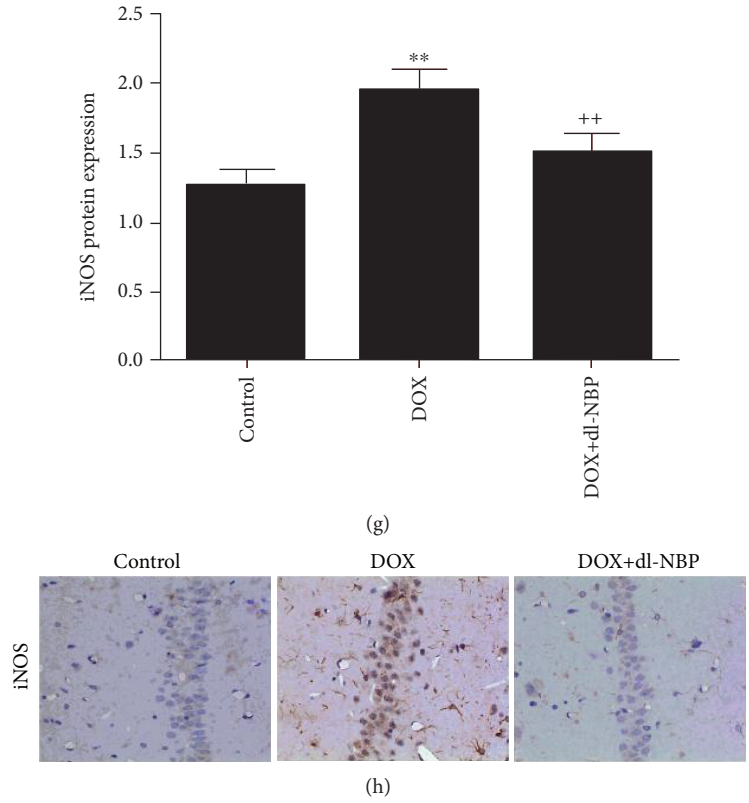

Figure 3: Effects of DOX and dl-NBP on neuroinflammation biomarkers: gene expression of IL-1β (a), IL-6 (b), and TNF-α (c); protein expression of IκB (e), p65 (f), and iNOS (g); and immunohistochemical staining of iNOS (h). Data are expressed as means ± SEM ($n = 8$). $^{*}p < 0.05$ and $^{**}p < 0.01$ compared to the control group. $^{+}p < 0.05$ and $^{++}p < 0.01$ compared to the DOX-injected group.

previous study demonstrated that the underlying mechanism of behavioral changes following DOX treatment and the antidepressant-like and neuroprotective effects of ω-3 PUFAs were closely related to the oxidative stress, neuroinflammation, and apoptotic status in the brain tissues [27]. Similarly, our present study showed that the supplementation with dl-NBP effectively restored anxiety- and depression-like behaviors induced by DOX. Thus, we further evaluated various markers of oxidative stress, ER stress, inflammation, and apoptosis in different groups.

The oxidative stress, which is consisted of oxidation system and antioxidant system, can cause oxidative damage and promote inflammatory reactions. In our study, the levels of NO and MDA were significantly increased after exposure to DOX, showing that DOX increased oxidative damage. Meanwhile, the antioxidant enzymes, including CAT, GR, GPx, and GSH, were all significantly decreased in DOX-challenged rats. DOX increased oxidation stress system and decreased antioxidant system, and the emergence of the redox imbalance led to oxidative damage of nerve cells, which is accompanied with cognitive dysfunction, anxiety, and depression-like behaviors. Furthermore, we clearly demonstrated the capability of dl-NBP to downregulate the levels of NO and MDA and upregulate the levels of GSH and activities of CAT, GR, and GPx, which acts as an antioxidant thereby reducing oxidative stress-induced apoptosis.

Neuroinflammation plays a critical role in the pathogenesis of brain disorders [42, 44]. iNOS, which produces large amounts of NO, is active during the inflammatory process [45], activating proinflammatory mediators, such as TNF-α and NF-κB, and subsequently induces brain neuroinflammation [43]. Proinflammatory cytokines such as TNF-α, IL-1β, IL-6, and iNOS have been demonstrated to play vital roles in inducing acute and chronic neurodegenerative disorders [42, 46]. We found that DOX provoked the generation of TNF-α, subsequently causing the activation of NF-κB and iNOS and increasing the gene expression of IL-1β and IL-6 and protein expression of p65, indicating severe inflammatory conditions in the hippocampus, and these inflammatory may result in neural death and behavioral changes. The treatment with dl-NBP significantly suppressed the DOX-induced increase of TNF-α, IL-1β, IL-6, p65, and iNOS expression in brain tissues.

ER is an organelle which plays as a key role in protein folding. Various destructive stimuli and pathological conditions such as hypoglycemia, inflammation, oxidative stress, and hypoxia may impair the ER function and consequently lead to the induction of a self-protecting signaling pathway known as unfolded protein response (UPR) [47]. The connection to the UPR is induction of cytokines and inflammation that have been linked to depression. The UPR acts on proinflammatory cytokines such as IL-8, IL-1β, and TNF-α, and these cytokines have been found to be upregulated in patients with major depression [48]. ER stress and ER stress-evoked inflammation form a vicious cycle which ultimately leads to neuronal cell death through apoptosis. To

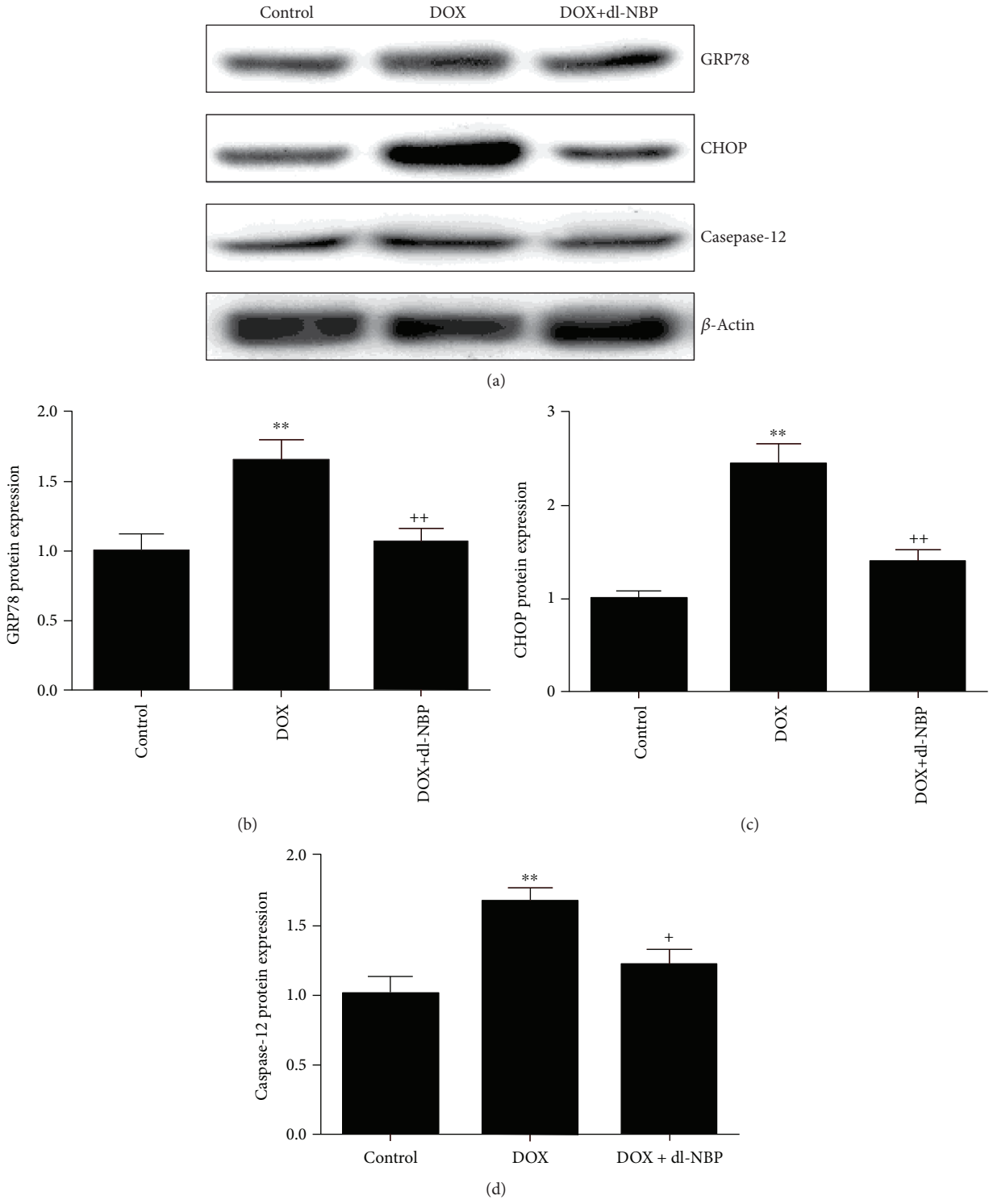

Figure 4: Effects of DOX and dl-NBP on ER stress. Protein expression of GRP78 (b), CHOP (c), and caspase-12 (d). Data are expressed as means ± SEM ($n = 8$). $^{**}p < 0.01$ compared to the control group. $^{+}p < 0.05$ and $^{++}p < 0.01$ compared to the DOX-injected group.

evaluate ER stress after DOX exposure, protein levels of ER stress markers such as GRP78, CHOP, and caspase-12 were measured in the hippocampus in the current study. CHOP is a transcriptional factor, which could decrease expression of the antiapoptotic molecules and increase the expression of proapoptotic molecules to trigger apoptotic cell death [19, 49, 50]. GRP78 is a heat shock protein family chaperone transcriptional factor which plays a key role in the regulation of ER functioning [11]. Caspase-12 is an apoptosis-associated protein. Previous evidence has demonstrated that these ER

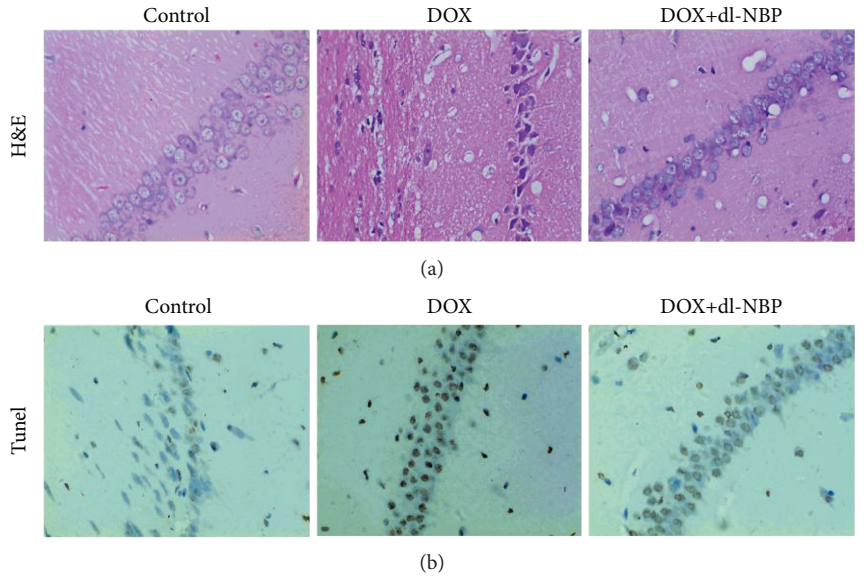

Figure 5: Effects of DOX and dl-NBP on histopathological changes and apoptotic markers. HE staining of different group (a) and TUNEL staining of different group (b).

stress-related proteins were also increased in the hippocampus of rat exposure to chronic unpredictable mild stress, a valid animal model of depression [38]. Our study found that dl-NBP alleviated the upregulation of CHOP, GRP-78, and caspase-12 in the hippocampus of rats exposed to DOX. Our results indicated that the potential antidepressant action of dl-NBP is endowed with its significant neuroprotective properties against DOX-induced hippocampal ER stress.

Our present study also found that DOX caused a significant increase in TUNEL-positive neurocytes, indicating severe DNA damage and neuronal death. Previous studies showed that DOX-induced neural apoptosis is closely related to depression [27]. Moreover, proinflammatory cytokines appear to contribute to depression-associated cell death through intrinsic apoptotic pathways, and neurotoxic free radicals are a second apoptosis-mediating factor associated with depressive disorder, suggesting that antioxidant and anti-inflammatory effects of dl-NBP could, in turn, indirectly contribute to its antiapoptotic effect. Although the study mainly focused on the neuroprotective effects of dl-NBP against DOX-induced neurotoxicity, it is important to note that the present study did not include dl-NBP-treated control animals, which is a major limitation of the study. Therefore, further studies are warranted to evaluate the baseline effect of the drug treatment to ensure its safety and efficacy.

5. Conclusion

In conclusion, our present study demonstrated that the DOX-induced behavioral anomalies might be the manifestations of oxidative stress, neuroinflammation, ER stress, and apoptosis in the hippocampus. The possible mechanisms under behavior-modulating and neuroprotective effects of dl-NBP are indicated to be at least partially associated with the antioxidant, anti-inflammatory, anti-ER stress, and anti-apoptotic actions in the brain. Thus, our study provides a new potential treatment for brain damage induced by chemotherapeutic drugs and paves the way for further studies to investigate other mechanisms underlying the behavior modulating and neuroprotective effects of dl-NBP.

Data Availability

The data used to support the findings of this study are available from the corresponding author upon request.

Conflicts of Interest

The authors declare no conflict of interest.

Authors' Contributions

Pei Jiang and Daxiong Xiang designed the study and wrote the protocol. Dehua Liao and Ruili Dang performed the experiments and analyzed the data. Pengfei Xu, Yingzhou Fu, Dunwu Yao, Wenxiu Han, and Lizhi Cao contributed to the reagents and materials. Dehua Liao drafted the manuscript. Pei Jiang and Dehua Liao revised the manuscript content. All authors read and approved the final manuscript.

Acknowledgments

This study was supported by the National Natural Science Foundation of China (no. 81603206), the Hunan Provincial Pharmaceutical Association Fund (no. hn2017005), and the Natural Science Foundation of Hunan Province (no. 2015JJ6062).

Supplementary Materials

Figure S1: the melting curve is shown as fluorescence versus temperature. *(Supplementary Materials)*

References

[1] J. T. R. Keeney, S. Miriyala, T. Noel, J. A. Moscow, D. K. St. Clair, and D. A. Butterfield, "Superoxide induces protein oxidation in plasma and TNF-α elevation in macrophage culture: insights into mechanisms of neurotoxicity following doxorubicin chemotherapy," *Cancer Letters*, vol. 367, no. 2, pp. 157–161, 2015.

[2] V. K. Todorova, Y. Kaufmann, L. J. Hennings, and V. S. Klimberg, "Glutamine regulation of doxorubicin accumulation in hearts versus tumors in experimental rats," *Cancer Chemotherapy and Pharmacology*, vol. 66, no. 2, pp. 315–323, 2010.

[3] A. I. Abushouk, A. Ismail, A. M. A. Salem, A. M. Afifi, and M. M. Abdel-Daim, "Cardioprotective mechanisms of phytochemicals against doxorubicin-induced cardiotoxicity," *Biomedicine & Pharmacotherapy*, vol. 90, pp. 935–946, 2017.

[4] M. Yagmurca, Z. Yasar, and O. Bas, "Effects of quercetin on kidney injury induced by doxorubicin," *Bratislava Medical Journal*, vol. 116, no. 8, pp. 486–489, 2015.

[5] J. F. Moruno-Manchon, N. E. Uzor, S. R. Kesler et al., "Peroxisomes contribute to oxidative stress in neurons during doxorubicin-based chemotherapy," *Molecular and Cellular Neurosciences*, vol. 86, pp. 65–71, 2018.

[6] S. Merzoug, M. L. Toumi, N. Boukhris, B. Baudin, and A. Tahraoui, "Adriamycin-related anxiety-like behavior, brain oxidative stress and myelotoxicity in male Wistar rats," *Pharmacology Biochemistry and Behavior*, vol. 99, no. 4, pp. 639–647, 2011.

[7] S. Merzoug, M. L. Toumi, and A. Tahraoui, "Quercetin mitigates Adriamycin-induced anxiety- and depression-like behaviors, immune dysfunction, and brain oxidative stress in rats," *Naunyn-Schmiedeberg's Archives of Pharmacology*, vol. 387, no. 10, pp. 921–933, 2014.

[8] C. E. Jansen, B. A. Cooper, M. J. Dodd, and C. A. Miaskowski, "A prospective longitudinal study of chemotherapy-induced cognitive changes in breast cancer patients," *Support Care Cancer*, vol. 19, no. 10, pp. 1647–1656, 2011.

[9] D. M. Bannerman, R. Sprengel, D. J. Sanderson et al., "Hippocampal synaptic plasticity, spatial memory and anxiety," *Nature Reviews Neuroscience*, vol. 15, no. 3, pp. 181–192, 2014.

[10] K. Sulakhiya, P. Kumar, A. Jangra et al., "Honokiol abrogates lipopolysaccharide-induced depressive like behavior by impeding neuroinflammation and oxido-nitrosative stress in mice," *European Journal of Pharmacology*, vol. 744, pp. 124–131, 2014.

[11] A. Jangra, C. S. Sriram, S. Dwivedi et al., "Sodium phenylbutyrate and edaravone abrogate chronic restraint stress-induced behavioral deficits: implication of oxido-nitrosative, endoplasmic reticulum stress cascade, and neuroinflammation," *Cellular and Molecular Neurobiology*, vol. 37, no. 1, pp. 65–81, 2017.

[12] H. A. Rizk, M. A. Masoud, and O. W. Maher, "Prophylactic effects of ellagic acid and rosmarinic acid on doxorubicin-induced neurotoxicity in rats," *Journal of Biochemical and Molecular Toxicology*, vol. 31, no. 12, 2017.

[13] S. Pal, M. Ahir, and P. C. Sil, "Doxorubicin-induced neurotoxicity is attenuated by a 43-kD protein from the leaves of *Cajanus indicus* L. via NF-κB and mitochondria dependent pathways," *Free Radical Research*, vol. 46, no. 6, pp. 785–798, 2012.

[14] J. Tangpong, M. P. Cole, R. Sultana et al., "Adriamycin-induced, TNF-α-mediated central nervous system toxicity," *Neurobiology of Disease*, vol. 23, no. 1, pp. 127–139, 2006.

[15] Y. Chen, Y. Tang, Y. Xiang, Y. Q. Xie, X. H. Huang, and Y. C. Zhang, "Shengmai injection improved doxorubicin-induced cardiomyopathy by alleviating myocardial endoplasmic reticulum stress and caspase-12 dependent apoptosis," *BioMed Research International*, vol. 2015, Article ID 952671, 8 pages, 2015.

[16] E. G. Vichaya, G. S. Chiu, K. Krukowski et al., "Mechanisms of chemotherapy-induced behavioral toxicities," *Frontiers in Neuroscience*, vol. 9, p. 131, 2015.

[17] Y. Zhang, W. Liu, Y. Zhou, C. Ma, S. Li, and B. Cong, "Endoplasmic reticulum stress is involved in restraint stress-induced hippocampal apoptosis and cognitive impairments in rats," *Physiology & Behavior*, vol. 131, pp. 41–48, 2014.

[18] L. Wei, L. Y. Kan, H. Y. Zeng et al., "BDNF/TrkB pathway mediates the antidepressant-like role of H_2S in CUMS-exposed rats by inhibition of hippocampal ER stress," *Neuro-Molecular Medicine*, vol. 20, no. 2, pp. 252–261, 2018.

[19] F. Cai, J. Liu, C. Li, and J. Wang, "Critical role of endoplasmic reticulum stress in cognitive impairment induced by microcystin-LR," *International Journal of Molecular Sciences*, vol. 16, no. 12, pp. 28077–28086, 2015.

[20] J. J. Min, X. L. Huo, Y. Xiang et al., "Protective effect of Dl-3n-butylphthalide on learning and memory impairment induced by chronic intermittent hypoxia-hypercapnia exposure," *Scientific Reports*, vol. 4, no. 1, p. 5555, 2014.

[21] P. Zhang, Z. F. Guo, Y. M. Xu, Y. S. Li, and J. G. Song, "*N*-Butylphthalide (NBP) ameliorated cerebral ischemia reperfusion-induced brain injury via HGF-regulated TLR4/NF-κB signaling pathway," *Biomedicine & Pharmacotherapy*, vol. 83, pp. 658–666, 2016.

[22] X. D. Yang, Z. D. Cen, H. P. Cheng et al., "L-3-n-Butylphthalide protects HSPB8 K141N mutation-induced oxidative stress by modulating the mitochondrial apoptotic and Nrf2 pathways," *Frontiers in Neuroscience*, vol. 11, p. 402, 2017.

[23] M. Estrada, C. Herrera-Arozamena, C. Perez et al., "New cinnamic – *N*-benzylpiperidine and cinnamic – *N*,*N*-dibenzyl(*N*-methyl)amine hybrids as Alzheimer-directed multitarget drugs with antioxidant, cholinergic, neuroprotective and neurogenic properties," *European Journal of Medicinal Chemistry*, vol. 121, pp. 376–386, 2016.

[24] Z. Liu, H. Wang, X. Shi et al., "DL-3-*n*-Butylphthalide (NBP) provides neuroprotection in the mice models after traumatic brain injury via Nrf2-ARE signaling pathway," *Neurochemical Research*, vol. 42, no. 5, pp. 1375–1386, 2017.

[25] H. M. Wang, T. Zhang, J. K. Huang, and X. J. Sun, "3-N-Butylphthalide (NBP) attenuates the amyloid-β-induced inflammatory responses in cultured astrocytes via the nuclear factor-κB signaling pathway," *Cellular Physiology and Biochemistry*, vol. 32, no. 1, pp. 235–242, 2013.

[26] X. Tian, W. He, R. Yang, and Y. Liu, "Dl-3-n-butylphthalide protects the heart against ischemic injury and H9c2 cardiomyoblasts against oxidative stress: involvement of mitochondrial function and biogenesis," *Journal of Biomedical Science*, vol. 24, no. 1, p. 38, 2017.

[27] Y. Q. Wu, R. L. Dang, M. M. Tang et al., "Long chain omega-3 polyunsaturated fatty acid supplementation alleviates doxorubicin-induced depressive-like behaviors and neurotoxicity in rats: involvement of oxidative stress and neuroinflammation," *Nutrients*, vol. 8, no. 4, p. 243, 2016.

[28] M. Tang, P. Jiang, H. Li et al., "Antidepressant-like effect of n-3 PUFAs in CUMS rats: role of tPA/PAI-1 system," *Physiology & Behavior*, vol. 139, pp. 210–215, 2015.

[29] A. Jangra, C. S. Sriram, and M. Lahkar, "Lipopolysaccharide-induced behavioral alterations are alleviated by sodium phenylbutyrate via attenuation of oxidative stress and neuroinflammatory cascade," *Inflammation*, vol. 39, no. 4, pp. 1441–1452, 2016.

[30] R. Dang, Y. Guo, L. Zhang, L. Chen, R. Yang, and P. Jiang, "Chronic stress and excessive glucocorticoid exposure both lead to altered neuregulin-1/ErbB signaling in rat myocardium," *Steroids*, vol. 112, pp. 47–53, 2016.

[31] R. Dang, H. Cai, L. Zhang et al., "Dysregulation of neuregulin-1/ErbB signaling in the prefrontal cortex and hippocampus of rats exposed to chronic unpredictable mild stress," *Physiology & Behavior*, vol. 154, pp. 145–150, 2016.

[32] H. Ohkawa, N. Ohishi, and K. Yagi, "Assay for lipid peroxides in animal tissues by thiobarbituric acid reaction," *Analytical Biochemistry*, vol. 95, no. 2, pp. 351–358, 1979.

[33] L. C. Green, D. A. Wagner, J. Glogowski, P. L. Skipper, J. S. Wishnok, and S. R. Tannenbaum, "Analysis of nitrate, nitrite, and [^{15}N]nitrate in biological fluids," *Analytical Biochemistry*, vol. 126, no. 1, pp. 131–138, 1982.

[34] M. S. Moron, J. Depierre, and B. Mannervik, "Levels of glutathione, glutathione reductase and glutathione *S*-transferase activities in rat lung and liver," *Biochimica et Biophysica Acta (BBA) - General Subjects*, vol. 582, no. 1, pp. 67–78, 1979.

[35] A. K. Sinha, "Colorimetric assay of catalase," *Analytical Biochemistry*, vol. 47, no. 2, pp. 389–394, 1972.

[36] D. Cattani, P. A. Cesconetto, M. K. Tavares et al., "Developmental exposure to glyphosate-based herbicide and depressive-like behavior in adult offspring: implication of glutamate excitotoxicity and oxidative stress," *Toxicology*, vol. 387, pp. 67–80, 2017.

[37] J. T. Rotruck, A. L. Pope, H. E. Ganther, A. B. Swanson, D. G. Hafeman, and W. G. Hoekstra, "Selenium: biochemical role as a component of glutathione peroxidase," *Science*, vol. 179, no. 4073, pp. 588–590, 1973.

[38] S.-Y. Liu, D. Li, H.-Y. Zeng et al., "Hydrogen sulfide inhibits chronic unpredictable mild stress-induced depressive-like behavior by upregulation of Sirt-1: involvement in suppression of hippocampal endoplasmic reticulum stress," *International Journal of Neuropsychopharmacology*, vol. 20, no. 11, pp. 867–876, 2017.

[39] J. P. Pei, L. H. Fan, K. Nan, J. Li, X. Q. Dang, and K. Z. Wang, "HSYA alleviates secondary neuronal death through attenuating oxidative stress, inflammatory response, and neural apoptosis in SD rat spinal cord compression injury," *Journal of Neuroinflammation*, vol. 14, no. 1, p. 97, 2017.

[40] E. Alsina, E. V. Macri, F. Lifshitz et al., "Efficacy of phytosterols and fish-oil supplemented high-oleic-sunflower oil rich diets in hypercholesterolemic growing rats," *International Journal of Food Sciences and Nutrition*, vol. 67, no. 4, pp. 441–453, 2016.

[41] A. M. Barbosa, P. . C. Francisco, K. Motta et al., "Fish oil supplementation attenuates changes in plasma lipids caused by dexamethasone treatment in rats," *Applied Physiology, Nutrition, and Metabolism*, vol. 41, no. 4, pp. 382–390, 2016.

[42] Y. Chtourou, B. Aouey, M. Kebieche, and H. Fetoui, "Protective role of naringin against cisplatin induced oxidative stress, inflammatory response and apoptosis in rat striatum via suppressing ROS-mediated NF-κB and P53 signaling pathways," *Chemico-Biological Interactions*, vol. 239, pp. 76–86, 2015.

[43] R. N. El-Naga, H. I. Ahmed, and E. N. Abd Al Haleem, "Effects of indole-3-carbinol on clonidine-induced neurotoxicity in rats: impact on oxidative stress, inflammation, apoptosis and monoamine levels," *NeuroToxicology*, vol. 44, pp. 48–57, 2014.

[44] T. C. Frank-Cannon, L. T. Alto, F. E. McAlpine, and M. G. Tansey, "Does neuroinflammation fan the flame in neurodegenerative diseases?," *Molecular Neurodegeneration*, vol. 4, no. 1, p. 47, 2009.

[45] M. Antosova, A. Strapkova, P. Mikolka, J. Mokry, I. Medvedova, and D. Mokra, "The influence of L-NAME on iNOS expression and markers of oxidative stress in allergen-induced airway hyperreactivity," *Advances in Experimental Medicine and Biology*, vol. 838, pp. 1–10, 2015.

[46] P. Eikelenboom, C. Bate, W. A. Van Gool et al., "Neuroinflammation in Alzheimer's disease and prion disease," *Glia*, vol. 40, no. 2, pp. 232–239, 2002.

[47] F. Lotrich, "Inflammatory cytokines, growth factors, and depression," *Current Pharmaceutical Design*, vol. 18, no. 36, pp. 5920–5935, 2012.

[48] M. A. Timberlake II and Y. Dwivedi, "Altered expression of endoplasmic reticulum stress associated genes in hippocampus of learned helpless rats: relevance to depression pathophysiology," *Frontiers in Pharmacology*, vol. 6, p. 319, 2015.

[49] K. Zhang and R. J. Kaufman, "From endoplasmic-reticulum stress to the inflammatory response," *Nature*, vol. 454, no. 7203, pp. 455–462, 2008.

[50] M. Qi, Y. Dang, Q. Xu et al., "Microcystin-LR induced developmental toxicity and apoptosis in zebrafish *(Danio rerio)* larvae by activation of ER stress response," *Chemosphere*, vol. 157, pp. 166–173, 2016.

Hindawi
Oxidative Medicine and Cellular Longevity
Volume 2018, Article ID 4010395, 21 pages
https://doi.org/10.1155/2018/4010395

Review Article

The Drug Developments of Hydrogen Sulfide on Cardiovascular Disease

Ya-Dan Wen,[1,2,3] **Hong Wang**,[3,4] **and Yi-Zhun Zhu**[3,5]

[1]*Department of Clinical Pharmacology, Xiangya Hospital, Central South University, Changsha, China*
[2]*Hunan Key Laboratory of Pharmacogenetics, Institute of Clinical Pharmacology, Central South University, Changsha, China*
[3]*Department of Pharmacology, Yong Loo Lin School of Medicine, National University of Singapore, Singapore*
[4]*Singapore Nuclear Research and Safety Initiative, National University of Singapore, Singapore*
[5]*Department of Pharmacology, Macau University of Science and Technology, Macau*

Correspondence should be addressed to Ya-Dan Wen; xiaoxiannv-a@163.com and Yi-Zhun Zhu; yzzhu@must.edu.mo

Received 30 March 2018; Accepted 27 May 2018; Published 29 July 2018

Academic Editor: Mohamed M. Abdel-Daim

The recognition of hydrogen sulfide (H_2S) has been evolved from a toxic gas to a physiological mediator, exhibiting properties similar to NO and CO. On the one hand, H_2S is produced from L-cysteine by enzymes of cystathionine γ-lyase (CSE) and cystathionine β-synthase (CBS), 3-mercaptopyruvate sulfurtransferase (3MST) in combination with aspartate aminotransferase (AAT) (also called as cysteine aminotransferase, CAT); on the other hand, H_2S is produced from D-cysteine by enzymes of D-amino acid oxidase (DAO). Besides sulfide salt, several sulfide-releasing compounds have been synthesized, including organosulfur compounds, Lawesson's reagent and analogs, and plant-derived natural products. Based on garlic extractions, we synthesized S-propargyl-L-cysteine (SPRC) and its analogs to contribute our endeavors on drug development of sulfide-containing compounds. A multitude of evidences has presented H_2S is widely involved in the roles of physiological and pathological process, including hypertension, atherosclerosis, angiogenesis, and myocardial infarcts. This review summarizes current sulfide compounds, available H_2S measurements, and potential molecular mechanisms involved in cardioprotections to help researchers develop further applications and therapeutically drugs.

1. Introduction

In an evolutionary perspective, the synthesis and catabolism of hydrogen sulfide (H_2S) by living organisms antedates the evolution of vertebrate. Bacteria and archaea produce and utilize the stinking gas as one of the essential sources for their survival and proliferation. For many decades, H_2S, the colorless gas with a strong odor of rotten gas, is recognized as a toxic gas and an environmental pollutant. The mechanism of its toxicity is a potent inhibition of mitochondrial cytochrome c oxidase, which is the important enzyme that is closely related with chemical energy in the form of adenosine triphosphate (ATP). Sulfide, together with cyanide, azide, and carbon monoxide (CO), all can inhibit cytochrome c oxidase which leads to chemical asphyxiation of cells.

In the last two decades, the perception of H_2S has been changed from that of a noxious gas to a gasotransmitter with vast potential in pharmacotherapy. At the end of the 1980s, endogenous H_2S is found in the brain [1]. Then, its enzymatic mechanism, physiological concentrations, and specific cellular targets were described in the year 1996 [2]. Subsequently, the physiological and pharmacological characters of H_2S were unveiled. Recently, H_2S, followed with NO and CO, is identified as the third gasotransmitter by Wang [3]. The three gases share some common features. They are all colorless and poisonous gases. With the exception of gas

Table 1: Comparison of nitric oxide, carbon monoxide, and hydrogen sulfide.

	Nitric oxide	Carbon monoxide	Hydrogen sulfide
Formula	NO	CO	H_2S
Color and odor	Colorless; a mild, sweet odor	Colorless; odorless	Colorless; smell like rotten egg
Free radical	Yes	No	No
Flammable	No	No	Yes
Toxicity	Yes	Yes	Yes
Inhibition of mitochondrial cytochrome c oxidase	Yes	Yes	Yes
Resources	L-arginine or nitrite	Protohaem IX	L/D-cysteine
Intermediate products	L-NG hydroxyarginine, citrulline	Biliverdin IX-α	Cystathionine, L-cysteine, α-ketobutyrate, and pyruvate
Enzymes	eNOS, iNOS, and nNOS	HO-1, HO-2, and HO-3	CBS, CSE, 3MST/AAT, and DAO
Vascular effect	Vasodilation, angiogenesis	Vasodilation, angiogenesis	Vasodilation, angiogenesis
Inhibition inflammation	Yes	Yes	Yes
Antiapoptosis	Yes	Yes	Yes
Haem effect	Yes	Yes	Yes
Molecular targets	Soluble guanylate cyclase (sGC)	Soluble guanylate cyclase (sGC)	K_{ATP} (ATP-gated potassium) channel
Targeting outcome	Increase cGMP, activate K_{Ca} channels and nitrosylation	Increase cGMP, activate K_{Ca} channels	Increase cGMP and cAMP, activate K_{ATP} channels and sulfhydration
Application on human	Pulmonary hypertension, lung transplantation, and ARDS	Not available	Not available

pressure in atmosphere, they can dissolve in water at different solubility. All these small signaling molecules possess significant physiological importance, like anti-inflammation and antiapoptosis. The similarities and differences of the features of NO, CO, and H_2S are summarized in Table 1.

This review is prepared for researchers, who are interested in H_2S and sulfide-containing compounds, on drug development of cardiovascular disease. Therefore, some key issues were discussed, like "donors and inhibitors" to support choosing the sulfide-releasing chemicals and specific inhibitors. Readers could depend on the precision of currently "measuring methods" to decide the analyzing techniques. H_2S on "inflammation," "redox status," and "cardiovascular disease" summarizes the currently novel findings of the effects of H_2S and underlying mechanisms.

2. Physical and Biological Characteristics

H_2S, a colorless and flammable gas with the characteristic foul odor of rotten eggs, is known for decades as a toxic gas and an environmental hazard. It is soluble in water (1 g in 242 ml at 20°C). In water or plasma, H_2S is a weak acid which hydrolyzes to hydrogen ion and hydrosulfide and sulfide ions as following: $H_2S \leftrightarrow H^+ + HS^- \leftrightarrow 2H^+ + S^{2-}$. The pKa at 37°C is 6.76. When H_2S is dissolved in physiological solution (pH 7.4, 37°C), it yields approximately 18.5% H_2S and 81.5% hydrosulfide anion (HS^-), as predicted by the Henderson-Hasselbalch equation [4]. H_2S could be oxidized to sulfur oxide, sulfate, persulfide, and sulfite. H_2S is permeable to plasma membranes as its solubility in lipophilic solvents is fivefold greater than in water. In other words, it is able to freely penetrate cells of all types.

The toxic effect of H_2S on living organisms has been recognized for nearly 300 years, and until recently, it was believed to be a poisonous environmental pollutant with minimal physiological significance. H_2S is more toxic than hydrogen cyanide and exposed to as little as 300 ppm in the air for just 30 min is fatal to human. The level of odor detection of sulfide by the human nose is at a concentration of 0.02–0.1 ppm, 400-fold lower than the toxic level. As a broad-spectrum toxicant, H_2S affects many organ systems including the lung, brain, and kidney.

H_2S is often produced through the anaerobic bacterial breakdown of organic substrates in the absence of oxygen, such as in swamps and sewers (anaerobic digestion). It also results from inorganic reactions in volcanic gases, natural gas, and some well waters. Digestion of algae, mushrooms, garlic, and onions is believed to release H_2S by chemical transformation and enzymatic reactions [5]. Structures of natural food-releasing H_2S on digestion are shown in Figure 1. Consuming mushrooms, garlic, and onions, which contain chemicals and enzymes responsible for the transformation of the sulfur compounds, is responsible for H_2S production in the human gut [6]. Human body produces small amounts of H_2S and uses it as a signaling molecule. In different species and organs, the concentration of H_2S varies in different levels. In Wistar rats, the normal blood level of H_2S is 10 μM [7]; while in Sprague-Dawley rats, the plasma level of H_2S increases to 46 μM [8]; in human, 10–100 μM H_2S in blood was reported [9]. The tissue level of H_2S is known to

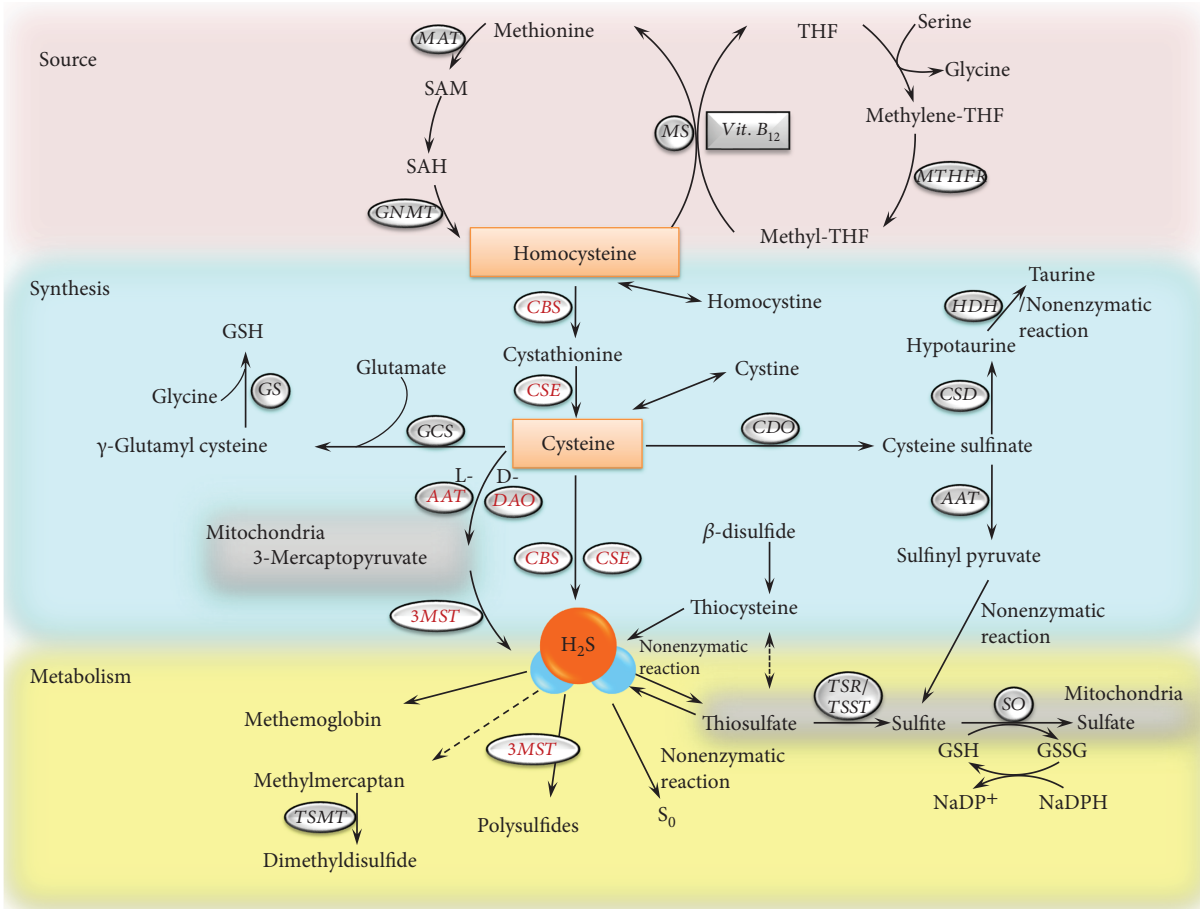

Figure 1: Synthesis and catabolism of H_2S. AAT: aspartate aminotransferase; CDO: cysteine dioxygenase; CSE: cystathionine γ-lyase; HDH: hypotaurine dehydrogenase; GCS: γ-glutamyl cysteine synthase; GS: glutathione synthase; MAT: methionine adenosyltransferase; MS: methionine synthase; S0: elemental sulfur; SAM: S-adenosylmethionine; THF: tetrahydrofolate; TSST: thiosulfate sulfurtransferase; CBS: cystathionine β-synthase; CSD: sulfinate decarboxylase; DAO: D-amino acid oxidase; H_2S: hydrogen sulfide; GNMT: glycine N-methyltransferase; GSH: glutathione; 3MST: 3-mercaptopyruvate sulfide transferase; MTHFR: methylenetetrahydrofolate reductase; SAH: S-adenosylhomocysteine; SO: sulfite oxidase; TSR: thiosulfate reductase; TSMT: thiol S-methyltransferase.

be higher than its circulating level. The concentration of endogenous H_2S has been reported up to 50–160 μM in the brains of rat, human, and bovine [1, 10, 11]. Significant amounts of H_2S are generated from vascular tissues, and this production varies among different types of vascular tissues. For instance, the homogenates of thoracic aorta yielded more H_2S than that of portal vein of rats [8]. Furne et al. reported that in situ tissue H_2S level through analyzing the gas space over rapidly homogenized mouse brain and liver was only 15 nM [12].

3. Synthesis and Catabolism of H_2S

H_2S is endogenously formed by both enzymatic and nonenzymatic pathways [3]. The enzymatic procedure of synthesizing H_2S, in mammalian tissues, is involved in two pyridoxal 5′-phosphate-dependent enzymes: cystathionine γ-lyase (CSE) and cystathionine β-synthase (CBS) [13–15]. As shown in Figure 1, H_2S is catalyzed from the desulfhydration of L-cysteine, a sulfur containing amino acid derived from alimentary sources, produced by the transsulfuration pathway of L-methionine to homocysteine or liberated from other endogenous proteins [16, 17]. As the intermediate, CBS catalyzes homocysteine together with serine to yield cystathionine, which is converted to cysteine, α-ketobutyrate, and NH_4^+ by CSE. The two pyridoxal 5′-phosphate-dependent enzymes both or either catalyze the conversion of cysteine to H_2S, pyruvate, and NH_4^+. CSE also could catalyze a β-disulfide elimination reaction that results in the production of thiocysteine, pyruvate, and NH_4^+. Thiocysteine is associated with cysteine or other thiols to form H_2S [18]. The two synthesis pathways of producing H_2S are illustrated in Figure 1.

The two enzymes are widespread in mammalian tissues and cells and also in many invertebrates and bacteria [19]. The activity of CSE is chiefly concentrated in the liver, heart, vessels, kidney, brain, small intestine, stomach, uterus, placenta, and pancreatic islets; whereas, the amount of CBS is mainly located in the brain, liver, kidney and ileum, uterus, placenta, and pancreatic islets [20]. The locations of H_2S-

Table 2: Characteristics of H_2S-producing enzymes.

	Cystathionine γ-lyase (CSE)	Cystathionine β-synthase (CBS)
Localization	Liver, heart, vessels, kidney, brain, adipose, small intestine, stomach, uterus, placenta, and pancreatic islets	Brain, liver, kidney and ileum, uterus, placenta, and pancreatic islets
Activators	Pyridoxal 5′-phosphate	Pyridoxal 5′-phosphate, S-adenosyl-L-methionine, and Ca^{2+}/calmodulin
Inhibitors	D,L-propargylglycine, β-cyano-L-alanine	Hydroxylamine, aminooxyacetate
Functional roles	H_2S production in the liver and smooth muscle	H_2S production in the brain and nervous system

producing enzymes are seen in Table 2. In several species, the liver is the common organ containing the two enzymes in abundance. According to the research of Zhao et al., the intensity rank of biosynthesis of H_2S by origin of exogenous cysteine in different rat blood vessels was tail artery > aorta > mesenteric artery [21].

A third enzymatic reaction contributing to H_2S production has recently been identified in brain and vascular endothelium, that is, 3-mercaptopyruvate sulfurtransferase (3MST) in combination with aspartate aminotransferase (AAT) (also called cysteine aminotransferase, CAT) [22, 23], seen in Figure 1. In mitochondria, L-cysteine and α-ketoglutarate as substrates can be converted to 3-mercaptopyruvate (3MP) by AAT; then, the intermediate product is converted to H_2S by 3MST [23]. In the brain, 3MST is found in neurons [24] and astrocytes [25], while CBS in astrocytes [24]. It could speculate that the two enzymes of catalyzing H_2S play different roles in the nervous system. In vascular tissues, 3MST could be detected in both endothelial cells and vascular smooth muscle cells (SMCs), while AAT just occurs in endothelial cells. From another perspective, only vascular endothelial cells in vessel could utilize the two enzymes to produce H_2S, whereas vascular SMCs likely absorb 3-mercaptopyruvate or other sources to generate H_2S which exerts as a vasodilator.

The fourth enzymatic pathway was recently reported by Shibuya et al. [26] that produces H_2S from D-cysteine by D-amino acid oxidase (DAO). Different from using L-cysteine to produce H_2S by CBS, CSE, and 3MST/AAT, which are pyridoxal 5′-phosphate- (PLP-) dependent enzymes, D-cysteine pathway generates H_2S by PLP-independent enzyme [27]. Similar to 3MST on mitochondria, DAO localizes to peroxisomes in mitochondrial fractions [28]. D-cysteine is metabolized by DAO in peroxisomes to achiral 3MP, which is also generated from L-cysteine by AAT [27, 29]. 3MP then is metabolized to final H_2S through 3MST, due to the vesicular trafficking between mitochondria and peroxisomes [30]. The key enzyme in new D-cysteine pathway, DAO was verified by DAO-selective antagonist I2CA, which suppressed the production of 3MP and H_2S from D-cysteine in concentration-dependent manner, but that from L-cysteine was not influenced by I2CA [26]. This new enzymatic H_2S-producing pathway is integrated into the part of "synthesis" in Figure 1.

The nonenzymatic route of yielding H_2S is the conversion of elemental sulfur and transformation of oxidation of glucose. The nonenzymatic route is presented in vivo, involving phosphogluconate (<10%), glycolysis (>90%), and glutathione (<5%) [3].

In the pathway of H_2S production, there are several important amino acids: homocysteine and D-cysteine. Besides the generation of H_2S pathway, homocysteine is related to folate cycle and methionine cycle [31], the latter of which is participated in methionine, SAM and SAH, as previously stated. As the bridge of the two cycles, homocysteine could be remethylated to methionine by interacting with methylenetetrahydrofolate (methyl-THF) and vitamin B_{12} as cofactor under the synthesis of methionine synthase (MS). Methyl-THF is transformed from methylenetetrahydrofolate (methylene-THF) by methylenetetrahydrofolate reductase (MTHFR). Tetrahydrofolate (THF) is generated by remethylation and converted to methylene-THF, thus integrated the folate cycle. In another cycle, methionine is transformed to S-adenosylmethionine (SAM) by methionine adenosyltransferase (MAT) and then is converted to S-adenosylhomocysteine (SAH), which is subsequently hydrolyzed to homocysteine by glycine N-methyltransferase (GNMT). The cycles of homocysteine can assist researchers to link the studies of upstream and downstream of H_2S, as illustrated in Figure 1. The second interesting amino acid is D-cysteine, because mammalian enzymes generally metabolize L-amino acids, except a little few like D-aspartate and D-serine [29]. Previously, D-cysteine is widely used as a negative control for L-cysteine until discovered as a highly effective H_2S-producing source by Hideo group [26]. As the key enzymes in D-cysteine pathway, DAO is localized in the cerebellum and kidney, together with 3MST [26]. After birth, the level of DAO increased then reached maximal at 8 weeks in mice, while the level of 3MST was quite high at birth but slightly reduced at 8 weeks in mice [27]. Taken together, the level of H_2S through D-cysteine pathway rose after birth and rocketed to maximal at 6 weeks [27]. The level of H_2S generated from L-cysteine was much lower than that from D-cysteine and remains in a certain amount over time. Additionally, the generation of H_2S from D-cysteine is 80 times more efficient than that from L-cysteine in the kidney [26]. Moreover, the generation of H_2S from D-cysteine in the kidney is 7 times higher than that in the cerebellum, which is the region producing highest level of H_2S from D-cysteine than other parts in the brain [26]. Since H_2S has presented significant therapeutic potentials on anti-inflammation, antioxidation, antiapoptosis, antimitochondrial dysfunction, and energy

reservation, the new D-cysteine pathway in the kidney and cerebellum may provide researchers new ideas of finding therapeutic approaches on brain and kidney diseases, such as kidney transplantation.

Cysteine metabolism is engaged in three major routes. Apart from the conversion of H_2S, one path is oxidation of -SH group by cysteine dioxygenase (CDO) to cysteine sulfinate, which is decarboxylated to hypotaurine by cysteine sulfinate decarboxylase (CSD) and then further transformed to taurine by a nonenzymatic reaction or by hypotaurine dehydrogenase (HDH) or which is converted to sulfinyl pyruvate, subsequently to sulfite and further sulfate. Another path from cysteine is synthesis GSH by glutathione synthase (GS) from γ-glutamyl cysteine, which is originated from cysteine and glutamate catalyzed by γ-glutamyl cysteine synthase (GCS). Besides H_2S, cysteine metabolism is integrated in Figure 1 for helping researchers to find out the potential associations.

The concentration of H_2S is not only determined by the rate of formation but also by degradation of H_2S. Dissolved gaseous H_2S is in a pH-dependent equilibrium, with hydrosulfide anions (HS^-) and sulfide anions (S^{2-}), which can be catabolized to any sulfur-containing molecule. Sulfide, via nonenzymatic route, is catabolized to thiosulfate, which could be catalyzed to sulfite by thiosulfate reductase (TSR) in the livers, brains, or kidneys, or by thiosulfate sulfurtransferase (TSST) in the livers, sequentially oxidized to sulfate via sulfite oxidase (SO) by a glutathione- (GSH-) dependent reaction. The last product is excreted in urine [32]. H_2S could be broken down by rhodanese, methylated to CH_3SH, sequestrated by methemoglobin, interacted with superoxide or NO, and scavenged by metallo- or disulfide-containing molecules such as oxidized glutathione [18, 19]. The major routes of degradation of H_2S through nonenzymatic oxidation of sulfide also yield elemental sulfur, polysulfides, dithionate, and polythionates. Among them, polysulfides could be produced through the enzymatic way via 3MST [33–35] and the chemical interaction of H_2S with NO [36]. The whole schematic version of source, synthesis, and metabolism of H_2S is depicted in Figure 1.

4. Donors and Inhibitors of H_2S

4.1. The Donors of H_2S

4.1.1. Sulfide-Containing Salts. Sodium hydrogen sulfide (NaHS) and disodium sulfide (Na_2S) are the common H_2S-releasing chemicals in research of hydrogen sulfide. These sodium salts purchased from pharmaceutical companies are usually aquo compounds, like $NaHS{\cdot}12H_2O$, $Na_2S{\cdot}9H_2O$, or anhydrous forms. The products of sodium hydrogen sulfide and disodium sulfide should be white. The pills with yellow color predicate the anhydrous forms have been converted to hygroscopic blocks and should not be purchased. White sulfide products are likely to have greater purity, but may contain sodium salts of thiosulfate or higher oxidation state sulfur oxyanions [37]. Contamination by trace metal ions may also be important, as these catalyze oxidation processes. The sulfides should therefore be reserved in a vacuum desiccator to minimize oxidation.

The solution of NaHS, at physical pH and room temperature, hydrolyzes to sodium ion, hydrosulfide as following: $NaHS \leftrightarrow Na^+ + HS^-$. Solutions of HS^- are sensitive to oxygen, converting mainly to polysulfides, indicated by the appearance of yellow color. Hence, solutions of fresh prepared NaHS should be clear and put to use immediately. The purity of sulfides could be measured by determining the sulfide content either by titration with bromate, as described in standard analytical chemistry texts, or by UV spectroscopy in the case of sodium hydrogen sulfide, at pH 9, which has an absorption maximum at 230 nm with a molar absorptivity of 7200 l/mol/cm [38].

Considering the unstable chemical properties of NaHS and Na_2S, some researchers introduce another donor of H_2S, calcium sulfide (CaS), which is more steady [39]. CaS can be found as one of the effective components in a traditional herb, named "hepar sulfuris calcareum," usually applied to homeopathic remedy. Oral administration of CaS will be decomposed to more H_2S in stomach acid environment. This review postulates CaS may carry out hypotension, arguing from its catabolism, relationship of calcium supplementation and blood pressure, dosage design, and traditional application of homeopathic remedy on infection.

4.1.2. H_2S-Releasing Molecules. Thioacetamide is an organosulfur compound with the formula C_2H_5NS. This white crystalline solid is soluble in water and serves as a source of sulfide ions in the synthesis of organic and inorganic compounds [40]. For lab safety, thioacetamide is carcinogen class 2B and has hepatotoxicity. Thioacetamide was widely used in classical qualitative inorganic analysis as an in situ source for sulfide ions.

Some research laboratories developed H_2S releasers. Lawesson's reagent is a chemical compound used in organic synthesis as a thiation agent and is also a H_2S releaser. Lawesson's reagent is first synthesized in 1956 during a systematic study of the reactions of arenes with P_4S_{10} [41]. After much time, it is first made popular by Sven-Olov Lawesson for introducing a thiation procedure as an example of a general synthetic method for the conversion of carbonyl to thiocarbonyl groups [41]. 2,4-Bis (4-methoxyphenyl)-1,3,2,4-dithiadiphosphetane 2,4-disulfide, Lawesson's reagent, has a four-membered ring of alternating sulfur and phosphorus atoms. Normally in higher temperatures, the central phosphorus/sulfur four-membered ring can open to form two reactive dithiophosphine ylides (R-PS2), which decompose to release H_2S. As its strong and unpleasant smell, it is best to prepare Lawesson's reagent within a fume hood and treat all glassware used with a decontamination solution before taking the glassware outside the fume hood.

Based on Lawesson's compound, a series of compounds are synthesized. Professor Moore's lab reports that morpholin-4-ium-4-methoxyphenyl (morpholino) phosphinodithioate (GYY4137) releases H_2S slowly both in vitro and in vivo. It has been proved that GYY4137 has vasodilator and antihypertensive activities and a useful H_2S-releasing chemical in the study of biological effects of H_2S [42]. In a later experiment, administration of GYY4137 to lipopolysaccharide- (LPS-) induced rats displays its anti-

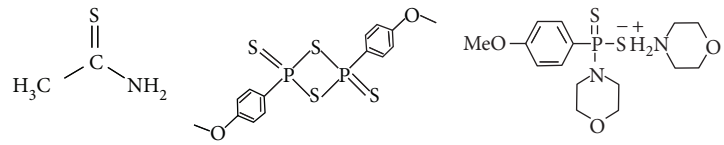

Figure 2: Structures of H_2S-releasing molecules.

inflammatory effect by increasing plasma anti-inflammatory cytokine IL-10 and reducing plasma proinflammatory cytokines (TNF-α, IL-1β, and IL-6) and nitrite/nitrate, C-reactive protein, and L-selectin [43]. Structures of H_2S-releasing molecules are shown in Figure 2.

Considering pharmacological effects and adverse effects of H_2S, some pharmaceutical factories join in working on H_2S donors which are made up of well-established parent compounds and H_2S-releasing moieties. CTG Pharma developed ACS series H_2S-releasing compounds to meet their interests on the aspects of hypertension, metabolic syndrome, thrombosis, and arthritis (http://www.ctgpharma.com). Antibe Therapeutics synthesizes several ATB series H_2S-releasing derivatives for the treatments of inflammatory bowel disease, joint pain, and irritable bowel syndrome (http://www.antibe-therapeutics.com). The compound, IK-1001, from the company Ikaria, is an injectable form of Na_2S, which is pure, pH neutral, and stable. IK-1001 has been used several basic studies and processed into clinical trials. One is a phase I safety trial for assessing pharmacokinetics of intravenous IK-1001 (ClinicalTrials.gov ID: NCT00879645). Another is a phase II efficacy trial which administers IK-1001 in patients undergoing surgery for a coronary artery bypass graft (ClinicalTrials.gov ID: NCT00858936). The effects of some H_2S-releasing compounds are shown in Table 3.

4.1.3. Natural Products Containing Sulfur. Digestion of algae, mushrooms, garlic, and onions is believed to form H_2S by chemical transformation and enzymatic reactions [5]. Structures of natural food-releasing H_2S on digestion are shown in Figures 2 and 3. Nearly all the allium families are sulfur-rich containing. Several publication reports enumerated functional activities of garlic. It exhibits hypolipidemic, antimicrobial, antiplatelet, and procirculatory effects [44–46]. It also demonstrates immune enhancement and provides anticancer, antimutagenic, and antiproliferative that are interesting in chemopreventive interventions. Additionally, aged garlic extract possesses hepatoprotective, neuroprotective, and antioxidative activities [47]. The major sulfur-containing compounds in intact garlic are γ-glutamyl-S-allyl-L-cysteines and S-allyl-L-cysteine sulfoxides (alliin). Both are abundant as sulfur compounds, and alliin is the primary odorless, sulfur-containing amino acid, a precursor of allicin, methiin, (+)-S-(trans-1-propenyl)-L-cysteine sulfoxide, and cycloalliin [48].

S-allylcysteine (SAC), a major transformed product from γ-glutamyl-S-allyl-L-cysteine, is a sulfur amino acid detected in the blood that is verified as both biologically active and bioavailable [49], as seen in Figure 3. SAC has been enumerated in several research investigations mediating protective effects in neural system and cardiovascular system by the inhibition of cell damage in the neuron, heart, and endothelium. In neural system, it is reported that SAC may attenuate Aβ-induced apoptosis [50] and destabilize Alzheimer's Aβ fibrils in vitro [51]. SAC prohibits cerebral amyloid, cerebral inflammation, and tau phosphorylation in Alzheimer's transgenic mouse model harboring Swedish double mutation [52]. In stroke-prone spontaneously hypertensive rats, intaking SAC diminishes incidence of stroke, impairs behavioral syndromes, and abates mortality induced by stroke [53]. SAC inhibits free radical production, lipid peroxidation, and neuronal damage in rat brain ischemia [54]. In cardiovascular system, SAC can help the acute myocardial infarction rats survived by significantly lowering mortality and reducing infarct size [55].

S-propyl-L-cysteine (SPC) and S-propargyl-L-cysteine (SPRC) are structural analogues of SAC, differing only in the propargyl and allyl moiety, respectively, while containing the same cysteine structure as shown in Figure 3. Wang et al., from our lab, reported that SPRC exhibited stronger cardioprotective effects than SAC in reducing mortality, increasing cell viability, reducing heart infarct size, lowering LDH and CK levels and activities, and having antioxidant properties [56]. These data suggest that the propargyl group of SPRC further increases the affinity and/or activity of SPRC towards the enzyme CSE as compared to SAC, where SPRC treatment is shown to have an increased CSE expression and activity to produce H_2S for coping with ischemic damage. This observation suggests that the cardioprotective effects involving the CSE/H_2S pathway were more effective using SPRC compared to SAC. Recently, our lab reported that SPRC showed neuroprotective effects of cognitive impairment and inhibition of neuronal ultrastructure damage in Aβ-induced rats, affords a beneficial action on anti-inflammatory pathways [57]. SPRC has been demonstrated the anticancer effect on gastric cancer at high doses 50 mg/kg/d and 100 mg/kg/d [58]. The effects of SAC and SPRC are shown in Table 3.

4.2. The Inhibitors and Regulators of H_2S. The production of H_2S from cysteine by tissue/cell homogenate is decreased by the presence of inhibitors of H_2S-producing enzymes, which are mainly attributed to CSE and CBS. CSE is also named as cysteine desulfhydrase [59]. The CBS locus is mapped to chromosome 21 (21q22.3) [60]. Several specific blockers for CSE and CBS are currently available. D,L-Propargylglycine (PAG) and b-cyano-L-alanine selectively inhibit CSE [8]. L-Cysteine metabolites, including ammonia, H_2S, and pyruvate, cannot inhibit CSE activity [61]. CBS is inhibited by hydroxylamine (HA) and aminooxyacetate (AOAA) albeit

Table 3: H_2S-releasing compounds used in basic scientific researches.

Compounds	Constituents	Effects on research fields
SAC	S-allylcysteine	Protection on cardiovascular and neural systems
SPRC	S-propargyl-cysteine	Anticancer, anti-inflammation, and antihypoxic/ischemia and impairs cognition and Aβ-induced neuronal damage
GYY4137	Morpholin-4-ium-4-methoxyphenyl (morpholino) phosphinodithioate	Antagonizes endotoxic shock though anti-inflammatory effects
ACS-6	A H_2S-donating sildenafil	Inhibits superoxide formation and $gp91^{phox}$ expression in porcine PAECs
ACS-14	A H_2S-releasing aspirin	Regulates redox imbalance, such as GSH formation, HO-1 promoter activity, and isoprostane suppression
ACS-15	A H_2S-releasing derivative of diclofenac	Arthritis
ACS-67	A H_2S-releasing derivative of latanoprost acid	Glaucoma; retinal ischemia
ATB-284	A H_2S-releasing derivative of trimebutine	Irritable bowel syndrome
ATB-337	A H_2S-releasing derivative of diclofenac	Gastrointestinal damage induced by NSAIDs
ATB-346	A H_2S-releasing derivative of naproxen	Acute and chronic joint pain
ATB-429	A H_2S-releasing derivative of mesalamine	Inflammatory bowel disease and antinociceptive and anti-inflammatory effects
IK 1001	Calcium-cross-linked alginate polymer	Suspended animation, multiple hypoxic/ischemic conditions, cardiac remodeling, and congestive heart failure

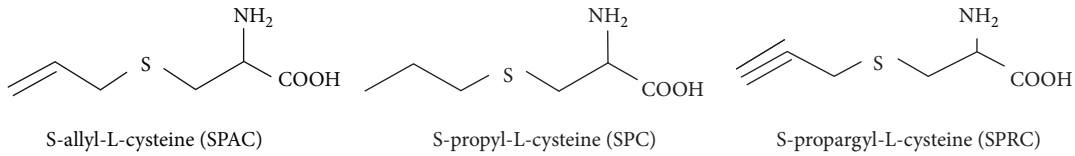

Figure 3: The chemical structures of SAC, SPC, and SPRC.

these chemicals are not selective inhibitors of CBS [2]. The relationships between H_2S-producing enzymes and their inhibitors are summarized in Table 2.

The currently known regulations of H_2S-producing enzymes are glutamate and its receptors, S-adenosylmethionine (SAM), hormones, and other gasotransmitters—NO and CO. In the brain, electrical stimulation and excitatory neurotransmitter, glutamate, rapidly increase CBS activity in Ca^{2+}/calmodulin-dependent manner [62]. Both α-amino-3-hydroxy-5-methyl-4-isoxazolepropionate (AMPA) glutamate receptors and N-methyl-D-aspartate (NMDA) are involved in this effect. SAM is an intermediate product of methionine metabolism and a major donor of methyl groups. This allosteric regulator can activate CBS by approximately twofold [2]. Sex hormones seem to regulate brain H_2S, since CBS activity and H_2S level are higher in male than in female mice and castration of male mice decreases H_2S formation [16]. Sodium nitroprusside, a nitric oxide donor, increases the activity of brain CBS *in vitro*; however, this effect is NO-independent and results from chemical modification of the enzyme's cysteine groups [63]. In contrast, NO itself may bind to and inactivate the CBS. Interestingly, CO is a much more potent CBS inhibitor than NO and it is suggested that CBS may be one of the molecular targets for CO in the brain [64, 65]. In homogenates of the rat aorta, NO donors acutely increase CSE-dependent H_2S generation in a cGMP-dependent manner [21]. Moreover, prolonged incubation of cultured vascular smooth muscle cells in the presence of NO donors increases CSE mRNA and protein levels [8]. The physiological significance of NO in the regulation of H_2S production is also supported by the observation that circulating H_2S level as well as CSE gene expression and enzymatic activity in the cardiovascular system are reduced in rats chronically treated with NOS inhibitor. Thus, NO is probably a physiological regulator of H_2S production in the cardiovascular system. Recently, the inhibitors of 3MST were selected by high-throughput screening (HTS) of a large chemical library (174,118 compounds) with the H_2S-selective fluorescent probe, HSip-1, which discovered compound 3 presented very high selectivity for 3MST over other H_2S/sulfane sulfur-producing enzymes and rhodanese [66]. This study provides these compounds as useful chemical tools for investigating the physiological roles of 3MST.

5. H_2S Measurements

5.1. Spectrophotometric Method. The principle of spectrophotometric method of H_2S depends on the formation of methylene blue. H_2S is chemiadsorbed by zinc acetate and transformed into stable zinc sulfide. The sulfide is recovered by extraction with water. In contact with an oxidizing agent such as ferric chloride in a strongly acid solution, it reacts with the N,N-dimethyl-p-phenylenediammonium

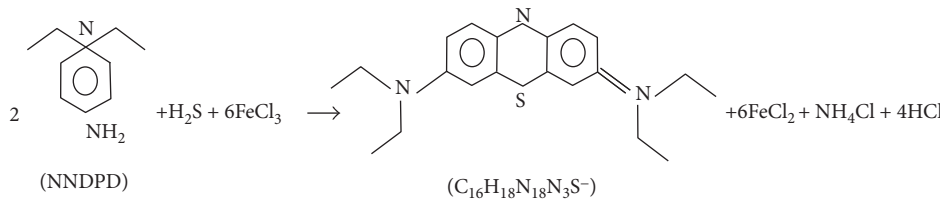

Figure 4: The equation of spectrophotometric method of H_2S.

(NNDPD) ion to yield methylene blue ($C_{16}H_{18}N_3SCl$). The equation is shown in Figure 4:

The methylene blue method has been designed to a different protocol. A common method is adding NNDPD and ferric chloride to the plasma or homogenized tissue and then developing color and colorimetric estimating immediately. Owing to the volatile character of H_2S, researchers modify the protocol, like using a filter paper to augment the contact surface and prolong the contact time [67, 68]. Based on published papers and previous experience, our lab revised the assay for H_2S by placing a sample in an airtight vessel with a central tube. The central tube contains a filter paper wick saturated with zinc acetate. The purpose of the filter paper wick is for trapping H_2S to zinc sulfide. The reactions are initiated by mixing of strong acid with the sample, which sulfide is driven out and adsorbed onto the wick. The driving time is usually 30–120 minutes which is modified based on lab condition and optimization in the sorts of samples. Reactions are stopped by injecting 0.5% trichloroacetic acid (TCA). After gas evolution and wick absorption, the sulfide in the central tube reacts with NNDPD in present of Fe^{2+} ion. The absorbance of the resulting solution at 670 nm was measured with a microplate reader. This method was improved by Ishigami et al. through the release of H_2S from acid-labile sulfur using acids as an artifact, which leads H_2S absorbed immediately and stored as bound sulfur [24].

This colorimetric method is not only widely used on the determination of H_2S on serum in animal experiment but also widely used on the activity of CSE/CBS enzyme on tissues or cells. The concentrations of H_2S are reflected on the different shades of color of methylene blue and calculated by the plotting H_2S standard curve.

Two points need to be made. Firstly, most researchers' assay H_2S using the spectrophotometric assay involves acidifying zinc acetate-treated (to "trap" free H_2S) biological samples in the presence of a dye and observing a color change. This assay actually measures total sulfide and not the gas H_2S. Secondly, H_2S is either broken down rapidly in the body by enzymes, sequestered by binding to hemoglobin, or can react chemically with a number of species abundant in tissues, including superoxide radical [69], hydrogen peroxide [67], peroxynitrite [70], and/or hypochlorite [71]. All in all, making reasonably accurate measurements of such an evanescent and reactive gas in biological tissues is difficult. Indeed, the chemical nature of gases such as H_2S, NO, and CO might render it nonsensical even to try and measure them in body fluids or tissues.

5.2. Sulfide Ion-Selective Electrode. A sulfide ion-selective electrode (SISE) is immersed in an aqueous solution containing the ions to be measured, together with a separate, external reference electrode. The electrochemical circuit is completed by connecting the electrodes to a sensitive millivoltmeter using special low-noise cables and connectors. A potential difference is developed across the SISE membrane when the sulfide ions diffuse through from the high concentration side to the lower concentration side.

At equilibrium, the membrane potential is mainly dependent on the concentration of the target ion outside the membrane and is described by the Nernst equation. Briefly, the measured voltage is proportional to the logarithm of the concentration, and the sensitivity of the electrode is expressed as the electrode slope in millivolts per decade of concentration. Thus, the electrodes can be calibrated by measuring the voltage in sulfide standard solution. Testing samples can then be determined by measuring the voltage and plotting the result on the calibration graph. The use of sulfide ion-selective electrode suffers from precipitation of metal sulfide, for example, sliver sulfide (Ag_2S) from the filling solution on the electrodes.

Reproducibility is limited by factors such as temperature fluctuations, drift, and noise. The electrode can be used at temperatures from 0 to 100°C and only used intermittently at temperatures above 80°C. Interfering ions, like mercury, must be absent from all sulfide sample. In aqueous solution, H_2S is dissolved into HS^- and S^{2-}. In acid solution, sulfide is chiefly in the form of H_2S, while in the intermediate pH range (up to approximately pH 12), almost all the sulfide is in the form HS^-. Only in very basic does the sulfide exist primarily as free ion (S^{2-}). The SISE from Thermo Scientific supplies sulfide antioxidant buffer could maintain a fixed level of H_2S.

Nevertheless, the alkaline condition of antioxidant buffer is regarded as an influencing factor to SISE measurements in plasma. Initially, mixing samples to antioxidant buffer is reported to generate protein desulfuration and artificially increased sulfide values [72]. It is also observed that placing 5% bovine serum albumin into antioxidant buffer leads to a surging reading of total sulfide measured by SISE in the first 20 minutes and following slow accumulation in 3 hours [73].

5.3. Fluorescent Probe Assays. Currently, there are more and more labs that choose to use fluorescent probes to assay the

concentrations of real-time H_2S, sensitively, selectively, and biologically compatible. There are 3 types of fluorescent probes for H_2S detections: reduction-based, nucleophilic-based, and metal sulfide-based.

Reaction-based fluorescent probes for H_2S detection are designed based on the reducing ability of H_2S [74]. The firstly developed fluorescent probes by Lippert and colleagues were probes SF1 and SF2 based on the H_2S-mediated reduction from an aryl azide to an aryl amine [75]. After adding NaHS for 1 hour, probes SF1 and SF2 detected 7- and 9-fold fluorescent increase, respectively. Probes SF4–7 were improved by the same lab with enhanced sensitivity and cellular retention [76]. The group of Peng and colleagues simultaneously reported another fluorescent probe DNS-Az through the reduction of a sulfonyl azide to a sulfonamide with faster kinetics than aryl azide reduction but less adaption [77]. Later, various fluorophores were developed for H_2S measurement with different colors and targeting specific organelles. Fluorescent probes SHS-M1 and SHS-M2 were reported by Bae et al. to detect mitochondrial moiety by incorporating triphenylphosphonium group [78]. SulpHensor by Yang et al. was designed to detect lysosome moiety due to the morpholine group [79]. AzMC was reported by Thorson et al. to screen CBS based on coumarin [80]. Other functional groups that can be reduced by H_2S were utilized in the design of fluorescent probes, like nitro group. Montoya and Pluth reported the fluorescent probe HSN-1, which incorporates a nitro group into the 1,8-naphthalimide scaffold, but with greater thiol cross-reactivity than azide probes [81]. This weakness was attenuated by Wang et al. that increased electron-rich aromatic system on the nitro-based probe [82]. The concept of H_2S-mediated reduction was extended to other fluorophore scaffolds by several laboratories [83–85].

Nucleophilic-based fluorescent probe for H_2S detection is designed based on the strong nucleophilic HS^- hydrolyzed from H_2S at physiological pH (pH = 7.4) [86]. Qian et al. used this concept to develop fluorescent probes, SFP-1 and SFP-2, which allowed fluorescence switching via HS^- addition to aldehyde and underwent an intermolecular Michael addition to unsaturated acrylate ester to form a thioacetal, producing stable tetrahydrothiophene with strong fluorescence [87]. Qian et al. designed the probes with an aldehyde group ortho to an α,β-unsaturated acrylate methyl ester on an aryl ring, which trapped H_2S and modulated a fluorescence response through decreased photoinduced electron transfer (PET) quenching of the product [87]. Disulfide bond cleaved by H_2S was utilized by Liu et al. and Peng et al. to develop WSP1–5, which persulfide group, like 2-thiopyridine, intramolecular nucleophilic attacked on the ester moiety to release great fluorophore [88, 89]. 50–500 μM H_2S in bovine plasma and 250 μM H_2S in cells could be detected by this probe. Reversible nucleophilic addition was exploited by Chen et al., as CouMC, to track real-time H_2S fluxes due to fast and potentially reversible fluorescence [90].

Metal sulfide-based fluorescent probe for H_2S detection is based on the phenomenon that heavy metal ions such as Fe^{3+} and Cu^{2+} quench the fluorescence of a nearby fluorophore [91]. Zinc sulfide complex was utilized to design a selective fluorescent probe of H_2S by Galardon et al. by releasing a coumarin dye [92]. Choi chose copper sulfide precipitation to design the fluorescent sulfide sensor [93]. Later, Sasakura et al. developed it to HSip-1, which possessed a cyclen macrocycle with fluorescein and binds Cu^{2+} to release unbound cyclen-AF, displaying greater fluorescence [94]. The measuring range of this probe for sulfide could be 10–100 μM. Hou et al. improved the copper-containing probe to a lower detection limit of 1.7 μM [95]. Another strength of metal precipitation-based probes is that they respond to turn on within seconds, allowing the real-time H_2S detection [96]. Researchers may choose one of these fluorescent probes depended on their facilities, reagents, targeted organelles, and sensitivity ranges.

5.4. Other Analyzing Methods. Carbon nanotube (CNT) was introduced by Wu et al. for measuring low-concentration and nanoquantity H_2S [97, 98]. One of the benefits of unfuctionalized CNT in analyzing H_2S is due to the special bond with H_2S, but other proteins kept in serum. H_2S concentrations are reflected by the intensity of the fluorescence of the unfuctionalized CNT, due to the two values in a linear relationship. The lowest H_2S concentration that can be tested is 20 μM and smallest quantity of H_2S is 0.5 μg. The series of experiments are trying to establish a new sensor to measure micro- or nanoquantity H_2S, comprising unfuctionalized CNT as a transducer and LSM fluorescence as a signal acquisition modality.

Polarography is a voltammetric measurement which makes use of the dropping mercury electrode or the static mercury drop electrode. The value of diffusion current depends on the speed of electroactive material (samples) diffusing to dropping mercury electrode. This principle contributes to the measurement of the concentration of analytes. Polarography is well known for the application of quantitative measurements of O_2 (polarographic oxygen sensor, POS) and NO (polarographic nitric oxide sensor, PNOS). By recent years of the appreciation of the third gasotransmitter, H_2S, several analytical methods are utilized, including polarography. A novel polarographic hydrogen sulfide sensor (PHSS) has been developed for the study of H_2S-producing rates and consumption in mammalian tissues, with resolution of 10 nM [99]. The polarographic sulfide sensor is also applied to the investigation of kinetics of sulfide metabolism in organisms living in sulfide-rich environment [100]. PHSS permits direct and simultaneous measurement of H_2S gas in biological fluids without sample preparation. PHSS has provided an alternative method for sulfide measurement.

Gas chromatography is a recent method described by Levitt et al. as a unique chemiluminescence-based technique to measure free and acid-labile H_2S in multiple tissues from mouse [101]. The tissues were first submerged in 50 mM glycine-NaOH buffer (pH 9.3) and homogenized. The homogenates were then transferred to syringes, which were sealed and flushed with N_2. The homogenate in alkaline extraction turns to acidification to pH 5.8 by adding sodium hydrogen phosphate solution (pH 5.5). After vigorous mixture, the gas space was removed to gas chromatography to analyze free H_2S concentration. Next, adding 50% trichloroacetic acid to the syringe, the gas was collected to test the

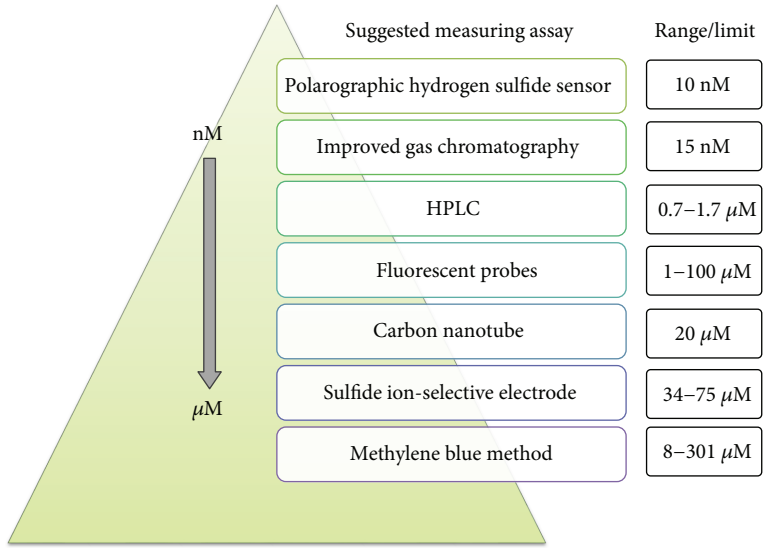

Figure 5: The ranges or limits of H_2S measurements.

acid-labile H_2S concentration. The flow rate of N_2 was 25 ml/min. The concentration of H_2S was calculated by the plotting H_2S standard curve.

High-performance liquid chromatography (HPLC) is used to separate the sulfide mixture. Togawa et al. reported that using monobromobimane (MBB) with dithiothreitol (DTT) reacted with bound sulfide to produce sulfide dibimane, which is separated from MBB by HPLC and detected by its fluorescent probes [102]. Recently, MBB assay without DTT was used to measure available H_2S in rat blood [103] and mouse plasma [104]. The ranges or limits of H_2S measurements are in Figure 5.

6. H_2S in Inflammation

Inflammation is an immune response to an injury or harmful stimuli, in order to self-protect the body from avoiding pathogen assaults and initiating healing process. However, the adaptive immune system fails to counter invading agents will turn to target host tissues, making deeply more serious damage. H_2S regulating inflammation and injury was initially contradictory, but in recent years, more studies supported that H_2S inhibited the process of inflammation, except at high concentration [105]. This mediator possibly exerts its anti-inflammatory effects through reduction of leukocyte-endothelial cell adhesion [106], action on ATP-sensitive K^+ channels [107], scavenging of toxic free radicals [108], elevation of cyclic AMP and/or cyclic GMP [70, 71], and inhibition of nuclear factor-κB (NF-κB) and proinflammatory cytokines (e.g., COX-2 [109], iNOS [110], and interleukin-(IL-) 1β, IL-6 [111]).

Various diseases could be found inflammatory response, like atherosclerosis, ischemia-reperfusion, and colitis. Contributing to anti-inflammatory molecular mechanisms of this novel gasotransmitter, it is not surprising that H_2S may participate in the process of resolution of a variety of inflammatory diseases. In atherosclerosis, H_2S exerts its potent inhibitor of leukocyte adherence to vascular endothelium [112]. Meanwhile, the generation of reactive oxygen species (ROS), activation of NF-κB, increased expressions of cell adhesion cytokines, and induction of apoptosis, which were all regarded as the key promoters of pathology, were all found suppressed by H_2S [112, 113]. These mechanisms of action described for H_2S may explain that H_2S can diminish the plaques in arteries and attenuate the atherosclerotic injury, suggesting the character of anti-inflammation of H_2S is a benefit for the vascular protection.

Ischemia-reperfusion (I/R) is identified as an acute endogenous inflammatory response that characterizes release of toxic free radicals, leucocyte-endothelial cell adhesion, and platelet-leucocyte aggregation [114]. In porcine myocardial I/R model, therapeutic sulfide improved myocardial function and diminished infarct size though decreased levels of inflammatory cytokines (IL-6, IL-8, and TNF-α), reduced left ventricular pressure, and improved coronary microvascular reactivity [115]. A similar tissue protection of H_2S was also found in hepatic I/R injury by inhibition of inflammation (lipid peroxidation, IL-10, ICAM-1, and TNF-α) and apoptosis (caspase-3, Fas, and Fas ligand) [116]. Another study suggested that the cardioprotective effects of H_2S may be mediated by opening the mitochondrial K_{ATP} channel and second window of protection caused by endotoxin [117].

Colitis is a one form of gastrointestinal inflammation and ulceration. Administration of H_2S-generating agents or precursor for H_2S synthesis, L-cysteine, has been shown to significantly accelerate ulcer healing [118, 119]. This ability of H_2S to enhance gastrointestinal resistance attracts investigators to exploit novel treatments of gastrointestinal injury and inflammation, like H_2S-releasing derivative of NSAIDs to reduce the adverse drug reaction of NASIDs, retarding gastrointestinal ulcer healing [120]. Evidence of H_2S in resolution of colitis in rats or mice studies showed that administration of H_2S donor significantly inhibited the severity of colitis with marked reduction of granulocyte infiltration into colonic tissue. In inflamed colon, H_2S production was highly increased via CSE, CBS, or other enzymatic

pathways [121, 122]. Once H_2S synthesis was inhibited, the colitis tended to worsen the inflammation with thickening of the smooth muscle, perforation of bowel wall, and even death [110].

7. H_2S in Redox Status

7.1. H_2S Direct Effects on Toxic Free Radicals. In a weak acid, H_2S dissociates in equilibrium with hydrosulfide anion (HS^-) and sulfide anion (S^{2-}). Under physiological conditions, the amounts of H_2S and HS^- are early equal within the cell, whereas extracellular fluid and plasma exist approximately the ratio of 20% H_2S, 80% HS^-, and 0% S^{2-}. HS^- is a potent one-electron reductant that eliminates free radicals by donating single electron. Hydrogen disulfide (H_2S_2), a kind of hydrogen polysulfide (H_2Sn), is the production of oxidation of HS^- by two-electron oxidants, like hypochlorous acid [123] and hydrogen peroxide [124]. Additionally, the chemical interaction between H_2S and NO also produced H_2Sn by activating transient receptor potential ankyrin 1 (TRPA1) channels [36]. H_2S_2, a highly reactive oxidizing chemical, generates H_2S by reacting with thiol [125] or disproportionation [123, 126]. H_2S_2 and H_2S_3 were reported to generate redox regulators Cys-SSH and GSSH via 3MST in the brain of wild-type mice but not in those of 3MST-KO mice [34, 35, 127, 128].

H_2S is considered as an endogenous reducing agent which is produced in response to oxidative stress [129, 130]. Evidence showed that H_2S is a highly reactive molecule and may easily react with other compounds, especially with reactive oxygen and nitrogen species. H_2S reacts with at least four different ROS: superoxide radical anion [69], hydrogen peroxide [67], peroxynitrite [70], and hypochlorite [71]. All these compounds are highly reactive, and their reactions with H_2S result in the protection of proteins and lipids against RNS/RNS-mediated damage [70, 71] and myocardial injury induced by homocysteine in rats [131].

7.2. H_2S Protects Mitochondria against Oxidative Stress. Mitochondrial injury is an important source of reactive oxygen species (ROS), which is involved in a range of pathologies, such as ischemia-reperfusion, atherosclerosis, and toxin exposure [132]. Under oxidative stress conditions, mitochondria will show unstable mitochondrial membrane potential ($\Delta\Psi m$), redox transitions, and negative changes in the mitochondrial permeability transition (MPT) pore and the inner membrane anion channel (IMAC) [133]. Our lab found that H_2S can reduce the H_2O_2-induced injury in HUVECs via increasing ATP production, saving mitochondrial ultrastructure, stabilizing mitochondrial membrane intact, decreasing ROS and MDA, and rising antioxidants. The same situation was also unveiled in H_2O_2-stimulated isolated rabbit aorta that H_2S ameliorated mitochondrial dysfunction through improving O_2 consumption and ATP production, protecting mitochondrial respiration chain complexes activities and matrix enzymes, decreasing mitochondrial membrane permeability, and inhibiting mitochondrial ROS levels. These effects of H_2S indicated that the antioxidative ability of H_2S is through increasing antioxidants and prohibiting ROS levels and also preserving mitochondrial function to reduce the production of toxic free radicals.

8. H_2S in Cardiovascular System

8.1. Hypertension. Before identified as the third gasotransmitter, H_2S has been speculated to regulate an array of physiological processes in regulating cardiovascular functions, distinctive from its toxicological effect. A great number of studies have been carried on investigation of the modulating of blood pressure by exogenous and endogenous H_2S. Early at the end of the last century, it is first reported that H_2S relaxes the contracted smooth muscles (SM) induced by 1 μM norepinephrine in rat thoracic aorta and portal vein [134]. The relaxations in these tested aortas and veins present a NaHS dose-dependent manner, but the potency of relaxation by exogenous H_2S in the thoracic aorta is less than the portal vein, even by 10^{-3} M NaHS, which are around 25% and 90%, respectively. The data also showed that the relaxation effects of H_2S and NO can be enhanced by each other. 30 μM NaHS can augment the loosening effect of NO by up to 13-fold. Thus, endogenous cysteine and glutathione do not have synergistic effect with NO. Subsequently, the vasorelaxant effect of H_2S was found *in vivo* of SD rats, ex vivo of aortic rings, and *in vitro* at rat aortic smooth muscle cells [15], which was a literature that first demonstrated the underlying mechanism of vasorelaxation, a consequence of opening K_{ATP}^+ channels. Interestingly, it has been found that H_2S induces endothelium-dependent vasorelaxation with many common mechanistic traits of hyperpolarizing factor [135]. CSE knockout mice lacked the methacholine-induced endothelium-dependent vasorelaxation in mesenteric arteries and showed higher resting membrane potential of SMCs, while hyperpolarization of SMCs induced by methacholine was observed in endothelium-intact mesenteric arteries at wild-type mice [136]. Administration of exogenous H_2S hyperpolarized both SMCs and vascular endothelial cells in wild-type and CSE knockout mice [136]. Removal of functional endothelium attenuated vasorelaxation of rat aorta [137] and rat mesenteric artery [138]. It appears that vasorelaxation of H_2S is induced on both SMCs and endothelial cells, instead of previous research discussions mainly focusing on SMCs.

A multitude of H_2S-induced vasodilation studies have investigated the activation of K_{ATP}^+ channels. One possible mechanism involved in the activation of K_{ATP}^+ channels by H_2S was opening K_{ATP}^+ channels and increasing K^+ currents resulted in hyperpolarizing membrane of smooth muscle cells [139]. The explanation of the opening of K_{ATP}^+ channels by H_2S was that cysteines on K_{ATP}^+ channels of SMCs were S-sulfhydrated, leading to hyperpolarization [140]. Cys43 of the inwardly rectifier (Kir) potassium channels subunit Kir 6.1 was sulfhydrated by NaHS, eliciting the binding to phospholipid phosphatidylinositol (4,5)-bisphosphate (PIP2) together with decreased association of ATP [140]. Additionally, the vasodilation effect of H_2S was inhibited significantly by either using a calcium-free bath solution or with the normal bath solution, but in the presence of nifedipine, a voltage-gated Ca^{2+} channel inhibitor, on aortic rings [8],

indicates that the vascular effects of H_2S are also likely mediated by the attenuation of intracellular inward Ca^{2+} currents. Not only H_2S hyperpolarizes ion channels on blood vessels to possess the relaxant effects but also endothelium generates H_2S by increasing catalytic activity of CSE through calcium-calmodulin, indicating that the H_2S formation may be involved in vascular activation to reduce blood pressure [141]. Moreover, H_2S exerts cardioprotective effect by relieving vascular structural remodeling observed during hypertension, including suppression of VSMC proliferation via the activation of cardiac extracellular signal-regulated kinase (ERK) and/or Akt pathway [137] and attenuation of collagen accumulation through reduction of collagen type I level, [3H] thymidine and [3H] proline incorporation, and [3H] hydroxyproline secretion in the SHRs [142] and through mitrogen-activated protein kinase (MAPK) pathway [143]. As endothelium-derived relaxing factors (EDRF), H_2S and NO have "cross-talk" on the calcium mobilization [144], activation of eNOS [145–148], PI3K/Akt signaling [145], soluble guanylate cyclase (sGC) [145, 149], and cGMP [150, 151]. However, whether NO is directly involved in the antihypertensive effects of H_2S has to be further investigated by a NO deficiency model induced to hypertension and treated by sulfide-rich compounds.

8.2. Atherosclerosis. Atherosclerosis is a chronic and slowly progressive cardiovascular disease that affects arterial blood vessels by thickening and hardening as consequences of the high plasma cholesterol concentrations, especially cholesterol in low-density lipoprotein [152]. Cholesterol deposition, lipid oxidization, cell adhesion, vascular inflammation, foam cell accumulation, smooth muscle cell migration, and plaque calcification are involved in different stages of the pathological process [153]. The cumulative plaques consequentially narrow the arterial lumen and restrict blood supply. Severe atherosclerotic lesions are the high risk factors of ischemic diseases such as stroke and heart attack [154].

Recent years, H_2S draws attentions from researchers by its cardiovascular protective effects, while there are not many studies on its effects on the progress of atherosclerosis. Fortunately, increasing evidence has indicated that H_2S plays a potentially significant role in a number of biological processes and potential cardiovascular protections, which suggest that H_2S may contribute to the inhibition of pathogenesis of atherosclerosis. First, H_2S shows inhibitory effects on the development of atherogenesis, such as oxidative stress, modificated oxidation of LDL, cell adhesion, and calcification. In vascular smooth muscle cells (SMCs), low levels of NaHS (30 or 50 μM), a donor of H_2S, decrease toxic reactive oxygen species, including $H_2O_2^-$, $ONOO^-$, and O_2^- [155]. At the same time, NaHS also enhances the functions of antioxidative enzymes. In addition, H_2S inhibits atherogenic modification of LDL-induced HOCl in vitro (such as oxidized LDL, shortened as oxLDL). As a potent atherogenic agent, oxLDL particle is an important product of atherogenic oxidation that stimulates endothelial cells to express various adhesion molecules for consequent inflammatory reactions and formation of foam cells. Therefore, inhibition of oxLDL by potential treatments of H_2S implies that H_2S may interfere atherosclerotic progress [156]. Furthermore, H_2S attenuates atherosclerotic lesions by reducing cell adhesion molecules, such as ICAM-1, involving the NF-κB pathway *in vivo* and *in vitro* [112]. Adhesion molecules are the significant causes to promote bindings between monocytes and T lymphocytes to endothelial cells, which will lead to sequential inflammation and advanced process. Reduced expressions of adhesion molecules prohibit monocytes migration and later inflammation, which may also benefit in ameliorate atherosclerotic lesions. Lastly, calcification, presented in the advanced process of atherosclerosis, is a potent factor of plaque stability. There was a study that found the link between H_2S and plaque calcification [157]. In calcified arteries, H_2S level, CSE activity, and CSE mRNA were downregulated, while after administration of H_2S, a dose response was shown in the decreased vascular calcium content, Ca^{2+} accumulation, alkaline phosphatase (ALP) activity, and aortic osteopontin (OPN) mRNA. These changes speculated the effect on atherogenesis of H_2S might be induced by suppressing vessel calcification.

Second, H_2S possesses vascular protective capacities from inhibition of proliferation of vascular cells, such as intima and SMCs, and angiosteosis. It has been demonstrated that H_2S suppresses neointima hyperplasia on rat carotid after balloon injury [158]. In another balloon-injured artery experiment, NaHS (30 μmol/kg bodyweight) enhances methacholine-induced vasorelaxation and significantly ameliorates neointimal lesion formation. Additionally, evidences are also pointing to the fact that H_2S relieves apoptosis and proliferation of SMCs [159]. SMCs migrate from the medial layer into the subendothelial space where they may proliferate, ingest modified lipoproteins, secrete extracellular matrix proteins, and contribute to lesion development. The suppression of proliferation of SMCs by H_2S can restrict atherosclerotic damages. Moreover, H_2S prevents the process of angiosteosis [143, 160, 161]. Angiosteosis, ossification or calcification of a vessel, is an advanced change in the pathology of atherosclerosis. Its development leads to the narrowing of the caliber of an artery, stimulates thrombosis, or even worse generates the abruption of unstable plaques. Vascular calcifications induced by vitamin D_3 and nicotine in rats are ameliorated by exogenous H_2S. The responses after administration of H_2S show the decreased calcium concentration in vessels, reduced expressions of angiosteosis, and accompanied acidic phosphatese and osteopontin.

Third, H_2S alleviates the vascular damage induced by an established risk factor, for instance, homocysteine. Homocysteine is an amino acid, biosynthesized from methionine and converted into cysteine and sulfur. Augmented levels of homocysteine in plasma, termed hyperhomocysteinemia, are considered as a high risk factor of atherogenesis. Early plaque development in apolipoprotein E-deficient mice, a knockout genetic model of atherosclerosis by 8 weeks high-cholesterol diet intake, could be enhanced by dietary supplementation with methionine or homocysteine [162]. A research shows that low concentrations of NaHS (30 or 50 μM), a H_2S donor, potentiates cell viability of rat aortic

SMCs by abating cytotoxicity and reactive oxygen species stimulated by hyperhomocysteinemia [163].

Although atherosclerosis is a chronic, systemic disease with multifactors involved in its initiation and progression, previous studies have shown that the specific characteristics and functions of H_2S may contribute to the inhibition of atherogenesis. The multiaspect recognitions of cardiovascular protective effects of H_2S provide a new avenue of antagonism towards this complicated cardiovascular disease.

8.3. Myocardial Injury. Plenty of work have documented that the CSE/H_2S pathway participates in the regulation of cardioprotective effects [155]. Administration of exogenous H_2S reduces "infarct-like" myocardial necrosis induced by isoproterenol in the rat [67, 164, 165]. This protection is accompanied with the reduced concentrations of H_2S in myocardium and plasma, decreased CSE protein activity, and upregulated CSE gene expression in myocardium [67]. NaHS attenuates the myocardial ischemic injury by evidences of reduced mortality and shrunk infarct size in vivo of rat and recovered SMC viability induced by hypoxia [67]. Further study discovers that 14 μmol/kg/d NaHS improves ECG and blood pressure and diminishes infarct size, as well as the greater survivin expression [165].

Oxidative stress injury is an important mechanism of myocardial injury. Direct or indirect antioxidative effects will lead to cardioprotection from myocardial ischemia. The data in above literature reveal that NaHS may antagonize MDA production *in vitro* of myocytes by oxygen free radicals or directly react with hydrogen peroxide and superoxide anions [166]. Another experiment also proves that H_2S provided profound protection against ischemic injury by significant decreases in infarct size, circulating troponin I levels, and oxidative stress [67]. The protections by Na_2S in early and late preconditioning are all though stimulating the increased antioxidants, which could be itemized to the elevated Nrf2 in early stage and increased expressions of heme oxygenase-1 and thioredoxin 1 in late preconditioning. The antioxidant effect of H_2S is also embodied in the preservation of mitochondrial functions and ultrastructure by Na_2S after myocardial ischemia-reperfusion (MI-R) injury [167]. These observations have been recently confirmed by cysteine analogues, SAC, SPC, and SPRC [168, 169]. The activities of superoxide dismutase (SOD), catalase (CAT), glutathione peroxidase (GPx), and glutathione redox status are preserved by cysteine analogues. The mitochondrial ultrastructure of cysteine analogues treatments appeared more normal than MI vehicle group. These evidences demonstrate the CSE/H_2S pathway is involved in reducing the deleterious effects of oxidative stress.

Furthermore, recent discoveries indicate the observed protection of H_2S is related to regulate leukocyte adhesion and leukocyte-mediated inflammation, increase anti-inflammatory cytokines, and reduce several proinflammatory cytokines [169]. The anti-inflammatory effect of H_2S is reflected in amplification of heat shock protein (HSP) 70, HSP 90, and cyclooxygenase-2 [115] and reduction of MPO activity [167], nuclear factor-κB (NF-κB), and interleukin (IL)-6, IL-8, and tumor necrosis factor-alpha (TNF-α) [167]. The cardioprotection of H_2S is associated with inhibition of cardiomyocyte apoptosis after myocardial injury. H_2S amplifies antiapoptosis proteins (Bcl-2, Bcl-xL) and inactivates proapoptogen (Bad) [115]. It is also suggested that H_2S ameliorates cardiomyocyte apoptosis after MI-R injury *in vitro* and *in vivo*, significant abatement of caspase-3 activity, and declining of the number of TUNEL positive nuclei, respectively [167].

Finally, multiple studies have elucidated a protective effect of K_{ATP} channel activators in myocardial MI-R injury [168]. By virtue of the relaxant effect of H_2S as an opener of K_{ATP} channels, it is easy to hypothesize that H_2S protects myocardial cells against ischemic injury. In the isolated Langendorff-perfused rat hearts, administrations of NaHS result in a dose-dependent limitation of infarct size induced by left coronary artery ligation and reperfusion, while this protective effect is abolished by K_{ATP} channel blockers [170]. There is a report that H_2S preconditioning presents cardioprotective effects against ischemia though signaling pathways of K_{ATP}/PKC/ERK1/2 and PI3K/Akt [171]. Researchers may investigate additional molecular mechanisms to explain this ischemic injury in hearts not limited on stereotyped mechanisms, such as oxidative stress or potassium channels.

8.4. H_2S in Angiogenesis. The term "angiogenesis" is referred to the physiological process of blood vessel growth or vessel sprouting [172]. Blood vessel growth can benefit for delivering nutrients and waste and supplying immune surveillance [172]. Insufficient vessel growth has been linked to stroke, myocardial infarction, ulcerative disorders, hair loss, preeclampsia, and neurodegeneration [173]. Embryonic development, menstrual cycle, hypoxia, inflammation, and tumor will stimulate angiogenic signals, such as vascular endothelial growth factor (VEGF), angiopoietin-2 (ANG-2), and fibroblast growth factors (FGFs) to sprout new endothelial cells and pericytes or vascular smooth muscle cells [173, 174].

H_2S has been displayed as an important regulator of angiogenesis through promoting endothelial proliferation, migration, and formations of tub-like structure and networks. Administration of H_2S increased proliferation and migration in bEnd3 microvascular endothelial cells and recovered microvessel sprouting in rat aortic rings of silencing CSE [145]. We discovered that SPRC, as a H_2S donor, enhanced HUVEC cell proliferation, adhesion, migration, and tube formation as well as the same effects in the rat aortic ring and Matrigel plug models [175]. In vivo studies of mouse hindlimb ischemia and rat myocardial ischemia provided additional evidence that SPRC ameliorated ischemic insults through augmenting angiogenesis [175]. Considering H_2S and NO share angiogenic effects, we synthesized H_2S-NO hybrid molecule, named ZYZ-803, to slowly release H_2S and NO [176]. As expected, ZYZ-803 presented significantly greater potency of angiogenesis than H_2S and NO alone [176]. Besides CSE-mediated effects, some studies showed that RNAi-mediated silencing CBS leads to a 40–50% decrease in HUVEC proliferation and 30% decrease in tube length on Matrigel [177]. Using AOAA, the CBS inhibitor developed a dose-dependent decrease of HUVEC proliferation

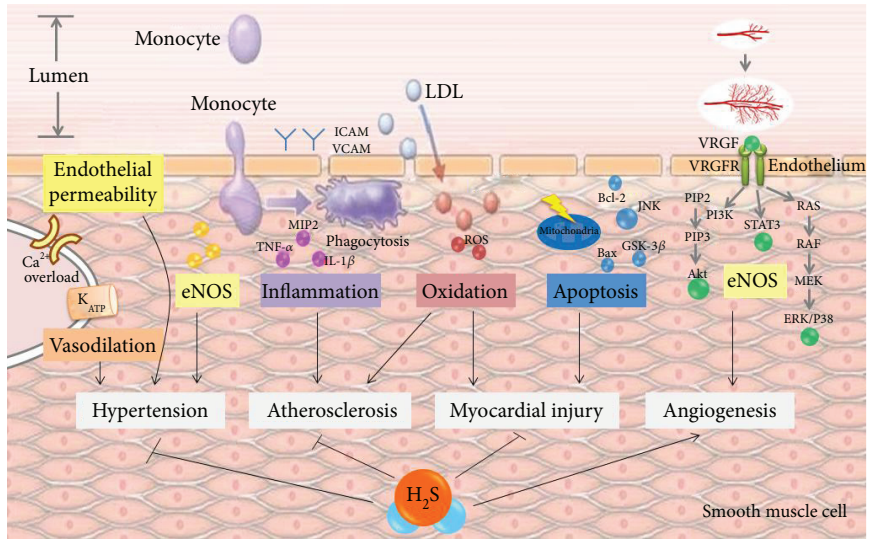

Figure 6: Schematic illustration of molecular mechanisms underlying H_2S-induced cardioprotection.

rate, indicating that CBS is also involved in mitogenic effects of H_2S [177]. Supplying 3MP, the 3MST substrate, facilitated wound healing and reserved mitochondrial functions which were associated with greater proliferation rates, proven by silencing 3MST to inhibit ECs growth and migration rates [178]. Taken together, H_2S may be a potential proangiogenic agent, which is independent of the three synthesizing enzymes.

To determine how H_2S regulates endothelial functions, most studies focused on the VEGF (also called as vascular permeability factor, VPF) signaling, which is the arguably crucial pathway in angiogenic responses both under healthy and pathophysiological circumstances [173, 179]. Silencing CSE and CSE inhibitor PAG reduced vessel length and branching stimulated by VEGF [145, 180]. Meanwhile, incubation of VEGF in HUVECs resulted in higher H_2S synthesis and level [180]. Additionally, H_2S presented as an endogenous stimulator of angiogenesis by increasing the activation of Akt, ERK, and p38, which are the downstreams of VEGF signaling [180]. Administration of glibenclamide, the K_{ATP} channel blocker, reduced H_2S-induced endothelial cells motility and prohibited H_2S-triggered activation of p38, indicating K_{ATP} channel was one of the H_2S targets and may locate at upstream of p38 in this motility process [180]. We first developed SPRC as the H_2S donor which activated and interacted with signal transducer and activator of transcription 3 (STAT3) to induce angiogenesis *in vitro* and *in vivo* [175]. We also discovered that ZYZ-803, releasing H_2S and NO, regulates angiogenesis through SIRT1/VEGF/cGMP pathway [176]. However, how the STAT3 links to Akt signaling, ERK/p38, and K_{ATP} channel still needs further investigations.

9. Conclusion and Perspectives

Over the last few decades, there are significant progress achieved in delineating the therapeutic potentials and molecular mechanisms underlying the actions of H_2S on cardiovascular diseases [181], seen in Figure 6. The evidences elaborated above indicate that H_2S derived from CSE, CBS, 3MST/AAT, or DAO reduces blood pressure, inhibits atherosclerotic progress, alleviates infarct myocardial injuries, and stimulates the angiogenic properties on endothelium. Therefore, several chemicals have been developed to test the therapeutical potentials for further drug development in human. In spite of compelling evidences in the literature for the role of exogenous and endogenous and H_2S in vessel and myocardial protection, several questions regarding to precise mechanisms and regulations of H_2S in the context of cardiovascular diseases need to be better understand. In quiescent, growing, and maturing vessels, does the generation of H_2S generated by different cell types have any interaction and which one plays the major role? Is the H_2S-mediated inflammation different in high blood pressure, angiogenesis, ischemic injury, and atherosclerosis? What is the exact manner of cross-talk between the three gas neurotransmitters, that is, NO, CO, and H_2S? Interestingly, some studies showed obvious discrepancy by suggesting vasoconstrictor effects of H_2S, instead of vasodilation actions. Further studies will be required to determine whether this discrepancy is due to dose of H_2S, vascular response, oxygen tension, or experimental models. Finally, the posttranslational level of H_2S-producing enzymes should be defined in the context of regulations and activities. After these tremendous growths of preclinical studies, we expect the sulfide-containing compounds will apply to clinics someday with considerable efficacy and safety.

Disclosure

This publication is an extension and based on the Dr. Ya-Dan Wen's thesis (http://scholarbank.nus.edu.sg/bitstream/10635/77716/1/Wen%20Yadan_HT090143H_PhD%20thesis-v2.pdf).

Conflicts of Interest

There is no conflict of interest declared by the authors.

Acknowledgments

This work has been funded by the Faculty Research Grant of MUST (FRG-17-06-SP), the Macau Science and Technology Development Fund (FDCT 055/2016/A2 and 039/2016/A), and the International Exchanges and Cooperation Projects of CSU-RF (201826).

References

[1] M. W. Warenycia, L. R. Goodwin, C. G. Benishin et al., "Acute hydrogen sulfide poisoning. Demonstration of selective uptake of sulfide by the brainstem by measurement of brain sulfide levels," *Biochemical Pharmacology*, vol. 38, no. 6, pp. 973–981, 1989.

[2] K. Abe and H. Kimura, "The possible role of hydrogen sulfide as an endogenous neuromodulator," *Journal of Neuroscience*, vol. 16, no. 3, pp. 1066–1071, 1996.

[3] R. Wang, "Two's company, three's a crowd: can H_2S be the third endogenous gaseous transmitter?," *The FASEB Journal*, vol. 16, no. 13, pp. 1792–1798, 2002.

[4] R. A. Dombkowski, M. J. Russell, and K. R. Olson, "Hydrogen sulfide as an endogenous regulator of vascular smooth muscle tone in trout," *American Journal of Physiology-Regulatory, Integrative and Comparative Physiology*, vol. 286, no. 4, pp. R678–R685, 2004.

[5] J. L. Wallace, "Hydrogen sulfide-releasing anti-inflammatory drugs," *Trends in Pharmacological Sciences*, vol. 28, no. 10, pp. 501–505, 2007.

[6] S. Fiorucci, E. Distrutti, G. Cirino, and J. L. Wallace, "The emerging roles of hydrogen sulfide in the gastrointestinal tract and liver," *Gastroenterology*, vol. 131, no. 1, pp. 259–271, 2006.

[7] J. Mason, C. J. Cardin, and A. Dennehy, "The role of sulphide and sulphide oxidation in the copper molybdenum antagonism in rats and guinea pigs," *Research in Veterinary Science*, vol. 24, no. 1, pp. 104–108, 1978.

[8] W. Zhao, J. Zhang, Y. Lu, and R. Wang, "The vasorelaxant effect of H_2S as a novel endogenous gaseous K_{ATP} channel opener," *The EMBO Journal*, vol. 20, no. 21, pp. 6008–6016, 2001.

[9] C. J. Richardson, E. A. M. Magee, and J. H. Cummings, "A new method for the determination of sulphide in gastrointestinal contents and whole blood by microdistillation and ion chromatography," *Clinica Chimica Acta*, vol. 293, no. 1-2, pp. 115–125, 2000.

[10] L. R. Goodwin, D. Francom, F. P. Dieken et al., "Determination of sulfide in brain tissue by gas dialysis/ion chromatography: postmortem studies and two case reports," *Journal of Analytical Toxicology*, vol. 13, no. 2, pp. 105–109, 1989.

[11] J. C. Savage and D. H. Gould, "Determination of sulfide in brain tissue and rumen fluid by ion-interaction reversed-phase high-performance liquid chromatography," *Journal of Chromatography B: Biomedical Sciences and Applications*, vol. 526, no. 2, pp. 540–545, 1990.

[12] J. Furne, A. Saeed, and M. D. Levitt, "Whole tissue hydrogen sulfide concentrations are orders of magnitude lower than presently accepted values," *American Journal of Physiology-Regulatory, Integrative and Comparative Physiology*, vol. 295, no. 5, pp. R1479–R1485, 2008.

[13] P. F. Erickson, I. H. Maxwell, L. J. Su, M. Baumann, and L. M. Glode, "Sequence of cDNA for rat cystathionine γ-lyase and comparison of deduced amino acid sequence with related Escherichia coli enzymes," *Biochemical Journal*, vol. 269, no. 2, pp. 335–340, 1990.

[14] G. Bukovska, V. Kery, and J. P. Kraus, "Expression of human cystathionine β-synthase in Escherichia coli: purification and characterization," *Protein Expression and Purification*, vol. 5, no. 5, pp. 442–448, 1994.

[15] R. Hosoki, N. Matsuki, and H. Kimura, "The possible role of hydrogen sulfide as an endogenous smooth muscle relaxant in synergy with nitric oxide," *Biochemical and Biophysical Research Communications*, vol. 237, no. 3, pp. 527–531, 1997.

[16] K. Eto and H. Kimura, "The production of hydrogen sulfide is regulated by testosterone and S-adenosyl-l-methionine in mouse brain," *Journal of Neurochemistry*, vol. 83, no. 1, pp. 80–86, 2002.

[17] M. Iciek, A. Bilska, L. Ksiazek, Z. Srebro, and L. Włodek, "Allyl disulfide as donor and cyanide as acceptor of sulfane sulfur in the mouse tissues," *Pharmacological Reports*, vol. 57, no. 2, pp. 212–218, 2005.

[18] C. Szabo, "Hydrogen sulphide and its therapeutic potential," *Nature Reviews Drug Discovery*, vol. 6, no. 11, pp. 917–935, 2007.

[19] L. Li and P. Moore, "Putative biological roles of hydrogen sulfide in health and disease: a breath of not so fresh air?," *Trends in Pharmacological Sciences*, vol. 29, no. 2, pp. 84–90, 2008.

[20] L. Bao, Č:. Vlček, V. Pačes, and J. P. Kraus, "Identification and tissue distribution of human cystathionine β-synthase mRNA isoforms," *Archives of Biochemistry and Biophysics*, vol. 350, no. 1, pp. 95–103, 1998.

[21] W. Zhao, J. F. Ndisang, and R. Wang, "Modulation of endogenous production of H_2S in rat tissues," *Canadian Journal of Physiology and Pharmacology*, vol. 81, no. 9, pp. 848–853, 2003.

[22] N. Shibuya, Y. Mikami, Y. Kimura, N. Nagahara, and H. Kimura, "Vascular endothelium expresses 3-mercaptopyruvate sulfurtransferase and produces hydrogen sulfide," *Journal of Biochemistry*, vol. 146, no. 5, pp. 623–626, 2009.

[23] N. Shibuya, M. Tanaka, M. Yoshida et al., "3-Mercaptopyruvate sulfurtransferase produces hydrogen sulfide and bound sulfane sulfur in the brain," *Antioxidants and Redox Signaling*, vol. 11, no. 4, pp. 703–714, 2009.

[24] M. Ishigami, K. Hiraki, K. Umemura, Y. Ogasawara, K. Ishii, and H. Kimura, "A source of hydrogen sulfide and a mechanism of its release in the brain," *Antioxidants and Redox Signaling*, vol. 11, no. 2, pp. 205–214, 2009.

[25] N. Nagahara, T. Ito, H. Kitamura, and T. Nishino, "Tissue and subcellular distribution of mercaptopyruvate sulfurtransferase in the rat: confocal laser fluorescence and immunoelectron microscopic studies combined with biochemical analysis," *Histochemistry and Cell Biology*, vol. 110, no. 3, pp. 243–250, 1998.

[26] N. Shibuya, S. Koike, M. Tanaka et al., "A novel pathway for the production of hydrogen sulfide from D-cysteine in mammalian cells," *Nature Communications*, vol. 4, no. 1, p. 1366, 2013.

[27] H. Kimura, "The physiological role of hydrogen sulfide and beyond," *Nitric Oxide*, vol. 41, pp. 4–10, 2014.

[28] S. J. Gould, G. A. Keller, and S. Subramani, "Identification of peroxisomal targeting signals located at the carboxy terminus of four peroxisomal proteins," *The Journal of Cell Biology*, vol. 107, no. 3, pp. 897–905, 1988.

[29] A. Hashimoto, T. Oka, and T. Nishikawa, "Anatomical distribution and postnatal changes in endogenous free D-aspartate and D-serine in rat brain and periphery," *European Journal of Neuroscience*, vol. 7, no. 8, pp. 1657–1663, 1995.

[30] U. Schumann and S. Subramani, "Special delivery from mitochondria to peroxisomes," *Trends in Cell Biology*, vol. 18, no. 6, pp. 253–256, 2008.

[31] R. Wang, "Hydrogen sulfide: a new EDRF," *Kidney International*, vol. 76, no. 7, pp. 700–704, 2009.

[32] J. E. Dominy and M. H. Stipanuk, "New roles for cysteine and transsulfuration enzymes: production of H_2S, a neuromodulator and smooth muscle relaxant," *Nutrition Reviews*, vol. 62, no. 9, pp. 348–353, 2004.

[33] Y. Kimura, Y. Mikami, K. Osumi, M. Tsugane, J. I. Oka, and H. Kimura, "Polysulfides are possible H_2S-derived signaling molecules in rat brain," *The FASEB Journal*, vol. 27, no. 6, pp. 2451–2457, 2013.

[34] Y. Kimura, Y. Toyofuku, S. Koike et al., "Identification of H_2S3 and H_2S produced by 3-mercaptopyruvate sulfurtransferase in the brain," *Scientific Reports*, vol. 5, no. 1, 2015.

[35] Y. Kimura, S. Koike, N. Shibuya, D. Lefer, Y. Ogasawara, and H. Kimura, "3-Mercaptopyruvate sulfurtransferase produces potential redox regulators cysteine- and glutathione-persulfide (Cys-SSH and GSSH) together with signaling molecules H_2S2, H_2S3 and H_2S," *Scientific Reports*, vol. 7, no. 1, article 10459, 2017.

[36] R. Miyamoto, S. Koike, Y. Takano et al., "Polysulfides (H_2Sn) produced from the interaction of hydrogen sulfide (H_2S) and nitric oxide (NO) activate TRPA1 channels," *Scientific Reports*, vol. 7, article 45995, 2017.

[37] K. Y. Chen and J. C. Morris, "Kinetics of oxidation of aqueous sulfide by oxygen," *Environmental Science and Technology*, vol. 6, no. 6, pp. 529–537, 1972.

[38] M. N. Hughes, M. N. Centelles, and K. P. Moore, "Making and working with hydrogen sulfide. The chemistry and generation of hydrogen sulfide in vitro and its measurement in vivo: a review," *Free Radical Biology and Medicine*, vol. 47, no. 10, pp. 1346–1353, 2009.

[39] Y. F. Li, C. S. Xiao, and R. T. Hui, "Calcium sulfide (CaS), a donor of hydrogen sulfide (H_2S): a new antihypertensive drug?," *Medical Hypotheses*, vol. 73, no. 3, pp. 445–447, 2009.

[40] N. Balasubramanian and K. Shanthi, "Development of simple permeation device for the generation of hydrogen sulfide," *The Analyst*, vol. 120, no. 8, pp. 2287–2289, 1995.

[41] I. Thomsen, K. Clausen, S. Scheibye, and S. O. Lawesson, "Thiation with 2, 4-bis (4-methoxyphenyl)-1, 3, 2, 4-dithiadiphosphetane 2, 4-disulfide: N-methylthiopyrrolidone," in *Organic Syntheses*, vol. 7, p. 372, Wiley & Sons, New York, 1990.

[42] L. Li, M. Whiteman, Y. Y. Guan et al., "Characterization of a novel, water-soluble hydrogen sulfide-releasing molecule (GYY 4137): new insights into the biology of hydrogen sulfide," *Circulation*, vol. 117, no. 18, pp. 2351–2360, 2008.

[43] L. Li, M. Salto-Tellez, C. H. Tan, M. Whiteman, and P. K. Moore, "GYY 4137, a novel hydrogen sulfide-releasing molecule, protects against endotoxic shock in the rat," *Free Radical Biology and Medicine*, vol. 47, no. 1, pp. 103–113, 2009.

[44] M. A. Huffman, "Animal self-medication and ethno-medicine: exploration and exploitation of the medicinal properties of plants," *Proceedings of the Nutrition Society*, vol. 62, no. 02, pp. 371–381, 2003.

[45] K. L. Miller, R. S. Liebowitz, and L. K. Newby, "Complementary and alternative medicine in cardiovascular disease: a review of biologically based approaches," *American Heart Journal*, vol. 147, no. 3, pp. 401–411, 2004.

[46] G. A. Benavides, G. L. Squadrito, R. W. Mills et al., "Hydrogen sulfide mediates the vasoactivity of garlic," *Proceedings of the National Academy of Sciences of the United States of America*, vol. 104, no. 46, pp. 17977–17982, 2007.

[47] M. S. Butt, M. T. Sultan, M. S. Butt, and J. Iqbal, "Garlic: nature's protection against physiological threats," *Critical Reviews in Food Science and Nutrition*, vol. 49, no. 6, pp. 538–551, 2009.

[48] H. Amagase, "Clarifying the real bioactive constituents of garlic," *Journal of Nutrition*, vol. 136, no. 3, pp. 716S–725S, 2006.

[49] H. Matsuura, "Phytochemistry of garlic horticultural and processing procedures," in *Nutraceuticals*, pp. 55–69, Food & Nutrition Press, Inc., 2008.

[50] Q. Peng, A. R. Buz'Zard, and B. H. Lau, "Neuroprotective effect of garlic compounds in amyloid-β peptide-induced apoptosis in vitro," *Medical Science Monitor*, vol. 8, no. 8, pp. BR328–BR337, 2002.

[51] V. B. Gupta and K. S. J. Rao, "Anti-amyloidogenic activity of S-allyl-l-cysteine and its activity to destabilize Alzheimer's β-amyloid fibrils in vitro," *Neuroscience Letters*, vol. 429, no. 2-3, pp. 75–80, 2007.

[52] N. B. Chauhan, "Effect of aged garlic extract on APP processing and tau phosphorylation in Alzheimer's transgenic model Tg 2576," *Journal of Ethnopharmacology*, vol. 108, no. 3, pp. 385–394, 2006.

[53] J.-M. Kim, N. Chang, W.-K. Kim, and H. S. Chun, "Dietary S-allyl-L-cysteine reduces mortality with decreased incidence of stroke and behavioral changes in stroke-prone spontaneously hypertensive rats," *Bioscience, Biotechnology, and Biochemistry*, vol. 70, no. 8, pp. 1969–1971, 2006.

[54] Y. Numagami and S. T. Ohnishi, "S-allylcysteine inhibits free radical production, lipid peroxidation and neuronal damage in rat brain ischemia," *Journal of Nutrition*, vol. 131, no. 3, pp. 1100S–1105S, 2001.

[55] S. C. Chuah, P. K. Moore, and Y. Z. Zhu, "S-allylcysteine mediates cardioprotection in an acute myocardial infarction rat model via a hydrogen sulfide-mediated pathway," *American Journal of Physiology-Heart and Circulatory Physiology*, vol. 293, no. 5, pp. H2693–H2701, 2007.

[56] Q. Wang, H. R. Liu, Q. Mu, P. Rose, and Y. Z. Zhu, "S-propargyl-cysteine protects both adult rat hearts and neonatal cardiomyocytes from ischemia/hypoxia injury: the contribution of the hydrogen sulfide-mediated pathway," *Journal of Cardiovascular Pharmacology*, vol. 54, no. 2, pp. 139–146, 2009.

[57] Q. H. Gong, L. L. Pan, X. H. Liu, Q. Wang, H. Huang, and Y. Z. Zhu, "S-propargyl-cysteine (ZYZ-802), a sulphur-containing amino acid, attenuates beta-amyloid-induced cognitive deficits and pro-inflammatory response: involvement of ERK1/2 and NF-κB pathway in rats," *Amino Acids*, vol. 40, no. 2, pp. 601–610, 2011.

[58] K. Ma, Y. Liu, Q. Zhu et al., "H_2S donor, S-propargyl-cysteine, increases CSE in SGC-7901 and cancer-induced mice: evidence for a novel anti-cancer effect of endogenous H_2S?," *PLoS One*, vol. 6, no. 6, article e20525, 2011.

[59] R. C. Simpson and R. A. Freedland, "Factors affecting the rate of gluconeogenesis from L cysteine in the perfused rat liver," *Journal of Nutrition*, vol. 106, no. 9, pp. 1272–1278, 1976.

[60] F. Skovby, N. Krassikoff, and U. Francke, "Assignment of the gene for cystathione β-synthase to human chromosome 21 in somatic cell hybrids," *Human Genetics*, vol. 65, no. 3, pp. 291–294, 1984.

[61] G. P. Kurzban, L. Chu, J. L. Ebersole, and S. C. Holt, "Sulfhemoglobin formation in human erythrocytes by cystalysin, an L-cysteine desulfhydrase from Treponema denticola," *Oral Microbiology and Immunology*, vol. 14, no. 3, pp. 153–164, 1999.

[62] H. Kimura, "Hydrogen sulfide as a neuromodulator," *Molecular Neurobiology*, vol. 26, no. 1, pp. 013–020, 2002.

[63] K. Eto and H. Kimura, "A novel enhancing mechanism for hydrogen sulfide-producing activity of cystathionine β-synthase," *Journal of Biological Chemistry*, vol. 277, no. 45, pp. 42680–42685, 2002.

[64] M. Puranik, C. L. Weeks, D. Lahaye et al., "Dynamics of carbon monoxide binding to cystathionine β-synthase," *Journal of Biological Chemistry*, vol. 281, no. 19, pp. 13433–13438, 2006.

[65] S. Taoka and R. Banerjee, "Characterization of NO binding to human cystathionine β-synthase: possible implications of the effects of CO and NO binding to the human enzyme," *Journal of Inorganic Biochemistry*, vol. 87, no. 4, pp. 245–251, 2001.

[66] K. Hanaoka, K. Sasakura, Y. Suwanai et al., "Discovery and mechanistic characterization of selective inhibitors of H_2S-producing enzyme: 3-mercaptopyruvate sulfurtransferase (3MST) targeting active-site cysteine persulfide," *Scientific Reports*, vol. 7, article 40227, 2017.

[67] B. Geng, L. Chang, C. Pan et al., "Endogenous hydrogen sulfide regulation of myocardial injury induced by isoproterenol," *Biochemical and Biophysical Research Communications*, vol. 318, no. 3, pp. 756–763, 2004.

[68] H. Yan, J. Du, and C. Tang, "The possible role of hydrogen sulfide on the pathogenesis of spontaneous hypertension in rats," *Biochemical and Biophysical Research Communications*, vol. 313, no. 1, pp. 22–27, 2004.

[69] H. Mitsuhashi, S. Yamashita, H. Ikeuchi et al., "Oxidative stress-dependent conversion of hydrogen sulfide to sulfite by activated neutrophils," *Shock*, vol. 24, no. 6, pp. 529–534, 2006.

[70] M. Whiteman, J. S. Armstrong, S. H. Chu et al., "The novel neuromodulator hydrogen sulfide: an endogenous peroxynitrite 'scavenger'?," *Journal of Neurochemistry*, vol. 90, no. 3, pp. 765–768, 2004.

[71] M. Whiteman, N. S. Cheung, Y. Z. Zhu et al., "Hydrogen sulphide: a novel inhibitor of hypochlorous acid-mediated oxidative damage in the brain?," *Biochemical and Biophysical Research Communications*, vol. 326, no. 4, pp. 794–798, 2005.

[72] K. R. Olson, "Is hydrogen sulfide a circulating "gasotransmitter" in vertebrate blood?," *Biochimica et Biophysica Acta (BBA) - Bioenergetics*, vol. 1787, no. 7, pp. 856–863, 2009.

[73] N. L. Whitfield, E. L. Kreimier, F. C. Verdial, N. Skovgaard, and K. R. Olson, "Reappraisal of H_2S/sulfide concentration in vertebrate blood and its potential significance in ischemic preconditioning and vascular signaling," *American Journal of Physiology-Regulatory, Integrative and Comparative Physiology*, vol. 294, no. 6, pp. R1930–R1937, 2008.

[74] D. C. Dittmer, "Hydrogen sulfide," in *Encyclopedia of Reagents for Organic Synthesis*, John Wiley & Sons, Ltd, 2001.

[75] A. R. Lippert, E. J. New, and C. J. Chang, "Reaction-based fluorescent probes for selective imaging of hydrogen sulfide in living cells," *Journal of the American Chemical Society*, vol. 133, no. 26, pp. 10078–10080, 2011.

[76] V. S. Lin, A. R. Lippert, and C. J. Chang, "Cell-trappable fluorescent probes for endogenous hydrogen sulfide signaling and imaging H_2O_2-dependent H_2S production," *Proceedings of the National Academy of Sciences*, vol. 110, no. 18, pp. 7131–7135, 2013.

[77] H. Peng, Y. Cheng, C. Dai et al., "A fluorescent probe for fast and quantitative detection of hydrogen sulfide in blood," *Angewandte Chemie International Edition*, vol. 50, no. 41, pp. 9672–9675, 2011.

[78] S. K. Bae, C. H. Heo, D. J. Choi et al., "A ratiometric two-photon fluorescent probe reveals reduction in mitochondrial H_2S production in Parkinson's disease gene knockout astrocytes," *Journal of the American Chemical Society*, vol. 135, no. 26, pp. 9915–9923, 2013.

[79] S. Yang, Y. Qi, C. Liu et al., "Design of a simultaneous target and location-activatable fluorescent probe for visualizing hydrogen sulfide in lysosomes," *Analytical Chemistry*, vol. 86, no. 15, pp. 7508–7515, 2014.

[80] M. K. Thorson, T. Majtan, J. P. Kraus, and A. M. Barrios, "Identification of cystathionine β-synthase inhibitors using a hydrogen sulfide selective probe," *Angewandte Chemie International Edition*, vol. 52, no. 17, pp. 4641–4644, 2013.

[81] L. A. Montoya and M. D. Pluth, "Selective turn-on fluorescent probes for imaging hydrogen sulfide in living cells," *Chemical Communications*, vol. 48, no. 39, pp. 4767–4769, 2012.

[82] R. Wang, F. Yu, L. Chen, H. Chen, L. Wang, and W. Zhang, "A highly selective turn-on near-infrared fluorescent probe for hydrogen sulfide detection and imaging in living cells," *Chemical Communications*, vol. 48, no. 96, article 11757, 11759 pages, 2012.

[83] W. Xuan, R. Pan, Y. Cao, K. Liu, and W. Wang, "A fluorescent probe capable of detecting H_2S at submicromolar concentrations in cells," *Chemical Communications*, vol. 48, no. 86, article 10669, 10671 pages, 2012.

[84] F. Yu, P. Li, P. Song, B. Wang, J. Zhao, and K. Han, "An ICT-based strategy to a colorimetric and ratiometric fluorescence probe for hydrogen sulfide in living cells," *Chemical Communications*, vol. 48, no. 23, pp. 2852–2854, 2012.

[85] C. Yu, X. Li, F. Zeng, F. Zheng, and S. Wu, "Carbon-dot-based ratiometric fluorescent sensor for detecting hydrogen sulfide in aqueous media and inside live cells," *Chemical Communications*, vol. 49, no. 4, pp. 403–405, 2013.

[86] Y. Takano, H. Echizen, and K. Hanaoka, "Fluorescent probes and selective inhibitors for biological studies of hydrogen sulfide- and polysulfide-mediated signaling," *Antioxidants & Redox Signaling*, vol. 27, no. 10, pp. 669–683, 2017.

[87] Y. Qian, J. Karpus, O. Kabil et al., "Selective fluorescent probes for live-cell monitoring of sulphide," *Nature Communications*, vol. 2, no. 1, 2011.

[88] C. Liu, J. Pan, S. Li et al., "Capture and visualization of hydrogen sulfide by a fluorescent probe," *Angewandte Chemie International Edition*, vol. 50, no. 44, pp. 10327–10329, 2011.

[89] B. Peng, W. Chen, C. Liu et al., "Fluorescent probes based on nucleophilic substitution-cyclization for hydrogen sulfide detection and bioimaging," *Chemistry - A European Journal*, vol. 20, no. 4, pp. 1010–1016, 2014.

[90] Y. Chen, C. Zhu, Z. Yang et al., "A ratiometric fluorescent probe for rapid detection of hydrogen sulfide in mitochondria," *Angewandte Chemie International Edition*, vol. 52, no. 6, pp. 1688–1691, 2013.

[91] R. J. Reiffenstein, W. C. Hulbert, and S. H. Roth, "Toxicology of hydrogen sulfide," *Annual Review of Pharmacology and Toxicology*, vol. 32, no. 1, pp. 109–134, 1992.

[92] E. Galardon, A. Tomas, P. Roussel, and I. Artaud, "New fluorescent zinc complexes: towards specific sensors for hydrogen sulfide in solution," *Dalton Transactions*, no. 42, pp. 9126–9130, 2009.

[93] M. G. Choi, S. Cha, H. Lee, H. L. Jeon, and S. K. Chang, "Sulfide-selective chemosignaling by a Cu^{2+} complex of dipicolylamine appended fluorescein," *Chemical Communications*, no. 47, pp. 7390–7392, 2009.

[94] K. Sasakura, K. Hanaoka, N. Shibuya et al., "Development of a highly selective fluorescence probe for hydrogen sulfide," *Journal of the American Chemical Society*, vol. 133, no. 45, pp. 18003–18005, 2011.

[95] F. Hou, J. Cheng, P. Xi et al., "Recognition of copper and hydrogen sulfide in vitro using a fluorescein derivative indicator," *Dalton Transactions*, vol. 41, no. 19, pp. 5799–5804, 2012.

[96] A. R. Lippert, "Designing reaction-based fluorescent probes for selective hydrogen sulfide detection," *Journal of Inorganic Biochemistry*, vol. 133, pp. 136–142, 2014.

[97] X. C. Wu, W. J. Zhang, D. Q. Wu, R. Sammynaiken, R. Wang, and Q. Yang, "Using carbon nanotubes to absorb low-concentration hydrogen sulfide in fluid," *IEEE Transactions on Nanobioscience*, vol. 5, no. 3, pp. 204–209, 2006.

[98] X. C. Wu, W. J. Zhang, R. Sammynaiken et al., "Measurement of low concentration and nano-quantity hydrogen sulfide in sera using unfunctionalized carbon nanotubes," *Measurement Science and Technology*, vol. 20, no. 10, article 105801, 2009.

[99] J. E. Doeller, T. S. Isbell, G. Benavides et al., "Polarographic measurement of hydrogen sulfide production and consumption by mammalian tissues," *Analytical Biochemistry*, vol. 341, no. 1, pp. 40–51, 2005.

[100] D. W. Kraus and J. E. Doeller, "Sulfide consumption by mussel gill mitochondria is not strictly tied to oxygen reduction: measurements using a novel polarographic sulfide sensor," *Journal of Experimental Biology*, vol. 207, no. 21, pp. 3667–3679, 2004.

[101] M. D. Levitt, M. S. Abdel-Rehim, and J. Furne, "Free and acid-labile hydrogen sulfide concentrations in mouse tissues: anomalously high free hydrogen sulfide in aortic tissue," *Antioxidants and Redox Signaling*, vol. 15, no. 2, pp. 373–378, 2011.

[102] T. Togawa, M. Ogawa, M. Nawata, Y. Ogasawara, K. Kawanabe, and S. Tanabe, "High performance liquid chromatographic determination of bound sulfide and sulfite and thiosulfate at their low levels in human serum by pre-column fluorescence derivatization with monobromobimane," *Chemical and Pharmaceutical Bulletin*, vol. 40, no. 11, pp. 3000–3004, 1992.

[103] E. A. Wintner, T. L. Deckwerth, W. Langston et al., "A monobromobimane-based assay to measure the pharmacokinetic profile of reactive sulphide species in blood," *British Journal of Pharmacology*, vol. 160, no. 4, pp. 941–957, 2010.

[104] X. Shen, C. B. Pattillo, S. Pardue, S. C. Bir, R. Wang, and C. G. Kevil, "Measurement of plasma hydrogen sulfide in vivo and in vitro," *Free Radical Biology and Medicine*, vol. 50, no. 9, pp. 1021–1031, 2011.

[105] J. L. Wallace, "Physiological and pathophysiological roles of hydrogen sulfide in the gastrointestinal tract," *Antioxidants and Redox Signaling*, vol. 12, no. 9, pp. 1125–1133, 2010.

[106] R. C. O. Zanardo, V. Brancaleone, E. Distrutti, S. Fiorucci, G. Cirino, and J. L. Wallace, "Hydrogen sulfide is an endogenous modulator of leukocyte-mediated inflammation," *The FASEB Journal*, vol. 20, no. 12, pp. 2118–2120, 2006.

[107] F. Spiller, M. I. L. Orrico, D. C. Nascimento et al., "Hydrogen sulfide improves neutrophil migration and survival in sepsis via K^{+}_{ATP} channel activation," *American Journal of Respiratory and Critical Care Medicine*, vol. 182, no. 3, pp. 360–368, 2010.

[108] E. Distrutti, L. Sediari, A. Mencarelli et al., "Evidence that hydrogen sulfide exerts antinociceptive effects in the gastrointestinal tract by activating K_{ATP} channels," *Journal of Pharmacology and Experimental Therapeutics*, vol. 316, no. 1, pp. 325–335, 2006.

[109] M. Bucci, A. Papapetropoulos, V. Vellecco et al., "Hydrogen sulfide is an endogenous inhibitor of phosphodiesterase activity," *Arteriosclerosis, Thrombosis, and Vascular Biology*, vol. 30, no. 10, pp. 1998–2004, 2010.

[110] J. L. Wallace, L. Vong, W. McKnight, M. Dicay, and G. R. Martin, "Endogenous and exogenous hydrogen sulfide promotes resolution of colitis in rats," *Gastroenterology*, vol. 137, no. 2, pp. 569–578.e1, 2009.

[111] E. Ekundi-Valentim, K. T. Santos, E. A. Camargo et al., "Differing effects of exogenous and endogenous hydrogen sulphide in carrageenan-induced knee joint synovitis in the rat," *British Journal of Pharmacology*, vol. 159, no. 7, pp. 1463–1474, 2010.

[112] Y. Wang, X. Zhao, H. Jin et al., "Role of hydrogen sulfide in the development of atherosclerotic lesions in apolipoprotein E knockout mice," *Arteriosclerosis, Thrombosis, and Vascular Biology*, vol. 29, no. 2, pp. 173–179, 2009.

[113] L. L. Pan, X. H. Liu, Q. H. Gong, D. Wu, and Y. Z. Zhu, "Hydrogen sulfide attenuated tumor necrosis factor-α-induced inflammatory signaling and dysfunction in vascular endothelial cells," *PLoS One*, vol. 6, no. 5, article e19766, 2011.

[114] H. K. Eltzschig and C. D. Collard, "Vascular ischaemia and reperfusion injury," *British Medical Bulletin*, vol. 70, no. 1, pp. 71–86, 2004.

[115] N. R. Sodha, R. T. Clements, J. Feng et al., "Hydrogen sulfide therapy attenuates the inflammatory response in a porcine model of myocardial ischemia/reperfusion injury," *Journal of Thoracic and Cardiovascular Surgery*, vol. 138, no. 4, pp. 977–984, 2009.

[116] K. Kang, M. Zhao, H. Jiang, G. Tan, S. Pan, and X. Sun, "Role of hydrogen sulfide in hepatic ischemia-reperfusion–induced injury in rats," *Liver Transplantation*, vol. 15, no. 10, pp. 1306–1314, 2009.

[117] A. Sivarajah, M. C. McDonald, and C. Thiemermann, "The production of hydrogen sulfide limits myocardial ischemia and reperfusion injury and contributes to the cardioprotective effects of preconditioning with endotoxin, but not ischemia in the rat," *Shock*, vol. 26, no. 2, pp. 154–161, 2006.

[118] J. L. Wallace, M. Dicay, W. McKnight, and G. R. Martin, "Hydrogen sulfide enhances ulcer healing in rats," *FASEB Journal*, vol. 21, no. 14, pp. 4070–4076, 2007.

[119] J. L. Wallace, G. Caliendo, V. Santagada, and G. Cirino, "Markedly reduced toxicity of a hydrogen sulphide-releasing derivative of naproxen (ATB-346)," *British Journal of Pharmacology*, vol. 159, no. 6, pp. 1236–1246, 2010.

[120] S. Fiorucci and L. Santucci, "Hydrogen sulfide-based therapies: focus on H_2S releasing NSAIDs," *Inflammation & Allergy - Drug Targets*, vol. 10, no. 2, pp. 133–140, 2011.

[121] K. L. Flannigan, K. D. McCoy, and J. L. Wallace, "Eukaryotic and prokaryotic contributions to colonic hydrogen sulfide synthesis," *American Journal of Physiology-Gastrointestinal and Liver Physiology*, vol. 301, no. 1, pp. G188–G193, 2011.

[122] G. R. Martin, G. W. McKnight, M. S. Dicay, C. S. Coffin, J. G. P. Ferraz, and J. L. Wallace, "Hydrogen sulphide synthesis in the rat and mouse gastrointestinal tract," *Digestive and Liver Disease*, vol. 42, no. 2, pp. 103–109, 2010.

[123] P. Nagy and C. C. Winterbourn, "Rapid reaction of hydrogen sulfide with the neutrophil oxidant hypochlorous acid to generate polysulfides," *Chemical Research in Toxicology*, vol. 23, no. 10, pp. 1541–1543, 2010.

[124] G. Rábai, M. Orbán, and I. R. Epstein, "Systematic design of chemical oscillators. 77. A model for the pH-regulated oscillatory reaction between hydrogen peroxide and sulfide ion," *The Journal of Physical Chemistry*, vol. 96, no. 13, pp. 5414–5419, 1992.

[125] B. L. Predmore, D. J. Lefer, and G. Gojon, "Hydrogen sulfide in biochemistry and medicine," *Antioxidants & Redox Signaling*, vol. 17, no. 1, pp. 119–140, 2012.

[126] I. N. Lykakis, C. Ferreri, and C. Chatgilialoglu, "The sulfhydryl radical (HS./S.-): a contender for the isomerization of double bonds in membrane lipids," *Angewandte Chemie International Edition*, vol. 46, no. 11, pp. 1914–1916, 2007.

[127] S. Koike, K. Kawamura, Y. Kimura, N. Shibuya, H. Kimura, and Y. Ogasawara, "Analysis of endogenous H_2S and H_2S n in mouse brain by high-performance liquid chromatography with fluorescence and tandem mass spectrometric detection," *Free Radical Biology and Medicine*, vol. 113, pp. 355–362, 2017.

[128] N. Nagahara, S. Koike, T. Nirasawa, H. Kimura, and Y. Ogasawara, "Alternative pathway of H_2S and polysulfides production from sulfurated catalytic-cysteine of reaction intermediates of 3-mercaptopyruvate sulfurtransferase," *Biochemical and Biophysical Research Communications*, vol. 496, no. 2, pp. 648–653, 2018.

[129] Y. Kimura and H. Kimura, "Hydrogen sulfide protects neurons from oxidative stress," *The FASEB Journal*, vol. 18, no. 10, pp. 1165–1167, 2004.

[130] Y. Kimura, Y. I. Goto, and H. Kimura, "Hydrogen sulfide increases glutathione production and suppresses oxidative stress in mitochondria," *Antioxidants and Redox Signaling*, vol. 12, no. 1, pp. 1–13, 2010.

[131] L. Chang, B. Geng, F. Yu et al., "Hydrogen sulfide inhibits myocardial injury induced by homocysteine in rats," *Amino Acids*, vol. 34, no. 4, pp. 573–585, 2008.

[132] M. P. Murphy, "How mitochondria produce reactive oxygen species," *Biochemical Journal*, vol. 417, no. 1, pp. 1–13, 2009.

[133] D. B. Zorov, M. Juhaszova, and S. J. Sollott, "Mitochondrial ROS-induced ROS release: an update and review," *Biochimica et Biophysica Acta-Bioenergetics*, vol. 1757, no. 5-6, pp. 509–517, 2006.

[134] M. Whiteman, L. Li, P. Rose, C. H. Tan, D. B. Parkinson, and P. K. Moore, "The effect of hydrogen sulfide donors on lipopolysaccharide-induced formation of inflammatory mediators in macrophages," *Antioxidants and Redox Signaling*, vol. 12, no. 10, pp. 1147–1154, 2010.

[135] G. Edwards, M. Feletou, and A. H. Weston, "Hydrogen sulfide as an endothelium-derived hyperpolarizing factor in rodent mesenteric arteries," *Circulation Research*, vol. 110, no. 1, pp. e13–e14, 2012.

[136] G. Tang, G. Yang, B. Jiang, Y. Ju, L. Wu, and R. Wang, "H_2S is an endothelium-derived hyperpolarizing factor," *Antioxidants and Redox Signaling*, vol. 19, no. 14, pp. 1634–1646, 2013.

[137] W. Zhao and R. Wang, "H_2S-induced vasorelaxation and underlying cellular and molecular mechanisms," *American Journal of Physiology-Heart and Circulatory Physiology*, vol. 283, no. 2, pp. H474–H480, 2002.

[138] Y. Cheng, J. F. Ndisang, G. Tang, K. Cao, and R. Wang, "Hydrogen sulfide-induced relaxation of resistance mesenteric artery beds of rats," *American Journal of Physiology-Heart and Circulatory Physiology*, vol. 287, no. 5, pp. H2316–H2323, 2004.

[139] S. Yuan, X. Shen, and C. G. Kevil, "Beyond a gasotransmitter: hydrogen sulfide and polysulfide in cardiovascular health and immune response," *Antioxidants & Redox Signaling*, vol. 27, no. 10, pp. 634–653, 2017.

[140] A. K. Mustafa, G. Sikka, S. K. Gazi et al., "Hydrogen sulfide as endothelium-derived hyperpolarizing factor sulfhydrates potassium channels," *Circulation Research*, vol. 109, no. 11, pp. 1259–1268, 2011.

[141] G. Yang, L. Wu, B. Jiang et al., "H_2S as a physiologic vasorelaxant: hypertension in mice with deletion of cystathionine γ-lyase," *Science*, vol. 322, no. 5901, pp. 587–590, 2008.

[142] X. Zhao, L.-K. Zhang, C.-Y. Zhang et al., "Regulatory effect of hydrogen sulfide on vascular collagen content in spontaneously hypertensive rats," *Hypertension Research*, vol. 31, no. 8, pp. 1619–1630, 2008.

[143] J. Du, Y. Hui, Y. Cheung et al., "The possible role of hydrogen sulfide as a smooth muscle cell proliferation inhibitor in rat cultured cells," *Heart and Vessels*, vol. 19, no. 2, pp. 75–80, 2004.

[144] F. Moccia, G. Bertoni, A. Florio Pla et al., "Hydrogen sulfide regulates intracellular Ca^{2+} concentration in endothelial cells from excised rat aorta," *Current Pharmaceutical Biotechnology*, vol. 12, no. 9, pp. 1416–1426, 2011.

[145] C. Coletta, A. Papapetropoulos, K. Erdelyi et al., "Hydrogen sulfide and nitric oxide are mutually dependent in the regulation of angiogenesis and endothelium-dependent vasorelaxation," *Proceedings of the National Academy of Sciences*, vol. 109, no. 23, pp. 9161–9166, 2012.

[146] M. Y. Ibrahim, N. M. Aziz, M. Y. Kamel, and R. A. Rifaai, "Sodium hydrosulphide against renal ischemia/reperfusion and the possible contribution of nitric oxide in adult male Albino rats," *Bratislava Medical Journal*, vol. 116, no. 11, pp. 681–688, 2015.

[147] L. Kram, E. Grambow, F. Mueller-Graf, H. Sorg, and B. Vollmar, "The anti-thrombotic effect of hydrogen sulfide is partly mediated by an upregulation of nitric oxide synthases," *Thrombosis Research*, vol. 132, no. 2, pp. e112–e117, 2013.

[148] B.-B. Tao, S. Y. Liu, C. C. Zhang et al., "VEGFR2 functions as an H_2S-targeting receptor protein kinase with its novel Cys 1045–Cys 1024 disulfide bond serving as a specific molecular switch for hydrogen sulfide actions in vascular endothelial cells," *Antioxidants & Redox Signaling*, vol. 19, no. 5, pp. 448–464, 2013.

[149] C. Szabo, "Hydrogen sulfide, an enhancer of vascular nitric oxide signaling: mechanisms and implications," *American Journal of Physiology-Cell Physiology*, vol. 312, no. 1, pp. C3–C15, 2017.

[150] M. Nishida, T. Sawa, N. Kitajima et al., "Hydrogen sulfide anion regulates redox signaling via electrophile sulfhydration," *Nature Chemical Biology*, vol. 8, no. 8, pp. 714–724, 2012.

[151] M. Nishida, T. Toyama, and T. Akaike, "Role of 8-nitro-cGMP and its redox regulation in cardiovascular electrophilic signaling," *Journal of Molecular and Cellular Cardiology*, vol. 73, pp. 10–17, 2014.

[152] A. Ghazalpour, S. Doss, X. Yang et al., "Thematic review series: the pathogenesis of atherosclerosis. Toward a biological network for atherosclerosis," *The Journal of Lipid Research*, vol. 45, no. 10, pp. 1793–1805, 2004.

[153] G. K. Hansson and Mechanisms of disease, "Inflammation, atherosclerosis, and coronary artery disease," *New England Journal of Medicine*, vol. 352, no. 16, pp. 1685–1695, 2005.

[154] R. B. Singh, S. A. Mengi, Y. J. Xu, A. S. Arneja, and N. S. Dhalla, "Pathogenesis of atherosclerosis-a multifactorial process," *Experimental and Clinical Cardiology*, vol. 7, no. 1, pp. 40–53, 2002.

[155] S.-K. Yan, T. Chang, H. Wang, L. Wu, R. Wang, and Q. H. Meng, "Effects of hydrogen sulfide on homocysteine-induced oxidative stress in vascular smooth muscle cells," *Biochemical and Biophysical Research Communications*, vol. 351, no. 2, pp. 485–491, 2006.

[156] H. Laggner, M. K. Muellner, S. Schreier et al., "Hydrogen sulphide: a novel physiological inhibitor of LDL atherogenic modification by HOCl," *Free Radical Research*, vol. 41, no. 7, pp. 741–747, 2007.

[157] N. Alexopoulos and P. Raggi, "Calcification in atherosclerosis," *Nature Reviews Cardiology*, vol. 6, no. 11, pp. 681–688, 2009.

[158] W. Qiao, T. Chaoshu, J. Hongfang, and D. Junbao, "Endogenous hydrogen sulfide is involved in the pathogenesis of atherosclerosis," *Biochemical and Biophysical Research Communications*, vol. 396, no. 2, pp. 182–186, 2010.

[159] Q. H. Meng, G. Yang, W. Yang, B. Jiang, L. Wu, and R. Wang, "Protective effect of hydrogen sulfide on balloon injury-induced neointima hyperplasia in rat carotid arteries," *American Journal of Pathology*, vol. 170, no. 4, pp. 1406–1414, 2007.

[160] G. Yang, X. Sun, and R. Wang, "Hydrogen sulfide-induced apoptosis of human aorta smooth muscle cells via the activation of mitogen-activated protein kinases and caspase-3," *The FASEB Journal*, vol. 18, no. 14, pp. 1782–1784, 2004.

[161] G. Yang, L. Wu, and R. Wang, "Pro-apoptotic effect of endogenous H_2S on human aorta smooth muscle cells," *The FASEB Journal*, vol. 20, no. 3, pp. 553–555, 2006.

[162] S.-y. WU, C.-s. Pan, B. Geng et al., "Hydrogen sulfide ameliorates vascular calcification induced by vitamin D3 plus nicotine in rats," *Acta Pharmacologica Sinica*, vol. 27, no. 3, pp. 299–306, 2006.

[163] J. Zhou, J. Moller, C. C. Danielsen et al., "Dietary supplementation with methionine and homocysteine promotes early atherosclerosis but not plaque rupture in ApoE-deficient mice," *Arteriosclerosis, Thrombosis, and Vascular Biology*, vol. 21, no. 9, pp. 1470–1476, 2001.

[164] Q. C. Yong, S. W. Lee, C. S. Foo, K. L. Neo, X. Chen, and J.-S. Bian, "Endogenous hydrogen sulphide mediates the cardioprotection induced by ischemic postconditioning," *American Journal of Physiology-Heart and Circulatory Physiology*, vol. 295, no. 3, pp. H1330–H1340, 2008.

[165] Y. Z. Zhu, Z. J. Wang, P. Ho et al., "Hydrogen sulfide and its possible roles in myocardial ischemia in experimental rats," *Journal of Applied Physiology*, vol. 102, no. 1, pp. 261–268, 2007.

[166] Y. Zhuo, P. F. Chen, A. Z. Zhang, H. Zhong, C. Q. Chen, and Y. Z. Zhu, "Cardioprotective effect of hydrogen sulfide in ischemic reperfusion experimental rats and its influence on expression of survivin gene," *Biological & Pharmaceutical Bulletin*, vol. 32, no. 8, pp. 1406–1410, 2009.

[167] J. W. Calvert, S. Jha, S. Gundewar et al., "Hydrogen sulfide mediates cardioprotection through Nrf 2 signaling," *Circulation Research*, vol. 105, no. 4, pp. 365–374, 2009.

[168] J. W. Elrod, J. W. Calvert, J. Morrison et al., "Hydrogen sulfide attenuates myocardial ischemia-reperfusion injury by preservation of mitochondrial function," *Proceedings of the National Academy of Sciences of the United States of America*, vol. 104, no. 39, pp. 15560–15565, 2007.

[169] Q. Wang, X. L. Wang, H. R. Liu, P. Rose, and Y. Z. Zhu, "Protective effects of cysteine analogues on acute myocardial ischemia: novel modulators of endogenous H_2S production," *Antioxidants and Redox Signaling*, vol. 12, no. 10, pp. 1155–1165, 2010.

[170] B. O'Rourke, "Myocardial K (ATP) channels in preconditioning," *Circulation Research*, vol. 87, no. 10, pp. 845–855, 2000.

[171] D. Johansen, K. Ytrehus, and G. F. Baxter, "Exogenous hydrogen sulfide (H_2S) protects against regional myocardial ischemia–reperfusion injury," *Basic Research in Cardiology*, vol. 101, no. 1, pp. 53–60, 2006.

[172] M. Potente, H. Gerhardt, and P. Carmeliet, "Basic and therapeutic aspects of angiogenesis," *Cell*, vol. 146, no. 6, pp. 873–887, 2011.

[173] P. Carmeliet and R. K. Jain, "Molecular mechanisms and clinical applications of angiogenesis," *Nature*, vol. 473, no. 7347, pp. 298–307, 2011.

[174] A. Katsouda, S. I. Bibli, A. Pyriochou, C. Szabo, and A. Papapetropoulos, "Regulation and role of endogenously produced hydrogen sulfide in angiogenesis," *Pharmacological Research*, vol. 113, no. Part A, pp. 175–185, 2016.

[175] J. Kan, W. Guo, C. Huang, G. Bao, Y. Zhu, and Y. Z. Zhu, "S-propargyl-cysteine, a novel water-soluble modulator of endogenous hydrogen sulfide, promotes angiogenesis through activation of signal transducer and activator of

transcription 3," *Antioxidants and Redox Signaling*, vol. 20, no. 15, pp. 2303–2316, 2014.

[176] Q. Hu, D. Wu, F. Ma et al., "Novel angiogenic activity and molecular mechanisms of ZYZ-803, a slow-releasing hydrogen sulfide–nitric oxide hybrid molecule," *Antioxidants & Redox Signaling*, vol. 25, no. 8, pp. 498–514, 2016.

[177] S. Saha, P. K. Chakraborty, X. Xiong et al., "Cystathionine β-synthase regulates endothelial function via protein S-sulfhydration," *The FASEB Journal*, vol. 30, no. 1, pp. 441–456, 2016.

[178] C. Coletta, K. Módis, B. Szczesny et al., "Regulation of vascular tone, angiogenesis and cellular bioenergetics by the 3-mercaptopyruvate sulfurtransferase/H_2S pathway: functional impairment by hyperglycemia and restoration by DL-α-lipoic acid," *Molecular Medicine*, vol. 21, no. 1, pp. 1–14, 2015.

[179] A.-K. Olsson, A. Dimberg, J. Kreuger, and L. Claesson-Welsh, "VEGF receptor signalling? In control of vascular function," *Nature Reviews Molecular Cell Biology*, vol. 7, no. 5, pp. 359–371, 2006.

[180] A. Papapetropoulos, A. Pyriochou, Z. Altaany et al., "Hydrogen sulfide is an endogenous stimulator of angiogenesis," *Proceedings of the National Academy of Sciences*, vol. 106, no. 51, pp. 21972–21977, 2009.

[181] Y. D. WEN, 2014, http://scholarbank.nus.edu.sg/bitstream/10635/77716/1/Wen%20Yadan_HT090143H_PhD%20thesis-v2.pdf.

Hindawi
Oxidative Medicine and Cellular Longevity
Volume 2018, Article ID 5167524, 8 pages
https://doi.org/10.1155/2018/5167524

Research Article

Lycopene: Hepatoprotective and Antioxidant Effects toward Bisphenol A-Induced Toxicity in Female Wistar Rats

Haidy G. Abdel-Rahman[1], **Heba M. A. Abdelrazek**[2], **Dalia W. Zeidan**[3], **Rasha M. Mohamed**[4] **and Aaser M. Abdelazim**[5,6]

[1]*Department of Clinical Pathology, Faculty of Veterinary Medicine, Suez Canal University, Ismailia, Egypt*
[2]*Department of Physiology, Faculty of Veterinary Medicine, Suez Canal University, Ismailia, Egypt*
[3]*Department of Home and Economics, Nutrition and Food Science Branch, Faculty of Education, Suez Canal University, Ismailia, Egypt*
[4]*Department of Forensic Medicine & Clinical Toxicology, Faculty of Medicine, Suez Canal University, Ismailia, Egypt*
[5]*Department of Biochemistry, Faculty of Veterinary Medicine, Zagazig University, Zagazig, Egypt*
[6]*Department of Basic Medical Sciences, College of Applied Medical Sciences, University of Bisha, Bisha, Saudi Arabia*

Correspondence should be addressed to Haidy G. Abdel-Rahman; haidy.galal@vet.suez.edu.eg

Received 23 November 2017; Revised 5 March 2018; Accepted 4 April 2018; Published 26 July 2018

Academic Editor: Rohit Saluja

Bisphenol A (BPA)—an endocrine disruptor xenoestrogen—is widely spread in the environment. Lycopene (LYC) is an antioxidant phytochemical carotenoid. The hereby study was designed to verify the deleterious effect of BPA on cyclic female rats' hepatic tissue as well as evaluation of the effect of LYC toward BPA hepatic perturbation. Twenty-eight female Wistar rats were allocated equally into four groups: control group, LYC group (10 mg/kg B.wt), BPA group (10 mg/kg B.wt), and BPA + LYC group (the same doses as former groups). The treatments were given daily via gavage to the rats for 30 days. The rats in BPA displayed high activities of serum liver enzymes with low levels of total proteins (TP) and albumin. Moreover, BPA induced hepatic oxidative stress via depletion of antioxidant enzymes concomitant with augmentation of lipid peroxidation, increased comet tail DNA %, and overexpression of caspase-3. Meanwhile, LYC administration reduced the cytotoxic effects of BPA on hepatic tissue, through improving the liver function biomarkers and oxidant-antioxidant state as well as DNA damage around the control values. These findings were confirmed by hepatic histopathological examination. Finally, LYC credited to have a noticeable protective effect versus BPA provoked oxidative injury and apoptosis of the liver tissue.

1. Introduction

Liver is the major organ in the body responsible for detoxification and metabolism, resulting in the production of free radicals, which are very reactive and unstable [1]. These products are eliminated by antioxidants that are naturally present in the tissue [2]. The imbalance between the free radical production and elimination leads to oxidative stress which can cause hepatic damage [3].

Bisphenol A (BPA)—an endocrine disruptor—is a monomer used in polycarbonate plastic industry and epoxy resins that lines cans of preserved food and beverages [4]. It can immigrate into food or water on heating [5]. Due to the wide spreading of the usage of BPA in manufacture, both animals and human are daily exposed to BPA hazardous effects [6]. BPA is metabolized primarily in the liver [7]. It has been reported that BPA can cause hepatic [8], renal [9], cerebral [10], and other organs damage by producing reactive oxygen species (ROS) [11]. Moreover, BPA lead to lipid peroxidation of the hepatic tissue by diminishing the endogenous antioxidant defense mechanism in male rats [12].

Antioxidants are present naturally in the living cells as superoxide dismutase, catalase, glutathione reductase, and glutathione oxidase [13] or are available in food such as carotenoids, polyphenols, and vitamins C and E [14]. Therefore, there is a dietary trend recommending increased intake of plant foods rich in antioxidants as an attempt to protect from diseases [15].

An interest has been aroused in utilizing natural products isolated from plants against chemical compounds generating tissue damage [16]. Lycopene (LYC) is a natural antioxidant and free radical scavenger lipophilic carotenoid present in food especially tomatoes giving it the red color [17]. LYC supplementation had been tested for its ameliorative effect against the harmful oxidative injury of tissues caused by environmental toxicants [18, 19]. Additionally, it can retrieve the peroxyl radicals, thus restraining lipid peroxidation pathway [20]. In view of the aforesaid literatures, the exposure of cyclic female rats to BPA has not been fully elucidated. Also, there has been no model exploring the effect of lycopene on BPA exposure; thus, the current study aimed at examining whether LYC has a potential protective action against BPA-induced hepatotoxicity in cyclic female rat model with concern to biochemical, oxidative stress, and antioxidant capacity in the liver tissue as well as histopathological alterations, percent of DNA in comet tail, and hepatic caspase-3 protein contents.

2. Materials and Methods

2.1. Animals and Experimental Design. Twenty-eight female Wistar rats weighing 94–100 g were bought from the Egyptian Organization for Biological Products and Vaccines, Helwan, Egypt. They were kept two weeks for accommodation prior to the onset of the experiment. Rats were kept in wire-topped cages and housed in a ventilated room under standardized housing conditions of natural light/dark rhythm, temperature $25 \pm 2^{\circ}$C, and humidity $48\% \pm 2$. Rats were given ad libitum diet and drinking water. The design of this experiment was approbated by the Research Ethical Committee of Faculty of Veterinary Medicine, Suez Canal University, Egypt. Rats were randomly allotted to four experimental groups, seven rats each. The 1st group received corn oil and considered as a control. The 2nd group was given LYC (NOW FOODS Co., USA) at a dose of 10 mg/kg B.wt [17] daily via gavage. The 3rd group was given BPA (Sigma-Aldrich Co., USA) at 10 mg/kg B.wt [21] daily via gavage. Finally, the 4th group was administrated both BPA and LYC at the same doses of the 2nd and 3rd groups daily via gavage. All treatments continued for 30 days.

2.2. Body and Liver Weights. Rats were weighed at the beginning of the experiment and then weighed at the end of the experiment. The body weight gain (B.wt.G) was calculated by subtracting the initial from the final body weight (F.B.wt). The relative liver weight was calculated as follows: absolute liver weight at the end of experiment/F.B.wt $\times$ 100.

2.3. Serum and Tissue Sampling. At the end of the experiment, female rats at luteal phase of estrous cycle (diestrus) were anesthetized via diethyl ether inhalation. Blood samples were collected from retroorbital venous plexus of the eye into clean plain tubes and left for clot formation, and then, sera were collected and stored at -20°C to evaluate immediate the hepatic function biomarkers and lipid profile.

Thereafter, rats were immolated by cervical dislocation. Liver, from each rat, was immediately enucleated, washed out with buffer saline, blotted by filter paper, and then weighed. A part of the liver from each rat was preserved in 10% neutral formalin for the histopathological and immunohistochemical investigations. The remaining parts were divided into two parts and kept at -80°C. The first part was used for liver tissue homogenate preparation to estimate antioxidant enzymes, lipid peroxidation, and cytochrome P450 reductase (CYPR450) assessments. The second part was used for single-cell suspensions followed by comet assay procedures.

2.4. Serum Biochemical Analysis

2.4.1. Hepatic Function Biomarker Assay. Serum alanine aminotransferase (ALT) and alkaline phosphatase (ALP) enzyme activities were assayed as described previously by Reitman and Frankel [22] and Tietz et al. [23]. Total protein (TP), albumin (Alb), and gamma glutamyl transferase (GGT) were estimated according to Gornall et al. [24], Westgard and Poquette [25], and Szasz [26], respectively. All the previously mentioned kits were purchased from DIACHEM Ltd. Co., Hungary.

2.4.2. Lipid Profile Assay. Lipid profile calorimetric kits were purchased from Diamond diagnostic Co., Egypt. Serum total cholesterol (TC) was determined by enzymatic method as demonstrated by Allain et al. [27], and triglycerides (TGs) were performed according to Fossati and Prencipe [28]. High-density lipoprotein cholesterol (HDL-c) and low-density lipoprotein cholesterol (LDL-c) were determined as described by Bachorik [29].

2.5. Antioxidants and Oxidative Stress Measurements

2.5.1. Preparation of Liver Homogenate. Liver tissues from different experimental groups were homogenized in ice cold 100 mM sodium phosphate-buffered saline (pH 7.4) and centrifuged at 5000 rpm for 30 min; thereafter, the obtained supernatants were kept at -80°C.

2.5.2. Hepatic Antioxidants and Lipid Peroxidation Levels. Glutathione peroxidase (GPx), superoxide dismutase (SOD), and malondialdehyde (MDA) were assayed in liver homogenate according to Paglia and Valentine [30], Nishikimi et al. [31], and Mihara and Uchiyama [32], respectively. Previous kits were purchased from LifeSpan BioSciences Inc., USA, for GPx and OxisResearch, USA, for SOD and MDA.

2.5.3. Cytochrome P450 Reductase (CYPR450). Cytochrome P450 reductase was estimated by using ELISA kit (CUSABIO, China). The procedures were followed according to the manufacturer's protocol.

2.6. Histopathological Examination. Paraffinized liver tissue blocks were processed and cut on a microtome at 5 μm thickness, then deparaffinized, and stained with hematoxylin and eosin (H&E) according to Drury and Wallington [33] in order to examine the hepatic histomorphological alterations.

2.7. Immunohistochemical (IHC) Evaluation of Caspase-3. Formalin-fixed paraffin-embedded specimens were cut into

Table 1: Effect of LYC on body and liver weights of BPA-intoxicated female Wistar rats.

Parameter	Experimental groups			
	Control	LYC	BPA	BPA + LYC
F.B.wt (g)	164.80 ± 4.58^{ab}	171.40 ± 9.60^{a}	142.40 ± 3.53^{b}	149.30 ± 11.81^{ab}
B.wt.G (g)	54.20 ± 4.51^{b}	70.40 ± 4.23^{a}	34.40 ± 4.72^{c}	53.90 ± 3.29^{b}
Abs. liver wt. (g)	5.97 ± 0.43	6.56 ± 0.52	5.39 ± 0.19	5.40 ± 0.49
Rel. liver wt. (%)	3.61 ± 0.18	3.81 ± 0.10	3.79 ± 0.09	3.62 ± 0.16

Values are expressed as means ± SE ($n = 7$) in every group. BPA: bisphenol A; LYC: lycopene; F.B.wt: final body weight; B.wt.G: body weight gain; Abs. liver wt.: absolute liver weight; Rel. liver wt.: relative liver weight. Within the same row, means with different superscript letters differ significantly at $P \leq 0.05$.

Table 2: Effect of LYC on serum biochemical hepatic markers in BPA-intoxicated female Wistar rats.

Parameter	Experimental groups			
	Control	LYC	BPA	BPA + LYC
ALT (U/l)	25.59 ± 0.10^{c}	25.09 ± 0.11^{c}	50.18 ± 1.05^{a}	35.68 ± 1.07^{b}
ALP (U/l)	66.93 ± 0.35^{c}	66.20 ± 0.49^{c}	93.19 ± 0.89^{a}	74.51 ± 1.62^{b}
GGT (U/l)	10.53 ± 0.12^{c}	10.43 ± 0.11^{c}	44.05 ± 0.79^{a}	20.95 ± 0.55^{b}
TP (g/dl)	6.10 ± 0.02^{a}	6.14 ± 0.01^{a}	4.94 ± 0.04^{c}	5.54 ± 0.03^{b}
Alb (g/dl)	4.60 ± 0.01^{a}	4.61 ± 0.01^{a}	3.64 ± 0.03^{c}	4.05 ± 0.03^{b}

Values are expressed as means ± SE ($n = 7$) in every group. BPA: bisphenol A; lycopene (LYC); ALT: alanine aminotransferase; ALP: alkaline phosphatase; GGT: gamma glutamyl transferase; TP: total protein; Alb: albumin. Within the same row, means with different superscript letters differ significantly at $P \leq 0.05$.

4 μm sections. After deparaffinization, sections were heated with an autoclave in Tris/HCl buffer (pH 9.0) for 20 min at room temperature for antigen retrieval. The sections were then incubated with 0.3% H_2O_2 in absolute methanol for 30 minutes and then incubated with primary antibody against caspase-3 (#PA1-29157, Thermo Fisher Scientific Co., USA) at concentration 1 : 1000. This was followed by sequential 60-minute incubations with secondary anti-rabbit antibody, Envision + System HRP-Labelled Polymer (Dako, USA), and visualization with liquid DAB (diaminobenzidine) substrate chromogen system (Dako, USA). All slides were lightly counterstained with hematoxylin for 30 seconds prior to dehydration and mounting [34].

2.8. Image Analysis of Caspase-3. Semi-quantitative method to assess the caspase-3 IHC staining intensity % from seven random fields/animal was proceeded using ImageJ program according to Elgawish et al. [35].

2.9. Liver Comet Assay. Single-cell suspensions were prepared from frozen livers according to the method described by Smith et al. [36]. The procedures for comet assay were followed as described by Abdelrazek et al. [37].

2.10. Statistical Analysis. Statistical analyses were made using SPSS software, v. 16.0 (SPSS Inc., IL, USA). All values were expressed as mean ± standard errors. One-way analysis of variance (ANOVA) followed by Duncan's multiple comparison tests was applied for analyzing values among groups. A probability level of $P < 0.05$ indicated significance.

3. Results

3.1. Body and Liver Weights. The rats in the BPA group showed numerically decreased F.B.wt than those in the control, although the decrease was not statistically significant. The decrease in body weight induced by BPA was slightly improved by LYC administration. Notwithstanding, the LYC-treated rats expressed significantly ($P < 0.05$) increased body weight in comparison with the BPA-treated rats. On the other hand, the B.wt.G of LYC rats was significantly ($P < 0.05$) increased in counter to the BPA rats which had significant reduction in B.wt.G when compared to the control rats. Moreover, BPA + LYC group was significantly ($P < 0.05$) improved than BPA group to a value comparable to control group. Concerning the absolute and relative liver weights, there were nonsignificant differences between groups (Table 1).

3.2. Serum Hepatic Function Biomarkers. Rats receiving BPA revealed significantly ($P < 0.05$) higher activities of serum ALT, ALP, and GGT enzymes and lower levels of TP and albumin than control rats. Meanwhile, BPA + LYC group exhibited significant ($P < 0.05$) improvement in these parameters when compared to the BPA group but still significantly ($P < 0.05$) differed from the control one. Rats supplemented with LYC only did not differ from the control group (Table 2).

3.3. Lipid Profile Assay. In the BPA-treated rats, the serum TC and LDL levels were significantly ($P < 0.05$) elevated in comparison with the control rats, whereas TC and LDL levels in rats receiving BPA + LYC were nonsignificantly altered compared to the control rats (Table 3).

3.4. Hepatic Antioxidative Status and Lipid Peroxidation. BPA significantly ($P < 0.05$) decreased GPx, SOD, and CYPR450 activities while increasing MDA level in comparison to control group. The SOD, GPx, and CYPR450 activities

Table 3: Effect of LYC on serum lipid profile in BPA-intoxicated female Wistar rats.

Parameter	Experimental groups			
	Control	LYC	BPA	BPA + LYC
TC (mg/dl)	102.00 ± 11.24^{b}	101.67 ± 11.85^{b}	146.33 ± 7.42^{a}	119.67 ± 4.09^{ab}
TGs (mg/dl)	81.00 ± 9.85^{ab}	73.00 ± 9.87^{b}	105.00 ± 2.52^{a}	97.67 ± 6.94^{ab}
HDL-c (mg/dl)	47.67 ± 3.93	52.00 ± 3.21	44.67 ± 3.71	47.33 ± 3.93
LDL-c (mg/dl)	52.53 ± 6.24^{b}	40.87 ± 6.91^{b}	83.13 ± 4.52^{a}	49.80 ± 5.31^{b}

Values are expressed as means ± SE ($n = 7$) in every group. BPA: bisphenol A; LYC: lycopene; TC: total cholesterol; TGs: triglycerides; HDL-c: high-density lipoprotein cholesterol; LDL-c: low-density lipoprotein cholesterol. Within the same row, means with different superscript letters differ significantly at $P \leq 0.05$.

Table 4: Effect of LYC on hepatic tissue antioxidant enzyme activities, lipid peroxidation level, caspase-3 immunoreactivity, and comet tail DNA % in BPA-intoxicated female Wistar rats.

Parameter	Experimental groups			
	Control	LYC	BPA	BPA + LYC
GPx (nmol/mg)	99.06 ± 3.79^{b}	108.85 ± 2.95^{a}	61.14 ± 0.90^{d}	88.62 ± 1.71^{c}
SOD (U/mg)	7.60 ± 1.50^{a}	7.62 ± 0.01^{a}	5.74 ± 0.05^{c}	6.74 ± 0.04^{b}
MDA (nmol/mg)	0.54 ± 0.00^{c}	0.52 ± 0.01^{c}	0.93 ± 0.02^{a}	0.72 ± 0.02^{b}
CYPR450 (ng/g)	3.86 ± 0.04^{a}	3.98 ± 0.01^{a}	2.44 ± 0.04^{c}	3.44 ± 0.08^{b}
Caspase-3 IRA (%)	35.62 ± 4.82^{c}	42.74 ± 5.71^{c}	77.04 ± 2.97^{a}	61.86 ± 3.09^{b}
Comet tail DNA (%)	6.68 ± 1.04^{c}	6.94 ± 1.29^{c}	25.05 ± 2.93^{a}	14.50 ± 2.61^{b}

Values are expressed as means ± SE ($n = 7$) in every group. BPA: bisphenol A; LYC: lycopene, GPx: glutathione peroxidase; SOD: superoxide dismutase, MDA: malondialdehyde, CYPR450: cytochrome P450 reductase; IRA: immunoreactive area. Within the same row, means with different superscript letters differ significantly at $P \leq 0.05$.

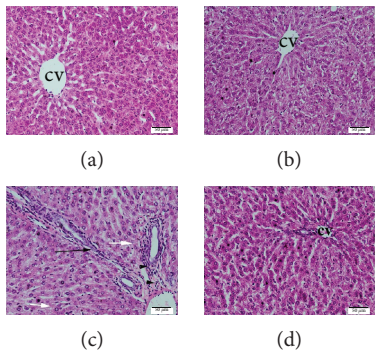

Figure 1: Histopathological sections of female Wistar rats. (a) Control group (b), LYC-treated (10 mg/kg) control, (c) BPA-treated (10 mg/kg) group, and (d) BPA (10 mg/kg) and LYC (10 mg/kg) cotreated group. (a) and (b) show normal hepatocytes arranged in radiating cords around central vein (cv). (c) The BPA-treated liver shows dilated vein, bridging fibrosis of portal areas (black arrow), mild leukocytic infiltration (arrowheads), and minute focal hepatocyte necrosis (white arrows). (d) BPA + LYC-treated liver shows amelioration of hepatic lesions with mildly vacuolization of hepatocytes.

were significantly ($P < 0.05$) elevated while MDA level was significantly ($P < 0.05$) diminished in the BPA + LYC group in contrast to BPA group, thus improving the oxidative effect of BPA on liver tissue. In the LYC group, nonsignificant changes occurred compared to the control group (Table 4).

3.5. Histopathological Examination of the Liver. The liver tissue of rats in the control and LYC groups showed normal hepatocytes with normal arrangement of hepatic cords around the central veins (Figures 1(a) and 1(b)). Livers of rats in BPA group exhibited fibrous expansion of some portal areas with occasional portal to portal bridging, foci of focal (spotty) lytic necrosis with dilated and congested central veins, and cytoplasmic vacuolization of hepatocytes with eccentric nuclei (Figure 1(c)), while rats in BPA + LYC group manifested no fibrous expansion of portal areas or necrosis with tendency for retaining normal hepatic architecture of hepatocytes accompanied with mild congestion of central vein (Figure 1(d)).

3.6. Immunohistochemical Evaluation (IHC) of the Liver. The different experimental groups in this study showed variable positive staining intensities of caspase-3 using DAB chromogen, where BPA group rats revealed significant ($P < 0.05$) higher positive cytoplasmic staining area % of caspase-3 in the hepatocytes (Figure 2(c) and Table 4) than control (Figure 2(a) and Table 4), while BPA + LYC group showed significantly ($P < 0.05$) lower caspase-3 staining area % (Figure 2(d) and Table 4) than BPA group.

3.7. Liver Comet Assay. Comet tail DNA % showed a significant ($P < 0.05$) elevation in BPA-treated group than in control. Administration of LYC with BPA significantly ($P < 0.05$) reduced comet tail % than BPA group.

4. Discussion

BPA is a monomer found in plastic goods and affects adversely many organs especially the liver through induction

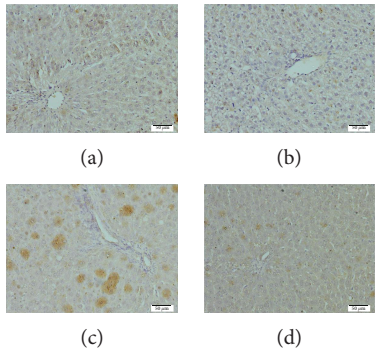

Figure 2: Immunohistochemical reaction of caspase-3 in livers of female Wistar rats. (a) Control group (b), LYC-treated (10 mg/kg) control, (c) BPA-treated (10 mg/kg) group, and (d) BPA (10 mg/kg) and LYC (10 mg/kg) cotreated group. Control and LYC groups show week immunoreactivity of caspase-3 while BPA-treated group exhibited higher immunoreactivity. The LYC coadministration with BPA shows amelioration of caspase-3 immunoreactivity than that in BPA alone.

of oxidation state. In this study, LYC was tested for its protective effect against the deleterious impacts induced by BPA in female rats' liver tissue. The present results demonstrated that BPA had no effect on body and liver weights. However, B.wt.G expressed significant decline in BPA-treated group than control while BPA + LYC showed improvement in B.wt.G to a level comparable to control. These results could be attributed to the toxic effect of BPA that could encounter several body homeostatic pathways, among which neuronal appetite loop in the brain [38], where BPA can easily cross blood brain barrier and have estrogenic effect [39]. Moreover, BPA can alter the antioxidant enzymes in different body systems [40, 41] as noted in the current study, thus could alter normal weight gain of the experimental rats. This can obviously illustrate the higher B.wt.G observed in BPA + LYC-treated group where LYC can alleviate oxidative stress [42] favor, cell-cell communication, and body performance in a positive manner [43, 44]. Our results were in harmony with Morrissey et al. [45] and Christiansen et al. [46] who recorded significant reduction in B.wt.G in BPA-treated female mice offspring and insignificant change in F.B.wt or organ weights of rats exposed to BPA, respectively. On the other hand, some reports in the literatures were inconsistent to our findings, where Rubin et al. [47] found significant increase in the body weight of Sprague Dawley female rats' offspring exposed to low BPA doses. The variation in results may be attributed to the diversity in diet composition, BPA exposure period, route and doses, and animal strain.

In our data, BPA expressed harmful effect on the liver evidenced by significant increase in the serum liver enzyme activities along with reduction in TP and albumin. The explanation of the higher hepatic enzyme activities could be due to altered hepatocytes' membrane permeability by BPA; thus, the cell membrane losses its functional integrity resulting in cellular leakage of these enzymes to circulation. This is augmented by the observed depletion in the activities of endogenous enzymatic antioxidants SOD, GPx, and CYPR450 that could increase hepatic membrane lipid peroxidation that disrupt its permeability [48]. Meanwhile, serum protein concentration is considered equilibrium between the rate of protein synthesis and breakdown. It is well known that BPA induces mitochondrial oxidative stress in the cell that results in protein damage [49], thus making protein damage more prominent than its synthesis. Moreover, administration of BPA disrupted hepatic integrity and functions where liver is considered the main organ involved in plasma protein biosynthesis [50]; thus, serum TP and albumin were declined. These obtained results were concurring with those recorded by Moon et al. [51], Geetharathan and Josthna [52], and Moustafa and Ahmed [53]. Fortunately, LYC reversed all abnormalities made by BPA intoxication and returned the values near normal. This finding harmonized with Sheriff and Devaki [54] and Jiang et al. [18] in other hepatic toxicity male rat models. Current results suggested that LYC consolidates hepatic cells' regeneration. Consequently, it strengthens the cellular membrane while diminishing the enzyme leakage and preserves its function in protein biosynthesis. The hepatic consolidating effect of LYC could be attributed to its ability for quenching of singlet oxygen and elimination of peroxyl radicals that was confirmed by the elevated antioxidant activities of SOD, GPx, and CYPR450 along with reduced MDA in BPA + LYC cotreated rats.

Administration of BPA in current study disrupted lipid metabolism that reflected negatively on serum profile results. Our results were in agreement with Moghaddam et al. [55] who recorded increased lipid profile in male mice treated with BPA for 4 weeks. BPA has the capability to disrupt the lipid metabolism [56] and trigger lipid accumulation through differentiation of 3T3-L1 fibroblasts into adipocytes [57]. The occurrence of abnormalities in lipid profile is considered the starting station for induction of oxidative stress and lipid peroxidation [58] that were observed in the current study. Administration of LYC with BPA, in this study, had improved the lipid profile. Jiang et al. [59, 18] confirmed our results as they suggested that LYC supplementation decreased TC, TGs, and LDL-c. LYC could decrease TC through diminishing cholesterol synthesis via inhibiting the hydroxy-methyl-glutaryl-coenzyme A reductase (HMGCoA), an enzyme controlling the rate of cholesterol formation besides declining LDL-c [60].

In our existing data, BPA evoked hepatic oxidative stress as it diminished activities of endogenous enzymatic antioxidant as SOD, GPx, and CYPR450 with increment in MDA which is an end product for lipid peroxidation. These results were in harmony with those obtained by Kabuto et al. [11], Asahi et al. [61], and Eid et al. [62]. The reduction in serum SOD activity could be due to excessive consumption in the autoxidation procedure induced by BPA in the liver. The decrease in SOD activity might lead to increase level of superoxide radicals which resulted in the inactivation of GPx [63], thus increasing hydrogen peroxide generation [11]. The observed increment in hepatic oxidative stress denoted by depletion of hepatic antioxidant enzymes could induce lipid peroxidation in hepatocytes' membrane, thus causing their damage [21, 64]. Moreover, the observed reduction in CYPR450, an essential enzyme for variable metabolic

processes of xenobiotics and BPA metabolism [65], led to persistence of active BPA metabolites which further increased ROS production [66].

Otherwise, LYC offered a reciprocal impact on the liver tissue manifested by raised SOD, GPx, and CYPR450 activities along with lowered MDA level in rats treated with BPA + LYC. The antioxidant activity of LYC could be attributed to being a beta carotene, where LYC had been proved to protect against protein, lipid, and DNA oxidation [67] through scavenging singlet oxygen [68] and peroxyl radicals [69], thus limiting MDA production as lipid peroxidation end product [70].

Histopathological investigations augmented the previous results, where BPA resulted in deleterious hepatic changes ranged from hepatocytes' vacuolization with eccentric nuclei to focal necrosis and fibrosis. These results were similar to those obtained by Eid et al. [62]. Current histopathological picture was confirmative for the oxidative stress and lipid peroxidation induction nature of BPA observed in this study. Oxidative stress and lipid peroxidation led to destruction of hepatocytes' cell membrane and liberation of hepatic enzymes as well as perturbation in hepatic capacity for protein biosynthesis. The usage of LYC, as antioxidant, produced pronounced hepatic protection that markedly ameliorated the severity of hepatic lesions and subsequently the hepatic functions.

Hepatic homeostasis is gained through a regular cell turnover involving apoptosis of hepatocytes [71]. The increase of apoptosis via increment of DNA strand breaks with DNA migration from the nucleus into the comet tail together with increment in caspase-3 protein content in BPA group is an attribution for various types of the observed liver pathology. Current results were parallel to the previous results of Abdel Samie et al. [72] and Eid et al. [62]. Our data suggested that BPA increased caspase-3 apoptosis and DNA tail fragment breaks via depletion of antioxidant activities and lipid peroxidation. The observed hepatic oxidative stress due to BPA administration could possibly damage DNA. The administration of LYC with BPA significantly decreased DNA fragment % in comet tail as well as caspase-3 immunoreactive area % than BPA group. These results were in agreement with Kurcer et al. [73]. The possible attribution for LYC antiapoptotic effect is its antioxidant power as it is known for its free radical scavenging effect that reduces lipid peroxidation, protein, and DNA damage [74, 75].

5. Conclusion

In conclusion, the current study demonstrated the protective effects of LYC versus BPA hepatic oxidative injury and apoptotic effect by means of MDA suppression with SOD and GPx activities' amelioration. Antioxidant effects of LYC led to overregulation of CYPR450 that cleared BPA metabolites rapidly and decreasing the exposure of hepatic cells to their harmful effects. All these effects downregulated hepatic caspase-3, thus reducing apoptosis and thus keeping hepatic integrity, and prevented the liberation of hepatic enzymes into the blood of female Wistar rats.

Conflicts of Interest

All authors have no competing interests to state.

Acknowledgments

Eternal thanks to Prof. Amina El Dessouki, Department of Pathology, for giving histopathology comments.

References

[1] D. Wu and A. I. Cederbaum, "Alcohol, oxidative stress, and free radical damage," *Alcohol Research & Health*, vol. 27, no. 4, pp. 277–284, 2003.

[2] D. W. Reische, D. A. Lillard, and R. R. Eitenmiller, "Antioxidants," in *Food lipids: Chemistry, Nutrition, and Biotechnology*, pp. 409–433, CRC Press, 2008.

[3] S. Li, H. Y. Tan, N. Wang et al., "The role of oxidative stress and antioxidants in liver diseases," *International Journal of Molecular Sciences*, vol. 16, no. 11, pp. 26087–26124, 2015.

[4] A. Schecter, N. Malik, D. Haffner et al., "Bisphenol A (BPA) in U.S. food," *Environmental Science & Technology*, vol. 44, no. 24, pp. 9425–9430, 2010.

[5] H. H. Le, E. M. Carlson, J. P. Chua, and S. M. Belcher, "Bisphenol A is released from polycarbonate drinking bottles and mimics the neurotoxic actions of estrogen in developing cerebellar neurons," *Toxicology Letters*, vol. 176, no. 2, pp. 149–156, 2008.

[6] B. S. Rubin, "Bisphenol A: an endocrine disruptor with widespread exposure and multiple effects," *The Journal of Steroid Biochemistry and Molecular Biology*, vol. 127, no. 1-2, pp. 27–34, 2011.

[7] J. B. Knaak and L. J. Sullivan, "Metabolism of bisphenol A in the rat," *Toxicology and Applied Pharmacology*, vol. 8, no. 2, pp. 175–184, 1966.

[8] A. Kourouma, C. Quan, P. Duan et al., "Bisphenol A induces apoptosis in liver cells through induction of ROS," *Advances in Toxicology*, vol. 2015, Article ID 901983, 10 pages, 2015.

[9] D. H. Krieter, B. Canaud, H. D. Lemke et al., "Bisphenol A in chronic kidney disease," *Artificial Organs*, vol. 37, no. 3, pp. 283–290, 2013.

[10] H. Kabuto, M. Amakawa, and T. Shishibori, "Exposure to bisphenol A during embryonic/fetal life and infancy increases oxidative injury and causes underdevelopment of the brain and testis in mice," *Life Sciences*, vol. 74, no. 24, pp. 2931–2940, 2004.

[11] H. Kabuto, S. Hasuike, N. Minagawa, and T. Shishibori, "Effects of bisphenol A on the metabolisms of active oxygen species in mouse tissues," *Environmental Research*, vol. 93, no. 1, pp. 31–35, 2003.

[12] W. M. Abdel-Waha, "Thymoquinone attenuates toxicity and oxidative stress induced by bisphenol A in liver of male rats," *Pakistan Journal of Biological Sciences*, vol. 17, no. 11, pp. 1152–1160, 2014.

[13] V. Bindhumol, K. C. Chitra, and P. P. Mathur, "Bisphenol A induces reactive oxygen species generation in the liver of male rats," *Toxicology*, vol. 188, no. 2-3, pp. 117–124, 2003.

[14] H. Sies and W. Stahl, "Vitamins E and C, beta-carotene, and other carotenoids as antioxidants," *The American Journal of Clinical Nutrition*, vol. 62, no. 6, pp. 1315S–1321S, 1995.

[15] A. H. Lichtenstein, L. J. Appel, M. Brands et al., "Diet and lifestyle recommendations revision 2006: a scientific statement from the American Heart Association Nutrition Committee," *Circulation*, vol. 114, no. 1, pp. 82–96, 2006.

[16] R. Szymanska, P. Pospisil, and J. Kruk, "Plant-derived antioxidants in disease prevention," *Oxidative Medicine and Cellular Longevity*, vol. 2016, Article ID 1920208, 2 pages, 2016.

[17] N. Rencuzogullari and S. Erdogan, "Oral administration of lycopene reverses cadmium-suppressed body weight loss and lipid peroxidation in rats," *Biological Trace Element Research*, vol. 118, no. 2, pp. 175–183, 2007.

[18] W. Jiang, M.-H. Guo, and X. Hai, "Hepatoprotective and antioxidant effects of lycopene on non-alcoholic fatty liver disease in rat," *World Journal of Gastroenterology*, vol. 22, no. 46, pp. 10180–10188, 2016.

[19] S. S. Palabiyik, P. Erkekoglu, N. D. Zeybek et al., "Protective effect of lycopene against ochratoxin A induced renal oxidative stress and apoptosis in rats," *Experimental and Toxicologic Pathology*, vol. 65, no. 6, pp. 853–861, 2013.

[20] G. W. Burton and K. U. Ingold, "Beta-carotene: an unusual type of lipid antioxidant," *Science*, vol. 224, no. 4649, pp. 569–573, 1984.

[21] Z. K. Hassan, M. A. Elobeid, P. Virk et al., "Bisphenol A induces hepatotoxicity through oxidative stress in rat model," *Oxidative Medicine and Cellular Longevity*, vol. 2012, Article ID 194829, 6 pages, 2012.

[22] S. Reitman and S. Frankel, "A colorimetric method for the determination of serum glutamic oxalacetic and glutamic pyruvic transaminases," *American Journal of Clinical Pathology*, vol. 28, no. 1, pp. 56–63, 1957.

[23] N. W. Tietz, C. A. Burtis, P. Duncan et al., "A reference method for measurement of alkaline phosphatase activity in human serum," *Clinical Chemistry*, vol. 29, no. 5, pp. 751–761, 1983.

[24] A. G. Gornall, C. J. Bardawill, and M. M. David, "Determination of serum proteins by means of the biuret reaction," *The Journal of Biological Chemistry*, vol. 177, no. 2, pp. 751–766, 1949.

[25] J. O. Westgard and M. A. Poquette, "Determination of serum albumin with the "SMA 12/60" by a bromcresol green dye-binding method," *Clinical Chemistry*, vol. 18, no. 7, pp. 647–653, 1972.

[26] G. Szasz, "A kinetic photometric method for serum γ-glutamyl transpeptidase," *Clinical Chemistry*, vol. 15, no. 2, pp. 124–136, 1969.

[27] C. C. Allain, L. S. Poon, C. S. Chan, W. Richmond, and P. C. Fu, "Enzymatic determination of total serum cholesterol," *Clinical Chemistry*, vol. 20, no. 4, pp. 470–475, 1974.

[28] P. Fossati and L. Prencipe, "Serum triglycerides determined colorimetrically with an enzyme that produces hydrogen peroxide," *Clinical Chemistry*, vol. 28, no. 10, pp. 2077–2080, 1982.

[29] P. S. Bachorik, "Measurement of low-density-lipoprotein cholesterol," in *Handbook of Lipoprotein Testing*, pp. 245–264, AACC Press, 2000.

[30] D. E. Paglia and W. N. Valentine, "Studies on the quantitative and qualitative characterization of erythrocyte glutathione peroxidase," *The Journal of Laboratory and Clinical Medicine*, vol. 70, no. 1, pp. 158–169, 1967.

[31] M. Nishikimi, N. Appaji Rao, and K. Yagi, "The occurrence of superoxide anion in the reaction of reduced phenazine methosulfate and molecular oxygen," *Biochemical and Biophysical Research Communications*, vol. 46, no. 2, pp. 849–854, 1972.

[32] M. Mihara and M. Uchiyama, "Determination of malonaldehyde precursor in tissues by thiobarbituric acid test," *Analytical Biochemistry*, vol. 86, no. 1, pp. 271–278, 1978.

[33] R. Drury and E. Wallington, "Preparation and fixation of tissues," in *Carleton's Histological Technique*, pp. 41–54, Oxford University Press, 1980.

[34] W. Haggag, E. Omara, S. Nada, H. Eleid, and H. Amra, "*Rhodotorula glutinis* and its two mutants ameliorate hepato-renal dysfunction induced by ochratoxin A on rats," *British Microbiology Research Journal*, vol. 4, no. 12, pp. 1392–1408, 2014.

[35] R. A. R. Elgawish, H. G. A. Rahman, and H. M. A. Abdelrazek, "Green tea extract attenuates CCl4-induced hepatic injury in male hamsters via inhibition of lipid peroxidation and p53-mediated apoptosis," *Toxicology Reports*, vol. 2, pp. 1149–1156, 2015.

[36] C. C. Smith, D. J. Adkins, E. A. Martin, and M. R. O'Donovan, "Recommendations for design of the rat comet assay," *Mutagenesis*, vol. 23, no. 3, pp. 233–240, 2008.

[37] H. Abdelrazek, M. Yusuf, S. Ismail, and R. Elgawish, "Effect of probiotic strains mixture administration on serum interleukins concentration, lymphocyte proliferation and DNA damage in rams," *Journal of Animal and Feed Sciences*, vol. 24, no. 4, pp. 302–307, 2015.

[38] E. Somm, V. M. Schwitzgebel, A. Toulotte et al., "Perinatal exposure to bisphenol A alters early adipogenesis in the rat," *Environmental Health Perspectives*, vol. 117, no. 10, pp. 1549–1555, 2009.

[39] G. N. Wade and J. E. Schneider, "Metabolic fuels and reproduction in female mammals," *Neuroscience & Biobehavioral Reviews*, vol. 16, no. 2, pp. 235–272, 1992.

[40] F. Vahdati Hassani, S. Mehri, K. Abnous, R. Birner-Gruenberger, and H. Hosseinzadeh, "Protective effect of crocin on BPA-induced liver toxicity in rats through inhibition of oxidative stress and downregulation of MAPK and MAPKAP signaling pathway and miRNA-122 expression," *Food and Chemical Toxicology*, vol. 107, Part A, pp. 395–405, 2017.

[41] D. Tiwari and G. Vanage, "Bisphenol A induces oxidative stress in bone marrow cells, lymphocytes, and reproductive organs of Holtzman rats," *International Journal of Toxicology*, vol. 36, no. 2, pp. 142–152, 2017.

[42] J. Chen, Y. Song, and L. Zhang, "Effect of lycopene supplementation on oxidative stress: an exploratory systematic review and meta-analysis of randomized controlled trials," *Journal of Medicinal Food*, vol. 16, no. 5, pp. 361–374, 2013.

[43] K. Sahin, M. Onderci, N. Sahin, M. F. Gursu, F. Khachik, and O. Kucuk, "Effects of lycopene supplementation on antioxidant status, oxidative stress, performance and carcass characteristics in heat-stressed Japanese quail," *Journal of Thermal Biology*, vol. 31, no. 4, pp. 307–312, 2006.

[44] H. Sies and W. Stahl, "Lycopene: antioxidant and biological effects and its bioavailability in the human," *Experimental Biology and Medicine*, vol. 218, no. 2, pp. 121–124, 1998.

[45] R. E. Morrissey, J. D. George, C. J. Price, R. W. Tyl, M. C. Marr, and C. A. Kimmel, "The developmental toxicity of bisphenol A in rats and mice," *Fundamental and Applied Toxicology*, vol. 8, no. 4, pp. 571–582, 1987.

[46] S. Christiansen, M. Axelstad, J. Boberg, A. M. Vinggaard, G. A. Pedersen, and U. Hass, "Low-dose effects of bisphenol A on

early sexual development in male and female rats," *Reproduction*, vol. 147, no. 4, pp. 477–487, 2014.

[47] B. S. Rubin, M. K. Murray, D. A. Damassa, J. C. King, and A. M. Soto, "Perinatal exposure to low doses of bisphenol A affects body weight, patterns of estrous cyclicity, and plasma LH levels," *Environmental Health Perspectives*, vol. 109, no. 7, pp. 675–680, 2001.

[48] N. Gahalain, J. Chaudhary, A. Kumar, S. Sharma, and A. Jain, "Lipid peroxidation: an overview," *International Journal of Pharmaceutical Sciences and Research*, vol. 2, no. 11, p. 2757, 2011.

[49] K. C. Chitra, C. Latchoumycandane, and P. P. Mathur, "Induction of oxidative stress by bisphenol A in the epididymal sperm of rats," *Toxicology*, vol. 185, no. 1-2, pp. 119–127, 2003.

[50] F. M. Shahbazian, M. Jacobs, and A. Lajtha, "Rates of protein synthesis in brain and other organs," *International Journal of Developmental Neuroscience*, vol. 5, no. 1, pp. 39–42, 1987.

[51] M. K. Moon, M. J. Kim, I. K. Jung et al., "Bisphenol A impairs mitochondrial function in the liver at doses below the no observed adverse effect level," *Journal of Korean Medical Science*, vol. 27, no. 6, pp. 644–652, 2012.

[52] T. Geetharathan and P. Josthna, "Effect of BPA on protein, lipid profile and immuno-histo chemical changes in placenta and uterine tissues of albino rat," *International Journal of Pharmaceutical and Clinical Research*, vol. 8, no. 4, pp. 260–268, 2016.

[53] G. G. Moustafa and A. A. M. Ahmed, "Impact of prenatal and postnatal exposure to bisphenol A on female rats in a two generational study: genotoxic and immunohistochemical implications," *Toxicology Reports*, vol. 3, pp. 685–695, 2016.

[54] S. A. Sheriff and T. Devaki, "Lycopene stabilizes liver function during D-galactosamine/lipopolysaccharide induced hepatitis in rats," *Journal of Taibah University for Science*, vol. 7, no. 1, pp. 8–16, 2013.

[55] H. S. Moghaddam, S. Samarghandian, and T. Farkhondeh, "Effect of bisphenol A on blood glucose, lipid profile and oxidative stress indices in adult male mice," *Toxicology Mechanisms and Methods*, vol. 25, no. 7, pp. 507–513, 2015.

[56] C. Casals-Casas and B. Desvergne, "Endocrine disruptors: from endocrine to metabolic disruption," *Annual Review of Physiology*, vol. 73, no. 1, pp. 135–162, 2011.

[57] H. Masuno, T. Kidani, K. Sekiya et al., "Bisphenol A in combination with insulin can accelerate the conversion of 3T3-L1 fibroblasts to adipocytes," *Journal of Lipid Research*, vol. 43, no. 5, pp. 676–684, 2002.

[58] O. E. Kelany, H. E. Khaled, A. M. El-Nahla, H. M. A. Abdelrazek, and M. M. Abdel-Daim, "Hepatoprotective and metabolic effects of dietary soy phytoestrogens against hyper caloric diet in cyclic female albino rats is mediated through estradiol receptors beta," *Biomedical and Pharmacology Journal*, vol. 10, no. 3, pp. 1061–1069, 2017.

[59] H. Jiang, Z. Wang, Y. Ma, Y. Qu, X. Lu, and H. Luo, "Effects of dietary lycopene supplementation on plasma lipid profile, lipid peroxidation and antioxidant defense system in feedlot Bamei lamb," *Asian-Australasian Journal of Animal Sciences*, vol. 28, no. 7, pp. 958–965, 2015.

[60] B. Fuhrman, A. Elis, and M. Aviram, "Hypocholesterolemic effect of lycopene and β-carotene is related to suppression of cholesterol synthesis and augmentation of LDL receptor activity in macrophages," *Biochemical and Biophysical Research Communications*, vol. 233, no. 3, pp. 658–662, 1997.

[61] J. Asahi, H. Kamo, R. Baba et al., "Bisphenol A induces endoplasmic reticulum stress-associated apoptosis in mouse non-parenchymal hepatocytes," *Life Sciences*, vol. 87, no. 13-14, pp. 431–438, 2010.

[62] J. I. Eid, S. M. Eissa, and A. A. El-Ghor, "Bisphenol A induces oxidative stress and DNA damage in hepatic tissue of female rat offspring," *The Journal of Basic & Applied Zoology*, vol. 71, pp. 10–19, 2015.

[63] J. Blum and I. Fridovich, "Inactivation of glutathione peroxidase by superoxide radical," *Archives of Biochemistry and Biophysics*, vol. 240, no. 2, pp. 500–508, 1985.

[64] A. Korkmaz, M. A. Ahbab, D. Kolankaya, and N. Barlas, "Influence of vitamin C on bisphenol A, nonylphenol and octylphenol induced oxidative damages in liver of male rats," *Food and Chemical Toxicology*, vol. 48, no. 10, pp. 2865–2871, 2010.

[65] A. V. Pandey and C. E. Fluck, "NADPH P450 oxidoreductase: structure, function, and pathology of diseases," *Pharmacology & Therapeutics*, vol. 138, no. 2, pp. 229–254, 2013.

[66] M. R. Namazi, "Cytochrome-P450 enzymes and autoimmunity: expansion of the relationship and introduction of free radicals as the link," *Journal of Autoimmune Diseases*, vol. 6, no. 1, p. 4, 2009.

[67] S. Agarwal and A. V. Rao, "Tomato lycopene and low density lipoprotein oxidation: a human dietary intervention study," *Lipids*, vol. 33, no. 10, pp. 981–984, 1998.

[68] J. R. Mein, F. Lian, and X. D. Wang, "Biological activity of lycopene metabolites: implications for cancer prevention," *Nutrition Reviews*, vol. 66, no. 12, pp. 667–683, 2008.

[69] W. Stahl and H. Sies, "Carotenoids and flavonoids contribute to nutritional protection against skin damage from sunlight," *Molecular Biotechnology*, vol. 37, no. 1, pp. 26–30, 2007.

[70] C. Liu, R. Wang, B. Zhang, C. Hu, and H. Zhang, "Protective effects of lycopene on oxidative stress, proliferation and autophagy in iron supplementation rats," *Biological Research*, vol. 46, no. 2, pp. 189–200, 2013.

[71] B. Fadeel, A. Ottosson, and S. Pervaiz, "Big wheel keeps on turning: apoptosome regulation and its role in chemoresistance," *Cell Death & Differentiation*, vol. 15, no. 3, pp. 443–452, 2008.

[72] H. A. Abdel Samie, S. A. Nassar, and Y. Hussein, "Ameliorative potential of selenium against bisphenol A-induced hepatotoxicity in rats," *Egyptian Journal of Hospital Medicine*, vol. 67, no. 1, pp. 444–454, 2017.

[73] M. A. Kurcer, Z. Kurcer, M. Koksal et al., "Effect of lycopene on caspase-3 enzyme activation in liver of methanol-intoxicated rats: comparison with fomepizole," *Journal of Medicinal Food*, vol. 13, no. 4, pp. 985–991, 2010.

[74] X. Zhao, G. Aldini, E. J. Johnson et al., "Modification of lymphocyte DNA damage by carotenoid supplementation in postmenopausal women," *The American Journal of Clinical Nutrition*, vol. 83, no. 1, pp. 163–169, 2006.

[75] W. Stahl and H. Sies, "Antioxidant activity of carotenoids," *Molecular Aspects of Medicine*, vol. 24, no. 6, pp. 345–351, 2003.

Hindawi
Oxidative Medicine and Cellular Longevity
Volume 2018, Article ID 8989676, 11 pages
https://doi.org/10.1155/2018/8989676

Research Article

Ascorbate Attenuates Oxidative Stress and Increased Blood Pressure Induced by 2-(4-Hydroxyphenyl) Amino-1,4-naphthoquinone in Rats

Javier Palacios,[1] **José Miguel Fonseca**,[1] **Fernando Ayavire**,[1] **Felipe Salas**,[1] **Mirko Ortiz**,[1] **Juan Marcelo Sandoval**,[1] **Julio Benites**,[1] **Chukwuemeka R. Nwokocha**,[2] **Ewaldo Zavala**,[3] **Adrián Paredes**,[4,5] **Iván Barría**,[5] **José Luis Vega**,[5] **and Fredi Cifuentes**[5]

[1]*Departamento de Ciencias Químicas y Farmacéuticas, Facultad Ciencias de la Salud, Universidad Arturo Prat, Iquique, Chile*
[2]*Department of Basic Medical Sciences, Physiology Section, Faculty of Medical Sciences, The University of the West Indies, Mona, Kingston 7, Jamaica*
[3]*Facultad de Farmacia y Bioquímica, Universidad Nacional de Trujillo, Trujillo, Peru*
[4]*Laboratorio de Química Biológica, Instituto Antofagasta (IA), Universidad de Antofagasta, Antofagasta, Chile*
[5]*Laboratorio de Fisiología Experimental (EPhyL), Instituto Antofagasta (IA), Universidad de Antofagasta, Antofagasta, Chile*

Correspondence should be addressed to Javier Palacios; clpalaci@unap.cl and Fredi Cifuentes; fredi.cifuentes@uantof.cl

Received 15 March 2018; Revised 15 May 2018; Accepted 7 June 2018; Published 26 July 2018

Academic Editor: Mohamed M. Abdel-Daim

Quinone derivatives like 2-(4-hydroxyphenyl) amino-1,4-naphthoquinone (Q7) are used as antitumor agents usually associated with adverse effects on the cardiovascular system. The objective of this study was to evaluate the cardioprotective effect of ascorbate on Q7-induced cardiovascular response in Wistar rats. In this study, blood pressure, vascular reactivity, and intracellular calcium fluxes were evaluated in cardiomyocytes and the rat aorta. We also measured oxidative stress through lipid peroxidation (TBARS), superoxide dismutase- (SOD-) like activity, and H_2O_2 generation. Oral treatment of rats with ascorbate (500 mg/kg) for 20 days significantly ($p < 0.05$) reduced the Q7-induced increase (10 mg/kg) in blood pressure and heart rate. The preincubation with ascorbate (2 mM) significantly ($p < 0.05$) attenuated the irregular beating of the atrium induced by Q7 (10^{-5} M). In addition, ascorbate induced endothelial vasodilation in the presence of Q7 in the intact aortic rings of a rat and reduced the cytosolic calcium levels in vascular smooth muscle cells. Ascorbate also reduced the Q7-induced oxidative stress *in vivo*. Ascorbate also attenuated Q7-induced SOD-like activity and increased TBARS levels. These results suggest a cardioprotective effect *in vivo* of ascorbate in animals treated orally with a naphthoquinone derivative by a mechanism involving oxidative stress.

1. Introduction

Naphthoquinone derivatives are widely distributed molecules in nature. Numerous antitumor therapeutic drugs are quinone-bearing molecules; these include anthracyclines, the 1,4-naphthoquinone pharmacophore group, and several synthetic compounds [1–4]. The therapeutic spectrum of action of quinone derivatives is very wide: leukemia, breast and lung cancer, lymphomas, and others [5].

Treatment of cancer with anthracycline derivatives has been very successful. However, these treatments generate increased cardiotoxic effects such as hypertension, heart failure, vascular complications, and cardiac arrhythmia [6]. Oxidative stress, DNA damage, senescence, and cell death are mechanisms causing anthracycline toxicity [7]. Cytotoxic and cardiotoxic effects of naphthoquinone derivatives involve the generation of reactive oxygen species (ROS) by a redox-cycling reaction [8–11]. Redox-cycling reaction occurs

through quinone reduction by 1 or 2 electrons from NADPH cytochrome P450 reductase, leading to a semiquinone-free radical that is reoxidized to the quinone in the presence of molecular oxygen, while oxygen is reduced to superoxide anion [12].

To reduce the cardiotoxic effects of anthracycline derivatives, researchers have evaluated its coadministration with molecules displaying antioxidant capacity. L-Carnitine supplementation was shown to reduce antioxidant defense with doxorubicin administration [13, 14]. In contrast, ascorbate plays a cardioprotective role in doxorubicin-induced cardiomyopathy by decreasing oxidative and/or nitrosative stress [15]. Phytochemical metabolites prevent oxidative stress by decreasing ROS generation, free radical scavenging activity, or improving the antioxidant effect of cells [16].

Ascorbate increases nitric oxide (NO) bioavailability in vascular endothelial tissue from dysfunctional patients. The protective effect of ascorbate on the vascular endothelium has been linked to the enhanced bioavailability of the tetrahydrobiopterin (BH_4) or the endothelial nitric oxide synthase (eNOS) activity [17]. The key role of an antioxidant agent relies on its ability to donate one or two electrons [18].

A previous study from our group showed that arylaminonaphthoquinone derivatives like Q7 (2-(4-hydroxyphenyl) amino-1,4-naphthoquinone) increased the formation of ROS and impaired the endothelial vasodilation in the rat aorta [19]. The objective of this investigation was to evaluate possible cardioprotective effects of ascorbate on the cardiotoxic response induced through chronic treatment with a naphthoquinone derivative Q7.

2. Materials and Methods

2.1. Drugs. The following drugs were used in this study: 2-(4-hydroxyphenyl) amino-1,4-naphthoquinone (Q7); acetylcholine (Sigma-Aldrich, USA); ascorbate (Asc) (Winkler, Santiago); phenylephrine (Sigma-Aldrich, USA); butylated hydroxytoluene (Merck, Darmstadt, Germany); pyrogallol (Sigma-Aldrich, USA); tetramethoxypropane (Sigma-Aldrich, USA); thiobarbituric acid (Merck, Darmstadt, Germany); and Tris-cacodylic acid (Sigma-Aldrich, USA). Drugs were dissolved in distilled deionized water. Acetylcholine solution in Krebs-Ringer bicarbonate (KRB) buffer was freshly prepared before each experiment.

2.2. Animals. Male and female Wistar rats (4 weeks of age, 150–170 g) from the Height Institute of Arturo Prat University of Iquique were used for this study. The animals were housed in light-cycled (8:00 to 20:00 hours) and temperature-controlled rooms. In addition, the rats were provided ad libitum access to drinking water and standard rat chow (Champion, Santiago). Since the female rats were sexually immature [20], no stages of the estrus cycle were observed by vaginal smear. In this study, 25 rats were randomly assigned into five groups of 5 animals each.

2.2.1. In Vivo Experiments. These include noninvasive blood pressure and ECG measurements. The oral treatment of animals consisted in a daily administration of a mixture of Q7 and/or ascorbate plus peanut butter for 20 days.

(i) Group 1 ($n = 5$; control) consists of rats treated with vehicle (peanut butter).

(ii) Group 2 ($n = 5$; Q7) consists of rats treated with Q7 (10 mg/kg).

(iii) Group 3 ($n = 5$; Q7 + Asc) consists of rats treated with Q7 (10 mg/kg) plus ascorbate (500 mg/kg).

(iv) Group 4 ($n = 5$; Asc) consists of rats treated with ascorbate (500 mg/kg).

2.2.2. In Vitro Experiments. This includes contractibility measurements in the isolated rat right atrium and thoracic aorta (Group 5, $n = 5$). Cytosolic calcium levels and H_2O_2 production were measured in rat cardiomyocytes and A7r5 cells. The tissues or cells were preincubated with Q7 (10^{-5} M) and/or ascorbate (0.125, 0.25, and 2 mM).

For groups 2, 3, and 4, the doses of Q7 and ascorbate were selected according to previous experiments using ECG of the normotensive rats in our laboratory and antitumor activity in mice was also observed [21]. For *in vitro* studies, the concentration of Q7 and ascorbate was selected according to our vascular reactivity experiments in the rat aorta [19].

The experiments of this study were conducted following the ARRIVE guidelines and Guide for the Care and Use of Laboratory Animals published by the National Institute of Health of the United States (NIH, publication revised in 2013) and the Ethics Committee of Arturo Prat University (CEC-17).

2.3. Blood Pressure and ECG Recording. The blood pressure and ECG measurements were simultaneously carried out on the rats, as previously described in our laboratory [22]. SBP was measured using the tail-cuff method (BIOPAC Systems) and AcqKnowledge 3.9.1 computer software program. The method of Erken et al. [23] was followed for measuring blood pressures. Animals were acclimatized for 20 min prior to the beginning of the experiment at room temperature (30–33°C). Then the pressure sensor cuffs and plethysmograph were placed on the tail of the animal. An average of 4 reading cycles of blood pressure measurements was made with the conscious animal per day.

For ECG recordings, the animals were anesthetized with ketamine (42 mg/kg, i.p.) and xylazine (5 mg/kg, i.p.). The needle electrodes were placed subcutaneously in bipolar configuration (DII). Measurements were done using the electrocardiographic amplifier (ECG100C BIOPAC) equipment and AcqKnowledge 3.9.1 computer software program.

2.4. Frequency of the Isolated Right Atrium. The isolated atrium experiment was carried out on rats as previously described in our laboratory [22]. The heart was isolated and placed in a cold (4°C) Krebs-Ringer bicarbonate (KRB) physiological buffered solution containing ($\times 10^{-3}$ M) 4.2 KCl, 1.19 KH_2PO_4, 120 NaCl, 25 Na_2HCO_3, 1.2 $MgSO_4$, 1.3 $CaCl_2$, and 5 D-glucose (pH 7.4, 37°C, 95% O_2, and 5% CO_2). The isolated right atrium of the rat was carefully fixed with a silk

thread into a moveable and static lever; the upper one was attached to an isometric transducer (Radnoti, California). PowerLab 8/35 (USA) was used for continuous recording of vascular tension (LabChart 8 program, ADInstruments). The passive tension of the atrium was 0.5 g.

2.5. Isolation of Neonatal Cardiac Myocytes. Neonatal rat cardiac myocytes were prepared as previously described [24]. Animals were decapitated and hearts were removed. Then atria were excised and the ventricles were minced in ice-cold PBS without Ca^{2+}/Mg^{2+}. Ventricular tissue was transferred to a new tube and subjected to overnight digestion (4°C, constant shaking) with 0.05% trypsin-EDTA solution (Gibco, NY, USA). A pelleted fraction was then subjected to digestion using collagenase type II (0.75 mg·mL^{-1}, 20 min) (Gibco, NY, USA). The collected enzyme solution was centrifuged, the supernatant was discarded, and the cardiac myocyte fraction was resuspended in a culture medium (DMEM high glucose/M199, 4 : 1) and preplated into a 60 mm dish for 1–3 hours. The preplating step removed fibroblasts and endothelial cells. Nonadherent cells were then collected, quantified, and plated in 2% gelatin-coated 35 mm glass bottom microdish (Ibidi GmbH, Munich, Germany). 3 μg/mL cytosine beta-D-arabinofuranoside was added to the culture medium for 12 hours to eliminate residual fibroblasts. Cultures were maintained in a humidified incubator at 37°C and 5% CO_2. Culture medium was changed every day.

2.6. Monitoring Cytosolic Ca^{2+} Signal on Isolation of Rat Neonatal Cardiac Myocytes. Cytosolic calcium was determined in rat neonatal cardiomyocytes according to Barría et al. [24]. The cells were washed with Krebs-Ringer bicarbonate buffer (KRB) containing ($\times 10^{-3}$ M) 4.2 KCl, 1.19 KH_2PO_4, 120 NaCl, 25 Na_2HCO_3, 1.2 $MgSO_4$, 1.3 $CaCl_2$, and 5 D-glucose (pH 7.4). Then they were loaded with 10^{-5} M Fluo-3 AM for 25 min at 37°C and then were again washed with KRB and incubated for 15 minutes at 37°C. Cells were studied in duplicate, preincubating for 20 min with Q7 (10^{-5} M) and/or ascorbate (2 mM) and then stimulating with phenylephrine (PE, 10^{-6} M). Fluo-3 fluorescence (506 nm excitation, 526 nm emission) was monitored every 5 seconds using a Leica TCS SP8 confocal microscope (Leica, Canada). Fluorescence intensity was analyzed by the ImageJ software (NIH software), which measured the selected region of interest (ROI). Fluorescence was expressed as arbitrary units, and for each value, the background intensity was subtracted.

2.7. Isolation of the Aortic Rings. Vascular reactivity was evaluated in the aortic rings according to Paredes et al. [25]. Rats were sacrificed by cervical dislocation. The thoracic aorta was quickly excised and placed in cold (4°C) physiological Krebs-Ringer bicarbonate buffer (KRB) containing ($\times 10^{-3}$ M) 4.2 KCl, 1.19 KH_2PO_4, 120 NaCl, 25 Na_2HCO_3, 1.2 $MgSO_4$, 1.3 $CaCl_2$, and 5 D-glucose and 1 liter of distilled water (pH 7.4). Rings (3-4 mm) were cut after connective tissue was cleaned out from the aorta, taking care to avoid endothelial damage. The aortic rings were equilibrated for 40 min in KRB at 37°C by constant bubbling with 95% O_2 and 5% CO_2.

2.8. Vascular Reactivity Experiments. To evaluate the vascular function of the endothelium, the vasodilation in response to 10^{-5} M ACh (muscarinic receptor agonist) in the precontracted aortic rings with 10^{-6} M PE was tested. According to the general use of the rat aorta as a pharmacological tool for *in vitro* analysis, the aortic rings were considered for a functional endothelial response if vasodilation was up to 70–80% [26]. Two aortic rings from the same animal were simultaneously studied in different organ baths, using different vasoactive substances (phenylephrine (PE), KCl, and acetylcholine (ACh)). The aortic rings were mounted on two 25-gauge stainless steel wires; the upper one was attached to an isometric transducer (Radnoti, California, USA). The volume of the organ bath was 10 mL. The transducer was connected to a PowerLab 8/35 (Colorado Springs, CO) for continuous recording of vascular tension using the LabChart Prov 8.1.2 computer program (ADInstruments). After the equilibration period for 40 min, the aortic rings were stabilized by three successive near-maximum contractions with KCl (6×10^{-2} M) for 10 min. The passive tension on the aortic rings was 1.0 g, which was determined with 6×10^{-2} M KCl [27].

2.9. Cytosolic Ca^{2+} Signal on Vascular Smooth Muscle Cell (A7r5). A7r5 cells were cultured in 35 mm culture dish according to the methodology described by Palacios et al. [19]. The cells were washed with Krebs-Ringer bicarbonate buffer (KRB) containing ($\times 10^{-3}$ M) 4.2 KCl, 1.19 KH_2PO_4, 120 NaCl, 25 Na_2HCO_3, 1.2 $MgSO_4$, 1.3 $CaCl_2$, and 5 D-glucose (pH 7.4). They were preincubated with 10^{-5} M Fluo-3 AM for 25 min at 37°C and then were again washed with KRB. Cells were studied in duplicate, preincubating for 20 min with Q7 (10^{-5} M) and/or ascorbate (2 mM) and then stimulating with phenylephrine (PE, 10^{-6} M). A fluorescence microplate reader equipped for excitation in the range of 506 nm and emission detection at 526 nm was used (Infinite® 200 TECAN (Männedorf, Switzerland).

2.10. Determination of Lipid Peroxidation Products in Serum. The thiobarbituric acid reactive substances (TBARS) were measured in serum of rat, according to Cifuentes et al. [27]. Briefly, 100 μL of the serum (10.9 ± 0.6 mg protein/mL) was taken and mixed with 200 μL of trichloroacetic acid 10% (TCA) and butylated hydroxytoluene 4% (BHT); this mixture was centrifuged, and then 140 μL of the supernatant was mixed with thiobarbituric acid (0.67%) and heated to 95°C for 1 hour. After cooling to room temperature, 280 μL of butanol-pyridine (15 : 1) was added and mixed and centrifuged at 3000g for 20 minutes; finally, the absorbance of the supernatant was measured at 532 nm in an Infinite 200 TECAN (Männedorf, Switzerland).

2.11. Determination of Superoxide Dismutase- (SOD-) Like Activity in Serum. The SOD-like activity in serum was determined according to the methodology by Marklund and Marklund [28]. Briefly, 20 μL of the serum (10.9 ± 0.6 mg protein/mL) was taken and mixed with 130 μL of 50 mM Tris-cacodylic acid buffer (pH 8.2), 20 μL of 1 mM EDTA, and 7 μL of pyrogallol (2 mM in 10 mM HCl). The absorbance

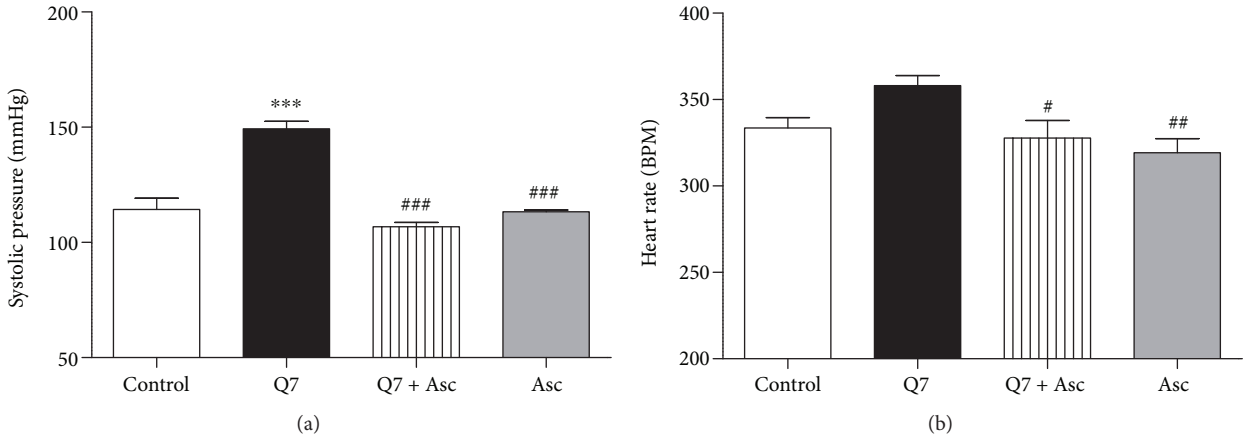

Figure 1: Hypotensive and bradycardic effects of ascorbate on normotensive rats chronically treated with Q7. The results show that oral administration of 500 mg/kg ascorbate (Asc) for 20 days decreased the systolic blood pressure (SBP) (a) and heart rate (HR) (b) in Q7-treated rats (10 mg/kg Q7). Values are mean ± standard error of the mean of 5 experiments in mmHg or BPM. Statistically significant differences: $^{***}p < 0.001$ versus control; $^{\#}p < 0.05$; $^{\#\#}p < 0.001$; and $^{\#\#\#}p < 0.01$ versus Q7.

was monitored at 420 nm and 37°C for 3 min with an Infinite 200 TECAN (Männedorf, Switzerland) against a reagent blank. The SOD-like activity was calculated as the change in absorbance per minute in the experimental sample versus the control sample. The SOD-like activity was expressed according to the equation $\% = (E - C) \times 100/E$, where E and C are autoxidation rates of pyrogallol in an experimental sample and control sample, respectively. When the activity was 100%, pyrogallol autoxidation was completely inhibited.

2.12. Determination of H_2O_2 in Vascular Smooth Muscle Cell. Vascular smooth muscle cells (A7r5) were cultured in petri dishes (35 mm). High-glucose and Dulbecco's modified Eagle's medium (DMEM) pyruvate was used as a medium culture. The Amplex® Red Kit (Invitrogen) was used for determination of H_2O_2 in culture cell, according to Song et al. [29]. The kit contains 10-acetyl-3,7-dihydroxyphenoxazine (Amplex Red) to detect H_2O_2. A fluorescence microplate reader equipped with Infinite 200 TECAN (Männedorf, Switzerland) for excitation in the range of 530–560 nm and emission detection at ~590 nm was used.

2.13. Statistical Analysis. GraphPad Prism 5 software was used, n represents the number of animals studied, and values were expressed as the mean ± standard error of the mean (SEM). For the statistical analysis of the groups, a one-way or two-way ANOVA was used as appropriate, followed by a Bonferroni post hoc test when necessary. A value p of <0.05 was considered statistically significant.

3. Results

3.1. Ascorbate Reverses the Increased Blood Pressure and Heart Rate Induced by Q7. To determine whether the findings of this study may have clinical implications, we measured arterial blood pressure in rats *in vivo*. As shown in Figure 1(a), the chronic treatment with Q7 (10 mg/kg) significantly increased the SBP compared to those of control rats (120 ± 1 mmHg control versus 149 ± 3 mmHg with Q7; $p < 0.001$). In contrast, chronic treatment with ascorbate (Asc) (500 mg/kg) after Q7 exposure significantly reduced the SBP (107 ± 2 mmHg with Q7 + Asc; $p < 0.001$), a similar value to that observed in rats treated with ascorbate alone (113 ± 1 mmHg with Asc; $p < 0.001$).

On the other hand, Figure 1(b) shows that chronic oral administration of ascorbate following Q7 treatment significantly reduced the heart rate (325 ± 6 BPM control versus 243 ± 3 BPM with Q7 + Asc; $p < 0.05$). Q7 treatment caused an increased HR compared with the control rats (364 ± 12 BPM with Q7).

3.2. Ascorbate Protects against the Negative Effect of Q7 on the Frequency of the Atrium. Although no mortality was detected in rats treated with Q7 at the dose used during this study, we found an elevation of ST segment observed in ECG from Q7-treated rats. As seen in Figure 2, oral administration of Q7 (10 mg/kg) significantly caused an elevation of ST segment (5.69 ± 0.36 mm control versus 16.58 ± 3.32 mm Q7 treated; $p < 0.001$). Ascorbate (500 mg/kg) decreased the elevation of ST segment in the presence of Q7 (6.75 ± 0.29 mm). We also evaluated the effect of ascorbate on the beating of the isolated rat atrium. As shown in Figure 3(a), acute treatment with 10^{-5} M Q7 induced an irregular beating of the isolated atrium of the rat, which was prevented when the isolated atria were preincubated with 2 mM ascorbate before addition of 10^{-5} M Q7 (Figure 3(b)).

3.3. Ascorbate Effects on the Increased Intracellular Calcium Induced by Q7 in the Cardiomyocytes. To investigate if the Q7-mediated effects were dependent on changes in intracellular calcium levels, we measured intracellular calcium levels in isolated rat cardiomyocytes. As shown in Figure 4, the administration of 10^{-5} M Q7 increased the intracellular calcium levels in rat cardiomyocytes, an effect that was not modified in the presence of 2 mM ascorbate. Moreover, an increase in intracellular calcium levels was also observed in cardiomyocytes perfused with 2 mM ascorbate but the

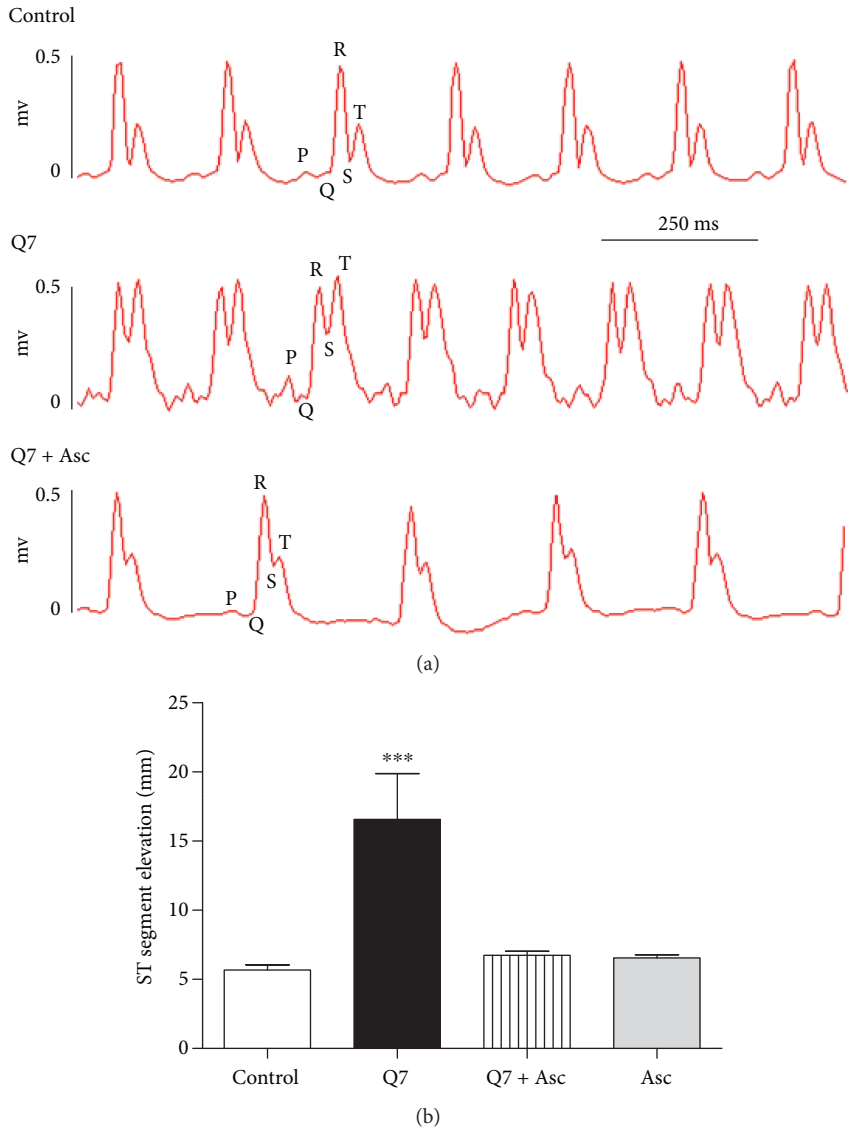

FIGURE 2: Original trace showing the electrocardiogram (a) and ST segment elevation in rats (b). Oral administration of ascorbate (500 mg/kg Asc) for 20 days decreased the ST segment elevation in Q7-treated rats (10 mg/kg Q7). Values are mean ± standard error of the mean of 5 experiments. Statistically significant differences: $^{***}p < 0.001$ versus control.

kinetics was substantially slower than that observed in response to Q7 (Figure 4(c)).

3.4. Ascorbate Improves the ACh-Induced Vasodilation and Decreases the Intracellular Calcium Level in the Presence of Q7 in the Rat Aorta. It is possible that the increase of blood pressure would occur through an increase of the vasoconstriction. Therefore, we analyzed the vascular response in the aortic rings of rats treated with Q7 and/or ascorbate. As shown in Figure 5(a), the vascular contractile response of the intact aortic rings to the alpha-adrenergic receptor agonist PE was significantly increased with Q7 (158 ± 11% control versus 228 ± 3% with Q7; PE 10^{-5} M; $p < 0.01$). Moreover, ascorbate slightly decreased the vascular contractile response to PE in the presence of Q7 (196 ± 10% with Q7 + Asc; PE 10^{-5} M). The aortic rings preincubated with 2 mM ascorbate (170 ± 8%) showed a similar response to PE compared with those of the control experiments.

We also assessed the endothelial ACh-induced vasodilatation in the intact aortic rings. As shown in Figure 5(b), the intact aortic rings in the presence of 2 mM ascorbate showed a complete relaxation in response to different doses of the muscarinic receptor agonist ACh (10^{-8} to 10^{-5} M). Preincubation of intact rings with 10^{-5} M Q7 significantly decreased the ACh-induced vasodilation (102 ± 6% control versus 28 ± 6% with Q7; ACh 10^{-5} M; $p < 0.001$). This negative effect of Q7 on the ACh-induced vasodilation was reverted, in part, by preincubation with ascorbate (65 ± 6% with Q7 + Asc; ACh 10^{-5} M). Nevertheless, sodium nitroprusside (SNP), a NO donor compound, caused a complete vasodilation even in the presence of 10^{-5} M Q7. These data were recently published from our laboratory [19].

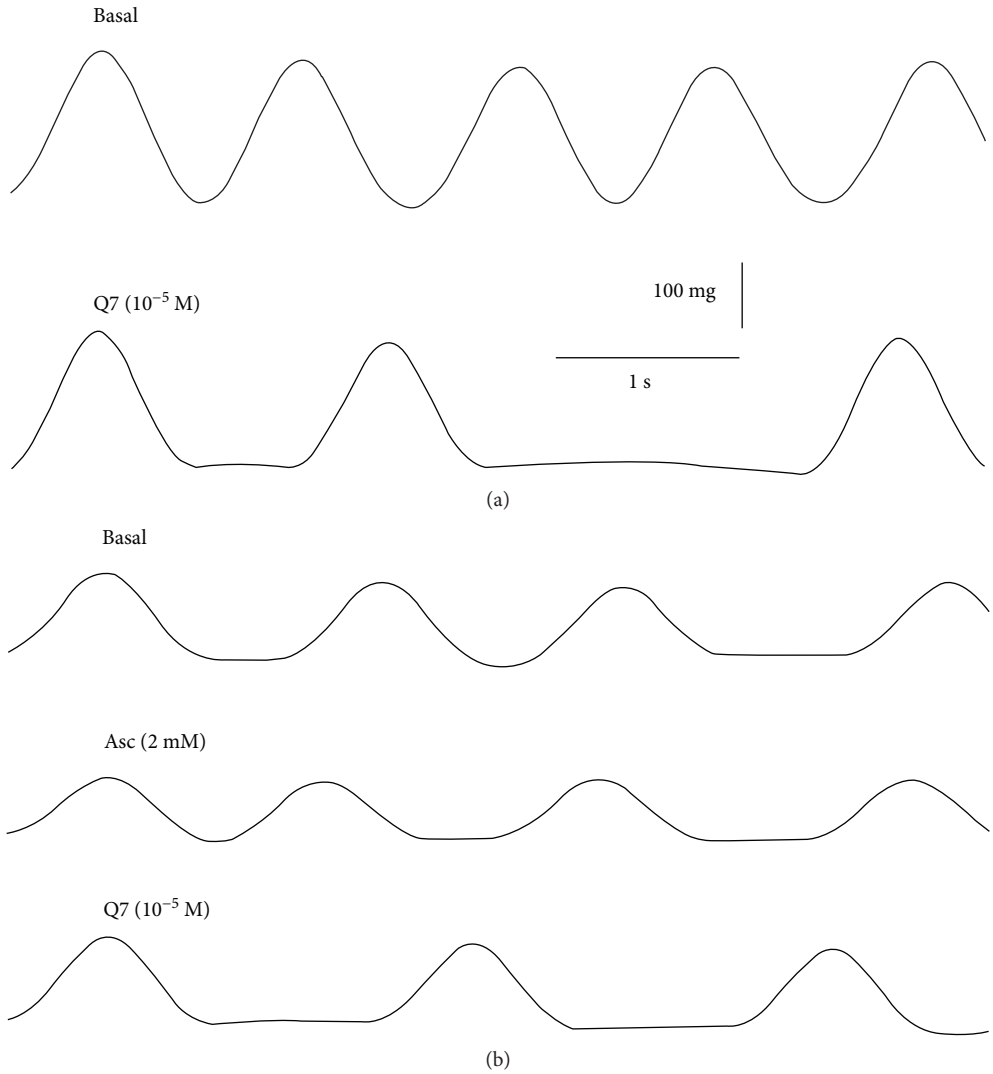

FIGURE 3: Original trace showing the time course of the frequency of the isolated right atrium. The addition of Q7 to the organ bath caused an irregular beating of the atrium (a), but the preincubation with 2 mM ascorbate before addition of 10^{-5} M Q7 induced regular-frequency beats of the atrium (b). Three independent experiments were performed.

In order to gain insight into the potential role of Q7 and ascorbate in the vascular contractile response to PE, determination of intracellular calcium was carried out in vascular smooth muscle cell culture (A7r5). We observed that preincubation of A7r5 cells with Q7 increased the intracellular calcium levels in response to 10^{-6} M PE (Table 1). In agreement with vascular contractile response to PE, preincubation with 2 mM ascorbate attenuated the increase in intracellular calcium levels caused by Q7. Ascorbate per se did not increase the intracellular calcium levels compared to control experiments (Table 1).

3.5. Increase of Oxidative Stress in Rats Treated with Q7: TBARS and SOD-Like Activity. Since 1,4-naphthoquinone derivatives produce oxidative stress, we analyzed the oxidative stress in serum samples from Q7-treated rats. TBARS assay and SOD-like activity were used as indicators of oxidative stress. As shown in Table 2, oral administration of Q7 significantly increased the TBARS in serum (26 ± 1 nM control versus 33 ± 2 nM Q7 treated; $p < 0.05$). In the same groups of animals, we confirmed that Q7 significantly decreased the SOD-like activity in serum ($159 \pm 49\%$ control versus $-193 \pm 100\%$ Q7 treated; $p < 0.05$). When the activity was ≥100%, pyrogallol autoxidation was completely inhibited, while the negative value means that adding Q7 accelerated it. Since the Q7 + Asc group did not significantly increase the TBARS level (Table 2) or decrease SOD-like activity in serum, suggesting that ascorbate treatment partially reduced the oxidative stress induced by Q7, the Asc-treated group did not show a significant increase in the TBARS level or decrease in SOD-like activity in serum samples compared to control samples.

3.6. Ascorbate, but Not Q7, Increases Production of H_2O_2 in A7r5 Cells. It has been suggested that Q7 induces ROS (O_2^- and H_2O_2) by a redox-cycling mechanism [11]. We measured H_2O_2 levels in A7r5 cells in response to Q7. As shown in Figure 6(a), Q7 (10^{-8} to 10^{-6} M) did not

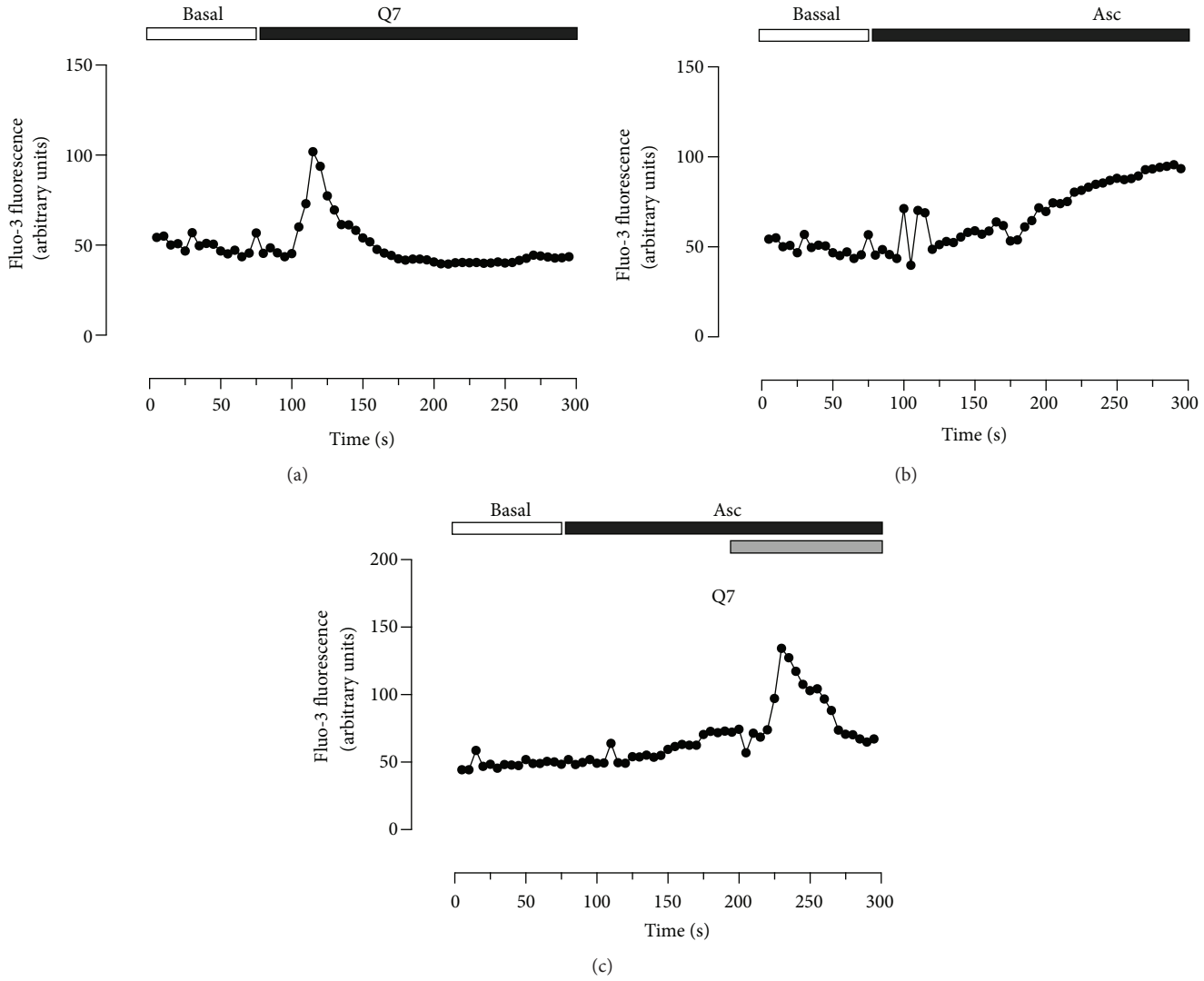

Figure 4: Effects of quinone and ascorbate on intracellular Ca^{2+} levels in rat cardiomyocytes. Quinone Q7 (10^{-5} M) increased intracellular calcium levels in rat cardiomyocytes (a), but ascorbate (Asc) (2 mM) did not prevent the increase of Q7-induced intracellular calcium (c). Effect of ascorbate on intracellular calcium levels in rat cardiomyocytes (b). Three independent experiments were performed.

increase the generation of H_2O_2 compared with basal levels (Figure 6(a)). However, ascorbate alone or in combination with Q7 (10^{-8} to 10^{-6} M) significantly increased ($p < 0.001$) the generation of H_2O_2 (0.21 ± 0.01 nM basal versus 2.76 ± 0.13 nM with 10^{-8} Q7; $p < 0.001$). Figure 6(b) shows that the effect of ascorbate on the generation of H_2O_2 was dose dependent (0.125, 0.25, and 2 mM).

4. Discussion

The focus of this study was to evaluate whether ascorbate counteracts the adverse cardiovascular effects and oxidative stress induced by a quinone derivative treatment. We found that oral treatment with ascorbate at physiological concentrations reduced the Q7-induced blood pressure in rats. This decrease in blood pressure was as a result of decreased HR and improved endothelial vasodilation in the intact aortic rings of the rat.

The increased Q7-induced SBP was significantly decreased after the treatment with ascorbate. The effect of Q7 is in agreement with other studies, which reported an increased SBP in juglone- (5-hydroxy-1,4-naphthoquinone-) treated mice for 14 days [30]. On the one hand, Q7 could increase the blood pressure by a mechanism dependent on oxidative stress. In fact, Q7 significantly increased lipid peroxidation (TBARS) and decreased the SOD-like activity in serum of rats. In previous studies, we demonstrated increased TBARS levels in rat aorta tissue [19] and in calf thymus DNA treated with Q7 [21]. These findings are in agreement with other reports showing that oral administration of high-dose ascorbate reduced the blood pressure and heart rate in dogs displaying ROS-induced myocardial damage [31].

It is possible that Q7-induced increase of blood pressure would occur through an increase of vasoconstriction or decrease of endothelial vasodilation. Q7 significantly increased the vascular contractile response to phenylephrine in the intact aortic rings and increased intracellular calcium

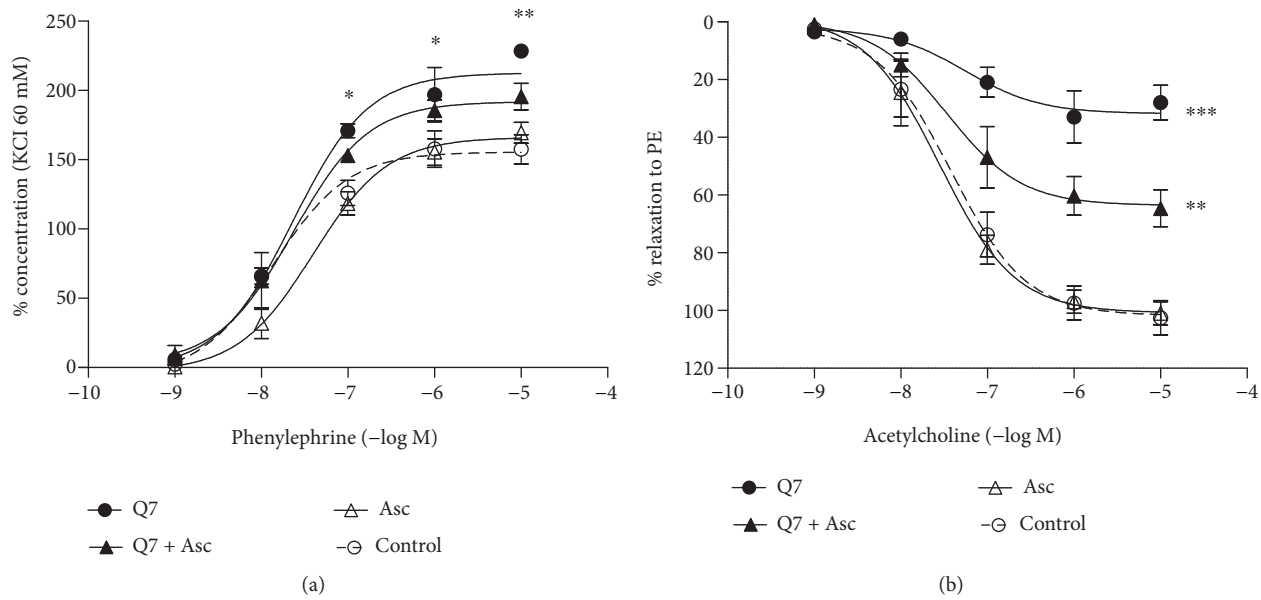

Figure 5: Effect of Q7 and ascorbate on the vascular response in the intact rat aorta. The quinone increased the contractile response to PE and impaired ACh-induced vasodilation. The concentration-response curves to PE (10^{-9} to 10^{-5} M) (a) and ACh (10^{-9} to 10^{-5} M) in the intact aortic rings of rats (b) in the presence or absence (control) of 10^{-5} M Q7 or 2 mM ascorbate (Asc). Arteries were preincubated with Q7 or ascorbate for 30 min. Values are mean ± standard error of the mean of 5 experiments. Statistically significant differences: $^{*}p < 0.05$, $^{**}p < 0.01$, and $^{***}p < 0.001$ versus control.

Table 1: Ascorbate decreases intracellular calcium levels in the presence of Q7 in vascular smooth muscle cells (A7r5). The A7r5 cells were preincubated with 10^{-5} M Q7 and/or 2 mM ascorbate (Asc) for 20 min.

	Control	Q7	Q7+Asc	Asc
Ca^{2+} signal (Fluo-3 fluorescence)	209 ± 15	296 ± 23*	230 ± 16	201 ± 10

Values are mean ± standard error of the mean of 3 experiments. Statistically significant differences: $^{*}p < 0.05$ versus control.

Table 2: Oral treatment with Q7 causes oxidative stress in rats. The SOD-like activity represents the autoxidation rate of pyrogallol in an experimental sample and control sample. When the activity is ≥100%, pyrogallol autoxidation is completely inhibited, while the negative value means that it is accelerated by adding Q7.

	Control	Q7	Q7 + Asc	Asc
TBARS (nM)	26 ± 1	33 ± 2*	30 ± 3	25 ± 1
SOD-like activity (%)	159 ± 49	−193 ± 100*	−36 ± 10	150 ± 39

Values are mean ± standard error of the mean of 5 experiments. Statistically significant differences: $^{*}p < 0.05$ versus control.

levels in vascular smooth muscle cells (A7r5). Interestingly, the preincubation with ascorbate before addition of Q7 blunted the increase of intracellular calcium caused by Q7 and significantly improved the endothelial vasodilation in the intact aortic rings of the rat. We observed that ACh-induced endothelial vasodilation was significantly decreased by Q7 but the vasodilation was reestablished with the addition of SNP (a NO donor) into intact rat aorta preparations in previously published data [19]. In the same previous study, we demonstrated that Q7 significantly reduced the ACh-induced NO generation in the intact aortic rings [19]. Other studies had reported that the preincubation of mouse aortic rings with 10^{-5} M juglone (5-hydroxy-1,4-naphthoquinone) decreased NO- and ACh-induced relaxation [30] and incubation of rat aortic rings with ascorbate restored vasodilation in L-nitro-L-arginine hypertensive rats [32].

Oxidative stress caused by Q7 is due to ROS generation through a redox-cycling mechanism [11]. The anion superoxide (O_2^-) induced by Q7 would react with endothelial NO and could produce peroxynitrite ($ONOO^-$). Quinones (i.e., doxorubicin and menadione) increase the generation of ROS, leading to the scavenging of NO [33–35]. Therefore, the decrease in the bioavailability of endothelial NO in blood vessels can explain the increase of the blood pressure as described above [19].

Ascorbate acts as a powerful antioxidant decreasing the oxidative stress in blood vessels by blunting the generation of ROS. Reduced levels of hydroxyl radical (HO^-) and O_2^- would result in a higher bioavailability of endothelial NO [17]. This is in agreement with reports that ascorbate reduces the level of ROS and improves the endothelial vasodilation in chronic smokers [36].

We found that oral treatment of rats with ascorbate attenuated the elevation of ST segment in ECG and irregular beating of the atrium induced by Q7. The elevation of ST

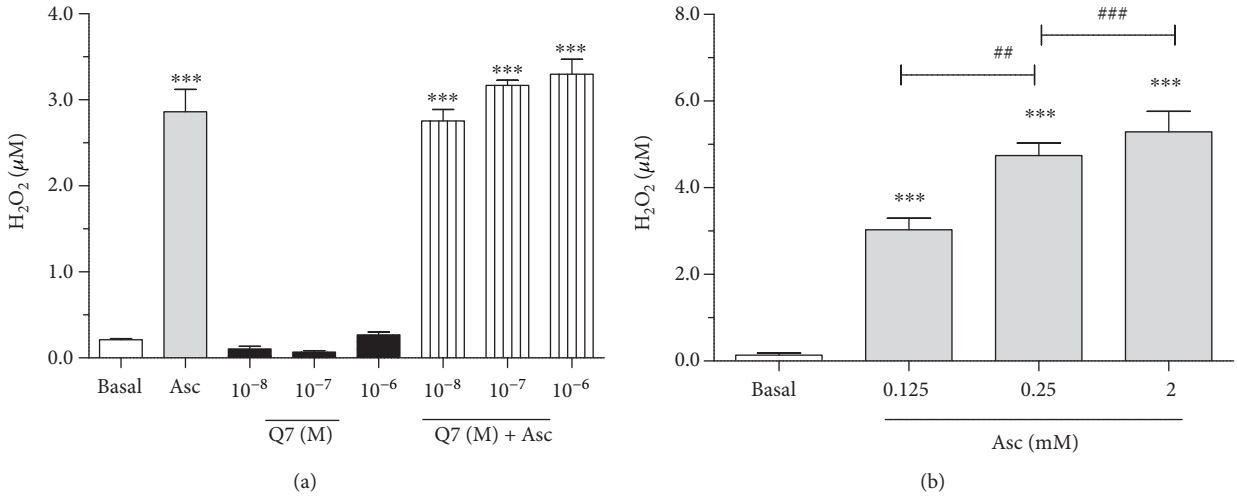

FIGURE 6: Effect of ascorbate and Q7 on the production of H_2O_2 in vascular smooth muscle cells (A7r5). The data shows the H_2O_2 generation in the presence of ascorbate and Q7 in A7r5 cells (a) and the effect of increasing doses of ascorbate on H_2O_2 generation (b). Ascorbate increased significantly the generation of H_2O_2 in a dose-dependent manner in A7r5 cells, while Q7 did not cause any change. Values are mean ± standard error of the mean of 3 experiments. Statistically significant differences: $^{***}p < 0.001$ versus basal; $^{\#\#}p < 0.01$, and $^{\#\#\#}p < 0.001$ versus 0.125 mM Asc.

segment represents a partial depolarization in the damaged cells of the heart, compared with the healthy myocardium [37]. Others studies reported that melatonin decreases the elevation of the ST segment on adriamycin-induced cardiotoxicity in rats [38]. To investigate if the cardiac activity in the presence of Q7 could be modulated by changes in intracellular calcium, further experiments were conducted in neonatal rat cardiac myocytes. The results showed that Q7 increased the intracellular calcium levels in rat cardiomyocytes and this Q7-mediated effect was not prevented by preincubation with ascorbate. Conversely, studies have shown that the preincubation with salvianolic acid B for 6 h prevented the doxorubicin-induced increase of the intracellular calcium levels and contractility in cardiomyocytes of rats [39]. Our results do not show a similar effect as that reported for salvianolic acid B, although it could be due to the lower preincubation time used in our experiments (few seconds prior to Q7 addition).

Since 1,4-naphthoquinone induces ROS by a redox-cycling mechanism [11] and Q7 is a 1,4-naphthoquinone derivative, the levels of TBARS, SOD-like activity, and H_2O_2 were determined in our experimental models. Although Q7 significantly increased oxidative stress (increased TBARS and decreased SOD-like activity) in serum samples of treated rats, it did not increase the production of H_2O_2 in vascular smooth muscle cells of the rat aorta (A7r5). Therefore, our data suggest that Q7 generated O_2^- and increased TBARS, but not H_2O_2. One explanation is that the formation of O_2^- and H_2O_2 induced by Q7 does not occur simultaneously. Alternatively, the low activity levels of superoxide dismutase enzyme (SOD) in cultured cells could mask the generation of H_2O_2 by Q7 [40], although this is unlikely as Q7 decreased SOD-like activity in serum samples.

Our results showed that high concentrations of ascorbate (0.125, 0.25, and 2 mM) significantly increased the generation of H_2O_2 in a dose-dependent manner in A7r5 cells. The formulation of culture medium (Dulbecco's modified Eagle's medium (DMEM)) has iron (0.25 mM Fe $(NO_3)_3$), which may act as an essential catalyzer through the process of autoxidation of ascorbate, leading to the higher generation of H_2O_2 [41].

Therefore, the route of administration of ascorbate is very important because of the potential generation of ROS. Intravenous infusion of high doses of ascorbate will increase the generation of ROS in the presence of serum iron; as such, ascorbate is considered a prooxidant substance [42] and useful for cancer treatment. Intraperitoneal or intravenous administration of ascorbate could peak concentrations between 3 and 8 mM in blood samples from rats [43]. In contrast, oral administration of high doses of ascorbate would achieve peaks up to 150 M in blood samples from rats [44].

We found that oral administration of ascorbate prevented the increase of Q7-induced TBARS levels and the decrease of SOD-like activity when compared to the Q7-treated group. The 4-hydroxyaniline substituent in Q7 has a low electron donating capacity and is similar to 1,4-naphthoquinone [45], leading to a lower O_2^- formation. In contrast, menadione (2-methyl-1,4-naphthoquinone) has a high electron donating capacity, leading to a higher O_2^- formation [40]. Our findings of TBARS levels and SOD-like activity could be attributed to the partial stabilization of the semiquinone radical species of Q7 by ascorbate, causing a change of redox-cycling process and a lower ROS generation.

In conclusion, oral treatment with ascorbate reduced the Q7-induced increase in blood pressure. This finding is consistent with a putative model in which ascorbate decreased the heart rate and improved endothelial vasodilation in quinone-treated rats. These are possibly mediated by an increase of the endothelial NO bioavailability and reduced calcium-dependent vascular contractile response in vascular smooth muscle cells. These results suggest an *in vivo* cardioprotective effect of oral ascorbate in animals treated with

naphthoquinone derivative, which is dependent on oxidative stress. *In vivo*, ascorbate partially reduced the Q7-induced oxidative stress. These findings could have interesting and potential clinical effects for a number of pathologies such as inflammatory disorders, diabetic blindness, cardiovascular and autoimmune diseases, and cancer [46]. More studies with naphthoquinones on cancer models may provide a better understanding of the mechanism underlying the amelioration of cardioprotection by ascorbate.

Data Availability

The data used to support the findings of this study are available from the corresponding author upon request.

Conflicts of Interest

The authors declare no conflict of interests.

Acknowledgments

Financial support by Universidad Arturo Prat (Iquique, Chile; VRIIP0006-17 and VRIIP0209-17 to Javier Palacios) and Universidad de Antofagasta (Antofagasta, Chile), Network for Extreme Environments Research project (NEXER), is gratefully acknowledged. This work was supported by a MINEDUC-UA project Code ANT 1755 to José Luis Vega. Iván Barría holds a CONICYT PhD fellowship, Chile. The authors are grateful to Dr. Marcelo Catalán and Dr. Pedro Buc-Calderon for the useful commentaries to improve the manuscript and Dr. Patricia Siqués and Dr. Julio Brito from the Institute of Health Studies, Universidad Arturo Prat, for the animals.

References

[1] S. L. de Castro, F. S. Emery, and E. N. da Silva Júnior, "Synthesis of quinoidal molecules: strategies towards bioactive compounds with an emphasis on lapachones," *European Journal of Medicinal Chemistry*, vol. 69, pp. 678–700, 2013.

[2] P. Kovacic and R. Somanathan, "Recent developments in the mechanism of anticancer agents based on electron transfer, reactive oxygen species and oxidative stress," *Anti-Cancer Agents in Medicinal Chemistry*, vol. 11, no. 7, pp. 658–668, 2011.

[3] E. M. Malik and C. E. Müller, "Anthraquinones as pharmacological tools and drugs," *Medicinal Research Reviews*, vol. 36, no. 4, pp. 705–748, 2016.

[4] V. K. Tandon and S. Kumar, "Recent development on naphthoquinone derivatives and their therapeutic applications as anticancer agents," *Expert Opinion on Therapeutic Patents*, vol. 23, no. 9, pp. 1087–1108, 2013.

[5] A. Jemal, R. Siegel, J. Xu, and E. Ward, "Cancer statistics, 2010," *CA: A Cancer Journal for Clinicians*, vol. 60, no. 5, pp. 277–300, 2010.

[6] E. T. H. Yeh and H. M. Chang, "Oncocardiology—past, present, and future: a review," *JAMA Cardiology*, vol. 1, no. 9, pp. 1066–1072, 2016.

[7] D. Cappetta, F. Rossi, E. Piegari et al., "Doxorubicin targets multiple players: a new view of an old problem," *Pharmacological Research*, vol. 127, pp. 4–14, 2018.

[8] L. Tabrizi and H. Chiniforoshan, "Designing new iridium(III) arene complexes of naphthoquinone derivatives as anticancer agents: a structure–activity relationship study," *Dalton Transactions*, vol. 46, no. 7, pp. 2339–2349, 2017.

[9] J. L. Bolton, M. A. Trush, T. M. Penning, G. Dryhurst, and T. J. Monks, "Role of quinones in toxicology," *Chemical Research in Toxicology*, vol. 13, no. 3, pp. 135–160, 2000.

[10] P. J. O'Brien, "Molecular mechanisms of quinone cytotoxicity," *Chemico-Biological Interactions*, vol. 80, no. 1, pp. 1–41, 1991.

[11] Y. Shang, C. Chen, Y. Li, J. Zhao, and T. Zhu, "Hydroxyl radical generation mechanism during the redox cycling process of 1,4-naphthoquinone," *Environmental Science & Technology*, vol. 46, no. 5, pp. 2935–2942, 2012.

[12] I. Wilson, P. Wardman, T. S. Lin, and A. C. Sartorelli, "One-electron reduction of 2- and 6-methyl-1,4-naphthoquinone bioreductive alkylating agents," *Journal of Medicinal Chemistry*, vol. 29, no. 8, pp. 1381–1384, 1986.

[13] O. A. Alshabanah, M. M. Hafez, M. M. Al-Harbi et al., "Doxorubicin toxicity can be ameliorated during antioxidant L-carnitine supplementation," *Oxidative Medicine and Cellular Longevity*, vol. 3, no. 6, 433 pages, 2010.

[14] R. E. L. Cabral, T. B. Mendes, V. Vendramini, and S. M. Miraglia, "Carnitine partially improves oxidative stress, acrosome integrity, and reproductive competence in doxorubicin-treated rats," *Andrology*, vol. 6, no. 1, pp. 236–246, 2018.

[15] G. Akolkar, D. da Silva Dias, P. Ayyappan et al., "Vitamin C mitigates oxidative/nitrosative stress and inflammation in doxorubicin-induced cardiomyopathy," *American Journal of Physiology-Heart and Circulatory Physiology*, vol. 313, no. 4, pp. H795–H809, 2017.

[16] A. I. Abushouk, A. Ismail, A. M. A. Salem, A. M. Afifi, and M. M. Abdel-Daim, "Cardioprotective mechanisms of phytochemicals against doxorubicin-induced cardiotoxicity," *Biomedicine & Pharmacotherapy*, vol. 90, pp. 935–946, 2017.

[17] A. Mortensen and J. Lykkesfeldt, "Does vitamin C enhance nitric oxide bioavailability in a tetrahydrobiopterin-dependent manner? In vitro, in vivo and clinical studies," *Nitric Oxide*, vol. 36, pp. 51–57, 2014.

[18] G. R. Buettner, "The pecking order of free radicals and antioxidants: lipid peroxidation, alpha-tocopherol, and ascorbate," *Archives of Biochemistry and Biophysics*, vol. 300, no. 2, pp. 535–543, 1993.

[19] J. Palacios, F. Cifuentes, J. A. Valderrama et al., "Modulatory effect of 2-(4-hydroxyphenyl)amino-1,4-naphthoquinone on endothelial vasodilation in rat aorta," *Oxidative Medicine and Cellular Longevity*, vol. 2016, Article ID 3939540, 12 pages, 2016.

[20] P. Sengupta, "The laboratory rat: relating its age with human's," *International Journal of Preventive Medicine*, vol. 4, no. 6, pp. 624–630, 2013.

[21] F. Ourique, M. R. Kviecinski, K. B. Felipe et al., "DNA damage and inhibition of Akt pathway in MCF-7 cells and Ehrlich tumor in mice treated with 1,4-naphthoquinones in combination with ascorbate," *Oxidative Medicine and Cellular Longevity*, vol. 2015, Article ID 495305, 10 pages, 2015.

[22] F. Cifuentes, A. Paredes, J. Palacios et al., "Hypotensive and antihypertensive effects of a hydroalcoholic extract from *Senecio nutans* Sch. Bip. (Compositae) in mice: chronotropic and negative inotropic effect, a nifedipine-like action," *Journal of Ethnopharmacology*, vol. 179, pp. 367–374, 2016.

[23] H. A. Erken, G. Erken, and O. Genç, "Blood pressure measurement in freely moving rats by the tail cuff method," *Clinical and Experimental Hypertension*, vol. 35, no. 1, pp. 11–15, 2013.

[24] I. Barría, J. Güiza, F. Cifuentes et al., "*Trypanosoma cruzi* infection induces pannexin-1 channel opening in cardiac myocytes," *The American Journal of Tropical Medicine and Hygiene*, vol. 98, no. 1, pp. 105–112, 2018.

[25] A. Paredes, J. Palacios, C. Quispe et al., "Hydroalcoholic extract and pure compounds from *Senecio nutans* Sch. Bip (Compositae) induce vasodilation in rat aorta through endothelium-dependent and independent mechanisms," *Journal of Ethnopharmacology*, vol. 192, pp. 99–107, 2016.

[26] M. Rameshrad, H. Babaei, Y. Azarmi, and D. F. Fouladi, "Rat aorta as a pharmacological tool for in vitro and in vivo studies," *Life Sciences*, vol. 145, pp. 190–204, 2016.

[27] F. Cifuentes, J. Bravo, M. Norambuena, S. Stegen, A. Ayavire, and J. Palacios, "Chronic exposure to arsenic in tap water reduces acetylcholine-induced relaxation in the aorta and increases oxidative stress in female rats," *International Journal of Toxicology*, vol. 28, no. 6, pp. 534–541, 2009.

[28] S. Marklund and G. Marklund, "Involvement of the superoxide anion radical in the autoxidation of pyrogallol and a convenient assay for superoxide dismutase," *European Journal of Biochemistry*, vol. 47, no. 3, pp. 469–474, 1974.

[29] C. Song, A. B. Al-Mehdi, and A. B. Fisher, "An immediate endothelial cell signaling response to lung ischemia," *American Journal of Physiology-Lung Cellular and Molecular Physiology*, vol. 281, no. 4, pp. L993–L1000, 2001.

[30] V. L. Chiasson, N. Munshi, P. Chatterjee, K. J. Young, and B. M. Mitchell, "Pin1 deficiency causes endothelial dysfunction and hypertension," *Hypertension*, vol. 58, no. 3, pp. 431–438, 2011.

[31] Y. Nishinaka, S. Sugiyama, M. Yokota, H. Saito, and T. Ozawa, "The effects of a high dose of ascorbate on ischemia-reperfusion-induced mitochondrial dysfunction in canine hearts," *Heart and Vessels*, vol. 7, no. 1, pp. 18–23, 1992.

[32] B. M. Mitchell, A. M. Dorrance, A. Ergul, and R. C. Webb, "Sepiapterin decreases vasorelaxation in nitric oxide synthase inhibition–induced hypertension," *Journal of Cardiovascular Pharmacology*, vol. 43, no. 1, pp. 93–98, 2004.

[33] J. Vásquez-Vivar, P. Martasek, N. Hogg, B. S. S. Masters, K. A. Pritchard, and B. Kalyanaraman, "Endothelial nitric oxide synthase-dependent superoxide generation from adriamycin," *Biochemistry*, vol. 36, no. 38, pp. 11293–11297, 1997.

[34] O. N. Bae, K. M. Lim, J. Y. Han et al., "U-shaped dose response in vasomotor tone: a mixed result of heterogenic response of multiple cells to xenobiotics," *Toxicological Sciences*, vol. 103, no. 1, pp. 181–190, 2008.

[35] C. Gerassimou, A. Kotanidou, Z. Zhou, D. D. C. Simoes, C. Roussos, and A. Papapetropoulos, "Regulation of the expression of soluble guanylyl cyclase by reactive oxygen species," *British Journal of Pharmacology*, vol. 150, no. 8, pp. 1084–1091, 2007.

[36] T. Heitzer, H. Just, and T. Münzel, "Antioxidant vitamin C improves endothelial dysfunction in chronic smokers," *Circulation*, vol. 94, no. 1, pp. 6–9, 1996.

[37] G. X. Yan, R. S. Lankipalli, J. F. Burke, S. Musco, and P. R. Kowey, "Ventricular repolarization components on the electrocardiogram: cellular basis and clinical significance," *Journal of the American College of Cardiology*, vol. 42, no. 3, pp. 401–409, 2003.

[38] A. Bilginoğlu, D. Aydın, S. Ozsoy, and H. Aygün, "Protective effect of melatonin on adriamycin-induced cardiotoxicity in rats," *Türk Kardiyoloji Derneği Arşivi*, vol. 42, no. 3, pp. 265–273, 2014.

[39] R. C. Chen, G. B. Sun, J. X. Ye, J. Wang, M. D. Zhang, and X. B. Sun, "Salvianolic acid B attenuates doxorubicin-induced ER stress by inhibiting TRPC3 and TRPC6 mediated Ca^{2+} overload in rat cardiomyocytes," *Toxicology Letters*, vol. 276, pp. 21–30, 2017.

[40] L. O. Klotz, X. Hou, and C. Jacob, "1,4-naphthoquinones: from oxidative damage to cellular and inter-cellular signaling," *Molecules*, vol. 19, no. 9, pp. 14902–14918, 2014.

[41] M. V. Clément, J. Ramalingam, L. H. Long, and B. Halliwell, "The in vitro cytotoxicity of ascorbate depends on the culture medium used to perform the assay and involves hydrogen peroxide," *Antioxidants & Redox Signaling*, vol. 3, no. 1, pp. 157–163, 2001.

[42] J. Du, J. J. Cullen, and G. R. Buettner, "Ascorbic acid: chemistry, biology and the treatment of cancer," *Biochimica et Biophysica Acta (BBA) - Reviews on Cancer*, vol. 1826, no. 2, pp. 443–457, 2012.

[43] L. H. Long and B. Halliwell, "Artefacts in cell culture: pyruvate as a scavenger of hydrogen peroxide generated by ascorbate or epigallocatechin gallate in cell culture media," *Biochemical and Biophysical Research Communications*, vol. 388, no. 4, pp. 700–704, 2009.

[44] Q. Chen, M. G. Espey, A. Y. Sun et al., "Ascorbate in pharmacologic concentrations selectively generates ascorbate radical and hydrogen peroxide in extracellular fluid in vivo," *Proceedings of the National Academy of Sciences of the United States of America*, vol. 104, no. 21, pp. 8749–8754, 2007.

[45] J. Benites, J. A. Valderrama, K. Bettega, R. C. Pedrosa, P. B. Calderon, and J. Verrax, "Biological evaluation of donor-acceptor aminonaphthoquinones as antitumor agents," *European Journal of Medicinal Chemistry*, vol. 45, no. 12, pp. 6052–6057, 2010.

[46] E. Aranda and G. I. Owen, "A semi-quantitative assay to screen for angiogenic compounds and compounds with angiogenic potential using the EA.hy926 endothelial cell line," *Biological Research*, vol. 42, no. 3, pp. 377–389, 2009.

Hindawi
Oxidative Medicine and Cellular Longevity
Volume 2018, Article ID 1261356, 12 pages
https://doi.org/10.1155/2018/1261356

Research Article

Protective Effects of Fullerene C_{60} Nanoparticles and Virgin Olive Oil against Genotoxicity Induced by Cyclophosphamide in Rats

Fayza M. Aly,[1] Amnah Othman,[2] and Mohie A. M. Haridy[3]

[1]*Department of Zoology, Faculty of Science, South Valley University, Qena 83523, Egypt*
[2]*Leibniz-Institut für Analytische Wissenschaften-ISAS-e.V., Bunsen-Kirchhoff-Straße 11, 44139 Dortmund, Germany*
[3]*Department of Pathology & Clinical Pathology, Faculty of Veterinary Medicine, South Valley University, Qena 83523, Egypt*

Correspondence should be addressed to Mohie A. M. Haridy; mohieharidy@svu.edu.eg

Received 10 March 2018; Revised 4 April 2018; Accepted 11 April 2018; Published 15 July 2018

Academic Editor: Simona G. Bungău

The potential effects of the fullerene C_{60} nanoparticle (C_{60}) as well as virgin olive oil (VOO) against the cyclophosphamide- (CP-) induced cytotoxic and mutagenic effects were evaluated by two main methods: molecular intersimple sequence repeat (ISSR) assay and cytogenetic biomarkers. Thirty adult male rats were divided to five groups (control, CP, C_{60}, CP + C_{60}, and CP + VOO). CP was i.p. injected with a single dose of 200 mg/kg; C_{60} and VOO were given orally (4 mg/kg dissolved in VOO and 1 ml, resp.) in alternative days for 20 days. The ISSR analysis revealed an increased in the DNA fragmentation level for liver and heart tissues represented by 21.2% and 32.6%, respectively, in the CP group. The DNA polymorphism levels were modulated and improved in CP + C_{60} (8.9% and 12%) and CP + VOO (9.8% and 12.7%) for hepatic and cardiac tissues, respectively. The bone marrow cytogenetic analysis revealed that C_{60} and VOO had significantly decreased the frequency of CP-induced chromosomal aberrations (chromosomal ring, deletion, dicentric chromosome, fragmentation, and polyploidy). Fullerene C_{60} and VOO have ability to reduce DNA damage and decrease chromosomal aberrations. In conclusion, fullerene C_{60} and VOO have protective effects against the CP-induced mutagenicity and genotoxicity. Fullerene C_{60} and VOO open an interesting field concerning their potential antigenotoxic agents against deleterious side effects of chemotherapeutics.

1. Introduction

Commonly used anticancer agents, for example, cyclophosphamide, are implicated as mutagenic agents against mammalian cells *in vivo* and *in vitro* [1, 2]. Cyclophosphamide causes cytotoxicity to normal cells in spite of its effective anticancer alkylating agent [3]. The active metabolites of cyclophosphamide, for example, phosphoramide mustard and acrolein, are responsible for accumulation of reactive oxygen species resulting in fragmentation of the DNA strand and an increasing in mutagenic DNA effects [4, 5]. The activated CP metabolites are responsible for inducing damage to DNA, RNA, proteins, and cytoplasmic membranes [6, 7]. Therefore, it is necessary to investigate an effective antioxidant that prevents the oxidative DNA damage and reduces the side effects of CP and other chemotherapeutic agents.

Recently, carbon nanotubes, especially fullerene, have received considerable attention in the field of biomedical research and applications due to their distinct electrical properties. The interactions between carbon nanotubes, proteins, nucleic acids, and cell membranes as well as their mutagenicity and antimutagenicity assays have been investigated in order to discover potential antimutagen and anticarcinogen potentials [8]. Evaluation of chromosomal aberration is an effective assay to detect the occurrence of the genotoxicity. Detection of chromosomal aberration is an indicator for an organism exposure to the genotoxic agent and the occurrence of DNA damage. Various types of mutagens can induce structural chromosomal aberrations via DNA strand breaks that may elevate the risk of developing tumors [9, 10]. It is necessary to approve potential drugs that can be used in protection and amelioration of cytotoxicity and DNA damage. The genotoxic effect of fullerene C_{60} (C_{60}) is controversial. C_{60} has genotoxic activity resulting in breaks of the DNA strand as well as oxidative damages of DNA in a concentration-dependent manner. The basic mechanisms of

its toxic effect are lipid peroxidation, oxidative stress dissemination, and genotoxicity [11–13]. It was found that C_{60} toxicity depends on their surface modifications, synthesis, concentration in the medium, and processing conditions. On the other hand, numerous studies found no mutagenic effect of C_{60} fullerene *in vivo* and *in vitro* [14–17]. C_{60} fullerene nanoparticle does not possess any genotoxic effect towards human lymphocytes. C_{60} was used in combination with doxorubicin (one of the most common anticancer therapeutic agents); C_{60} reduced the genotoxic effect of doxorubicin in healthy human lymphocytes [18]. Furthermore, C_{60} possesses an ability to prevent oxidative stress dissemination due to the nanosize [19, 20].

Olive oil-containing meals reduce the risk of many diseases and malignant tumors, as they have antioxidative, anti-inflammatory, and anticarcinogenic effects [21]. Oleuropein and hydroxytyrosol are important components of virgin olive oil (VOO); they have anticancer activity through reducing DNA oxidation, arresting the cell cycle, and inducing apoptosis in tumor cells [22]. High consumption of VOO in the Mediterranean diet has been suggested to be responsible for protection of DNA against perioxidation and hence reduction in cancer incidence. So, it was found that DNA and RNA oxidation in Northern European regions is higher compared with that in central and Southern regions. These findings support the assumption that VOO consumption may explain the decreased incidence of cancer in south European than those in North regions [23]. It is necessary to investigate the effect of C_{60} nanoparticle and VOO separately and in combination against CP-induced genotoxicity. Therefore, the objective of this study is to assess the effect of C_{60} as well as VOO on CP-induced genotoxicity in rats based on detection of DNA damage by intersimple sequence repeat (ISSR) analysis of liver and heart tissues and detection of chromosomal aberrations in bone marrow cells by mitotic analysis technique.

2. Materials and Methods

2.1. Animals, Experimental Design, and Sampling. Thirty male albino rats (weighing 180–200 g, 2-month old) were housed in Animal House Facility (South Valley University, Qena, Egypt). Rats were housed under normal nutritional and laboratory conditions for one week for acclimatization. Animals were kept in the ventilated room under controlled laboratory conditions of normal light-dark cycle (12 h light/dark) and temperature (25 ± 2°C). Food and water were provided ad libitum. Rats were divided into 5 groups ($n = 6$ rats each group) as follows: (i) control group received placebo intraperitoneal (i.p.) injection; (ii) CP group was injected i.p. with a single dose of CP (200 mg/kg dissolved in 2 ml distilled water (DW)); (iii) C_{60} group was given orally of C_{60} (4 mg/kg dissolved in 1 ml VOO) in alternative days for 20 days according to [24, 25]; (iv) CP + C_{60} group was injected i.p. with a single dose of CP (200 mg/kg dissolved in 2 ml DW) and given orally 4 mg/kg dissolved in 1 ml VOO of C_{60} in alternative days for 20 days; and (v) CP + VOO group was injected i.p. with a single dose of CP (200 mg/kg dissolved in 2 ml DW and treated orally with VOO (1 ml in alternative days for 20 days). The experimental animal protocols were carried out by following the guidelines for animal care and were approved by the Ethical Animal Care and Use Committee from the Faculty of Veterinary Medicine, South Valley University, Egypt (application number: VetEg.0465R-2017-2018). After 45 days, the treatments were stopped and rats were left for 24 hours, then three animals from each group were sacrificed. Efforts were maximized to minimize pain suffering of animals. The animals were scarified by cervical dislocation under deep anesthesia using diethyl ether. The whole liver and heart were collected in Carnoy's solution for fixation and frozen at −80°C until used for DNA extraction. Bone marrow aspiration for cytogenetic analysis was performed in all rats.

2.2. Chemicals and Fullerene C_{60} Preparation. Cyclophosphamide (Endoxan) was delivered as vials (Baxter Oncology, Halle, Germany), and VOO was commercially purchased (Colavita Extra Virgin Olive Oil Company, New Jersey, USA). Mixture of fullerene C_{60} (99.9% purity) (Shanghai Boyle Chemical Co. Ltd., China) and VOO was prepared according to Baati et al. [24] and Elshater et al. [25] as follows: one gram of C_{60} was dissolved in VOO (200 ml), stirred at ambient temperature in dark for 15 days, and centrifuged (5000 rpm) for 1 h. Using 0.25 μm Millipore filters, the supernatant was filtered through and administered immediately.

2.3. DNA Extraction. Carnoy's fixed and frozen liver and heart tissues were used for DNA extraction using QIAamp DNA Mini Kit (Qiagen, Santa Clarita, CA). DNA fragmentation in liver and heart tissues was carried out according to the kit manufacturer's protocol. Briefly, liver or heart tissues (20 mg) were grinded in hypotonic lysis buffer (400 μl; 10 mM Tris base, 1 mM EDTA, and 0.2% Triton X-10), and the cells were centrifuged (10,000 rpm) at 4°C for 5 min. The supernatant (containing small DNA fragments) was mixed with equal volumes of 0.5 M NaCl and absolute isopropyl alcohol for precipitation of DNA. Mixture was stored at −20°C overnight, then centrifuged (11,000 rpm) at 4°C for 15 min. Ethanol (200 μl of 70%) was used for washing the pellet; then, the pellet was loaded into the elution column and washed twice with buffer, and the DNA was isolated using elution buffer. The eluted DNA was stored at −20°C until use [26].

2.4. Polymerase Chain Reaction of ISSR Analysis. Five primers (Eurofins, Germany) (Table 1) were used in intersimple sequence repeat (ISSR) analysis, and PCR cycling was performed in a TakaRa Thermal Cycler (Takara Bio Inc., Shiga, Japan). For ISSR analysis, PCR amplification reactions [27] were used in a volume of 25 μl (1X of Green GoTaq® Flexi Buffer, primer (25 pucM), dNTPs (200 μM, Promega), $MgCl_2$ (1.5 mM), GoTaq Flexi DNA Polymerase (1 U, Promega), template DNA (25 ng), and up to 25 μl DW). The reactions were carried out in the following conditions: initial denaturation process (1 cycle) was performed at 94°C for 5 min; annealing (40 cycles) was carried out at 94°C for 45 sec, 45°C for 50 sec, and 72°C for 1.5 min; and lastly, extension (1 cycle) was done at 72°C for 7 min.

Table 1: The primer code and nucleotide sequences.

Primer	Primer sequence 5′-3′
ISSR-1	5′-ACACACACACACACACYA-3′
ISSR-2	5′-AGAGAGAGAGAGAGAGYT-3′
ISSR-3	5′-CTCCTCCTCCTCCTCTT-3′
ISSR-4	5′-CTCTCTCTCTCTCTCTCG-3′
ISSR-5	5′-TCTCTCTCTCTCTCTCA-3′

Nucleotide code: A = adenine, C = cytosine, G = guanine, T = thymine, and Y = Cor T.

2.5. Agarose Gel Electrophoresis. PCR products were analyzed using agarose gel electrophoresis (1.5%) and visualized with ethidium bromide (10 μg/μl) staining. The gels were exposed to UV light and photographed using a Molecular Imager® Gel Doc™ System with Image Lab™ Software, Bio-Rad. The size of the DNA fragments was estimated based on a DNA ladder (100 to 2000 bp, MBI, Fermentas). The presence or absence of each band was treated as binary character in a data matrix, that is, coded 1 and 0, respectively, The amplification products were scored as (1) for the presence and (0) for the absence of the bands and were compared to the bands in the control group to determine the genetic alterations across the other treated groups. The appearance of new bands and disappearance of existed bands in comparison with the control group are considered DNA polymorphism. Percentage of polymorphism is calculated according to this equation: number of polymorphic DNA band × 100/ total number of bands.

2.6. Preparation of Chromosome for Chromosomal Aberration Analysis. Microscopic slides for mitotic chromosomal spread were prepared as described by Yosida and Amano [28]. Rats were injected i.p. with colchicines (0.05%) and then euthanized 2 h later. Femurs of rats were removed, and the bone marrow cells were aspirated from both femurs in warmed hypotonic solution (5-6 ml of 0.56% KCl) for 30 min. The aspirate was centrifuged, and the supernatant was decanted. The resultant cellular mass was fixed three times in a mixture of (3 : 1) methanol-glacial acetic acid. Slides were prepared by dropping the cell suspension onto ethanol-cold slides and flaming them slightly. The slides were stained with Giemsa (10%) in phosphate buffer (pH 6.8). In each group, approximately 250 metaphase spreads were analyzed and the structural chromosomal aberrations per cell were counted. Different types of chromosomal aberrations such as chromosomal ring, chromatid deletion, dicentric chromosomes, chromosome fragments, and polyploidy chromosomes were accounted. The data was expressed as chromosomal aberration percentage (%) in each group using the following formula: chromosomal aberration % = total number of chromosomal aberrations × 100/total number of counted metaphase spreads (250).

2.7. Statistical Analysis. Statistical analysis was carried out using the Student's *t*-test (two-tailed) with SPSS 24 software. Chromosomal aberrations are expressed as mean ± SE. Differences were considered as significant when $P < 0.05$.

3. Results

3.1. Genotoxic Changes in Hepatic and Cardiac Tissues. ISSR analysis of the hepatic and cardiac tissues was performed to assess the genotoxicity of CP and the effect of C_{60} and VOO on CP-induced genotoxicity in rats. Numbers of ISSR bands ranged between 8 and 15 and 9 and 17 in hepatic and cardiac tissues, respectively (Figures 1 and 2, Table 2). The amplified bands had molecular weight of genomic DNA ranged between 160 and 1400 bp for both the hepatic and cardiac tissues, with 12 band average per primer (Figures 1 and 2, Table 2). In the control group, there were 57 ISSR bands in liver samples, compared to 52, 57, 56, and 61 bands in CP, C_{60}, CP + C_{60}, and CP + VOO groups, respectively. The CP group exhibited the highest number of lost bands. The number of lost bands caused by CP was decreased after treatment with C_{60} or VOO (Table 2). CP-induced loss in bands has been improved through treatment with C_{60}, as well as VOO.

In cardiac tissues, ISSR bands were 53, 46, 53, 50, and 55 in control, CP, C_{60}, CP + C_{60}, and CP + VOO groups, respectively (Figure 2, Table 2). Similarly, rats treated with CP had the highest number of ISSR band loss, and treatment with C_{60} or VOO decreased the band loss and recovered to control levels. Treatment with C_{60} and VOO improved the CP-induced genotoxicity. Furthermore, cardiac muscles were more affected by genotoxic effects of CP than hepatic tissues, and the rate of improvement due to treatment with C_{60} was lower than that observed in hepatic tissue.

The highest polymorphic bands were produced by the ISSR-3 and ISSR-1 primers (71.4% and 50% in hepatic and cardiac tissues, resp.) in the CP group (Table 3), whereas the lowest polymorphic bands were produced by ISSR-5 and ISSR-2 (0% and 9.1%) in hepatic and cardiac tissues, respectively (Table 3).

3.2. Attenuation of CP-Induced Polymorphism in Hepatic and Cardiac Tissues after Treatment with Fullerene C_{60} and VOO. Genetic analysis revealed that CP induced 11 polymorphic bands out of 52 bands (21.2% polymorphism) detected in the hepatic tissues (Table 3). In cardiac tissues, CP produced 15 polymorphic bands out of 46 bands (32.6% polymorphism) (Table 3). In contrast, the percentages of polymorphism in fullerene C_{60} (7%), CP + C_{60} (8.9%), and CP + VOO (9.8%) were lower than those recorded in CP (21.2%) in liver tissues (Table 3). Band polymorphism in cardiac tissues is recorded in Table 3. The percentages of polymorphism were 32.6, 11.3, 12, and 12.7% in cardiac tissues of CP, C_{60}, CP + C_{60}, and CP + VOO groups, respectively. Livers and hearts from rats exposed to C_{60} dissolved in VOO (C_{60} group) showed 7% and 11.3% polymorphisms, respectively (Table 3). These results indicate that polymorphisms induced by CP can be attenuated by C_{60} or VOO (in CP + C_{60} and CP + VOO groups).

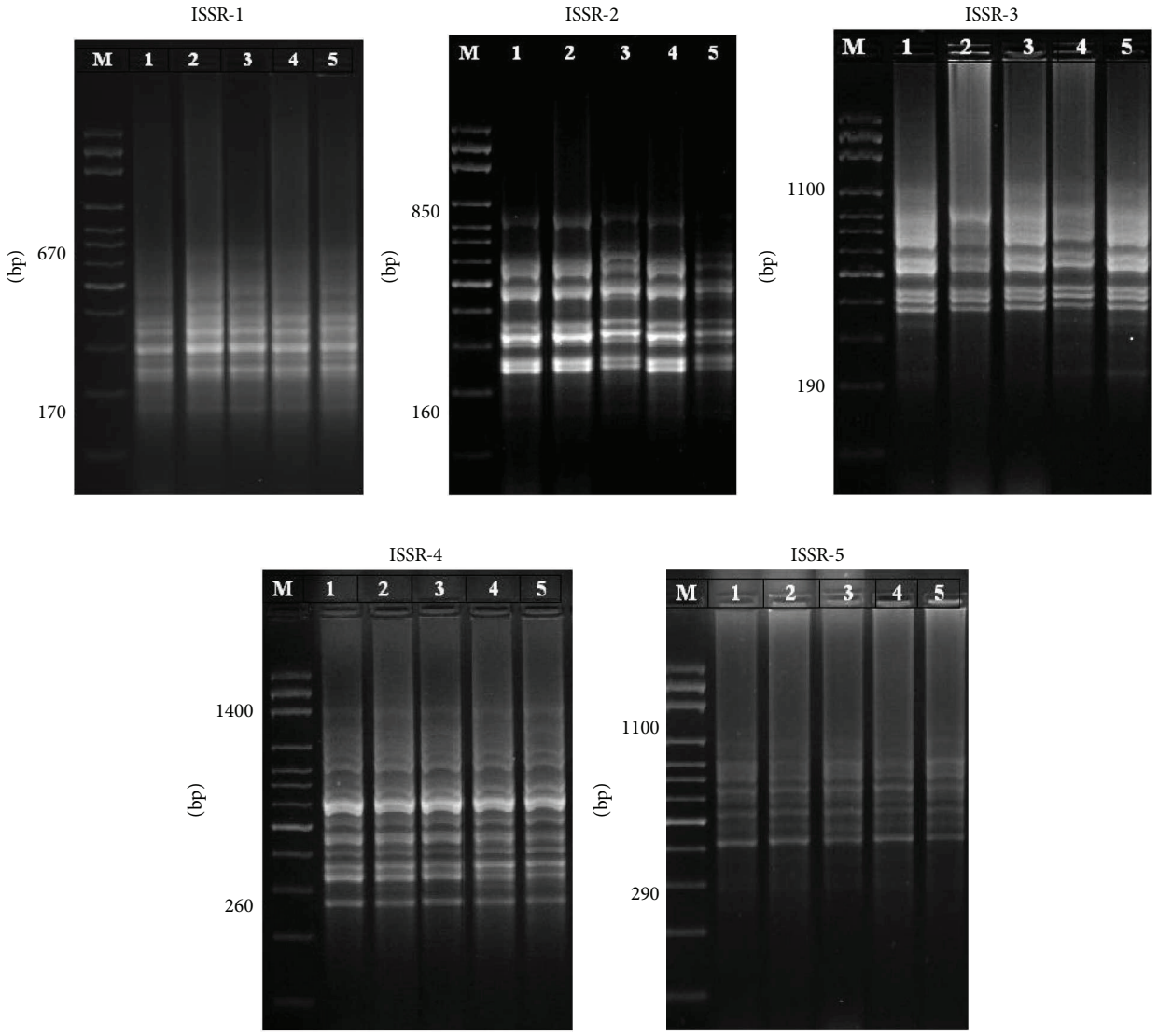

Figure 1: PCR products of liver genomic DNA after treatments with cyclophosphamide, fullerene nanoparticles (C_{60}), and virgin olive oil; lane M: DNA marker; lane 1: control; lane 2: CP group; lane 3: C_{60} group; lane 4: CP + C_{60} group; and lane 5: CP + VOO group.

Comparison of polymorphism percentages in cardiac muscles in all groups with those of hepatic tissues indicated that cardiac muscles (32.6% in CP) were more sensitive to CP genotoxicity than hepatic tissues (21.2% in CP) and the latter was better in response to the effect of C_{60} and VOO in moderation, reduction, or attenuation of CP toxic effects. Moreover, treatment with C_{60} was more effective than with VOO in improving the CP-induced genetic toxicity.

3.3. Cyclophosphamide-Induced Chromosomal Aberrations and Effect of C_{60} and VOO. The chromosomal alterations in bone marrow cells due to CP, C_{60}, and VOO were recorded. The CP group had the highest level (23.00 ± 14.28) of aberrant chromosomes (Figure 3, Table 4) in comparison to other treated groups. The major chromosomal aberrations were the formation of chromosomal rings (40.0%) (Table 4, Figure 3). Dicentric chromosomes (Figures 3(d) and 3(g)), chromosomal fragments (Figure 3(e)), chromatid deletions (Figures 3(c), 3(e), and 3(f)), and polyploidy were recorded after CP treatment, representing 4.00%, 3.5%, 6.0%, and 4.0%, respectively. Rats cotreated with CP and C_{60} or VOO reduced significantly the percentage of chromosomal aberrations when compared to those with CP alone. The frequencies of total chromosomal aberrations were 0.40 ± 0.24, 23.0 ± 14.28, 8.20 ± 3.29, 10.40 ± 5.10, and 11.20 ± 6.23 in control-, CP-, C_{60}-, CP + C_{60}-, and CP + VOO-treated animals, respectively. The percentages of total aberrant chromosomes were 1, 57.5, 20.5, 26.0, and 28% in control, CP, C_{60}, CP + C_{60}, and CP + VOO groups, respectively (Table 4). Phenotype of chromosomal ring was reduced significantly after treatment with C_{60} or VOO (Table 4, Figure 3). Other chromosomal changes such as deletion, dicentric chromosome, fragmentation, and polyploidy were reduced in number and percentage in treatment groups (C_{60}, CP + C_{60}, and

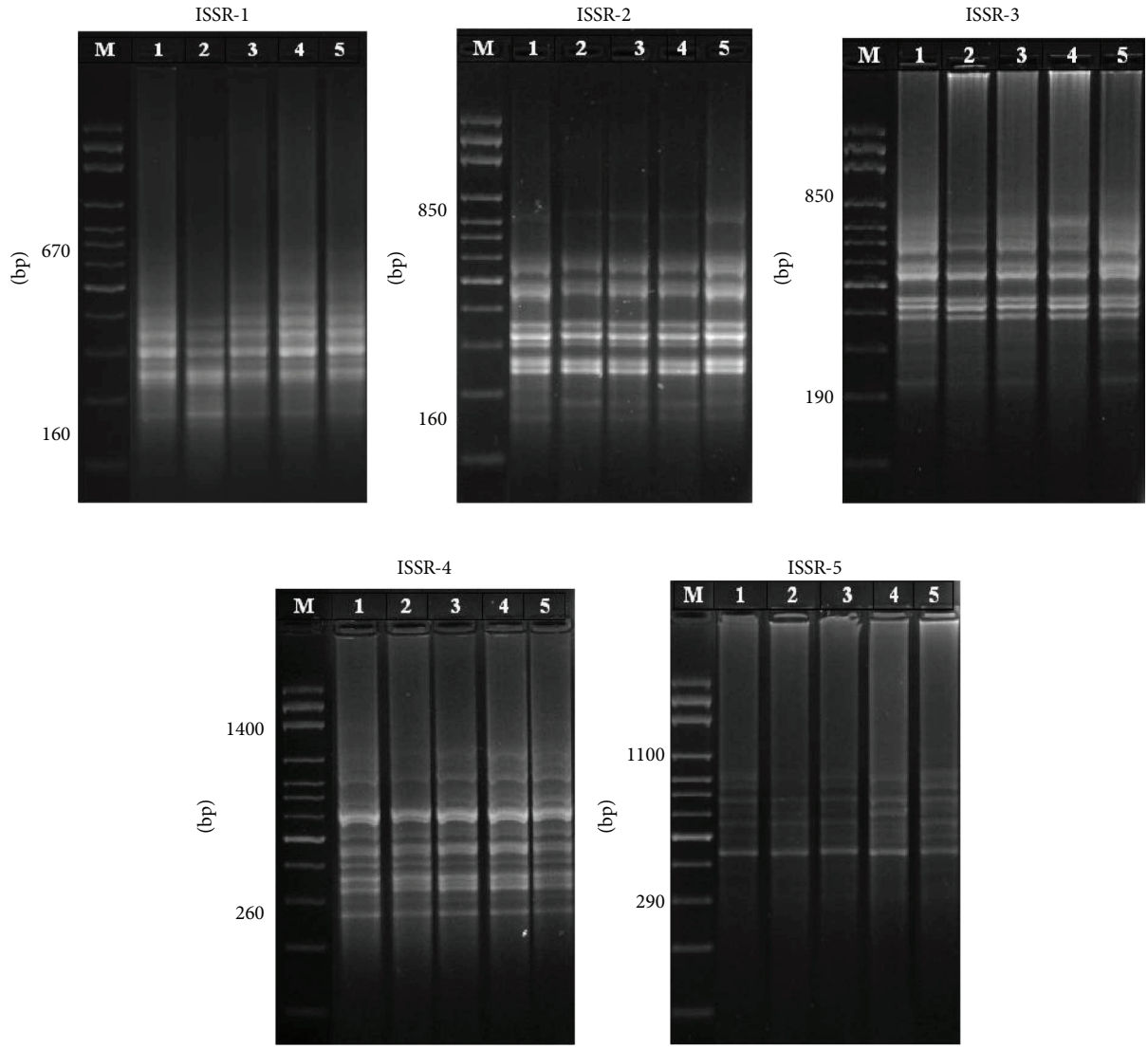

Figure 2: PCR products of heart genomic DNA after treatments with CP, fullerene nanoparticles (C_{60}), and virgin olive oil; lane M: DNA marker; lane 1: control; lane 2: CP group; lane 3: C_{60} group; lane 4: CP + C_{60} group; and lane 5: CP + VOO group.

CP + VOO) compared with those in the CP group (Table 4, Figure 3). The total numbers of aberrant chromosomes in 250 bone marrow cells were 2, 115, 41, 52, and 56 in control, CP, C_{60}, CP + C_{60}, and CP + VOO, respectively (Table 4). C_{60} and VOO significantly reduced chromosomal aberrations (50% reduction or more) in comparison with CP-treated rats.

4. Discussion

CP is used as a cancer chemotherapy alkylating agent. Active compounds of CP are acrolein and phosphoramide which are responsible for reducing the growth of cancerous cells by acting at the DNA level [29]. On the other hand, CP can enhance secondary tumors in healthy human tissues such as urinary bladder tumors as well as metastasis occasionally [30, 31]. CP, as a prooxidant, is used for treatment for a long time which leads to oxidative stress through generation of free radicals. After CP treatment, antioxidant enzyme activities decreased and lipid peroxidation increased [32]. Moreover, CP-induced genotoxicity is a dose-dependent manner. Although CP is used as an anticancer drug which is necessary to kill the carcinogenic cells, the increase use of CP in the treatment period leads to cytotoxicity of healthy cells in the body [5]. CP chemotherapy induces a variety of changes in DNA and proteins that lead to imbalance in cell division. In the present study, CP decreased the DNA level and increased the chromosomal aberrations in rat tissues. Most of chemotherapeutic agents and CP cause gene mutations, chromosomal aberrations, and rearrangements in somatic and germ cells of experimental animals [33]. Protection against CP chemotherapy-induced genotoxicity is a hot research point. Many mechanisms have been adopted to deal with CP genotoxicity, and several antimutagens were recorded acting in rodents and may be active in human too [34]. The objective of the current study was to assess the effect of fullerene C_{60} nanoparticles as well as VOO to

Table 2: Number and frequency of the obtained bands using ISSR in liver and heart tissues after treatment with CP, C_{60}, and VOO.

Primers	Total band numbers	Mobility range (bp)	Number of bands					Band frequency (mean ± SE)
			Control	CP	C_{60}	CP + C_{60}	CP + VOO	
Rat liver								
ISSR-1	11	170–670	10	11	11	11	11	0.98 ± 0.02
ISSR-2	14	160–850	12	11	14	10	14	0.81 ± 0.07
ISSR-3	13	190–1000	13	7	10	12	13	0.85 ± 0.06
ISSR-4	15	260–1400	14	15	14	15	15	0.97 ± 0.03
ISSR-5	8	290–1000	8	8	8	8	8	1.00 ± 0.00
Sum			**57**	**52**	**57**	**56**	**61**	
Rat heart								
ISSR-1	9	160–670	10	10	10	11	11	0.82 ± 0.08
ISSR-2	11	160–850	12	11	11	11	12	0.95 ± 0.05
ISSR-3	11	190–850	12	9	12	7	10	0.83 ± 0.06
ISSR-4	17	260–1400	12	11	13	14	15	0.87 ± 0.06
ISSR-5	11	290–1000	7	5	7	7	**7**	0.83 ± 0.10
Sum			**53**	**46**	**53**	**50**	**55**	

ameliorate CP-induced genotoxicity. Previous studies were demonstrating an improved effect of some extracts and chemicals such as garlic and *Ocimum sanctum* on the chromosomal aberrations [35, 36]. This study investigated the antigenotoxic activity of fullerene C_{60} as well as VOO in rat tissues by two main methods, molecular assays and cytogenetic biomarkers using DNA fragmentation assay in liver and heart tissues and chromosomal aberrations in bone marrow cells, respectively. CP produced severe mutations in DNA strands and chromosomes giving the ability to fairly judge on the DNA repair and cytogenetic activity of C_{60} and VOO in rats *in vivo*. CP induced loss of ISSR bands that decreased by cotreatment with C_{60} or VOO. CP-induced loss in bands has been improved through treatment with C_{60}, as well as VOO. Moreover, treatment with C_{60} was more effective than with VOO in improving the CP-induced genetic toxicity because the percentages of DNA polymorphism in hepatic and cardiac tissues were 8.9% and 9.8% and 12 and 12.7% in CP + C_{60} and CP + VOO groups, respectively. Fullerene C_{60} causes no damage in DNA strands and had no impact on the level of aberrant chromosomes *in vivo* and *in vitro* [15, 37, 38]. In the present study, C_{60} and VOO induced an improved DNA level and decreased the chromosomal aberration in CP + C_{60} or CP + VOO compared to that in the CP group. Fullerene nanoparticles (C_{60}) possess an ability to protect against oxidative stress and may decrease mutagenic activity, due to the nanosize [19, 20, 39]. In contrast, few reports stated that C_{60} possesses genotoxic activity in different animal tissues where it induces breaks and oxidative damages of in the DNA strand [12, 13, 40, 41]. In the present study, C_{60} improved the lost ISSR bands in both hepatic (57 and 56 in C_{60} and CP – C_{60}, resp.) and cardiac (53 and 50 in C_{60} and CP – C_{60}, resp.) tissues when compared to those of CP (52 and 46), respectively. Moreover, C_{60} decreased the percentage of DNA polymorphism in hepatic (7% and 8.9% in C_{60} and CP – C_{60}, resp.) and cardiac (11.3% and 12% in C_{60} and CP – C_{60}, resp.) tissues when compared to that of CP (21.2% and 32.6%), respectively. Effect of C_{60} on tissues *in vivo* and *in vitro* studies depends on the size of nanoparticles, the given dose, duration of exposure, and type of cells [41, 42]. In the present study, low dose of C_{60} was 4 mg/kg dissolved in VOO as those recorded by Baati et al. [24] and Elshater et al. [25] as low doses are protective against oxidative stress.

Effect of C_{60} on CP-induced hepatotoxicity was more effective than its effect on CP-induced cardiotoxicity and triggered a better response against genotoxicity in the liver than in the heart. Comparison of polymorphism percentages in cardiac muscles in all groups with those of hepatic tissues indicated that cardiac muscles (32.6% in CP) were more sensitive to CP genotoxicity than hepatic tissues (21.2% in CP). Cardiac muscles were worse in response to the effect of C_{60} and VOO than hepatic tissue in moderation, reduction, or attenuation of CP toxic effects.

The chromosomal aberration is an important parameter for investigating the protective effects of antigenotoxic agents on chemical and drug-induced toxicity. C_{60} had no genotoxic effects, and it induced antigenotoxic effects at subcytotoxic concentrations on human lymphocytes, presented by the decreased in micronuclei and chromosomal aberration frequency [37, 38]. Moreover, C_{60} prevents the toxic effect of doxorubicin (chemotherapeutic agent) on normal cells and possesses no genotoxic effect on human lymphocytes [18]. C_{60} has a potential antioxidative effect against CP-induced hepatotoxicity [25]. In the present work, in spite of C_{60} induced few genotoxic features represented by a few number of chromosomal aberration, for example, chromosomal ring, chromosomal fragments, and chromatid deletions, C_{60} had a protective effect against CP-induced genotoxicity. C_{60} as well as VOO decreased the number and types of aberrant chromosomes in CP + C_{60} and CP + VOO groups, respectively, when compared to the treatment by CP alone. Similar findings have been approved by C_{60} and VOO against cadmium-induced genotoxicity [43]. Fullerene C_{60} and VOO significantly ameliorate cadmium chloride-induced genotoxicity in hepatic and renal tissues. Moreover, they

Table 3: Detected polymorphism for the ISSR primer in hepatic and cardiac tissues of rats after treatment with CP, C_{60}, and VOO.

Primer	CP			C_{60}			CP + C_{60}			CP + VOO		
	Bands (number)	Polyploidy (number)	Polymorphism (%)	Bands (number)	Polyploidy (number)	Polymorphism (%)	Bands (number)	Polyploidy (number)	Polymorphism (%)	Bands (number)	Polyploidy (number)	Polymorphism (%)
Liver												
ISSR-1	11	1	9.1	11	0	0	11	0	0	11	1	9.1
ISSR-2	11	4	36.4	14	0	0	10	4	40	14	4	28.6
ISSR-3	7	5	71.4	10	3	30	12	1	8.3	13	0	0
ISSR-4	15	1	6.7	14	1	7.1	15	0	0	15	1	6.7
ISSR-5	8	0	0	8	0	0	8	0	0	8	0	0
Sum	52	11	21.2	57	4	7	56	5	8.9	61	6	9.8
Heart												
ISSR-1	10	5	50	10	1	10	11	0	0	11	0	0
ISSR-2	11	1	9.1	11	1	9.1	11	1	9.1	12	1	8.3
ISSR-3	9	3	33.3	12	2	16.7	7	3	42.9	10	2	20
ISSR-4	11	4	36.4	13	2	15.4	14	1	7.1	15	3	20
ISSR-5	5	2	40	7	0	0	7	1	14.3	7	1	14.3
Sum	46	15	32.6	53	6	11.3	50	6	12	55	7	12.7

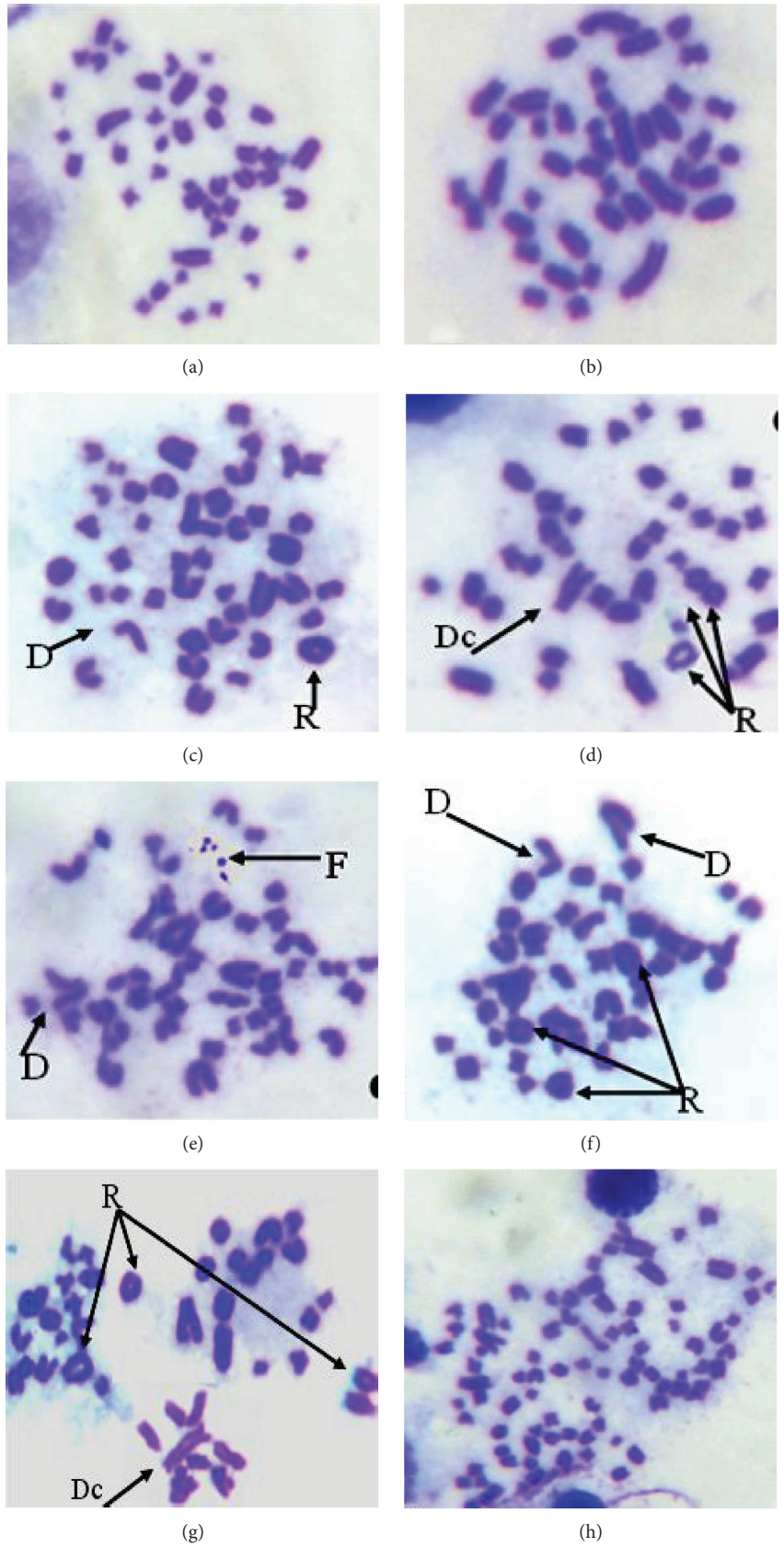

Figure 3: Metaphase-chromosomal aberrations in bone marrow cells showing the effect of CP treatment in group 2; (a and b) normal metaphase. Deletion in chromatid (*D*), ring chromosomes (*R*), dicentric chromosome (D_c), and fragment chromosomes (*F*), and polyploidy in chromosome numbers was observed in (h).

Table 4: Chromosomal aberrations in rat bone marrow cells after treatment with CP, C_{60}, and VOO.

Groups	Aberration cells (number)	Chromosomal aberration					Total aberrations		Average number of aberration (mean ± SEM)
		R (number)	*D* (number)	D_c (number)	*F* (number)	Poly (number)	Number	%	
Control	2	1	1	—	—		2	1.00	0.40 ± 0.24
CP	95	80	12	8	7	8	115	57.5	23.00 ± 14.28*
C_{60}	25	20	10	6	1	4	41	20.5	8.20 ± 3.29*
CP + C_{60}	36	30	10	7	3	2	52	26.0	10.40 ± 5.10*
CP + VOO	45	36	7	3	5	5	56	28.0	11.20 ± 6.23*

R = ring chromosome, *D* = deletion in chromatid, D_c = dicentric chromosome, *F* = fragmentation chromosomes, and Poly = polyploidy chromosomes. Values are mean of replicates ± SEM. *Significant at $P < 0.05$.

reversed the chromosomal alterations caused by cadmium chloride toxicity on bone marrow [43].

Moreover, VOO had an antigenotoxic impact on rat tissues. Our molecular studies on ISSR in hepatic and cardiac tissues as well as cytogenetic of bone marrow cells indicated that VOO alleviated CP-induced genotoxicity. Similarly, Fabiani et al. [22] reported that olive oil has a protective activity against cancer through arrest of the cell cycle and induction of apoptosis in tumor cells and also it has cytotoxic as well as cytoprotective compounds with potential pharmaceutical properties. VOO has a potential antioxidative effect, and it protects DNA from damage induced by a toxic material or a chemotherapeutic agent [21, 44, 45]. This study displays the antioxidant and antigenotoxic activities of fullerene C_{60} nanoparticle and olive oil and its antimutagenic impacts in reducing the DNA damage, which can be occurred in healthy cells as side effect of the treatment with cyclophosphamide.

5. Conclusion

The present study investigated the antigenotoxic activity of C_{60} as well as VOO in hepatic and cardiac tissues of a rat after induction of genotoxicity by CP. Two main methods were performed molecular ISSR assay and cytogenetic biomarkers using DNA fragmentation of liver and heart tissues and chromosomal aberrations in bone marrow cells, respectively. CP made severe mutations in DNA strands and chromosomal aberration; in contrast, DNA band numbers return to the control level as well as the chromosomal aberration frequency decreased significantly after C60 and VOO treatments. This study investigated the antigenotoxic activities of C_{60} nanoparticle and VOO and its antimutagenic impacts in reducing the DNA damage in healthy cells (C_{60} group) and after genotoxicity (CP + C_{60} and CP + VOO groups). Virgin olive oil has potent antigenotoxic effect compared with C_{60}. Cardiac muscles were more susceptible to CP-induced genotoxicity and less responsive to C_{60} and VOO treatments than hepatic tissues. These findings highlight the principles for the future research possibilities to design and develop C_{60}- and VOO-related drugs combined to CP and other chemotherapeutics, which might minimize the side effects caused by the commonly used chemotherapeutic agent.

Data Availability

The data used to support the findings of this study are available from the corresponding author upon request.

Conflicts of Interest

The authors declare that there are no conflicts of interest to disclose.

References

[1] B. Szikriszt, Á. Póti, O. Pipek et al., "A comprehensive survey of the mutagenic impact of common cancer cytotoxics," *Genome Biology*, vol. 17, no. 1, p. 99, 2016.

[2] C. D. Glen and Y. E. Dubrova, "Exposure to anticancer drugs can result in transgenerational genomic instability in mice," *Proceedings of the National Academy of Sciences of the United States of America*, vol. 109, no. 8, pp. 2984–2988, 2012.

[3] D. J. Kim, E. J. Kim, T. Y. Lee, J. N. Won, M. H. Sung, and H. Poo, "Combination of poly-gamma-glutamate and cyclophosphamide enhanced antitumor efficacy against tumor growth and metastasis in a murine melanoma model," *Journal of Microbiology and Biotechnology*, vol. 23, no. 9, pp. 1339–1346, 2013.

[4] M. U. Rehman, M. Tahir, F. Ali et al., "Cyclophosphamide-induced nephrotoxicity, genotoxicity, and damage in kidney genomic DNA of Swiss albino mice: the protective effect of Ellagic acid," *Molecular and Cellular Biochemistry*, vol. 365, no. 1-2, pp. 119–127, 2012.

[5] J. Deng, Y.-F. Zhong, Y.-P. Wu et al., "Carnosine attenuates cyclophosphamide-induced bone marrow suppression by reducing oxidative DNA damage," *Redox Biology*, vol. 14, pp. 1–6, 2018.

[6] I. A. Al-Nasser, "In vivo prevention of cyclophosphamide-induced Ca^{2+} dependent damage of rat heart and liver mitochondria by cyclosporin A," *Comparative Biochemistry and Physiology Part A: Molecular & Integrative Physiology*, vol. 121, no. 3, pp. 209–214, 1998.

[7] P. T. Sudharsan, Y. Mythili, E. Selvakumar, and P. Varalakshmi, "Lupeol and its ester ameliorate the cyclophosphamide provoked cardiac lysosomal damage studied in rat," *Molecular and Cellular Biochemistry*, vol. 282, no. 1-2, pp. 23–29, 2006.

[8] E. Gebhart, "Anticlastogenicity in cultured mammalian cells," *Mutation Research/Fundamental and Molecular Mechanisms of Mutagenesis*, vol. 267, no. 2, pp. 211–220, 1992.

[9] A. K. Patlolla and P. B. Tchounwou, "Cytogenetic evaluation of arsenic trioxide toxicity in Sprague–Dawley rats," *Mutation Research/Genetic Toxicology and Environmental Mutagenesis*, vol. 587, no. 1-2, pp. 126–133, 2005.

[10] J. Kour, M. N. Ali, H. A. Ganaie, and N. Tabassum, "Amelioration of the cyclophosphamide induced genotoxic damage in mice by the ethanolic extract of *Equisetum arvense*," *Toxicology Reports*, vol. 4, pp. 226–233, 2017.

[11] A. Dhawan, J. S. Taurozzi, A. K. Pandey et al., "Stable colloidal dispersions of C60 fullerenes in water: evidence for genotoxicity," *Environmental Science & Technology*, vol. 40, no. 23, pp. 7394–7401, 2006.

[12] N. R. Jacobsen, G. Pojana, P. White et al., "Genotoxicity, cytotoxicity, and reactive oxygen species induced by single-walled carbon nanotubes and C_{60} fullerenes in the FE1-Muta™Mouse lung epithelial cells," *Environmental and Molecular Mutagenesis*, vol. 49, no. 6, pp. 476–487, 2008.

[13] S. N. Al-Subiai, V. M. Arlt, P. E. Frickers et al., "Merging nano-genotoxicology with eco-genotoxicology: an integrated approach to determine interactive genotoxic and sub-lethal toxic effects of C_{60} fullerenes and fluoranthene in marine mussels, *Mytilus* sp," *Mutation Research/Genetic Toxicology and Environmental Mutagenesis*, vol. 745, no. 1-2, pp. 92–103, 2012.

[14] L. P. Zakharenko, I. K. Zakharov, E. A. Vasiunina, T. V. Karamysheva, A. M. Danilenko, and A. A. Nikiforov, "Determination of the genotoxicity of fullerene C60 and fullerol using the method of somatic mosaics on cells of *Drosophila melanogaster* wing and SOS-chromotest," *Genetika*, vol. 33, no. 3, pp. 405–409, 1997.

[15] N. Shinohara, K. Matsumoto, S. Endoh, J. Maru, and J. Nakanishi, "*In vitro* and *in vivo* genotoxicity tests on fullerene C_{60} nanoparticles," *Toxicology Letters*, vol. 191, no. 2-3, pp. 289–296, 2009.

[16] T. Mori, H. Takada, S. Ito, K. Matsubayashi, N. Miwa, and T. Sawaguchi, "Preclinical studies on safety of fullerene upon acute oral administration and evaluation for no mutagenesis," *Toxicology*, vol. 225, no. 1, pp. 48–54, 2006.

[17] M. Ema, T. Imamura, H. Suzuki, N. Kobayashi, M. Naya, and J. Nakanishi, "Genotoxicity evaluation for single-walled carbon nanotubes in a battery of *in vitro* and *in vivo* assays," *Journal of Applied Toxicology*, vol. 33, no. 9, pp. 933–939, 2013.

[18] K. S. Afanasieva, S. V. Prylutska, A. V. Lozovik et al., "C(60) fullerene prevents genotoxic effects of doxorubicin in human lymphocytes in vitro," *The Ukrainian Biochemical Journal*, vol. 87, no. 1, pp. 91–98, 2015.

[19] S. V. Prylutska, I. I. Grynyuk, O. P. Matyshevska, Y. I. Prylutskyy, U. Ritter, and P. Scharff, "Anti-oxidant properties of C_{60} fullerenes *in vitro*," *Fullerenes, Nanotubes and Carbon Nanostructures*, vol. 16, no. 5-6, pp. 698–705, 2008.

[20] S. V. Prylutska, I. I. Grynyuk, S. M. Grebinyk et al., "Comparative study of biological action of fullerenes C_{60} and carbon nanotubes in thymus cells," *Materialwissenschaft Und Werkstofftechnik*, vol. 40, no. 4, pp. 238–241, 2009.

[21] T. Saber, M. Farag, and R. Cooper, "Ameliorative effect of extra virgin olive oil on hexavalent chromium-induced nephrotoxicity and genotoxicity in rats," *Revue de Médecine Vétérinaire*, vol. 166, pp. 11–19, 2015.

[22] R. Fabiani, A. de Bartolomeo, P. Rosignoli, M. Servili, G. F. Montedoro, and G. Morozzi, "Cancer chemoprevention by hydroxytyrosol isolated from virgin olive oil through G1 cell cycle arrest and apoptosis," *European Journal of Cancer Prevention*, vol. 11, no. 4, pp. 351–358, 2002.

[23] A. Machowetz, H. E. Poulsen, S. Gruendel et al., "Effect of olive oils on biomarkers of oxidative DNA stress in Northern and Southern Europeans," *The FASEB Journal*, vol. 21, no. 1, pp. 45–52, 2007.

[24] T. Baati, F. Bourasset, N. Gharbi et al., "The prolongation of the lifespan of rats by repeated oral administration of [60] fullerene," *Biomaterials*, vol. 33, no. 19, pp. 4936–4946, 2012.

[25] A. A. Elshater, M. A. M. Haridy, M. M. A. Salman, A. S. Fayyad, and S. Hammad, "Fullerene C_{60} nanoparticles ameliorated cyclophosphamide-induced acute hepatotoxicity in rats," *Biomedicine & Pharmacotherapy*, vol. 97, pp. 53–59, 2018.

[26] E. Zietkiewicz, A. Rafalski, and D. Labuda, "Genome fingerprinting by simple sequence repeat (SSR)-anchored polymerase chain reaction amplification," *Genomics*, vol. 20, no. 2, pp. 176–183, 1994.

[27] K. Sharaf-Eldeen, M. El-Ezabi, and A. Al-Bohaissi, "The molecular changes of hepatocytes in tilapia zillh under the effect of the agricultural and industrial pollution in the river Nile, Egypt," *Egyptian Journal of Aquatic Biology and Fisheries*, vol. 10, no. 2, pp. 55–67, 2006.

[28] T. H. Yosida and K. Amano, "Autosomal polymorphism in laboratory bred and wild Norway rats, *Rattus norvegicus*, found in Misima," *Chromosoma*, vol. 16, no. 6, pp. 658–667, 1965.

[29] A. Emadi, R. J. Jones, and R. A. Brodsky, "Cyclophosphamide and cancer: golden anniversary," *Nature Reviews Clinical Oncology*, vol. 6, no. 11, pp. 638–647, 2009.

[30] A. Shimizu, T. Ueda, Y. Furuya et al., "Cyclophosphamide-induced bladder cancer in a patient with Wegener granulomatosis," *The Japanese Journal of Urology*, vol. 90, no. 1, pp. 53–56, 1999.

[31] L. Strzadala, J. Rak, E. Ziolo, H. Kusnierczyk, and C. Radzikowski, "Potentiation of cyclophosphamide-induced enhancement of experimental metastasis by splenectomy," *Archivum Immunologiae et Therapiae Experimentalis*, vol. 37, pp. 399–403, 1989.

[32] B. Popov, S. Georgieva, and V. Gadjeva, "Modulatory effects of total extract of *Haberlea rhodopensis* against the cyclophosphamide induced genotoxicity in rabbit lymphocytes in vivo," *Trakia Journal of Sciences*, vol. 9, pp. 52–58, 2011.

[33] M. Murata, T. Suzuki, K. Midorikawa, S. Oikawa, and S. Kawanishi, "Oxidative DNA damage induced by a hydroperoxide derivative of cyclophosphamide," *Free Radical Biology & Medicine*, vol. 37, no. 6, pp. 793–802, 2004.

[34] C. Sushma and K. Rudrama Devi, "Antigenotoxic effects of *Aegle marmelos* fruit extract in cyclophosphamide induced chromosomal aberrations and aberrant sperms in germ cells of Swiss albino mice," *International Journal of Pure & Applied Bioscience*, vol. 3, no. 5, pp. 178–183, 2015.

[35] Y. Shukla and P. Taneja, "Antimutagenic effects of garlic extract on chromosomal aberrations," *Cancer Letters*, vol. 176, no. 1, pp. 31–36, 2002.

[36] D. Dutta, S. Saravana Devi, K. Krishnamurthi et al., "Modulatory effect of distillate of *Ocimum sanctum* leaf extract (Tulsi) on human lymphocytes against genotoxicants," *Biomedical and Environmental Sciences*, vol. 20, p. 226, 2007.

[37] J. Vávrová, M. Řezáčová, and J. Pejchal, "Fullerene nanoparticles and their anti-oxidative effects: a comparison to other radioprotective agents," *Journal of Applied Biomedicine*, vol. 10, no. 1, pp. 1–8, 2012.

[38] J. Mrđanović, S. Jungić, S. Šolajić, V. Bogdanović, and V. Jurišić, "Effects of orally administered antioxidants on micronuclei and sister chromatid exchange frequency in workers professionally exposed to antineoplastic agents," *Food and Chemical Toxicology*, vol. 50, no. 8, pp. 2937–2944, 2012.

[39] C. A. Theriot, R. C. Casey, V. C. Moore et al., "Dendro[C60]-fullerene DF-1 provides radioprotection to radiosensitive mammalian cells," *Radiation and Environmental Biophysics*, vol. 49, no. 3, pp. 437–445, 2010.

[40] Y. Su, J. Xu, P. Shen et al., "Cellular uptake and cytotoxic evaluation of fullerenol in different cell lines," *Toxicology*, vol. 269, no. 2-3, pp. 155–159, 2010.

[41] K. Aschberger, H. J. Johnston, V. Stone et al., "Review of fullerene toxicity and exposure—appraisal of a human health risk assessment, based on open literature," *Regulatory Toxicology and Pharmacology*, vol. 58, no. 3, pp. 455–473, 2010.

[42] H. J. Johnston, G. R. Hutchison, F. M. Christensen, K. Aschberger, and V. Stone, "The biological mechanisms and physicochemical characteristics responsible for driving fullerene toxicity," *Toxicological Sciences*, vol. 114, no. 2, pp. 162–182, 2010.

[43] F. M. Aly, A. M. Kotb, M. A. M. Haridy, and S. Hammad, "Impacts of fullerene C60 and virgin olive oil on cadmium-induced genotoxicity in rats," *Science of The Total Environment*, vol. 630, pp. 750–756, 2018.

[44] E. T. Mohammed, K. S. Hashem, and M. R. A. Rheim, "Biochemical study on the impact of *Nigella sativa* and virgin olive oils on cadmium-induced nephrotoxicity and neurotoxicity in rats," *Journal of Investigational Biochemistry*, vol. 3, no. 2, pp. 71–78, 2014.

[45] L. Nousis, P.-T. Doulias, N. Aligiannis et al., "DNA protecting and genotoxic effects of olive oil related components in cells exposed to hydrogen peroxide," *Free Radical Research*, vol. 39, no. 7, pp. 787–795, 2005.

Hindawi
Oxidative Medicine and Cellular Longevity
Volume 2018, Article ID 6703296, 14 pages
https://doi.org/10.1155/2018/6703296

Research Article

Protective Effects of Miswak (*Salvadora persica*) against Experimentally Induced Gastric Ulcers in Rats

Mohamed A. Lebda,[1] **Ali H. El-Far**,[2] **Ahmed E. Noreldin**,[3] **Yaser H. A. Elewa**,[4,5] **Soad K. Al Jaouni**,[6] **and Shaker A. Mousa**[7]

[1]*Biochemistry Department, Faculty of Veterinary Medicine, Alexandria University, Alexandria 22758, Egypt*
[2]*Biochemistry Department, Faculty of Veterinary Medicine, Damanhour University, Damanhour 22511, Egypt*
[3]*Histology and Cytology Department, Faculty of Veterinary Medicine, Damanhour University, Damanhour 22511, Egypt*
[4]*Histology and Cytology Department, Faculty of Veterinary Medicine, Zagazig University, Zagazig, Egypt*
[5]*Laboratory of Anatomy, Department of Biomedical Sciences, Graduate School of Veterinary, Hokkaido University, Sapporo, Japan*
[6]*Department of Pediatric Hematology/Oncology, King Abdulaziz University Hospital and Scientific Chair of Yousef Abdul Latif Jameel of Prophetic Medicine Application, Faculty of Medicine, King Abdulaziz University, Jeddah 21589, Saudi Arabia*
[7]*Pharmaceutical Research Institute, Albany College of Pharmacy and Health Sciences, Rensselaer, NY 12144, USA*

Correspondence should be addressed to Mohamed A. Lebda; lebdam1979@alexu.edu.eg
and Ali H. El-Far; ali.elfar@damanhour.edu.eg

Received 10 March 2018; Revised 26 April 2018; Accepted 24 May 2018; Published 9 July 2018

Academic Editor: Rohit Saluja

Gastric ulcers are among the most broadly perceived illnesses affecting individuals. Alcohol consumption is the main cause of gastric ulceration. This study assessed the protective effects of *Salvadora persica* (SP) extract against ethanol-induced gastric ulcer and elucidated the conceivable underlying mechanisms involved. For this purpose, 40 rats were allotted into 4 equal groups (control, ethanol- (EtOH-) treated, and SP-treated "SP200 and SP400" groups). The control and EtOH-treated groups were given phosphate buffer saline (PBS), and both the SP200 and SP400 groups were given SP extract dissolved in PBS at doses of 200 and 400 mg/kg b.w., respectively. All treatments were given orally for 7 constitutive days. On the 8th day, all rats were fasted for 24 h followed by oral gavage of PBS in the control group and chilled absolute ethanol solution (5 ml/kg b.w.) in the EtOH- and SP-treated groups to induce gastric lesions. One hour later, the rats were sacrificed and the stomachs were harvested. Gross and microscopic examinations of the EtOH-treated group showed severe gastric hemorrhagic necrosis, submucosal edema, destruction of epithelial cells, and reduced glycoprotein content at the mucus surface. These pathological lesions were defeated by SP extract treatment. Administration of SP extract modulated the oxidative stress and augmented the antioxidant defenses. The elevated ethanol-expressed tumor necrosis factor-α (TNF-α) and interleukin-1β (IL-1β) genes, as well as bcl-2-like protein 4 (Bax) and inducible nitric oxide synthase (iNOS), were diminished in the SP-treated group. Curiously, SP extract upregulated endothelial nitric oxide synthase (eNOS) and transforming growth factor-β1 (TGF-β1) gene expression comparable to that of the EtOH-treated rats. Aggregately, SP exerted antiulcer activities in ethanol-induced gastric ulcer rat models via modulation of oxidant/antioxidant status, mitigation of proinflammatory cytokines, and apoptosis, as well as remodeling of both NOS isoforms.

1. Introduction

Gastric ulceration mainly occurs as a result of disharmony between 5 inverse factors at the gastric mucosa [1]. Inducing factors include alcohol, nonsteroidal anti-inflammatory drugs, smoking, stress, and *Helicobacter pylori* [2]. This is in contrast to the gastroprotective factors that are attributed to adequate secretion of mucus and prostaglandins, maintenance of anti-inflammatory and antioxidative agents, and normal mucosal blood flow [3].

Ethanol is one of the forceful factors that prompt gastric ulcer and is used as a model for assessment of the gastro-defensive effects of various drugs and natural products [4]. The oxidative stress that leads to the production of reactive oxygen species (ROS) along with the decline in antioxidative enzymes at the gastric mucosa induced by ethanol ingestion is implicated in the pathogenesis of ethanol-induced gastric ulceration [5]. Alcohol consumption induces gastric mucosal damage and apoptosis through tumor necrosis factor-α (TNF-α) signaling and ROS formation [6]. TNF-α, an initiating proinflammatory cytokine, has a critical role in the pathogenesis of gastric ulcer via inflammation and injury inducement [7]. Alcohol-induced gastric damage has been mediated through hypersecretion of gastric acid [8], proinflammatory cytokines and ROS generation [9], apoptosis induction, and depletion of nitric oxide (NO) and prostaglandin E2 [10]. NO, a vasodilator that is synthesized from the amino acid arginine by two NO synthases, has a dual function at the gastric mucosal level. One of them is the endothelial nitric oxide synthase (eNOS) that produces NO to assist gastric ulcer healing mainly through stimulation of blood vessels' formation, increasing blood flow, and anti-inflammatory action [11], while NO generated from inducible nitric oxide synthase (iNOS) functions in gastric ulcer induction via the formation of ROS and toxic effects on cells [12].

Alleviation of gastric aggressive mediators and progression of gastric preservative factors are considered as therapeutic tools for the healing of gastric ulcer [13]. The mechanism of the healing process encompasses the restoration of the gastro-defensive factors' balance, generation of gastric mucosal cells and blood vessels, matrix reconstruction, antioxidation, and anti-inflammation [14].

Natural products have attracted scientific attention as prophylactic alternatives for gastric ulcer [15]. *Salvadora persica* L. (SP), also known as miswak, a Salvadoraceae family member, has been used mainly as natural toothbrushes [16]. SP-lyophilized decoction has a protective action on gastric ulcer induced by acetylsalicylic acid in rats [17]. Soliman et al. [18] reported that SP root extract attenuated oxidative stress, restored antioxidant enzymes, and reduced glutathione (GSH) level in rats exposed to lead acetate. Also, Nomani et al. [19] showed that the anti-inflammatory activity of SP extract is mediated via the down-regulation of TNF-α mRNA expression in inflammatory bowel disease-induced rats. Further, the most potent inflammatory factors IL-1β, TNF-α, and TGF-β1 were decreased in rat serum subjected to carrageenan-induced paw edema pretreated with SP extract [20].

In view of previously published data concerning the mechanistic factors of gastric ulcer healing, the current study was designed to evaluate the effects of SP aqueous extract on proinflammatory cytokines, nitric oxide synthases, apoptotic pathways, and oxidative/antioxidative pathways involved in ethanol-induced gastric ulcer in rats.

2. Materials and Methods

2.1. Ethics Statement. The experiments were done in compliance with the rules set by the Ethics Committee at the Faculty of Veterinary Medicine, Alexandria University, Egypt. All efforts were made to minimize the suffering of rats during experimentation and sampling.

Table 1: Ingredients of basal diet.

Ingredients	g/kg diet
Corn flour	529.5
Casein	200
Sucrose	100
Soybean oil	70
Cellulose	50
Mineral mix	35
Vitamin mix	10
L-Cysteine	3
Choline	2.5

2.2. Chemicals and Reagents. Absolute ethanol (EtOH) solution was purchased from Sigma-Aldrich Co. (St. Louis, MO, USA). Polyclonal rabbit anti-mouse iNOS antibody (1 : 100; Cat: ab15323), monoclonal rabbit anti-human Bax antibody (1 : 300; Cat: ab32503), polyclonal rabbit anti-mouse IL-1β antibody (1 : 250; Cat: ab9722), and polyclonal rabbit anti-human CD3 antibody (1 : 100; Cat: ab5690) were purchased from Abcam Co., Cambridge, UK.

Kits for malondialdehyde (MDA), GSH, total superoxide dismutase (T.SOD), catalase (CAT), glutathione peroxidase (GPx), and glutathione S-transferase (GST) were obtained from Biodiagnostic Co. (Dokki, Giza, Egypt). Total RNA extraction and SYBR Green Master Mix kits were purchased from Qiagen Co., Germany. cDNA kit was obtained from Promega Co., Madison, WI, USA.

2.3. Plant Extraction. SP roots were purchased from the local market in Alexandria, Egypt, and authenticated at the Botany Department, Agriculture Faculty, Alexandria University. One kg of SP roots was cut into small pieces, air dried, and ground into fine powder and then extracted in distilled water for 48 h at 25°C. After centrifugation at 1435 ×g for 15 min, the resulting supernatants were filtered through Whatman number 1 filter paper and the filtrates were concentrated using a rotary evaporator at 40°C [21]. The obtained fine extract powder was subdivided into small portions in brown bottles and freshly prepared before supplementation to rats.

2.4. Gas Chromatography-Mass Spectrometry (GC-MS) Analysis of SP Phytochemicals in Extract. SP extract was dissolved in N,O-Bis(trimethylsilyl)trifluoroacetamide and injected into a Trace GC Ultra-ISQ mass spectrometer with a direct capillary column TG-5MS (30 m × 0.25 mm × 0.25 μm). The GC was equipped with splitless mode/30 s with helium as a carrier gas. The temperature of the GC oven was maintained at 45°C for 30 s. The oven temperature was gradually raised to 235°C at a rate of 8°C/min and maintained at 235°C for 7.07 min. The MS ion source temperature was 150°C and mass spectra were obtained at 70 eV [22].

Table 2: Primer sequences.

Gene symbol	Gene description	GenBank accession number	Sequence	Annealing temperature (°C)
Actb	β-Actin	NM_031144.3	F: TGTTGTCCCTGTATGCCTCT R: TAATGTCACGCACGATTTCC	60
eNOS	Endothelial nitric oxide synthase	NC_005103.4	F: TCTTCAAGGACCTACCTCAGGC R: GCTAAGGCAAAGCTGCTAGGTC	60
TGF-β1	Transforming growth factor-β1	NM_021578.2	F: CCAACTACTGCTTCAGCTCCACA R: TGTACTGTGTGTCCAGGCTCCAAA	58
TNF-α	Tumor necrosis factor-α	NM_012675.3	F: GACCCTCACACTCAGATCATCTTCT R: TTGTCTTTGAGATCCATGCCATT	60
IL-1β	Interleukin-1β	NM_031512.2	F: CACCTCTCAAGCAGAGCACAG R: GGGTTCCATGGTGAAGTCAAC	60

Separated compounds were identified by comparing their mass spectra to the Wiley Registry 8e.

2.5. Animal Study Design and Induction of Gastric Ulcer. Forty male adult rats weighing between 240 and 250 g were purchased from the Animal Breeding Unit, Medical Research Institute, Alexandria University. Animals were housed in clean metal cages under optimum conditions proportionate to the Institutional Guideline for Care and Use of Laboratory Animals: temperature: $21 \pm 2^{\circ}$C, humidity: $56 \pm 5\%$, 12 h light/dark cycle, and free access to water and to diet as listed in Table 1.

Rats were allocated into the control group ($n = 20$), SP200 ($n = 10$) group that received SP extract 200 mg/kg b.w., and SP400 ($n = 10$) group that received SP extract 400 mg/kg b.w. [23, 24]. SP extract was dissolved in phosphate buffer saline (PBS) and given orally to the SP200 and SP400 groups for 7 days while the control group received only PBS. On the 8th day, all rats were fasted for 24 h followed by administration of ethanol by gastric tube to induce gastric lesions to 10 rats of the control group and all rats in the SP200 and SP400 groups; rats were gavaged with chilled absolute ethanol solution 5 ml/kg b.w. according to the method described by Park et al. [25]. The remaining 10 rats of the control group were gavaged with PBS and kept as negative control. One hour following the induction of gastric lesions, the rats were sacrificed under anesthesia with intravenous injection of sodium pentobarbital (30 mg/kg).

2.6. Macroscopic Examination of Gastric Mucosa. Stomachs of anesthetized rats from each group were opened along the greater curvature and rinsed with normal saline (NaCl 0.9%) followed by gross examination for assessment of any abnormal lesions and then photographed. The length of each lesion in mm was measured according to Bozkurt et al. [26], and the gastric ulcer index (UI) was calculated according to the method described by Das and Banerjee [27].

2.7. Histological Screening of Gastric Mucosa. Stomachs were flushed with PBS pH 7.4 and fixed in 4% paraformaldehyde in 0.1 M phosphate buffer. Fixed specimens were processed using the conventional paraffin embedding technique including dehydration through ascending grades of ethanol and clearing in 3 changes of xylene and melted paraffin and ended by embedding in paraffin wax at 65°C. Paraffin blocks were sectioned into 4 μm thickness sections. These sections were stained with hematoxylin and eosin (H&E) stain according to the method described by Bancroft and Layton [28] and Periodic acid–Schiff (PAS) stain according to Pearse [29]. The section images were taken with a digital camera (Leica EC3, Leica, Germany) connected to a microscope (Leica DM500).

Table 3: Phytochemical analysis of *S. persica* extract by GC-MS.

Retention time (min)	Phytochemicals	Area (%)
5.52	Chavicol	1.18
10.18	Oleic acid	1.97
12.31	3-Penten-2-one	4.24
15.58	Tristrimethylsilyl ether derivative of 1,25-dihydroxyvitamin D2	3.94
16.24	Retinoic acid	1.31
16.78	Palmitic acid	13.19
17.27	Androst-7-ene-6,17-dione	9.56
19.05	Methyl alpha-D-glucopyranoside	4.09
19.32	α-Linolenic acid	1.77
20.83	Tributyl acetylcitrate	5.24
23.78	Hexa-t-butylselenatrisiletane	6.97
26.33	Lycopene	16.56
27.45	Pregn-16-ene-11,14,18,20-tetrol	1.73
28.46	Lycoxanthin	1.61
	Ingredients less than 1.00%	26.64

2.8. Determination of Gastric Mucosal Malondialdehyde and Antioxidant Parameters. Gastric tissues were homogenized with PBS to prepare 10% (w/v) homogenate and divided into 3 aliquots; one was used for the estimation of the MDA level. The second aliquot was deproteinized by adding 10% trichloroacetic acid and centrifuged, and the supernatant was used for the determination of reduced glutathione level, while the third aliquot was centrifuged and used to determine the antioxidant enzyme activities in the supernatant. All procedures were performed using commercial kits (Biodiagnostic Co.) according to the manufacturer's instructions.

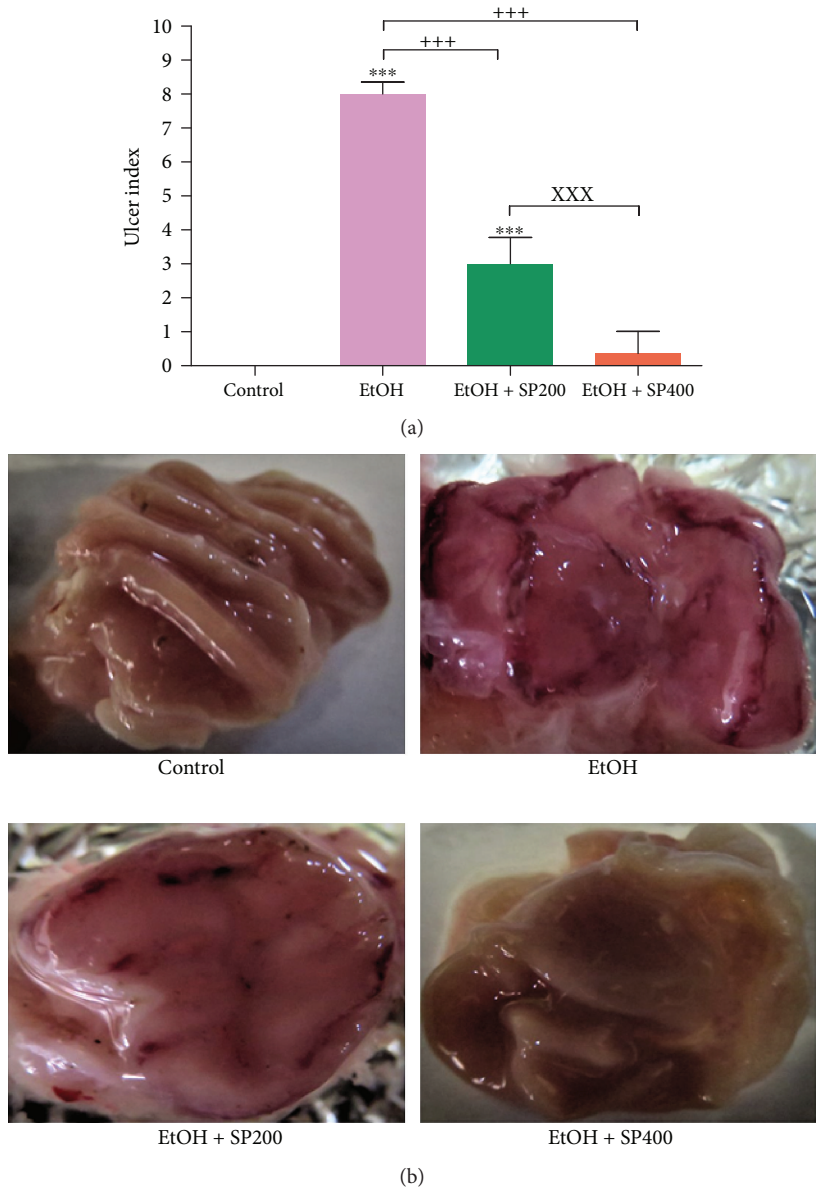

Figure 1: Gastric ulcer index (a) and macroscopic finding of gastric mucosal lesions (b) in rats exposed to ethanol-induced gastric ulcer and treated with *S. persica* extract. EtOH: ethanol-induced gastric ulcer; EtOH + SP200: ethanol-gastric ulcer treated with *S. persica* extract 200 mg/kg b.w.; EtOH + SP400: ethanol-gastric ulcer treated with *S. persica* extract 400 mg/kg b.w. Data are expressed as mean ± SE ($n = 5$), and the statistical analysis was done with one-way ANOVA, followed by Tukey's post hoc test multiple comparisons. $^{***}P < 0.001$ versus control, $^{+++}P < 0.001$ versus EtOH, and $^{xxx}P < 0.001$ versus EtOH + SP400.

2.9. Relative Expression of Proinflammatory Cytokine and Endothelial Nitric Oxide Synthase. Total RNA was isolated from 100 mg gastric tissue samples in all groups using an RNA extraction kit (Qiagen Inc., Germantown, MD, USA). qRT-PCR was performed in a real-time PCR machine using one-step SYBR Green RT-PCR Master Mix (Qiagen Inc.) and ready-made primers of TNF-α, IL-1β, TGF-β1, eNOS, and β-actin as housekeeping reference genes (Table 2). Thermal cycling conditions were retention time step at 50°C/10 min for cDNA synthesis followed by inactivation step at 95°C/15 min. For gene amplification, conditions were 45 cycles of 95°C/15 s, 58–60°C/30 s, and 60°C/1 min, followed by 60°C/10 min. Analysis of relative gene expression was estimated using the $2^{-\Delta\Delta Ct}$ method [30].

2.10. Immunohistochemical Examination of Bax, iNOS, IL-1β, and CD3 Proteins. Briefly, 4 μm thick paraffin sections were prepared and deparaffinized using xylene, rehydrated in graded alcohols, and finally washed with distilled water. Antigen retrieval was done in the case of anti-iNOS, anti-Bax, and anti-CD3 by heating in 10 mM citrate buffer (pH 6.0) for 20 min at 95°C with no antigen retrieval for anti-IL-1β, followed by washing with distilled water. Deactivation of endogenous peroxidase was carried out using 3%

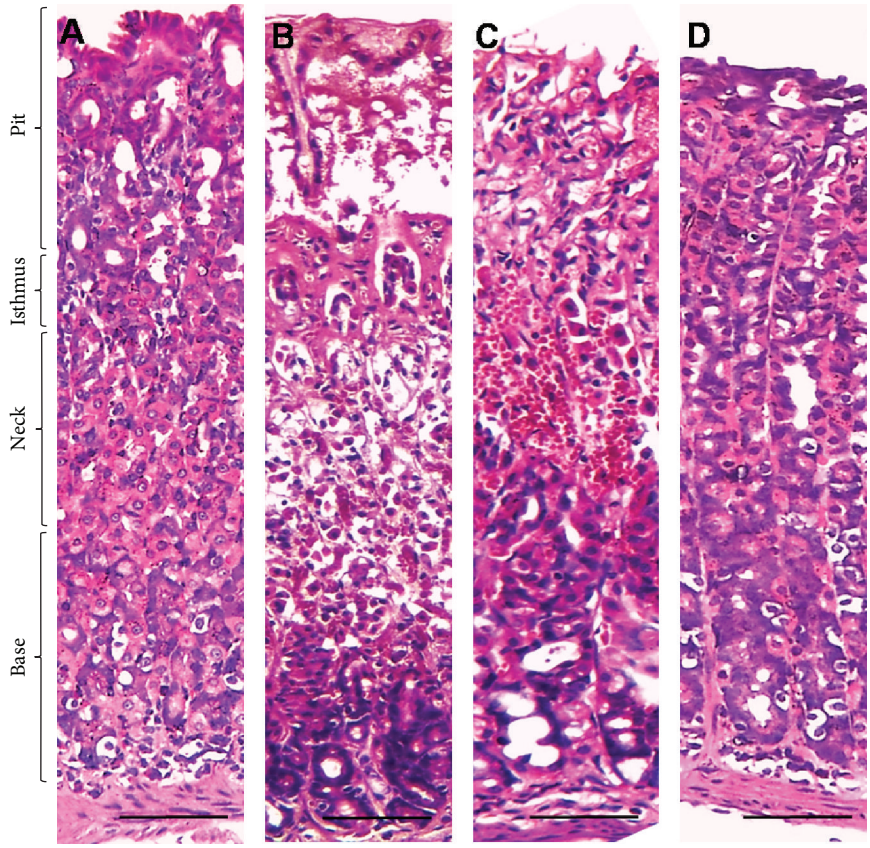

Figure 2: Light microscopic images of gastric mucosa. (a) The control group showed normal histologic appearance of all parts of the gastric wall. (b) The EtOH-induced gastric ulcer group revealed severe degeneration, necrosis, and hemorrhage of gastric base, neck, and isthmus with sloughing of gastric pits. (c) The EtOH-induced gastric ulcer and treated with *S. persica* at a dose of 200 mg/kg b.w. group showed moderated degeneration and hemorrhage in the gastric neck, isthmus, and pits with slight vacuolation in the gastric neck. (d) The EtOH-induced gastric ulcer and treated with *S. persica* at a dose of 400 mg/kg b.w. group showed normal histologic appearance of all gastric portions with only slight vacuolation. Scale bar = 50 μm.

H_2O_2 in absolute methanol for 30 min at 4°C. After washing with PBS, the nonspecific reaction was blocked with 10% normal blocking serum for 60 min at room temperature. The sections were incubated at 4°C overnight with the specific primary antibody: monoclonal rabbit anti-human Bax antibody (Abcam, Cat: ab32503); polyclonal rabbit anti-mouse iNOS antibody (Abcam, Cat: ab15323, Cambridge, UK); polyclonal rabbit anti-mouse IL-1β antibody (Abcam, Cat: ab9722); and polyclonal rabbit anti-human CD3 antibody (Abcam, Cat: ab5690) diluted in 1.5% BSA/PBS (pH 7.2) at 1 : 100; 1 : 300; 1 : 250; and 1 : 100, respectively. For negative control sections, PBS was used instead of the primary antibody. After washing with PBS, the sections were incubated with biotin-conjugated goat anti-rabbit IgG antiserum (Histofine kit, Nichirei Corp.) for 60 min and then washed with PBS, followed by incubation with streptavidin-peroxidase conjugate (Histofine kit, Nichirei Corp.) for 30 min. The streptavidin-biotin complex was visualized with 3,3′-diaminobenzidine tetrahydrochloride (DAB) H_2O_2 solution, pH 7.0, for 3 min. Then sections were washed in distilled water and Mayer's hematoxylin was used as a counterstain. The section images were taken with a digital camera (Leica EC3, Leica, Germany) connected to a microscope (Leica DM500).

2.11. Statistical Analysis. Data were analyzed with one-way ANOVA followed by Tukey's post hoc test multiple comparisons using GraphPad Prism 5 (GraphPad Software, San Diego, CA, USA). The data of oxidative and antioxidant status were analyzed with one-way ANOVA followed by Duncan's post hoc test multiple comparisons using the SPSS programming tool (IBM SPSS. 201, Coppell, TX, USA).

3. Results

3.1. GC-MS Analysis of S. persica Extract. Phytochemical ingredients of SP extract detected with GC-MS analysis are listed in Table 3 and Figure S1. The SP extract contained many ingredients with antioxidant potentials such as lycopene (16.56%), α-linolenic acid (1.77%), oleic acid (1.97%), lycoxanthin (1.61%), and retinoic acid (1.31%).

3.2. Macroscopic Examination of Gastric Mucosa. Normal appearance of gastric mucosal epithelium and folding in the control group is shown in Figure 1. Rats exposed to EtOH

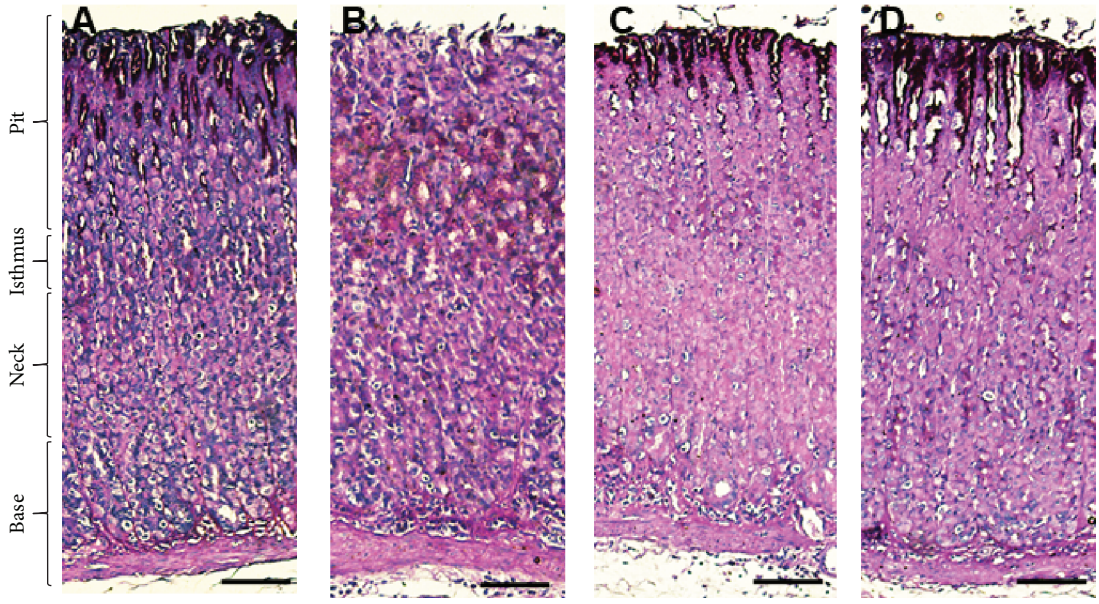

Figure 3: Light micrograph of histochemical staining of periodic acid–Schiff (PAS) in rats. (a) Control rats revealed intense PAS reaction at the surface mucous epithelium in the pit region. (b) No PAS reaction at the surface mucous epithelium in the pit region and moderate PAS reaction at the mucous cells in the pit and isthmus region of EtOH-induced gastric injury. (c) Lower distribution of PAS reacting cells in the SP200-protected group than those observed in the control group concentrated mainly in the pit region. (d) Similar distribution of PAS reacting cells in the SP400-protected group to the control group concentrated in the pit region. Scale bar = 50 μm.

Table 4: Oxidative stress and antioxidative profile in ethanol-induced gastric ulcer rat model pretreated with *S. persica* extract.

	MDA (nmol/g)	GSH (μmol/g)	T.SOD (U/g)	CAT (U/g)	GPX (U/g)	GST (U/g)
Control	101.3 ± 8.2^{a}	16.8 ± 1.6^{c}	75.4 ± 7.8^{c}	11.2 ± 2.6^{c}	46.9 ± 7.6^{c}	143.2 ± 12.4^{c}
EtOH	111.5 ± 7.6^{a}	14.2 ± 1.4^{d}	70.5 ± 5.4^{c}	9.8 ± 1.1^{d}	41.7 ± 8.9^{c}	131.8 ± 15.8^{c}
EtOH + SP200	83.7 ± 8.9^{b}	18.6 ± 2.1^{b}	85.4 ± 7.1^{b}	13.6 ± 2.3^{b}	63.8 ± 8.7^{b}	165.7 ± 13.3^{b}
EtOH + SP400	74.3 ± 9.1^{b}	22.9 ± 1.9^{a}	96.8 ± 6.4^{a}	16.7 ± 2.2^{a}	72.9 ± 6.3^{a}	181.2 ± 11.8^{a}

Values are expressed as mean ± SEM. The means within the same column carrying different superscript letters are significantly different at $P < 0.05$ as determined with one-way ANOVA, followed by Duncan's post hoc test multiple comparisons. EtOH: ethanol-induced gastric ulcer group; EtOH + SP200: ethanol-induced gastric ulcer pretreated with *S. persica* extract at a dose of 200 mg/kg b.w.; EtOH + SP400: ethanol-induced gastric ulcer pretreated with *S. persica* extract at a dose of 400 mg/kg b.w.

revealed severe gastric mucosal congestion and hemorrhage, loose mucosal folds, and thinning and ballooning of the gastric wall with serious ulcers. However, treatment with SP extract significantly reduced the ethanol-induced gastric lesions, moderated congestion and petechial hemorrhage, improved the gastric mucosal folding, and lowered the ulcer index at an SP extract dose of 200 mg/kg, while the high dose of 400 mg/kg caused more alleviation in these lesions as compared to normal ones.

3.3. Histological Findings. Light microscopic examination of the gastric mucosa stained with H&E showed a normal structure of all gastric portions in the control group (Figure 2). Contrary to the control, ethanol produced gastric damage as manifested by intense degeneration, necrosis, and hemorrhages in almost all parts of the gastric wall, severe submucosal edema, and sloughing of gastric pits. Interestingly, treatment with SP extract significantly reduced the degeneration and hemorrhage induced by ethanol, indicating protective action that was evident with the high dose of 400 mg/kg b.w.

An augmented level of PAS staining was observed at the surface of the mucosal epithelium in the pit region in the control group (Figure 3), indicating high glycoprotein contents. However, negative PAS staining of the surface mucosal epithelium showed low reactivity at the mucosa cells in the pit and isthmus regions among those in the alcohol-treated group. Notably, there was moderate distribution of PAS-reacting cells mainly at the pit region in SP200-treated rats, and an intense reaction was observed in SP400-treated rats resembling those in the control rats.

3.4. Oxidative Damage and Antioxidative Biomarkers. The levels of antioxidant GSH (14.2 ± 1.4 μmol/g tissue) and CAT (9.8 ± 1.1 U/g tissue) were significantly reduced in the EtOH group relative to control. Notably, SP extract intake in a dose-dependent manner significantly attenuated the gastric MDA level and motivated the enzymatic and

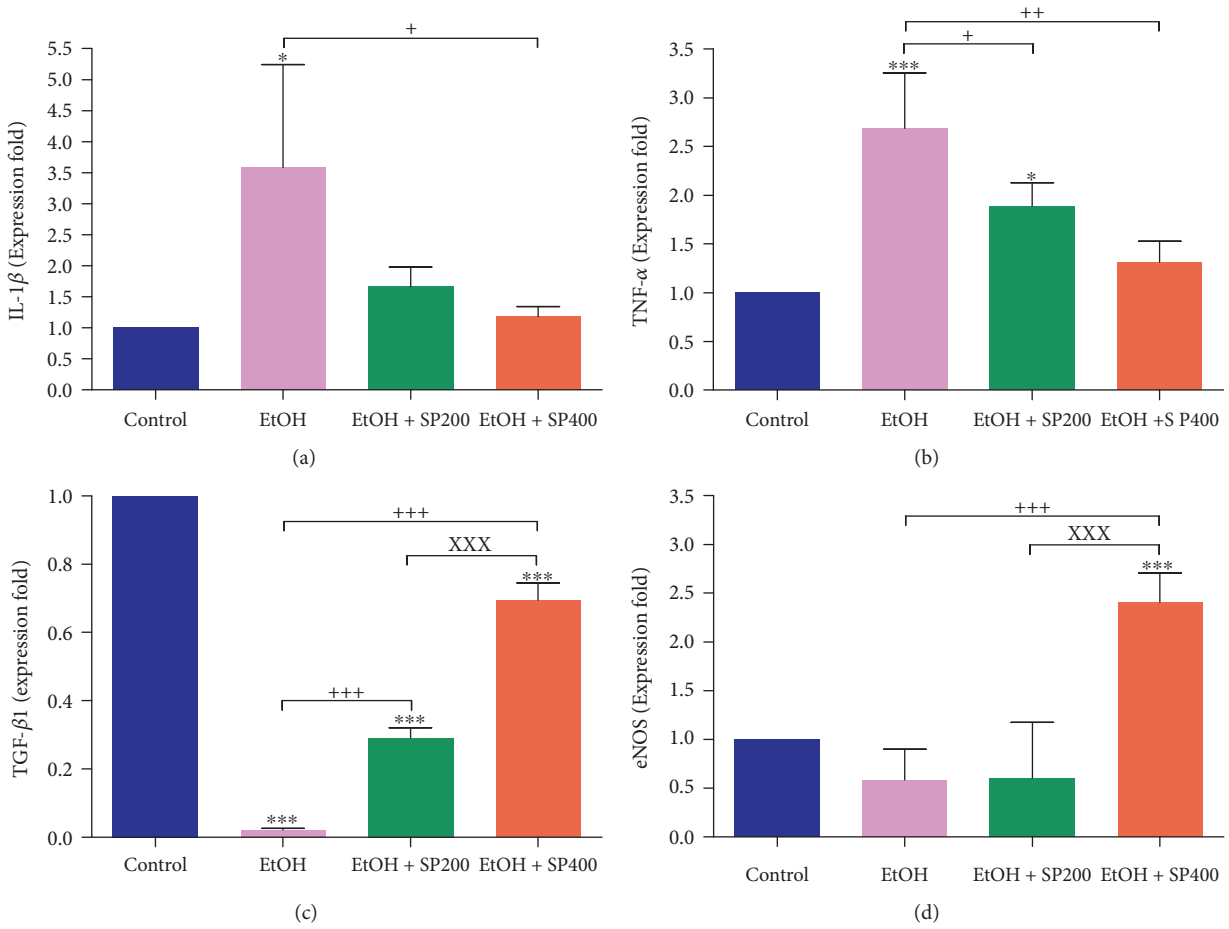

Figure 4: Reverse transcription polymerase chain reaction (RT-PCR) validation of (a) IL-1β, (b) TNF-α, (c) TGF-β1, and (d) eNOS. IL-1β: interleukin-1 beta; TNF-α: tumor necrosis factor-alpha: TGF-β1: transforming growth factor beta; eNOS: endothelial nitric oxide synthase; CON: control; EtOH: ethanol-treated group; EtOH + SP200: ethanol-treated and treated with *S. persica* at a dose of 200 mg/kg b.w.; EtOH + SP400: ethanol-treated and treated with *S. persica* at a dose of 400 mg/kg b.w. $^{*}P < 0.05$ and $^{***}P < 0.001$ versus control. $^{+}P < 0.05$, $^{++}P < 0.01$, and $^{+++}P < 0.001$ versus EtOH. $^{xxx}P < 0.001$ versus EtOH + SP400. Statistical analysis was done with one-way ANOVA, followed by Tukey's post hoc test multiple comparisons. Error bars represent SE. Samples ($n = 5$).

nonenzymatic antioxidant levels $P < 0.05$ when compared to EtOH-treated rats, suggesting antioxidative characteristics of the SP extract (Table 4).

3.5. Gastric IL-1β, TNF-α, TGF-β1, and eNOS Relative Expression. Ethanol intake significantly upregulated the proinflammatory cytokines' expression: TNF-α (2.7-fold) ($P < 0.001$) and IL-1β (3.5-fold) ($P < 0.05$). It also reduced the expression of TGF-β1 (0.02-fold) ($P < 0.001$) and insignificantly downregulated eNOS (0.6-fold), elucidating the inflammatory condition as compared to control (Figure 4). Pretreatment with SP extract significantly downregulated both proinflammatory cytokines in a dose-dependent manner comparable to the EtOH-treated group while causing an elevation in the relative expression of TGF-β1 and eNOS $P < 0.001$, which is more pronounced at the high dose of SP extract in comparison to the control group.

3.6. Immunohistochemical Detection of Bax, iNOS, IL-1β, and CD3 Proteins. Immunohistochemical analysis revealed an overexpression of Bax, IL-1β, iNOS, and CD3 proteins in the ethanol-treated group as indicated by high distribution of IL-1β-, Bax-, and iNOS-immunopositive cells in the base, neck, isthmus, and mucous surface of the pit region as compared to negative or low distribution of immunopositive cells in the control group (Figures 5–7), while CD3-immunopositive cells distributed at the margin of the inflammation that was extensive in the alcohol group penetrated all epithelial layers (Figure 8). Interestingly, pretreatment with SP extract significantly reduced the immunopositive staining of IL-1β, Bax, CD3, and eNOS in a dose-dependent manner in the EtOH group, elucidating reduced expression of these proteins.

4. Discussion

The current study highlights the antiulcerative effect of SP aqueous extract against EtOH-induced gastric ulceration in rats. This antiulcerative potential might be due to the antioxidant ingredients found in SP aqueous extract such as lycopene [31], α-linolenic acid [32], oleic acid [33], lycoxanthin [34], and retinoic acid [35].

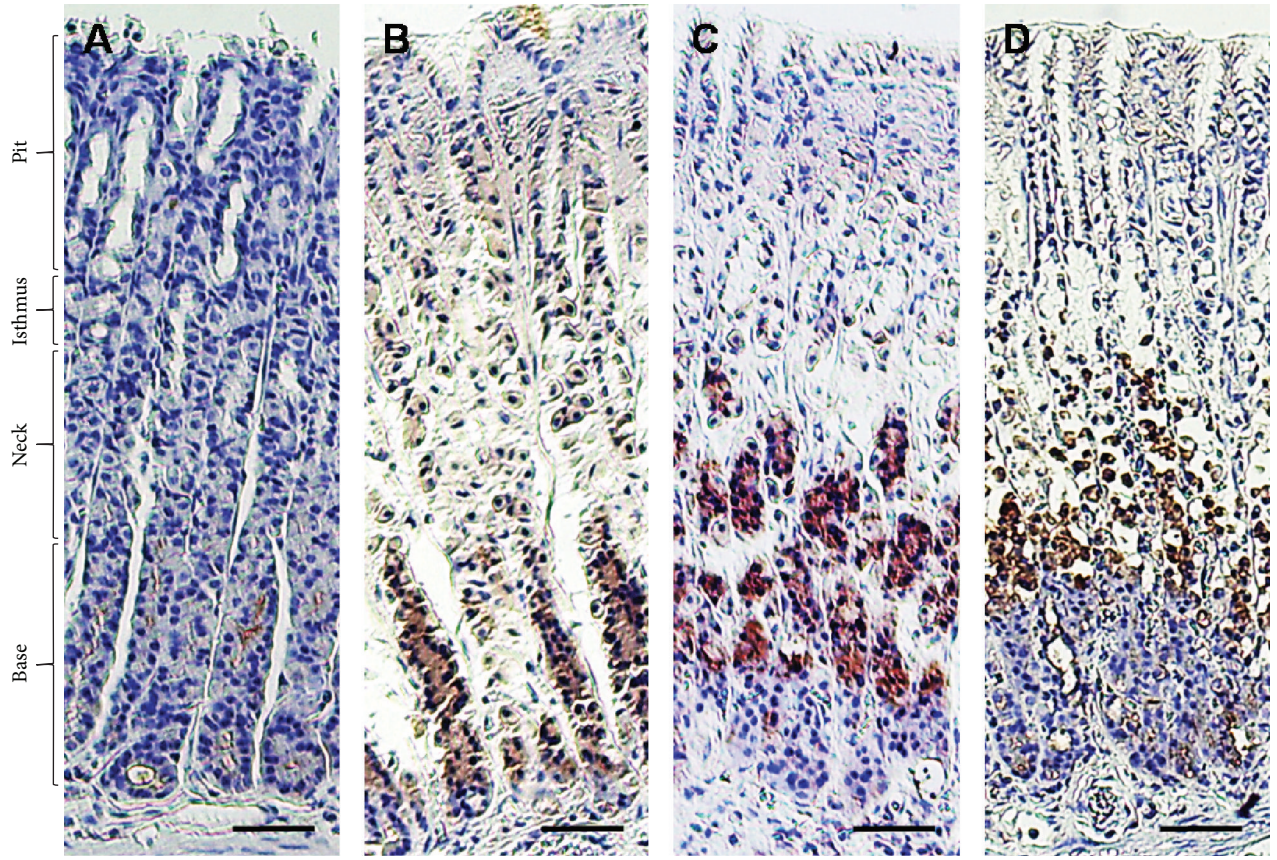

Figure 5: Immunohistochemical reactivity of Bax in rats exposed to induced gastric ulcer and treated with *S. persica* extract. (a) Control group, (b) EtOH-induced gastric ulcer group, (c) EtOH-induced gastric ulcer and treated with *S. persica* at a dose of 200 mg/kg b.w. group, and (d) EtOH-induced gastric ulcer and treated with *S. persica* at a dose of 400 mg/kg b.w. group. Scale bar = 50 μm.

Short-term exposure to ethanol-induced gastric damage, hemorrhagic erosions, and increased gastric ulcer index (UI) was confirmed by our histological findings: hemorrhagic degeneration, submucosal edema, shedding of gastric pits, and decreased glycoproteins in the gastric mucosal surface. These results are similar to those obtained by Yang et al. [36] who stated that ethanol had an immense effect on the gastric mucosa represented by severe hyperemia, inflammatory cell infiltration, loss of epithelial cells, and cell erosions. In addition to hemorrhage, epithelial exfoliation, submucosal edema [37], and mucosal friability [38] were recognized. In a recent study, interrupted gastric mucosa, neutrophil infiltration, glandular cell nuclear intensification, and acute hemorrhage were the major histological findings following ethanol exposure in rats [39].

The collective mechanisms implicated in the gastric damaging effect induced by ethanol are due to the perturbation of the antioxidant system, recruitment of inflammatory cascade and apoptosis, and disturbance of nitric oxide synthases. Results of the present study revealed that ethanol stimulated slight production of MDA accompanied by the minimization of both enzymatic and nonenzymatic antioxidants in gastric tissues. Antonisamy et al. [5] revealed that the imbalance between prooxidant and antioxidant molecules is the major contributor of ethanol-induced gastric damage. Park et al. [25] reported that ethanol had dual effects on the gastric mucosa: direct action through damaging the mucosal membranes, cytotoxic dehydration, and generation of inflammatory signaling pathways and an indirect action via neutrophil infiltration with subsequent inflammation and induction of oxidative stress and apoptosis. Alcohol consumption catalyzed the formation of MDA in the gastric tissue with a reduction in SOD, CAT enzymatic activities [40], and GPX activity [41]. Treatment with SP extract caused a decline in the gastric MDA level and enhanced the enzymatic and nonenzymatic antioxidants. The antioxidant activity of SP may be attributed to its high content of furan derivatives, vitamin C, tannins, saponins, and flavonoids [42, 43].

The data of the current study showed an upregulation of gene expression of proinflammatory cytokines: TNF-α and IL-1β in the gastric mucosa of the EtOH-treated rats. In the same context, Katary and Salahuddin [44] reported the enhancement of gene expression and mucosal levels of TNF-α along with increased mucosal levels of IL-1β after ethanol consumption in rats. The gastric inflammatory condition has been associated with the release of TNF-α, which activates the immune cells and other proinflammatory cytokines and increases the NF-κB expression [45]. TNF-α could trigger gastric tissue damage mediated through the activation of neutrophil migration into the gastric tissue associated with retardation of gastric ulcer healing [37]. Inevitably, alcohol resulted in the augmentation of the proinflammatory

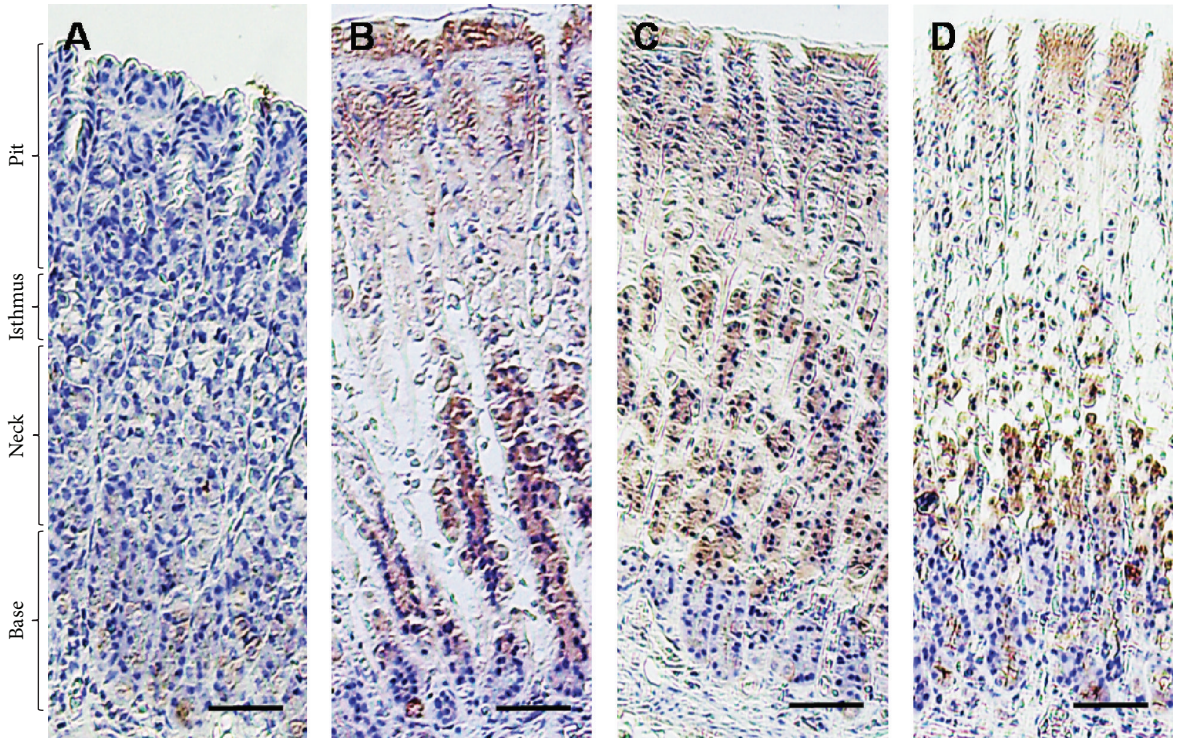

Figure 6: Immunohistochemical reactivity of iNOS in rats exposed to induced gastric ulcer and treated with *S. persica* extract. (a) Control group, (b) EtOH-induced gastric ulcer group, (c) EtOH-induced gastric ulcer and treated with *S. persica* at a dose of 200 mg/kg b.w. group, and (d) EtOH-induced gastric ulcer and treated by *S. persica* at a dose of 400 mg/kg b.w. group. Scale bar = 50 μm.

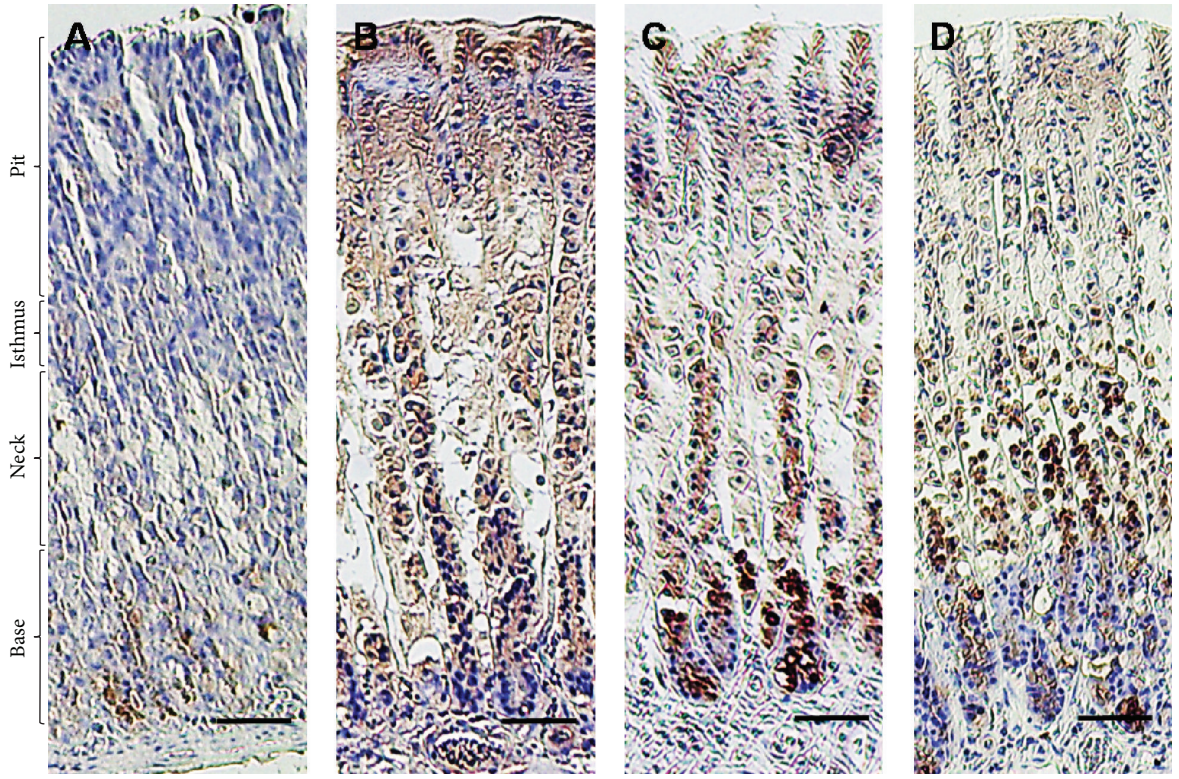

Figure 7: Immunohistochemical reactivity of IL-1β in rats exposed to induced gastric ulcer and treated with *S. persica* extract. (a) Control group, (b) EtOH-induced gastric ulcer group, (c) EtOH-induced gastric ulcer and treated with *S. persica* at a dose of 200 mg/kg b.w. group, and (d) EtOH-induced gastric ulcer and treated with *S. persica* at a dose of 400 mg/kg b.w. group. Scale bar = 50 μm.

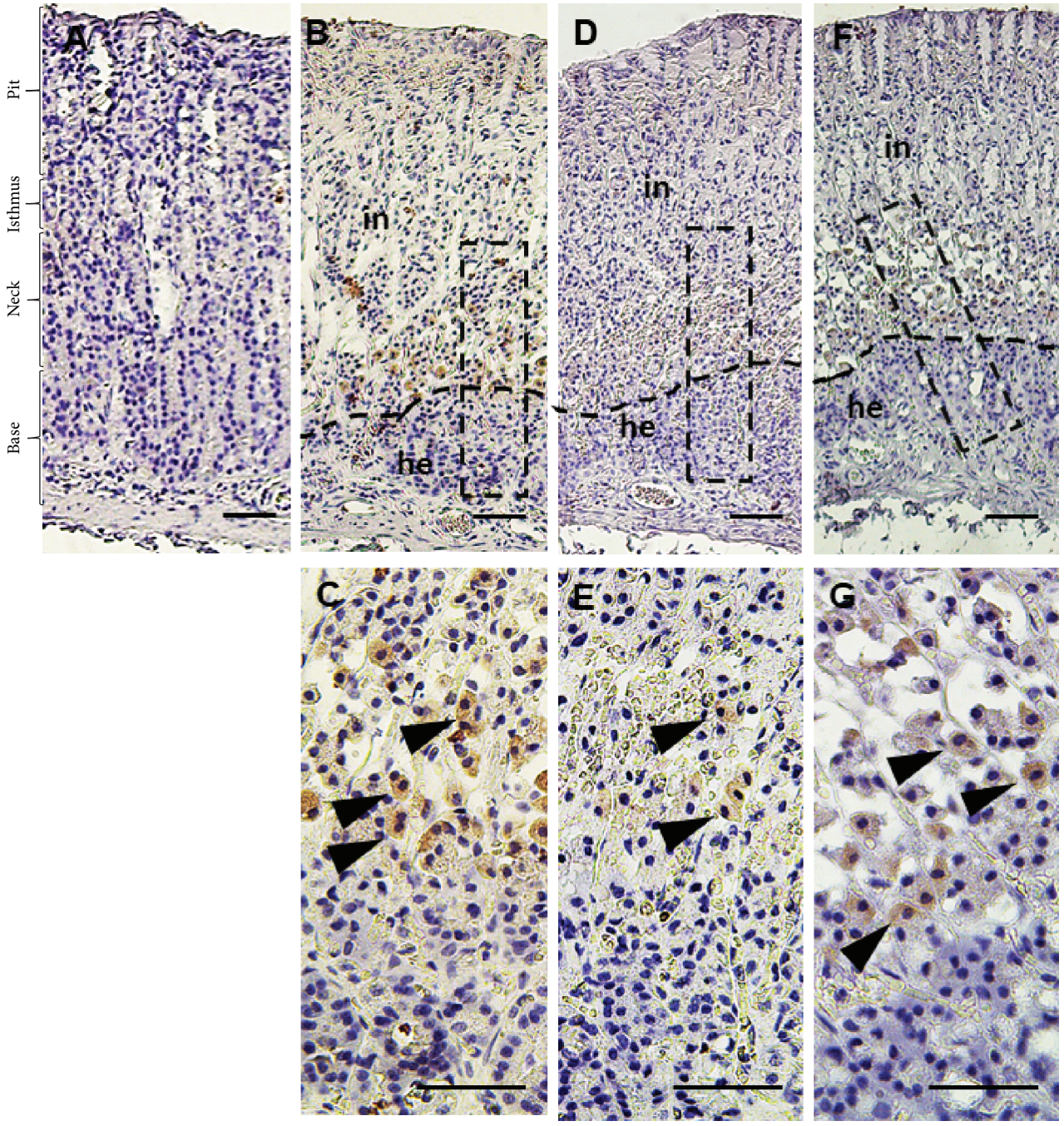

Figure 8: Immunohistochemical reactivity of CD3 in rats exposed to induced gastric ulcer and treated with *S. persica* extract. (a) Control group, (b-c) EtOH-induced gastric ulcer group, (d-e) EtOH-induced gastric ulcer and treated with *S. persica* at a dose of 200 mg/kg b.w. group, and (f-g) EtOH-induced gastric ulcer and treated with *S. persica* at a dose of 400 mg/kg b.w. group. Scale bar = 50 μm.

cytokines: TNF-α participating in gastric ulcer via boosting apoptosis, NF-κB, iNOS, and neutrophil infiltration and IL-1β arousing the oxidative stress inflicting the gastric damage [46]. Meanwhile, TNF-α promotes the release of oxygen free radicals and other proinflammatory cytokines, causing destruction of cell membrane stability and leading to gastric tissue injuries [36].

TGF-β1 coordinates different signaling pathways including adhesion, cell proliferation, angiogenesis, and production of extracellular matrix components [47]. Our data revealed low expression of TGF-β1 in the EtOH-treated group, while SP extract mitigated the inflammatory effect of ethanol on the gastric tissue, which is in compliance with the results of Monforte et al. [17] who showed that the antiulcer activity of SP decoction against acetylsalicylic acid-induced gastric ulcer in rats resulted in a significant reduction of UI via anti-inflammatory activity. Furthermore, the serum proinflammatory cytokine IL-1β, IL-6, and TNF-α levels

were significantly decreased following the administration of ethyl acetate extract of SP in a gastric ulcer model [20].

Apoptosis induction was evidenced in the current study by increased protein expression of the proapoptotic Bax after EtOH exposure. Ye et al. [48] reported that the gastric damage induced by ethanol might be due, to a certain extent, to the enhancement of the apoptotic pathway. The proapoptotic protein Bax signals the initiation of apoptosis [4], causing cytochrome-C release followed by caspase cascade activation and finally apoptotic cell death [49]. Notably, Al Batran et al. [50] implied that ethanol-triggered gastric injury was in part due to the enhancement of apoptosis in subsequent mucosal epithelial cell loss. The attenuation of lipid peroxidation and TNF-α secretion resulted in inhibition of the gastric apoptosis [4]. The antioxidative and anti-inflammatory activities of SP reflected the inhibition of the apoptotic pathway, providing another explanation of its antiulcer activity.

Ethanol evoked the protein expression of iNOS and the decline of the gene expression of eNOS in gastric tissue. A high concentration of NO generated from iNOS was involved in the gut tissue damage during the inflammatory conditions [51]. Nagai et al. [52] indicated that iNOS-produced NO had a critical role in the enhancement of gastric ulcer. Activation of iNOS expression was associated with gastric ulcer and chronic ulcerative colitis in affected patients, suggesting a detrimental effect due to the excessive production of NO on the pathogenesis of these conditions [53]. In contrast, eNOS-derived NO plays a central role in gastric ulcer healing via the maintenance of gastric epithelium, mucosal blood flow, and mucus secretion and synthesis [54]. The present results are comparable to those of Pan et al. [55] who reported that ethanol activated iNOS and the inhibitory effect on eNOS gene expression. Furthermore, ethanol provoked the gene expression of TNF-α, IL-1β, and iNOS, inflicting the immense effect of the generated NO on gastric ulcer formation [56]. This phenomenon was initiated via the NF-κB pathway where the production of proinflammatory cytokines TNF-α and IL-1β, upregulation of iNOS gene expression, and release of NO were enhanced by activated NF-κB during gastric ulcer formation [57]. However, pretreatment with SP extract significantly reduced the protein expression of iNOS and upregulated eNOS gene expression in gastric tissue exposed to EtOH, indicating an antiulcerative effect. NO derived from highly expressed iNOS in the ulcerated stomach had no role in the healing process modulation. On the contrary, eNOS-originated NO might enhance the formation of new blood vessels assisting the gastric ulcer healing [11]. This hypothesis suggested the involvement of NO generated from eNOS isoforms in the healing process of gastric ulcers. This mechanism emphasizes the pivotal role that NO plays in the liberation of vasoactive peptides and in the stimulation of cGMP in gastric tissue [58]. NO-stimulated cGMP led to relaxation of mouse gastric smooth muscles and prevented the cytotoxic effect of EtOH on the gastric parietal cells [59]. Also, eNOS-originated NO established the protection and healing of gastric ulcer via augmentation of mucus and bicarbonate secretions, promotion of blood flow, and angiogenesis [60]. CD3 proteins are receptors characteristic for T lymphocyte populations. Bamford et al. [61] detected an increase of CD3 expression in gastric inflammation caused by infection of *H. pylori*. Our results showed the increase of intensity of CD3-expressed cells in the EtOH-treated group that decreased in the SP-treated groups suggesting the effective role of SP in decreasing the symptoms of inflammation that resulted from alcohol exposure. This supports our histological PAS staining that was used to evaluate the level of glycoprotein, mucin, and subsequent mucus content; intense mucin staining in the mucosal cell layer reflects high mucus content in the SP-treated groups, suggesting a protective effect.

5. Conclusion

SP aqueous extract alleviated serious gastric mucosal ulcerations induced by ethanol and emphasized its efficacy as an antiulcer protectant. The underlying mechanism of its activity is through the enhancement of the antioxidative defense system, minimization of proinflammatory cytokines and apoptotic pathway, augmentation of mucus content, and redesign of the NOS isoforms supporting the antioxidant, anti-inflammatory, and antiapoptotic effects of SP favoring the healing and prevention of gastric ulcers.

Data Availability

All data generated or analyzed during this study are included in this article and its supplementary information files.

Ethical Approval

The experiments were done following the Ethics Committee recommendations at the Faculty of Veterinary Medicine, Alexandria University, Egypt.

Conflicts of Interest

The authors declare that they have no competing interests.

Authors' Contributions

Mohamed A. Lebda, Ali H. El-Far, Ahmed E. Noreldin, and Yaser H. A. Elewa contributed equally to the experimental design, experimental work, data analysis, manuscript writing, and manuscript revisions. Shaker A. Mousa and Soad K. Al Jaouni contributed to the design, manuscript writing, and manuscript revisions.

Acknowledgments

The authors express many thanks to Kelly A. Keating (Pharmaceutical Research Institute, Albany College of Pharmacy and Health Sciences) for the brilliant language revision.

Supplementary Materials

Figure S1: GC-MS chromatogram showing the area % of *S. persica* extract phytoconstituents at different retention times. *(Supplementary Materials)*

References

[1] L. Laine, K. Takeuchi, and A. Tarnawski, "Gastric mucosal defense and cytoprotection: bench to bedside," *Gastroenterology*, vol. 135, no. 1, pp. 41–60, 2008.

[2] J. M. Kang, P. J. Seo, N. Kim et al., "Analysis of direct medical care costs of peptic ulcer disease in a Korean tertiary medical center," *Scandinavian Journal of Gastroenterology*, vol. 47, no. 1, pp. 36–42, 2011.

[3] Y.-F. Zheng, J.-H. Xie, Y.-F. Xu et al., "Gastroprotective effect and mechanism of patchouli alcohol against ethanol, indomethacin and stress-induced ulcer in rats," *Chemico-Biological Interactions*, vol. 222, pp. 27–36, 2014.

[4] S. I. Abdelwahab, "Protective mechanism of gallic acid and its novel derivative against ethanol-induced gastric ulcerogenesis: involvement of immunomodulation markers, Hsp70 and Bcl-2-associated X protein," *International Immunopharmacology*, vol. 16, no. 2, pp. 296–305, 2013.

[5] P. Antonisamy, P. Subash-Babu, A. Albert-Baskar et al., "Experimental study on gastroprotective efficacy and mechanisms of luteolin-7-O-glucoside isolated from *Ophiorrhiza mungos* Linn. in different experimental models," *Journal of Functional Foods*, vol. 25, pp. 302–313, 2016.

[6] W.-c. Zhao, Y.-s. Xu, G. Chen, Y. Guo, D.-y. Wang, and G.-b. Meng, "*Veronicastrum axillare* alleviates ethanol-induced injury on gastric epithelial cells via downregulation of the NF-kB signaling pathway," *Gastroenterology Research and Practice*, vol. 2017, Article ID 7395032, 8 pages, 2017.

[7] X. Chang, F. Luo, W. Jiang et al., "Protective activity of salidroside against ethanol-induced gastric ulcer via the MAPK/NF-κB pathway in vivo and in vitro," *International Immunopharmacology*, vol. 28, no. 1, pp. 604–615, 2015.

[8] D. Laloo, S. K. Prasad, S. Krishnamurthy, and S. Hemalatha, "Gastroprotective activity of ethanolic root extract of *Potentilla fulgens* Wall. ex Hook," *Journal of Ethnopharmacology*, vol. 146, no. 2, pp. 505–514, 2013.

[9] X. Mei, D. Xu, S. Xu, Y. Zheng, and S. Xu, "Novel role of Zn(II)–curcumin in enhancing cell proliferation and adjusting proinflammatory cytokine-mediated oxidative damage of ethanol-induced acute gastric ulcers," *Chemico-Biological Interactions*, vol. 197, no. 1, pp. 31–39, 2012.

[10] P. Antonisamy, P. Subash-Babu, A. A. Alshatwi et al., "Gastroprotective effect of nymphayol isolated from Nymphaea stellata (Willd.) flowers: contribution of antioxidant, anti-inflammatory and anti-apoptotic activities," *Chemico-Biological Interactions*, vol. 224, pp. 157–163, 2014.

[11] L. Ma and J. L. Wallace, "Endothelial nitric oxide synthase modulates gastric ulcer healing in rats," *American Journal of Physiology-Gastrointestinal and Liver Physiology*, vol. 279, no. 2, pp. G341–G346, 2000.

[12] C. H. Cho, "Current roles of nitric oxide in gastrointestinal disorders," *Journal of Physiology-Paris*, vol. 95, no. 1–6, pp. 253–256, 2001.

[13] H. Suo, X. Zhao, Y. Qian et al., "Lactobacillus fermentum Suo attenuates HCl/ethanol induced gastric injury in mice through its antioxidant effects," *Nutrients*, vol. 8, no. 3, p. 155, 2016.

[14] A. S. Tarnawski, "Cellular and molecular mechanisms of gastrointestinal ulcer healing," *Digestive Diseases and Sciences*, vol. 50, Supplement 1, pp. S24–S33, 2005.

[15] L. Pinheiro Silva, C. Damacena de Angelis, F. Bonamin et al., "*Terminalia catappa* L.: a medicinal plant from the *Caribbean pharmacopeia* with anti-*Helicobacter pylori* and antiulcer action in experimental rodent models," *Journal of Ethnopharmacology*, vol. 159, pp. 285–295, 2015.

[16] P. Salehi and S. H. Momeni Danaie, "Comparison of the antibacterial effects of persica mouthwash with chlorhexidine on Streptococcus mutans in orthodontic patients," *DARU Journal of Pharmaceutical Sciences*, vol. 14, no. 4, pp. 178–182, 2006.

[17] M. T. Monforte, N. Miceli, M. R. Mondello, R. Sanogo, A. Rossitto, and E. M. Galati, "Antiulcer activity of Salvadora persica on experimental ASA-induced ulcer in rats: ultrastructural modifications," *Pharmaceutical Biology*, vol. 39, no. 4, pp. 289–292, 2008.

[18] G. A. Soliman, M. A. Ganaie, H. N. Althurwi, F. F. Albaqami, M. A. Salkini, and M. S. Abdel-Kader, "Extract of *Salvadora persica* roots attenuates lead acetate-induced testicular oxidative stress in rats," *Journal of Pharmacy & Pharmacognosy Research*, vol. 5, no. 4, pp. 238–250, 2017.

[19] M. Nomani, M. J. Hosseini, M. Vazirian, A. Nomani, and H. R. Monsef-Esfahani, "Evaluation of anti-inflammatory effect of *Salvadora persica* in IBD-induced rat," *Research Journal of Pharmacognosy*, vol. 4, p. 27, 2017.

[20] A. Y. Ibrahim, S. E. el-Gengaihi, H. M. Motawea, and A. A. Sleem, "Anti-inflammatory activity of *Salvadora persica* L. against carrageenan induced paw oedema in rat relevant to inflammatory cytokines," *Notulae Scientia Biologicae*, vol. 3, no. 4, pp. 22–28, 2011.

[21] A.-M. Fouda and A. R. Youssef, "Antiosteoporotic activity of *Salvadora persica* sticks extract in an estrogen deficient model of osteoporosis," *Osteoporosis and Sarcopenia*, vol. 3, no. 3, pp. 132–137, 2017.

[22] R. Albabtain, M. Azeem, Z. Wondimu, T. Lindberg, A. K. Borg-Karlson, and A. Gustafsson, "Investigations of a possible chemical effect of *Salvadora persica* chewing sticks," *Evidence-Based Complementary and Alternative Medicine*, vol. 2017, Article ID 2576548, 10 pages, 2017.

[23] M. S. Hooda, R. Pal, A. Bhandari, and J. Singh, "Antihyperglycemic and antihyperlipidemic effects of *Salvadora persica* in streptozotocin-induced diabetic rats," *Pharmaceutical Biology*, vol. 52, no. 6, pp. 745–749, 2014.

[24] W. Filimban, N. ElSawy, E. A. Header, and M. El-Boshy, "Evaluation of aqueous extract of *Salvadora persica* and *Glycyrrhiza glabra* in treatment of gastric ulcer," *Jokull Journal*, vol. 65, no. 5, pp. 275–293, 2015.

[25] S. W. Park, T. Y. Oh, Y. S. Kim et al., "*Artemisia asiatica* extracts protect against ethanol-induced injury in gastric mucosa of rats," *Journal of Gastroenterology and Hepatology*, vol. 23, no. 6, pp. 976–984, 2008.

[26] A. Bozkurt, M. Yuksel, G. Haklar, H. Kurtel, B. C. Yegen, and I. Alican, "Adenosine protects against indomethacin-induced gastric damage in rats," *Digestive Diseases and Sciences*, vol. 43, no. 6, pp. 1258–1263, 1998.

[27] D. Das and R. K. Banerjee, "Effect of stress on the antioxidant enzymes and gastric ulceration," *Molecular and Cellular Biochemistry*, vol. 125, no. 2, pp. 115–125, 1993.

[28] J. D. Bancroft and C. Layton, "The hematoxylin and eosin," in *Theory Practice of Histological Techniques*, S. K. Suvarna, C. Layton, and J. D. Bancroft, Eds., Churchill Livingstone of El Sevier, Philadelphia, PA, USA, 7th edition, 2013.

[29] A. G. E. Pearse, *Histochemistry, Theoretical and Applied, Preparative and Optical Technology*, Churchill-Livingstone, Edinburgh, 4th edition, 1980.

[30] J. S. Yuan, A. Reed, F. Chen, and C. N. Stewart Jr., "Statistical analysis of real-time PCR data," *BMC Bioinformatics*, vol. 7, no. 1, p. 85, 2006.

[31] C. Hanson, E. Lyden, J. Furtado et al., "Serum lycopene concentrations and associations with clinical outcomes in a cohort of maternal-infant dyads," *Nutrients*, vol. 10, no. 2, p. 204, 2018.

[32] É. Fortin, R. Blouin, J. Lapointe, H. V. Petit, and M.-F. Palin, "Linoleic acid, α-linolenic acid and enterolactone affect lipid oxidation and expression of lipid metabolism and antioxidant-related genes in hepatic tissue of dairy cows," *British Journal of Nutrition*, vol. 117, no. 09, pp. 1199–1211, 2017.

[33] J. S. Perona, C. Arcemis, V. Ruiz-Gutierrez, and A. Catala, "Effect of dietary high-oleic-acid oils that are rich in antioxidants on microsomal lipid peroxidation in rats," *Journal of Agricultural and Food Chemistry*, vol. 53, no. 3, pp. 730–735, 2005.

[34] Y. Bellik, L. Boukraâ, H. Alzahrani et al., "Molecular mechanism underlying anti-inflammatory and anti-allergic activities of phytochemicals: an update," *Molecules*, vol. 18, no. 1, pp. 322–353, 2013.

[35] R. Edge and T. Truscott, "Singlet oxygen and free radical reactions of retinoids and carotenoids—a review," *Antioxidants*, vol. 7, no. 1, p. 5, 2018.

[36] Y. Yang, B. Yin, L. Lv et al., "Gastroprotective effect of aucubin against ethanol-induced gastric mucosal injury in mice," *Life Sciences*, vol. 189, pp. 44–51, 2017.

[37] K. Amirshahrokhi and A.-R. Khalili, "The effect of thalidomide on ethanol-induced gastric mucosal damage in mice: involvement of inflammatory cytokines and nitric oxide," *Chemico-Biological Interactions*, vol. 225, pp. 63–69, 2015.

[38] M. Umamaheswari, K. AsokKumar, A. Somasundaram, T. Sivashanmugam, V. Subhadradevi, and T. K. Ravi, "Xanthine oxidase inhibitory activity of some Indian medical plants," *Journal of Ethnopharmacology*, vol. 109, no. 3, pp. 547–551, 2007.

[39] Y. Zhang, H. Wang, N. Mei et al., "Protective effects of polysaccharide from *Dendrobium nobile* against ethanol-induced gastric damage in rats," *International Journal of Biological Macromolecules*, vol. 107, Part A, pp. 230–235, 2018.

[40] C. Xu, C. Ding, N. Zhou, X.-M. Ruan, and B.-X. Guo, "A polysaccharide from *Aloe vera* L. var. *chinensis* (Haw.) Berger prevents damage to human gastric epithelial cells in vitro and to rat gastric mucosa in vivo," *Journal of Functional Foods*, vol. 24, pp. 501–512, 2016.

[41] A. Paulrayer, A. Adithan, J. Lee et al., "*Aronia melanocarpa* (black chokeberry) reduces ethanol-induced gastric damage via regulation of HSP-70, NF-κB, and MCP-1 signaling," *International Journal of Molecular Sciences*, vol. 18, no. 6, p. 1195, 2017.

[42] S. A. Mohamed and J. A. Khan, "Antioxidant capacity of chewing stick miswak *Salvadora persica*," *BMC Complementary and Alternative Medicine*, vol. 13, no. 1, 2013.

[43] M. A. Farag, S. Fahmy, M. A. Choucry, M. O. Wahdan, and M. F. Elsebai, "Metabolites profiling reveals for antimicrobial compositional differences and action mechanism in the toothbrushing stick "miswak" *Salvadora persica*," *Journal of Pharmaceutical and Biomedical Analysis*, vol. 133, pp. 32–40, 2017.

[44] M. A. Katary and A. Salahuddin, "Gastroprotective effect of punicalagin against ethanol-induced gastric ulcer: the possible underlying mechanisms," *Biomarkers Journal*, vol. 3, p. 3, 2017.

[45] S. K. Yadav, B. Adhikary, S. Chand, B. Maity, S. K. Bandyopadhyay, and S. Chattopadhyay, "Molecular mechanism of indomethacin-induced gastropathy," *Free Radical Biology & Medicine*, vol. 52, no. 7, pp. 1175–1187, 2012.

[46] S. Verma and V. L. Kumar, "Attenuation of gastric mucosal damage by artesunate in rat: modulation of oxidative stress and NFκB mediated signaling," *Chemico-Biological Interactions*, vol. 257, pp. 46–53, 2016.

[47] P. Shang, W. Liu, T. Liu et al., "Acetyl-11-keto-β-boswellic acid attenuates prooxidant and profibrotic mechanisms involving transforming growth factor-β1, and improves vascular remodeling in spontaneously hypertensive rats," *Scientific Reports*, vol. 6, no. 1, 2016.

[48] H.-H. Ye, K.-J. Wu, S.-J. Fei et al., "Propofol participates in gastric mucosal protection through inhibiting the toll-like receptor-4/nuclear factor kappa-B signaling pathway," *Clinics and Research in Hepatology and Gastroenterology*, vol. 37, no. 1, pp. e3–e15, 2013.

[49] X.-J. Luo, B. Liu, Z. Dai et al., "Expression of apoptosis-associated microRNAs in ethanol-induced acute gastric mucosal injury via JNK pathway," *Alcohol*, vol. 47, no. 6, pp. 481–493, 2013.

[50] R. Al Batran, F. Al-Bayaty, M. M. Jamil Al-Obaidi et al., "In vivo antioxidant and antiulcer activity of *Parkia speciosa* ethanolic leaf extract against ethanol-induced gastric ulcer in rats," *PLoS One*, vol. 8, no. 5, article e64751, 2013.

[51] M. D. Barrachina, J. P. Panes, and J. V. Esplugues, "Role of nitric oxide in gastrointestinal inflammatory and ulcerative diseases: perspective for drugs development," *Current Pharmaceutical Design*, vol. 7, no. 1, pp. 31–48, 2001.

[52] N. Nagai, T. Fukuhata, Y. Ito, S. Usui, and K. Hirano, "Involvement of interleukin 18 in indomethacin-induced lesions of the gastric mucosa in adjuvant-induced arthritis rat," *Toxicology*, vol. 255, no. 3, pp. 124–130, 2009.

[53] W. Li, H. Huang, X. Niu, T. Fan, Q. Mu, and H. Li, "Protective effect of tetrahydrocoptisine against ethanol-induced gastric ulcer in mice," *Toxicology and Applied Pharmacology*, vol. 272, no. 1, pp. 21–29, 2013.

[54] Y. Li, W. P. Wang, H. Y. Wang, and C. H. Cho, "Intragastric administration of heparin enhances gastric ulcer healing through a nitric oxide-dependent mechanism in rats," *European Journal of Pharmacology*, vol. 399, no. 2-3, pp. 205–214, 2000.

[55] L.-r. Pan, Q. Tang, Q. Fu, B.-r. Hu, J.-z. Xiang, and J.-q. Qian, "Roles of nitric oxide in protective effect of berberine in ethanol-induced gastric ulcer mice1," *Acta Pharmacologica Sinica*, vol. 26, no. 11, pp. 1334–1338, 2005.

[56] J.-W. Song, C.-S. Seo, T.-I. Kim et al., "Protective effects of Manassantin A against ethanol-induced gastric injury in rats," *Biological & Pharmaceutical Bulletin*, vol. 39, no. 2, pp. 221–229, 2016.

[57] S. A. El-Maraghy, S. M. Rizk, and N. N. Shahin, "Gastroprotective effect of crocin in ethanol-induced gastric injury in rats," *Chemico-Biological Interactions*, vol. 229, pp. 26–35, 2015.

[58] X. E. Yu and Q. N. Luo, "Protective effects of exogenous nitric oxide on acid-ethanol induced gastric ulcer in Guinea-pig," *World Chinese Journal of Digestology*, vol. 8, p. 224, 2000.

[59] D. Jimenez, M. J. Martin, D. Pozo et al., "Mechanisms involved in protection afforded by L-arginine in ibuprofen-induced

gastric damage: role of nitric oxide and prostaglandins," *Digestive Diseases and Sciences*, vol. 47, no. 1, pp. 44–53, 2002.

[60] L. Zhang, J. W. Ren, C. C. M. Wong et al., "Effects of cigarette smoke and its active components on ulcer formation and healing in the gastrointestinal mucosa," *Current Medicinal Chemistry*, vol. 19, no. 1, pp. 63–69, 2012.

[61] K. B. Bamford, X. Fan, S. E. Crowe et al., "Lymphocytes in the human gastric mucosa during *Helicobacter pylori* have a T helper cell 1 phenotype," *Gastroenterology*, vol. 114, no. 3, pp. 482–492, 1998.

Hindawi
Oxidative Medicine and Cellular Longevity
Volume 2018, Article ID 9506543, 12 pages
https://doi.org/10.1155/2018/9506543

Research Article

Hepatoprotective Activity of Vitamin E and Metallothionein in Cadmium-Induced Liver Injury in *Ctenopharyngodon idellus*

Yajiao Duan,[1] Jing Duan,[1] Yang Feng,[1] Xiaoli Huang,[1] Wei Fan,[2] Kaiyu Wang,[3] Ping Ouyang,[3] Yongqiang Deng,[4] Zongjun Du,[1] Defang Chen,[1] Yi Geng,[3] and Shiyong Yang[1]

[1]*Department of Aquaculture, Sichuan Agricultural University, Wenjiang, Sichuan 611130, China*
[2]*Neijiang City Academy of Agricultural Sciences, Neijiang, Sichuan 641000, China*
[3]*College of Animal Science and Veterinary Medicine, Sichuan Agricultural University, Wenjiang, Sichuan 611130, China*
[4]*Animal Disease Prevention and Control Center of Sichuan Province, Chengdu, Sichuan 610000, China*

Correspondence should be addressed to Xiaoli Huang; hxldyq@126.com

Received 11 November 2017; Revised 21 January 2018; Accepted 15 February 2018; Published 11 April 2018

Academic Editor: Mohamed M. Abdel-Daim

As an environmental and industrial pollutant, cadmium (Cd) can cause a broad spectrum of toxicological effects. Multiple organs, especially the liver, are considerably affected by Cd in both humans and animals. We investigated the protective effects of metallothionein (MT) and vitamin E (VE) supplementation on Cd-induced apoptosis in the grass carp (*Ctenopharyngodon idellus*) liver. Grass carp were divided into four groups: the control group, Cd + phosphate-buffered saline (PBS) group, Cd + VE group, and Cd + MT group. All fish were injected with $CdCl_2$ on the first day and then VE, MT, and PBS were given 4 days postinjection, respectively. The results showed that Cd administration resulted in liver poisoning in grass carp, which was expressed as an increase in Cd contents, malondialdehyde (MDA) concentration, percentage of hepatocyte apoptosis, and apoptosis-related gene mRNA transcript expression. However, VE and MT treatments protected against Cd-induced hepatotoxicity in grass carp by decreasing Cd contents, lipid peroxidation, and histological damage and reducing the percentage of hepatocyte apoptosis by regulating related mRNA transcript expression. These data demonstrate that oxidative stress and activation of the caspase signaling cascade play a critical role in Cd-induced hepatotoxicity. However, VE and MT alleviate Cd-induced hepatotoxicity through their antioxidative and antiapoptotic effects, and MT has a more powerful effect than VE.

1. Introduction

Cadmium (Cd) is a widespread environmental toxin and occupational pollutant and was listed as one of the most toxic substances to human health and the most malicious carcinogen by the Agency for Toxic Substances and Disease Registry and the International Agency for Research on Cancer, respectively [1, 2]. Cd can endanger human and animal health by causing multiple organ damage [3–5], which may result in prostate, lung, and testes cancer in humans [6] and kidney, liver, bone, and brain injury, as well as immune and cardiovascular system impairment [7].

Free Cd, which can cause human poisoning, is mainly taken into the body via food [8]. Fish is known to be the richest source of toxic trace elements in humans, and these animals live in contaminated water and bioaccumulate Cd through the food chain [9]. Cd generally enters an aquatic organism's body, accumulates in the body via the blood circulation, and binds to the sulfhydryl groups of proteins [10]. Thus, Cd can be transferred to humans following the ingestion of aquatic organisms. This issue is critical in Cd intoxication research, not only for the aquaculture industry but also for human health [9].

The mechanisms of Cd-induced damage in organisms are mainly related to apoptosis and oxidative stress [11–16]. Glutathione [17], cysteine [10], anthocyanin [18], zinc and selenium [19], and other drugs have been found to protect organisms against Cd-induced damage by reducing apoptosis

and blocking oxidative stress pathways. Vitamin E (VE) is a primary liposoluble antioxidant, which may play an important role in scavenging free oxygen radicals and stabilizing cell membranes, thus maintaining cell permeability [20]. In addition, metallothionein (MT), a ubiquitous metal-binding protein, is an endogenous detoxification factor in organisms and is highly conserved in evolution, and can reduce damage by chelating Cd [21]. Furthermore, the translocation of MT to the nucleus is probably associated with the protection of cells by resisting DNA damage and apoptosis as well as gene transcription during different stages of the cell cycle [22]. However, it is unclear whether MT can protect fish from damage through these pathways. It is necessary to determine whether VE and MT have protective effects and which drug has the best effect against Cd-induced damage in fish.

Liver is one of the primary target organs of Cd and is extremely sensitive to both acute and chronic Cd exposures [23]. Grass carp (*Ctenopharyngodon idellus*) aquaculture accounts for 18.10% of the total products from freshwater fisheries worldwide each year [24]. Cd-induced chronic diseases such as rickets, deformities, and liver toxicity can seriously jeopardize the grass carp cultivation industry [25]. Therefore, we have created an "intoxication–detoxification" comparative grass carp model to determine whether Cd-induced liver injury can be prevented by exogenous VE and MT supplementation. The underlying protective mechanism was also investigated.

2. Materials and Methods

2.1. Chemicals and Their Preparation. $CdCl_2$ was obtained from MOLBASE (Shanghai) Biotechnology Co. Ltd. VE (liposoluble; purity 99%) and MT-2 (pure rabbit liver MT powder; purity 99%) were purchased from Shanghai Shou Feng Industrial Co. Ltd. and Sigma-Aldrich Company (Beijing, China), respectively. All other chemicals were of analytical grade or the highest grade available and obtained from local companies.

$CdCl_2$ and MT were dissolved in sterilized PBS. Liposoluble VE was dissolved in sterilized phosphate-buffered saline (PBS) and emulsified using an ultrasonic crusher until milky.

2.2. Experimental Carp. Grass carp of similar weight (50 ± 3.4 g) and length (15 ± 2.5 cm) were purchased from a fish farm in Meishan, Sichuan, China. The fish were acclimatized in the laboratory for 2 weeks before experimentation. The carp were exposed to a light : dark cycle of 12 h : 12 h, an uninterrupted oxygen supply to ensure more than 5 mg/L dissolved oxygen, pH of 6.5–8.5, ammoniacal nitrogen and nitrite maintained at 0–0.02 mg/L, the water in the tanks was pretreated with UV light and an aeration process, and 20% of the culture water was renewed every day. The fish were fed with commercial pellets (Tongyi Company, Suzhou, China) twice a day for 2 weeks. Fish that has a bright body color and is responsive, robust, and healthy were selected for experimentation. All animal handling procedures were approved by the Animal Care and Use Committee of Sichuan Agricultural University, following the guidelines of the animal experiments of Sichuan Agricultural University, under permit number DY-S20144657.

Table 1: The LC_{50} of Cd in grass carp.

Concentration of $CdCl_2$ (μmol/kg)	Injected concentration (μmol/kg)	The number of deaths	Mortality rate	LC_{50} (μmol/kg)
420.709	20	8	80%	
294.994	20	8	80%	
206.845	20	6	60%	
145.036	20	4	40%	199.631
101.696	20	3	30%	
71.3081	20	1	10%	
0	20	0	0	

2.3. Establishment of the "Intoxication–Detoxification" Model

2.3.1. Determination of the LC_{50} of Cd in Grass Carp. To assess the lethal concentration 50% (LC_{50}) of $CdCl_2$, similar body weight (54 ± 4.2 g) grass carp ($n = 60$) were divided into six groups (10 fish/group). Our previous study found that large amounts of precipitate covered the surface of skin and gills and led to dyspnea during $CdCl_2$ contaminated water; therefore, $CdCl_2$ was administered by intraperitoneal injection. The nominal concentrations of Cd tested were 71.308, 101.696, 145.036, 206.845, 294.994, and 420.709 μmol/kg. The experiment in each group was repeated three times, and the number of dead fish in 96 h was recorded. No food was provided during the test. The LC_{50} was determined with the Karber method [26]. The results showed that the mortality rate rose as the concentration increased within 96 h in the different groups. No deaths were recorded in the control group. According to the modified Kobvgguffer method [27], the LC_{50} was 199.631 μmol/kg (Table 1).

2.3.2. Challenge and Detoxification Reagent Injection. As previously reported [28], 1/10 LC_{50} was used as the subacute concentration in the present study. Challenged fish ($n = 450$) were divided into three groups and each group included three parallel tanks. Another 150 control fish were also divided into three parallel tanks (Figure 1). $CdCl_2$ was injected into the challenged fish ($n = 450$) intraperitoneally during the challenge period. Healthy fish ($n = 150$) not given $CdCl_2$ were included as controls. On the 4th day post Cd injection, challenged fish were medicated with 4 mL/kg PBS, 20 IU/kg VE [29], and 2.1 mg/kg MT [30], respectively. Liver samples were collected after treatment on the 4th, 8th, 12th, and 16th days postchallenge.

2.4. Histological Analysis. Six fish in each group were necropsied at 4, 8, 12, and 16 days. Liver tissues were fixed in 10% neutral formalin and routinely processed in paraffin. Liver tissues were also trimmed into cassettes, dehydrated in graded ethanol solutions, cleared in xylene, and embedded in paraffin wax. Sections of 5 μm for hematoxylin and eosin (H&E) staining were prepared prior to microscopic analysis.

2.5. Determination of the Cd Content in the Liver. All glass containers used in the trial were soaked in 10% nitric acid for 24 h and then rinsed several times with deionized water. The grass carp liver ($n = 6$) was sampled on the 4th, 8th,

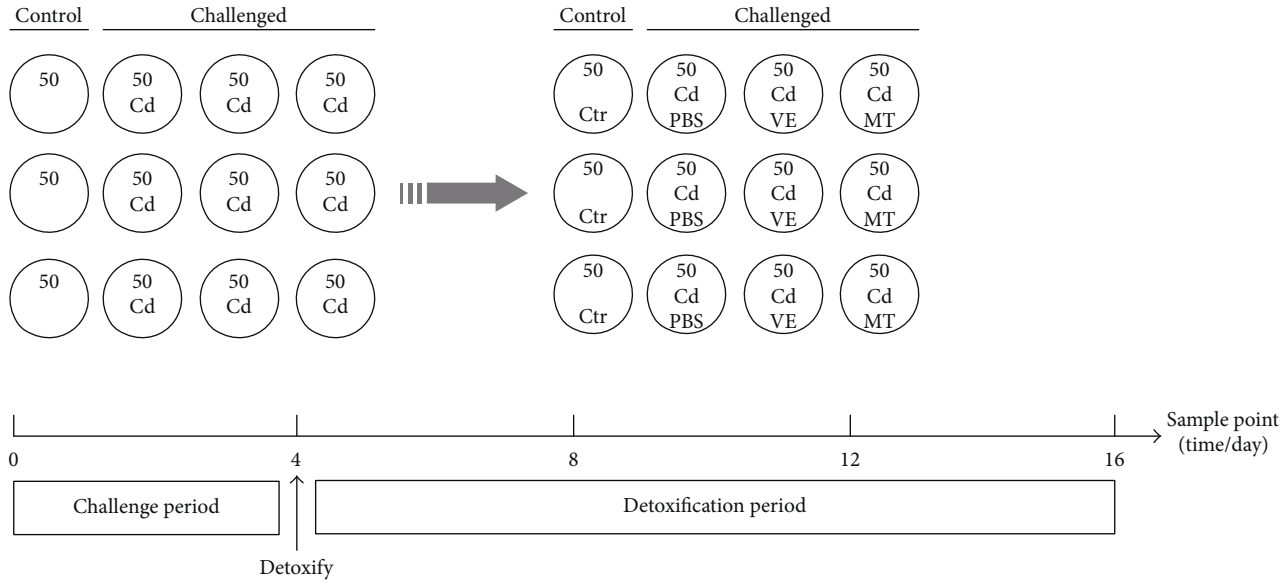

Figure 1: Study design showing the challenge model based on a three-parallel-tank system. Each group included 150 fish divided into three parallel tanks.

12th, and 16th days, treated immediately with liquid nitrogen, and then stored at −80°C. The liver tissue was placed in a 25 mL stopper flask, and a few clean glass spheres were added to prevent splashing. The tissue was incubated with 2 mL mixed acid ($HNO_3 : HClO_4 = 4 : 1$) overnight and then transferred to an 18°C sand bath to digest, until the color of the liquid was clear. The liver tissue was then transferred to a volumetric flask and detected using an AA680 Shimadzu (Kyoto, Japan) flame atomic absorption spectrometer [31, 32], under the following conditions: wavelength of 228.8 nm, crack 0.5 nm, lamp current 6 mA, drying at 100°C for 20 s, ashing at 300°C for 15–20 s and an atomization at 1500°C. The results were calculated according to the following formula:

$$X = \frac{(\mathrm{A1} - \mathrm{A2}) \times V \times 1000}{M \times 1000}, \quad (1)$$

where X (μg/kg) is the Cd content in the liver, A1 (μg/mL) is the Cd content in the sample, A2 (μg/mL) is the Cd content in the reagent blank, V (mL) is the total volume after sample treatment, and M (g) is the sample mass.

2.6. Determination of the MDA Content in the Liver. MDA is a breakdown product of the oxidative degradation of cell membrane lipids and is generally considered an indicator of lipid peroxidation [33]. Lipid peroxidation was evaluated by measuring MDA concentrations using a spectrophotometer to determine the color produced during the reaction of thiobarbituric acid with MDA. At 4, 8, 12, and 16 days, six fish in each group were anesthetized and immediately necropsied. Livers were immediately removed and stored at 0°C in 0.65% NaCl solution. Approximately 1 g liver tissue was homogenized with 9 mL 0.65% NaCl solution in a homogenizer on ice. The homogenates were then centrifuged at 3500g at 4°C, and total protein in the supernatant was determined with a protein quantification kit (A045-2) (NJJCBIO, Nanjing, China). The activity of MDA (A003-2) in the supernatant was determined using a commercial kit (NJJCBIO, Nanjing, China), according to the manufacturer's instructions.

2.7. Liver Cell Apoptosis Measurement. At 4, 8, 12, and 16 days, six fish from each group were anesthetized by MS-222. The livers were then sampled to determine the percentage of apoptotic cells using flow cytometry [34]. The livers were immediately minced to form a cell suspension and filtered through a 300-mesh nylon screen. Cells were washed twice with cold PBS, and the cell pellet was resuspended at a concentration of 1×10^6 cells/mL in PBS. Then, 5 μL of annexin V-fluorescein isothiocyanate (V-FITC) (BD Pharmingen, Franklin Lakes, New Jersey, USA) and 5 μL of propidium iodide (PI) (BD Pharmingen) were added into the 100 μL cell suspension, respectively. The cells were then incubated with annexin V-FITC/PI in the dark for 15 min at room temperature. Apoptotic cells were examined by flow cytometry (BD FACSCalibur). The data were analyzed using Expo 32 software (Beckman Coulter, Kraemer Boulevard, Brea, California, USA).

2.8. Quantitative Real-Time Polymerase Chain Reaction (qPCR) Analysis. At 4, 8, 12, and 16 days, six fish from each group were anesthetized by MS-222. Livers were sampled, placed in RNA/DNA protector solution (TaKaRa, Dalian, China), and stored at 4°C. The livers were then homogenized by crushing with a mortar and pestle and stored at −80°C.

Total RNA was isolated from livers with a TRIzol reagent (TaKaRa). Complementary DNA (cDNA) was synthetized from 1 μg of RNA using the PrimeScript™ RT reagent kit with gDNA eraser (RR047A, TaKaRa). qPCR was performed using an SYBR green real-time PCR kit (TaKaRa, Kusatsu, Japan) and a thermocycler (Bio-Rad, Hercules, California,

Table 2: Primers of various genes detected with qPCR.

Gene	Abbreviation		Primer sequence (5′–3′)	Acc. number
B-cell lymphoma 2	*Bcl-2*	F	GAGATGGCGTCCCAGGTAGAT	JQ713862
		R	GCCAATCCAAGCACTTTCGT	
Bcl-2 associated X	*Bax*	F	CAGCCATAAACGTCTTGCGC	JQ793788
		R	GTCGGTTGAAGAGCAGAGTCATTTA	
Caspase-3	*CASP3*	F	AGTCGCTGTGCTTCATTTGTTT	JQ793789
		R	CGGTCTCCTCTGAACAGGCTA	
Caspase-9	*CASP9*	F	CCTACTCAACCTTTCCAGGCTATG	KT239368
		R	TCATCTGTGGCAACATTCTCCTT	
Apoptosis-inducing factor	*AIF*	F	CATGAAGCGAATGATGGAGAAGT	KR872830
		R	CAAAGTCCCTGTAGTTGATGGTGT	
Glucose-regulated protein-78	*Grp78/BiP*	F	CTGACCTGAAGAAGTCTGACATCG	FJ436356
		R	GAAGGCTCTTTGCCGTTGAA	
Caspase-8	*CASP8*	F	ATGGTAATCTGGTTGAAATCCGTG	KP145003
		R	TCCTTGGCAGGCTTGAATGA	
β-Actin	*ACTB*	F	GCTCTGCTATGTGGCTCTTGACT	DQ211096
		R	CAATGGTGATGACCTGTCCGT	
18S ribosomal RNA	*RNA18S*	F	ACCCATTGGAGGGCAAGTCT	EU047719
		R	CTCCCGAGATCCAACTACAAGC	

USA). *β-Actin* and *18S ribosomal RNA* were used as reference genes to determine the relative expression of target genes, which was the invariant expression in the grass carp liver in our previous validation. The primers used for qPCR are listed in Table 2.

For qPCR, the 25 μL reaction mixture contained 12.5 μL SYBR green PCR master mix, 8.5 μL diethylpyrocarbonate-treated water, 1.0 μL of forward primer, 1.0 μL of reverse primer, and 2 μL cDNA. The following program conditions were used for the reactions: 3 min at 95°C for 1 cycle, samples were amplified for 40 cycles at 95°C for 10 s, melting temperature of a specific primer pair for 30 s, followed by 10 s at 95°C, and 72°C for 10 s. To distinguish between specific and nonspecific reaction products, a melting curve was obtained at the end of each run. The $2^{-\Delta\Delta CT}$ method was used to calculate relative changes in mRNA transcript expression from the qPCR results ($\Delta CT = CT_{\text{target gene}} - CT_{\beta\text{-actin}}$, $\Delta\Delta CT = \Delta CT_{\text{experimental}} - \Delta CT_{\text{control}}$) [35].

2.9. Statistical Analysis. The results are expressed as the mean value ($n = 6$) and standard deviation. The significance of differences was analyzed by variance analysis. The analysis was performed using one-way analysis of variance while the *t*-test was applied to determine whether the differences between groups were significant (SPSS v.20.0, IBM Corp., Armonk, New York, USA). A value of $P < 0.05$ was considered significant, while a $P < 0.01$ was considered highly significant.

3. Results

3.1. VE and MT Protected Cell Morphological Integrity in the Liver. Under normal conditions, grass carp hepatocytes had normal morphology and growth, and there were no significant morphological changes in the hepatopancreas (Figures 2(a)–2(c)). After Cd treatment, hepatic sinusoids were congested on the 4th day (Figure 2(d)). On the 12th day, the number of inflammatory cells was elevated in the blood vessels and hepatic sinusoids (Figure 2(e)). Interstitial edema was also noted following Cd challenge. In the final stage of the challenge, various degrees of necrosis and apoptosis in hepatic cells and pancreatic cells were observed (Figure 2(f)).

No obvious congestion in hepatic sinusoids was seen in the VE and MT groups (Figures 2(g) and 2(j)). Inflammatory cells gradually decreased with prolonged detoxification (Figures 2(h) and 2(k)). Simultaneously, interstitial edema in hepatopancreatic tissues also recovered following 12 days of detoxification. In addition, apoptotic and necrotic hepatic cells and pancreatic cells were significantly reduced and gradually recovered (Figures 2(i) and 2(l)).

3.2. MT, but Not VE, Decreased Cd Accumulation to Protect the Liver. To further assess the protective effect of VE and MT in the liver, we evaluated the Cd content in the liver under different treatments. Significant accumulation of Cd was seen in the liver after the Cd challenge ($P < 0.01$) compared with the control group, which reached a maximum value on the 8th day (Figure 3). After detoxification, the VE group showed no significant difference in the Cd content compared with the PBS group, which indicated that VE may protect the liver by a different mechanism, such as antioxidation. However, Cd accumulation in the liver in the MT group was significantly reduced compared with that in the PBS group ($P < 0.01$). Furthermore, the Cd content in the VE group was not statistically different to that in the MT group until the 8th day.

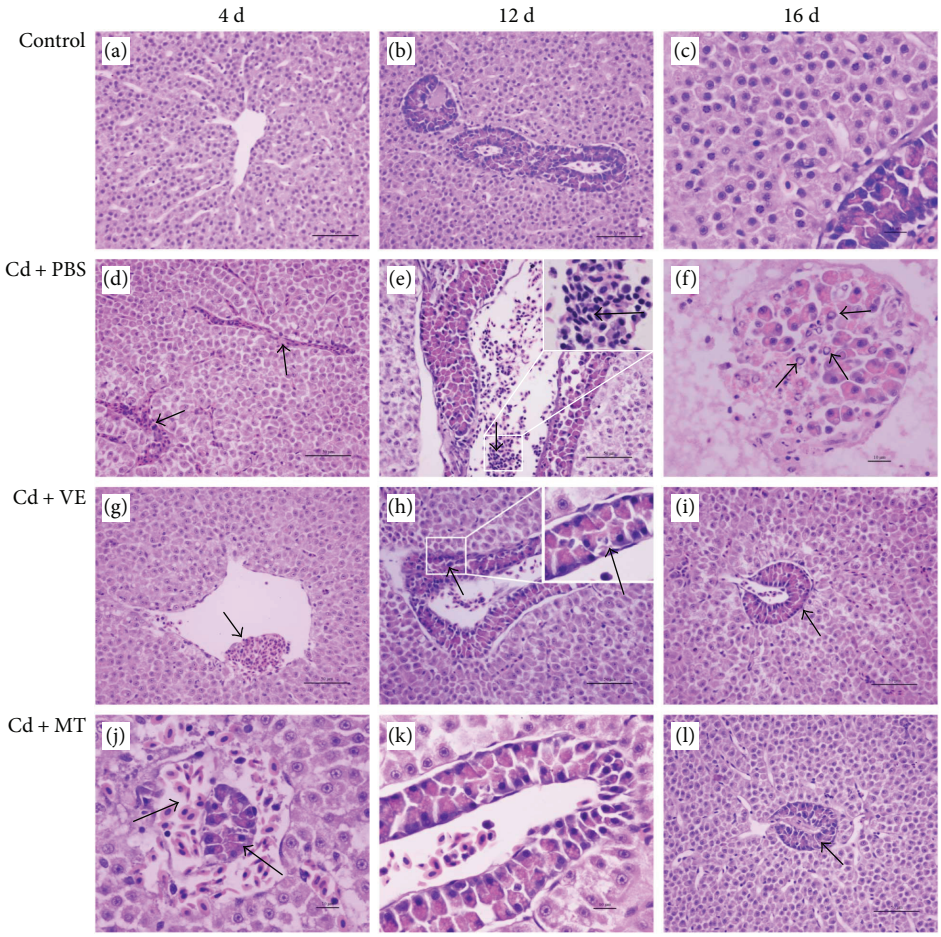

Figure 2: Histopathological changes in the livers induced by cadmium and detoxification-treated livers collected on the 4th, 12th, and 16th days after challenge with cadmium and treatment with VE and MT. (a–c) The liver of the control group. (d–f) Histopathological changes in the liver in the PBS group with time. (d) The arrow shows congestion in hepatic sinusoids. (e) The number of inflammatory cells increased in the blood vessels and hepatic sinusoids on the 12th and 16th days postchallenge. The arrow shows inflammatory cells. (f) Necrotic and apoptotic cells present in pancreatic cells. The arrows show cell degeneration and necrosis. (g–i) Histopathological changes in the liver in the VE group with time. (g) Hyperemia did not significantly improve during the Cd challenge in the VE group on the 4th day. The arrows show red blood cells. (h, i) Hepatopancreas recovered on the 12th and 16th days in the VE group. The arrows show pancreatic cells restored. (j–l) Histopathological changes in the liver in the MT group with time. (j) Hyperemia did not significantly improve during the Cd challenge in the MT group on the 4th day. The arrows show pancreas congestion. (k, l) Inflammatory cells decreased on the 12th and 16th days and hepatopancreas damage recovered. The arrows show red cells in the pancreas decreased.

3.3. MT Is Better Than VE in Protecting the Liver by Eliminating Cd-Induced Lipid Peroxidation. Following the Cd challenge, there was significant accumulation of MDA in the liver of grass carp injected with $CdCl_2$ (Figure 4). As the Cd challenge time increased, the MDA content in the PBS group increased up to the 8th day and then declined, which indicated that the liver was also involved in detoxification, although the effect was minimal. During detoxification, it was apparent that VE and MT hastened the recovery of MDA; however, MT was superior to VE in this recovery. Both VE and MT significantly reduced the MDA content compared with PBS ($P < 0.01$) on the 8th day. Although this ability declined in the late stages of detoxification, the effect of MT was also significant compared with that of PBS. However, the effect of VE on reducing MDA was only statistically significant after the 12th day (Figure 4). Furthermore, MDA in the MT group was significantly different to that in the VE group after the 12th day.

3.4. MT Had a Greater Effect Than VE in Inhibiting Cd-Induced Apoptosis of Liver Cells in Hepatoprotection. Apoptosis was detected by flow cytometry. Liver cells were examined by counting the total percentage of early apoptotic liver cells and late apoptotic liver cells (Figure 5). Cd induced apoptosis during the challenge period in the PBS group compared with the controls ($P < 0.01$). However, apoptosis was reduced following detoxification by VE and MT in the Cd-challenged group ($P < 0.01$), which indicated that VE and MT played a role in the inhibition of liver cell apoptosis caused by Cd. The PBS group also showed recovery of liver cell apoptosis at the end of the Cd challenge, and both VE and MT hastened this recovery on the 8th day.

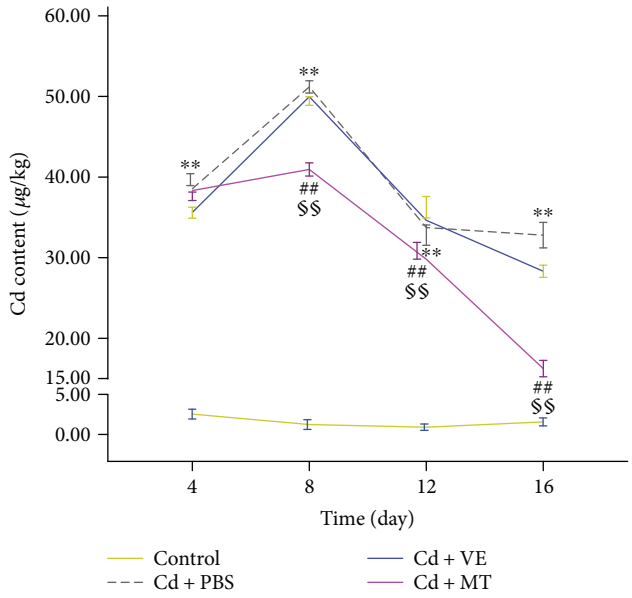

Figure 3: Change in the Cd content (μg/kg wet weight) in the liver of grass carp in four experimental groups. Data are presented as means ± standard deviation. $^{*}P < 0.05$ or $^{**}P < 0.01$ represents a significant difference or highly significant difference between the control group and the PBS group. $^{\#}P < 0.05$ or $^{\#\#}P < 0.01$ represents a significant difference or highly significant difference between the PBS group and the VE/MT group. $^{\S}P < 0.05$ or $^{\S\S}P < 0.01$ represents a significant difference or a highly significant difference between the VE group and the MT group. $n = 6$ in each group.

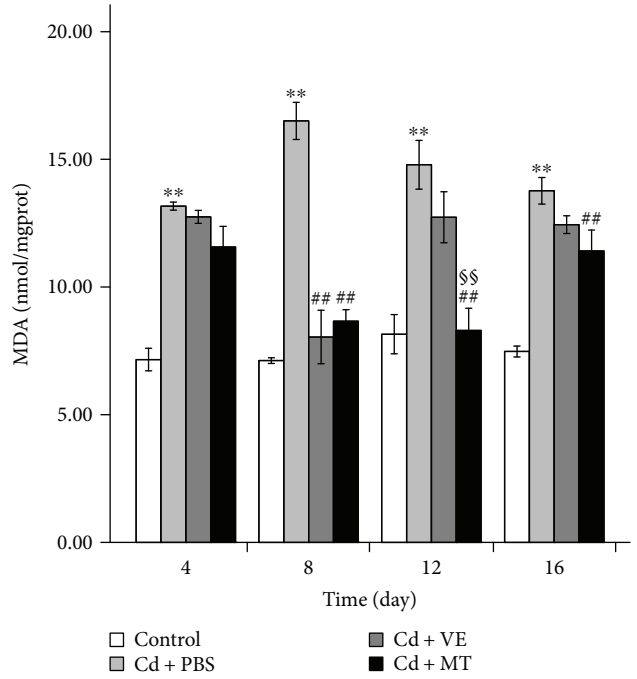

Figure 4: Assessment of MDA in the liver of grass carp in different groups. Data are presented as means ± standard deviation. $^{*}P < 0.05$ or $^{**}P < 0.01$ represents a significant difference or highly significant difference between the control group and the PBS group. $^{\#}P < 0.05$ or $^{\#\#}P < 0.01$ represents a significant difference or highly significant difference between the PBS group and the VE/MT group. $^{\S}P < 0.05$ or $^{\S\S}P < 0.01$ represents a significant difference or a highly significant difference between the VE group and the MT group. $n = 6$ in each group.

3.5. VE and MT Reversed the Expression of Apoptosis-Related Genes to Inhibit Apoptosis. To investigate the mechanism of MT and VE in inhibiting hepatocyte apoptosis to protect the grass carp liver, we determined the mRNA transcript expression of several apoptosis-related genes at different times. Compared with the control group, *caspase-3* mRNA expression in the PBS group was significantly increased up to the 12th day and then sharply decreased in the last few days of the Cd challenge. Compared with the PBS group, *caspase-3* expression was downregulated in the VE and MT groups on the 12th and 16th days (Figure 6(a)), and there was a significant difference between the VE/MT group and the PBS group on the 12th day ($P < 0.01$). These results suggest that VE and MT play a role in inhibiting apoptosis as they both inhibited *caspase-3* expression, which is a widely accepted apoptotic terminal gene [36]. Therefore, the mRNA transcript expression of *caspase-3* in the MT group was significantly different to that in the VE group on the 16th day.

To better understand how VE and MT regulate *caspase-3* expression, we detected several main genes of three major apoptotic pathways [37]. These three genes, *caspase-8*, *caspase-9*, and *Grp78/BiP*, showed a high level of mRNA transcript expression after the Cd challenge (Figures 6(b)–6(d). However, *caspase-8* showed no significant change until the 16th day, and *Grp78/BiP* mRNA expression only increased early in the Cd challenge. This may indicate that Cd-induced apoptosis was mainly through the mitochondrial pathway rather than the death receptor pathway and endoplasmic reticulum stress pathway. VE and MT reduced the expression of *caspase-9* but not *caspase-8* or *Grp78/BiP* to diminish the expression of *caspase-3* ($P < 0.01$).

We also investigated other apoptosis-related genes during the Cd challenge and VE/MT stimulation to confirm our findings that VE/MT inhibit liver cell apoptosis. Compared with the controls, the mRNA transcript expression of *AIF* (Figure 6(e)) and *Bax* (Figure 6(f)) was significantly enhanced in the PBS group after the Cd challenge, despite the fact that the expression of *AIF* increased continuously, while *Bax* increased up to the 8th day and then declined. Compared with the PBS group, a significant decrease ($P < 0.01$) in *Bax* expression in the VE and MT groups was observed in the liver of grass carp from the 8th to the 16th day. It was reduced by almost 5-fold compared with the PBS group on the 8th day and showed a good antiapoptotic effect. The mRNA transcript expression of *AIF* was also significantly decreased ($P < 0.01$) in the VE and MT groups. In addition, *AIF* expression in the MT group was significantly different ($P < 0.05$) to that in the VE group on the 12th day. Moreover, as an antiapoptosis gene [38], *Bcl-2* mRNA transcript expression levels in the PBS group showed a decline within the first 4 days and then an increase compared with the control group. *Bcl-2* in the VE and MT groups was significantly higher

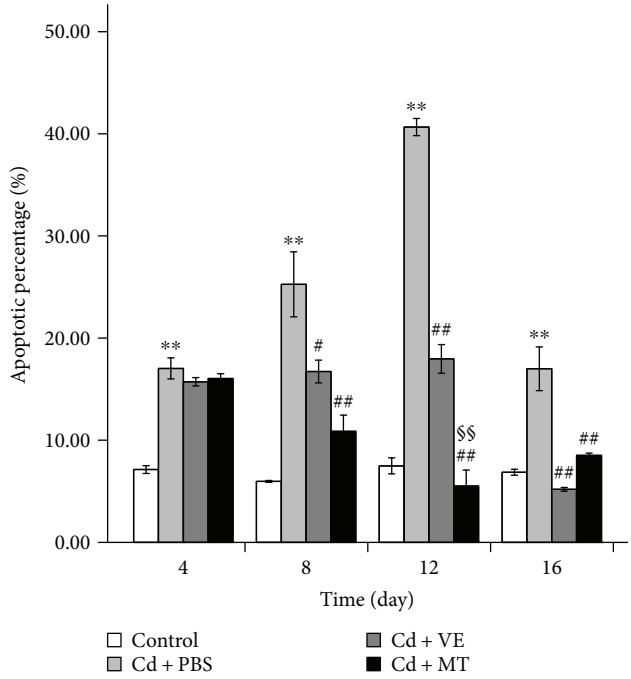

Figure 5: Percentage changes in liver cell apoptosis. Data are presented as means ± standard deviation. $^{*}P < 0.05$ or $^{**}P < 0.01$ represents a significant difference or highly significant difference between the control group and the PBS group. $^{\#}P < 0.05$ or $^{\#\#}P < 0.01$ represents a significant difference or highly significant difference between the PBS group and the VE/MT group. $^{\S}P < 0.05$ or $^{\S\S}P < 0.01$ represents a significant difference or a highly significant difference between the VE group and the MT group. $n = 6$ in each group.

($P < 0.05$ or $P < 0.01$) than that in the PBS group on the 8th day (Figure 6(g)). Furthermore, the greatest recovery of *Bcl-2* was seen in the MT group on the 8th day compared with the other groups. VE and MT significantly accelerated the upregulation of *Bcl-2* mRNA transcript expression.

4. Discussion

Heavy metals contained in food products have a negative impact on human health, as it will be chronic if the food they consume contains heavy metals. The International Codex Alimentarius Commission's (CAC) limit of Cd is 0.05 mg/kg in fruits and vegetables, 0.1 mg/kg in beans and cereals (CAC, CODEX STAN 193-1995). The limit standard of heavy metal residues in food in China stipulates that the limit of Cd concentration is 0.03 mg/kg in fruits, 0.05 mg/kg in vegetables and eggs, and 0.1 mg/kg in aquatic products (limit of contaminants in food, GB2762-2012). However, many aquatic organisms have a very strong enrichment capacity for Cd, and many fish in contaminated areas are seriously overstandard [39]. Even in some places, the Cd content of fish was as high as 37.867 mg/kg [40]. Previous studies found that the LC_{50} of Cd in mice was only 3.2 mg/kg [41] and 15 mg/kg in rabbits [42], which means that residual Cd in some fish may kill the mice or rabbit directly. Therefore, the problem of Cd in fish seriously involves the food safety issues.

Water is the main natural route of exposure to metal pollution in fish. However, our previous study found that large amounts of precipitate covered the surface of the skin and gills and led to dyspnea during Cd water-contaminated exposure. The potential reason for this is not yet clear, but we speculate that Cd may act on the mucus of fish. Therefore, it was difficult to determine whether the death of fish was caused by hypoxia or by Cd poisoning. Moreover, the precipitate also reduced the concentration of Cd in the water environment markedly and may have interfered with the experimental results. To avoid this interference, we delivered the drugs intraperitoneally in the present study.

Currently, to identify therapies, more and more studies have focused on exogenous drugs for Cd-induced damage. In previous studies, VE [43] and MT [44] were used in rats and mice for detoxification. Moreover, VE has also been used in chickens as an antidote [45]. However, to date, these drugs have not been studied in aquatic species with regard to protection against Cd-induced damage. Therefore, we selected exogenous VE and MT to evaluate their protective effects on Cd-induced intoxication in grass carp. The results showed that all the experimental fish demonstrated significant poisoning after the Cd challenge, which resulted in severe oxidative stress and apoptosis in the grass carp liver, with gradual accumulation of Cd in the liver. The accumulation of Cd in the liver reached $51.176 \pm 1.070\ \mu$g/kg, although accumulation slowed down during the latter part of the Cd challenge. We speculate that a potential reason for this may be due to the body's own detoxification system, such as the antioxidation and self-repair mechanisms. Following Cd challenge, the body's antioxidant enzyme activity increased, and both apoptosis- and antiapoptosis-related gene mRNA transcript expressions changed in order to protect the body against damage. Furthermore, after VE and MT addition, recovery in the detoxification groups was significantly accelerated and similar to the control group within a short period of time. These findings provide a theoretical basis for the treatment and prevention of toxicity caused by heavy metals, which may benefit humans.

Previous studies have shown that Cd is distributed via the blood circulation where it is bound to red blood cells and plasma proteins, mainly albumin, after being absorbed into the body. The liver is a major organ where Cd is distributed [46]. In animal studies, an acute dose of Cd caused severe liver injury and was the major toxic effect [12]. Widespread hepatocellular damage including congestion in mice was caused by Cd [47]. In addition, hepatocellular dissociation, degenerative changes including swelling, hydropic degeneration, hypertrophy and necrosis were seen in the Cd-challenged freshwater fish *Ophiocephalus striatus* [48]. In the present study, severe liver damage including congestion, cytoplasmic dissolution, nuclear debris, and increased inflammatory cell infiltration was observed. This provides further evidence that the liver, which is a sensitive organ, is affected by Cd. Moreover, VE and MT can protect the liver against Cd-induced damage.

Cd can be absorbed into the blood and binds with albumin and other high molecular weight proteins. When the bound Cd is overloaded, free Cd^{2+} will accumulate in

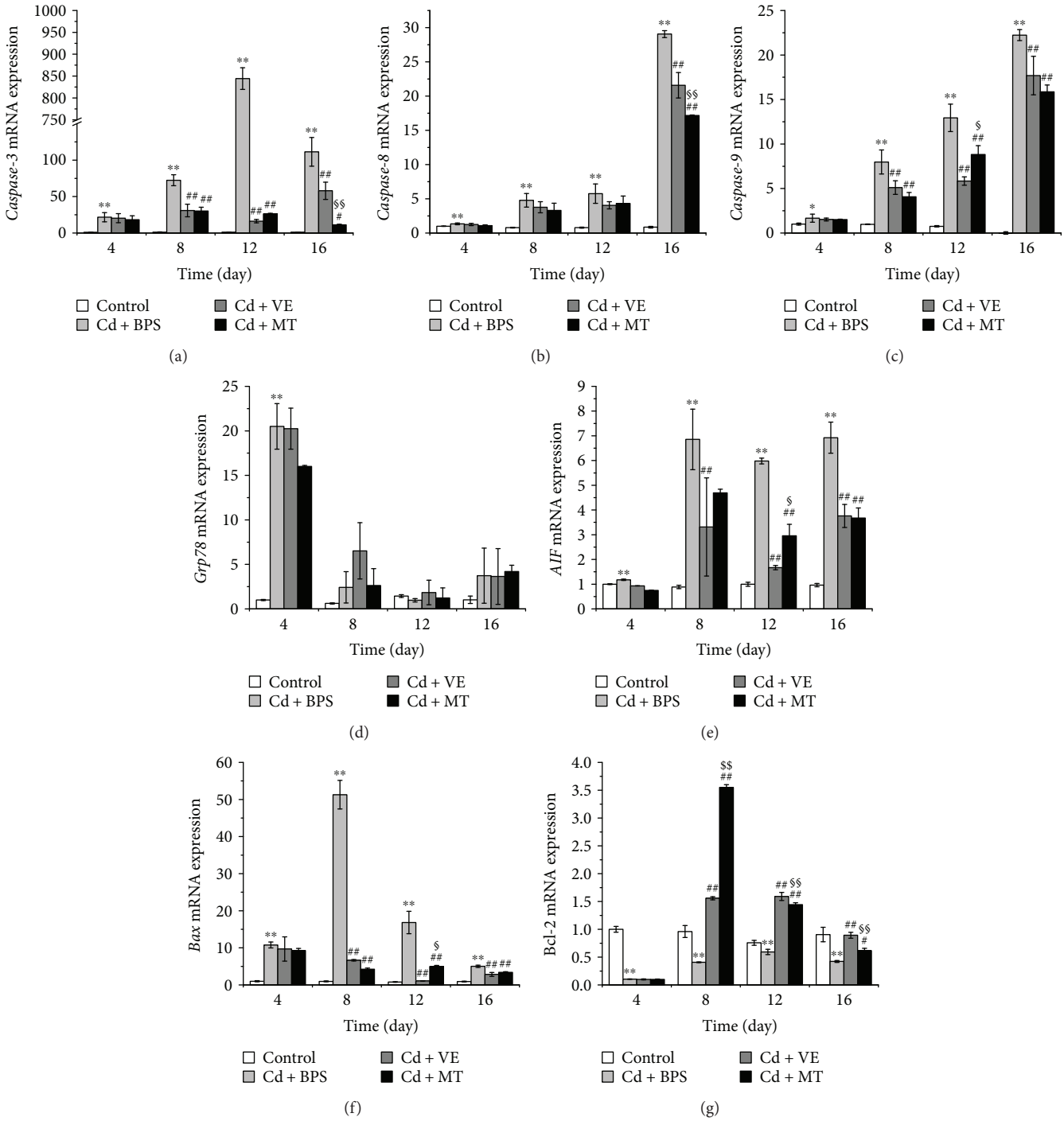

Figure 6: The mRNA expression levels of *caspase-3*, *caspase-8*, *caspase-9*, *Grp78*, *AIF*, *Bax*, and *Bcl-2* in the liver. (a) *Caspase-3*, (b) *caspase-8*, (c) *caspase-9*, (d) *Grp78*, (e) *AIF*, (f) *Bax*, and (g) *Bcl-2*. Data are presented as means ± standard deviation. $^{*}P < 0.05$ or $^{**}P < 0.01$ represents a significant difference or highly significant difference between the control group and the PBS group. $^{\#}P < 0.05$ or $^{\#\#}P < 0.01$ represents a significant difference or highly significant difference between the PBS group and the VE/MT group. $^{\S}P < 0.05$ or $^{\S\S}P < 0.01$ represents a significant difference or a highly significant difference between the VE group and the MT group. $n = 6$ in each group.

various tissues and organs and is eventually delivered to the liver, which is a detoxification organ [49, 50]. However, redundant Cd is likely to cause severe liver damage [51]. In the present study, the Cd content in the liver was measured under different experimental conditions. In our research, the accumulation of Cd in the liver increased with time. However, we also found that Cd then decreased after reaching a certain level in the Cd-challenged grass carp liver. This may be due to the body's self-protection mechanism. The previous study showed that hepatic subcellular Cd was less distributed in nuclei, mitochondria, and microsomes, and more Cd was found in the cytosol in MT-transgenic mice

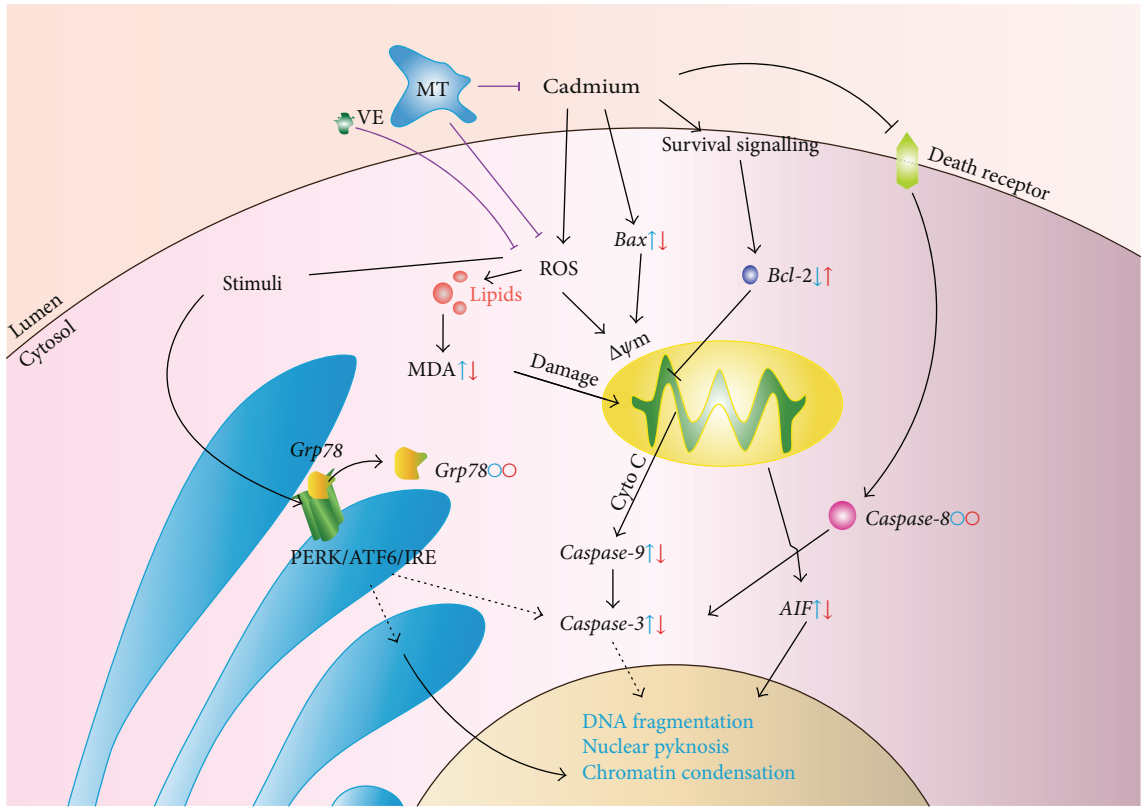

Figure 7: VE and MT protect cells from apoptosis by reducing the Cd content and/or antioxidation. Cd mainly induced apoptosis of liver cells via the induction of the mitochondrial apoptosis pathway rather than the other two pathways; MT mainly inhibited apoptosis by inhibiting Cd accumulation (I) and antioxidation (II), while VE mainly inhibited apoptosis by antioxidation (III). Blue: apoptosis-related gene mRNA transcript expression after Cd challenge, with respect to the controls. Red: apoptosis-related gene mRNA transcript expression after VE/MT supplementation, with respect to the PBS group. The direction of the arrows represents expression of the gene (up or down). The circle represents no significant difference.

compared with wild-type mice [52]. MT has the ability to chelate [21], therefore, we speculate that the grass carp protects itself by endogenous MT chelating Cd.

Free radicals, which can be generated by Cd, can cause lipid peroxidation [14]. We determined the MDA content to investigate whether Cd caused similar oxidative damage in the grass carp liver. Many studies have shown that MDA concentrations always increase with elevated lipid oxidation, which reflects the level of lipid peroxidation [53] as well as the level of peroxides in the body. Exposure to Cd can result in an excessive generation of MDA [45]. In addition, Cd derived from chicken ovarian follicles showed elevated Cd-induced MDA generation [33]. Moreover, the increase in MDA in broilers caused by Cd at a concentration of 25 mg/L was time-dependent during the 6-week trial [54]. In our research, we also found that MDA was elevated following Cd challenge in grass carp, which indicated that Cd caused severe oxidative damage. VE, as a typical antioxidant, has excellent antioxidative activity. A previous study demonstrated that VE had a protective role in relation to the toxic effects of Cd on hematological indices and lipid peroxide concentration in rats [20]. Furthermore, MT also had an antioxidative effect beyond its chelation function, which reduced the content of free radicals in the rat liver [55]. In the present study, a highly significant reduction in MDA was found in the livers from the VE and MT groups on the 8th day compared with the PBS group, which indicated that these two drugs can recover the antioxidant capacity of the body, and that they can protect the liver by decreasing lipid peroxidation due to the reduced production of MDA. In addition, the content of MDA in the MT group was significantly different to that in the VE group on the 12th day, which indicated that MT had a better effect in reducing the MDA content.

We observed cell apoptosis in the Cd-challenged group, which then recovered in the VE/MT groups as shown by histopathology. To further confirm that VE and MT can reduce Cd-induced apoptosis, we determined the apoptotic ratio in each experimental group using flow cytometry. The results showed that VE and MT diminished the apoptosis caused by Cd, and MT was more efficient than VE. Previous research showed that apoptosis is mainly controlled by three major apoptotic pathways: the mitochondrial pathway, death receptor pathway, and endoplasmic reticulum pathway [37]. The apoptotic machinery is well conserved among vertebrates [56]. A similar apoptotic pathway also exists in fish [56–59]. To investigate how VE and MT were regulated to suppress Cd-induced apoptosis, we determined the changes in a number of apoptosis-related genes in the Cd-induced and VE/MT treatment groups. The expression

of *caspase-3*, *Bax*, *caspase-9*, *AIF*, and *Bcl-2* was determined to evaluate the apoptotic level associated with the mitochondrial pathway [60–66]. One study suggested that *caspase-8* is located downstream of the death receptor pathway [67]. *Grp78*/*BiP* is the major endoplasmic reticulum partner with Ca^{2+} binding and antiapoptotic properties in vivo [29]. Our findings showed that Cd induced apoptosis of grass carp liver cells by activating the mitochondrial pathway via upregulation of the expression of *caspase-3*, *Bax*, *caspase-9*, and *AIF* and downregulation of *Bcl-2* expression. We showed Cd-induced apoptosis by inducing the mitochondrial pathway. VE and MT were able to regulate these genes to inhibit apoptosis. Nevertheless, VE and MT had no significant effect on *caspase-8* and *Grp78*/*BiP* mRNA expression, with the exception of a significant effect on the 16th day on *caspase-8* expression. These findings indicated that VE and MT had no obvious effect on the death receptor pathway and endoplasmic reticulum pathway. We conclude that Cd mainly accumulated in cells and initially produced reactive oxygen species then rapidly activated downstream apoptotic genes, which ultimately led to apoptosis. These findings suggested that MT had a stronger hepatoprotective effect than VE in Cd-induced liver injury (Figure 7).

Conflicts of Interest

The authors declare no competing financial interests.

Authors' Contributions

All authors read and approved the final manuscript. Yajiao Duan, Jing Duan, and Yang Feng contributed equally to this work.

Acknowledgments

This research was supported by grants: Sichuan Agricultural Science and Technology Achievements Transformation Fund (no. 15NZ0008). The authors would like to thank Mr. Guo Wang who kindly provided the grass carp used in the experiments. They also thank the International Science Editing (http://www.internationalscienceediting.com) for editing this manuscript.

References

[1] M. Hutton and C. Symon, "The quantities of cadmium, lead, mercury and arsenic entering the U.K. environment from human activities," *Science of the Total Environment*, vol. 57, pp. 129–150, 1986.

[2] M. P. Waalkes, "Cadmium carcinogenesis in review," *Journal of Inorganic Biochemistry*, vol. 79, no. 1-4, pp. 241–244, 2000.

[3] D. X. Tan, R. Hardeland, K. Back, L. C. Manchester, M. A. Alatorre-Jimenez, and R. J. Reiter, "On the significance of an alternate pathway of melatonin synthesis via 5-methoxytryptamine: comparisons across species," *Journal of Pineal Research*, vol. 61, no. 1, pp. 27–40, 2016.

[4] S. Hu, Z. Su, J. Jiang et al., "Lead, cadmium pollution of seafood and human health risk assessment in the coastline of the southern China," *Stochastic Environmental Research and Risk Assessment*, vol. 30, no. 5, pp. 1379–1386, 2016.

[5] D. Bagchi, M. Bagchi, E. A. Hassoun, and S. J. Stohs, "Cadmium-induced excretion of urinary lipid metabolites, DNA damage, glutathione depletion, and hepatic lipid peroxidation in Sprague-Dawley rats," *Biological Trace Element Research*, vol. 52, no. 2, pp. 143–154, 1996.

[6] G. Bertin and D. Averbeck, "Cadmium: cellular effects, modifications of biomolecules, modulation of DNA repair and genotoxic consequences (a review)," *Biochimie*, vol. 88, no. 11, pp. 1549–1559, 2006.

[7] W. R. García-Niño and J. Pedraza-Chaverrí, "Protective effect of curcumin against heavy metals-induced liver damage," *Food and Chemical Toxicology*, vol. 69, pp. 182–201, 2014.

[8] S. A. Mansour and M. M. Sidky, "Ecotoxicological studies. 3. Heavy metals contaminating water and fish from Fayoum Governorate, Egypt," *Food Chemistry*, vol. 78, no. 1, pp. 15–22, 2002.

[9] P. Morcillo, M. A. Esteban, and A. Cuesta, "Heavy metals produce toxicity, oxidative stress and apoptosis in the marine teleost fish SAF-1 cell line," *Chemosphere*, vol. 144, pp. 225–233, 2016.

[10] D. Quig, "Cysteine metabolism and metal toxicity," *Alternative Medicine Review*, vol. 3, no. 4, pp. 262–270, 1998.

[11] J. K. Angeli, C. A. Cruz Pereira, T. de Oliveira Faria, I. Stefanon, A. S. Padilha, and D. V. Vassallo, "Cadmium exposure induces vascular injury due to endothelial oxidative stress: the role of local angiotensin II and COX-2," *Free Radical Biology & Medicine*, vol. 65, pp. 838–848, 2013.

[12] K. C. Wu, J. J. Liu, and C. D. Klaassen, "Nrf2 activation prevents cadmium-induced acute liver injury," *Toxicology and Applied Pharmacology*, vol. 263, no. 1, pp. 14–20, 2012.

[13] H. Zhang, S. Sun, S. Guan, and J. Zhao, "Preventive effects of vitamin C and polysaccharides in *Dioscrea opposita* Thunb. on cadmium-induced liver injury in mice," *Medicinal Plant*, vol. 5, no. 6, pp. 36–38, 2014.

[14] H. Hagar and W. Al Malki, "Betaine supplementation protects against renal injury induced by cadmium intoxication in rats: role of oxidative stress and caspase-3," *Environmental Toxicology and Pharmacology*, vol. 37, no. 2, pp. 803–811, 2014.

[15] J. Wang, C. Jiang, M. Alattar et al., "Oxidative injury induced by cadmium sulfide nanoparticles in A549 cells and rat lungs," *Inhalation Toxicology*, vol. 27, no. 12, pp. 649–658, 2015.

[16] S. Liu, F. P. Xu, Z. J. Yang, M. Li, Y. H. Min, and S. Li, "Cadmium-induced injury and the ameliorative effects of selenium on chicken splenic lymphocytes: mechanisms of oxidative stress and apoptosis," *Biological Trace Element Research*, vol. 160, no. 3, pp. 340–351, 2014.

[17] P. D. B. Adamis, D. S. Gomes, M. L. C. C. Pinto, A. D. Panek, and E. C. A. Eleutherio, "The role of glutathione transferases in cadmium stress," *Toxicology Letters*, vol. 154, no. 1-2, pp. 81–88, 2004.

[18] E. Kowalczyk, A. Kopff, P. Fijałkowski et al., "Effect of anthocyanins on selected biochemical parameters in rats exposed to cadmium," *Acta Biochimica Polonica*, vol. 50, no. 2, pp. 543–548, 2003.

[19] M. Banni, L. Chouchene, K. Said, A. Kerkeni, and I. Messaoudi, "Mechanisms underlying the protective effect of zinc and selenium against cadmium-induced oxidative stress in zebrafish *Danio rerio*," *Biometals*, vol. 24, no. 6, pp. 981–992, 2011.

[20] B. I. Ognjanović, S. Z. Pavlović, S. D. Maletić et al., "Protective influence of vitamin E on antioxidant defense system in the blood of rats treated with cadmium," *Physiological Research*, vol. 52, p. 563, 2003.

[21] C. D. Klaassen, J. Liu, and S. Choudhuri, "Metallothionein: an intracellular protein to protect against cadmium toxicity," *Annual Review of Pharmacology and Toxicology*, vol. 39, no. 1, pp. 267–294, 1999.

[22] A. Formigari, P. Irato, and A. Santon, "Zinc, antioxidant systems and metallothionein in metal mediated-apoptosis: biochemical and cytochemical aspects," *Comparative Biochemistry and Physiology Part C: Toxicology & Pharmacology*, vol. 146, no. 4, pp. 443–459, 2007.

[23] S. Xu, H. Pi, Y. Chen et al., "Cadmium induced Drp1-dependent mitochondrial fragmentation by disturbing calcium homeostasis in its hepatotoxicity," *Cell Death & Disease*, vol. 4, no. 3, article e540, 2013.

[24] Y. Rao and J. Su, "Insights into the antiviral immunity against grass carp (*Ctenopharyngodon idellus*) reovirus (GCRV) in grass carp," *Journal of Immunology Research*, vol. 2015, Article ID 670437, 18 pages, 2015.

[25] D. G. Sfakianakis, E. Renieri, M. Kentouri, and A. M. Tsatsakis, "Effect of heavy metals on fish larvae deformities: a review," *Environmental Research*, vol. 137, pp. 246–255, 2015.

[26] C. Karber, "Karber's method of determining LD_{50}," *Biological Standardization*, pp. 37–40, 1937.

[27] J. Sun, "Practical combined method for computing the median lethal dose (LD_{50})," *Yao Hsueh Hsueh Pao (China)*, p. 10, 1963.

[28] K. S. Rajkumar, N. Kanipandian, and R. Thirumurugan, "Toxicity assessment on haemotology, biochemical and histopathological alterations of silver nanoparticles-exposed freshwater fish *Labeo rohita*," *Applied Nanoscience*, vol. 6, no. 1, pp. 19–29, 2016.

[29] A. S. Lee, "GRP78 induction in cancer: therapeutic and prognostic implications," *Cancer Research*, vol. 67, no. 8, pp. 3496–3499, 2007.

[30] A. Kukner, N. Colakoglu, H. Kara, H. Oner, C. Özogul, and E. Ozan, "Ultrastructural changes in the kidney of rats with acute exposure to cadmium and effects of exogenous metallothionein," *Biological Trace Element Research*, vol. 119, no. 2, pp. 137–146, 2007.

[31] M. E. Conti and F. Botrè, "The content of heavy metals in food packaging paper: an atomic absorption spectroscopy investigation," *Food Control*, vol. 8, no. 3, pp. 131–136, 1997.

[32] B. Mansouri, M. Ebrahimpour, and H. Babaei, "Bioaccumulation and elimination of nickel in the organs of black fish (*Capoeta fusca*)," *Toxicology and Industrial Health*, vol. 28, no. 4, pp. 361–368, 2012.

[33] Y. Jia, J. Lin, Y. Mi, and C. Zhang, "Quercetin attenuates cadmium-induced oxidative damage and apoptosis in granulosa cells from chicken ovarian follicles," *Reproductive Toxicology*, vol. 31, no. 4, pp. 477–485, 2011.

[34] A. W. M. Boersma, K. Nooter, R. G. Oostrum, and G. Stoter, "Quantification of apoptotic cells with fluorescein isothiocyanate-labeled annexin V in Chinese hamster ovary cell cultures treated with cisplatin," *Cytometry*, vol. 24, no. 2, pp. 123–130, 1996.

[35] K. J. Livak and T. D. Schmittgen, "Analysis of relative gene expression data using real-time quantitative PCR and the $2^{-\Delta\Delta CT}$ method," *Methods*, vol. 25, no. 4, pp. 402–408, 2001.

[36] C. A. Odonkor and S. Achilefu, "Modulation of effector caspase cleavage determines response of breast and lung tumor cell lines to chemotherapy," *Cancer Investigation*, vol. 27, no. 4, pp. 417–429, 2009.

[37] M. Affara, B. Dunmore, C. Savoie et al., "Understanding endothelial cell apoptosis: what can the transcriptome, glycome and proteome reveal?," *Philosophical Transactions of the Royal Society B: Biological Sciences*, vol. 362, no. 1484, pp. 1469–1487, 2007.

[38] Y. W. Mao, H. Xiang, J. Wang, S. Korsmeyer, J. Reddan, and D. W. C. Li, "Human *bcl-2* gene attenuates the ability of rabbit lens epithelial cells against H_2O_2-induced apoptosis through down-regulation of the αB-crystallin gene," *Journal of Biological Chemistry*, vol. 276, no. 46, article 43435, 43445 pages, 2001.

[39] P. Tarzan, *Cadmium and Lead Content in Aquatic Ecosystem, Brackiswater Ponds and Fish in Areas Affected Lapindo Mud*, Yogyakarta State University, 2014.

[40] A. Abubakar, A. Uzairu, P. A. Ekwumemgbo, and O. J. Okunola, "Evaluation of heavy metals concentration in imported frozen fish *Trachurus murphyi* species sold in Zaria market, Nigeria," *American Journal of Chemistry*, vol. 4, no. 5, pp. 137–154, 2014.

[41] Y. Tanaka, R. Tanaka, and T. Kashimoto, "Effect of cysteine on the fate of cadmium in rats-LD_{50} and transition of cadmium," *Food Hygiene and Safety Science (Shokuhin Eiseigaku Zasshi)*, vol. 24, no. 2, pp. 194–200_1, 1983.

[42] N. Ghosh and S. Bhattacharya, "Thyrotoxicity of the chlorides of cadmium and mercury in rabbit," *Biomedical and Environmental Sciences*, vol. 5, no. 3, pp. 236–240, 1992.

[43] S. V. S. Rana and S. Verma, "Protective effects of GSH, vitamin E, and selenium on lipid peroxidation in cadmium-fed rats," *Biological Trace Element Research*, vol. 51, no. 2, pp. 161–168, 1996.

[44] L. B. Yu, J. F. Gong, and X. Y. Huang, "The renovating effect of extract of plant-metallothionein to cadmium-induced oxidative damage in mice," *Journal of Xinjiang Medical University*, 2005.

[45] M. Cinar, A. Yigit, and G. Eraslan, "Effects of vitamin C or vitamin E supplementation on cadmium induced oxidative stress and anaemia in broilers," *Revue de Médecine Vétérinaire*, vol. 161, pp. 449–454, 2010.

[46] Y. Liu, J. Liu, and C. D. Klaassen, "Metallothionein-null and wild-type mice show similar cadmium absorption and tissue distribution following oral cadmium administration," *Toxicology and Applied Pharmacology*, vol. 175, no. 3, pp. 253–259, 2001.

[47] H. Jin, F. Jin, J. X. Jin et al., "Protective effects of *Ganoderma lucidum* spore on cadmium hepatotoxicity in mice," *Food and Chemical Toxicology*, vol. 52, pp. 171–175, 2013.

[48] U. E. Bais and M. V. Lokhande, "Effect of cadmium chloride on histopathological changes in the freshwater fish *Ophiocephalus striatus (Channa)*," *International Journal of Zoological Research*, vol. 8, no. 1, pp. 23–32, 2012.

[49] J. Liu, W. C. Kershaw, Y. P. Liu, and C. D. Klaassen, "Cadmium-induced hepatic endothelial cell injury in inbred strains of mice," *Toxicology*, vol. 75, no. 1, pp. 51–62, 1992.

[50] T. Yamano, L. A. DeCicco, and L. E. Rikans, "Attenuation of cadmium-induced liver injury in senescent male Fischer 344 rats: role of Kupffer cells and inflammatory cytokines," *Toxicology and Applied Pharmacology*, vol. 162, no. 1, pp. 68–75, 2000.

[51] J. C. van Dyk, G. M. Pieterse, and J. H. J. van Vuren, "Histological changes in the liver of *Oreochromis mossambicus* (Cichlidae) after exposure to cadmium and zinc," *Ecotoxicology and Environmental Safety*, vol. 66, no. 3, pp. 432–440, 2007.

[52] Y. P. Liu, J. Liu, M. B. Iszard, G. K. Andrews, R. D. Palmiter, and C. D. Klaassen, "Transgenic mice that overexpress metallothionein-I are protected from cadmium lethality and hepatotoxicity," *Toxicology and Applied Pharmacology*, vol. 135, no. 2, pp. 222–228, 1995.

[53] I. M. Drake, N. P. Mapstone, C. J. Schorah et al., "Reactive oxygen species activity and lipid peroxidation in *Helicobacter pylori* associated gastritis: relation to gastric mucosal ascorbic acid concentrations and effect of *H. pylori* eradication," *Gut*, vol. 42, no. 6, pp. 768–771, 1998.

[54] Z. Erdogan, S. Erdogan, S. Celik, and A. Unlu, "Effects of ascorbic acid on cadmium-induced oxidative stress and performance of broilers," *Biological Trace Element Research*, vol. 104, no. 1, pp. 019–032, 2005.

[55] M. Yoshida, Y. Saegusa, A. Fukuda, Y. Akama, and S. Owada, "Measurement of radical-scavenging ability in hepatic metallothionein of rat using in vivo electron spin resonance spectroscopy," *Toxicology*, vol. 213, no. 1-2, pp. 74–80, 2005.

[56] M. Yamashita, "Apoptosis in zebrafish development," *Comparative Biochemistry and Physiology Part B: Biochemistry and Molecular Biology*, vol. 136, no. 4, pp. 731–742, 2003.

[57] F. U. Dawar, X. Hu, L. Zhao et al., "Transcriptomic analysis reveals differentially expressed genes and a unique apoptosis pathway in channel catfish ovary cells after infection with the channel catfish virus," *Fish & Shellfish Immunology*, vol. 71, pp. 58–68, 2017.

[58] Y. Zhu, Q. Fan, H. Mao, Y. Liu, and C. Hu, "GRP78 from grass carp (*Ctenopharyngodon idellus*) provides cytoplasm protection against thermal and Pb^{2+} stress," *Fish & Shellfish Immunology*, vol. 34, no. 2, pp. 617–622, 2013.

[59] H. L. Huang, J. L. Wu, M. H. C. Chen, and J. R. Hong, "Aquatic birnavirus-induced ER stress-mediated death signaling contribute to downregulation of bcl-2 family proteins in salmon embryo cells," *PLoS One*, vol. 6, no. 8, article e22935, 2011.

[60] E. Eldering and R. A. W. vanLier, "B-cell antigen receptor-induced apoptosis: looking for clues," *Immunology Letters*, vol. 96, no. 2, pp. 187–194, 2005.

[61] I. M. Ghobrial, T. E. Witzig, and A. A. Adjei, "Targeting apoptosis pathways in cancer therapy," *CA: A Cancer Journal for Clinicians*, vol. 55, no. 3, pp. 178–194, 2005.

[62] J. D. Ly, D. R. Grubb, and A. Lawen, "The mitochondrial membrane potential ($\Delta\psi_m$) in apoptosis; an update," *Apoptosis*, vol. 8, no. 2, pp. 115–128, 2003.

[63] Y.-L. P. Ow, D. R. Green, Z. Hao, and T. W. Mak, "Cytochrome *c*: functions beyond respiration," *Nature Reviews Molecular Cell Biology*, vol. 9, no. 7, pp. 532–542, 2008.

[64] R. C. Taylor, S. P. Cullen, and S. J. Martin, "Apoptosis: controlled demolition at the cellular level," *Nature Reviews Molecular Cell Biology*, vol. 9, no. 3, pp. 231–241, 2008.

[65] Y. Tsujimoto, J. Cossman, E. Jaffe, and C. Croce, "Involvement of the bcl-2 gene in human follicular lymphoma," *Science*, vol. 228, no. 4706, pp. 1440–1443, 1985.

[66] C. Candé, F. Cecconi, P. Dessen, and G. Kroemer, "Apoptosis-inducing factor (AIF): key to the conserved caspase-independent pathways of cell death?," *Journal of Cell Science*, vol. 115, no. 24, pp. 4727–4734, 2002.

[67] W. C. Earnshaw, L. M. Martins, and S. H. Kaufmann, "Mammalian caspases: structure, activation, substrates, and functions during apoptosis," *Annual Review of Biochemistry*, vol. 68, no. 1, pp. 383–424, 1999.

Hindawi
Oxidative Medicine and Cellular Longevity
Volume 2018, Article ID 6926712, 9 pages
https://doi.org/10.1155/2018/6926712

Research Article

Oxidative Stress in the Muscles of the Fish Nile Tilapia Caused by Zinc Oxide Nanoparticles and Its Modulation by Vitamins C and E

Aaser M. Abdelazim,[1,2] **Islam M. Saadeldin**,[3,4] **Ayman Abdel-Aziz Swelum**,[3,5] **Mohamed M. Afifi**,[1,6,7] **and Ali Alkaladi**[6]

[1]*Department of Biochemistry, Faculty of Veterinary Medicine, Zagazig University, Zagazig 44519, Egypt*
[2]*Department of Basic Medical Sciences, College of Applied Medical Sciences, University of Bisha, Bisha, Saudi Arabia*
[3]*Department of Animal Production, College of Food and Agricultural Science, King Saud University, Riyadh 11451, Saudi Arabia*
[4]*Department of Physiology, Faculty of Veterinary Medicine, Zagazig University, Zagazig 44519, Egypt*
[5]*Department of Theriogenology, Faculty of Veterinary Medicine, Zagazig University, Zagazig 44519, Egypt*
[6]*Department of Biological Science, Faculty of Science, University of Jeddah, Jeddah, Saudi Arabia*
[7]*University of Jeddah Center for Scientific and Medical Research, University of Jeddah, Jeddah, Saudi Arabia*

Correspondence should be addressed to Islam M. Saadeldin; isaadeldin@ksu.edu.sa

Received 19 November 2017; Revised 25 January 2018; Accepted 31 January 2018; Published 5 April 2018

Academic Editor: Simona G. Bungău

The effects of zinc oxide nanoparticles (ZnONPs) on antioxidants in Nile tilapia muscles and the protective role of vitamins C and E were examined. Two hundred males of Nile tilapia were held in aquaria (10 fishes/aquarium). Fishes were divided into 5 groups: 40 fishes in each group; the first group was the control; the 2nd and 3rd groups were exposed to 1 and 2 mg/L of ZnONPs, respectively; and the 4th and 5th group were exposed to 1 and 2 mg/L of ZnONPs and treated with a (500 mg/kg diet) mixture of vitamin C and E mixture (250 mg/kg diet of each). Muscles were collected on the 7th and 15th day of treatments. Muscle malondialdehyde, reduced glutathione levels, superoxide dismutase (SOD), catalase (CAT), reduced glutathione (GR), glutathione peroxidase (GPx), and glutathione-*S*-transferase (GST) activities were measured after treatments. Relative quantification of SOD, CAT, GR, GPx, and GST mRNA transcripts was detected in the muscles. Results showed that MDA and GSH concentration; SOD, CAT, GR, GPx, and GST activities; and mRNA expression were significantly decreased in groups exposed to ZnONPs. Vitamins C and E significantly ameliorated the toxic effects of ZnONPs. In conclusion, vitamins C and E have the ability to ameliorate ZnONP oxidative stress toxicity in Nile tilapia.

1. Introduction

Despite their useful properties, nanoparticle hazards on the biological system are poorly understood up till now [1–3]. The wide production and huge use of nanoparticles facilitate their possibility to induce hazards, for example, the use of nanoparticles in water waste treatment leads to their spread in the aquatic environment inducing a huge hazard for both human and aquatic beings [4]. The hazards of nanoparticles (NPs) generally and zinc oxide nanoparticles (ZnONPs) especially in aquatic environment may be related to their ability to induce an oxidative stress [5]. Furthermore, the generation of reactive oxygen species (ROS) could be influenced by the size and shape of NPs as well as the experimental conditions [6]. Several studies have examined the effect of ZnONPs on aquatic environment. Cytotoxicity and genotoxicity on the freshwater molluscan bivalve *Coelatura aegyptiaca* have been approved [7]. Moreover, the embryotoxicity of ZnONPs to marine medaka, *Oryzias melastigma*, was explored [8]. Additionally, changes in the transcriptional profile in larval zebrafish exposed to ZnONPs have been reported [9]. Now, there is a great concern that ZnONPs have a powerful effect on the aquatic environment and organisms. Antioxidant enzymes have been used as a biomarker for detection of contamination of Nile tilapia and its possibility to be potential candidates for tissue toxicity biomarkers of

pollutants [10]; also, they have been used as biochemical markers for short-term exposure to diesel oil, pure biodiesel, and biodiesel blends in Nile tilapia [11]. This gave us the light to examine these antioxidant enzymes as targets for ZnONP exposure in Nile tilapia (*Oreochromis niloticus*). We especially chose Nile tilapia for our study due to its importance as an economical source of food and its varied systems of cultivation in developed countries [12]. The activity and expression profile of antioxidant enzymes under the effect of ZnONPs as well as the protective role of vitamins C and E were studied. We preferred to examine both vitamin C and E due to their important antioxidant capacity. The importance of vitamin C on fish health has been approved [13], while on the other hand, vitamin E has been used to control cyanotoxin [14], and both vitamin E and C have been used to control the hazards of metal toxicity in Nile tilapia [15]. At this moment, there is unclear role for both vitamin E and C to compete the toxicity originated form NP exposure. Only one recent study has showed the protective role of vitamin E alone against exposure to ZnONPs in Nile tilapia [16]. This gives us the impetus to validate their role to overcome the ZnONP toxicity on tilapia.

2. Material and Methods

2.1. Fish Preparation and Management. Two hundred males of *O. niloticus*, weight 90 ± 5 g, length 15 ± 3 cm, were obtained from Abrahem El-Solimani farms for fish, Kholes, KSA. The fishes were held in twenty glass boxes ($n = 10$ individuals/box), with 100 liters of water (pH 7.16 ± 0.3, 0.52 mM $CaCl_2$, and 0.24 mM $MgCl_2$) that was changed daily, a continuous system of water aeration (Eheim Liberty 150 Bio-Espumador cartridges). Temperature was maintained at 28 ± 2°C and O_2 at 7.0 ± 0.5 mg/L. Fishes were fed on fish diet containing proteins (31%), carbohydrates (37%), lipids (6%), fibers (2.5%), total phosphorus (1.5%), ash (12%), α-tocopherol (200 mg/kg diet), vitamin D3 (1700 IU/kg diet), and vitamin A (10,000 IU/kg diet). Daily change of water was established to eliminate any residuals of food or NPs. Institutional and national guidelines for the care and use of fisheries were followed.

2.2. Fish Grouping and Induction of ZnONP Toxicity. The fishes were randomly divided into 5 groups, 40 fishes in each group triplicate; the first group served as control (C) and the 2nd and 3rd groups were exposed to ZnONPs of 1 and 2 mg/L (T1 and T2), respectively. This dosage was determined in review of the related literature [17, 18]. The 4th and 5th group were exposed to ZnONPs of 1 and 2 mg/L and treated with a mixture of vitamins C and E in a dose of 500 mg/kg diet (250 mg of each), T1 + V and T2 + V, respectively. After 7 and 15 days of exposure, there was no mortality, and twenty fishes of each group were randomly selected and were anesthetized on ice. The muscles were removed, frozen in liquid nitrogen, and stored at −80°C until experimental procedures.

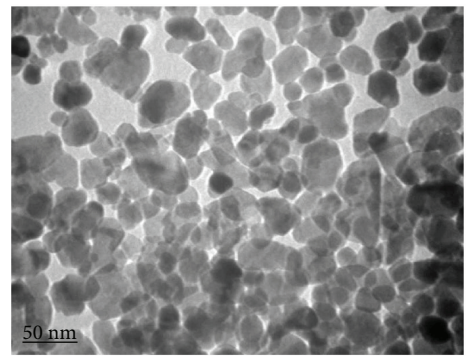

Figure 1: Transmission electron microscopic (TEM) photomicrograph of ZnONPs, which shows that the APS is 30 ± 5 nm.

Table 1: Oligonucleotide sequences of primers for examined antioxidant enzymes.

Gene	Forward 5′->3′	Reverse 5′->3′	Amplicon size (pb)
CAT	tcctgaatgaggaggagcga	atcttagatgaggcggtgatg	**232**
SOD	ggtgccctggagcccta	atgcgaagtcttccactgtc	**377**
GPx	ccaagagaactgcaagaga	caggacacgtcattcctacac	**180**
GR	cattaccgagacgcggagtt	cagttggctcaggatcatttgt	**420**
GST	taatgggagagggaagatgg	ctctgcgatgtaattcagga	**640**
β-actin	caatgagaggttccgttgc	aggattccataccaaggaagg	**280**

2.3. Preparation and Characterization of ZnONP Particle Suspensions. ZnONPs were obtained in the form of dispersion from Sigma-Aldrich, Steinheim, Germany (CAS number 1314-13-2), of concentration 50 wt.% in H_2O; average particle size (APS) was <35 nm Figure 1. The particle size distribution (hydrodynamic diameter) was <100 nm using dynamic light scattering (DLS) technique, pH 7 ± 0.1(for aqueous systems), and density 1.7 ± 0.1 g mL^{-1} at 25°C. Suspensions of ZnONPs in a concentration of 1 and 2 mg/L were daily prepared (JL-360, Shanghai, USA) for 20 min. To characterize the ZnONP shape and size, a small drop of aqueous ZnONP solution was air dried by directly placing onto a mesh of carbon-coated copper grid then examined under transmission electron microscope (TEM) (JEM-1011, JEOL, Japan). The concentration of ZnONPs in the exposure solution was quantified by inductively coupled plasma mass spectrometry (ICP-MS) at zero, 12, and 24 h of exposure to verify the exposure concentration is the same as the prepared concentrations (Supplemental Table 1).

2.4. Tissue Preparations. Trunk muscle homogenate was prepared from each sample without pooling according to [19], where 0.5 g of each muscle homogenization was performed using a solution formed from 5 mL of 0.1 M potassium phosphate buffer (pH 6.5) containing 20% (v/v) glycerol, 1 mM EDTA, and 1.4 mM dithioerythritol, centrifuged at 3000 rpm/5 m; then, the supernatant was used for biochemical assays.

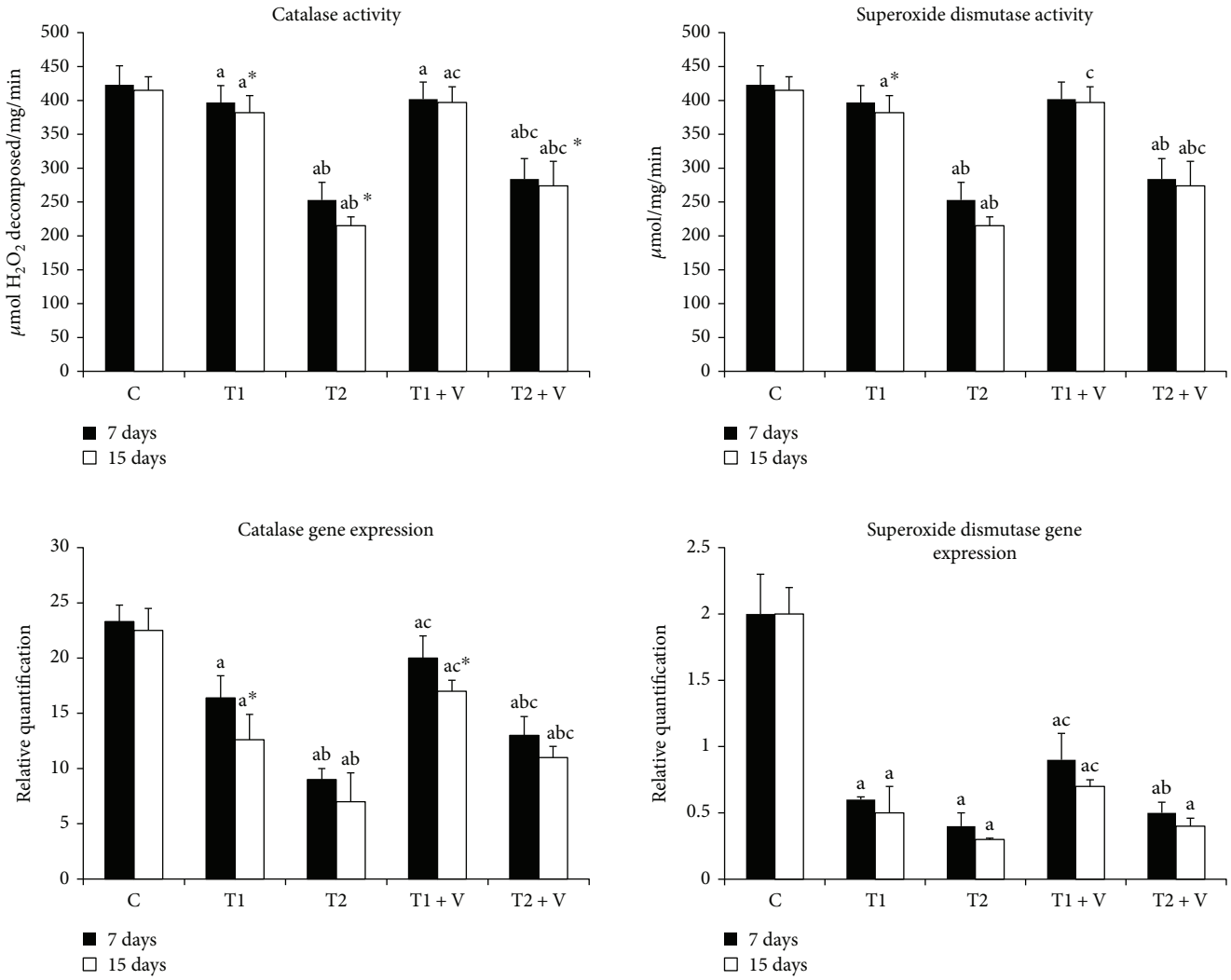

Figure 2: Activities and mRNA expression of muscle antioxidant enzymes, catalase, and superoxide dismutase in the (C) control group and in those (T1) exposed to 1 mg/L of zinc oxide nanoparticles, (T2) exposed to 1 mg/L of zinc oxide nanoparticles, (T1 + V) exposed to 1 mg/L of zinc oxide nanoparticles with a mixture of both vitamin C and E, and (T2 + V) exposed to 2 mg/L of zinc oxide nanoparticles with a mixture of both vitamin C and E. Values are expressed as mean ± SD ($n = 20$). Significant levels ($p < 0.05$) observed are as follows: a = in comparison to control group, b = when 2 mg ZnONP groups versus 1 mg ZnONP groups are compared, and c = when ZnONPs + vitamin groups versus their respective ZnONP groups are compared. *When 15-day-treated groups are compared with their respective 7-day-treated groups.

2.5. Malondialdehyde (MDA), Reduced Glutathione (GSH), and Antioxidant Enzyme Activity Analysis. The biochemical levels of MDA [20] and GSH [21] and the activities of SOD [22], CAT [23], GR [24], GPx [25], and GST [26] were determined in the muscles of all experimental fishes. Details about the biochemical analysis were included in Supplemental Methods.

2.6. Antioxidant Enzyme mRNA Expression Levels by RT-PCR. Muscle SOD, CAT, GPx, GR, and GST gene expression was quantified using real-time PCR. RNA was isolated from the muscles using the RNeasy Mini Kit (Qiagen) (Cat. number 74104). 0.5 μg of total RNA was used for production of cDNA using Qiagen Long Range 2 Step RT-PCR Kit (Cat. number 205920). Five μL of total cDNA was mixed with 12.5 μL of 2x SYBR® Green PCR mix with ROX from BioRad and 10 pmol/μL of each forward and reverse primer for the measured genes. Primer3 software was used for primer design (The Whitehead Institute, http://bioinfo.ut.ee/primer3-0.4.0/) as per the published *O. niloticus* SOD, CAT, GPx, GR, GST, and β-actin gene sequences (JF801727.1, JF801726.1, FF280316.1, XM_003445184, EU234530, and EF206801), respectively, of NCBI database; all primers were provided by Sigma-Aldrich (Sigma-Aldrich Chemie GmbH, Steinheim, Germany) and are shown in Table 1. PCR reactions were carried out in a thermal cycler (AbiPrism 7300) (Applied Biosystems, USA). The quantitative fold increase in genes was determined in relation to β-actin mRNA gene and calculated by the $2^{-\mathrm{DD\ CT}}$ method.

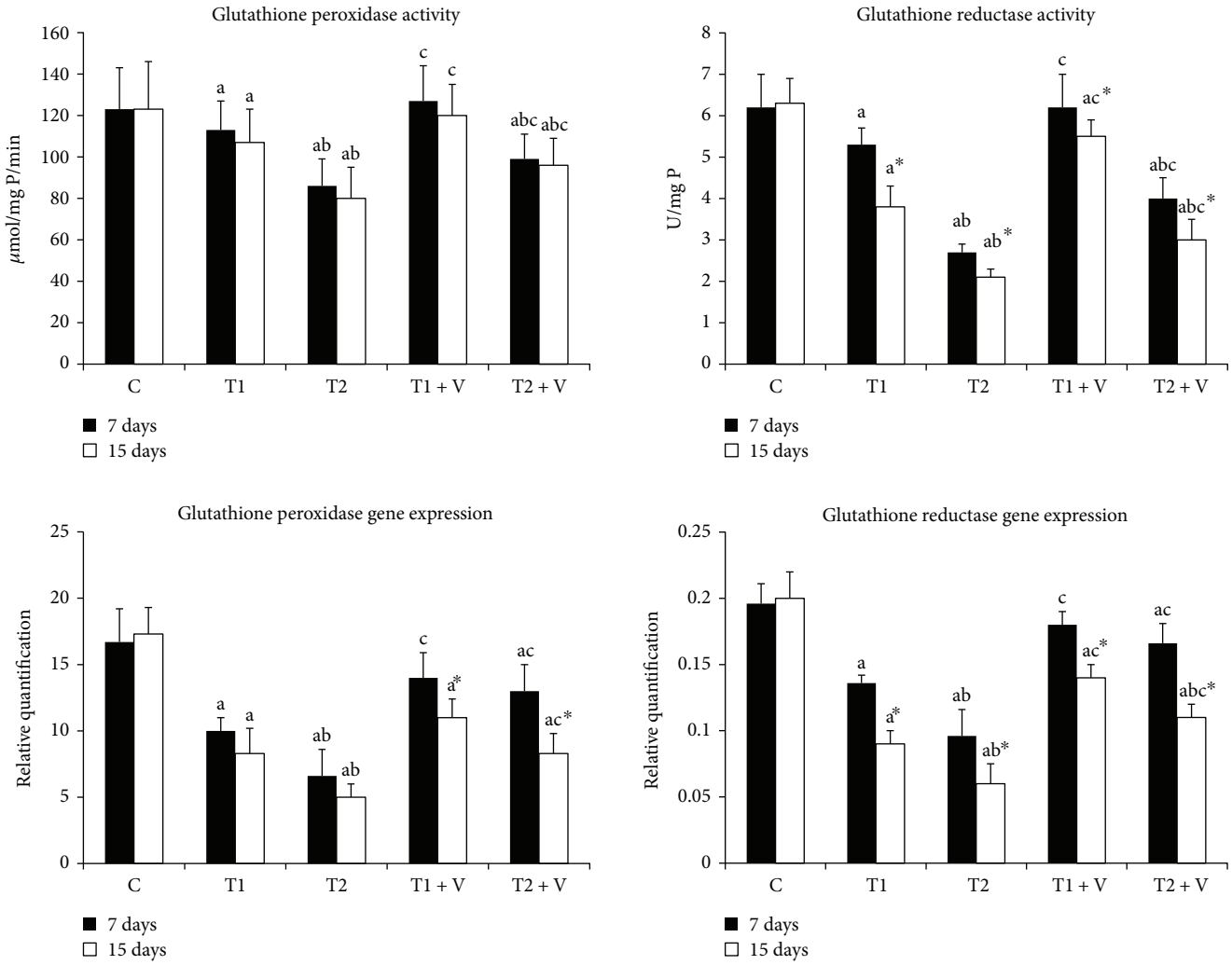

Figure 3: Activities and mRNA expression of muscle antioxidant enzymes glutathione peroxidase and glutathione reductase in the (C) control group and in those (T1) exposed to 1 mg/L of zinc oxide nanoparticles, (T2) exposed to 1 mg/L of zinc oxide nanoparticles, (T1 + V) exposed to 1 mg/L of zinc oxide nanoparticles with a mixture of both vitamin C and E, and (T2 + V) exposed to 2 mg/L of zinc oxide nanoparticles with a mixture of both vitamin C and E. Values are expressed as mean ± SD ($n = 20$). Significant levels ($p < 0.05$) observed are as follows: a = in comparison to control group, b = when 2 mg ZnONP groups versus 1 mg ZnONP groups are compared, and c = when ZnONPs + vitamin groups versus their respective ZnONP groups are compared. *When 15-day-treated groups are compared with their respective 7-day-treated groups.

2.7. Statistical Analysis. Statistical Package for Social Science (SPSS Inc., Chicago, IL, version 20, USA) was used to analyze all data. The data were expressed as mean ± SD. One-way analysis of variance (ANOVA) was used to a comparison among groups. For intergrouping homogeneity, Duncan's test was used. Statistical significance was set at $P \leq 0.05$.

3. Results

3.1. Effects of ZnONPs on Antioxidant Enzyme Activities and Gene Expression in Fish Muscles. The activities of antioxidant enzymes in the muscle tissues are shown in Figures 2–4. ZnONPs significantly inhibited CAT, SOD (Figure 2), GPx, GR (Figure 3), and GST (Figure 4) activities in muscles of ZnONP-exposed groups when compared to their control ($p < 0.05$). Supplementation of vitamin C and E mixture significantly ameliorated the enzyme activities to a similar level when compared with their control of nontreated fishes ($p < 0.05$). ZnONPs induced a significant repression of the relative mRNA expression of SOD and CAT (Figure 2), GPx and GR (Figure 3), and GST (Figure 4) in the muscles of exposed groups when compared with their control ($p < 0.05$). Supplementation of vitamin C and E mixture caused a significant induction in the antioxidant enzyme relative mRNA expression in muscles if compared with exposed nontreated fishes ($p < 0.05$).

3.2. Effects of ZnONPs on the Level of Reduced Glutathione (GSH) and MDA in Fish Muscles. ZnONPs induced a significant decline in the concentration of GSH (Figure 5) in the

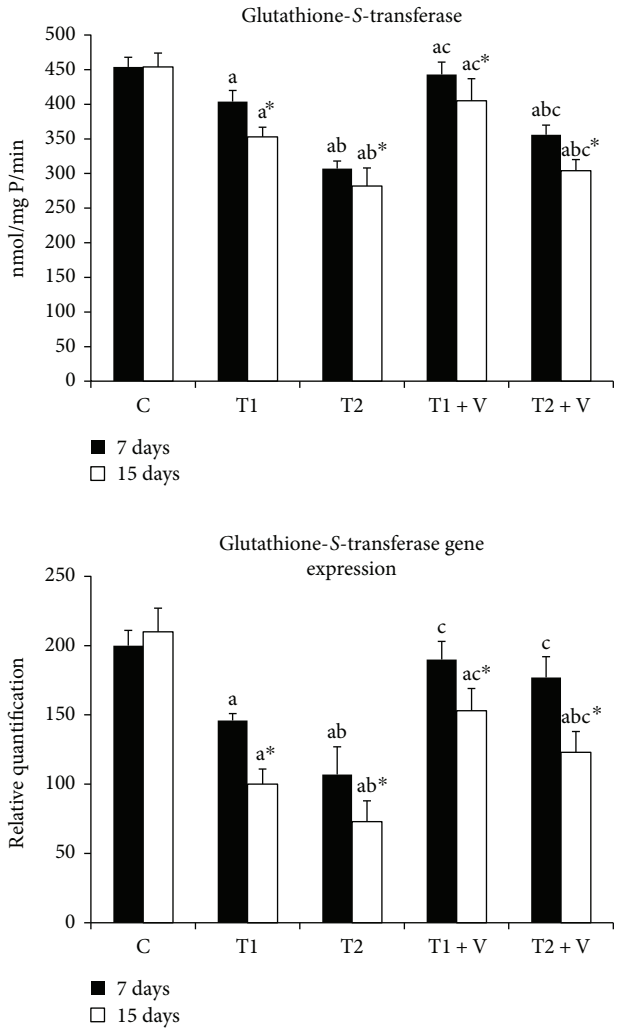

Figure 4: Activities and mRNA expression of muscle antioxidant enzymes glutathione-*S*-transferase in the (C) control group and those (T1) exposed to 1 mg/L of zinc oxide nanoparticles, (T2) exposed to 1 mg/L of zinc oxide nanoparticles, (T1+V) exposed to 1 mg/L of zinc oxide nanoparticles with a mixture of both vitamin C and E, and (T2+V) exposed to 2 mg/L of zinc oxide nanoparticles with a mixture of both vitamin C and E. Values are expressed as mean ± SD (n=20). Significant levels ($p < 0.05$) observed are as follows: a = in comparison to control group, b = when 2 mg ZnONP groups versus 1 mg ZnONPs groups are compared, and c = when ZnONPs + vitamin groups versus their respective ZnONPs groups are compared. *When 15-day-treated groups are compared with their respective 7-day-treated groups.

muscles of exposed groups when compared with their control. Supplementation of vitamins C and E induced an increase in its level in exposed groups when compared with nontreated groups. ZnONPs also induce a significant increase in the concentration of MDA (Figure 5) in the muscles of exposed fishes when compared with their control. Supplementation of vitamins C and E did not induce significant changes of MDA in exposed groups when compared with the nontreated groups. In the same time, increase in the duration of exposure leads to increase of the generation of MDA in the muscles of exposed fishes.

4. Discussion

In the present study, we evaluated the possible effect of ZnONPs on the antioxidant system in *Oreochromis niloticus*. We also validated the use of antioxidants as bioindicators for NP exposure. The high exposure of humans and animals to NPs is the main subject that motivates us to do this work. There is great importance for such study. First, to the best of our knowledge, this is the first record about the sublethal effect of ZnONPs in Nile tilapia. Second, it is important to assess the oxidative stress risk resulted from ZnONP exposure, not only in aquatic organisms but also for human and all consummated beings. Third, we aimed to evaluate the possible protective role of vitamins C and E for of the ZnONP exposure drawbacks. The minimal effective dose (1 mg/L) of ZnONPs was used and it was duplicated (2 mg/L) for intensifying their effects. We selected muscles as a target for our study as it has been approved to be the main site for NPs deposition [5]. Moreover, muscles are the main consumed part of fish so their effect will directly reflected on human health.

4.1. Effects of ZnONPs on Antioxidant Enzyme Activities, Glutathione, and Lipid Peroxide Levels in Fish Muscles. The current study has showed a great effect of ZnONPs on the antioxidant enzyme activities and their mRNA expression in the muscles of *O. niloticus*. In general, NPs can induce their toxicity through many mechanisms; much of NPs have an oxidant power through production of reactive oxygen species (ROS) or through its power to inhibit cells antioxidant system [27, 28]. Our results showed a decline in superoxide dismutase (SOD), catalase (CAT), glutathione peroxidase (GPx), glutathione reductase (GR), and glutathione-*S*-transferase (GST) activities, respectively, in ZnONP-exposed groups. Therefore, our results could indicate the involvement of oxidative stress in response to ZnONPs. The concept of involvement of ZnONPs in the oxidative stress development has been recently approved in other organisms that have been exposed to NPs rather than *O. niloticus* [7, 29–36]. All these recent observations strengthen our concept of the involvement of ZnONPs in elevation of oxidative stress in fishes. Furthermore, our results showed that ZnONP effects were directly proportional to the period of exposure and in a dose-dependent manner.

4.1.1. Effect of ZnONP Exposure on SOD and CAT Activities and mRNA Expression Levels. SOD and CAT are used as potent markers for early detection of environmental oxidative pollution; their activity was significantly reduced in ZnONP-exposed groups. The reduction of SOD and CAT activities and their mRNA expression has been used as an indicator for oxidant eradication [37]. In the same line of our study, the same observations were found in Chinook salmon cells exposed to 10–60 μg/mL of titanium oxide NPs [38]; in the brain of *O. niloticus* and *Tilapia zilli* exposed to 2 and 4 mg/L of silver NPs [39]; in the liver of adult Japanese medaka exposed to nanoiron [40]; in Mozambique tilapia, *Oreochromis mossambicus*, exposed to nickel NPs [41]; in heart and gill cell lines of *Catla catla* and gill cell line

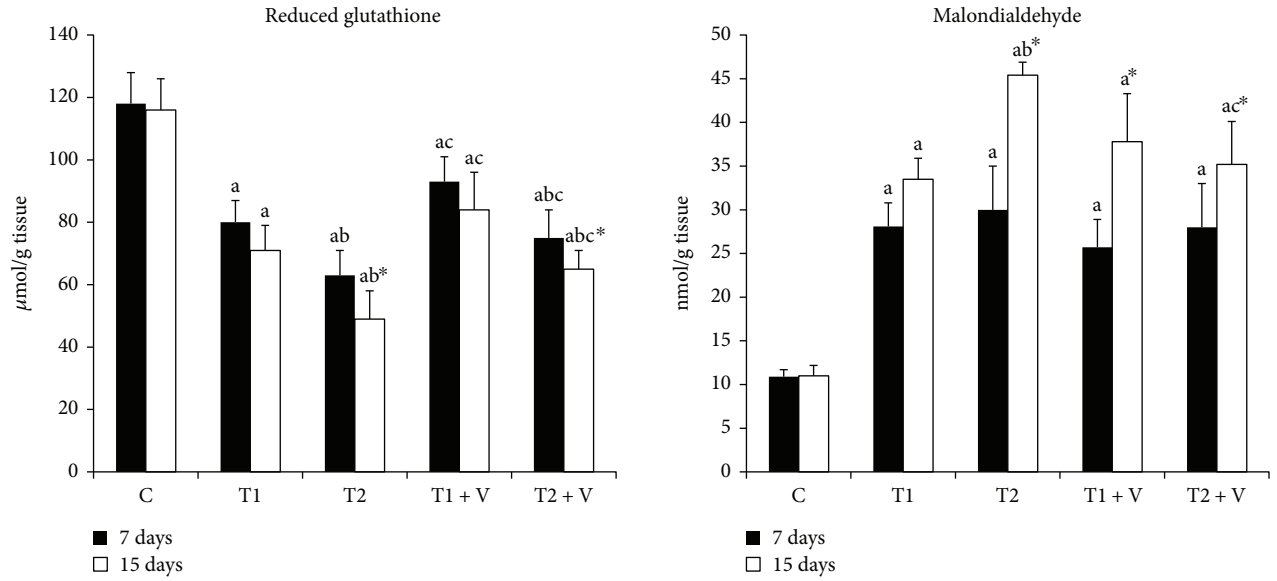

Figure 5: Level of malondialdehyde and reduced glutathione in the (C) control group and those (T1) exposed to 1 mg/L of zinc oxide nanoparticles, (T2) exposed to 1 mg/L of zinc oxide nanoparticles, (T1+V) exposed to 1 mg/L of zinc oxide nanoparticles with a mixture of both vitamin C and E, and (T2+V) exposed to 2 mg/L of zinc oxide nanoparticles with a mixture of both vitamin C and E. Values are expressed as mean ± SD ($n = 5$). Significant levels ($p < 0.05$) observed are as follows: a = in comparison to control group, b = when 2 mg ZnONP groups versus 1 mg ZnONP groups are compared, and c = when ZnONPs + vitamin groups versus their respective ZnONP groups are compared. *When 15-day-treated groups are compared with their respective 7-day-treated groups.

of *Labeo rohita* exposed to silver NPs [42]; and in *Carassius auratus* exposed to 20, 40, 80, 160, and 230 mg/L of a mixture of copper NPs, zinc oxide NPs, and cerium oxide NPs and individual NP, respectively [43], while our results regarding SOD and CAT activities have come in contrary to previous studies conducted on a freshwater fish, *Carassius auratus*, livers and gills exposed to 10 μg/mL of ZnONPs [44] and Chinook salmon cells exposed to 10–60 μg/mL of copper oxide NPs [45].

4.1.2. Effect of ZnONP Exposure on GPx, GR, and GST Activities and GSH Levels and mRNA Expression Levels. Our results showed a significant decline in GPx, GR, and GST activities and their mRNA expression levels in ZnONP-exposed groups. Previous studies have showed the same observations regarding these enzyme activities and/or mRNA expression levels. The effect of 2 and 4 mg/L of silver NPs on *O. niloticus and T. zillii* was studied; the GPx, GR, and GST activities and expression have been declined in the fish brain [39]. The same results have been obtained in the cells of Chinook salmon exposed to 10–60 μg/mL of copper oxide NPs [45]. In the same line, GST was declined in the livers of *Carassius auratus and Danio rerio* following exposure to 0, 0.01, 0.1, 1, 10, and 100 mg/L of titanium oxide NPs [46]. From the previously mentioned, we can say that antioxidant enzyme activities have tended to be increased after a short time of NP exposure, while longer time of exposure can lead to inhibition of their activities and moreover their production. In our study, we have observed that the activities of enzymes at 7-day exposure period were higher than the activities after 14-day exposure. Our data come in the same line of the observations of [44]. The activities of GPx, GR, and GST were directly proportional to the GSH levels. This was also clear from our data, which has showed a low level of muscle GSH in the exposed groups. Usually, the level of GSH is directly proportional to GPx, GR, and GST activities, and this has been approved in the previous studies [5, 18, 38, 47–51].

4.1.3. Effect of ZnONP Exposure on Malondialdehyde (MDA) Levels. Our results showed high levels of lipid MDA in the muscles of exposed fishes. The levels of malondialdehyde (MDA) as a potent marker for LPOs have been used in the present study. In the same line of our data, other authors also have proved high generation of MDA under ZnONP exposure [44, 52] and under other NP exposure [48, 50, 53]. In general, MDA has been considered a potent indicator for oxidative stress generation; the approved ability of ZnONPs to generate an oxidative stress has led directly to the increase of MDA levels in the tissues of the affected organism. The level of MDA was usually increased with the increase of exposure duration, and this was approved in our study. We can establish a concept here; the ability of NPs to induce toxicity to aquatic organisms depended on their doses, the duration of exposure, and their accessibility and distribution in organisms' tissues. Authors have approved that the gills, livers, brains, and muscles were the most affected fish parts when they are exposed to NPs. From our point of view, the muscles were considered the most important tissues, as they are the most consumed tissue by human beings. ZnONPs have induced an oxidative stress in the

muscles of Nile tilapia, and alleviating this toxic effect is an important issue.

4.2. Effect of Vitamins C and E as Protective Agents for ZnONP Exposure. Vitamin C scavenged superoxide anion by forming semidehydroascorbate radical which is subsequently reduced by GSH [54], while vitamin E has the ability to stop lipid peroxidation in the cell membrane. It does this by two ways: first by unsaturated fatty acid interaction and second by preserving the protein peptide chains [55]. In addition, it scavenges O_2, H_2O_2, (OH^-) radicals, and (O^-) radicals. The ability of both vitamin C and E to overcome the oxidative stress generated in the cells has now become a clear issue. Also, both vitamins have been known to have active pharmacological action, and they were therapeutically used in treatment of many oxidative stress-based diseases [56]. However, the challenge here is as follows: are they able to overcome the oxidative stress generated from exposure to sublethal doses of NPs? In the present study, we examined this. The results showed that there was a significant neutralization in the antioxidant system; the activities of SOD, CAT, GPx, GR, and GST started to return to normal as control with amelioration in the GSH levels and reduction in LPOs was observed in all fishes fed vitamin E and C mixture. This confirms the ability of both vitamin C and E to fight the oxidative damage results from ZnONP exposure. Our results were confirmed by previous observations; recently, vitamin C has been used to prepare a ligand for cerium oxide NPs as promising tool for facilitating NP detections in tissues [57]. This explained how much it has the power for binding of NPs; this illustrated the efficacy of vitamin C to tight bind to NPs and do its action. In the same line of our study, vitamin C and E mixture have the ability to correct some hematological and biochemical disorders in *O. niloticus* exposed to sublethal doses of ZnONPs [58]. In addition, vitamin E and vitamin C have induced protection against the cytotoxicity of silicon NPs [59]. This come in the same line of our finding. Moreover, the existence of NPs themselves could increase the activities of both vitamin C and E [60].

In conclusion, sublethal doses of ZnONPs were able to induce an oxidative stress in the muscles of *O. niloticus*, and a mixture of vitamins C and E was able to alleviate the oxidative stress generated due to exposure to ZnONPs.

Conflicts of Interest

The authors declare that they have no competing interests.

Authors' Contributions

All authors shared in the design and implementation of this study. All authors read and approved the final manuscript.

Acknowledgments

The authors extend their appreciation to the Deanship of Scientific Research at King Saud University for funding this work through the Research Group Project (no. RG-1438-018).

Supplementary Materials

Supplementary 1. Supplemental Table 1: the actual ZnONP concentrations (mg/L) in the exposure water.

Supplementary 2. Supplemental Methods (Biochemical assays).

References

[1] L. Chupani, H. Niksirat, J. Velíšek et al., "Chronic dietary toxicity of zinc oxide nanoparticles in common carp (*Cyprinus carpio* L.): tissue accumulation and physiological responses," *Ecotoxicology and Environmental Safety*, vol. 147, pp. 110–116, 2018.

[2] K. Isoda, R. Nagata, T. Hasegawa et al., "Hepatotoxicity and drug/chemical interaction toxicity of nanoclay particles in mice," *Nanoscale Research Letters*, vol. 12, no. 1, p. 199, 2017.

[3] B. J. Shaw and R. D. Handy, "Physiological effects of nanoparticles on fish: a comparison of nanometals versus metal ions," *Environment International*, vol. 37, no. 6, pp. 1083–1097, 2011.

[4] R. J. Aitken, M. Q. Chaudhry, A. B. A. Boxall, and M. Hull, "Manufacture and use of nanomaterials: current status in the UK and global trends," *Occupational Medicine*, vol. 56, no. 5, pp. 300–306, 2006.

[5] M. Connolly, M. Fernandez, E. Conde, F. Torrent, J. M. Navas, and M. L. Fernandez-Cruz, "Tissue distribution of zinc and subtle oxidative stress effects after dietary administration of ZnO nanoparticles to rainbow trout," *Science of The Total Environment*, vol. 551-552, pp. 334–343, 2016.

[6] C. Peng, W. Zhang, H. Gao et al., "Behavior and potential impacts of metal-based engineered nanoparticles in aquatic environments," *Nanomaterials*, vol. 7, no. 12, 2017.

[7] S. R. Fahmy and D. A. Sayed, "Toxicological perturbations of zinc oxide nanoparticles in the *Coelatura aegyptiaca* mussel," *Toxicology and Industrial Health*, vol. 33, no. 7, pp. 564–575, 2017.

[8] Y. Cong, F. Jin, J. Wang, and J. Mu, "The embryotoxicity of ZnO nanoparticles to marine medaka, *Oryzias melastigma*," *Aquatic Toxicology*, vol. 185, pp. 11–18, 2017.

[9] R. O. Kim, J. S. Choi, B. C. Kim, and W. K. Kim, "Comparative analysis of transcriptional profile changes in larval zebrafish exposed to zinc oxide nanoparticles and zinc sulfate," *Bulletin of Environmental Contamination and Toxicology*, vol. 98, no. 2, pp. 183–189, 2017.

[10] C. D. S. Carvalho, V. A. Bernusso, H. S. S. D. Araújo, E. L. G. Espíndola, and M. N. Fernandes, "Biomarker responses as indication of contaminant effects in *Oreochromis niloticus*," *Chemosphere*, vol. 89, no. 1, pp. 60–69, 2012.

[11] L. Nogueira, A. L. M. Sanches, D. G. H. da Silva, V. C. Ferrizi, A. B. Moreira, and E. A. de Almeida, "Biochemical biomarkers in Nile tilapia (*Oreochromis niloticus*) after short-term exposure to diesel oil, pure biodiesel and biodiesel blends," *Chemosphere*, vol. 85, no. 1, pp. 97–105, 2011.

[12] R. W. Ponzoni, N. H. Nguyen, H. L. Khaw, A. Hamzah, K. R. A. Bakar, and H. Y. Yee, "Genetic improvement of Nile tilapia (*Oreochromis niloticus*) with special reference to the work conducted by the WorldFish Center with the GIFT strain," *Reviews in Aquaculture*, vol. 3, no. 1, pp. 27–41, 2011.

[13] V. V. Trichet, E. Santigosa, E. Cochin, and J. Gabaudan, "The effect of vitamin C on fish health," in *Dietary Nutrients,*

Additives, and Fish Health, pp. 151–171, John Wiley & Sons, Inc, Hoboken, NJ, USA, 2015.

[14] R. Guzmán-Guillén, A. I. Prieto Ortega, D. Gutiérrez-Praena et al., "Vitamin E pretreatment prevents histopathological effects in tilapia (*Oreochromis niloticus*) acutely exposed to cylindrospermopsin," *Environmental Toxicology*, vol. 31, no. 11, pp. 1469–1485, 2016.

[15] A. S. A. Harabawy and Y. Y. I. Mosleh, "The role of vitamins A, C, E and selenium as antioxidants against genotoxicity and cytotoxicity of cadmium, copper, lead and zinc on erythrocytes of Nile tilapia, *Oreochromis niloticus*," *Ecotoxicology and Environmental Safety*, vol. 104, pp. 28–35, 2014.

[16] H. Ghafari Farsani, H. Binde Doria, H. Jamali, S. Hasanpour, N. Mehdipour, and G. Rashidiyan, "The protective role of vitamin E on *Oreochromis niloticus* exposed to ZnONP," *Ecotoxicology and Environmental Safety*, vol. 145, pp. 1–7, 2017.

[17] L. Hao and L. Chen, "Oxidative stress responses in different organs of carp (*Cyprinus carpio*) with exposure to ZnO nanoparticles," *Ecotoxicology and Environmental Safety*, vol. 80, pp. 103–110, 2012.

[18] H. Kaya, F. Aydin, M. Gurkan et al., "Effects of zinc oxide nanoparticles on bioaccumulation and oxidative stress in different organs of tilapia (*Oreochromis niloticus*)," *Environmental Toxicology and Pharmacology*, vol. 40, no. 3, pp. 936–947, 2015.

[19] P. Chen, B. A. Powell, M. Mortimer, and P. C. Ke, "Adaptive interactions between zinc oxide nanoparticles and *Chlorella* sp.," *Environmental Science & Technology*, vol. 46, no. 21, pp. 12178–12185, 2012.

[20] A. C. Gasparovic, M. Jaganjac, B. Mihaljevic, S. B. Sunjic, and N. Zarkovic, "Assays for the measurement of lipid peroxidation," *Methods in Molecular Biology*, vol. 965, pp. 283–296, 2013.

[21] H. Esterbauer and K. H. Cheeseman, "Determination of aldehydic lipid peroxidation products: malonaldehyde and 4-hydroxynonenal," *Methods in Enzymology*, vol. 186, pp. 407–421, 1990.

[22] F. Paoletti and A. Mocali, "Determination of superoxide dismutase activity by purely chemical system based on NAD(P)H ooxidation," *Methods in Enzymology*, vol. 186, pp. 209–220, 1990.

[23] H. Aebi, "Catalase in vitro," *Methods in Enzymology*, vol. 105, pp. 121–126, 1984.

[24] E. Beutler, "Effect of flavin compounds on glutathione reductase activity: in vivo and in vitro studies," *The Journal of Clinical Investigation*, vol. 48, no. 10, pp. 1957–1966, 1969.

[25] I. Carlberg and B. Mannervik, "Glutathione reductase," *Methods in Enzymology*, vol. 113, pp. 484–490, 1985.

[26] M. C. J. Wilce and M. W. Parker, "Structure and function of glutathione *S*-transferases," *Biochimica et Biophysica Acta (BBA) - Protein Structure and Molecular Enzymology*, vol. 1205, no. 1, pp. 1–18, 1994.

[27] I. Marisa, V. Matozzo, M. Munari et al., "In vivo exposure of the marine clam *Ruditapes philippinarum* to zinc oxide nanoparticles: responses in gills, digestive gland and haemolymph," *Environmental Science and Pollution Research*, vol. 23, no. 15, pp. 15275–15293, 2016.

[28] G. Vale, K. Mehennaoui, S. Cambier, G. Libralato, S. Jomini, and R. F. Domingos, "Manufactured nanoparticles in the aquatic environment-biochemical responses on freshwater organisms: a critical overview," *Aquatic Toxicology*, vol. 170, pp. 162–174, 2016.

[29] S. Ansar, M. Abudawood, S. S. Hamed, and M. M. Aleem, "Exposure to zinc oxide nanoparticles induces neurotoxicity and proinflammatory response: amelioration by hesperidin," *Biological Trace Element Research*, vol. 175, no. 2, pp. 360–366, 2017.

[30] S. C. Asani, R. D. Umrani, and K. M. Paknikar, "Differential dose-dependent effects of zinc oxide nanoparticles on oxidative stress-mediated pancreatic β-cell death," *Nanomedicine*, vol. 12, no. 7, pp. 745–759, 2017.

[31] H. Falfushynska, L. Gnatyshyna, O. Horyn, I. Sokolova, and O. Stoliar, "Endocrine and cellular stress effects of zinc oxide nanoparticles and nifedipine in marsh frogs *Pelophylax ridibundus*," *Aquatic Toxicology*, vol. 185, pp. 171–182, 2017.

[32] D. D. Guo, Q. Li, H. Y. Tang, J. Su, and H. S. Bi, "Zinc oxide nanoparticles inhibit expression of manganese superoxide dismutase via amplification of oxidative stress, in murine photoreceptor cells," *Cell Proliferation*, vol. 49, no. 3, pp. 386–394, 2016.

[33] J. Hou, G. You, Y. Xu et al., "Antioxidant enzyme activities as biomarkers of fluvial biofilm to ZnO NPs ecotoxicity and the Integrated Biomarker Responses (IBR) assessment," *Ecotoxicology and Environmental Safety*, vol. 133, pp. 10–17, 2016.

[34] L. Khorsandi, E. Mansouri, M. Orazizadeh, and Z. Jozi, "Curcumin attenuates hepatotoxicity induced by zinc oxide nanoparticles in rats," *Balkan Medical Journal*, vol. 33, no. 3, pp. 252–257, 2016.

[35] C. T. Ng, L. Q. Yong, M. P. Hande et al., "Zinc oxide nanoparticles exhibit cytotoxicity and genotoxicity through oxidative stress responses in human lung fibroblasts and *Drosophila melanogaster*," *International Journal of Nanomedicine*, vol. 12, pp. 1621–1637, 2017.

[36] D. Soni, D. Gandhi, P. Tarale, A. Bafana, R. A. Pandey, and S. Sivanesan, "Oxidative stress and genotoxicity of zinc oxide nanoparticles to *Pseudomonas* species, human promyelocytic leukemic (HL-60), and blood cells," *Biological Trace Element Research*, vol. 178, no. 2, pp. 218–227, 2017.

[37] I. Moreno, S. Pichardo, A. Jos et al., "Antioxidant enzyme activity and lipid peroxidation in liver and kidney of rats exposed to microcystin-LR administered intraperitoneally," *Toxicon*, vol. 45, no. 4, pp. 395–402, 2005.

[38] K. Srikanth, E. Pereira, A. C. Duarte, I. Ahmad, and J. V. Rao, "Assessment of cytotoxicity and oxidative stress induced by titanium oxide nanoparticles on Chinook salmon cells," *Environmental Science and Pollution Research*, vol. 22, no. 20, pp. 15571–15578, 2015.

[39] M. Afifi, S. Saddick, and O. A. Abu Zinada, "Toxicity of silver nanoparticles on the brain of *Oreochromis niloticus* and *Tilapia zillii*," *Saudi Journal of Biological Sciences*, vol. 23, no. 6, pp. 754–760, 2016.

[40] H. Li, Q. Zhou, Y. Wu, J. Fu, T. Wang, and G. Jiang, "Effects of waterborne nano-iron on medaka (*Oryzias latipes*): antioxidant enzymatic activity, lipid peroxidation and histopathology," *Ecotoxicology and Environmental Safety*, vol. 72, no. 3, pp. 684–692, 2009.

[41] C. Jayaseelan, A. Abdul Rahuman, R. Ramkumar et al., "Effect of sub-acute exposure to nickel nanoparticles on oxidative stress and histopathological changes in Mozambique tilapia, *Oreochromis mossambicus*," *Ecotoxicology and Environmental Safety*, vol. 107, pp. 220–228, 2014.

[42] G. Taju, S. Abdul Majeed, K. S. N. Nambi, and A. S. Sahul Hameed, "In vitro assay for the toxicity of silver nanoparticles using heart and gill cell lines of *Catla catla* and gill cell line of *Labeo rohita*," *Comparative Biochemistry and Physiology Part C: Toxicology & Pharmacology*, vol. 161, pp. 41–52, 2014.

[43] J. Xia, H. Z. Zhao, and G. H. Lu, "Effects of selected metal oxide nanoparticles on multiple biomarkers in *Carassius auratus*," *Biomedical and Environmental Sciences*, vol. 26, no. 9, pp. 742–749, 2013.

[44] M. Benavides, J. Fernandez-Lodeiro, P. Coelho, C. Lodeiro, and M. S. Diniz, "Single and combined effects of aluminum (Al_2O_3) and zinc (ZnO) oxide nanoparticles in a freshwater fish, *Carassius auratus*," *Environmental Science and Pollution Research*, vol. 23, no. 24, pp. 24578–24591, 2016.

[45] K. Srikanth, E. Pereira, A. C. Duarte, and J. V. Rao, "Evaluation of cytotoxicity, morphological alterations and oxidative stress in Chinook salmon cells exposed to copper oxide nanoparticles," *Protoplasma*, vol. 253, no. 3, pp. 873–884, 2016.

[46] M. S. Diniz, A. P. A. de Matos, J. Lourenço et al., "Liver alterations in two freshwater fish species (*Carassius auratus* and *Danio rerio*) following exposure to different TiO_2 nanoparticle concentrations," *Microscopy and Microanalysis*, vol. 19, no. 5, pp. 1131–1140, 2013.

[47] T. Fang, L. P. Yu, W. C. Zhang, and S. P. Bao, "Effects of humic acid and ionic strength on TiO_2 nanoparticles sublethal toxicity to zebrafish," *Ecotoxicology*, vol. 24, no. 10, pp. 2054–2066, 2015.

[48] M. S. Khan, N. A. Qureshi, F. Jabeen, M. S. Asghar, M. Shakeel, and M. Fakhar -e -Alam, "Eco-friendly synthesis of silver nanoparticles through economical methods and assessment of toxicity through oxidative stress analysis in the *Labeo Rohita*," *Biological Trace Element Research*, vol. 176, no. 2, pp. 416–428, 2017.

[49] T. Sovova, D. Boyle, K. A. Sloman, C. Vanegas Perez, and R. D. Handy, "Impaired behavioural response to alarm substance in rainbow trout exposed to copper nanoparticles," *Aquatic Toxicology*, vol. 152, pp. 195–204, 2014.

[50] T. Wang, X. Chen, X. Long, Z. Liu, and S. Yan, "Copper nanoparticles and copper sulphate induced cytotoxicity in hepatocyte primary cultures of *Epinephelus coioides*," *PLoS One*, vol. 11, no. 2, article e0149484, 2016.

[51] Y. Yuan, S. Ge, H. Sun et al., "Intracellular self-assembly and disassembly of ^{19}F nanoparticles confer respective "off" and "on" ^{19}F NMR/MRI signals for legumain activity detection in zebrafish," *ACS Nano*, vol. 9, no. 5, pp. 5117–5124, 2015.

[52] A. Nadhman, M. I. Khan, S. Nazir et al., "Annihilation of *Leishmania* by daylight responsive ZnO nanoparticles: a temporal relationship of reactive oxygen species-induced lipid and protein oxidation," *International Journal of Nanomedicine*, vol. 11, pp. 2451–2461, 2016.

[53] M. Ates, V. Demir, R. Adiguzel, and Z. Arslan, "Bioaccumulation, subacute toxicity, and tissue distribution of engineered titanium dioxide nanoparticles in goldfish (*Carassius auratus*)," *Journal of Nanomaterials*, vol. 2013, Article ID 460518, 6 pages, 2013.

[54] D. V. Ratnam, D. D. Ankola, V. Bhardwaj, D. K. Sahana, and M. N. V. R. Kumar, "Role of antioxidants in prophylaxis and therapy: a pharmaceutical perspective," *Journal of Controlled Release*, vol. 113, no. 3, pp. 189–207, 2006.

[55] G. A. Pascoe, M. W. Fariss, K. Olafsdottir, and D. J. Reed, "A role of vitamin E in protection against cell injury. Maintenance of intracellular glutathione precursors and biosynthesis," *European Journal of Biochemistry*, vol. 166, no. 1, pp. 241–247, 1987.

[56] A. K. Jain, N. K. Mehra, and N. K. Swarnakar, "Role of antioxidants for the treatment of cardiovascular diseases: challenges and opportunities," *Current Pharmaceutical Design*, vol. 21, no. 30, pp. 4441–4455, 2015.

[57] A. Othman, D. Andreescu, D. P. Karunaratne, S. V. Babu, and S. Andreescu, "Functional paper-based platform for rapid capture and detection of CeO_2 nanoparticles," *ACS Applied Materials & Interfaces*, vol. 9, no. 14, pp. 12893–12905, 2017.

[58] A. Alkaladi, N. A. M. N. el-Deen, M. Afifi, and O. A. A. Zinadah, "Hematological and biochemical investigations on the effect of vitamin E and C on *Oreochromis niloticus* exposed to zinc oxide nanoparticles," *Saudi Journal of Biological Sciences*, vol. 22, no. 5, pp. 556–563, 2015.

[59] S. Bhattacharjee, L. H. J. D. E. Haan, N. M. Evers et al., "Role of surface charge and oxidative stress in cytotoxicity of organic monolayer-coated silicon nanoparticles towards macrophage NR8383 cells," *Particle and Fibre Toxicology*, vol. 7, no. 1, p. 25, 2010.

[60] C. E. Astete, D. Dolliver, M. Whaley, L. Khachatryan, and C. M. Sabliov, "Antioxidant poly(lactic-*co*-glycolic) acid nanoparticles made with α-tocopherol–ascorbic acid surfactant," *ACS Nano*, vol. 5, no. 12, pp. 9313–9325, 2011.

Hindawi
Oxidative Medicine and Cellular Longevity
Volume 2018, Article ID 1056173, 13 pages
https://doi.org/10.1155/2018/1056173

Research Article

The Ameliorating Effect of Berberine-Rich Fraction against Gossypol-Induced Testicular Inflammation and Oxidative Stress

Samar R. Saleh,[1,2] Rana Attia,[1] and Doaa A. Ghareeb[1,2,3]

[1]*Biochemistry Department, Faculty of Science, Alexandria University, Alexandria, Egypt*
[2]*Pharmaceutical and Fermentation Industries Development Centre, City for Scientific Research and Technology Applications, Alexandria, Egypt*
[3]*Biological Sciences Department, Faculty of Science, Beirut Arab University, Beirut, Lebanon*

Correspondence should be addressed to Doaa A. Ghareeb; d.ghareeb@yahoo.com

Received 22 December 2017; Accepted 17 February 2018; Published 3 April 2018

Academic Editor: Agnieszka Najda

This study was aimed at evaluating the efficacy of berberine-rich fraction (BF) as a protective and/or a therapeutic agent against inflammation and oxidative stress during male infertility. Sexually mature Sprague-Dawley male rats were divided into five groups treated with either corn oil, BF (100 mg/kg BW, orally, daily for 30 days), gossypol acetate (5 mg/kg BW, i.p.) eight times for 16 days, BF alone for 14 days then coadministered with gossypol acetate for the next 16 days (protected group), or gossypol acetate for 16 days then treated with BF for 30 days (treated group). All animals completed the experimental period (46 days) without obtaining any treatments in the gap period. Sperm parameters, oxidative index, and inflammatory markers were measured. Gossypol injection significantly decreased the semen quality and testosterone level that resulted from the elevation of testicular reactive oxygen and nitrogen species (TBARS and NO), TNF-α, TNF-α-converting enzyme, and interleukins (IL-1β, IL-6, and IL-18) by 230, 180, 12.5, 97.9, and 300%, respectively, while interleukin-12 and tissue inhibitors of metalloproteinases-3 were significantly decreased by 59 and 66%, respectively. BF (protected and treated groups) significantly improved the semen quality, oxidative stress, and inflammation associated with male infertility. It is suitable to use more advanced studies to validate these findings.

1. Introduction

Infertility is the disability of a couple to achieve pregnancy after one year without intercourse precautions [1]. Male infertility is found to contribute 45%–50% of infertility cases [2]. Africa and Central/Eastern Europe were considered to have the highest rates of infertility [3]. Many factors are known to impair male infertility, including varicocele, testicular failure, treatment with radiation, and illicit drugs [4]. Infertility produces psychological stress as a couple fails achieve the expected goal of reproduction, causing disappointment and frustration that is attributed to generalized increased oxidative stress levels [5]. Oxidative stress is a well-known causative factor involved in the etiology of male infertility [6, 7]. Oxidative stress arises when reactive oxygen species (ROS) or free radical production overwhelms the endogenous antioxidant defense of the male reproductive tract [1, 8]. ROS have destructive effects on semen quality by disrupting the integrity of sperm nuclear DNA and ATP production [1]. The spermatozoal cell membrane contains a high abundance of polyunsaturated fatty acids representing the most vulnerable target for free radical damage and lipid peroxidation and, hence, influencing the sperm viability, count, motility, and morphology [9]. Inflammation could be linked to oxidative stress, and as oxidative stress primarily occurs, it can further induce inflammation and vice versa; thus, they strengthen each other, causing destructive effects to the cells [10, 11].

Cytokines, including interleukins (ILs) and tumor necrosis factor alpha (TNF-α), are important mediators of immunity and can be contributed in numerous physiological processes in the male reproductive tract [2]. Cytokines have

different effects on the semen quality and sperm function. IL-1β, IL-6, and IL-18 are proinflammatory cytokines, can be produced by specific cells in the male reproductive system (such as testicular somatic cells and Sertoli cells), are included in the inflammatory reaction, and can induce apoptosis [2], while IL-12 improves male fertility due to its immunomodulatory properties [12]. It is involved in the induction and maintenance of the immune response during both cell-mediated (helper T1) and humoral responses (helper T2) [13] and regulating antigen-presenting activity and natural killer cell activity [14]. TNF-α has destructive effects on sperm [8], and the TNF-α-converting enzyme (TACE; ADAM-17) is an enzyme involved in the proteolytic liberation of TNF-α from the pro-TNF-α molecule. Since ADAM-17 was found to be inhibited by tissue inhibitors of metalloproteinases-3 (TIMP-3); TIMP-3 are important factors involved in the regulation of the inflammatory process and the disease progression [15].

Antioxidants quench free radicals and protect gonadal cells and mature spermatozoa from ROS production and oxidative damage [9]. According to the World Health Organization (WHO), developing countries make use of herbal medicinal products for a variety problems due to their safety and the side effects of chemical drugs [16]. Berberine is an isoquinoline alkaloid that belongs to the structural class of protoberberines [17] and is present in roots, rhizomes, and stem bark of the *Berberis* species that belongs to the Berberidaceae family. Berberine is the most active constituent in *Berberis vulgaris* [18–20]. Several studies have indicated that berberine acts as a natural medicine with multiple biochemical and pharmacological activities [21, 22] including anti-inflammatory [23], antioxidant [24], antidepressant [25, 26], anticancer [27], hypoglycemic, hypolipidemic [22], and antimicrobial activities [19].

Gossypol was used as antifertility agent in male rats. Gossypol is a very toxic crystalline polyphenolic compound and is found in the highest concentration in the seeds of cotton plants [28]. Gossypol induces oxidative stress by the imbalance between antioxidants and prooxidants, resulting in the accumulation of ROS [29]. Oral gossypol acetate was found to reduce the levels of serum testosterone and luteinizing hormone in a dose- and duration-dependent manner [30]. Gossypol acts directly on testes and induces azoospermia or oligospermia [31]. Furthermore, gossypol blocked cAMP formation in sperms, which subsequently decreased sperm motility [32]. It also reduced the secretory activity of accessory sex glands [33]. Therefore, gossypol was used as an efficient male contraceptive drug [34].

The present study was aimed at assessing the therapeutic and/or protective effects of BF against the inflammation process produced during male infertility induced in rats by using gossypol acetate. The study will demonstrate its effect on biochemical blood parameters (TBARS, GSH, testosterone, cholesterol, glucose, and albumin), semen quality (sperm count, motility, morphology, α- glucosidase activity, and fructose level), and finally the inflammatory markers [testicular TBARS, NO, TNF-α, ADAM-17, TIMP-3, and interleukins (IL-1β, IL-6, IL-12, and IL-18)].

2. Materials and Methods

2.1. Plant Collection and Preparation of Ethanol Extract and Different Fractions. Barberry roots were purchased and authenticated by Professor Salma El-dareir, Botany Department, Faculty of Science, Alexandria University, Egypt. This classification was dependent on the data about the plant published in the Dargon Herbarium. Barberry roots were subjected to steam distillation, and the ethanol extract was prepared as described by [27]. The extract was lyophilized and the obtained powder (35 g, ethanolic extract) was dissolved in 1% HCl and then filtrated. The pH of the filtrate was optimized to 8 by using concentrated NH_4OH. The tertiary alkaloids were extracted from the previous solution by using chloroform, and this fraction (chloroform fraction) was evaporated and lyophilized (25 g). The obtained powder was dissolved in the minimum amount of chloroform and then was subjected to a silica gel 100–200 mesh column. A berberine-rich fraction (2.5 g) was obtained by using gradient elution with $CHCl_3$: MeOH (9 : 1; 8 : 2) and finally methanol [35]. The presence of berberine in the fraction was identified using TLC, melting point [36], HPLC [27], and ^{1}H-NMR [37]. The obtained powder was dissolved in polyethylene glycol (20%) to be administrated to rats.

2.2. Preparation of Gossypol Acetate. The Egyptian cottonseeds (Giza 70) were collected with the help of Professor Ali Aisa Nawar, Department of Crop Science, Faculty of Agriculture, Alexandria University, Egypt. The collected seeds were cleaned and crushed; the decorticated kernels were mashed by a meat chopper and finally extracted with peroxide-free ether by percolation. Briefly, the decorticated kernels (1 kg) were defatted by petroleum ether for at least 2 h at room temperature (RT), then filtrated by using a Bűchner funnel and dried. The dried kernels were soaked in peroxide-free ether at RT, overnight in the dark. The oil-ether extract was filtrated as mentioned above, and the extract was concentrated by using rotary evaporator (Büchi, Switzerland). Glacial acetic acid was added to the extract (1 : 1, v/v) and stirred thoroughly, and the gossypol acetate crystals were precipitated overnight. The crystals were collected and stored in refrigerator until use [38].

2.3. Animal Experimental Design. Thirty albino sexually mature Sprague-Dawley male rats, about 10–12 weeks of age (100–130 g body weight), were purchased from the experimental animal house of the Faculty of Science, Cairo University, and housed in the animal house of the physiology department of the Faculty of Medicine, Alexandria University. The animals were grouped (six rats/cage), under standard laboratory conditions with water and food provided ad libitum. All animal experiments were performed following the ethical standards according to the *Guide for the Care and Use of Laboratory Animals* of the National Institutes of Health (Institute of Laboratory Animal Resources 1996) in the Faculty of Medicine, Alexandria University, Egypt.

The healthy experimental animals were equally divided into five groups (Figure 1). Group 1 (control) received corn oil (0.5 ml, intraperitoneally) eight times for 16 days. Group

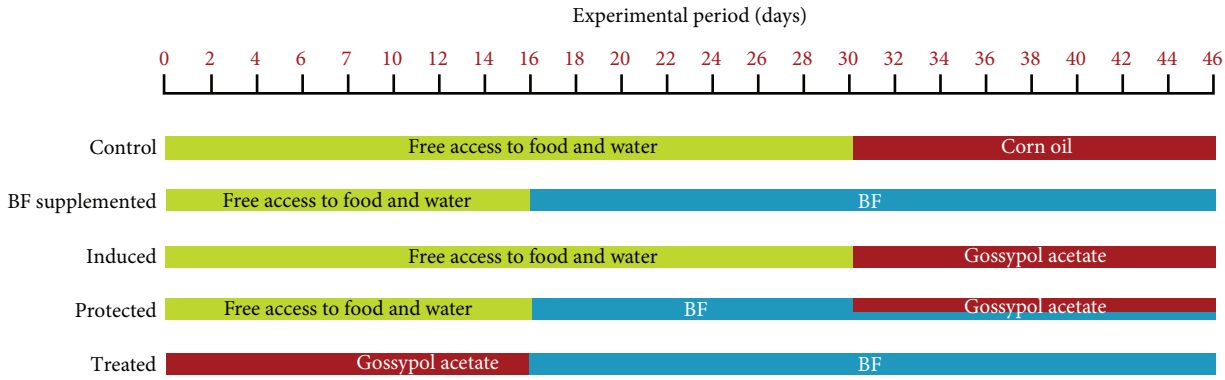

Figure 1: An illustration of the experimental design groups. Corn oil (0.5 ml, intraperitoneally) eight times for 16 days, BF (100 mg/kg BW, orally by gavage) daily for 30 days, and gossypol acetate (5 mg/kg BW, intraperitoneally, dissolved in corn oil) eight times for 16 days. Green colour indicates free access to food and water, red colour indicates the administration of corn oil or gossypol acetate, and blue colour indicates treatment with BF.

2 (BF supplemented) received BF (100 mg/kg BW, orally by gavage) daily for 30 days. Group 3 (induced) received gossypol acetate (5 mg/kg BW, intraperitoneally, dissolved in corn oil) eight times for 16 days. Group 4 (protected) was administered BF alone for 2 weeks and then was coadministered with gossypol acetate for the next 16 days. Group 5 (treated) received gossypol acetate for 16 days and then was treated with BF for 30 days. The doses of BF and gossypol acetate were as mentioned in groups 2 and 3, respectively (Figure 1). Experimental animals in groups 1, 2, 3, and 4 were allowed free access to water and food without any treatments until the 16th day for groups 2 and 4 for and until the 30th day for groups 1 and 3.

At the end of the experiment (after 46 days), the rats were fasted for eight hours and then the blood was collected from the eye canthus to measure the blood glucose level. Rats were allowed to complete fasting overnight and then decapitated to collect the blood and testes. Sera were isolated and stored at −20°C.

2.4. Preparation of Testicular and Epididymal Tissues. After decapitation, one testis was removed and most of the parenchyma (2/3) was weighed. A 10% (w/v) homogenate of testis tissues in 0.1 M phosphate buffer saline (PBS), pH 7.4, was prepared by using a mortar in an ice bath and centrifuged at 10,000*g* for 20 min at 4°C. The supernatant was collected and stored for further biochemical investigations. The second testis and one epididymis were postfixed overnight in 10% neutral buffered formalin for histopathological study. The second epididymis was isolated, washed, crushed in 2 ml Ham's F-10 medium (0.5% bovine serum albumin, BSA), and incubated at 37°C for the estimation of the spermatozoal quality by automated examination by MiraLab's Computer Aided Semen Analysis System (CASA, WLJY 9000, Beijing Weili New Century Science and Tech. Dev. Co. Ltd., China) [39]. Methylene blue and eosin red stains were used, respectively, for studying the sperm morphology.

2.5. Biochemical Assays. Serum-reduced glutathione (GSH) and TBARS as well as testicular TBARS and nitric oxide levels were determined according to Jollow et al. [40], Tappel and Zalkin [41], and Menaka et al. [42], respectively. Testosterone level was determined in serum by using an ELISA commercial kit [43], and the levels of glucose [44], cholesterol [45], and albumin [46] were also measured in the serum by using commercial kits (Biosystems S.A., Spain).

2.6. Semen Parameters. Sperm count, motility, and morphology index were assessed using CASA. Alpha-glucosidase activity and fructose level are important parameters related to semen quality. Alpha-glucosidase activity was measured by using the method of Han and Srinivasan [47], in which the specific activity (IU/mg) of the enzyme was defined as micromoles (μmol) of *p*-nitrophenol released per min per milligram (mg) of protein. The semen fructose level was determined according to Foreman et al. [48].

2.7. Determination of Sperm Inflammatory Markers. Testicular IL-1β, IL-6, IL-12, and IL-18 were estimated by using enzyme-linked immunosorbent assay (ELISA) kits (Koma Biotech–Korea), and testicular TNF-α, ADAM-17, and TIMP-3 were determined by Sun Red (England) ELISA kits. Precoated wells with the captured antibodies were washed four times with the washing buffer. Standard or samples (100 μl) were added to each well in duplicate, covered, and incubated at RT for 2 h. The plates were then washed four times and 100 μl of the diluted detection antibody was added per well, covered, and incubated at RT for 2 h. 100 μl of streptavidin-HRP was added to each well and incubated for 30 min at RT for a proper colour development. The plates were washed and 100 μl of the substrate solution (3,3′,5,5′-tetramethylbenzidine, TMB) was added to each well and incubated for 30 min at RT. The reaction was terminated by adding 100 μl of the stop solution (H_2SO_4, 5%) to each well, and the colour developed was read at 450 nm on a plate reader (Sanofi Diagnostics Pasteur, France).

2.8. Histopathological Changes. The testes and epididymides of the control and experimental groups were removed, postfixed overnight in 10% neutral buffered formalin, dehydrated in ascending grades of alcohol (70%, 80%, 95%, and absolute alcohol), and cleaned by immersion in xylene followed by

impregnation in melted paraffin wax for 1–2 h. Sections 5 μm thick were cut by using a rotary microtome. Finally, the sections were stained with conventional hematoxylin and eosin (H&E) stain for examination under a light microscope of any histopathological changes. The histopathological study was carried out in the Histopathology Department, Faculty of Medicine, Alexandria University.

2.9. Statistical Analysis. Data was analysed by one-way analysis of variance (ANOVA) using the Primer of Biostatistics (Version 5) software program. The significance of means ± SD was detected between groups by a post hoc test (Tukey) at $p < 0.05$.

3. Results

3.1. Characterization of Berberine-Rich Fraction. Table 1 shows the berberine concentration in different prepared samples, and BF had the highest concentration (0.89 mg/mg extract). The melting point of berberine chloride was 190°C and that of the berberine base was 165°C. Both the chloroform fraction and BF had the same berberine spot equal distance as shown in TLC results in Figure 2. Table 2 presents the ^{1}H-NMR (DMSO/TMS) showing δ: 3.17 (2H, t, H 5), 4.03 (3H, s, H 10-OCH_3), 4.05 (3H, s, H 9-OCH_3), 4.89 (2H, t, $J = 5.35$ Hz, H 6), 6.14 (2H, s, 3-OCH_2O), 7.06 (1H, s, H 4), 7.77 (1H, s, H 1), 7.96 (1H, d, H 12), 8.17 (1H, d, $J = 8.4$ Hz, H 11), 8.90 (1H, s, H 13), and 9.85 (1H, s, H 8) as our team previously published [36].

3.2. Effect of Berberine-Rich Fraction on Blood Parameters. Serum GSH, TBARS, testosterone, cholesterol, glucose, and albumin levels were measured to assess the effect of BF alone or in combination with gossypol on rats' fertility. The administration of BF to healthy rats showed no significant change in the levels of GSH, testosterone, or albumin compared to the normal control group. While it significantly decreased the levels of TBARS, cholesterol, and glucose compared with those of the control group as shown in Table 3, gossypol acetate-injected rats (induced group) had a significantly increased TBARS level and decreased GSH, testosterone, cholesterol, glucose, and albumin levels compared to the control group. BF coadministration with gossypol acetate (protected group) significantly decreased the TBARS level and increased GSH, testosterone, cholesterol, glucose, and albumin levels compared to the induced group, at $p < 0.05$. The treatment with BF (treated group) normalized the TBARS level and significantly enhanced the GSH, testosterone, cholesterol, glucose, and albumin levels, approaching the control levels (Table 3).

3.3. Effect of Berberine-Rich Fraction on Semen Quality. The BF-supplemented group showed normal sperm motility and had significantly improved sperm count and morphology compared with the control group. In addition, BF administration significantly increased the α-glucosidase activity compared to that of the control group. The male infertility-induced group showed a highly significant decrease in the sperm count, inhibited sperm motility, and a marked change in the sperm morphology to irregular shapes compared to the control group. Gossypol acetate injection also significantly inhibited the α-glucosidase activity and significantly decreased the semen fructose level compared with the control group. The BF-protected and BF-treated groups had significantly improved sperm count, motility, and morphology as well as significantly increased α-glucosidase activity and semen fructose level compared to the induced group ($p < 0.05$), with their values approaching the values of the control group, as shown in Figure 3.

Table 1: The berberine concentration in different prepared samples.

Extract	Berberine concentration (mg/mg extract)
Ethanolic extract	0.6
Chloroform fraction	0.73
Berberine-rich fraction	0.89

3.4. Effect of Berberine-Rich Fraction on the Testicular Inflammatory Markers. Figures 4 and 5 demonstrate that the administration of BF to healthy rats resulted in a non-significant change in the levels of testicular TBARS, NO, TIMP-3, and interleukins (IL-1β and IL-18) compared to the normal control group, at $p < 0.05$. It also significantly decreased TNF-α, ADAM-17, and IL-6 while it increased IL-12 compared to that of the control group (at $p < 0.05$). Gossypol-induced male infertility markedly and significantly increased the levels of testicular TBARS, NO, TNF-α, ADAM-17, and interleukins (IL-1β, IL-6, and IL-18) while significantly decreasing the levels of both TIMP-3 and IL-12 compared with those of the control group. A significant decrease in the levels of testicular TBARS, NO, ADAM-17, TNF-α, and interleukins (IL-18, IL-6, and IL-1β) as well as a significant increase in the levels of TIMP-3 and IL-12 was observed in the BF-protected and BF-treated groups compared to the gossypol-induced group. In addition, the administration of BF after gossypol injection (treated group) normalized the levels of testicular TIMP-3, TBARS, and interleukins (IL-1β and IL-6), approaching the values of the control group.

3.5. Histological Changes in Testicular and Epididymal Tissues of Different Experimental Groups. Figures 6(a)–6(d) show that the control healthy and BF-supplemented rats had normal and well-organized seminiferous tubules, and they show all stages of spermatogenesis till the stage of sperm formation. They also have normal epididymal ducts. On the other hand, the testicular tissue of the gossypol-treated group (Figure 6(e)) shows an accumulation of immature germ cells in the lumen and defects in spermatogenesis and sperm formation. Furthermore, it shows an increase in intracellular gaps due to disruption in cell-cell contacts in the seminiferous epithelium compared to the control one. Moreover, the epididymal section (Figure 6(f)) revealed leukocytic infiltration, congestion, and edema. The BF-protected group shows almost near-normal spermatogenesis with sperm formation in the testicular sections (Figure 6(g)) and mild interstitial inflammation and edema in the epididymal sections (Figure 6(h)). The testicular section of the BF-treated

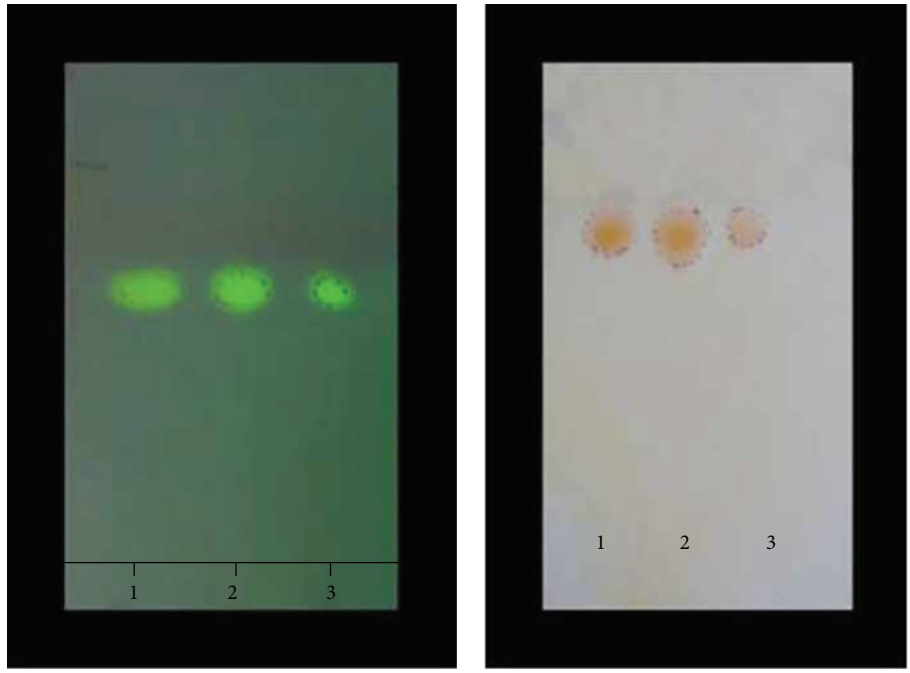

(a) (b)

Figure 2: TLC identification of standard berberine chloride (spot 1), chloroform fraction (spot 2), and isolated berberine base (Spot 3).

Table 2: ^{1}H-NMR (DMSO/TMS) chemical shifts of isolated berberine in ppm [36].

Proton	δ (ppm)
H 5	3.17 (2H, t)
H 10-OCH_3	4.03 (3H, s)
H 9-OCH_3	4.05 (3H, s)
H 6	4.89 (2H, t, J = 5.35 Hz)
H 2,3-OCH_2O	6.14 (2H, s)
H 4	7.06 (1H, s)
H 1	7.77 (1H, s)
H 12	7.96 (1H, d, J = 8.4 Hz)
H 11	8.17 (1H, d, J = 8.4 Hz)
H 13	8.90 (1H, s)
H 8	9.85 (1H, s)

group (Figure 6(i)) revealed a marked improvement in spermatogenesis in all stages till sperm formation compared with those observed in the control one, but little interstitial inflammation was observed in the epididymal section (Figure 6(j).

4. Discussion

Male infertility is considered to be one of the most critical health problems that are expected to increase [49]. Multiple lifestyle and environmental factors contributed to the etiology of male infertility including cigarette smoking, alcohol, heavy metals, pesticides, radiation, and illicit drugs; these factors are growing in number and are widely spread [50, 51]. In this study, BF (89%) was shown to be a leading therapy for this problem by controlling the inflammatory markers that are produced in the case of male infertility and that result in a destructive damage to sperm and reduction in the semen quality.

Gossypol is a toxic phenolic compound extracted from cottonseeds [28, 38]. Deleterious effects of gossypol on fertility have been widely reported in the literature [29, 52]. The intraperitoneal injection of gossypol acetate significantly reduced the semen quality as evidenced by the decrease in the sperm count and motility and changed the sperm morphology as well as inhibited the α-glucosidase activity compared with those of the control group. Alpha-glucosidase activity is widely used as an indicative marker for sperm count as alpha-glucosidase is produced by the epididymis, so a low level of α-glucosidase indicates epididymal obstruction [53]. Gossypol administration significantly reduced the enzyme activity in all segments of the epididymis [54]. The major antifertility effect of gossypol is to inhibit sperm production and motility; this inhibitory action has been attributed to a dramatic drop in the production of mitochondrial ATP [29]. Furthermore, gossypol induces oxidative stress by promoting the formation of ROS and lipid peroxides, which negatively affected plasma membrane permeability, ATPase activity, and glucose transport in sperms [55, 56]. In the present study, gossypol injection significantly elevated serum and testicular TBARS and NO levels as well as depleted the antioxidant capacity (GSH) and serum glucose level, resulting in the damage of sperm membrane. These results are in concert with the reports from El-Sharaky et al. [38] and Santana et al. [29] that demonstrated the reproductive damage caused by gossypol-induced oxidative stress in rats and that from Chen et al. [52] that reported a lowered serum glucose level after gossypol treatment.

Table 3: Effect of berberine-rich fraction on blood parameters of different experimental groups.

Groups	TBARS (nmol/ml)	GSH (mg/ml)	Testosterone (ng/ml)	Cholesterol (mg/dl)	Glucose (mg/dl)	Albumin (g/dl)
Control	0.49 ± 0.01	0.38 ± 0.01	3.7 ± 0.21	110 ± 5.2	95 ± 2.4	3.5 ± 0.2
BF supplemented	0.44 ± 0.02*	0.37 ± 0.02	3.8 ± 0.15	90 ± 1.6*	80 ± 3.1*	3.4 ± 0.1
Induced	0.58 ± 0.03*	0.29 ± 0.01*	0.36 ± 0.23*	65 ± 2.3*	65 ± 2.1*	2.9 ± 0.04*
Protected	0.52 ± 0.03#	0.32 ± 0.06#	3.2 ± 0.34#	75 ± 1.9*#	75 ± 2.8*#	3.3 ± 0.05 #
Treated	0.49 ± 0.05#	0.30 ± 0.08#	3.4 ± 0.16#	85 ± 3.9*#	82 ± 2.6*#	3.1 ± 0.2#

Values represent the mean ± SD of 6 rats. *$p \leq 0.05$ versus control. #$p \leq 0.05$ versus induced group. ANOVA (one-way) followed by Tukey's test.

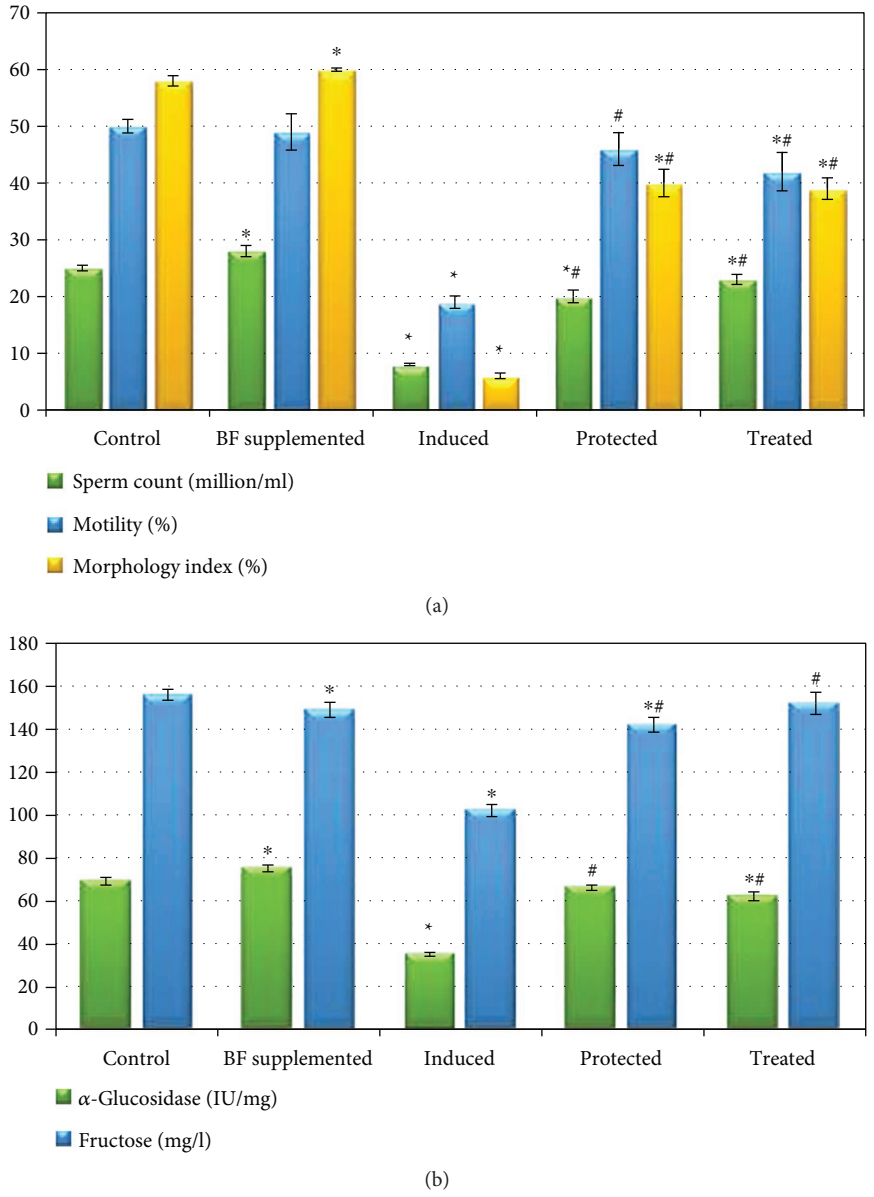

Figure 3: Effects of berberine-rich fraction on sperm parameters. Graph (a) shows sperm count, motility, and morphology index. Graph (b) shows α-glucosidase activity and fructose level. Values represent the mean ± SD of 6 rats. *$p \leq 0.05$ versus control group. #$p \leq 0.05$ versus induced group. One-way ANOVA followed by Tukey's test was used.

Free radical overproduction enhances proinflammatory gene expression and is associated with inflammatory reactions. On the other hand, inflammatory cells increased the generation of ROS, leading to exaggerated oxidative stress that impairs sperm function [8, 11]. The proinflammatory cytokines TNF-α, IL-1α and IL-1β may have certain

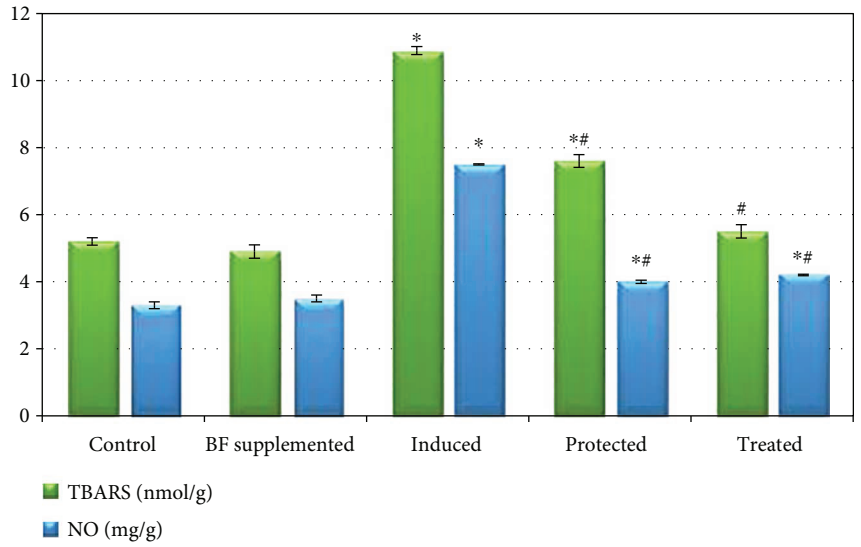

Figure 4: Effect of berberine-rich fraction on sperm prooxidants. Values represent the mean ± SD of 6 rats. $^{*}p \leq 0.05$ versus control group. $^{\#}p \leq 0.05$ versus induced group. One-way ANOVA followed by Tukey's test was used.

physiological functions in the male genital tract. However, the elevated levels of these cytokines compared with the normal one, as seen during the inflammation process, are very harmful to sperm production [8]. Increasing the generation of ROS induces ADAM-17 expression and results in TNF-α proteolytic cleavage, which in turn increases ROS production, induces oxidative stress, promotes lipid peroxidation, causes destructive damage sperm cell membrane, decreases sperm motility, and induces apoptosis [57]. TIMP-3 is an inhibitor for ADAM-17 and negatively controls its activity [15]. Thus, the balance between ADAM-17 and TIMP-3 expression can control the inflammation process. In addition, IL-18 was found to stimulate the *cytotoxic* activity of T cells and natural killer cells and stimulates the production of IL-6 and TNF-α [58]. On the other hand, Naz and Evans [12] suggested a significant correlation between IL-12 levels and fertility as these improve the count and normal morphology of sperm in the semen. Therefore, male infertility may be attributed to its derangement. The destruction of testicular tissues, in the case of infertility, lowered the production of IL-12 and negatively affected the sperm count and motility [12]. In agreement with the earlier findings, gossypol acetate injection significantly increased the levels of testicular ADAM-17, TNF-α, and interleukins (IL-1β, IL-6, and IL-18), while it decreased TIMP-3 and IL-12 levels compared with those of the control group. TNF-α affects the androgenic receptor controlling testosterone activity; it decreases the production of testosterone and reduces the sperm function [2].

Testosterone, as a steroid hormone, is essential for spermatogenesis [5]. Gossypol was found to induce the regression of Leydig cells, resulting in a significant decrease in the level of serum testosterone and reduced libido [56]. Furthermore, testosterone regulates the formation of seminal fructose, as it controls the activity and function of the accessory glands that are responsible for fructose secretion. Fructose is an important source of energy for sperms and is required for sperm motility [59]. Thus, the decreased level of semen fructose is due to gossypol-induced depletion in the testosterone level. In addition, gossypol decreased the serum level of cholesterol, which is consistent with the studies by Nwoha and Aire [60] and Obeidy et al. [61], who reported that gossypol altered the serum lipoprotein metabolism.

Antioxidants can contribute to the protection of cells and tissues against the deleterious effects of free radicals [9]. The toxicological effect of gossypol was reversed by the treatment of animals with berberine-rich fraction. Berberine (BBR) is one of the most potent ingredients in *Berberis vulgaris*, characterized by a diversity of pharmacological effects [17, 22] including antioxidant and anti-inflammatory properties in a variety of tissues including kidney, liver, pancreas, and adipose tissue. BBR administration reduced the oxidative stress markers (TBARS) and evaluated the antioxidant enzymes (GSH, GPx, and SOD) in diabetic animals [24]. In the present study, the oral administration of BF successfully reversed most of the hazardous effects of gossypol on semen characteristics. BF significantly enhanced the sperm count, motility, and morphology as well as improved α-glucosidase activity and increased the semen fructose level. BF has antioxidant properties, as confirmed by the reduction of TBARS and NO levels as well as the elevation of the reduced level of glutathione, and can be considered one of the most potent antioxidant agents, protecting the cell against ROS destructive damage [62]. These results confirmed the potent antioxidant capacity of BF as mentioned previously [27, 63, 64].

The oral administration of BF either with or after gossypol acetate injection represented an ameliorative effect against the analysed inflammatory markers. Previously, BBR showed a potent anti-inflammatory effect by suppressing the production of inflammatory mediators such as TNF-α, COX-2, IL-1β, IL-6, NO, and inducible nitric oxide synthase (iNOS) as well as by the inhibition of arachidonic

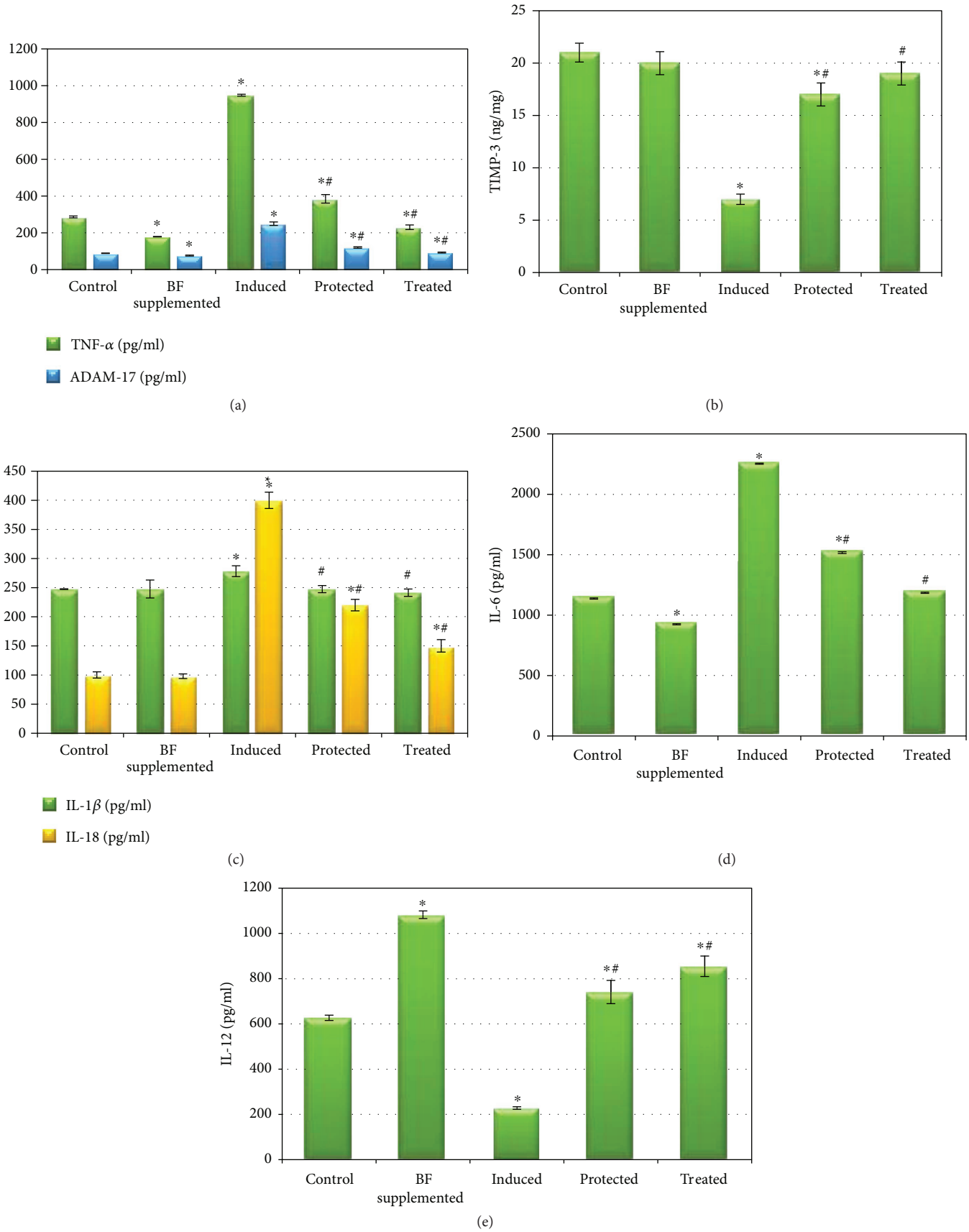

Figure 5: Effect of berberine-rich fraction on sperm inflammatory markers. Values represent the mean ± SD of 6 rats. $^{*}p \leq 0.05$ versus control group. $^{\#}p \leq 0.05$ versus induced group. One-way ANOVA followed by Tukey's test was used.

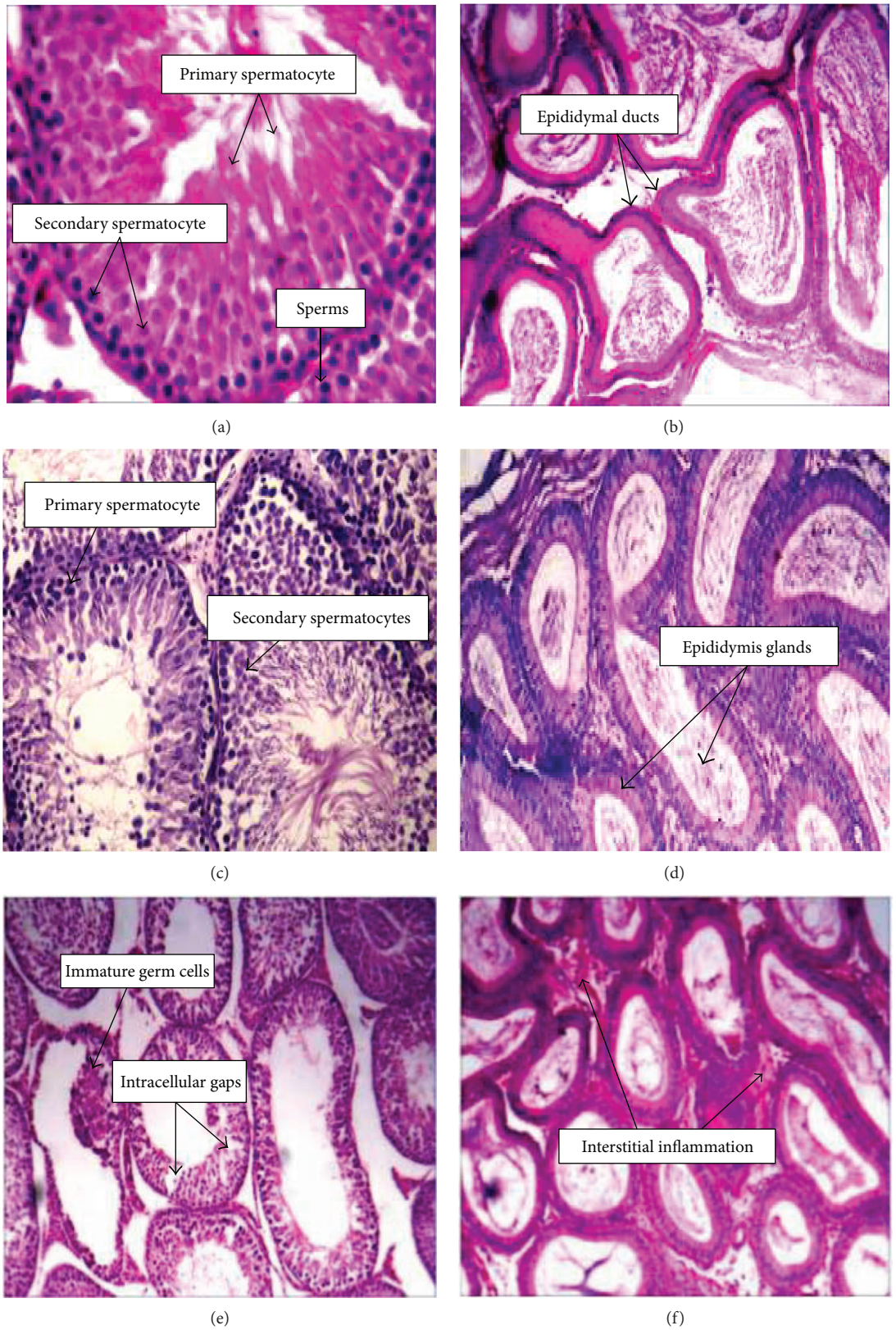

Figure 6: Continued.

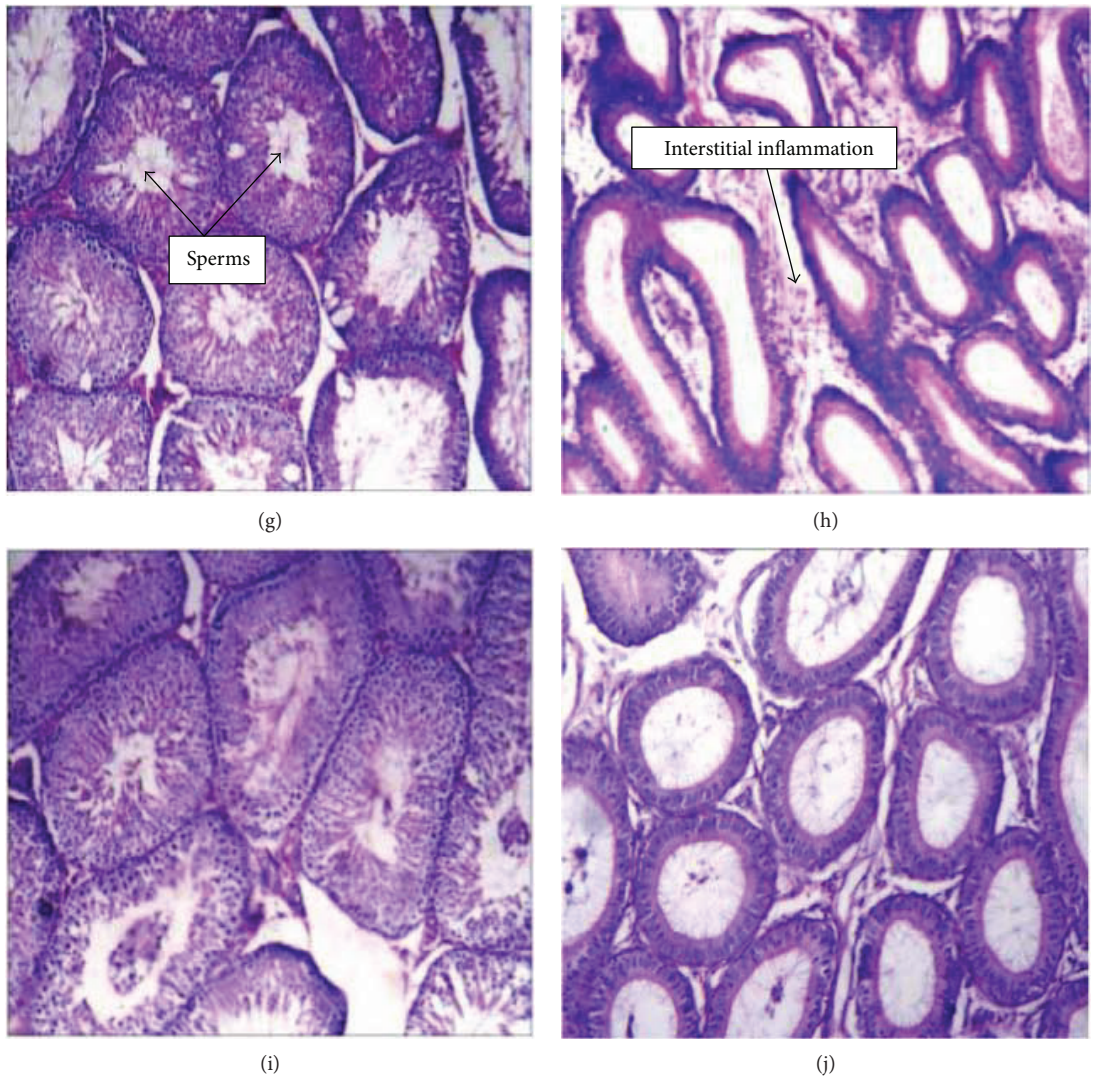

Figure 6: The histological examination of both testicular and epididymal tissues of different treated groups compared to the control one. (Magnification of a and c: ×40; magnification of b, d, e, f, g, h, i, and j: ×10). Testicular (a) and epididymal tissues (b) of control group. Testicular (c) and epididymal tissues (d) of berberine-rich fraction (100 mg/kg orally) supplemented group. Testicular (e) and epididymal tissues (f) of gossypol-induced group (5 mg/kg, 8 times). Testicular (g) and epididymal tissues (h) of berberine-rich fraction (100 mg/kg orally) protected group. Testicular (i) and epididymal tissues (j) of berberine-rich fraction (100 mg/kg orally) treated group.

acid metabolism [23, 24, 65, 66]. In addition, BBR was found to inhibit the activator protein-1 (AP-1, a key transcription factor in inflammation) [67] and inhibit DNA synthesis in active lymphocytes, resulting in the inhibition of lymphocyte transformation [68].

The obtained biochemical results were confirmed by the histological study where gossypol intraperitoneal injection resulted in a marked histological alterations in the testicular and epididymal tissues including depressed spermatogenesis, degenerative germ cells, and vacuoles (in testicular section) as well as leukocytic infiltration and edema (in epididymal section), which are in agreement with the El-Sharaky et al. [38]. A normal histological structure of a rat's testis and epididymis was observed in both control and BF-supplemented animals. Almost near-normal spermatogenesis with sperm formation in the testicular sections and little mild interstitial inflammation in the epididymal sections were observed in BF-protected and BF-treated groups.

In conclusion, the mechanism of gossypol-induced toxicity on rats' testes contributed to the induction of oxidative stress and inflammatory responses, leading to cell membrane damage and reduced sperm count, motility, and morphology. The administration of BF to animals was shown to be effective in preventing oxidative damage and inflammation induced by gossypol. Thus, the use of BF can be suggested as a palliative measure in animals subjected to poisoning by gossypol. However, further studies must be done to confirm the anti-inflammatory effect of BF by using different experimental models. Moreover, the concentration of active metabolite (berberine) must be measured in the testicular tissue and the pharmacokinetics of BF should be investigated in rats.

Conflicts of Interest

The authors declare that the research was conducted without any conflict of interest for each author, and the authors alone are responsible for the content and writing of the paper.

Acknowledgments

This research was supported by the Alexandria University Research Fund under the Research Enhancement Program (ALEX REP 2011-2012).

References

[1] S. Bisht, M. Faiq, M. Tolahunase, and R. Dada, "Oxidative stress and male infertility," *Nature Reviews Urology*, vol. 14, no. 8, pp. 470–485, 2017.

[2] A. Havrylyuk, V. Chopyak, Y. Boyko, I. Kril, and M. Kurpisz, "Cytokines in the blood and semen of infertile patients," *Central European Journal of Immunology*, vol. 40, no. 3, pp. 337–344, 2015.

[3] A. Agarwal, A. Mulgund, A. Hamada, and M. R. Chyatte, "A unique view on male infertility around the globe," *Reproductive Biology and Endocrinology*, vol. 13, no. 1, p. 37, 2015.

[4] H. J. Wiser, J. Sandlow, and T. S. Köhler, "Causes of male infertility," in *Male Infertility: Contemporary Clinical Approaches, Andrology, ART & Antioxidants*, S. J. Parekattil and A. Agarwal, Eds., pp. 3–14, Springer New York, New York, NY, USA, 2012.

[5] A. A. Oremosu and E. N. Akang, "Impact of alcohol on male reproductive hormones, oxidative stress and semen parameters in Sprague–Dawley rats," *Middle East Fertility Society Journal*, vol. 20, no. 2, pp. 114–118, 2015.

[6] M. Adewoyin, M. Ibrahim, R. Roszaman et al., "Male infertility: the effect of natural antioxidants and phytocompounds on seminal oxidative stress," *Diseases*, vol. 5, no. 4, p. 9, 2017.

[7] A. Agarwal and A. D. Bui, "Oxidation-reduction potential as a new marker for oxidative stress: correlation to male infertility," *Investigative and Clinical Urology*, vol. 58, no. 6, pp. 385–399, 2017.

[8] A. Azenabor, A. O. Ekun, and O. Akinloye, "Impact of inflammation on male reproductive tract," *Journal of Reproduction & Infertility*, vol. 16, no. 3, pp. 123–129, 2015.

[9] A. Agarwal, G. Virk, C. Ong, and S. S. du Plessis, "Effect of oxidative stress on male reproduction," *The World Journal of Men's Health*, vol. 32, no. 1, pp. 1–17, 2014.

[10] O. Sarkar, J. Bahrainwala, S. Chandrasekaran, S. Kothari, P. P. Mathur, and A. Agarwal, "Impact of inflammation on male fertility," *Frontiers in Bioscience*, vol. E3, pp. 89–95, 2011.

[11] S. K. Biswas, "Does the interdependence between oxidative stress and inflammation explain the antioxidant paradox?," *Oxidative Medicine and Cellular Longevity*, vol. 2016, Article ID 5698931, 9 pages, 2016.

[12] R. K. Naz and L. Evans, "Presence and modulation of interleukin-12 in seminal plasma of fertile and infertile men," *Journal of Andrology*, vol. 19, no. 3, pp. 302–307, 1998.

[13] M. R. Gazvani, M. Bates, G. Vince, S. Christmas, D. I. Lewis-Jones, and C. Kingsland, "Follicular fluid concentrations of interleukin-12 and interleukin-8 in IVF cycles," *Fertility and Sterility*, vol. 74, no. 5, pp. 953–958, 2000.

[14] F. Fairbanks, M. S. Abrão, S. Podgaec, J. A. Dias Jr, R. M. de Oliveira, and L. V. Rizzo, "Interleukin-12 but not interleukin-18 is associated with severe endometriosis," *Fertility and Sterility*, vol. 91, no. 2, pp. 320–324, 2009.

[15] A. Cesaro, A. Abakar-Mahamat, P. Brest et al., "Differential expression and regulation of ADAM17 and TIMP3 in acute inflamed intestinal epithelia," *American Journal of Physiology-Gastrointestinal and Liver Physiology*, vol. 296, no. 6, pp. G1332–G1343, 2009.

[16] M. Ekor, "The growing use of herbal medicines: issues relating to adverse reactions and challenges in monitoring safety," *Frontiers in Pharmacology*, vol. 4, p. 177, 2014.

[17] M. Imenshahidi and H. Hosseinzadeh, "*Berberis vulgaris* and berberine: an update review," *Phytotherapy Research*, vol. 30, no. 11, pp. 1745–1764, 2016.

[18] M. Rahimi-Madiseh, Z. Lorigoini, H. Zamani-Gharaghoshi, and M. Rafieian-Kopaei, "*Berberis vulgaris*: specifications and traditional uses," *Iran J Basic Med Sci*, vol. 20, no. 5, pp. 569–587, 2017.

[19] S. K. Battu, M. A. Repka, S. Maddineni, A. G. Chittiboyina, M. A. Avery, and S. Majumdar, "Physicochemical characterization of berberine chloride: a perspective in the development of a solution dosage form for oral delivery," *AAPS PharmSciTech*, vol. 11, no. 3, pp. 1466–1475, 2010.

[20] S. Lee, H. J. Lim, J. H. Park, K. S. Lee, Y. Jang, and H. Y. Park, "Berberine-induced LDLR up-regulation involves JNK pathway," *Biochemical and Biophysical Research Communications*, vol. 362, no. 4, pp. 853–857, 2007.

[21] Y. S. Chai, J. Hu, F. Lei et al., "Effect of berberine on cell cycle arrest and cell survival during cerebral ischemia and reperfusion and correlations with p53/cyclin D1 and PI3K/Akt," *European Journal of Pharmacology*, vol. 708, no. 1–3, pp. 44–55, 2013.

[22] B. Pang, L. H. Zhao, Q. Zhou et al., "Application of berberine on treating type 2 diabetes mellitus," *International Journal of Endocrinology*, vol. 2015, Article ID 905749, 12 pages, 2015.

[23] C. L. Kuo, C. W. Chi, and T. Y. Liu, "The anti-inflammatory potential of berberine in vitro and in vivo," *Cancer Letters*, vol. 203, no. 2, pp. 127–137, 2004.

[24] Z. Li, Y. N. Geng, J. D. Jiang, and W. J. Kong, "Antioxidant and anti-inflammatory activities of berberine in the treatment of diabetes mellitus," *Evidence-based Complementary and Alternative Medicine*, vol. 2014, Article ID 289264, 12 pages, 2014.

[25] W. H. Peng, K. L. Lo, Y. H. Lee, T. H. Hung, and Y. C. Lin, "Berberine produces antidepressant-like effects in the forced swim test and in the tail suspension test in mice," *Life Sciences*, vol. 81, no. 11, pp. 933–938, 2007.

[26] S. K. Kulkarni and A. Dhir, "On the mechanism of antidepressant-like action of berberine chloride," *European Journal of Pharmacology*, vol. 589, no. 1–3, pp. 163–172, 2008.

[27] A. E. Abd El-Wahab, D. A. Ghareeb, E. E. Sarhan, M. M. Abu-Serie, and M. A. El Demellawy, "*In vitro* biological assessment of *Berberis vulgaris* and its active constituent, berberine: antioxidants, anti-acetylcholinesterase, anti-diabetic and anticancer effects," *BMC Complementary and Alternative Medicine*, vol. 13, no. 1, p. 218, 2013.

[28] I. C. N. Gadelha, N. B. S. Fonseca, S. C. S. Oloris, M. M. Melo, and B. Soto-Blanco, "Gossypol toxicity from cottonseed products," *The Scientific World Journal*, vol. 2014, Article ID 231635, 11 pages, 2014.

[29] A. T. Santana, M. Guelfi, H. C. D. Medeiros, M. A. Tavares, P. F. V. Bizerra, and F. E. Mingatto, "Mechanisms involved in reproductive damage caused by gossypol in rats and protective effects of vitamin E," *Biological Research*, vol. 48, no. 1, p. 43, 2015.

[30] M. A. Hadley, Y. C. Lin, and M. Dym, "Effects of gossypol on the reproductive system of male rats," *Journal of Andrology*, vol. 2, no. 4, pp. 190–199, 1981.

[31] S. P. Xue, "Gossypol contraception and mechanism of action," in *Male Fertility and Its Regulation*, T. J. Lobl and E. S. E. Hafez, Eds., Springer Netherlands, Dordrecht, Netherlands, 1985.

[32] P. M. Zavos and P. N. Zarmakoupis-Zavos, "The inhibitory effects of gossypol on human sperm motility characteristics: possible modes of reversibility of those effects," *The Tohoku Journal of Experimental Medicine*, vol. 179, no. 3, pp. 167–175, 1996.

[33] I. N. Nair and D. A. Bhiwgade, "Effect of gossypol on pituitary reproductive axis: ultrastructural and biochemical studies," *Indian Journal of Experimental Biology*, vol. 28, no. 8, pp. 724–732, 1990.

[34] Y. X. Liu, "Control of spermatogenesis in primate and prospect of male contraception," *Archives of Andrology*, vol. 51, no. 2, pp. 77–92, 2005.

[35] D. Pradhan, B. Prativa, and K. A. Suri, "Isolation of berberine from *Berberis vulgaris* Linn. and standardization of aqueous extract by RP-HPLC," *International Journal of Herbal Medicine*, vol. 1, no. 2, pp. 106–111, 2013.

[36] M. Abd El-Salam, H. Mekky, E. M. B. El-Naggar, D. Ghareeb, M. El-Demellawy, and F. El Fiky, "Biological activities of *Berberis vulgaris* constituents: cytotoxicity, antihepatitis C virus and anti-acetylcholine esterase," *Journal of Pharmaceutical Biology*, vol. 6, no. 2, pp. 89–97, 2016.

[37] M. Abd El-Salam, H. Mekkya, E. M. B. El-Naggar, D. Ghareeb, M. El-Demellawy, and F. El-Fiky, "Hepatoprotective properties and biotransformation of berberine and berberrubine by cell suspension cultures of *Dodonaea viscosa* and *Ocimum basilicum*," *South African Journal of Botany*, vol. 97, pp. 191–195, 2015.

[38] A. S. El-Sharaky, A. A. Newairy, N. M. Elguindy, and A. A. Elwafa, "Spermatotoxicity, biochemical changes and histological alteration induced by gossypol in testicular and hepatic tissues of male rats," *Food and Chemical Toxicology*, vol. 48, no. 12, pp. 3354–3361, 2010.

[39] C. Yeung, F. Pérez-Sánchez, C. Soler, D. Poser, S. Kliesch, and T. G. Cooper, "Maturation of human spermatozoa (from selected epididymides of prostatic carcinoma patients) with respect to their morphology and ability to undergo the acrosome reaction," *Human Reproduction Update*, vol. 3, no. 3, pp. 205–213, 1997.

[40] D. J. Jollow, J. R. Mitchell, N. Zampaglione, and J. R. Gillette, "Bromobenzene-induced liver necrosis. Protective role of glutathione and evidence for 3,4-bromobenzene oxide as the hepatotoxic metabolite," *Pharmacology*, vol. 11, no. 3, pp. 151–169, 1974.

[41] A. L. Tappel and H. Zalkin, "Inhibition of lipide peroxidation in mitochondria by vitamin E," *Archives of Biochemistry and Biophysics*, vol. 80, no. 2, pp. 333–336, 1959.

[42] K. Menaka, A. Ramesh, B. Thomas, and N. S. Kumari, "Estimation of nitric oxide as an inflammatory marker in periodontitis," *Journal of Indian Society of Periodontology*, vol. 13, no. 2, pp. 75–78, 2009.

[43] A. Chen, J. J. Bookstein, and D. R. Meldrum, "Diagnosis of a testosterone-secreting adrenal adenoma by selective venous catheterization," *Fertility and Sterility*, vol. 55, no. 6, pp. 1202-1203, 1991.

[44] M. Hjelm and C. H. Verdier, "Determination of serum glucose by glucose oxidase method," *Scandinavian Journal of Clinical and Laboratory Investigation*, vol. 15, pp. 415–428, 1963.

[45] D. Watson, "A simple method for the determination of serum cholesterol," *Clinica Chimica Acta*, vol. 5, no. 5, pp. 637–643, 1960.

[46] B. T. Doumas, W. Ard Watson, and H. G. Biggs, "Albumin standards and the measurement of serum albumin with bromcresol green," *Clinica Chimica Acta*, vol. 258, no. 1, pp. 21–30, 1997.

[47] Y. W. Han and V. R. Srinivasan, "Purification and characterization of β-glucosidase of *Alcaligenes faecalis*," *Journal of Bacteriology*, vol. 100, no. 3, pp. 1355–1363, 1969.

[48] D. Foreman, L. Gaylor, E. Evans, and C. Trella, "A modification of the Roe procedure for determination of fructose in tissues with increased specificity," *Analytical Biochemistry*, vol. 56, no. 2, pp. 584–590, 1973.

[49] N. Pandiyan and S. D. Khan, "A clinical approach to male infertility," in *Male Infertility: A Clinical Approach*, K. Gunasekaran and N. Pandiyan, Eds., Springer India, New Delhi, India, 2017.

[50] F. Sohrabvand, M. Jafari, M. Shariat, F. Haghollahi, and M. Lotfi, "Frequency and epidemiologic aspects of male infertility," *Acta Medica Iranica*, vol. 53, no. 4, pp. 231–235, 2015.

[51] R. Sharma, K. R. Biedenharn, J. M. Fedor, and A. Agarwal, "Lifestyle factors and reproductive health: taking control of your fertility," *Reproductive Biology and Endocrinology*, vol. 11, no. 1, p. 66, 2013.

[52] G. Chen, R. Wang, H. Chen, L. Wu, R. S. Ge, and Y. Wang, "Gossypol ameliorates liver fibrosis in diabetic rats induced by high-fat diet and streptozocin," *Life Sciences*, vol. 149, pp. 58–64, 2016.

[53] W. Krause and C. Bohring, "Why do we determine α-glucosidase activity in human semen during infertility work-up?," *Andrologia*, vol. 31, no. 5, pp. 289–294, 1999.

[54] N. R. Kalla, S. Kaur, N. Ujwal, U. Mehta, H. Joos, and J. Frick, "Alpha-glucosidase activity in the rat epididymis under different physiological conditions," *International Journal of Andrology*, vol. 20, no. 2, pp. 92–95, 1997.

[55] J. Wang, L. Jin, X. Li et al., "Gossypol induces apoptosis in ovarian cancer cells through oxidative stress," *Molecular BioSystems*, vol. 9, no. 6, pp. 1489–1497, 2013.

[56] M. Y. El-Mokadem, T. A. Taha, M. A. Samak, and A. M. Yassen, "Alleviation of reproductive toxicity of gossypol using selenium supplementation in rams," *Journal of Animal Science*, vol. 90, no. 9, pp. 3274–3285, 2012.

[57] D. A. Ghareeb and E. M. E. Sarhan, "Role of oxidative stress in male fertility and idiopathic infertility: causes and treatment," *Journal of Diagnostic Techniques and Biomedical Analysis*, vol. 2, p. 1, 2014.

[58] M. Feldmann and J. Saklatvala, "Proinflammatory cytokines," in *Cytokine Reference*, J. J. Oppen-heim and M. Feldman, Eds., pp. 291–305, Academic Press, New York, NY, USA, 2001.

[59] H. I. Al-Daghistani, A.-W. R. Hamad, M. Abdel-Dayem, M. Al-Swaifi, and M. Abu Zaid, "Evaluation of serum testosterone, progesterone, seminal antisperm antibody, and fructose

levels among Jordanian males with a history of infertility," *Biochemistry Research International*, vol. 2010, Article ID 409640, 8 pages, 2010.

[60] P. U. Nwoha and T. A. Aire, "Reduced level of serum cholesterol in low protein-fed Wistar rats administered gossypol and chloroquine," *Contraception*, vol. 52, no. 4, pp. 261–265, 1995.

[61] A. Obeidy, I. Fities, and D. Sheriff, "The effect of gossypol on serum lipoproteins of adult rats," *Hormone and Metabolic Research*, vol. 21, no. 12, pp. 649–651, 1989.

[62] Z. Radak, Z. Zhao, E. Koltai, H. Ohno, and M. Atalay, "Oxygen consumption and usage during physical exercise: the balance between oxidative stress and ROS-dependent adaptive signaling," *Antioxidants & Redox Signaling*, vol. 18, no. 10, pp. 1208–1246, 2013.

[63] J. Laamech, J. el-Hilaly, H. Fetoui et al., "*Berberis vulgaris* L. effects on oxidative stress and liver injury in lead-intoxicated mice," *Journal of Complementary and Integrative Medicine*, vol. 14, no. 1, 2017.

[64] V. Pongkittiphan, W. Chavasiri, and R. Supabphol, "Antioxidant effect of berberine and its phenolic derivatives against human fibrosarcoma cells," *Asian Pacific Journal of Cancer Prevention*, vol. 16, no. 13, pp. 5371–5376, 2015.

[65] L. R. Pan, Q. Tang, Q. Fu, B. R. Hu, J. Z. Xiang, and J. Q. Qian, "Roles of nitric oxide in protective effect of berberine in ethanol-induced gastric ulcer mice," *Acta Pharmacologica Sinica*, vol. 26, no. 11, pp. 1334–1338, 2005.

[66] F. Zhu, F. Wu, Y. Ma et al., "Decrease in the production of beta-amyloid by berberine inhibition of the expression of beta-secretase in HEK293 cells," *BMC Neuroscience*, vol. 12, no. 1, pp. 125–125, 2011.

[67] K. Fukuda, Y. Hibiya, M. Mutoh, M. Koshiji, S. Akao, and H. Fujiwara, "Inhibition of activator protein 1 activity by berberine in human hepatoma cells," *Planta Medica*, vol. 65, no. 4, pp. 381–383, 1999.

[68] K. Ckless, J. L. Schlottfeldt, M. Pasqual, P. Moyna, J. A. P. Henriques, and M. Wajner, "Inhibition of in-vitro lymphocyte transformation by the isoquinoline alkaloid berberine," *The Journal of Pharmacy and Pharmacology*, vol. 47, no. 12A, pp. 1029–1031, 1995.

Hindawi
Oxidative Medicine and Cellular Longevity
Volume 2018, Article ID 4950705, 11 pages
https://doi.org/10.1155/2018/4950705

Research Article

Di-2-pyridylhydrazone Dithiocarbamate Butyric Acid Ester Exerted Its Proliferative Inhibition against Gastric Cell via ROS-Mediated Apoptosis and Autophagy

Xingshuang Guo,[1] Yun Fu,[2] Zhuo Wang,[1] Tingting Wang,[2] Cuiping Li,[2] Tengfei Huang,[2] Fulian Gao,[1] and Changzheng Li[2,3]

[1]*Department of Histology and Embryology, Xinxiang Medical University, Xinxiang, Henan 453003, China*
[2]*Laboratory of Molecular Medicine, Xinxiang Medical University, Xinxiang, Henan 453003, China*
[3]*Department of Molecular Biology and Biochemistry, Xinxiang Medical University, Xinxiang, Henan 453003, China*

Correspondence should be addressed to Fulian Gao; gfl@xxmu.edu.cn and Changzheng Li; changzhenl@yahoo.com

Received 15 November 2017; Revised 22 January 2018; Accepted 7 February 2018; Published 25 March 2018

Academic Editor: Mohamed M. Abdel-Daim

Diversified biological activities of dithiocarbamates have attracted widespread attention; improving their feature or exploring their potent action of mechanism is a hot topic in medicinal research. Herein, we presented a study on synthesis and investigation of a novel dithiocarbamate, DpdtbA (di-2-pyridylhydrazone dithiocarbamate butyric acid ester), on antitumor activity. The growth inhibition assay revealed that DpdtbA had important antitumor activity for gastric cancer (GC) cell lines ($IC_{50} = 4.2 \pm 0.52\,\mu M$ for SGC-7901, $3.80 \pm 0.40\,\mu M$ for MGC-803). The next study indicated that growth inhibition is involved in ROS generation in mechanism; accordingly, the changes in mitochondrial membrane permeability, apoptotic genes, cytochrome *c*, bax, and bcl-2 were observed, implying that the growth inhibition of DpdtbA is involved in ROS-mediated apoptosis. On the other hand, the upregulated p53 upon DpdtbA treatment implied that p53 could also mediate the apoptosis. Yet the excess generation of ROS induced by DpdtbA led to cathepsin D translocation and increase of autophagic vacuoles and LC3-II, demonstrating that autophagy was also a contributor to growth inhibition. Further investigation showed that DpdtbA could induce cell cycle arrest at the G1 phase. This clearly indicated the growth inhibition of DpdtbA was via triggering ROS formation and evoking p53 response, consequently leading to alteration in gene expressions that are related to cell survival.

1. Introduction

Gastric cancer (GC) ranks as one of the fifth most common malignancies in the world, and more than half of cases are reported annually in East Asia [1, 2]. Resection may benefit certain patients, but mostly transiently due to metastasis. Chemotherapy is still the main treatment for advanced GC [3]. It has been demonstrated that 5-year overall survival increased by 6% with chemotherapy compared to that of surgical treatment alone [4]. However, the side effects and resistance of chemotherapeutic agents limit their wide use, thus requiring alternative drugs.

Enzymes are important biological macromolecules involved in many biological processes. Almost half of all enzymes associate with a particular metal ion to function [5], such as cytochrome oxidase, zinc-copper superoxide dismutase, and lysyl oxidase, and several transcription factors require copper for activity [6]. It is well documented that cancer cells have an increased demand for iron and copper to maintain robust cell proliferation and metastasis; thus, disturbing the metal requirement of cancer cells by chelators has been an alternative option for cancer therapy [7].

Dithiocarbamates have received attention because of its multiple biological activities and strong affinity toward metal ions, which aroused an interest to probe their potent applications on disease treatment [8]. However, the strong affinity toward transition metals, especially to copper and zinc ions, may also bring undesirable consequences, such as direct

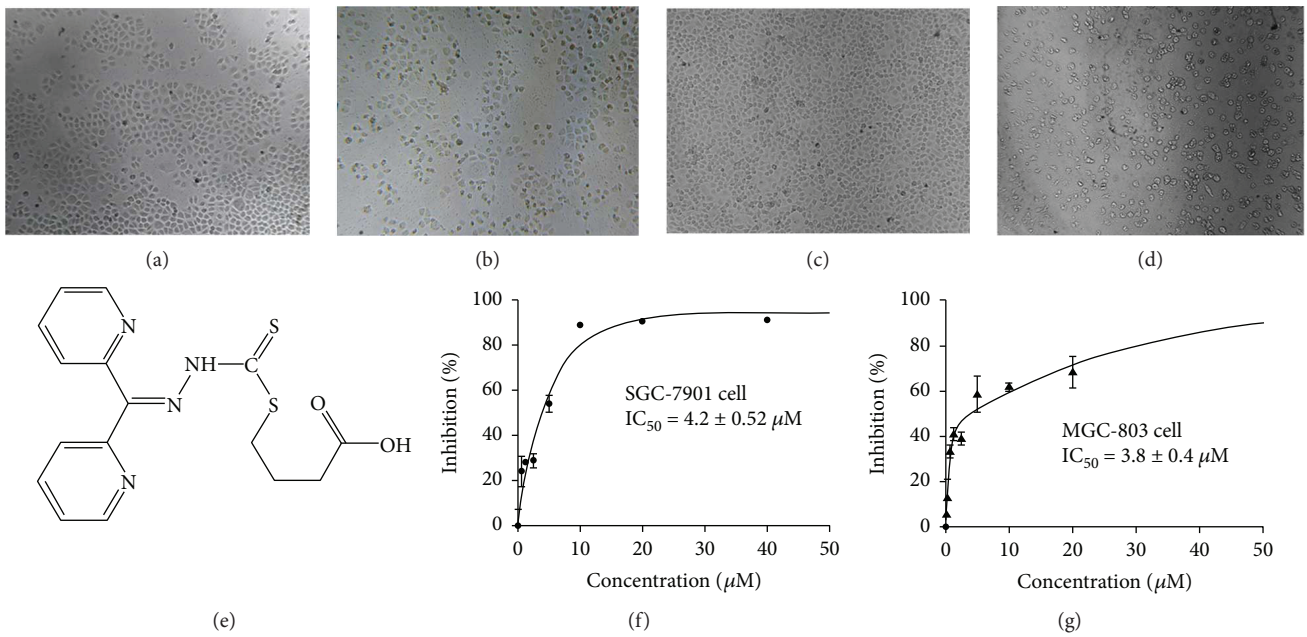

Figure 1: The chemical structure and growth inhibition of DpdtbA. The effect of DpdtbA on morphology. SGC-7901 cells: (a) control and (b) 5 μM DpdtbA after 16 h treatment. MGC-803 cells: (c) control and (d) 5 μM DpdtbA treatment after 16 h treatment. (e) Structure of DpdtbA. (f) Proliferation inhibition of DpdtbA against SGC-7901 cell line ($IC_{50} = 4.2 \pm 0.52\,\mu$M). (g) Proliferation inhibition of DpdtbA against MGC-803 cell line ($IC_{50} = 3.8 \pm 0.4\,\mu$M).

inactivation of enzymes that are required for cell growth [9–11]. To achieve the optimal therapeutic index, a reasonable balance is needed between cytotoxicity and affinity to metal ions for dithiocarbamates; thus, structural modification of dithiocarbamate is an active field. Dithiocarbazate is a widely used intermediate that can react with aldehyde and ketone derivatives, as well as alkylating agents; the resulting dithiocarbamate derivatives are more stable. We previously reported that *S*-propionic or acetic acid ester of di-pyridylhydrazone dithiocarbamate had excellent antitumor activity but has lesser activity for their copper complexes; this situation was rare in literatures [12, 13]. Analysis of structure-activity relationship revealed that *S*-propionic acid of the dithiocarbamate was better than *S*-acetic acid; however, a reversed phenomenon was found for their complexes in growth inhibition, which aroused an interest to further probe the effect of length of carbon chain on biological activity. To extend our knowledge of the new dithiocarbamate derivatives, in this study, di-pyridylhydrazone dithiocarbamate *S*-butyric acid (DpdtbA) was further prepared and characterized by MS and NMR. Next, its antiproliferative effect was evaluated on gastric cancer cell lines, as like other dithiocarbamates we have reported previously, the new prepared DpdtbA also showed excellent antitumor activity; thus, its underlying mechanism was preliminarily investigated. In vitro ROS assay revealed that DpdtbA could induce ROS generation, which triggered p53 response; consequently, the apoptotic genes and externalization of phosphatidylserine were altered, supporting the finding that induced apoptosis was p53 mediated. The excess ROS generated by DpdtbA also caused autophagy, protease leakage from lysosome, and cell cycle arrest, implying that ROS played important roles in the proliferation inhibition.

2. Results

2.1. Proliferation Inhibition of DpdtbA. DpdtbA was prepared as described previously [12], with the difference being that 4-bromine butyric acid was used in the last step-reaction. The resulting dithiocarbamate, di-2-pyridylhydrazone dithiocarbamate butyric acid ester (DpdtbA), was characterized by NMR and MS spectra (see Materials and Methods); the structure of DpdtbA is shown in Figure 1(e). HPLC and NMR indicated that it has adequate purity (>95%) for biological assay (Figure S1). Next, we assessed the growth inhibition of DpdtbA against gastric cancer cell lines, SGC-7901 and MGC-803; the dose-response curves are depicted in Figure 1. As shown in Figures 1(f) and 1(g), DpdtbA had significant growth inhibition with $IC_{50} = 4.20 \pm 0.52\,\mu$M for SGC-7901 and $3.80 \pm 0.40\,\mu$M for MGC-803. The cell dependence was not obvious, but the maximal inhibition was slightly different. For SGC-7901 cells, the maximal inhibition (~80%) was achieved at ~10 μM, but 40 μM DpdtbA is required for same inhibition of MGC-803 (Figures 1(f) and 1(g)). The morphology changes when exposure of the agent to the investigated cells was also recorded; rounded cells were observed for both cell lines (compare Figures 1(b) and 1(d) with Figures 1(a) and 1(c)).

2.2. DpdtbA Induced a ROS-Dependent Growth Inhibition. Generation of reactive oxygen species (ROS) in mechanism is involved in many chemotherapeutic agents; thus, the

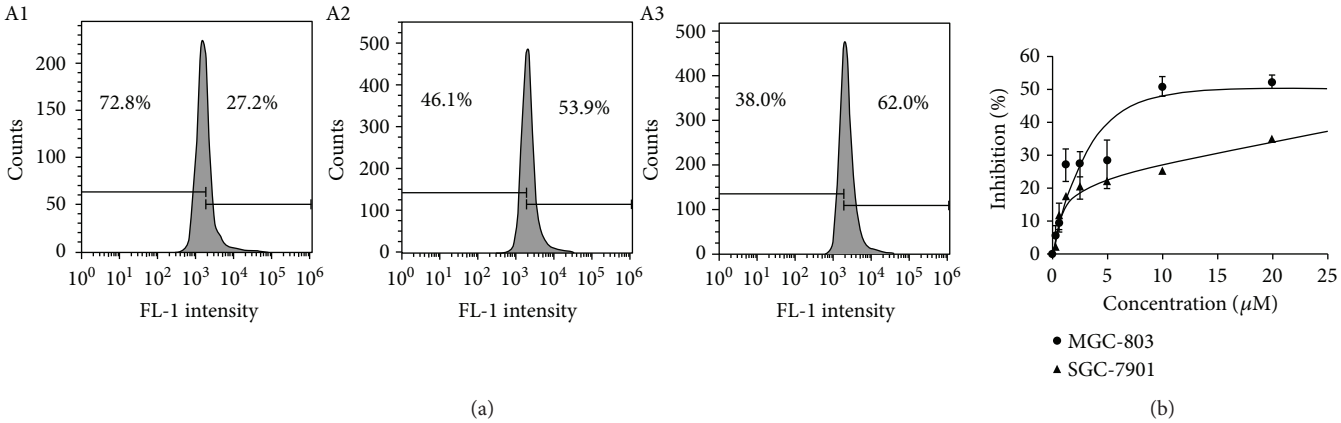

Figure 2: DpdtbA induced ROS generation and growth inhibition in the presence of NAC. (a) MGC-803 cells used for ROS assay (24 h incubation): (A1) DMSO, (A2) 2.5 μM DpdtbA, and (A3) 5 μM DpdtbA. (b) Growth inhibition of DpdtbA in the presence of 1.5 mM NAC.

ability of ROS production was assessed. DCFH-DA is frequently used to determine ROS; the populations in different fluorescence intensities were measured by flow cytometry. As shown in Figure 2, ROS increased with increasing DpdtbA (Figure 2(A2 and A3)). To determine whether ROS correlated with growth inhibition, a ROS scavenger, NAC (*N*-acetyl-L-cysteine), was introduced into the growth inhibition assay. As shown in Figure 2(b), the inhibitory effect of DpdtbA against both cell lines in the presence of NAC was significantly attenuated. For SGC-7901 cell, DpdtbA caused ~85% growth inhibition at low concentration (10 μM) but ~30% growth inhibition at higher concentration (20 μM) in the presence of 1.5 mM NAC (Figures 1(f) and 2(b)); similar for MGC-803 cell, IC_{50} was increased by ~3-fold in the presence of NAC (Figures 1(g) and 2(b)). This clearly indicated that the growth inhibition displayed by DpdtbA was ROS dependent.

2.3. DpdtbA and Its Copper Complex Induced Cellular Apoptosis. The excess intracellular ROS correlating with apoptosis has been well documented; the elevated ROS level implies that the action of the agent may be involved in apoptosis induction. To measure the apoptosis populations at early and late stages, the annexin V/propidium iodide (PI) staining was performed, which measures externalization of phosphatidylserine on the cell surface of apoptotic cells specifically. As shown in Figure 3, DpdtbA induced early apoptosis and later apoptosis of GC cells in a concentration-dependent manner; that is, the population of apoptosis was increased from 4.8 to 46.5% for SGC-7901 cells and from 5.6 to 35.0% for MGC-803 cells (Figures 3(a) and 3(b)).

To further support involvement of apoptosis, Western blotting was employed to determine changes in apoptotic genes. The excess ROS generally lead to apoptosis through changes in the expression of bcl-2 family proteins; thus, the alterations of bcl-2 and bax proteins before and after treatment with DpdtbA at different concentrations were measured. As shown in Figure 4, the upregulated bax and downregulation Bcl-2 were observed when DpdtbA treated SGC-7901 and MGC-803 cells in contrast to that of control (Figures 4(a) and 4(b)). Accordingly, the relative ratios of bax/bcl-2 were also generated for comparative purposes; clearly, the related ratios were elevated with increased concentration of DpdtbA (Figures 4(c) and 4(d)). In addition, the other apoptotic genes, caspase-8 and cytochrome *c*, were also observed to be upregulated; this was in agreement with the result of externalization of phosphatidylserine from flow cytometry (Figure 3), implying that the apoptosis was involved in the growth inhibition caused by DpdtbA.

To determine whether the alterations of apoptotic proteins correlated with ROS generation, the decreased ratio of bax/bcl-2 would be indicative when scavenging ROS. Thus, a ROS scavenger, NAC (*N*-acetyl-L-cysteine), was employed. In view of a similar tendency toward DpdtbA treatment in both gastric cell lines, the MGC-803 cell line was chosen and treated by either DpdtbA alone or combined with NAC; the related changes of the apoptotic genes are shown in Figure 5. It was clear that the NAC did decrease the ratio of bax/bcl-2 in contrast to the DpdtbA treatment only (Figure 5(b)). In addition, the other apoptosis-related proteins, cyt *c* and caspase-8, were also downregulated upon addition of NAC. Similarly, DpdtbA changed the mitochondrial membrane permeability (Figure S2); this indicated that the agent-induced apoptosis was ROS dependent. Since ROS is involved in growth inhibition, in response to ROS, p53 might be activated; upregulation of p53 when treated by the agent was observed but downregulation in combination with NAC (Figure 5(a)), implying that p53 played a role in the growth inhibition.

To further determine the role of p53 in the growth inhibition, a p53 inhibitor, pifithrin-α (PFT-α), was employed; accordingly, the MGC-803 cells were treated with either DpdtbA alone or in combination with PFT-α; p53 and other apoptotic proteins were evaluated by immunoblotting. As shown in Figure 6, the addition of PFT-α attenuated the increases of p53, cyt *c*, caspase-8 (Figure 6(a)), and ratio of bax/bcl-2 (Figure 6(b)), indicating that p53 did play a role in the process of induced apoptosis.

2.4. DpdtbA Induced Change in Lysosomal Membrane Permeability (LMP) and Autophagy Response. Lysosome is a

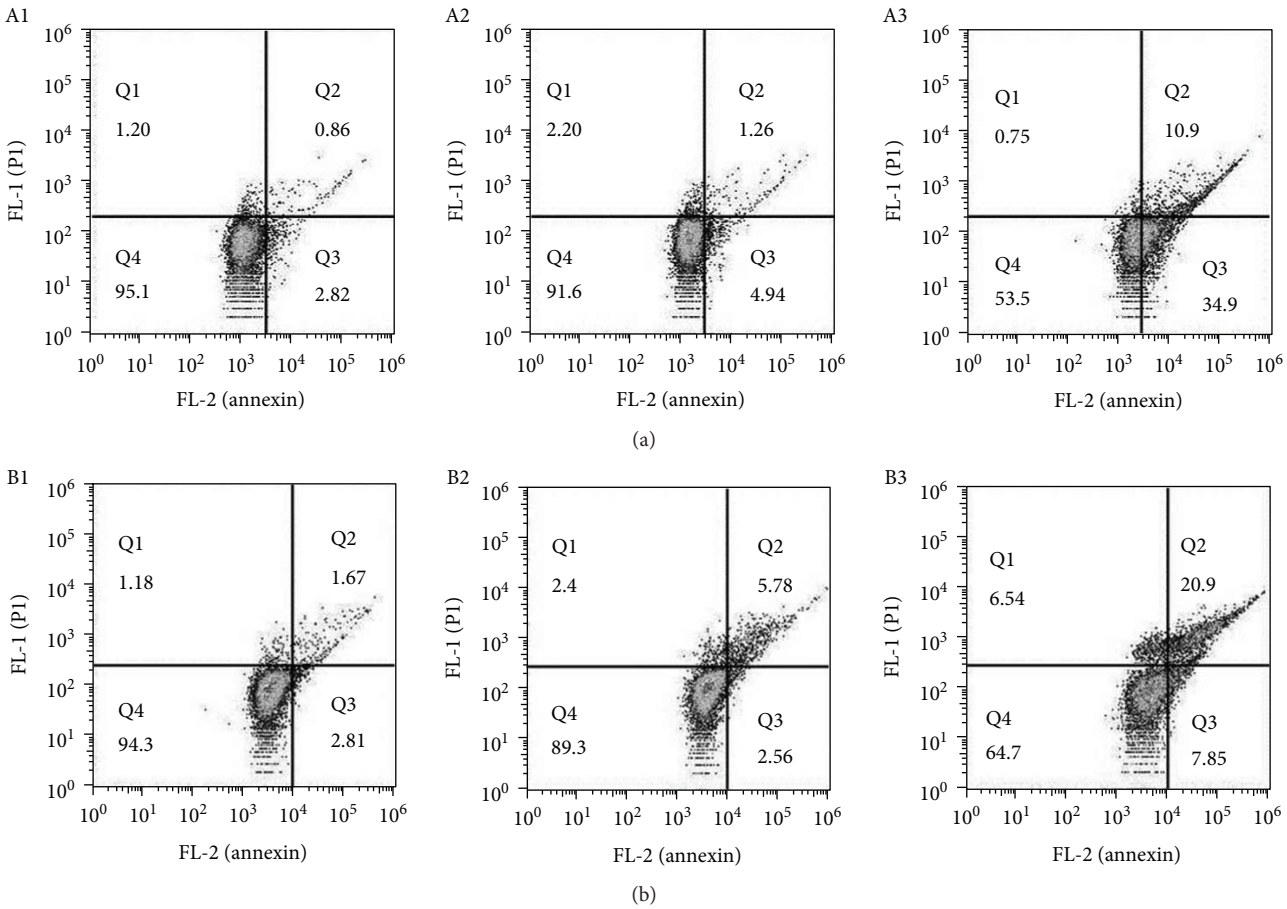

Figure 3: Flow cytometry analysis of apoptosis of GC cell lines. DpdtbA was incubated with the cells for 24 h. All attached cells were collected and double stained with annexin V and propidium iodide (PI) using a kit from Dojindo Laboratories following the manufacturer's instructions. (a) SGC-7901: (A1) DMSO, (A2) 2.5 μM DpdtbA, and (A3) 5.0 μM DpdtbA. (b) MGC-803: (B1) DMSO, (B2) 2.5 μM DpdtbA, and (B3) 5.0 μM DpdtbA.

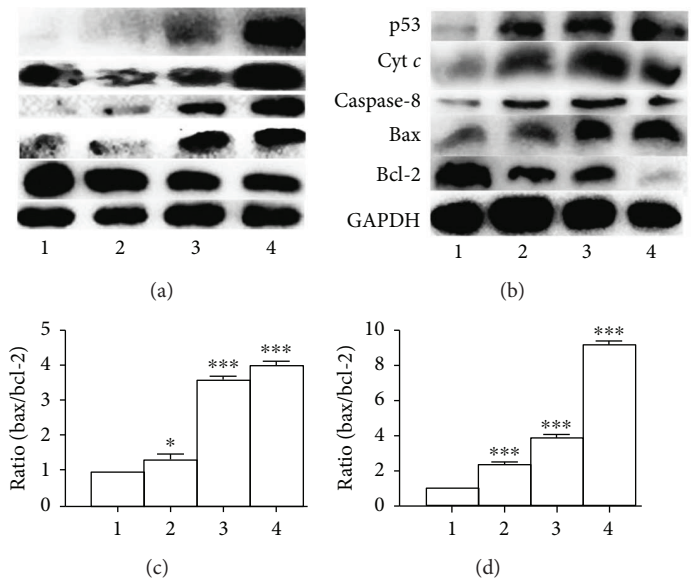

Figure 4: Western blotting analysis of changes of apoptosis-related genes. (a) MGC-803 and (b) SGC-7901: 1 = DMSO; 2 = 1.25 μM DpdtbA; 3 = 2.5 μM DpdtbA; 4 = 5 μM DpdtbA. (c) Normalized ratio of bax/bcl-2 (MGC-803). (d) Normalized ratio of bax/bcl-2 (SGC-7901) ($^{*}p < 0.05$; $^{***}p < 0.01$; one-way ANOVA).

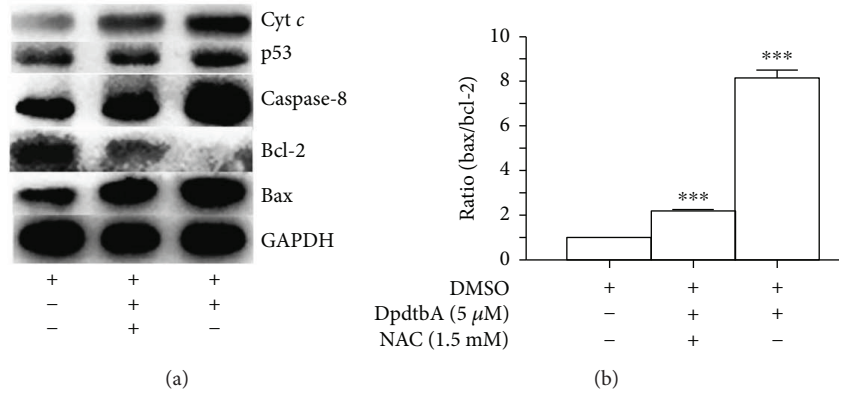

Figure 5: The effect of NAC on expressions of apoptotic genes of MGC-803 cells. (a) Western blotting analyses of apoptotic genes; (b) the changes in ratio of bax/bcl-2 in the presence or absence of NAC (***$p < 0.01$; one-way ANOVA).

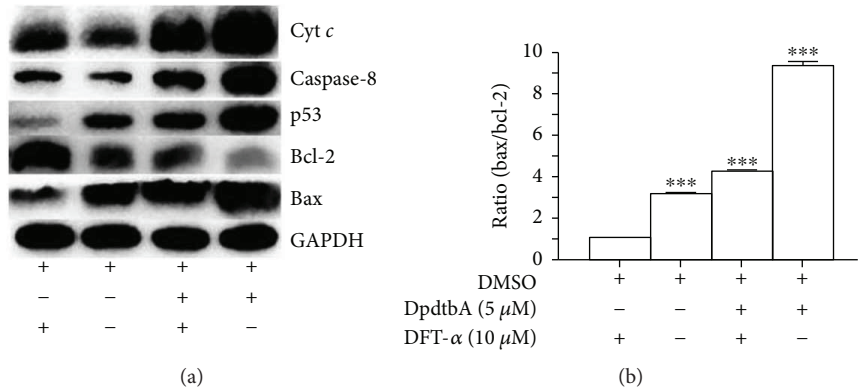

Figure 6: p53 played a role in DpdtbA-induced apoptosis. (a) Western blotting analyses of apoptotic genes when the MGC-803 cells treated with either DpdtbA alone or combined with p53 inhibitor; (b) the changes in ratio of bax/bcl-2 in different conditions (***$p < 0.01$; one-way ANOVA).

subcellular compartment that contained a host of hydrolytic enzymes and is responsible for digesting long-lived proteins and organelles, so the lysosomal membrane integrity is an important factor for maintaining its function. Some chemotherapeutic agents caused apoptosis and alteration of lysosomal membrane permeability; DpdtbA might have a similar action. To test the hypothesis, LysoTracker Red that can accumulate within lysosomes was employed to assess the lysosome membrane permeability [13]. As shown in Figure 7, the red fluorescence intensities of MGC-803 cells increased when DpdtbA was increased compared to those of nontreated cells, indicating that more LysoTracker Red accumulated in lysosomes and LMP was altered (Figures 7(b) and 7(c)). Since the alteration of the permeability, we questioned whether cathepsin release also occurred. To determine the possibility, cathepsin D was evaluated by immunofluorescence technique. As shown in Figure 7, the granular-stained cathepsin D was observed in the untreated cells (Figure 7(d)) and a diffusion pattern in the DpdtbA-treated cells (Figure 7(e)), indicating that cathepsin D was released from lysosome to cytosol, implying that apoptosis has occurred. A similar result from a Western blotting analysis further supported the increase of cathepsin D in cytosol, consistent with that reported previously [14].

Apoptosis associated with release and translocation of cathepsin has been realized [15], which may have stemmed from induced ROS generation. DpdtbA could produce excess ROS in response to the oxidative stress, and a response to autophagy might occur. Thus, the formation of autophagosome was measured by acridine orange staining. As shown in Figures 8(a)–8(c), the red granular fluorescence in the acidic vacuoles was observed in the agent-treated groups and in a concentration-dependent manner, indicating that more autophagic vacuoles were formed. To confirm the above result, 3-methyladenine (3-MA), an autophagy inhibitor, was introduced in the assay; clearly, the red granular fluorescence in the acidic vacuoles decreased in contrast to that of the agent only (Figures 8(b)–8(e)). To ensure the reliability of the results, the formation of autophagic vacuoles or autophagosomes was further analyzed by monodansylcadaverine (MDC) staining via flow cytometer and microcopy techniques (Figures S3 and S4) [16]. As shown in Figure S3, the fluorescence intensities of MDC were increased with treatment of DpdtbA and decreased with addition of 3-MA or NAC, and the trend in fluorescence intensity was similar to that of acridine orange staining (Figures 8(a)–8(e)). A similar situation was found during morphologic observation (Figure S4). This supported that

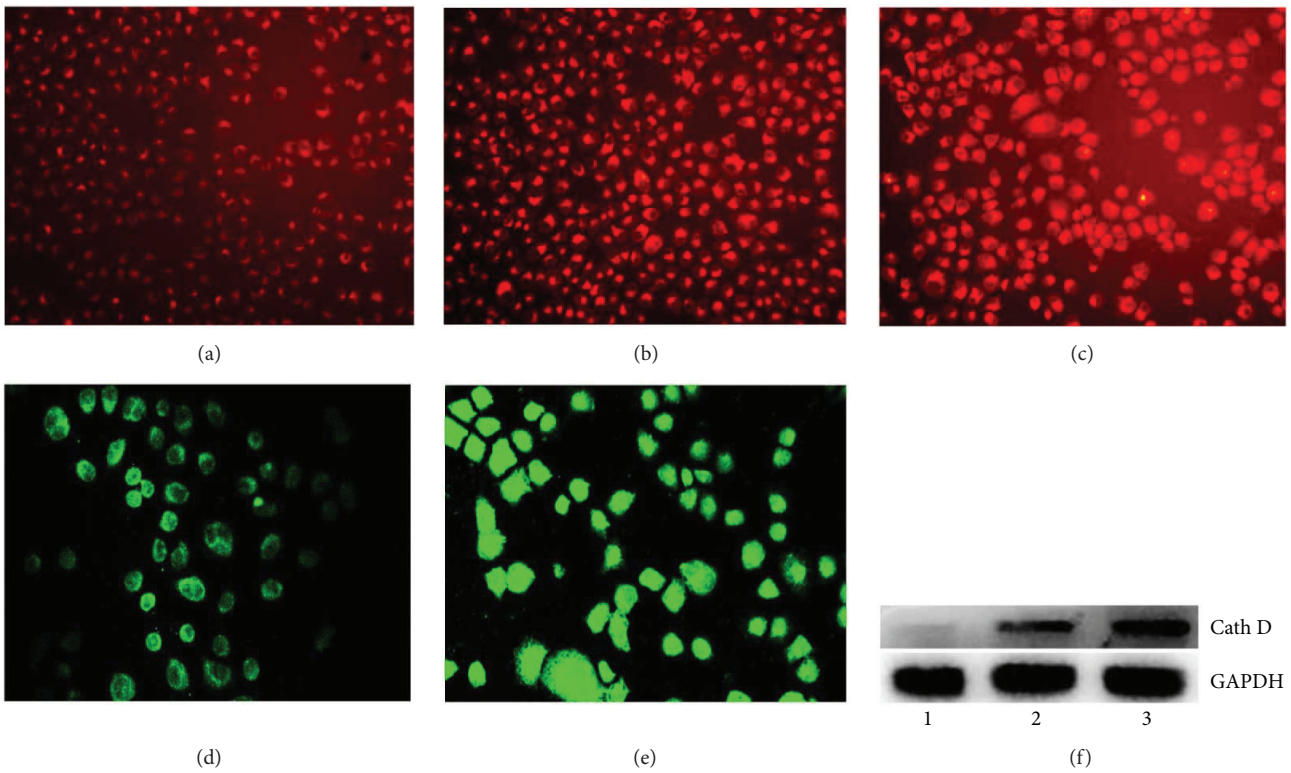

Figure 7: DpdtbA-induced change in lysosomal membrane permeability and cathepsin D translocation. LysoTracker Red-stained MGC-803 cells (objective size 10×10): (a) control, (b) 2.5 μM DpdtbA, and (c) 5.0 μM DpdtbA. The enhanced fluorescence intensities of the cells clearly indicated the alteration of LMP. Immunofluorescence detection of cathepsin D in MGC-803 cells (objective size 10×20): (d) control cells and (e) 2.5 μM DpdtbA. (f) Western blotting analysis of cathepsin D in cytosol.

autophagy occurred. Furthermore, the molecular evidence of autophagy occurrence was from measurement of LC3-II (microtubule-associated protein light chain 3), an autophagosome marker. As expected, the increase of LC3-II was observed when DpdtbA was exposed to the cells (Figure 8(f), line 2), but with addition of 3-MA or NAC, the LC3-II decreased or disappeared (Figure 8(f), line 1, line 3), indicating that DpdtbA indeed induced autophagy (Figure 8).

2.5. The Effect of DpdtbA on Cell Cycle. ROS induce cell cycle delay at the G1/S boundary [17]. We therefore evaluated the effect of DpdtbA on the cell cycle distribution using propidium iodide staining via flow cytometry. As shown in Figure 9, DpdtbA caused an accumulation of the GC cells in the G1 phase, and the percentage at the G1 phase significantly increased from 43.6 to ~70% during 24 h insult of the agent with both cell lines (Figures 9(a) and 9(b)), indicating that DpdtbA can disturb cell cycle and arrest the cells at the G1 phase as do other iron chelators [18].

3. Discussion

Transition metals, such as iron, that require to maintain viability and to support proliferation of almost all kinds of cells [19] play important roles in biosystem. Those metals locate either in proteins as cofactor or in cytosol as free form in metal labile pool. Clearly, chelators can disturb homeostasis of the metals, accordingly producing different biological effects. Cancer cells have higher iron demand than have normal cells, and depleting iron will be favorable to inhibit proliferation of cancer cells; thus, chelation therapy is a promising strategy. Dithiocarbamate derivatives have strong affinity toward transition metals; pyrrolidine dithiocarbamate (PDTC) is a representative compound, exhibiting diverse biological effects [20–22]. In view of instability and stronger affinity toward transition metals, especially zinc and copper ions, the thiol-modified dithiocarbamate derivatives were prepared to enhance their stability and improve their biological activity [23, 24]. In the present study, a new synthesized dithiocarbamate derivative (DpdtbA) showed better antitumor activity against gastric cell lines. In view of its good activity, the underlying mechanism was preliminarily investigated. Generally, antitumor drugs used clinically exert one of their actions via generating excess ROS, which causes oxidative damage of protein and nucleic acids, consequently resulting in cell death [25, 26]. DpdtbA may have a similar action. As expected, DpdtbA indeed has the ability to generate ROS at a cellular level (Figure 2). Next, we questioned whether the increased ROS correlated to the growth inhibition; thus a ROS scavenger, NAC, was employed in the proliferation assay. Clearly, addition of NAC could attenuate the cytotoxicity of DpdtbA (or increase viability of gastric cells), indicating that there was a ROS-dependent

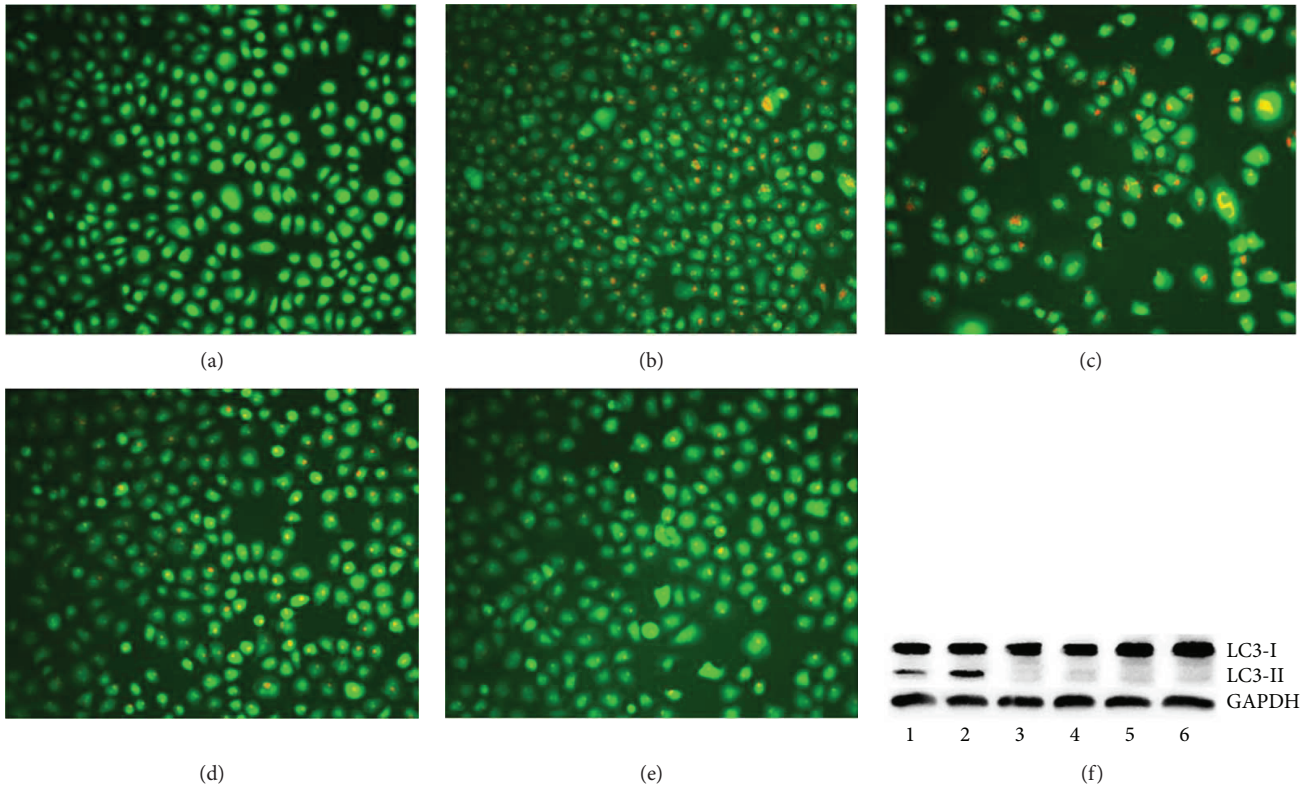

Figure 8: DpdtbA-induced autophagy in MGC-803 cells. Stained by acridine orange: (a) control, (b) 2.5 μM DpdtbA, (c) 5 μM DpdtbA, (d) 2.5 μM DpdtbA + 3-MA (2 mM), and (e) 5 μM DpdtbA + 3-MA (2 mM). (f) Western blotting: 1 = 5 μM DpdtbA plus 1.5 μM NAC; 2 = 5 μM DpdtbA; 3 = 5 μM DpdtbA plus 1.5 mM 3-MA; 4 = DMSO control; 5 = 1.5 mM NAC; 6 = 1.5 mM 3-MA.

growth inhibition, which was in agreement with that reported previously [27, 28]. The correlation between ROS and apoptosis has been well investigated; one of the molecular events upon apoptosis is externalization of phosphatidylserine, which can be revealed by the annexin V/propidium iodide (PI) staining though flow cytometric analysis [29]. The cytometric data showed that the DpdtbA induced early apoptosis and later apoptosis in a concentration-dependent manner (Figure 3). The evidence from Western blotting analysis also supported involvement of apoptosis due to the upregulation of bax, p53, and caspases and downregulation of bcl-2 after DpdtbA exposure to the cells (Figure 4). This situation is frequently observed in cells subjected to drug treatments [30]. The aforementioned changes in the apoptotic proteins may stem from ROS generation. To conform to the relevance, an antioxidant, NAC, was used to scavenge ROS; accordingly the extent of apoptosis was attenuated, indicating that ROS indeed play an important role in apoptosis induced by DpdtbA (Figure 5). p53 is a housekeeper gene that responds to external stimulus or oxidative stress; the upregulated p53 implied that it might be involved in the regulation of expression of bcl-2 family [31]. In this study, DpdtbA upregulated p53 protein expression, downregulated antiapoptotic protein bcl-2 expression, promoted proapoptotic protein bax expression, and triggered cell apoptosis via intrinsic and extrinsic pathways (Figure 6) [32]. Moreover, p53 can directly induce bax and bak oligomerization [33]; thus, the higher ratio of bax/bcl-2 would be favorable for bax oligomerization, consequently translocating the oligomerized bax to the mitochondrial membrane, which releases cytochrome *c* and causes mitochondrial cell death. Some forms of apoptosis have been found to be associated with a lysosomal pathway [34]. Similarly, the translocation of bax oligomer to lysosomal membrane causing the release of cathepsins from the lysosomal lumen to the cytosol has been also observed [35, 36]. Cathepsin D normally resides within lysosomes and endosomes but can be translocated to the cytoplasm under stress conditions, where it initiates apoptosis [37]. In the present study, this phenomenon of translocation of cathepsin D was also found (Figure 7), which was consistent with that reported previously [38]. The relocation of lysosomal cathepsins induces apoptotic signaling and leads to lysosomal cell death [39]; this clearly indicated that growth inhibition induced by DpdtbA is involved in apoptosis.

Autophagy plays an important role in cell survival by removing misfolded or aggregated proteins, clearing damaged organelles, and eliminating intracellular pathogens [40]. ROS-triggered apoptosis and autophagy have been well documented [41]. DpdtbA induced excess ROS production; accordingly, autophagy may be also involved. Figures 8(b) and 8(c) showed that the accumulated red granular

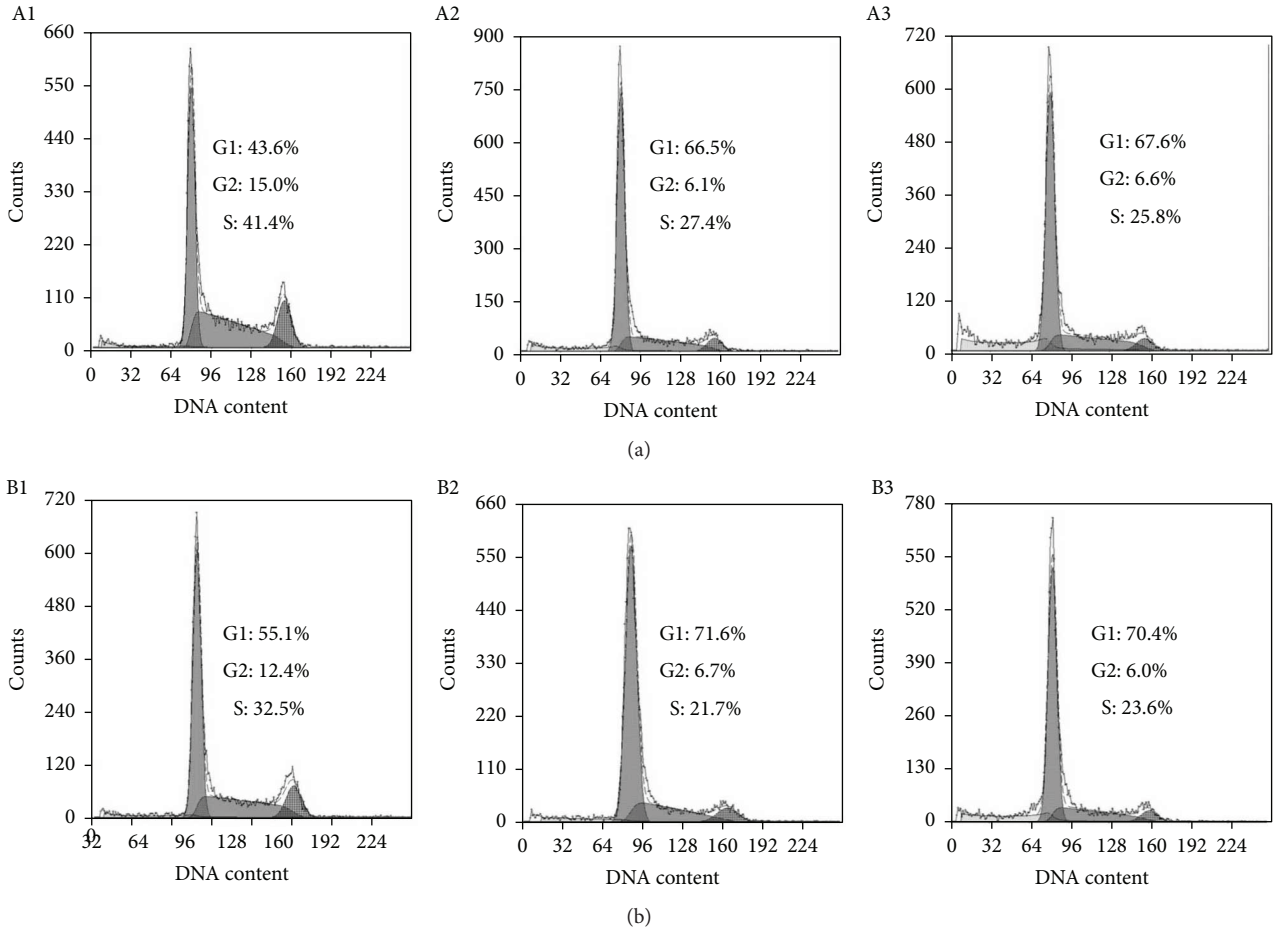

Figure 9: Cell cycle distribution of GC cells following treatment with various concentrations of DpdtbA. (a) SGC-7901: (A1) control, (A2) 2.50 μM DpdtbA, and (A3) 5.0 μM DpdtbA. (b) MGC-803: (B1) control, (B2) 2.5 μM DpdtbA, and (B3) 5.0 μM DpdtbA.

fluorescence in the acidic vacuoles in DpdtbA-treated cells was increased but decreased with the addition of an autophagy inhibitor (3-MA) (Figures 8(d) and 8(e)); a similar result was from flow cytometric analysis based on MDC staining (Figure S3). These data clearly showed that autophagosomes were increased; that is, autophagy was activated when DpdtbA was exposed to the cells. Interestingly, with the addition of a ROS scavenger, NAC, autophagy induced by DpdtbA was attenuated, indicating that occurrence of autophagy was triggered by ROS, which was consistent with findings of literatures [40, 41]. LC3 is an autophagosome molecular marker; the increase of LC3-II and decrease of LC3-I indicated that autophagy was activated. In the present study, DpdtbA induced the change in LC3, and the changes were attenuated by an addition of either autophagy inhibitor or ROS scavenger (Figure 8(f)). The aforementioned data demonstrated that autophagy made a contribution to the growth inhibition induced by DpdtbA. ROS generation leads to cell cycle delay. The cell cycle analysis revealed that DpdtbA could induce cell cycle arrest at the G1 phase as reported for other iron chelators (Figure 9) [18, 42]. Generally, iron chelators exhibit ribonucleotide reductase inhibition and then disturb cellular DNA synthesis [43]; therefore, cell cycle arrest caused by the agent was also partly a contributor to growth inhibition. It was noted that the DpdtbA-induced cell cycle arrest may be cell line dependent because its analogue, DpdtpA, led to cell cycle arrest in the S phase for hepatoma carcinoma cell line [12].

In conclusion, DpdtbA exhibited significant antiproliferative activity against gastric cells; it may stem from induction of ROS generation, subsequently provoking p53 response and triggering apoptosis, autophagy, lysosomal cell death, and cell cycle arrest. Therefore, ROS may be an initiator in the growth inhibition.

4. Materials and Methods

4.1. General Information. MTT, acridine orange, di-2-pyridylketone, pifithrin-α, and monodansylcadaverine (MDC) were purchased from Sigma-Aldrich. LC3 antibody was obtained from Proteintech Group (Wuhan, China), caspase-8, GAPDH, bax, cytochrome *c*, and bcl-2 were purchased from Boster (Wuhan, China). RPMI 1640 and fetal bovine serum were purchased from Zhejiang Tianhang Biological Technology Co. Ltd.

4.2. Preparation of Di-2-pyridylhydrazone Dithiocarbamate S-Butyric Acid (DpdtbA). DpdtbA (chemical name generated by ACD/Labs, 3-[({2-[di(pyridin-2-yl)methylidene]hydrazinyl}carbonothioyl)sulfanyl]butyric acid) was made as reported previously [12]. Briefly, the hydrazine dithiocarbamate was synthesized by reaction of equimolar carbon disulfide (1 mmol) with hydrazine (1 mmol) in KOH containing ethanol (10 ml) on an ice bath for 1 h. Then the reaction mixture without further separation was mixed with equimolar di-2-pyridylketone (1 mmol); the resulting mixture was refluxed for 1 h. After being cooled, the red-brown solid was filtered and washed with cold ethanol. TLC showed one pot (ethyl acetate/petroleum ether = 3 : 1). Next, the red-brown (di-2-pyridylhydrazone dithiocarbamate, 1 mmol) was dissolved in absolute ethanol (5 ml) and reacted with 4-bromo butyric acid at room temperature for 1 h; the yellow solid was filtered and washed with ethanol. TLC traced (ethyl acetate/petroleum ether = 3 : 1). mp: 158.7°C. ^{1}H NMR (Ascend™ 400 spectroscope, Bruker, Switzerland), ppm: 14.93 (s, NH), 8.86 (d, H, $J = 4$ Hz), 8.63 (d, H, $J = 4$ Hz), 8.03 (m, 2H, $J = 8$ Hz), 7.98 (d, H, $J = 8$ Hz), 7.64 (dd, H, $J = 4$ Hz), 7.60 (d, H, $J = 8$ Hz), 7.54 (dd, H, $J = 4$ Hz), 3.27 (tri, 2H, $J = 8$ Hz), 2.37 (tri, H, $J = 8$ Hz), 1.91 (tri, H, $J = 8$ Hz); ^{13}C NMR (Ascend 400 spectroscope, Bruker, Switzerland), ppm: 199.98, 174.28, 155.08, 150.98, 149.18, 148.68, 138.34, 137.96, 128.10, 125.80, 124.93, 124.14, 33.10, 24.26. ESI-MS ($C_{16}H_{16}N_4S_2O_2$ (cal/obs): M + Na: 383.0615 (383.0606).

4.3. Cytotoxicity Assay (MTT Assay). A 10 mM DpdtbA in 80% DMSO was diluted to the required concentration with culture. The MTT assay was conducted as previously described [9]. Briefly, 5×10^3/ml MGC-803 (or SGC-7901) cells in exponential phase was seeded equivalently into a 96-well plate, and the various amount of DpdtbA was added after the cells adhered. After 48 h incubation at 37°C in a humidified atmosphere of 5% CO_2, 10 μl MTT solution (5 mg/ml) was added to each well, followed by further 4 h incubation. The cell culture was removed, and 100 μl DMSO was added in each well to dissolve the formazan crystals. The measurement of absorptions of the solution that was related to the number of live cells was performed on a microplate reader (MK3, Thermo Scientific) at 570 nm. Percent growth inhibition was defined as percent absorbance inhibition within appropriate absorbance in each cell line. The same assay was performed in triplicate. Morphologic study was conducted under inverted microscope (Shanghai Batuo Instrument Co. Ltd., Shanghai, China); the photographs of SGC-7901 and MGC-803 cells treated by DpdtbA (2.5 or 5.0 μM for 16 or 48 h) were recorded (objective size: 10×20).

4.4. ROS Detection In Vivo. As described in MTT assay, the MGC-803 cells were treated by DpdtbA for 24 h. The cells were collected by centrifugation after trypsinization. Following PBS washing, the cell pellets were resuspended in serum-free culture medium containing H_2DCF-DA and incubated for 30 min. Finally, the medium containing H_2DCF-DA was removed by centrifugation and washed with PBS, and the cells were resuspended in PBS. The intracellular ROS assay was performed on a flow cytometer (Becton Dickinson, USA).

4.5. Flow Cytometric Analysis of Apoptosis. Cells were seeded into a 6-well plate and treated as described above for the cell viability assay. The cells were treated with different concentrations of the agent (2.5 and 5.0 μM DpdtbA) for 24 h. Then the cell culture was removed, following PBS washing and trypsin digestion; finally, the annexin V and propidium iodide (a kit from Dojindo Laboratories, Kumamoto, Japan) were added as recommended by the company. The stained cells were subjected to cytoflow analysis (Becton Dickinson, USA).

4.6. Western Blotting Analysis. The protocol used for Western blotting was as previously reported [10]; briefly, 1×10^7 MGC-803 (or SGC-7901) cells treated with or without DpdtbA was scraped off in lysis buffer (50 mM Tris-HCl, pH 8.0, 150 mM NaCl, 1.0% NP-40, 10% glycerol, and protease inhibitors) on ice for 30 min, following spin down by centrifugation at 14,000 ×g. The clear supernatant was stored at −80°C. The protein concentration was determined using a colorimetric Bio-Rad DC protein assay on a microplate reader MK3 at 570 nm. Proteins (30 μg) were separated on a 13% sodium dodecyl sulfate-polyacrylamide gel at 200 V for 1 h. Then, the separated proteins were subsequently transferred onto a PVDF membrane at 60 V for 1 h. The membrane was washed three times with Tris-buffered saline (TBS) and was then blocked for 2 h in TBS containing 0.1% Tween-20 and 5% nonfat skimmed milk. The membrane was incubated at 4°C overnight with the primary monoantibody used at a dilution of 1 : 300 in TBS plus 0.1% Tween-20 (TBST). The membrane was washed several times with TBST and was subsequently incubated with HRP-conjugated secondary antibody (1 : 2000 in TBST) for 1 h at room temperature. After another wash of the membrane with TBST, the protein bands were detected using a supersensitive ECL solution (Boster Biological Technology Co. Ltd.) and visualized on an Amersham Imager 600 (GE Healthcare Life Sciences, Fairfield, USA).

4.7. DpdtbA Induced Changes in Lysosomal Membrane Permeability and Autophagy. The SGC-7901 cells were seeded into a 24-well flask and treated as described above for the cell viability assay. The cells were treated with different concentrations of DpdtbA (2.5 and 5.0 μM DpdtbA) for 24 h. For detection of the acidic cellular compartment, acridine orange (or LysoTracker Red; Invitrogen) was used, which emits bright-red fluorescence in acidic vesicles but green fluorescence in the cytoplasm and nucleus. After treatment of the cells with the agent, acridine orange was then added at a final concentration of 1 μg/ml (the concentration of LysoTracker Red, as recommended) for a period of 15 min. Following PBS washing, the fluorescent micrographs were captured using an inverted fluorescence microscope (Shanghai Lengguang Technology Co. Ltd., Shanghai, China) or a laser confocal fluorescence microscope (Zeiss LSM 510 Confocal Inverted Microscope, Jena, Germany).

4.8. Cell Cycle Analysis. The SGC-7901 or MGC-803 cells (1×10^5) were seeded in a 6-well plate and incubated for 24 h at 37°C (5% CO_2). The medium was replaced with fresh medium supplemented or not (control) with the agent (2.5 and 5.0 μM). After 24 h of incubation, the cells were harvested with trypsin, followed by washing with PBS, fixed in 70% ethanol, and stored at −20°C. To stain the cellular nuclear DNA, the cells were suspended in 0.5 ml PBS containing 50 μg/ml propidium iodide (PI) and 100 μg/ml RNase after removing the 70% ethanol and washing with PBS. And then the cell suspension was incubated at 37°C for 30 min. DNA flow cytometry was performed in duplicate with a FACSCalibur flow cytometer (Becton Dickinson, USA). For each sample, 10,000 events were collected, and fluorescent signal intensity was recorded and analyzed by CellQuest and ModiFit (Becton Dickinson).

Conflicts of Interest

The authors declare no conflict of interest.

Authors' Contributions

Xingshuang Guo, Yun Fu, and Zhuo Wang performed the experiments; they contributed equally to this work. Changzheng Li and Fulian Gao conceived and designed the experiments. Tingting Wang and Tengfei Huang performed synthesis and purification of DpdtbA. Cuiping Li analyzed the data. Changzheng Li prepared and wrote the paper.

Acknowledgments

The present study was supported by grants awarded by the Natural Science Foundation of China (no. 21571153) and the Henan Science and Technology Agency (nos. 122102310197 and 152300410118).

Supplementary Materials

Figure S1: purity of DpdtbA was determined by HPLC. Figure S2: alteration of MMP with increased DpdtbA. (A) DMSO; (B) 2.5 μM DpdtbA; (C) 5.0 μM DpdtbA. Figure S3: the flow cytometric analysis of formation of autophagic vacuoles. (A) DMSO control; (B) 5 μM DpdtbA; (C) 5.0 μM DpdtbA + 1.5 mM 3-MA; (D) 5.0 μM DpdtbA + 1.5 NAC. Figure S4: the microscopic analysis of formation of autophagic vacuoles. (A) DMSO control; (B) 5 μM DpdtbA; (C) 5.0 μM DpdtbA + 1.5 mM 3-MA; (D) 5.0 μM DpdtbA + 1.5 NAC (objective size: 10×10). *(Supplementary Materials)*

References

[1] B. Vincenzi, M. Imperatori, M. Silletta, E. Marrucci, D. Santini, and G. Tonini, "Emerging kinase inhibitors of the treatment of gastric cancer," *Expert Opinion on Emerging Drugs*, vol. 20, no. 3, pp. 479–493, 2015.

[2] X. Lin, Y. Zhao, W. M. Song, and B. Zhang, "Molecular classification and prediction in gastric cancer," *Computational and Structural Biotechnology Journal*, vol. 13, pp. 448–458, 2015.

[3] W. Liu, Y. Lu, X. Chai et al., "Antitumor activity of TY-011 against gastric cancer by inhibiting Aurora A, Aurora B and VEGFR2 kinases," *Journal of Experimental & Clinical Cancer Research*, vol. 35, no. 1, p. 183, 2016.

[4] GASTRIC (Global Advanced/Adjuvant Stomach Tumor Research International Collaboration) Group, X. Paoletti, K. Oba et al., "Benefit of adjuvant chemotherapy for resectable gastric cancer: a meta-analysis," *JAMA*, vol. 303, no. 17, pp. 1729–1737, 2010.

[5] K. J. Waldron, J. C. Rutherford, D. Ford, and N. J. Robinson, "Metalloproteins and metal sensing," *Nature*, vol. 460, no. 7257, pp. 823–830, 2009.

[6] G. Vivoli, M. Bergomi, S. Rovesti, M. Pinotti, and E. Caselgrandi, "Zinc, copper, and zinc- or copper-dependent enzymes in human hypertension," *Biological Trace Element Research*, vol. 49, no. 2-3, pp. 97–106, 1995.

[7] V. Corcé, S. G. Gouin, S. Renaud, F. Gaboriau, and D. Deniaud, "Recent advances in cancer treatment by iron chelators," *Bioorganic & Medicinal Chemistry Letters*, vol. 26, no. 2, pp. 251–256, 2016.

[8] M. Frezza, S. Hindo, D. Chen et al., "Novel metals and metal complexes as platforms for cancer therapy," *Current Pharmaceutical Design*, vol. 16, no. 16, pp. 1813–1825, 2010.

[9] S. S. Sadhu, E. Callegari, Y. Zhao, X. Guan, and T. Seefeldt, "Evaluation of a dithiocarbamate derivative as an inhibitor of human glutaredoxin-1," *Journal of Enzyme Inhibition and Medicinal Chemistry*, vol. 28, no. 3, pp. 456–462, 2013.

[10] M. T. Elskens and M. J. Penninckx, "In vitro inactivation of yeast glutathione reductase by tetramethylthiuram disulphide," *European Journal of Biochemistry*, vol. 231, no. 3, pp. 667–672, 1995.

[11] C. S. I. Nobel, M. Kimland, D. W. Nicholson, S. Orrenius, and A. F. G. Slater, "Disulfiram is a potent inhibitor of proteases of the caspase family," *Chemical Research in Toxicology*, vol. 10, no. 12, pp. 1319–1324, 1997.

[12] T. Wang, Y. Fu, T. Huang et al., "Copper ion attenuated the antiproliferative activity of di-2-pyridylhydrazone dithiocarbamate derivative; however, there was a lack of correlation between ROS generation and antiproliferative activity," *Molecules*, vol. 21, no. 12, p. 1088, 2016.

[13] T. Wang, Y. Liu, Y. Fu et al., "Antiproliferative activity of di-2-pyridylhydrazone dithiocarbamate acetate partly involved in p53 mediated apoptosis and autophagy," *International Journal of Oncology*, vol. 51, no. 6, pp. 1909–1919, 2017.

[14] L. Emert-Sedlak, S. Shangary, A. Rabinovitz, M. B. Miranda, S. M. Delach, and D. E. Johnson, "Involvement of cathepsin D in chemotherapy-induced cytochrome *c* release, caspase activation, and cell death," *Molecular Cancer Therapeutics*, vol. 4, no. 5, pp. 733–742, 2005.

[15] A. C. Johansson, H. Appelqvist, C. Nilsson, K. Kågedal, K. Roberg, and K. Ollinger, "Regulation of apoptosis-associated lysosomal membrane permeabilization," *Apoptosis*, vol. 15, no. 5, pp. 527–540, 2010.

[16] D. B. Munafó and M. I. Colombo, "A novel assay to study autophagy: regulation of autophagosome vacuole size by amino acid deprivation," *Journal of Cell Science*, vol. 114, no. 20, pp. 3619–3629, 2001.

[17] W. Xiao, Y. Jiang, Q. Men et al., "Tetrandrine induces G1/S cell cycle arrest through the ROS/Akt pathway in EOMA cells and inhibits angiogenesis in vivo," *International Journal of Oncology*, vol. 46, no. 1, pp. 360–368, 2015.

[18] G. Siriwardana and P. A. Seligman, "Iron depletion results in Src kinase inhibition with associated cell cycle arrest in neuroblastoma cells," *Physiological Reports*, vol. 3, no. 3, article e12341, 2015.

[19] C. Zhang, "Essential functions of iron-requiring proteins in DNA replication, repair and cell cycle control," *Protein & Cell*, vol. 5, no. 10, pp. 750–760, 2014.

[20] A. M. Komarov, I. T. Mak, and W. B. Weglicki, "Iron potentiates nitric oxide scavenging by dithiocarbamates in tissue of septic shock mice," *Biochimica et Biophysica Acta (BBA) - Molecular Basis of Disease*, vol. 1361, no. 3, pp. 229–234, 1997.

[21] D. Moellering, J. McAndrew, H. Jo, and V. M. Darley-Usmar, "Effects of pyrrolidine dithiocarbamate on endothelial cells: protection against oxidative stress," *Free Radical Biology & Medicine*, vol. 26, no. 9-10, pp. 1138–1145, 1999.

[22] F. D. Nicuolo, S. Serini, A. Boninsegna, P. Palozza, and G. Calviello, "Redox regulation of cell proliferation by pyrrolidine dithiocarbamate in murine thymoma cells transplanted in vivo," *Free Radical Biology & Medicine*, vol. 31, no. 11, pp. 1424–1431, 2001.

[23] Y. Li, H. Qi, X. Li, X. Hou, X. Lu, and X. Xiao, "A novel dithiocarbamate derivative induces cell apoptosis through p53-dependent intrinsic pathway and suppresses the expression of the E6 oncogene of human papillomavirus 18 in heLa cells," *Apoptosis*, vol. 20, no. 6, pp. 787–795, 2015.

[24] Y. C. Zheng, L. Z. Wang, L. J. Zhao et al., "1,2,3-Triazole-dithiocarbamate hybrids, a group of novel cell active SIRT1 inhibitors," *Cellular Physiology and Biochemistry*, vol. 38, no. 1, pp. 185–193, 2016.

[25] M. Donadelli, I. Dando, T. Zaniboni et al., "Gemcitabine/cannabinoid combination triggers autophagy in pancreatic cancer cells through a ROS-mediated mechanism," *Cell Death & Disease*, vol. 2, no. 4, article e152, 2011.

[26] M. Chripkova, F. Zigo, and J. Mojzis, "Antiproliferative effect of indole phytoalexins," *Molecules*, vol. 21, no. 12, p. 1626, 2016.

[27] P. Y. Chou, M. M. Lee, S. Y. Lin, and M. J. Sheu, "Pipoxolan exhibits antitumor activity toward oral squamous cell carcinoma through reactive oxygen species-mediated apoptosis," *Anticancer Research*, vol. 37, no. 11, pp. 6391–6400, 2017.

[28] X. Shi, Y. Zhao, Y. Jiao, T. Shi, and X. Yang, "ROS-dependent mitochondria molecular mechanisms underlying antitumor activity of *Pleurotus abalonus* acidic polysaccharides in human breast cancer MCF-7 cells," *PLoS One*, vol. 8, no. 5, article e64266, 2013.

[29] S. H. Lee, X. W. Meng, K. S. Flatten, D. A. Loegering, and S. H. Kaufmann, "Phosphatidylserine exposure during apoptosis reflects bidirectional trafficking between plasma membrane and cytoplasm," *Cell Death & Differentiation*, vol. 20, no. 1, pp. 64–76, 2013.

[30] F. Gillardon, H. Wickert, and M. Zimmermann, "Up-regulation of *bax* and down-regulation of *bcl-2* is associated with kainate-induced apoptosis in mouse brain," *Neuroscience Letters*, vol. 192, no. 2, pp. 85–88, 1995.

[31] J. D. Amaral, J. M. Xavier, C. J. Steer, and C. M. Rodrigues, "The role of p53 in apoptosis," *Discovery Medicine*, vol. 9, no. 45, pp. 145–152, 2010.

[32] Y. Chen, M. B. Azad, and S. B. Gibson, "Methods for detecting autophagy and determining autophagy-induced cell death," *Canadian Journal of Physiology and Pharmacology*, vol. 88, no. 3, pp. 285–295, 2010.

[33] S. Paglin, T. Hollister, T. Delohery et al., "A novel response of cancer cells to radiation involves autophagy and formation of acidic vesicles," *Cancer Research*, vol. 61, no. 2, pp. 439–444, 2001.

[34] H. Erdal, M. Berndtsson, J. Castro, U. Brunk, M. C. Shoshan, and S. Linder, "Induction of lysosomal membrane permeabilization by compounds that activate p53-independent apoptosis," *Proceedings of the National Academy of Sciences of the United States of America*, vol. 102, no. 1, pp. 192–197, 2005.

[35] P. Boya and G. Kroemer, "Lysosomal membrane permeabilization in cell death," *Oncogene*, vol. 27, no. 50, pp. 6434–6451, 2008.

[36] A. Serrano-Puebla and P. Boya, "Lysosomal membrane permeabilization in cell death: new evidence and implications for health and disease," *Annals of the New York Academy of Sciences*, vol. 1371, no. 1, pp. 30–44, 2016.

[37] K. Kagedal, U. Johansson, and K. Ollinger, "The lysosomal protease cathepsin D mediates apoptosis induced by oxidative stress," *The FASEB Journal*, vol. 15, no. 9, pp. 1592–1594, 2001.

[38] C. Marques, C. S. F. Oliveira, S. Alves et al., "Acetate-induced apoptosis in colorectal carcinoma cells involves lysosomal membrane permeabilization and cathepsin D release," *Cell Death & Differentiation*, vol. 4, no. 2, article e507, 2013.

[39] M. Leist and M. Jäättelä, "Triggering of apoptosis by cathepsins," *Cell Death & Differentiation*, vol. 8, no. 4, pp. 324–326, 2001.

[40] D. Glick, S. Barth, and K. F. Macleod, "Autophagy: cellular and molecular mechanisms," *Journal of Pathology*, vol. 221, no. 1, pp. 3–12, 2010.

[41] L. Li, G. Ishdorj, and S. B. Gibson, "Reactive oxygen species regulation of autophagy in cancer: implications for cancer treatment," *Free Radical Biology & Medicine*, vol. 53, no. 7, pp. 1399–1410, 2012.

[42] G. Siriwardana and P. A. Seligman, "Two cell cycle blocks caused by iron chelation of neuroblastoma cells: separating cell cycle events associated with each block," *Physiological Reports*, vol. 1, no. 7, article e00176, 2013.

[43] J. Heath, J. Weiss, C. Lavau, and D. Wechsler, "Iron deprivation in cancer—potential therapeutic implications," *Nutrients*, vol. 5, no. 12, pp. 2836–2859, 2013.

Hindawi
Oxidative Medicine and Cellular Longevity
Volume 2018, Article ID 8296451, 10 pages
https://doi.org/10.1155/2018/8296451

Research Article

Protective Effect of Boswellic Acids against Doxorubicin-Induced Hepatotoxicity: Impact on Nrf2/HO-1 Defense Pathway

Bassant M. Barakat,[1] **Hebatalla I. Ahmed**,[1] **Hoda I. Bahr**,[2] **and Alaaeldeen M. Elbahaie**[3]

[1]*Department of Pharmacology and Toxicology, Faculty of Pharmacy (Girls), Al-Azhar University, Cairo, Egypt*
[2]*Department of Biochemistry, Faculty of Veterinary Medicine, Suez Canal University, Ismailia, Egypt*
[3]*Department of Clinical Oncology and Nuclear Medicine, Faculty of Medicine, Suez Canal University, Ismailia, Egypt*

Correspondence should be addressed to Bassant M. Barakat; bassant.barakat@yahoo.com

Received 8 October 2017; Accepted 19 December 2017; Published 6 February 2018

Academic Editor: Simona G. Bungău

The current study aimed to investigate the potential protective role of boswellic acids (BAs) against doxorubicin- (DOX-) induced hepatotoxicity. Also, the possible mechanisms underlying this protection; antioxidant, as well as the modulatory effect on the Nrf2 transcription factor/hem oxygenase-1 (Nrf2/HO-1) pathway in liver tissues, was investigated. Animals were allocated to five groups: group 1: the saline control, group 2: the DOX group, animals received DOX (6 mg/kg, i.p.) weekly for a period of three weeks, and groups 3–5: animals received DOX (6 mg/kg, i.p.) weekly and received protective doses of BAs (125, 250, and 500 mg/kg/day). Treatment with BAs significantly improved the altered liver enzyme activities and oxidative stress markers. This was coupled with significant improvement in liver histopathological features. BAs increased the Nrf2 and HO-1 expression, which provided protection against DOX-induced oxidative insult. The present results demonstrated that BAs appear to scavenge ROS and inhibit lipid peroxidation and DNA damage of DOX-induced hepatotoxicity. The antioxidant efficacy of BAs might arise from its modulation of the Nrf2/HO-1 pathway and thereby protected liver from DOX-induced oxidative injury.

1. Introduction

Organ dysfunction is common within cancer patients, and hepatic dysfunction has a great impact on the patient outcome leading to a health-care burden [1]. Doxorubicin (DOX) is a widely used chemotherapeutic agent, possessing a broad spectrum of antineoplastic effects against various tumor types and hematological malignancies [2]. Although DOX is a successful cancer chemotherapeutic, side effects limit the clinical utility of DOX-based therapy, including dose-dependent chronic cardiotoxicity, myelosuppression [3], and hepatotoxicity [4]. While the full mechanism of DOX-related cytotoxicities is not fully understood, it has been demonstrated that oxidative stress plays an essential role in DOX-induced toxicity [5]. Reactive oxygen species (ROS) can damage liver membranes causing the release of liver enzymes. Thus, controlling the oxidative injury by different agents is extensively appreciated.

Recently, the protective properties of pentacyclic triterpenoids have gained increasing attention. For instance, oleanolic and ursolic acids are triterpenoids extensively distributed in food and remedial plants [6] and exhibiting protective properties against liver injury in experimental models [7]. Additionally, it was documented that ursolic acid promotes neuroprotection after cerebral ischemia in mice by triggering the NF-E2-related factor 2 (Nrf2) pathway [8].

Boswellia serrata resin extracts show an antioxidant activity in a diversity of experimental diseases including ulcerative colitis [9], myocardial I/R injury [10], and pulmonic fibrosis [11]. Acetyl 11-keto-b-boswellic acid (AKBA) is a pentacyclic triterpenoid compound. It is known as the most significant component of *Boswellia serrata* resin [12]. AKBA has a structural similarity to ursolic acid, and interestingly, one study affirmed that AKBA has greater antioxidant activity in mice than ursolic acid [13]. Consequently, it may promote some of its protective effects via activating the

Nrf2 pathway, a hypothesis which was proved recently by Zhang et al. [14].

It was shown that Nrf2 is involved in regulating the expression of genes encoding antioxidant proteins and detoxifying enzymes of phase 2 through a promoter sequence termed the antioxidant response element. The importance of Nrf2 and its downstream proteins such as NAD(P)H, glutathione S-transferases, and heme oxygenase-1 (HO-1) has been evidenced in guarding against chemically induced oxidative stress causing cellular insult in several organs [15–17]. Among these genes, many studies have concentrated on the regulation and action of HO-1 as it has been proven to have the highest antioxidant response elements on its promoter. HO-1 catalyzes the first and rate-limiting step in heme breakdown and generation of the antioxidants biliverdin and bilirubin [18, 19].

Taking altogether, the profitable features of triterpenoids and the probable role of the Nrf2/HO-1 pathway, our hypothesis is that BAs may offer a protective effect against hepatotoxicity of DOX. We tested if this putative protective effect involves the stimulation of the Nrf2/HO-1 pathway.

2. Materials and Methods

2.1. Chemicals and Drugs. A standardized *B. serrata* extract containing 65% BAs in the form of a tablet preparation was purchased from Advance Physician Formulas Inc. (California, USA). Tablets were grid and suspended in distilled water. Adricin vial containing 2 mg/ml of DOX was obtained from EIMC United Pharmaceuticals (Cairo, Egypt), and dilution was done with saline solution.

2.2. Animals. Animal experiments were licensed and performed according to the rules of the research ethics committee at the Faculty of Pharmacy, Al-Azhar University, and complied with the National Institutes of Health Guide for the Care and Use of Laboratory Animals. We used male Swiss albino mice weighing 21–25 g. Mice were fed a regular chow diet with water ad libitum and maintained in a clean room with normal light and dark cycles. Animals were purchased from the Modern Veterinary Office in Cairo.

2.3. Design of the Experiment. Mice were equally and randomly assigned into five groups, eight animals per group: group 1: animals were injected with saline weekly [16 ml/kg, i.p.] and received distilled water [12 ml/kg/day] orally; group 2 (DOX group): DOX was given to animals every week (6 mg/kg, i.p.) [20] in addition to distilled water [12 ml/kg/day p.o.]; and groups 3, 4, and 5: animals received DOX (6 mg/kg, i.p.) every week and were treated with three doses of BAs [125, 250, and 500 mg/kg/day, p.o.]. All treatment regimens were continued for 3 weeks.

The intraperitoneal route was used for injecting DOX and saline weekly in a volume of 16 ml/kg whereas the oral gavage needle was used to administer BAs and distilled water daily in a total volume of 12 ml/kg. Generally, DOX or saline was given at days 1, 8, and 15 of the experiment. However, BAs started on day 1 and extended to day 21.

2.4. Blood and Sample Collection. At the last day of the experiment, mice were sacrificed by cervical dislocation after being anesthetized with ketamine (80 mg/kg, i.p.). Samples of blood were collected in dry tubes and centrifuged at 1200 ×g. Serum samples were then collected in clean Eppendorf tubes and kept at −20°C to be utilized later in biochemical assays.

For the evaluation of liver function, serum alanine aminotransferase (ALT) and aspartate aminotransferase (AST) activities were determined by enzymatic colorimetric kits from Biodiagnostic (Egypt). Readings for the reaction colors were obtained using an ultraviolet-visible spectrophotometer (UV-1601-PC; Shimadzu, Japan).

Then, each mouse abdomen was opened, and liver was separated and washed in cold phosphate-buffered saline (pH = 7.4). One liver portion was utilized for DNA extraction used in DNA laddering assay, and another one was stored at −80°C for the preparation of tissue homogenate (prepared as 10% *w*/*v*).

2.5. Determination of Oxidative Stress Markers. Frozen liver samples were homogenized in phosphate-buffered saline (pH 7.4) by the aid of a Teflon homogenizer. Tissue homogenates were then put in a cooling centrifuge at 2000 ×g for 10 min. The supernatants were used for malondialdehyde (MDA) determination which has been identified as the product of lipid peroxidation that reacts with thiobarbituric acid (TBA) in acidic medium at 95°C to give pink product measured by a spectrophotometer at wave length equals 534 nm using tetramethoxypropane as a standard [21, 22].

2.6. Western Blot Analysis for Nrf2, HO-1, and Cleaved Caspase-3. The frozen tissues were homogenized and lysed using ice-cold lysis buffer (10% glycerol, 2% SDS in 62 mM Tris-HCl, pH 6.8) containing a cocktail of protease inhibitors (Sigma-Aldrich, St. Louis, MO). The protein content in the collected protein lysates was quantified using the Bradford method [23]. Equal amounts of total protein were resolved under denaturing conditions by sodium dodecyl sulfate-polyacrylamide gel electrophoresis (SDS-PAGE) and then transferred into nitrocellulose membranes. Blocking was done with 6% non-fat dry milk in TBS-Tween buffer for 3 h at 4°C; then the nitrocellulose membranes were incubated at 4°C overnight with the primary antibodies against the target proteins (Nrf2, HO-1, and cleaved caspase-3). For Nrf2, we used Human/Mouse/Rat Nrf2 Antibody Monoclonal Mouse IgG2B Clone number 383727 from R and D Systems Inc. (Minneapolis, USA), for HO-1, we used (A-3): sc-136960 antibody from Santa Cruz Biotechnology Inc. (Dallas, Texas, USA), and for cleaved caspase-3, we used cleaved caspase-3 (Asp175) antibody from Cell Signaling Technology (Danvers, MA, USA). Again, the membranes were incubated with β-actin monoclonal antibody for 1 h on a roller shaker at 4°C. Membranes were then washed 5 times (5 min each) in TBS-Tween buffer in order to get rid of the excess primary antibodies after which they were incubated with an appropriate horseradish peroxidase-conjugated secondary antibodies for another 1 h at 37°C. The bands were scanned using ChemiDoc scanner, and then the densitometric intensity of each band was quantified.

Table 1: Effect of three weekly doses of doxorubicin (6 mg/kg) alone or in combination with boswellic acids (125, 250, or 500 mg/kg/day) on serum ALT and AST in mice.

Groups	ALT (unit/l)	AST (unit/l)
Saline	59.17 ± 14.39 (%CV = 24.31)	84.17 ± 17.41 (%CV = 20.68)
Doxorubicin (6 mg/kg/week)	158.83 ± 28.14[a] (%CV = 17.72)	191.33 ± 45.26[a] (%CV = 23.66)
Doxorubicin (6 mg/kg/week) + BAs (125 mg/kg)	110.83 ± 22.46[b] (%CV = 20.27)	158.17 ± 27.59[b] (%CV = 17.44)
Doxorubicin (6 mg/kg/week) + BAs (250 mg/kg)	91.33 ± 8.71[b] (%CV = 9.54)	129.33 ± 18.03[b] (%CV = 13.94)
Doxorubicin (6 mg/kg/week) + BAs (500 mg/kg)	72.2 ± 12.81[bc] (%CV = 17.79)	125.67 ± 10.78[bc] (%CV = 8.58)

Mice were injected with doxorubicin (DOX, 18 mg/kg i.p.) in combination with boswellic acids (BAs, 125, 250, or 500 mg/kg). Data are mean ± SD, and analysis was done by one-way ANOVA followed by Tukey's post hoc test. [a]Compared to the saline group. [b]Compared to the DOX group. [c]Compared to the doxorubicin + BAs (125 mg/kg) group. P value < 0.05.

2.7. DNA Fragmentation Analysis for Detecting Apoptosis. The liver gnomic DNA was extracted by a Bio Basic EZ-10 spin column genomic DNA kit (Markham, Canada). The diluted samples of extracted genomic DNA (90 ng/ml) were resolved by 0.8% (*w*/*v*) agarose gel electrophoresis for 2 h (90 V and 110 mA) and visualized by ethidium bromide staining using UV illumination. The 100 bp DNA ladder, a ready to use molecular weight marker, was purchased from Solis Biodyne (Tartu, Estonia). The gel was imaged using a gel documentation system; then analysis was done using Gel Docu advanced version 2 software.

2.8. Histopathological Examination. For the investigation of histopathological abnormalities, specimens were taken from the biggest lobe of the liver, fixed with 10% formaldehyde, and embedded in paraffin. From these paraffin blocks, tissue sections were cut and stained with hematoxylin and eosin (H and E). Histological examination for hepatic tissues was done by an expert pathologist who was blinded to the experimental groups. Abnormal histopathological findings were evaluated using a semiquantitative method according to standards proposed by the Knodell histology activity index scoring system [24]. In brief, it grades necroinflammation and fibrosis on a scale of 0 to 22, including 0 to10 for the periportal and/or bridging necrosis, 0 to 4 for intralobular degeneration and focal necrosis, 0 to 4 for portal inflammation, and 0 to 4 for fibrosis.

2.9. Statistical Analysis of the Results. Data were expressed as the mean ± SD and analyzed using the Statistical Package of Social Sciences (Chicago, IL, USA). Differences among means were tested for significant differences employing one-way analysis of variance (ANOVA) test followed by Bonferroni's multiple comparison test in order to determine differences between each pair of study groups. Statistical significance was considered at $P < 0.05$.

3. Results

Results indicated that injecting DOX in a dose of 6 mg/kg weekly increased serum liver enzyme level; ALT and AST activities increased to 158.83 ± 11.49 and 191.33 ± 18.48 versus 59.17 ± 5.87 and 84.17 ± 7.11 in group 1 (saline control), respectively. Combining BAs with DOX (groups 3, 4, and 5) reduced the serum liver enzyme activities in comparison to group 2 (DOX control). The effect of BAs (500 mg/kg) was significantly different from the lowest dose (125 mg/kg) (Table 1).

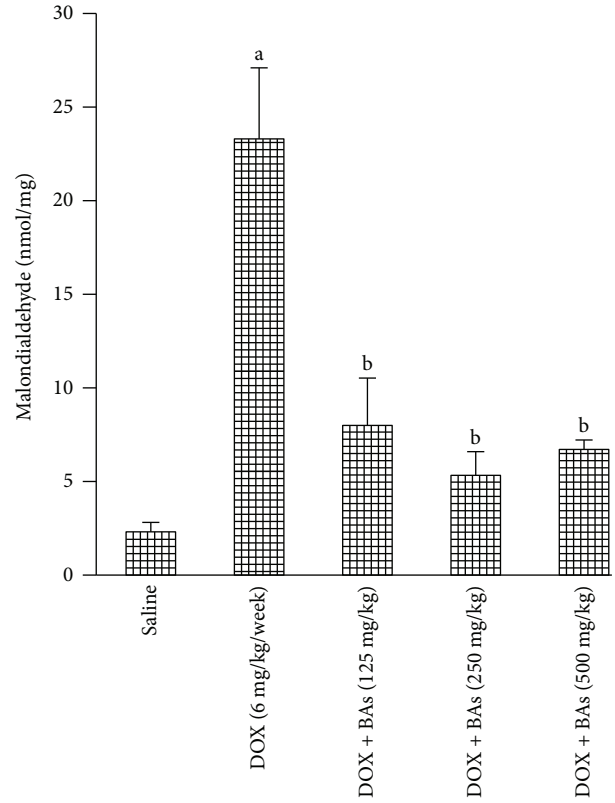

Figure 1: Malondialdehyde level in liver tissue in experimental groups. Mice were injected with doxorubicin (DOX, 18 mg/kg i.p.) in combination with boswellic acids (BAs, 125, 250, or 500 mg/kg). Data are the mean ± SD, and analysis was done by one-way ANOVA followed by Tukey's post hoc test. [a]P value < 0.05 compared to the saline group; [b]P value < 0.05 compared to the DOX group.

Furthermore, hepatic MDA levels increased 10-fold in group 2 (DOX control) as compared with group 1 (saline control). Therapeutic doses of BAs (groups 3, 4, and 5) decreased the MDA level to one-third of the value recorded in group 1 (DOX control) (Figure 1).

Western blot analysis indicated downregulation in genes encoding for Nrf2 and HO-1 {0.2 and 0.3 of the value

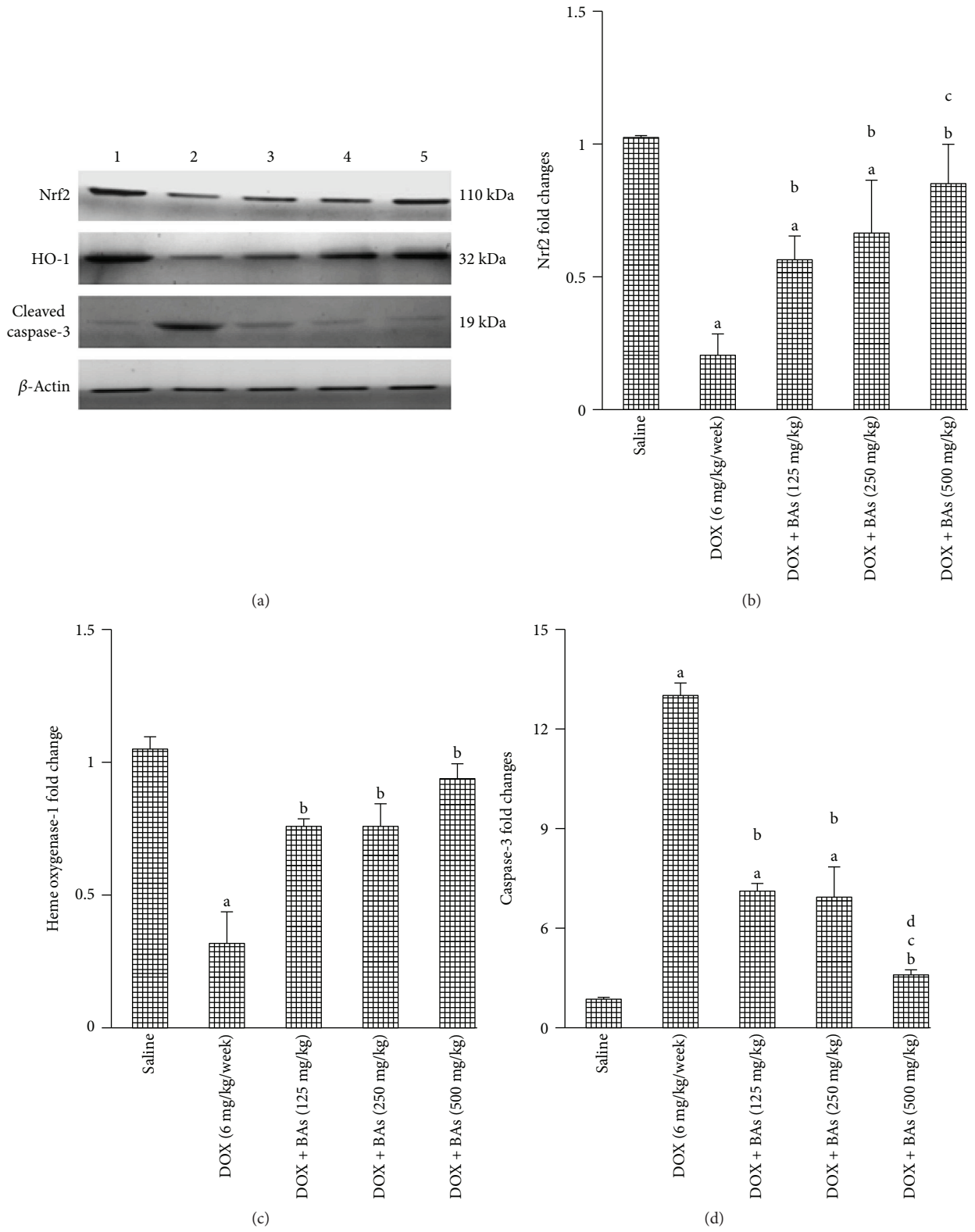

Figure 2: Western blot analysis for Nrf2, heme oxygenase-1, and cleaved caspase-3. (a) Western blots for the measured factors in comparison to β-actin, lane 1 (saline), lane 2 (DOX control), and lanes 3, 4, and 5 (DOX in combination with BAs (125, 250, or 500 mg/kg). Column charts for fold changes in Nrf2 (b), heme oxygenase-1 (c), and cleaved caspase-3 (d). DOX: doxorubicin; BAs: boswellic acids; HO-1: heme oxygenase-1. Data are the mean ± SD, and analysis was done by one-way ANOVA followed by Tukey's post hoc test. ^{a}P value < 0.05 compared to the saline group, ^{b}P value < 0.05 compared to the DOX group, ^{c}P value < 0.05 compared to the doxorubicin + BAs (125 mg/kg) group, and ^{d}P value < 0.05 compared to the doxorubicin + BAs (250 mg/kg) group.

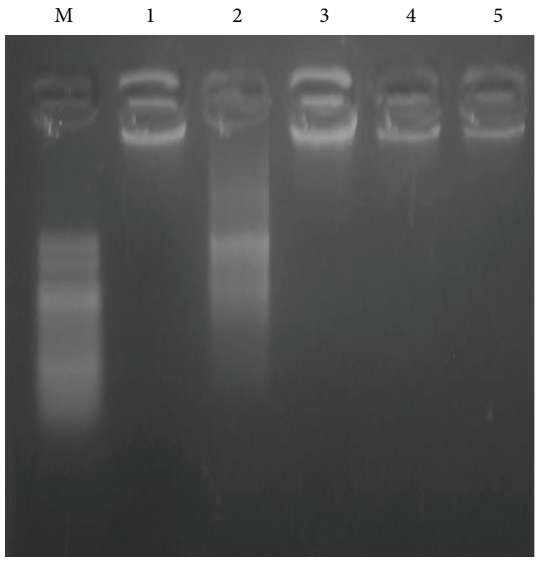

Figure 3: An agarose gel electrophoresis. Image shows DNA fragmentation. Lane M is a DNA marker with 100 bp. Lane 1 shows intact DNA in the saline-treated group. Lane 2 shows DNA streaks of DNA fragmentation in the doxorubicin group. Lanes 3, 4, and 5 show intact DNA in mice treated with BAs (125, 250, or 500 mg/kg) along with DOX. DOX: doxorubicin; BAs: boswellic acids.

reported with group 1 (saline control)} (Figures 2(a)–2(c)) and upregulation in gene encoding for cleaved caspase-3 in group 2 (DOX control—12.45-fold increase) versus group 1 (saline control) (Figures 2(a) and 2(d)). Coadministration of BAs with DOX increased the expression of Nrf2 gene in comparison to the DOX control group. The expression of Nrf2 gene in group 5 (DOX + BAs/500 mg/kg) was significantly greater than that in group 3 (DOX + BAs/125 mg/kg). Similarly, these combinations upregulated HO-1 compared to group 2 (DOX control) (Figures 2(b) and 2(c)). Further, the addition of BAs in all used doses (groups 3, 4, and 5) to DOX regimen differentially downregulated cleaved caspase-3 expression if compared to the DOX control group (group 2). Further, BAs/500 mg/kg/day (group 5) downregulated cleaved caspase-3 expression to a greater extent compared to either of the lower doses (groups 3 and 4) when added to DOX regimen (Figure 2(d)).

Agarose gel electrophoresis for DNA demonstrated normal intact DNA in saline control (group 1) and apoptotic DNA fragments in DOX control (group 2). Groups of mice that received a combination of BAs with DOX (groups 3, 4, and 5) showed less apoptosis and DNA fragmentation when compared to DOX control (group 2) (Figure 3).

Representative hepatic histology for all treatment groups is presented in Figure 4. Normal hepatic sections from saline-treated mice (group 1) showed normal polyhedral hepatic cells which are arranged in cords that are radically arranged around the central veins (Figure 4(a)). However, section from group 2 (doxorubicin control/6 mg/kg/week) showed marked necrosis of hepatocytes (N), hepatic cells with obscure and fiberized boundary with inflammatory cell infiltration (black arrow), dilatation, and congestion of central veins and portal blood vessels (CO) (Figure 4(b)). Moreover, nuclear pyknosis (white arrow), diffuse vacuolar degeneration (black arrow), and severe congestion of portal blood vessels (co) along with lymphocytic infiltration (black arrow), proliferation of bile duct, and fibrosis were very clear (Figure 4(c)). Sections from the liver of DOX + BAs- (125 mg/kg/day) treated group (group 3) showed hepatic cells with focal areas of vacuolar degeneration (black arrow) (Figure 4(d)).

Sections from the liver of group 4 (DOX + BAs/250 mg/kg/day) which revealed normal hepatocytes and vacuolar degeneration ranging from mild to moderate degree (arrow head) and mild hyperemia in the sinusoids (black arrow) are shown in Figure 4(e). On the other hand, Figure 4(f) shows sections from the liver of group 5 (DOX + BAs/500 mg/kg/day) revealing normal tissue architecture and cellular details with few mild vacuolar degeneration (black arrow).

Scoring of histopathological finding of H and E-stained liver section in group 2 (DOX control) demonstrated the greatest score for necrosis, lymphocytic infiltration, nuclear pyknosis, vacuolar degeneration, and congested blood vessels with a total score equal to 18.67 comparing to 0.00 in group 1 (saline control). In groups 3 and 4 (DOX + BAs/125 or 250 mg/kg/day), moderate degrees of necrosis, lymphocytic infiltration, nuclear pyknosis, vacuolar degeneration, and congested blood vessels were observed with a total score equal to 8.67 and 4.67, respectively. Meanwhile, group 5 which is treated with the highest dose of BAs (500 mg/kg/day) in combination with DOX expressed a mild level of necrosis, lymphocytic infiltration, nuclear pyknosis, vacuolar degeneration, and congested blood vessels with a total score equal to 0.67 (Table 2).

4. Discussion

A few specialists propose that 66% of natural plants especially therapeutic ones have an incredible antioxidant potential [25]. Acetylation of cellular proteome linking to proapoptotic domain could be changed by ROS in different experiments [26]. BAs are known as mitigating agents against atherosclerosis, hepatotoxicity, and hyperlipidemia [27] and known for their antioxidant and anti-inflammatory activities [1]. Therefore, BAs are considered promising agents in protection against toxic insults involving generation of ROS. Doxorubicin is a standout among the most broadly utilized anticancer drugs, showing action against a wide assortment of tumors. Nonetheless, its symptoms and critical toxicities display a major problem in cancer treatment that requires careful administration and close monitoring for patients' health. This incited us to address in more prominent subtle elements the part and defensive system of BAs in DOX-initiated liver oxidative damage and the resulting improvement of hepatic injury in mice. Doxorubicin-induced hepatotoxicity is well documented in a variety of animal models [5, 28–30]. And, although it might be comparatively minor from a clinician's perspective than its well-established cardiotoxicity, indeed, it still represents a major problem knowing that DOX is extensively metabolized by the liver to the major metabolite

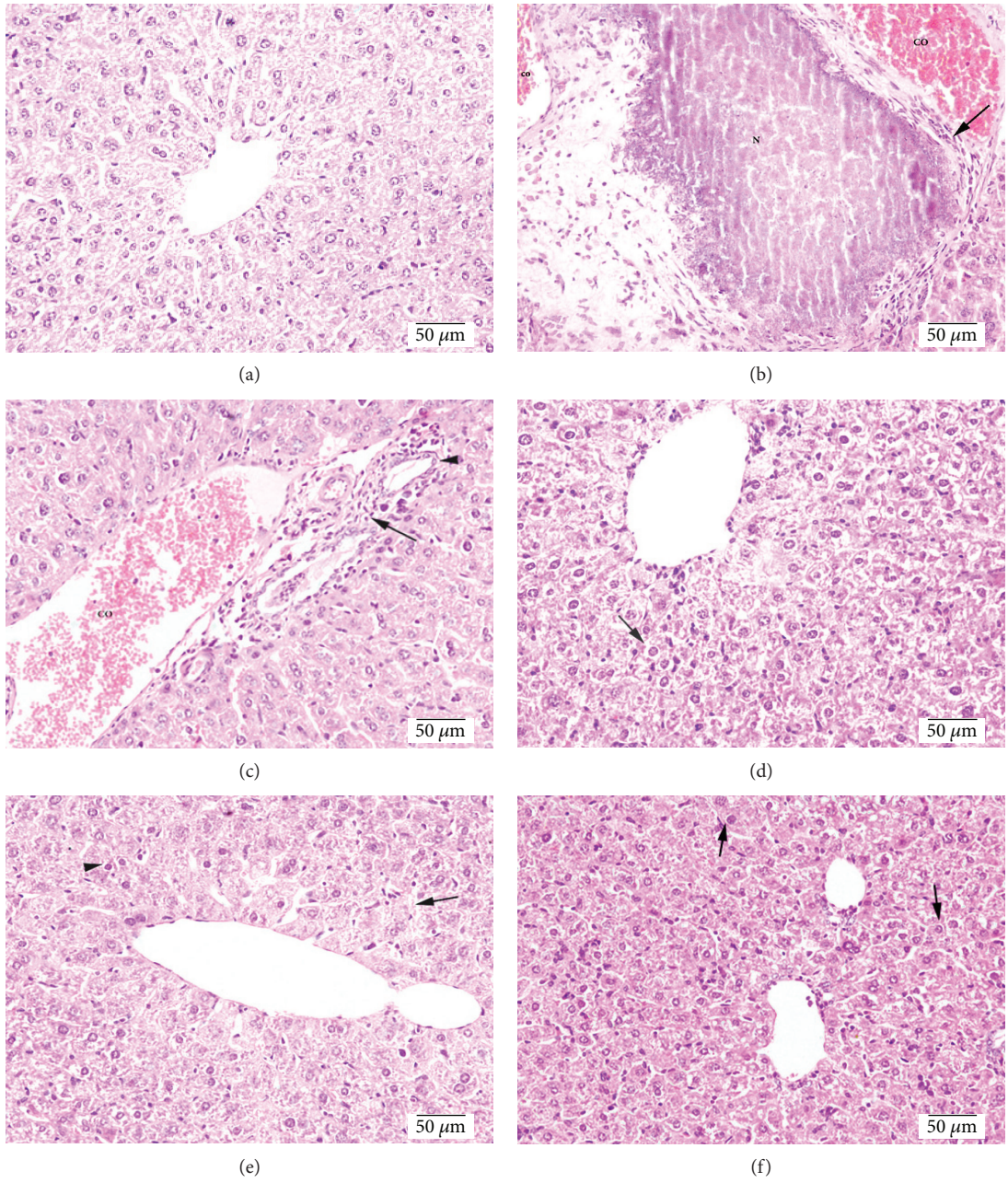

Figure 4: Photomicrographs for hepatic sections stained with hematoxylin and eosin. (a) Section of the liver from the saline group showing normal polyhedral hepatic cells which are arranged in cords that are radically arranged around the central veins. (b) Liver section from the DOX- (6 mg/kg/week) treated group showing marked necrosis of hepatocytes (N), hepatic cell which indicated obscure and fiberized boundary with inflammatory cell infiltration (black arrow), dilatation, and congestion of central veins and portal blood vessels (CO). (c) Section of the liver from the DOX control group showing nuclear pyknosis (white arrow), diffuse vacuolar degeneration (black arrow), and severe congestion of portal blood vessels (co) along with lymphocytic infiltration (black arrow), proliferation of bile duct, and fibrosis. (d) Liver section from mice treated with DOX (6 mg/kg/week) + BAs (125 mg/kg/day) demonstrating hepatic cells showing focal areas of vacuolar degeneration (black arrow). (e) Liver section from mice treated with DOX (6 mg/kg/week) + BAs (250 mg/kg/day) showing normal hepatocytes, mild to moderate vacuolar degeneration (arrow head), and mild hyperemia in the sinusoids (black arrow). (f) Sections from mice treated with DOX (6 mg/kg/week) + BAs (500 mg/kg/day) showing fairly normal tissue architecture and cellular details with mild vacuolar degeneration (black arrow).

doxorubicinol and several hepatotoxic aglycone metabolites [31, 32]. In our study, we selected a dosage regimen and an administration schedule that was previously used by Ali et al. [20] and was proven to cause cardiac toxic effects alongside the antitumor effects.

In the present work, the DOX-treated group prompted increments in the activity of ALT and AST enzymes as compared to the saline-treated group representing clinically significant liver damage that was further confirmed by our histological results. This finding was consistent with several

Table 2: Histopathological score of hepatic tissues from mice treated with three weekly doses of doxorubicin (6 mg/kg) alone or in combination with boswellic acids (125, 250, or 500 mg/kg/day). Scoring for hepatic tissues stained with hematoxylin and eosin was performed as 0 = absent; 1 = low or weak; 2 = mild; 3 = moderate; and 4 = high or frequent, and the total score was calculated from these. Presented results are the mean ± SD and were analyzed using one-way ANOVA followed by Bonferroni's post hoc test at $P < 0.05$.

Groups	Necrosis	Lymphocytic infiltration	Nuclear pyknosis	Vacuolar degeneration	Congested blood vessels	Total score	Mean ± SD
Saline	0.00 ± 0.00	0.00 ± 0.00	0.00 ± 0.00	0.00 ± 0.00	0.00 ± 0.00	**0**	0.00 ± 0.00
Doxorubicin (6 mg/kg/week)	3.67 ± 0.58[a] (%CV = 15.8)	3.33 ± 1.15[a] (%CV = 34.5)	3.67 ± 0.58[a] (%CV = 15.8)	4.00 ± 0.00[a] (%CV = 0.00)	4.00 ± 0.00[a] (%CV = 0.00)	**18.67[a]**	3.73 ± 0.59[a] (%CV = 15.8)
Doxorubicin (6 mg/kg/week) + BAs (125 mg/kg)	1.67 ± 0.58[b] (%CV = 34.7)	1.33 ± 0.58[b] (%CV = 43.6)	2.00 ± 1.00[b] (%CV = 50)	2.00 ± 0.00[b] (%CV = 0.00)	1.67 ± 0.58[b] (%CV = 34.7)	**8.67[b]**	1.73 ± 0.59[b] (%CV = 34.1)
Doxorubicin (6 mg/kg/week) + BAs (250 mg/kg)	0.67 ± 0.58[c] (%CV = 86.6)	1 ± 0.00[b] (%CV = 0.00)	0.67 ± 0.58[c] (%CV = 86.6)	1.33 ± 0.58[c] (%CV = 43.6)	1 ± 1.00[b] (%CV = 100)	**4.67[c]**	0.93 ± 0.59[c] (%CV = 34.1)
Doxorubicin (6 mg/kg/week) + BAs (500 mg/kg)	0.00 ± 0.00 (%CV = 0.00)	0.00 ± 0.00 (%CV = 0.00)	0.00 ± 0.00 (%CV = 0.00)	0.67 ± 0.58[d] (%CV = 86.6)	0.00 ± 0.00 (%CV = 0.00)	**0.67[d]**	0.13 ± 0.35[d] (%CV = 269.2)

[a]Compared to the saline group. [b]Compared to the DOX group. [c]Compared to the doxorubicin + BAs (125 mg/kg) group. [d]Compared to the doxorubicin + BAs (250 mg/kg) group. P value < 0.05.

past reports on DOX-prompted hepatotoxicity and apoptosis in patients enduring some forms of liver injury upon DOX administration [33, 34]. The exact mechanism of DOX-prompted hepatotoxicity is not totally explained. Most reviews support the free radical-induced oxidative stress mechanism, as it can be interpreted by the chemical structure of DOX possessing a tendency to generate superoxide anions and peroxynitrite radicals during hepatic drug metabolism [35]. This evokes ROS-initiated lipid peroxidation favoring hepatocyte damage and creating ALT and AST spillage into serum.

This work has investigated specific exposure responses, including focal infiltration by inflammatory cells, proliferation of bile duct, and fibrosis on liver biopsies demonstrating that DOX induces liver harm. These histopathological changes together with the elevated liver enzyme activities recorded in the DOX-treated group are significantly decreased in the DOX- and BAs-treated groups, suggesting protection from the cell damage produced by DOX. Speculations in regard to the mechanism underlying DOX hepatic damage may likewise lay on lessened hepatic HO-1, Nrf2 protein expression, and elevated MDA level favoring oxidative stress with hepatocyte apoptosis.

Here, these mechanisms were initially proposed to be part of the downregulation of hepatic Nrf2 expression. Firstly, reduced glutathione is able to react with cysteine residues in proteins to form disulfides and this chemical process is known as S-glutathionylation [36]. Curiously, S-glutathionylation can modulate Nrf2 gene expression [37]. Under stress conditions, hepatic metabolites upregulate Nrf-2 expression. Further, hepatic gene expression of many antioxidant and phase II/conjugation enzymes involving HO-1 is primarily induced by Nrf-2 tied to ARE/EpRE after being released from Keap1 and translocated to the nucleus [38–40]. And as presented in our results, Nrf2/HO-1 protein has been highly expressed in group 1 (saline group) which can be attributed to the fact that even in normal cells, ROS are produced but in a controlled fashion to help in different physiological processes within the cell [41]. However, the molecular mechanism of action of Nrf2 in the regulation of physiological oxidative stress, detoxification, and removal of numerous exogenous and some endogenous chemicals is expected to be very well functioning in normal cells [42]. Additionally, the expression of Nrf2 has been observed throughout the human tissue, with high expression in detoxification organs, especially the liver [43]. Steady with many lines of confirmation [38, 44] that underscored, antioxidant enzymes were actuated in response to mild oxidative stress. Yet insignificant cellular damage could be known as chemotherapy for cancer treatment. Hereinafter, it was referred to that HO-1 has been downregulated in response to potent ROS production by DOX as noted in many different experimental models [45–47]. Overall, our data highlighted that elevated MDA and downregulated Nrf2/HO-1 protein expression in DOX-treated mice was ameliorated by BAs coadministration. An effect was significantly demonstrated with the three doses of BAs. This finding might be ascribed to free radical-scavenging properties of BAs that are in concurrence with those got by others [48].

Bearing in mind these data, another proposed mechanism of DOX-induced hepatotoxicity may be attributed to hepatocytes' apoptosis that is confirmed in this study by DNA gel electrophoresis showing significant DNA degradation in the doxorubicin-challenged group compared to normal in addition to increased caspase-3 protein expression. A toxic effect was significantly attenuated by the addition of BAs in all used doses (125, 250, and 500 mg/kg/day). The observed DNA damage is in concurrence with that reported previously [49]. Indeed, the very well-known lipophilic properties of DOX and its DNA-binding capacity are responsible for the high concentrations accumulated in hepatic nucleus favoring DNA damage [34]. Unlike the past outcomes highlighting that DOX treatment did not invigorate hepatic caspase-3, caspase-8, and caspase-9 activation or PARP-1 cleavage [50], our data and others suggest that DOX actuates apoptosis signaling in response to ROS production [20, 51].

Taking altogether, we thus find that BAs are valuable in minimizing DOX-promoted hepatic oxidative damage. BAs downregulated hepatic MDA level and upregulated Nrf-2

protein expression and afterward initiated HO-1 expression. Additionally, it provokes geno-defensive impact by downregulating cleaved caspase-3 protein expression which in turn limits DNA fragmentation. Therefore, this complementary medicinal plant can adequately restrain hepatic damage in DOX-treated mice. It might be noted that some of the investigated parameters were ameliorated in a dose-response manner (e.g., Nrf-2, HO-1, and cleaved caspase-3) while others were not (e.g., MDA) which might be attributed to being more sensitive to the antioxidant effect of BAs than the others. Supporting our work, data published by Kruger et al. [52] have detailed that the metabolic active elements of BAs go about as antioxidants and chelate metals involved in oxidative stress pathways. Another clarification is managed by Hartmann et al. [9] who proposed that BAs possess antioxidant effects restraining MDA production in acute experimental colitis. In addition, previous findings accentuated that BAs evoke antioxidant properties that fortify the Nrf2/HO-1 defense pathway [8, 14].

Since the past works highlighted the stimulant action of BAs on the Nrf2/HO-1 pathway in addition to the inhibitory impacts on MDA production and caspase-3 expression, along these lines, we here can depict the hepatic apoptotic inhibitory impact of BAs by attenuating both initiation and execution phases of apoptosis through its antioxidant properties.

Finally, perhaps one of the considerations when coadministering DOX and an antioxidant agent is that whether this agent would interfere with the desired tumor cell death. However, it has been documented that DOX toxicity in cancer cells primarily occurs through DNA intercalation and damage [53], whereas its cardiotoxicity or hepatotoxicity mainly occurs by generating oxygen free radicals, which can be inhibited by free radical scavengers [54–56]. This difference in DOX-mediated toxicity in cancer and normal cells can be used to improve the antitumor effects of DOX with combinatorial approaches that allow protecting normal cells without affecting the desired oncolytic activity. Another investigated concept is that the defensive mechanisms of many cancer cells are known to be impaired. This makes tumor cells unable to utilize the extra antioxidants in a repair capacity leading to cell death [57]. Furthermore, if we consider the induction of Nrf2 expression in cancer cells by BAs, this will increase the chemosensitivity of anticancer agents since Nrf2 is widely debated for a dual role in chemosensitive and chemoprotective mechanisms [58].

5. Conclusions

Oxidative stress is viewed as the real occasion fundamental DOX hepatic harmfulness. Our outcomes in this study propose that doxorubicin administration is joined by indications of oxidative damage, including elevated hepatic MDA level in accordance with DNA fragmentation, caspase-3 protein expression, HO-1, and Nrf2 protein downregulation. In this work, BAs were capable of deactivating ROS, repressing lipid peroxidation and DNA damage. We also highlighted that the antioxidant effects of BAs involve the regulation of the HO-1/Nrf2 defense pathway and subsequently protect the liver from DOX-induced toxicity. Further studies are also needed to test the corresponding terminal doxorubicin blood concentrations across the dose groups to demonstrate consistency of exposure to strengthen follow-up studies.

Abbreviations

ALT: Alanine aminotransferase
AST: Aspartate aminotransferase (AST)
BAs: Boswellic acids
DOX: Doxorubicin
MDA: Malondialdehyde
Nrf2: Transcription factor/heme oxygenase-1 (Nrf2/HO-1)
ROS: Reactive oxygen species.

Conflicts of Interest

None of the authors have conflicts of interest to declare.

Acknowledgments

The authors wish to acknowledge Professor Dr. Laila Rashid of the Department of Biochemistry, Faulty of Medicine, Cairo University, for the technical support.

References

[1] D. Superfin, A. A. Iannucci, and A. M. Davies, "Commentary: oncologic drugs in patients with organ dysfunction: a summary," *The Oncologist*, vol. 12, no. 9, pp. 1070–1083, 2007.

[2] A. H. Thippeswamy, A. Shirodkar, B. C. Koti et al., "Protective role of *Phyllantus niruri* extract in doxorubicin-induced myocardial toxicity in rats," *Indian Journal of Pharmacology*, vol. 43, no. 1, pp. 31–35, 2011.

[3] I. Craig Henderson and E. Frei 3rd, "Adriamycin cardiotoxicity," *American Heart Journal*, vol. 99, no. 5, pp. 671–674, 1980.

[4] R. Injac, M. Perse, M. Cerne et al., "Protective effects of fullerenol $C_{60}(OH)_{24}$ against doxorubicin-induced cardiotoxicity and hepatotoxicity in rats with colorectal cancer," *Biomaterials*, vol. 30, no. 6, pp. 1184–1196, 2009.

[5] J. Kolarovic, M. Popovic, J. Zlinská, S. Trivic, and M. Vojnovic, "Antioxidant activities of celery and parsley juices in rats treated with doxorubicin," *Molecules*, vol. 15, no. 9, pp. 6193–6204, 2010.

[6] L. O. Somova, A. Nadar, P. Rammanan, and F. O. Shode, "Cardiovascular, antihyperlipidemic and antioxidant effects of oleanolic and ursolic acids in experimental hypertension," *Phytomedicine*, vol. 10, no. 2-3, pp. 115–121, 2003.

[7] J. Liu, "Pharmacology of oleanolic acid and ursolic acid," *Journal of Ethnopharmacology*, vol. 49, no. 2, pp. 57–68, 1995.

[8] L. Li, X. Zhang, L. Cui et al., "Ursolic acid promotes the neuroprotection by activating Nrf2 pathway after cerebral ischemia in mice," *Brain Research*, vol. 1497, pp. 32–39, 2013.

[9] M. R. Hartmann, M. I. Morgan Martins, J. Tieppo, H. S. Fillmann, and N. P. Marroni, "Effect of *Boswellia serrata* on antioxidant status in an experimental model of colitis rats induced by acetic acid," *Digestive Diseases and Sciences*, vol. 57, no. 8, pp. 2038–2044, 2012.

[10] S. M. Elshazly, D. M. Abd El Motteleb, and N. N. Nassar, "The selective 5-LOX inhibitor 11-keto-β-boswellic acid protects

against myocardial ischemia reperfusion injury in rats: involvement of redox and inflammatory cascades," *Naunyn-Schmiedeberg's Archives of Pharmacology*, vol. 386, no. 9, pp. 823–833, 2013.

[11] E. Ali and S. Mansour, "Boswellic acids extract attenuates pulmonary fibrosis induced by bleomycin and oxidative stress from gamma irradiation in rats," *Chinese Medicine*, vol. 6, no. 1, p. 36, 2011.

[12] H. Safayhi, T. Mack, J. Sabieraj, M. I. Anazodo, L. R. Subramanian, and H. P. Ammon, "Boswellic acids: novel, specific, nonredox inhibitors of 5-lipoxygenase," *The Journal of Pharmacology and Experimental Therapeutics*, vol. 261, no. 3, pp. 1143–1146, 1992.

[13] M. C. Yin, M. C. Lin, M. C. Mong, and C. Y. Lin, "Bioavailability, distribution, and antioxidative effects of selected triterpenes in mice," *Journal of Agricultural and Food Chemistry*, vol. 60, no. 31, pp. 7697–7701, 2012.

[14] Y. Zhang, J. Jia, Y. Ding et al., "Alpha-boswellic acid protects against ethanol-induced gastric injury in rats: involvement of nuclear factor erythroid-2-related factor 2/heme oxygenase-1 pathway," *The Journal of Pharmacy and Pharmacology*, vol. 68, no. 4, pp. 514–522, 2016.

[15] K. Chan and Y. W. Kan, "Nrf2 is essential for protection against acute pulmonary injury in mice," *Proceedings of the National Academy of Sciences of the United States of America*, vol. 96, no. 22, pp. 12731–12736, 1999.

[16] A. Enomoto, K. Itoh, E. Nagayoshi et al., "High sensitivity of Nrf2 knockout mice to acetaminophen hepatotoxicity associated with decreased expression of ARE-regulated drug metabolizing enzymes and antioxidant genes," *Toxicological Sciences*, vol. 59, no. 1, pp. 169–177, 2001.

[17] J. W. Fahey, X. Haristoy, P. M. Dolan et al., "Sulforaphane inhibits extracellular, intracellular, and antibiotic-resistant strains of *Helicobacter pylori* and prevents benzo[*a*]pyrene-induced stomach tumors," *Proceedings of the National Academy of Sciences of the United States of America*, vol. 99, no. 11, pp. 7610–7615, 2002.

[18] L. E. Otterbein, M. P. Soares, K. Yamashita, and F. H. Bach, "Heme oxygenase-1: unleashing the protective properties of heme," *Trends in Immunology*, vol. 24, no. 8, pp. 449–455, 2003.

[19] Q. Lin, S. Weis, G. Yang et al., "Heme oxygenase-1 protein localizes to the nucleus and activates transcription factors important in oxidative stress," *The Journal of Biological Chemistry*, vol. 282, no. 28, pp. 20621–20633, 2007.

[20] S. A. Ali, S. A. Zaitone, and Y. M. Moustafa, "Boswellic acids synergize antitumor activity and protect against the cardiotoxicity of doxorubicin in mice bearing Ehrlich's carcinoma," *Canadian Journal of Physiology and Pharmacology*, vol. 93, no. 8, pp. 695–708, 2015.

[21] K. Satoh, "Serum lipid peroxide in cerebrovascular disorders determined by a new colorimetric method," *Clinica Chimica Acta*, vol. 90, no. 1, pp. 37–43, 1978.

[22] H. Ohkawa, N. Ohishi, and K. Yagi, "Assay for lipid peroxides in animal tissues by thiobarbituric acid reaction," *Analytical Biochemistry*, vol. 95, no. 2, pp. 351–358, 1979.

[23] M. M. Bradford, "A rapid and sensitive method for the quantitation of microgram quantities of protein utilizing the principle of protein-dye binding," *Analytical Biochemistry*, vol. 72, no. 1-2, pp. 248–254, 1976.

[24] R. G. Knodell, K. G. Ishak, W. C. Black et al., "Formulation and application of a numerical scoring system for assessing histological activity in asymptomatic chronic active hepatitis," *Hepatology*, vol. 1, no. 5, pp. 431–435, 1981.

[25] D. Krishnaiah, R. Sarbatly, and R. Nithyanandam, "A review of the antioxidant potential of medicinal plant species," *Food and Bioproducts Processing*, vol. 89, no. 3, pp. 217–233, 2011.

[26] A. V. Pointon, T. M. Walker, K. M. Phillips et al., "Doxorubicin *in vivo* rapidly alters expression and translation of myocardial electron transport chain genes, leads to ATP loss and caspase 3 activation," *PLoS One*, vol. 5, no. 9, article e12733, 2010.

[27] M. Z. Siddiqui, "*Boswellia serrata*, a potential antiinflammatory agent: an overview," *Indian Journal of Pharmaceutical Sciences*, vol. 73, no. 3, pp. 255–261, 2011.

[28] J. Psotov, S. Chlopcikova, F. Grambal, V. Simanek, and J. Ulrichova, "Influence of silymarin and its flavonolignans on doxorubicin-iron induced lipid peroxidation in rat heart microsomes and mitochondria in comparison with quercetin," *Phytotherapy Research*, vol. 16, pp. S63–S67, 2002.

[29] N. A. El-Shitany, S. El-Haggar, and K. El-Desoky, "Silymarin prevents adriamycin-induced cardiotoxicity and nephrotoxicity in rats," *Food and Chemical Toxicology*, vol. 46, no. 7, pp. 2422–2428, 2008.

[30] A. Rašković, N. Stilinović, J. Kolarović, V. Vasović, S. Vukmirović, and M. Mikov, "The protective effects of silymarin against doxorubicin-induced cardiotoxicity and hepatotoxicity in rats," *Molecules*, vol. 16, no. 12, pp. 8601–8613, 2011.

[31] C. M. Camaggi, R. Comparsi, E. Strocchi, F. Testoni, B. Angelelli, and F. Pannuti, "Epirubicin and doxorubicin comparative metabolism and pharmacokinetics. A cross-over study," *Cancer Chemotherapy and Pharmacology*, vol. 21, no. 3, pp. 221–228, 1988.

[32] P. E. Ganey, F. C. Kauffman, and R. G. Thurman, "Oxygen dependent hepatotoxicity due to doxorubicin: role of reducing equivalent supply in perfused rat liver," *Molecular Pharmacology*, vol. 34, no. 5, pp. 695–701, 1988.

[33] Y.-Y. Zhang, C. Meng, X.-M. Zhang et al., "Ophiopogonin D attenuates doxorubicin-induced autophagic cell death by relieving mitochondrial damage in vitro and in vivo," *The Journal of Pharmacology and Experimental Therapeutics*, vol. 352, no. 1, pp. 166–174, 2015.

[34] O. Tacar, P. Sriamornsak, and C. R. Dass, "Doxorubicin: an update on anticancer molecular action, toxicity and novel drug delivery systems," *Journal of Pharmacy and Pharmacology*, vol. 65, no. 2, pp. 157–170, 2013.

[35] T. G. Neilan, S. L. Blake, F. Ichinose et al., "Disruption of nitric oxide synthase 3 protects against the cardiac injury, dysfunction, and mortality induced by doxorubicin," *Circulation*, vol. 116, no. 5, pp. 506–514, 2007.

[36] A. Martinez-Ruiz and S. Lamas, "Signalling by NO-induced protein S-nitrosylation and S-glutathionylation: convergences and divergences," *Cardiovascular Research*, vol. 75, no. 2, pp. 220–228, 2007.

[37] H. J. Forman, K. J. A. Davies, and F. Ursini, "How do nutritional antioxidants really work: nucleophilic tone and parahormesis versus free radical scavenging *in vivo*," *Free Radical Biology & Medicine*, vol. 66, pp. 24–35, 2014.

[38] K. Z. Guyton and T. W. Kensler, "Prevention of liver cancer," *Current Oncology Reports*, vol. 4, no. 6, pp. 464–470, 2002.

[39] N. Li, J. Alam, M. I. Venkatesan et al., "Nrf2 is a key transcription factor that regulates antioxidant defense in macrophages

and epithelial cells: protecting against the proinflammatory and oxidizing effects of diesel exhaust chemicals," *The Journal of Immunology*, vol. 173, no. 5, pp. 3467–3481, 2004.

[40] T. W. Kensler, N. Wakabayashi, and S. Biswal, "Cell survival responses to environmental stresses via the Keap1-Nrf2-ARE pathway," *Annual Review of Pharmacology and Toxicology*, vol. 47, no. 1, pp. 89–116, 2007.

[41] T. Finkel, "Signal transduction by reactive oxygen species," *The Journal of Cell Biology*, vol. 194, no. 1, pp. 7–15, 2011.

[42] Q. Ma, "Xenobiotic-activated receptors: from transcription to drug metabolism to disease," *Chemical Research in Toxicology*, vol. 21, no. 9, pp. 1651–1671, 2008.

[43] W. Tang, Y. F. Jiang, M. Ponnusamy, and M. Diallo, "Role of Nrf2 in chronic liver disease," *World Journal of Gastroenterology*, vol. 20, no. 36, pp. 13079–13087, 2014.

[44] C. R. Wolf, "Chemoprevention: increased potential to bear fruit," *Proceedings of the National Academy of Sciences of the United States of America*, vol. 98, no. 6, pp. 2941–2943, 2001.

[45] C. A. Piantadosi, M. S. Carraway, A. Babiker, and H. B. Suliman, "Heme oxygenase-1 regulates cardiac mitochondrial biogenesis via Nrf2-mediated transcriptional control of nuclear respiratory factor-1," *Circulation Research*, vol. 103, no. 11, pp. 1232–1240, 2008.

[46] F. Bernuzzi, S. Recalcati, A. Alberghini, and G. Cairo, "Reactive oxygen species-independent apoptosis in doxorubicin-treated H9c2 cardiomyocytes: role for heme oxygenase-1 down-modulation," *Chemico-Biological Interactions*, vol. 177, no. 1, pp. 12–20, 2009.

[47] T. Satoh, S. R. McKercher, and S. A. Lipton, "Nrf2/ARE-mediated antioxidant actions of pro-electrophilic drugs," *Free Radical Biology & Medicine*, vol. 66, pp. 45–57, 2014.

[48] M. K. Tawfik, "Anti-aggregatory effect of boswellic acid in high-fat fed rats: involvement of redox and inflammatory cascades," *Archives of Medical Science*, vol. 6, no. 6, pp. 1354–1361, 2016.

[49] S. S. Ahmad, S. F. Idris, G. A. Follows, and M. V. Williams, "Primary testicular lymphoma," *Clinical Oncology*, vol. 24, no. 5, pp. 358–365, 2012.

[50] A. J. Dirks-Naylor, S. A. Kouzi, J. D. Bero, N. T. Tran, S. Yang, and R. Mabolo, "Effects of acute doxorubicin treatment on hepatic proteome lysine acetylation status and the apoptotic environment," *World Journal of Biological Chemistry*, vol. 5, no. 3, pp. 377–386, 2014.

[51] R. Guo, J. Lin, W. Xu et al., "Hydrogen sulfide attenuates doxorubicin-induced cardiotoxicity by inhibition of the p38 MAPK pathway in H9c2 cells," *International Journal of Molecular Medicine*, vol. 3, pp. 644–650, 2013.

[52] P. Kruger, R. Daneshfar, G. P. Eckert et al., "Metabolism of boswellic acids in vitro and in vivo," *Drug Metabolism and Disposition*, vol. 36, no. 6, pp. 1135–1142, 2008.

[53] O. Hovorka, V. Subr, D. Větvička et al., "Spectral analysis of doxorubicin accumulation and the indirect quantification of its DNA intercalation," *European Journal of Pharmaceutics and Biopharmaceutics*, vol. 76, no. 3, pp. 514–524, 2010.

[54] K. Shimpo, T. Nagatsu, K. Yamada et al., "Ascorbic acid and adriamycin toxicity," *The American Journal of Clinical Nutrition*, vol. 54, no. 6, pp. 1298S–1301S, 1991.

[55] R. Chinery, J. A. Brockman, M. O. Peeler, Y. Shyr, R. D. Beauchamp, and R. J. Coffey, "Antioxidants enhance the cytotoxicity of chemotherapeutic agents in colorectal cancer: a p53-independent induction of $p21^{WAF1/CIP1}$ via C/EBPβ," *Nature Medicine*, vol. 3, no. 11, pp. 1233–1241, 1997.

[56] P. Mukhopadhyay, M. Rajesh, S. Bátkai et al., "Role of superoxide, nitric oxide, and peroxynitrite in doxorubicin-induced cell death in vivo and in vitro," *American Journal of Physiology Heart and Circulatory Physiology*, vol. 296, no. 5, pp. H1466–H1483, 2009.

[57] T. D. Oberley and L. W. Oberley, "Antioxidant enzyme levels in cancer," *Histology and Histopathology*, vol. 12, no. 2, pp. 525–535, 1997.

[58] M. C. Jaramillo and D. D. Zhang, "The emerging role of the Nrf2-Keap1 signaling pathway in cancer," *Genes & Development*, vol. 27, no. 20, pp. 2179–2191, 2013.